THE PHARMACOLOGICAL AND CELLULAR EFFECTS OF HUMAN SOMATOSTATIN RECEPTOR HOMO- AND HETERODIMERIZATION

By

MICHAEL GRANT

Department of Pharmacology and Therapeutics

McGill University

Montreal, Canada

June 2008

A thesis submitted to the Faculty of Graduate Studies and Research

In partial fulfillment for the Degree of

DOCTOR of PHILOSOPHY

Your file Votre référence
ISBN: 978-0-494-66304-2
Our file Notre référence
ISBN: 978-0-494-66304-2

It is a capital mistake to theorize before one has the data. Insensibly one begins to twist facts to suit theories, instead of theories to suit facts.

– Sherlock Holmes

ABSTRACT

Somatostatin (SST) is a peptide hormone that was originally identified in the hypothalamus and subsequently found throughout the central nervous system and in various peripheral organs. Generally classified as an inhibitory factor, SST is secreted by endocrine, neuronal and immune cells and acts to regulate cell secretion, neurotransmission and cell proliferation. There are five receptor-subtypes known to engage SST, termed SSTR1-5, all belonging to the superfamily of G-protein coupled receptors (GPCRs). Within the past few years, there has been a preponderance of evidence to suggest the importance of GPCR dimerization in receptor-biogenesis, regulation and pharmacology. It has been previously reported in our laboratory, that human (h) SSTR5 homo- and heterodimerizes with hSSTR1 in an agonist-regulated manner. However, it was unclear as to the contribution of each subtype in the formation of the hSSTR1/hSSTR5 heterodimer, the possible molecular determinants involved and the effects of heterodimerization on the pharmacology of the receptors. Furthermore, the dimerization properties of other hSSTRs including their heterodimerization remain undetermined. Here, we demonstrate that agonist binding to hSSTR5 and not hSSTR1 modulates the formation of the heterodimer, with particular emphasis on its carboxyl-terminal tail in specifying the interaction. We also determined the mechanics of the hSSTR2 homodimer, unlike the previous hSSTRs investigated, forms constitutive dimers that dissociate into monomers following activation with agonist. This feature is important for receptor trafficking, as preventing their dissociation impairs agonist-mediated endocytosis. Lastly, we investigated the heterodimerization of hSSTR2 and hSSTR5, an interaction that, like the hSSTR1/hSSTR5 heterodimer, is subtype-specific, requiring selective-activation of hSSTR2 and not hSSTR5. The heterodimer exhibited enhanced signalling characteristics including, prolonged activation of MAP kinases and an increase in the induction of the cyclin-dependent kinase inhibitor $p27^{Kip1}$. These enhanced properties of the heterodimer conferred an extended growth inhibitory response. Dimerization of GPCRs, with particular emphasis on heterodimers, generates novel receptors with unique properties distinct from those of the individual receptor

monomers/homodimers. An understanding on the mechanisms involved in GPCR dimerization could provide a rationale in future drug design.

RÉSUMÉ

La somatostatine (SST) est une hormone qui a été identifiée premièrement dans l'hypothalamus et retrouvée plus tard dans le système nerveux central et divers organes périphériques. SST est sécrétée par les neurones, les cellules endocriniennes et immunitaires et agit comme inhibiteur des voies impliquées dans la neurotransmission, la sécrétion et la prolifération des cellules. Il existe cinq sous-types de récepteurs de SST, nommés SSTR1 à 5, tous appartenant à la famille des récepteurs couplés aux protéines G (RCPG). De nombreuses études suggèrent que la dimérisation des RCPG est importante pour la biogenèse, la régulation et la pharmacologie de ses récepteurs. Précédemment, nous avons rapporté que la forme humaine du récepteur sous-type 5 de la somatostatine (hSSTR5) homodimèrise tout en présentant la capacité de former des hétérodimères avec hSSTR1 après son activation par SST. Cependant, nous connaissons peu sur la contribution de chaque sous-type dans la formation de l'hétérodimère hSSTR1/hSSTR5, sur les facteurs moléculaires qui y sont impliqués et les effets de l'hétérodimèrisation sur la pharmacologie des récepteurs. De plus, la dimérisation des autres sous-types de hSSTR et leur hétérodimèrisation restent indéterminées. Dans cette étude, nous démontrons que la liaison spécifique de l'agoniste au récepteur hSSTR5 module l'hétérodimèrisation dépendante elle-même du domaine C-terminal du récepteur. Nous avons aussi déterminé les mécanismes de formation de l'homodimère du récepteur hSSTR2 qui possède la particularité unique de se dissocier en monomère après l'activation par un agoniste. Cet aspect est essentiel dans l'internalisation des récepteurs. Enfin, nous avons étudié l'hétérodimèrisation des récepteurs hSSTR2 et hSSTR5 dont l'interaction est sous-type-spécifique et exige seulement l'activation du hSSTR2. Nous avons identifié que l'hétérodimère hSSTR2/hSSTR5 est impliqué dans la signalisation, il induit l'activation prolongée des MAP kinases et augmente l'induction de $p27^{Kip1}$. Ces propriétés de l'hétérodimère confèrent une réponse prolongée et inhibitrice de la croissance. La dimérisation des RCPG, tout particulièrement des hétérodimères, permet de générer des récepteurs originaux avec des propriétés uniques et distinctes des autres

récepteurs monomères/homodimères. Une compréhension des mécanismes impliqués dans la dimérisation des RCPG pourrait être une étape essentielle pour la conception des drogues futures.

ACKNOWLEDGEMENTS

This thesis is a dedication to the memory of Dr. Yogesh C. Patel (1942-2003). His relentless devotion to science and to the field of Somatostatin was deeply inspiring. I am grateful to have been a part of his legacy.

I would also like to thank Dr. Ujendra Kumar, whom after Dr. Patel's passing had continued in his stead. It was his support and belief in me as a student/scientist that gave me the needed encouragement to continue forward.

I thank Dr. Brian Collier, my academic advisor turned co-supervisor, for his thoughtful insight and understanding.

I would also like to thank Dr. Geoffrey Hendy for his support.

Thanks to all of my family, friends and co-workers, whom without their support, this would not have been possible.

Special thanks to Garo Yeretssian who aided me in the translation of my abstract.

Finally, I would like to thank the financial support I received throughout the years from the McGill University Health Center Research Institute and the Fonds de la recherche en santé du Québec.

CONTRIBUTIONS OF AUTHORS

This thesis is assembled in accordance with the regulations of the Faculty of Graduate Studies and Research, McGill University. It is written in a manuscript-based format and comprises three original manuscripts in their entirety in Section 4. The contribution of each author is as follows:

SECTION 4A) Grant, M., Patel, R.C. and Kumar, U. (2004) The role of subtype-specific ligand binding and the C-tail domain in dimer formation of human somatostatin receptors. *J Biol Chem*, **279**, 38636-38643.

The candidate was responsible for most of the work in this manuscript, including the conceptualization and design of each experiment. R.C. Patel aided in the interpretation of the pbFRET results. U. Kumar contributed to the assembly of the manuscript and supervised the project.

SECTION 4B) Grant, M., Collier, B. and Kumar, U. (2004) Agonist-dependent dissociation of human somatostatin receptor 2 dimers: a role in receptor trafficking. *J Biol Chem*, **279**, 36179-36183.

The candidate was responsible for most of the work in this manuscript, including the conceptualization and design of each experiment. B. Collier and U. Kumar contributed to the assembly of the manuscript and supervised the project.

SECTION 4C) Grant, M., Alturaihi, H., Jaquet, P., Collier, B. and Kumar, U. (*in revision*) Cell Growth Inhibition and Functioning of Human Somatostatin Receptor Type 2 are Modulated by Receptor Heterodimerization. *Mol Endocrinol.*

The candidate was responsible for most of the work in this manuscript, including the conceptualization and design of each experiment. H. Alturaihi assisted me in the MAPK experiments. P. Jaquet aided in the interpretation of the results and B. Collier and U. Kumar supervised the project.

TABLE OF CONTENTS

LIST OF FIGURES & TABLES

ABBREVIATIONS

BRET	Bioluminescence resonance energy transfer
cAMP	Cyclic adenosine monophosphate
cGMP	Cyclic guanosine monophosphate
CHO	Chinese hamster ovary
CNS	Central nervous system
CST	Cortistatin
C-tail	Carboxyl-terminal segment
D2R	Dopamine receptor subtype-2
EGF	Epidermal growth factor
ER	Endoplasmic reticulum
ERK	Extracellular signal-regulated kinase
FBS	Foetal bovine serum
FCS	Fluorescence correlation spectroscopy
FGF	Fibroblast growth factor
FITC	Fluorescein isothiocyanate
FRET	Fluorescence resonance energy transfer
GABA	Gamma-aminobutyric acid
$GABA_BR$	Metabotropic glutamate receptor
GDP	Guanosine diphosphate
GFP	Green fluorescent protein
GH	Growth hormone
GHRH	Growth hormone-releasing hormone
GPCR	G-protein coupled receptor
GRK	G-protein coupled receptor kinase
GTP	Guanosine triphosphate
HA	Hemagglutinin
HEK	Human embryonic kidney

hSSTR	human somatostatin receptor
IGF-I	Insulin growth factor-I
IL	Intracellular loop
JAK	Janus kinase
MAPK	Mitogen-activated protein kinase
μOR	mu-opioid receptor
NHE-1	Sodium/hydrogen exchanger
OR	Opioid receptor
PCA	Protein complementation assay
pbFRET	Photobleaching FRET
PPSST	Preprosomatostatin
PTPases	Phosphotyrosine phosphatases
PTX	Pertussis toxin
rSSTR	rattus somatostatin receptor
Rh	Rhodamine
Rluc	Renilla luciferase
SST, SRIF	Somatostatin
SSTR	Somatostatin receptor
T3	Triiodothyronine
T4	Thyroxine
T1R	Taste receptor
TM	Transmembrane domain
TSH	Thyroid-stimulating hormone
TR	Texas red
trFRET	Time resolved FRET
wt	wild-type
YFP	Yellow fluorescent protein

SECTION 1: PRELUDE

The physiological function and survival of cells is dependent on their ability to respond appropriately to stimuli within their surrounding environment. The communication that occurs with the environment and even between neighbouring cells is achieved primarily by cell surface receptors that are responsible for organizing complex networks of intracellular signalling proteins. The largest and most diverse family of cell surface receptors is the G-protein coupled receptor (GPCR) superfamily. The human genome comprises approximately 1000 members that respond to an astonishing variety of extracellular stimuli namely light, ions, small molecules, peptides, hormones and proteins. Upon activation, GPCRs initiate a cascade of responses by regulating a class of three-subunit proteins termed G-proteins, named for their binding to guanosine triphosphate (GTP). However, evidence has demonstrated GPCR signalling independent of G-protein activation, underscoring the complex nature of these receptors. It is estimated that over 50% of the drugs on the market today are targeted against GPCRs. This translates into annual revenues in excess of $40 billion, representing a valuable player in the human therapeutic market. It is no wonder why research in developing new and more potent drugs directed against GPCRs is ongoing. A better understanding on the structure, function and signalling pathways of GPCRs could improve the treatment of various diseases.

SECTION 2: RATIONALE AND OBJECTIVES

The biological effects of somatostatin (SST) were first encountered unexpectedly in the late 1960's. In two unrelated studies, one by Krulich et al. [Krulich et al., 1968] who reported on a growth hormone (GH)-releasing inhibitory substance from hypothalamic extracts and the other, by Hellman and Lernmark [Hellman and Lernmark, 1969], on the presence of a potent insulin inhibitory factor from the extracts of pigeon pancreatic islets. However, the inhibitory substance was not officially identified until 1973 by Guillemin's group [Brazeau et al., 1973]. In both synthetic and naturally occurring forms, this tetradecapeptide originally coined as somatotropin release-inhibitory factor (SRIF, SST-14) was shown by Brazeau et al. to be the substance in controlling hypothalamic GH release. This single achievement not only pioneered SST research but was also duly recognized, as Guillemin shared the 1977 Nobel Prize in Medicine. The following years bequeathed an exponential increase in SST-related studies. It soon became clear that SST-synthesis was not restricted to the hypothalamus. Its production is widely distributed throughout the central nervous system (CNS), peripheral neurons, the gastrointestinal tract and the pancreatic islets of Langerhans [Arimura et al., 1975; Dubois, 1975; Hokfelt et al., 1975; Luft et al., 1974; Orci et al., 1975; Patel and Reichlin, 1978; Pelletier et al., 1975; Polak et al., 1975]. In fact, SST-like immunoreactivity can be found throughout various tissues of vertebrates and invertebrates, including the plant kingdom {*reviewed in* [Patel, 1992; Tostivint, 2004]}. Given its broad anatomical distribution, it is no wonder why SST produces a wide spectrum of biological effects. Generally regarded as an inhibitory factor, SST can function either locally on neighbouring cells or distantly through the circulation, to regulate such physiological processes as glandular secretion, neurotransmission, smooth muscle contractility, nutrient absorption and cell division {*reviewed in* [Barnett, 2003; Patel, 1992; Patel, 1999; Patel et al., 2001; Reichlin, 1983a; Reichlin, 1983b]}.

These extraordinary efforts into the biology of SST could not have been possible if it were not for the availability of stable and potent analogs, given that SST has an extremely short plasma half-life [Weckbecker et al., 2003]. In 1978, while working at Sandoz (later Novartis, Basel, Switzerland), Vale et al. reported on the first SST-analog, an octapeptide with full SST-like biological activity, derived from a cyclic cysteine-bridged hexapeptide backbone [Vale et al., 1978]. Further modification of the peptide by the introduction of two D-amino acid isomers and L-threoninol at the C-terminal, provided increased metabolic stability even in the midst of aggressive media such as gastric juices at elevated temperatures [Bauer et al., 1982]. This improved octapeptide was coded as SMS 201-995 or octreotide, and developed under the name Sandostatin®. In 1988, Sandostatin gained its first FDA approval for the symptomatic treatment of gastroenteropancreatic tumours. Today, the inhibitory actions of SST-analogs are applied in several clinical scenarios, including, the suppression of tumoural hormone hyper-secretion (acromegaly, neuroendocrine tumours, pancreatic tumours, carcinoid tumours), gastrointestinal bleeding, dumping syndrome and pancreatitis {*reviewed in* [Lamberts et al., 1996; Weckbecker et al., 2003]}.

Despite the marked achievement in the development of octreotide, it was not until the early 1990's, that the structure of the first SST receptor (SSTR) emerged by molecular cloning [Yamada et al., 1992]. Subsequent cloning revealed five distinct SSTR genes, an amount that was greater than predicted from pharmacological and biochemical criteria at the time {*reviewed in* [Patel, 1997; Patel et al., 1995; Reisine and Bell, 1995]}. The conceptualization behind the development and successful deployment of octreotide, was only later identified by its preferential-binding to SSTR2 [Patel, 1997; Reisine and Bell, 1995; Weckbecker et al., 2003], as many tumours express this receptor-subtype [Gardette et al., 2004; Hofland and Lamberts, 2003; Lamberts et al., 2002]. Rational approaches to developing peptide and non-peptide analogs that bind more selectively soon followed {*reviewed in* [Weckbecker et al., 2003]}. However, it soon became clear that SSTRs would often show overlapping patterns of distribution in a tissue specific manner, which raised questions on the relevance of receptor-co-expression and the importance of target specificity, given the similarities in receptor-signalling. Nevertheless, reports have surfaced describing activation of putative second messengers as well as differential

cellular and physiological responses in cells bearing more than one receptor-subtype when treated with SST agonists [Ben-Shlomo et al., 2005; Bruns et al., 2002; Cattaneo et al., 2000; Danila et al., 2001; Fedele et al., 2007; Florio et al., 2003b; Jaquet et al., 2005; Jaquet et al., 2000; Ren et al., 2003; Saveanu et al., 2001; Saveanu et al., 2006; Shimon et al., 1997a; Shimon et al., 1997b; Tulipano et al., 2001; Zatelli et al., 2004; Zatelli et al., 2005a]. Recently, the trafficking and desensitization of SSTR2 following its selective activation was shown to be affected when SSTR5 was co-expressed, however the mechanism for this behaviour had yet to be described [Sharif et al., 2007].

All five SSTR subtypes are members of the superfamily of G-protein coupled receptors (GPCRs) {*reviewed* in [Olias et al., 2004; Patel, 1999]}. An abounding amount of reports has challenged the age-old notion that GPCRs exist and function as monomeric entities at the cell surface. It is now clear that many {*reviewed in* [Bai, 2004; Breitwieser, 2004; Franco et al., 2003; Hansen and Sheikh, 2004; Kroeger et al., 2003; Milligan, 2008; Prinster et al., 2005; Terrillon and Bouvier, 2004]} but not all GPCRs function exclusively as dimers [Bayburt et al., 2007; Grant et al., 2004b; Gripentrog et al., 2003; James et al., 2006; Meyer et al., 2006; Patel et al., 2002a; Rasmussen et al., 2007; Whorton et al., 2007; Whorton et al., 2008]. SSTRs are no exception, as our laboratory including others have demonstrated their ability to form both homo- and heterodimers, with members of the same or distantly related receptor-families [Baragli et al., 2007; Duran-Prado et al., 2007; Grant et al., 2004a; Grant et al., 2004b; Patel et al., 2002a; Pfeiffer et al., 2001; Pfeiffer et al., 2002; Rocheville et al., 2000a; Rocheville et al., 2000b]. This thesis investigates the functional and pharmacological relevance of human (h) SSTR dimerization and is a continuation on the ground work described by M. Rocheville [Rocheville, M (2002) Ph.D. thesis (McGill University, Montreal, Canada)], in our laboratory.

M. Rocheville had previously characterized the homodimerization of hSSTR5 and determined it to be regulated by agonist-binding [Rocheville et al., 2000b]. This was demonstrated using both Western blotting and photobleaching fluorescence resonance energy transfer (pbFRET) microscopy, a technique implemented in our laboratory to study the dimerization of GPCRs {*reviewed in* [Patel et al., 2002b]}. She had also

indirectly shown that hSSTR5 could heterodimerize with hSSTR1 using a functional complementation assay, where a signalling defective hSSTR5 could regain functionality when co-expressed alongside a functional hSSTR1 [Rocheville et al., 2000b]. Furthermore, she had extended the repertoire of hSSTR signalling, by demonstrating the ability of hSSTR5 to heterodimerize with the dopamine D2 receptor, enhancing the pharmacological properties of both receptor-subtypes [Rocheville et al., 2000a]. Following my introduction into the laboratory, we had demonstrated using both pbFRET microscopy and the more sophisticated two-photon fluorescence correlation spectroscopy approach, that although hSSTR5 can heterodimerize with hSSTR1 in an agonist-regulated manner, hSSTR1 remains monomeric when expressed separately despite treatment with agonist [Patel et al., 2002a]. Nevertheless, given the inability of hSSTR1 to homodimerize, it remained unclear as to whether its selective-activation could stabilize hSSTR1/hSSTR5 heterodimers, what molecular determinants may be involved in SSTR dimerization and the effects of hSSTR1/hSSTR5 heterodimerization on the pharmacology of the receptors. In addition, the dimerization properties of the remaining hSSTR family including the possible pharmacological, cellular or physiological impact on biology have yet to be reported.

SECTION 3: GENERAL INTRODUCTION

A) Somatostatin and its Receptor Family

Somatostatin processing

It has been over three decades since the discovery of somatostatins (SSTs), a family of cyclopeptide hormones that are mainly produced by normal endocrine, gastrointestinal, immune and neuronal cells {*reviewed in* [Barnett, 2003; Brazeau et al., 1973; Patel, 1992; Patel, 1999; Patel et al., 2001; Reichlin, 1983a; Reichlin, 1983b]}. SST is synthesized as two bioactive products, the form originally identified in the hypothalamus consisting of 14 amino acids, SST-14, and its congener, SST-28, subsequently discovered to contain an extension at the N-terminus [Pradayrol et al., 1980] (Fig. 3.1A, B). Elucidation of the biosynthesis of both forms of SST, like other protein hormones [Hook et al., 1994], revealed a larger inactive precursor molecule, preprosomatostatin (PPSST), which is processed by post-translational enzymatic cleavage to yield the active polypeptides [Goodman et al., 1981; Goodman et al., 1980; Joseph-Bravo et al., 1980; Oyama et al., 1980; Patzelt et al., 1980; Shields, 1980; Zingg and Patel, 1982]. In the early 1980s, development of recombinant DNA technology, allowed for the isolation and cloning of human and rat cDNAs encoding PPSST [Funckes et al., 1983; Goodman et al., 1982; Shen et al., 1982]. This work revealed the sequence and structure of PPSST, a polypeptide consisting of 116 amino acids. Enzymes implicated in the processing of PSST belong to the subtilisin/kexin-related, Ca^{2+}-dependent class of serine proteinases, collectively termed precursor convertases [Seidah and Chretien, 1999; Zhou et al., 1999]. Although there are seven known mammalian precursor convertases, a

Figure 3.1.

Somatostatin processing.

A, Prosomatostatin is processed into two bioactive forms, SST-14 and SST-28. ***B***, Amino acid sequence of somatostatin isoforms depicting the cysteine bridge maintaining its cyclic structure and the pharmacophore (red).

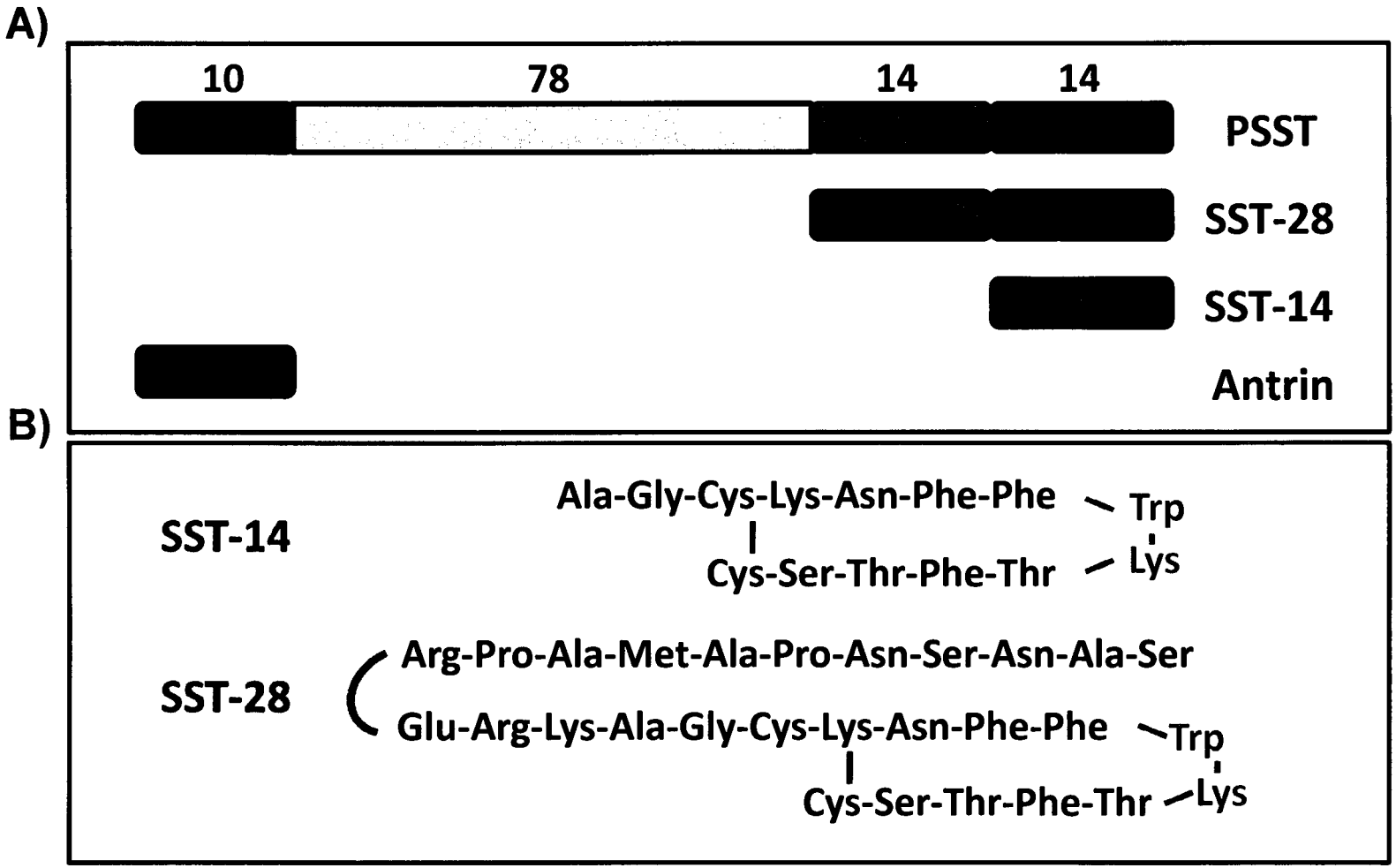
A)
10
78
14
14
PSST
SST-28
SST-14
Antrin
B)
SST-14
Ala-Gly-Cys-Lys-Asn-Phe-Phe
Trp
Cys-Ser-Thr-Phe-Thr
Lys
SST-28
Arg-Pro-Ala-Met-Ala-Pro-Asn-Ser-Asn-Ala-Ser
Glu-Arg-Lys-Ala-Gly-Cys-Lys-Asn-Phe-Phe
Trp
Cys-Ser-Thr-Phe-Thr
Lys

select few have been shown important in PSST processing {*reviewed in* [Mouchantaf et al., 2004]}. Processing of PSST primarily occurs at the C-terminal end generating the two bioactive forms. SST-14 is generated by dibasic cleavage at an Arg-Lys residue, whereas endoproteolysis of a monobasic Arg site produces SST-28 [Bersani et al., 1989; Patel and O'Neil, 1988]. In addition, a secondary monobasic site was determined in PSST, cleavage of which results in the generation of a 10-amino acid peptide termed antrin ($PSST_{1-10}$), named after its initial discovery in the gastric antrum, for which it showed the highest concentration [Benoit et al., 1987]. Although antrin has no known function, it has been isolated in all SST-producing tissues [Rabbani and Patel, 1990; Ravazzola et al., 1989].

Due to differential processing of PSST, various mixtures of SST-14 and SST-28 are produced in mammalian tissues [Patel et al., 1981]. SST-14 is largely present in pancreatic islets, stomach and neural tissues; it is the prominent form in the retina, peripheral nerves and enteric neurons [Patel et al., 1981]. In the brain, SST-28 accounts for approximately 20 to 30% of total SST-like immunoreactivity. In the periphery, SST-28 synthesis predominates in intestinal mucosal cells as the terminal biosynthetic product following PSST processing [Baskin and Ensinck, 1984; Patel et al., 1981]. Although only SST-14 and SST-28 are the known biologically active forms of PSST, other products have been identified in circulation following processing, however; their biological function remains uncertain as they are devoid of any known activity [Ensinck et al., 1989; Patel and O'Neil, 1988; Patel et al., 1981; Rabbani and Patel, 1990; Ravazzola et al., 1989; Shoelson et al., 1986].

Somatostatin distribution

The production of SST occurs at high densities in cells throughout the CNS, the peripheral nervous system, the endocrine pancreas and the gut, in addition; to small numbers in the thyroid, adrenals, submandibular glands, kidney, prostate, placenta, blood vessel walls and immune cells [Aguila et al., 1991; Arimura et al., 1975; Dubois, 1975; Finley et al., 1981; Fuller and Verity, 1989; Hokfelt et al., 1975; Johansson et al., 1984;

Patel, 1992; Patel and Reichlin, 1978; Pelletier et al., 1975; Polak et al., 1975; Reichlin, 1983a; Reichlin, 1983b]. Within the CNS, neurons and fibers positive for SST are abundantly dotted, the notable exception being the cerebellum [Finley et al., 1981; Johansson et al., 1984]. More specifically, brain regions such as the hypothalamus, the deep layers of the cortex, the limbic system and all levels of the major sensory pathway are rich in SST-producing neurons. In a subpopulation of C cells in the thyroid, SST coexists with calcitonin [Reichlin, 1983a; Reichlin, 1983b]. At least in rats, total body SST can be divided as follows: gut accounts for the majority of SST, approximately 65%, the brain for ~25%, the pancreas for ~5%, while the remaining organs account for the residual 5% [Patel and Reichlin, 1978].

Somatostatin physiology

The physiological role of hypothalamic SST is well established {*reviewed in* [Barnett, 2003; Patel, 1992; Patel, 1999]}. As early as week 10 of gestation, SST is detected in the foetal hypothalamus [Bugnon et al., 1978]. It is there where its release regulates the secretion of GH from the pituitary, the counterbalance being growth hormone-releasing hormone (GHRH), which is detected in the hypothalamus at week 18 of gestation [Bresson et al., 1984]. In adults, GH secretion occurs at a basal rate throughout the day. The major role of hypothalamic SST is the tonic inhibition of both basal and GHRH-stimulated secretion of GH from anterior pituitary somatotrophs [Barinaga et al., 1985]. Somatostatinergic neurons emanate from the anterior hypothalamus and project to the median eminence, where SST is released into hypophyseal portal vessels to interact with pituitary somatotrophs [Barnett, 2003; Patel, 1992]. SST and GHRH pathways interact with each other at both their point of convergence at the level of the pituitary and through direct neural connections within the hypothalamus [Horvath et al., 1989]. Thus, SST inhibits the secretion of GH via a direct interaction on the pituitary and indirectly through suppression of GHRH release [Katakami et al., 1988; Tannenbaum et al., 1990]. Two secretory feedback loops exist that modulate SST release: the short loop, where SST is negatively regulated by GHRH

[Katakami et al., 1988] but subject to positive-feedback by GH [Berelowitz et al., 1981a]; the long loop, where insulin growth factor type 1 (IGF-I) produced by GH acting on the liver, provides a positive influence [Berelowitz et al., 1981b]. This mechanism in regulating GH release is further supported in SST knockout mice, as nadir GH levels are consistently higher in these animals compared to their wild-type counterparts [Low et al., 2001]. In addition, secretion of hypothalamic SST can be further promoted by dopamine, substance P, neurotensin, glucagon, hypoglycaemia, various amino acids, acetylcholine, α_2-adrenergic agonists, vasoactive intestinal polypeptide (VIP) and cholecystokinin; it is however inhibited by glucose [Berelowitz et al., 1982; Chihara et al., 1979; Reichlin, 1983a]. Similar mechanisms also exist in the hypothalamic control of thyroid-stimulating hormone (TSH) secretion [Arimura and Schally, 1976; Ferland et al., 1976; James et al., 1997; Reichlin, 1983a; Reichlin, 1983b; Rodriguez-Arnao et al., 1981; Samuels et al., 1992; Siler et al., 1974; Tanjasiri et al., 1976; Vale et al., 1975].

In addition to its actions on the pituitary, SST functions as a neurotransmitter in the brain with effects on cognition, locomotor, sensory and autonomic functions {*reviewed in* [Barnett, 2003; Epelbaum et al., 1994; Patel, 1992; Reichlin, 1983a; Reichlin, 1983b]} (Fig. 3.2). SST inhibits the release of dopamine from the midbrain, the secretions of norepinephrine, thyroid-releasing hormone, corticotrophin-releasing hormone including its own secretion from the hypothalamus. As previously indicated, it inhibits both the basal and stimulated secretion of GH and TSH, but has no effects on the release of luteinising hormone, follicle-stimulating hormone, prolactin or adrenal corticotrophin hormone under normal physiological conditions. SST has direct effects on the thyroid by inhibiting the release of T4, T3 and calcitonin from thyroid parafollicular cells stimulated by TSH. It acts on the adrenals to inhibit angiotensin II stimulated aldosterone secretion and acetylcholine stimulated medullary catecholamine secretion. SST inhibits the secretion of renin in the kidneys when stimulated by hypovolemia, including the inhibition of antidiuretic hormone-mediated water absorption. Within the gastrointestinal tract, virtually every gut hormone has been shown to be inhibited by SST including gastric acid, pepsin, bile and colonic fluid. SST also has a generalized suppressive effect on the motor activity within the gastrointestinal tract, such that it

Figure 3.2.

Schematic depicting the hormonal actions of somatostatin.

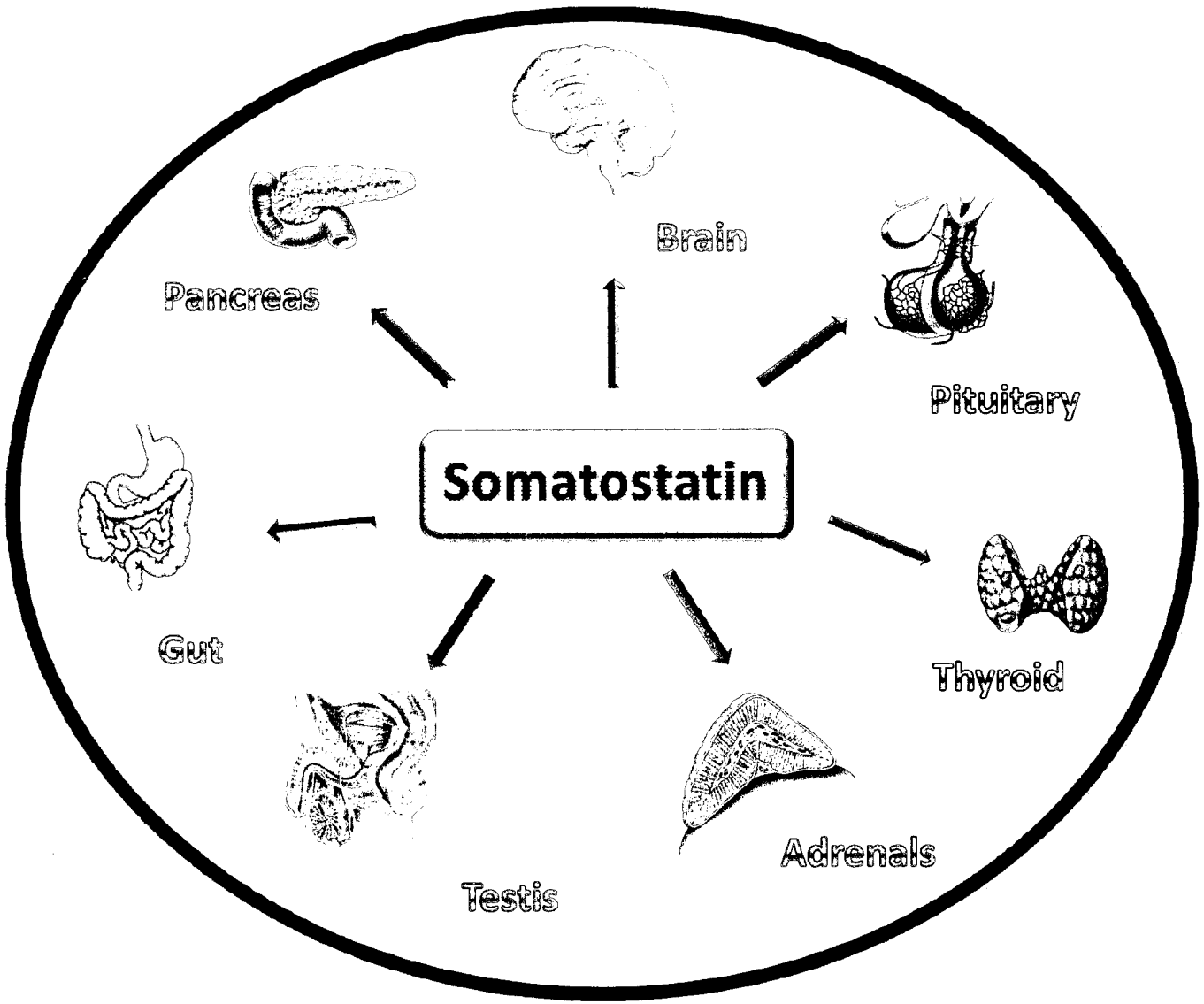
Somatostatin
Brain
Pancreas
Pituitary
Gut
Thyroid
Testis
Adrenals

inhibits gastric emptying, gallbladder contraction and small intestinal segmentation. In the pancreas, SST is an endogenous islet hormone. Its actions on the pancreas were first noted within the year of its discovery by two groups, following infusion in humans and baboons [Alberti et al., 1973; Koerker et al., 1974]. Somatostatin regulates the secretion of hormones from several tissues, including neurotransmission. When synthesized and released from δ cells of pancreatic islets, SST causes suppression of the synthesis and secretion of both insulin and glucagon, including the inhibition of pancreatic polypeptide [Ballian et al., 2006; German et al., 1990; Kendall et al., 1995; Kleinman et al., 1995; Nelson-Piercy et al., 1994; Philippe, 1993; Redmon et al., 1994; Zhang et al., 1991] (Fig. 2.2). SST is also known to block the release of several growth factors and cytokines [Blum et al., 1992; Elliott et al., 1994; Hayry et al., 1993]. More recently, the antisecretory properties of SST were demonstrated to affect ghrelin release [Barkan et al., 2003]. Additional effects of SST include vasoconstriction and an antiproliferative effect on immune, intestinal mucosal, cartilage and bone precursor cells [Aguila et al., 1996; Karalis et al., 1994; Patel, 1992; Reichlin, 1983a; Reichlin, 1983b; Takeba et al., 1997; Weiss et al., 1981]. Interestingly, a downregulation in SST expression has been associated with Alzheimer's disease. The brains of mice that were deficient in SST showed a greater accumulation of $A\beta_{42}$, the main contributor to Alzheimer's disease, due to a decrease in neprilysin activity [Saito et al., 2005]. When either SST was administered or neprilysin was directly activated, decreases in the aggregation of $A\beta_{42}$ was observed [Saito et al., 2005].

Somatostatin regulation

Given its widespread distribution and its interaction with various bodily systems, it is no wonder that SST can be regulated by a broad array of secretagogues; from ions and nutrients to neuropeptides, neurotransmitters, hormones, growth factors and cytokines {*reviewed in* [Barnett, 2003; Patel, 1992; Patel et al., 2001; Reichlin, 1983a; Reichlin, 1983b]. For instance, membrane depolarization stimulates SST release from both neurons and peripheral SST-secreting cells. However, the effects of nutrients such as

glucose, amino acids and lipids, on SST secretion appears to be tissue-specific, a predominant feature in the triggering of SST release from δ cells in pancreatic islets. Contrarily, the secretion of hypothalamic SST is inhibited by glucose but insensitive to aminogenic agents. On the other hand, gut SST is promoted by luminal but not circulating nutrients. The effects of glucocorticoids are distinct, however, and employ a biphasic effect on SST secretion: stimulatory at low doses and inhibitory at high doses. Almost every neurotransmitter or neuropeptide tested has been shown to exert some sort of effect on SST secretion with a certain degree of tissue specificity. In particular, glucagon, GH-releasing hormone, neurotensin, corticotrophin-releasing hormone, calcitonin gene-related peptide and bombesin are potent stimulators of SST secretion, while opiate and GABA are inhibitors [Epelbaum et al., 1994; Patel, 1992; Patel et al., 2001]. With regards to the hormones investigated, thyroid, GH, IGF-I and insulin augment SST release from the hypothalamus [Barnett, 2003; Patel, 1992; Patel et al., 2001]; insulin, leptin and epinephrine inhibits its release from the pancreas and hypothalamus respectively [Barnett, 2003; Patel, 1992; Patel et al., 2001]. Inflammatory mediators have also shown differential effects on SST secretion: IL-1, IL-6, IL-10, INF-γ and TNF-α stimulate SST release while TGF-β inhibits it [Elliott, 2004; Quintela et al., 1997; Scarborough et al., 1989].

In addition to modulating SST secretion, many of the same agents also regulate gene expression. For instance, various members of the growth factor and cytokine family, glucocorticoids, testosterone, estradiol, insulin, leptin, TGF-β and NMDA receptor agonists affect steady state SST mRNA levels {*reviewed in* [Patel, 1992; Patel, 1999; Patel et al., 2001]}. The typical transcriptional unit of a mammalian SST gene consists of two exons separated by an intron {*reviewed in* [Patel et al., 2001; Vallejo, 2004]. Several intracellular mediators are known to affect SST gene function and include, cAMP, cGMP, nitric oxide, Ca^{2+} and activators of protein kinase C [Aguila, 1994; Frankel et al., 1982; Kanatsuka et al., 1981; Montminy et al., 1986; Patel et al., 1991]. Immediately upstream of the start transcription site contains a variant of the TATA box element, followed by a cAMP response element (CRE), two glucocorticoid response element (GRE) nonconsensus sequences and an insulin response element.

Tissue-specific promoter elements are also present that work in concert with the CRE to impart high levels of constitutive gene activity. Finally, two silencer elements located within the promoter mediate repression of SST gene transcription [Patel et al., 2001; Vallejo, 2004].

A new member in the somatostatin family?

A little over a decade ago, cDNA encoding a peptide was cloned from rat brain tissue with structural similarity to SST [Tostivint et al., 1996]. This new peptide termed cortistatin (CST), due to its predominantly cortical expression, is synthesized from a larger precursor molecule, preprocortistatin. Enzymatic cleavage gives rise to two products, CST-14 and CST-29. Of the fourteen amino acids pertaining to CST-14, eleven are identical to SST-14. A human form was also identified, but unlike the rat homolog, it contains seventeen residues (hCST-17) [Fukusumi et al., 1997]. However, unlike SST, CST has potent sleep-promoting activities when infused into rat brain ventricles, a property achieved by its antagonizing effect on the neurotransmitter acetylcholine on cortical excitability [de Lecea et al., 1996]. Recently, CST mRNA has been demonstrated in various peripheral organs and hence, not restricting its expression to the CNS [Dalm et al., 2004; Papotti et al., 2003; Xidakis et al., 2007]. Furthermore, a biological relevance for CST outside the CNS has been recently confirmed, as similar observations have been obtained in comparison to SST-analogs in measures of endocrine function [Gottero et al., 2004].

Somatostatin receptors

The identification of high-affinity plasma membrane SST receptors (SSTRs), was first described in 1978, using the rat pituitary GH_4C_1 cell line by whole-cell binding analysis [Schonbrunn and Tashjian, 1978]. However, it was soon apparent that more than one class of SSTR existed, based upon differential binding affinities and potencies for SST-14 and SST-28 in brain, pituitary and islet cells [Mandarino et al., 1981; Srikant and

Patel, 1981]. These studies including one by Tran et al., further categorized SSTRs into two subclasses based on their affinity for the then available SST-analogs octreotide and seglitide: SRIF I, that bound SST-analogs and SRIF II, the group that was insensitive to these compounds [Reisine and Bell, 1995; Tran et al., 1985]. Using a variety of techniques such as binding analysis, covalent crosslinking and purification of solubilised receptor including in vivo and in vitro autoradiography, the expression of SSTRs was demonstrated at various densities in the brain, gut, pituitary, thyroid, adrenals, endocrine and exocrine pancreas, kidneys and immune cells {*reviewed in* [Olias et al., 2004; Patel, 1997; Patel, 1999; Patel et al., 1995; Reisine and Bell, 1995]}. Several tumour cell lines have also demonstrated to be rich sources of SSTRs and include, AtT-20 mouse pituitary tumour cells, hamster insulinoma and Rin m5F islet tumour cells, AR42J and Mia PaCa pancreatic tumour cells and human breast cancer, neuroblastoma, glioma, leukemic and myeloma cell lines {*reviewed in* [Patel, 1997; Patel, 1999; Patel et al., 1995; Reisine and Bell, 1995]}. Photoaffinity labelling and purification studies, revealed the existence of several SSTR species in the range of 32-85 kDa in a tissue-specific manner [Patel et al., 1995; Patel et al., 1990; Reisine and Bell, 1995].

Fourteen years following the discovery of high-affinity SSTR binding sites on whole-cell membranes [Schonbrunn and Tashjian, 1978], the first SSTR sequence was resolved by molecular cloning [Yamada et al., 1992]. It was not long before the identity of five distinct SSTR genes become available {*reviewed in* [Olias et al., 2004; Patel, 1997; Patel, 1999; Patel et al., 1995; Reisine and Bell, 1995]. Using the mRNA from human islets, the first two SSTRs were cloned and termed SSTR1 and SSTR2 [Yamada et al., 1992]. The sequences of the remaining SSTRs were soon elucidated (SSTR3, SSTR4 and SSTR5) as identified in human and rodent tissue [Patel, 1997; Patel et al., 1996; Patel et al., 1995]. SSTRs encoded from the human genome are all nonallelic, and map to separate loci on different chromosomes. With the exception of SSTR2, which gives rise to two spliced variants, SSTR2A and SSTR2B, SSTRs are intronless. SSTR2A and SSTR2B differ only in the length of their carboxy-terminal segments (C-terminus). All SSTR subtypes display seven α helical transmembrane (TM) segments typified by G-protein coupled receptor (GPCR) topology (Fig. 3.3). GPCRs are grouped into three

Figure 3.3.

Schematic representation of the structure of SSTR2A.

Possible glycosylation and phosphorylation sites including a palmitoyl membrane-anchorage site are shown.

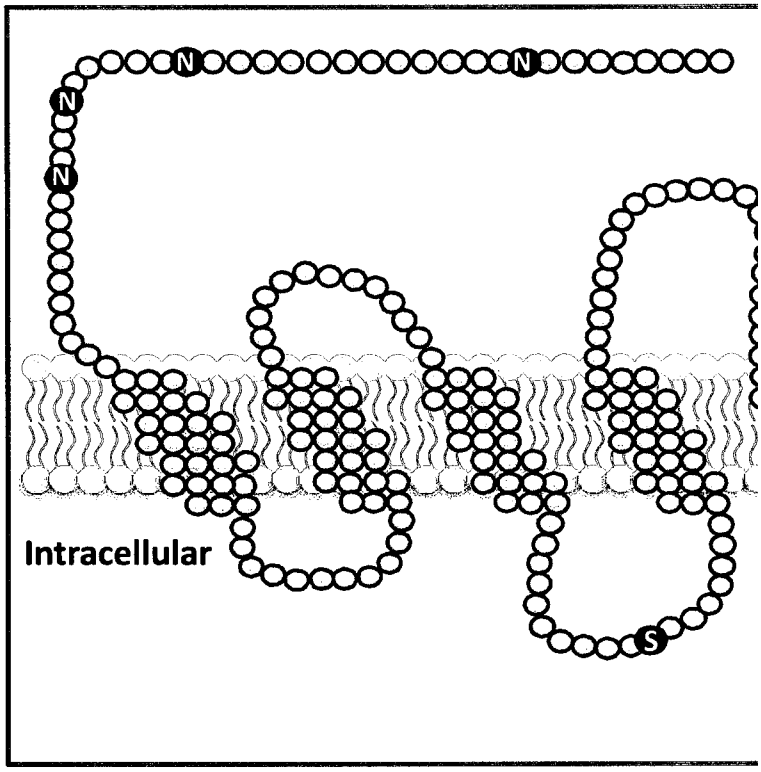
N
N
N
N
Intracellular
S

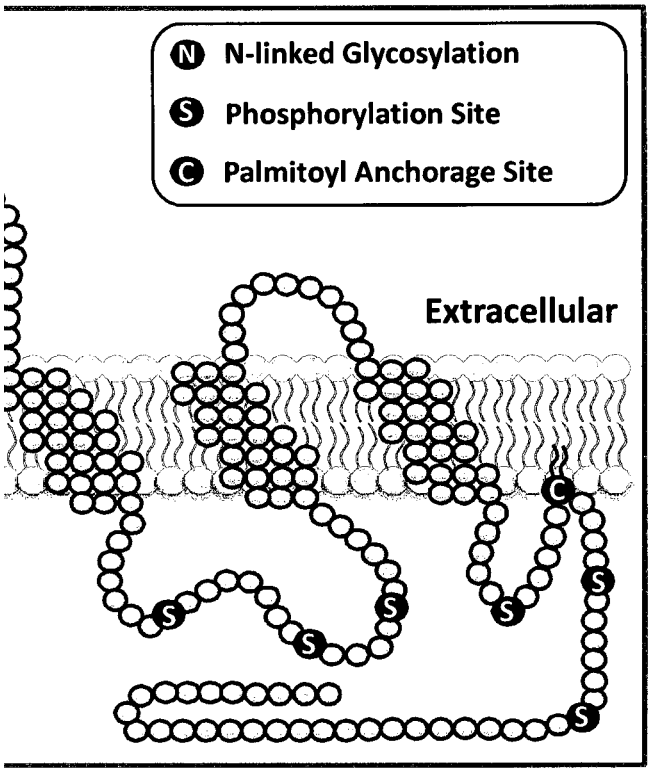
N N-linked Glycosylation
S Phosphorylation Site
C Palmitoyl Anchorage Site
Extracellular
C
S
S
S
S
S
S

distinct families, A, B and C on the basis of their sequence similarity. Family A, the largest group, also known as the rhodopsin-like family, includes rhodopsin, the adrenergic receptors, the olfactory and many other non-olfactory members including the SSTR family. Family B, consists of approximately two dozen members including the gastrointestinal peptide hormone receptor family (secretin, glucagon, vasoactive intestinal peptide and growth-hormone releasing hormone), corticotrophin-releasing hormone, calcitonin and parathyroid hormone receptors. Family C, which contains only a few members including, the metabotropic glutamate receptor family, the $GABA_B$ receptor and the calcium-sensing and taste receptors. This family of GPCRs is typified by a large extracellular amino terminus, which appears critical for ligand binding.

SSTRs range in size from 356 to 391 amino acid residues and have an overall sequence identity of 39-57%, with most of their divergence presented in the amino- and C-terminal segments [Patel, 1997; Patel, 1999; Patel et al., 1996; Reisine and Bell, 1995]. A highly conserved motif, YANSCANPI/VLY, in the seventh TM has been identified in all SSTR subtypes in every species, and serves as a signature sequence for this family of receptors. N-linked glycosylation sites have been identified within the amino-terminus and second extracellular loop (ECL) of all five human (h) SSTRs. Several putative phosphorylation recognition sites have been identified in the C-terminus, second and third intracellular loops (ILs) for protein kinase A, protein kinase C and calmodulin kinase II for all hSSTRs. Interestingly, hSSTR3 is the only hSSTR that does not contain a cysteine residue downstream from the seventh TM for purposes of palmitylation and hence membrane anchoring however, it does possess an unusually long C-terminus, which may be a characteristic of its unique signalling properties [Sharma et al., 1996; Sharma et al., 1999; Sharma and Srikant, 1998a]. In addition to these classical GPCR features [Pierce et al., 2002; Qanbar and Bouvier, 2003], various others have been identified including a PDZ (postsynaptic density-95/discs large/ZO-1) recognition domain in the C-terminus of all SSTR subtypes [Kreienkamp et al., 2004]. Several PDZ interacting proteins have been discovered, specific to each of the five subtypes, presumably implicated in the chaperoning, scaffolding and transport of SSTRs [Kreienkamp et al., 2004].

Development of somatostatin receptor ligands

All five hSSTR subtypes bind SST-14 and SST-28 with nanomolar affinity, the exception is hSSTR5, which binds SST-28 with a 5- to 10-fold higher affinity than SST-14 (see Table 3.1). CST also interacts with all five SST receptors with nanomolar affinities [Spier and de Lecea, 2000]. Administration of SST produces a wide spectrum of effects that occur mainly at the site of injection and are short-lived. This is the result of peptidases found in blood and tissues [Benuck and Marks, 1976; Marks et al., 1976], making the circulation half-life of SST extremely short (1.1 to 3 min) [Schusdziarra et al., 1977]. Not surprisingly, circulating SST levels are relatively low, ranging between 14 and 32.5 pg/ml [Ensinck et al., 1989; Gyr et al., 1987; Peeters et al., 1981; Penman et al., 1981; Shoelson et al., 1986; Skamene and Patel, 1984; Tsuda et al., 1981; Vasquez et al., 1982]. An intense investigation has surrounded the development of compounds with selective actions and metabolic stability to be used in both investigational and clinical settings [Lamberts et al., 1991; Reisine and Bell, 1995; Weckbecker et al., 2003]. Various hexa- and octapeptide derivatives were synthesized, the most potent of which maintained the β-turn of the original SST molecule, the biologically active core or pharmacophore. Structure-function studies determined that amino acid residues Phe^{7}, Trp^{8}, Lys^{9} and Thr^{10}, are necessary for biological activity, although residues Phe^{7} and Thr^{10} could undergo minor substitution. The first FDA approved SST analog SMS 201-995 (octreotide, Sandostatin®), is an octapeptide, BIM 23014 (lanreotide, Somatuline®), eventually followed. These analogs are prepared in long-acting formulations for diagnosis and treatment of various disorders including, gastrointestinal, islet cell, gut and pituitary tumours [Lamberts et al., 1991; Lamberts et al., 1996; Weckbecker et al., 2003]. Both lanreotide and octreotide exhibit high-affinity binding to SSTR2 and intermediate binding to SSTR3 and SSTR5 (see Table 3.1). In 2005, RC160 (vapreotide, Sanvar®), an

Table 3.1.

Binding-affinities of endogenous, synthetic and non-peptide somatostatin agonists.

Binding Constants (nM)					
Agonists	***Receptors***				
	SSTR1	**SSTR2**	**SSTR3**	**SSTR4**	**SSTR5**
Endogenous					
SST-14	0.1-2.26	0.2-1.3	0.3-1.6	0.3-1.8	0.2-0.9
SST-28	0.1-2.2	0.2-4.1	0.3-6.1	0.3-7.9	0.05-0.4
hCST-17	7	0.6	0.6	0.5	0.4
Synthetic					
Octreotide	290-1140	0.4-2.1	4.4-34.5	>1000	5.6-32
Lanreotide	500-2330	0.5-1.8	43-107	66-2100	0.6-14
Vapreotide	>1000	5.4	31	45	0.7
SCH-275	3.2-4.3	>1000	>1000	4.3-874	>1000
SOM-230	9.3	1	15	100	0.16
Non-peptide					
L-797,591	1.4	>1000	>1000	170	>1000
L-779,976	>1000	0.05	729	310	>1000
L-796,778	>1000	>10000	24	>1000	>1000
L-803,087	199	>1000	>1000	0.7	>1000
L-817,818	3.3	52	64	82	0.4

Adapted from [Florio, 2008; Patel, 1999].

SST-analog with similar binding affinities to SSTR2, 3 and 5 like lanreotide and octreotide but moderate affinity to SSTR4 [Patel, 1999], was granted approval for indication of acute oesophageal variceal bleeding secondary to portal hypertension [Patch and Burroughs, 2002]. In an attempt to reduce size but maintain metabolic stability, an SST mimic was achieved based on a cyclohexapeptide template termed MK-678 (seglitide), showing slightly higher-affinity and selectivity to SSTR2 than SSTR3 and SSTR5. As previously mentioned, SSTR2, -3 and -5 can be categorized as group SRIF I, based upon their ability to bind octapeptide analogs, however, analogs that bind receptors in group SRIF II (SSTR1 and SSTR4), would only become available in the mid 90's [Liapakis et al., 1996]. The analog Des-AA^{1,2,5}[D-Trp^{8} IAMP^{9}] SST (SCH-275), was reported to have high-affinity for SSTR1 and moderate affinity for SSTR4 [Liapakis et al., 1996; Patel, 1997] (see Table 3.1). Recently, the highly potent and stable cyclohexapeptide SOM230, designed by Novartis, is a near-universal agonist, the first of its kind, demonstrating high-affinity for SSTR1, 2, 3, and 5 [Bruns et al., 2002; Weckbecker et al., 2002]. SOM230 has demonstrated to be effective in regulating pituitary control in rats, dogs and monkeys including its control in patients with acromegaly and Cushing disease [Bruns et al., 2002; Labeur et al., 2006; Weckbecker et al., 2002; Weckbecker et al., 2003]. Despite the achievement of SSTR-analogs with group selectivity, there has been moderate success in the development of peptide analogs with receptor-specificity. Several analogs have been devised however; there specificity in targeting receptor-subtype ranges between 20-50 fold [Olias et al., 2004; Patel, 1999; Weckbecker et al., 2003]. A breakthrough in SST agonist design came from the Merck Research Group, using the backbone of peptide agonists for molecular modelling; they constructed subtype-selective nonpeptide agonists by combinatorial chemistry [Rohrer et al., 1998]. Of the five nonpeptide agonists, three of the compounds, L-797,591, L-779,976 and L-803,087 display high-selectivity and low nanomolar binding affinity for SSTR1, SSTR2 and SSTR4 respectively. The compound L-796,778 binds to SSTR3 with approximately 50-fold selectivity while the SSTR5 subtype-agonist, L-817,818, displays dual selectivity for SSTR1 (see Table 3.1).

With respect to the development of SST antagonists, the field has been lagging. The first SST peptide antagonist developed, CYN-154806, a cyclic octapeptide, displayed high-affinity for SSTR2 however, exhibited intermediate affinity for SSTR5 [Bass et al., 1996; Feniuk et al., 2000]. Unfortunately, follow up studies demonstrated near full agonism in a cAMP-accumulation assay [Nunn et al., 2003]. Using the same backbone design as CYN-154806, a high-affinity SSTR3 antagonist was developed and inhibited the effects of SST-14 in a functional assay for cAMP [Reubi et al., 2000]. In a unique design, open-chain octapeptide antagonists BIM 23056, BIM 23627 and BIM 23454 selected for their preferentially binding to SSTR5 and SSTR2 respectively, however, both compounds do show partial affinities for the other subtypes to various degrees [Shimon et al., 1997a; Tulipano et al., 2002]. The first high-affinity nonpeptide antagonist was designed for SSTR3 with greater than 1000-fold selectivity [Poitout et al., 2001]. An SSTR1 nonpeptide antagonist SRA880, was recently characterized in vitro to have modest selectivity of up to 100-fold [Hoyer et al., 2004].

Somatostatin receptor localization

The expression of SSTR subtypes has been well characterized in human and rodent tissue including various tumours and tumour cell lines by a multitude of techniques such as Northern blot, RT-PCR, ribonuclease protection assay, *in situ* hybridization and immunocytochemistry have been extensively reviewed elsewhere [Barnett, 2003; Gardette et al., 2004; Kreienkamp et al., 2004; Moller et al., 2003; Patel, 1997; Patel, 1999; Patel et al., 1996; Patel et al., 1995; Reisine and Bell, 1995]. The distribution is widespread, with localization throughout the CNS, periphery, often overlapping in subtype expression depending on tissue- and species-type. The mRNA expression of SSTR1-5 in the rat has been localized to brain regions such as the cerebral cortex, striatum, hippocampus, amygdale, olfactory bulb and preoptic area [Bruno et al., 1993]. Comparing the individual expression patterns of each receptor-subtype revealed SSTR1 to predominate in the brain, with expression in the pituitary, islets and adrenals. SSTR2 is also abundantly expressed throughout the brain, including the pituitary, islets

and adrenals. SSTR3 is densely expressed in the cerebellum but in moderate amounts throughout the rest of the brain. However, it is highly expressed in the spleen, kidneys and the liver. Compared to the other SSTR subtypes, SSTR4 is poorly expressed in the brain. It is however abundant in the heart and occurs at moderate levels in the lungs and islets. SSTR5 is sparsely expressed throughout the brain but is especially prominent in the pituitary, intestine and islets.

As previously mentioned, co-expression of SSTR subtypes is often seen to various degrees depending on tissue and cell type {*reviewed in* [Barnett, 2003; Gardette et al., 2004; Kreienkamp et al., 2004; Moller et al., 2003; Patel, 1997; Patel, 1999; Patel et al., 1996; Patel et al., 1995; Reisine and Bell, 1995]}. Overlapping patterns of SSTR distribution has been demonstrated throughout the CNS. Colocalization of SSTR1 and SSTR2 mRNA can be found in GHRH-producing arcuate neurons [Tannenbaum et al., 1998]. In the adult human pituitary, SSTR1, 2, 3 and 5 are expressed whereas all five are found in the pituitary of rats [Bruno et al., 1993; Day et al., 1995; O'Carroll and Krempels, 1995; Panetta and Patel, 1995]. Although the five receptors have been identified in the pituitary, the primary subtypes expressed are SSTR5 and SSTR2 [Day et al., 1995; Kimura et al., 1998]. In the periphery, human pancreatic islets were shown to express all five subtypes but colocalization was strongly identified for SSTR1 and SSTR5 in insulin-secreting β-cells, to a lesser extent SSTR1 and SSTR2 [Kumar et al., 1999]. The same authors also reported on the colocalization of SSTR2 and SSTR5 in glucagon-producing α-cells, an occurrence that was only identified in up to a third of the population. Elsewhere, in rat testis, SSTR1-3 displayed overlapping distribution patterns in Sertoli and germ cells, a property that was dependent on the stage of the seminiferous epithelium cycle [Zhu et al., 1998].

The expression of SSTRs in neoplastic tissue has been the forefront of current day investigation, as their densities are found to be much higher than in normal tissue. The first evidence for the expression of SSTRs in human tumours appeared as early as 1984 in GH-secreting pituitary adenomas [Reubi and Landolt, 1984]. The identification of differential SSTR subtypes initially appeared in 1987 from autoradiographic studies on neuroendocrine tumours [Reubi et al., 1987]. Since then, many tumours have been shown

to express SSTRs, a characteristic often exploited for both diagnostic and treatment purposes [Barnett, 2003; Gardette et al., 2004; Kreienkamp et al., 2004; Moller et al., 2003; Patel, 1997; Patel, 1999; Patel et al., 1996; Patel et al., 1995; Reisine and Bell, 1995; Reubi et al., 2004]. SSTRs are often highly expressed in neuroendocrine tumours, in particular, GH-secreting pituitary adenomas and gastroenteropancreatic tumours. Several other tumours known to express SSTRs include neoplasias of the brain, breast carcinomas, lymphomas, renal cell cancers, mesenchymal tumours, prostatic, ovarian, gastric, hepatocellular and nasopharyngeal carcinomas. Although the most prevalent subtype expressed in human tumours is hSSTR2, the appearance of other subtypes is often found, a property originally identified in pituitary adenomas [Greenman and Melmed, 1994a; Greenman and Melmed, 1994b; Miller et al., 1995; Panetta and Patel, 1995; Schaer et al., 1997] and gastroenteropancreatic tumours [Jais et al., 1997; Schaer et al., 1997; Wulbrand et al., 1998]. Over the past several years, a profusion of studies have been published addressing the variable expression of SSTR subtypes in a large variety of cancers [Barnett, 2003; Gardette et al., 2004; Kreienkamp et al., 2004; Moller et al., 2003; Patel, 1997; Patel, 1999; Patel et al., 1996; Patel et al., 1995; Reisine and Bell, 1995; Reubi et al., 2004]. The knowledge gained by these studies has been instrumental not only for investigational purposes but to decipher the use of SST-analogs in both diagnostic (tumour imaging by radio-labelled analogs) [Kwekkeboom et al., 2004] and therapeutic applications.

Regulation of somatostatin receptor genes

One major factor affecting the potency of SST is the expression of cell surface receptors. Hormones have been shown to have a profound impact on SSTR gene regulation. For instance, oestrogen induces SST binding sites in cultured rat prolactinoma cells via up-regulation of SSTR2 and SSTR3 [Visser-Wisselaar et al., 1997]. Similarly, both in vitro and in vivo studies have demonstrated the ability of oestrogen to induce the transcription and up-regulation of SSTR2 and SSTR3 in rat pituitary cells [Djordjijevic et al., 1998; Kimura et al., 1998]. While SSTR1 transcripts were found to be up-regulated

by both oestrogen [Kimura et al., 1998] and testosterone [Senaris et al., 1996] in the rat pituitary, SSTR5 mRNA was in fact down-regulated [Kimura et al., 1998]. In MCF-7 breast cancer cells, oestrogen was reported to simulate SSTR2 gene expression [Xu et al., 1996]. In two other breast cancer cell lines T47D and ZR75-1, oestrogen was found to increase and decrease SSTR binding sites respectively [Van Den Bossche et al., 2004]. Investigation on the subtypes involved by Western blotting revealed an up-regulation of SSTR2 in T47D cells and a down-regulation of SSTR5 in ZR75-1 cells following oestrogen treatment [Van Den Bossche et al., 2004]. In mouse TtT-97 thyrotrophic tumour cells, thyroid hormone increases the synthesis of SSTR1 and SSTR5 transcripts [James et al., 1997]. The effects of glucocorticoids on SSTR gene expression are somewhat unique: transient exposure induces SSTR1 and SSTR2 mRNA, while prolonged exposure inhibits transcription [Xu et al., 1995]. Other factors affecting SSTR gene transcription include cAMP, gastrin, epidermal growth factor and even SST itself [Bruno et al., 1994a; Patel et al., 1993; Vidal et al., 1994]. Finally, food deprivation and even diabetes in rat models have shown decreases in mRNA transcripts for SSTR1, 2 and 3 in the pituitary and SSTR5 in the hypothalamus [Bruno et al., 1994b]. Investigation on the promotors of each subtype and specific elements involved in their regulation has been described [Meyerhof, 1998; Moller et al., 2003; Olias et al., 2004; Patel, 1999].

Somatostatin receptor signalling

The signal transduction pathway of SSTRs is rather complex however, for the most part, it begins by activation of G-proteins. In the classical model of GPCR activation, agonist-binding induces a conformational change that transcends to G-proteins resulting in their activation {*reviewed in* [Lefkowitz, 2004; Pierce et al., 2002]}. The G-protein is comprised of three subunits: the α subunit (Gα) and the β and γ subunits (Gβγ) which are tightly bound. There are fifteen α subunits, five β subunits and fourteen γ subunits known to date. Activation of the G-protein heterotrimer is preceeded by the nucleotide exchange of GDP for GTP, resulting in the dissociation of the complex and allowing the Gα and Gβγ subunits to be free to propagate their signal. The G-proteins are

generally referred to by their Gα subunits and therefore, can be classified under four categories based on function: $G\alpha_s$, stimulate adenylate cyclase; $G\alpha_{i/o}$, inhibit adenylate cyclase and activate inwardly rectifying potassium channels; $G\alpha_q$, activate phospholipase C_β; and G_{12}, activate Rho guanine-nucleotide exchange factors.

Binding of SSTRs by SST ligands modulates the activates of several key enzymes, including adenylate cyclase, phosphotyrosine phosphatases (PTPases) and mitogen-activated protein kinase (MAPK) along with changes in the intracellular levels of calcium and potassium ions, as typified by activation of calcium and potassium channels, including the regulation of the sodium/proton antiporter (Fig. 3.4) [Barnett, 2003; Csaba and Dournaud, 2001; Moller et al., 2003; Olias et al., 2004; Patel, 1997; Patel, 1999; Patel et al., 1996; Patel et al., 1995; Reisine and Bell, 1995]. The type of signal that prevails is dependent on several factors such as the SSTR subtype(s) expressed, signalling elements, SSTR internalization, desensitization, and/or receptor crosstalk. The ability of SST to block regulated secretion from various cell types is typified in part by its effects on the synthesis and release of two important mediators, cAMP and calcium respectively. Adenylate cyclase was the first effector enzyme to be identified and regulated by SSTRs [Patel et al., 1994]. All five SSTR subtypes negatively couple to the enzyme by activating pertussis-toxin (PTX) sensitive $G\alpha_i$ G-proteins, a property observed in various cell types [Meyerhof, 1998]. In an attempt to elucidate the most relevant G-protein subtypes involved in SSTR-mediated inhibition of adenylate cyclase, the subtypes $G\alpha_{i1}$, $G\alpha_{i2}$ and $G\alpha_{i3}$ were identified, as determined by targeted-disruption using either antiserum or G-protein antisense plasmids [Gu and Schonbrunn, 1997; Liu et al., 1994; Tallent and Reisine, 1992]. SSTRs are coupled to several types of potassium channels and include the delayed rectifier, inward rectifier, ATP-sensitive potassium channels and large-conductance calcium-activated BK channels [Akopian et al., 2000; de Weille et al., 1989; Sims et al., 1991; Wang et al., 1989; White et al., 1991]. The G-protein subtype $G\alpha_{i3}$ and possibly its interacting βγ dimer pair are implicated in potassium channel regulation [Takano et al., 1997]. SSTRs have also been shown to directly modulate high-voltage-dependent calcium channels via $G\alpha_{o2}$ [Ikeda and Schofield, 1989; Kleuss et al., 1991]. SSTRs may also inhibit calcium currents by

Figure 3.4.

Schematic representation of SSTR signalling pathways.

SSTR signalling cascades leading to the modulation of hormone secretion, cell growth and apoptosis are shown.

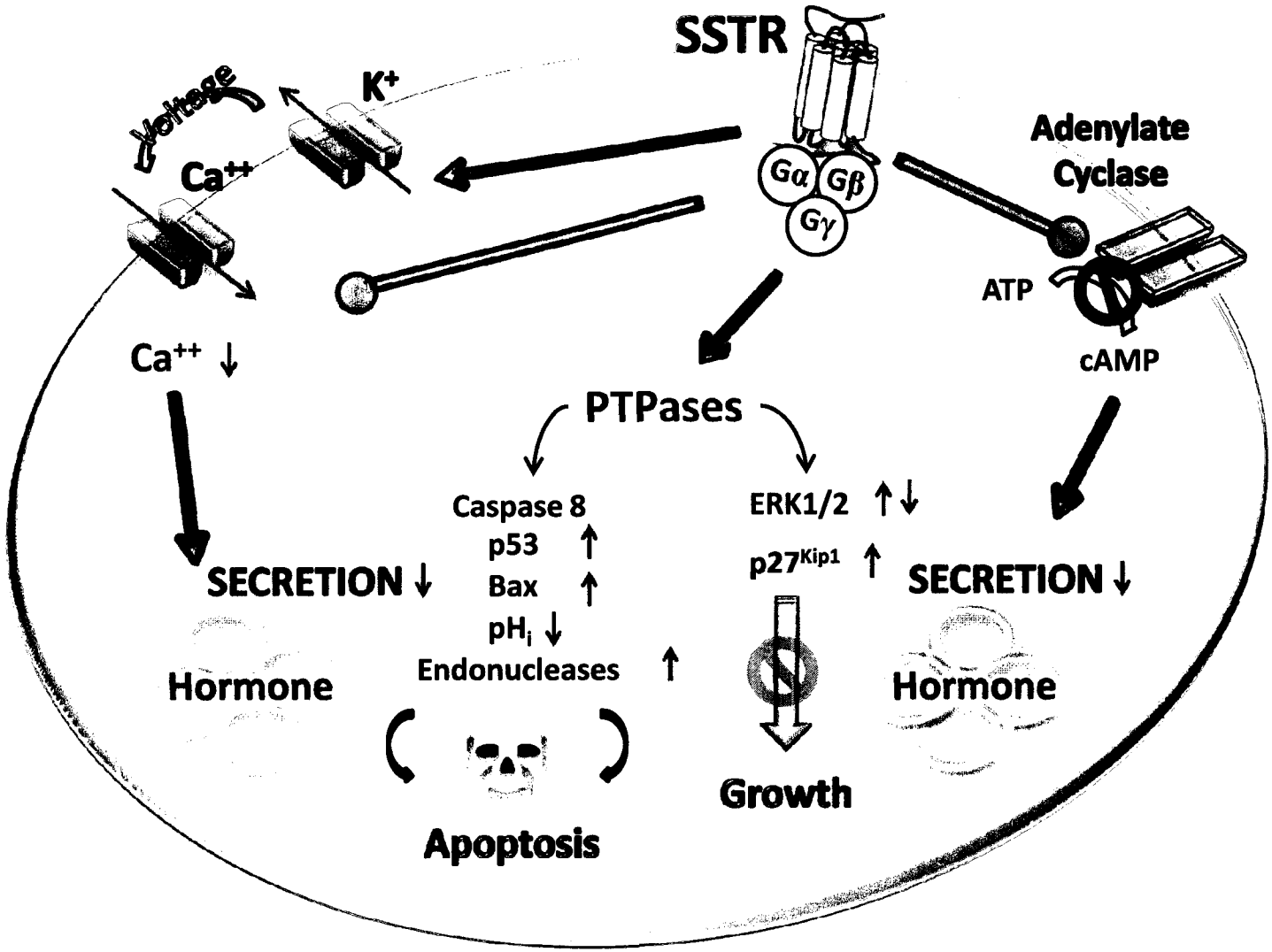
SSTR
Voltage
K+
Ca++
Gα
Gβ
Gγ
Adenylate Cyclase
ATP
cAMP
Ca++ ↓
PTPases
Caspase 8
p53 ↑
Bax ↑
pHi ↓
Endonucleases ↑
ERK1/2 ↑↓
p27Kip1 ↑
SECRETION ↓
SECRETION ↓
Hormone
Hormone
Growth
Apoptosis

activation of cGMP protein kinase, through the induction of cGMP to regulate channel phosphorylation [Meriney et al., 1994]. Aside from regulating channels to control ion flux, SSTRs have also been shown to couple to Na^+/H^+ exchangers (NHEs) [Barber et al., 1989; Hou et al., 1994; Lin et al., 2003; Smalley et al., 1998; Ye et al., 1999] to modulate such features as cell adhesion, migration and proliferation [Putney et al., 2002]. SSTR1 was the first subtype to specifically-regulate NHE-1, decreasing the extracellular acidification rate (ECAR) when transfected in either fibroblast Ltk^- or HEK-293 cells [Hou et al., 1994]. It was later determined that SSTR3 and SSTR4 also contribute but not SSTR2 and SSTR5 [Lin et al., 2003].

SSTRs activate a number of phosphatases that have been implicated in cell growth {*reviewed in* [Csaba and Dournaud, 2001; Moller et al., 2003; Olias et al., 2004; Patel, 1999]}. For instance, the SH2 domain containing tyrosine phosphatases, SHP-1 and SHP-2, which play a role in cell growth and differentiation, are known to be recruited by various SSTR subtypes. Both phosphatases are rapidly recruited to the membrane of breast cancer cells upon stimulation with SST [Srikant and Shen, 1996]. More specifically, SHP-1 has been demonstrated to co-precipitate with SSTR2 in a constitutive manner, suggesting its importance in the formation of signalling complexes [Hortala et al., 2003; Lopez et al., 1997]. Furthermore, the activation of SHP-1 was shown to be highly dependent on the recruitment of SHP-2 through phosphorylation of tyrosine residues present at the C-terminal portion of the receptor, implying the importance of both phosphatases in SSTR signalling [Ferjoux et al., 2003]. A receptor-like PTP known as PTPη, has also been demonstrated to be an important player in the cytostatic effects of SST, particularly since its expression is necessary for the control of thyroid tumor and human glioma cells [Florio et al., 2001; Florio et al., 1997; Massa et al., 2004a; Massa et al., 2004b]. Recently, a signalling complex involving JAK2, SHP-2 and c-src was demonstrated in the SSTR1-mediated activation of PTPη [Arena et al., 2007]. In addition to tyrosine phosphatases, the activation of serine/threonine phosphatases has also been demonstrated to be recruited by SSTRs. Modulation of the N- and L-type calcium channels and potassium channels have been shown to be dependent on the activation of

phosphatase 2A (PP2A) and calcineurin (PP2B) in several cell types such as sympathetic neurons, pancreatic alpha cells and pituitary tumour cells. Evidence on the importance of PP2B recruitment by SSTR activation comes from studies on the regulation of neurotransmitter release and exocytosis in sympathetic neurons and pancreatic alpha cells respectively [Gromada et al., 2001; White et al., 1991; Zhu and Yakel, 1997].

Several important yet recently identified signalling cascades found downstream of SSTR activation are the mitogen-activated protein kinases (MAPK) [Bousquet et al., 2001; Csaba and Dournaud, 2001; Moller et al., 2003; Olias et al., 2004; Patel, 1999; Weckbecker et al., 2003]. SSTR activation [Florio et al., 1999; Lahlou et al., 2003] or inhibition [Cattaneo et al., 1999; Dent et al., 1997; Douziech et al., 1999; Florio et al., 2001; Florio et al., 2003a] of MAPKs has been demonstrated to be mediated by PTPases. In case of SSTR5, the inhibition of MAPKs was related to the activation of a cGMP-dependent pathway when expressed in CHO-K1 cells [Cordelier et al., 1997]. In addition to PTPases, recruitment of phosphoinositide-3 kinase has also been shown fundamental in the activation of MAPKs. For instance, studies involving human SSTR4 [Smalley et al., 1999], rat SSTR2B [Sellers et al., 2000] or mouse SSTR2A [Lahlou et al., 2003] have underscored its relevance.

Relevance of SSTRs in cancer

As previously mentioned, a number of cancer cells overexpress SSTRs, with more than one subtype often being expressed. As early as the 1980s, the antiproliferative effects of the SST-analog octreotide were being recognized for treatment of hyper-secreting tumours of the pancreas, intestine and pituitary {*reviewed in* [Lamberts et al., 1991; Lamberts et al., 1996; Weckbecker et al., 1993]}. It was noted that not only was treatment blocking hormone secretion but was also causing variable tumour shrinkage through a distinct antiproliferative effect. The antiproliferative effects of SST demonstrated in normal dividing cells such as intestinal mucosal cells, activated lymphocytes, inflammatory cells, as well as in experimental tumour models for example solid tumours of transplanted rat mammary carcinomas and finally cultured cells derived

from both endocrine and epithelial tumours (pituitary, thyroid, breast, prostate, colon, pancreas, lung and brain) {*reviewed in* [Csaba and Dournaud, 2001; Lamberts et al., 2002; Moller et al., 2003; Olias et al., 2004; Patel, 1999; Weckbecker et al., 2003; Zatelli et al., 2006]}. The antiproliferative effects of SST on normal or transformed cells can be directed by cell growth arrest and/or apoptosis; several SSTR signalling pathways have been implicated (Fig. 3.4).

A large body of evidence implicates PTPs as central mediators in the antiproliferative effects of SSTRs. SSTR subtypes activate different PTPs, resulting in varying effects on downstream effectors such as MAPKs, ultimately, regulating the induction of cyclin-dependent kinase inhibitors $p27^{Kip1}$ and $p21^{Cip1/Waf1}$. In the mid 80's, a role for PTPases in SST-mediated antiproliferation of pancreatic cancer cells was postulated on the basis of an inhibition toward epidermal growth factor receptor phosphorylation patterns [Hierowski et al., 1985]. All five receptor subtypes display some capacity to activate PTPs [Buscail et al., 1994; Florio et al., 1994; Reardon et al., 1997; Sharma et al., 1996; Sharma et al., 1999], whether the PTPases are cytosolic [Bousquet et al., 1998; Florio et al., 2000; Reardon et al., 1997; Srikant and Shen, 1996] or membrane localized as demonstrated with PTPη [Florio et al., 2001; Florio et al., 1997; Massa et al., 2004a; Massa et al., 2004b]. An increase in the PTP SHP-1 has been reported in several different cancer cell lines including pituitary adenomas, pancreatic cancers, medullary, breast and prostate carcinomas following SST treatment [Douziech et al., 1999; Ferjoux et al., 2000; Thangaraju et al., 1999; Theodoropoulou et al., 2006; Zapata et al., 2002; Zatelli et al., 2005b]. Consequently, SHP-1 activation is a critical factor in SSTR2-mediated cell growth arrest [Bousquet et al., 1998; Lopez et al., 1997; Theodoropoulou et al., 2006]. In fact, a multi-effector complex between c-src and SHP-2 was determined central in the recruitment and activation of SHP-1 following stimulation of SSTR2 [Ferjoux et al., 2003]. Ultimately, SHP-1 activation results in growth factor receptor signalling inhibition by dephosphorylating its substrates [Bousquet et al., 1998; Lopez et al., 1997]. Other inhibitory pathways of SHP-1 include the activation of nNOS by its dephosphorylation, resulting in an increase in cGMP formation and subsequent induction of $p27^{Kip1}$ and cell cycle arrest [Lopez et al., 2001].

In a similar vein, activation of SSTR1 has also been shown to recruit SHP-2 and c-src for its antiproliferative activity [Florio et al., 2000; Florio et al., 1999; Reardon et al., 1997]. Activation of SHP-2 by SSTR1 was reported to orchestrate antiproliferation by mediating the dephosphorylation of growth factor receptors for EGF, insulin and platelet derived growth factor (PDGF), with the consequent inhibition of Ras and MAPK activity [Cattaneo et al., 2000]. However, unlike SSTR2, the final effector PTP for SSTR1 is not SHP-1 but the membrane-bound PTPη [Arena et al., 2007; Florio et al., 2001; Florio et al., 1997; Massa et al., 2004a; Massa et al., 2004b].

Recently, SSTR2 was shown to inhibit the activity of phosphatidyl inositol 3 kinase (PI3K), thereby, preventing the activation of AKT in both pituitary and insulinoma tumor cells [Grozinsky-Glasberg et al., 2008a; Theodoropoulou et al., 2006]. The PI3K/Akt signalling pathway has been demonstrated to poromote the survival, proliferation, angiogenisis and motility for tissue invasion of cancer cells and therefore, provides an important target in tumor control [Altomare and Testa, 2005].

Although typically involved in cell growth and proliferation [Dhanasekaran et al., 1995], the activation of the MAPKs as demonstrated via distinct SSTRs can be associated with cell growth inhibition [Alderton et al., 2001; Florio et al., 1999; Lahlou et al., 2003; Sellers et al., 2000]. Stimulation of SSTR2 was shown to inhibit the proliferation of CHO-K1 cells by activating two members of the MAPK family, extracellular-regulated kinase-1 and -2 (ERK1/2) and p38, upstream the activation of the cyclin-dependent protein kinase inhibitor $p21^{cip}1$/WAF1 [Alderton et al., 2001; Sellers et al., 2000]. Similar findings were also reported upon activation of SSTR1 [Florio et al., 1999]. Contrarily, the antiproliferative actions of SSTR5 do not require activation of MAPKs but rather inhibition [Cordelier et al., 1997]. Pathways suggested to be implicated in SSTR5-mediated antiproliferation include one involving phospholipase C/inositol phospholipid/Ca^{2+} [Buscail et al., 1995] and the other involving the induction of the retinoblastoma tumour suppressor protein (Rb) and p21 [Sharma et al., 1999]. In rare instances, SST may actually stimulate cell growth, an anomaly shown to occur by MAPK activation via human SSTR4 [Sellers et al., 2000].

In addition to the cytostatic effects of SST, apoptosis or programmed cell death, has also been observed to contribute to the antiproliferative response following treatment. Apoptosis was first demonstrated in AtT-20 and MCF-7 cells when treated with octreotide [Pagliacci et al., 1991; Sharma and Srikant, 1998b; Srikant, 1995]. In MCF-7 cells, SHP-1 is necessary for SSTR-mediated apoptotic signalling [Liu et al., 2000; Sharma and Srikant, 1998b]. Because both cell types express more than one SSTR, it is not possible to assign which subtype may be contributing to apoptosis. When CHO-K1 cells were individually transfected with each receptor-subtype, apoptosis was uniquely triggered by human SSTR3 [Sharma et al., 1996]. The events preceding apoptosis following hSSTR3 activation include activation of tumour suppressor protein p53 and pro-apoptotic protein Bax [Sharma et al., 1996]. However, recent reports have described p53-independent apoptosis via SSTR2 in HL-60, human pancreatic adenocarcinoma and human somatotroph tumour cells [Ferrante et al., 2006; Guillermet et al., 2003; Teijeiro et al., 2002].

Unlike the direct effects of SST on tumor cell proliferation mentioned above, SST can indirectly control tumor growth and development by inhibiting angiogenesis. Antiangiogenic activity was first described by Woltering et al., using a chicken corioallanthoic membrane model, a property that was further supported by the findings conducted *in vitro* and *in vivo* with SST and its analogs [Albini et al., 1999; Barrie et al., 1993; Danesi et al., 1997; Danesi and Del Tacca, 1996; Dasgupta and Mukherjee, 2000; Florio et al., 2003a; Garcia de la Torre et al., 2002; Koizumi et al., 2002; Murray et al., 2004; Zalatnai and Timar, 2002]. Three different pathways have been proposed and may operate concurrently to achieve the antiangiogenic activity of SSTRs. First, activation of SSTRs may directly inhibit the proliferation, migration and invasion of endothelial cells to the tumor. Second, SST may regulate the secretion of angiogenic promoting factors such as vascular endothelial growth factor (VEGF) and basic fibroblast growth factor (bFGF). Third, SST may modulate the activation of monocytes, cells that are although important in the immune response, their migration in the peritumoral region can produce pro-angiogenic factors resulting in neovascularisation (*reviewed in* [Florio, 2008]. SST may also indirectly regulate tumor growth by inhibiting the synthesis and/or secretion of

growth factors and hormones such as EGF, transforming growth factor, insulin, prolactin, GH and IGF-I [Susini and Buscail, 2006].

The first conclusive evidence that SST-analogs can have antiproliferative properties in the clinic, came from a multicenter randomized trial recruiting 32 acromegalic patients with hyper-secreting pituitary adenomas [Thapar et al., 1997]. These patients demonstrated an 83% reduction in mean growth fraction when compared to untreated controls, suggesting that octreotide had exerted an antineoplastic effect on somatotroph adenomas. In a separate study by Losa et al., the Ki-67 index, a nuclear protein expressed only in dividing cells, was significantly lower in the GH hyper-secreting adenomas of patients pre-treated with octreotide compared to untreated controls [Losa et al., 2001]. Many trials have since been undertaken demonstrating the effects of SST-analog therapy on tumour shrinkage in acromegalic patients. Typically, patients receiving SST-analogs as primary therapy show reductions of up to 50% in tumour volume [Bevan, 2005; Melmed et al., 2005]. In regards to the antiproliferative effects of SST-analogs in the treatment of patients with other types of tumors evidence is scanty. In approximately half of patients with gastrointestinal neuroendocrine tumors, stabilization of tumor growth was apparent for duration of 8-16 months however, tumor shrinkage was achieved in only 10%-20% of cases [Eriksson and Oberg, 1999]. In a study with patients diagnosed with malignant gastrinoma, treatment with the long-acting formulation of octreotide demonstrated an antiproliferative response in approximately 50% of the subjects [Shojamanesh et al., 2002]. Although SST-analogs are effective in the symptomatic treatment of neuroendocrine tumors, a family of tumors which originate from various endocrine glands including the pituitary, parathyroid, adrenals, endocrine islets, in addition to exocrine cells from the digestive and respiratory tracts [Grozinsky-Glasberg et al., 2008b; Grozinsky-Glasberg et al., 2008c], SST-analog therapy is rarely curative.

Agonist-regulation of somatostatin receptors

The initial responses following activation of SSTRs diminish with continued exposure to SST [Csaba and Dournaud, 2001; Moller et al., 2003; Olias et al., 2004; Patel, 1997; Patel, 1999]. This feature is shared by many GPCRs and is a requirement for terminating signalling. This process can be divided into two general steps: desensitization and internalization. Desensitization is the result of rapid attenuation of receptor function, usually by phosphorylation of its c-tail, causing uncoupling of the receptor from its respective G-protein. This property can be mediated by second-messenger kinases, such as protein kinase A or protein kinase C, or through a distinct family of G-protein-coupled receptor kinases termed GRKs, and is typically followed by internalization [Pierce et al., 2002; Premont and Gainetdinov, 2007]. Internalization is a process by which the receptor is redistributed away from the surface and brought into the cell, also known as endocytosis {*reviewed in* [Claing et al., 2002; Pierce et al., 2002]}. The process of internalization can be divided into three different pathways: clathrin-coated pits, caveolae, and uncoated vesicles [Claing et al., 2002; Pierce et al., 2002]. The least understood method by which GPCRs internalize involves caveolae. This mechanism involves membrane invaginations that are rich in both caveolin and cholesterol [Nichols, 2003]. Several GPCRs have been demonstrated to undergo caveolae-dependent internalization and include the endothelin and vasoactive intestinal peptide receptors [Claing et al., 2000] in addition to the chemokine receptors [Neel et al., 2005]. The most investigated and best-understood mechanism involved in GPCR internalization is the β-arrestin-dependent mediated pathway, which occurs via clathrin-coated vesicles [Claing et al., 2002; Lefkowitz and Shenoy, 2005; Pierce et al., 2002]. There are two subtypes of β-arrestin, β-arrestin-1 and β-arrestin-2, both of which are ubiquitously expressed. A third type of arrestin known as visual arrestin is exclusively expressed in the retina where it was originally identified [Lefkowitz and Shenoy, 2005; Pierce et al., 2002]. This process of internalization is initiated by the recruitment of β-arrestin to the phosphorylated portion of the receptor [Lohse et al., 1990]. This in turn engages the receptor into the clathrin-coated pit machinery, as β-arrestin is known to interact with several components involved in this process including the heavy chain of

clathrin itself, the β2-adaptin subunit of the clathrin adaptor protein AP-2, the small guanosine triphosphatase ARF6 and its guanine nucleotide exchange factor ARNO, the N-ethylmaleimide-sensitive fusion protein (NSF) in addition to constituents of the inner leaflet of the cell membrane itself [Claing et al., 2002; Lefkowitz and Shenoy, 2005; Pierce et al., 2002]. The final step to internalization requires the actions of a GTPase known as dynamin, as it is responsible for pinching off the pits to generate endosomes. There are two general types of β-arrestin-mediated internalization that depend on its avidity for the receptor: class A, β-arrestins bind transiently to the receptor, target it to clathrin-coated pits and dissociate during receptor-internalization; class B, β-arrestin remains tightly bound to the receptor and does so throughout the internalization process for extended periods of time, from which the receptor can be sorted to lysosomes where it is degraded. The end result is that class A receptors, such as the β_2-adrenergic receptor, are recycled more quickly to the cell surface, as their fate is not tied to β-arrestin sorting; whereas class B receptors, for example, the V_2R vasopressin receptor, are slowly recycled and often end up being degraded [Claing et al., 2002; Lefkowitz and Shenoy, 2005; Pierce et al., 2002].

In the early 1980's, it was appreciated that SSTRs can undergo agonist-induced uncoupling from their G-proteins, a property demonstrated in AtT-20 cells [Reisine and Axelrod, 1983]. It wasn't long before agonist-induced internalization was documented and shown to occur in cells from the rat anterior pituitary and islet, mouse AtT-20 cells and human pituitary and islet tumour cells [Amherdt et al., 1989; Hofland et al., 1999; Hofland et al., 1995; Morel et al., 1985]. However, a rather unusual occurrence developed following prolonged agonist exposure (24-48 hrs) in GH_4C_1 and Rin m5f cells, SSTRs were found to increase at the cell surface [Presky and Schonbrunn, 1988; Sullivan and Schonbrunn, 1988]. Although the underlying mechanisms are still unclear, agonist-induced up-regulation has been observed by several other GPCRs [Cox et al., 1995; Hukovic et al., 1996; Ng et al., 1997; Presky and Schonbrunn, 1988; Tannenbaum et al., 2001] and may play a role in long-term drug therapy. A hunt for the specific receptor-subtypes mitigating these events is underway. The results are confounding, as studies have revealed differences that were not only dependent on receptor-subtype but also the

species from which the receptor is derived. Despite these differences, two important conclusions can be made based upon the subgroup of SSTRs examined: SRIF1 receptors (SSTR2, SSTR3 and SSTR5) internalize readily following agonist treatment, whereas SRIF2 receptors (SSTR1 and SSTR4) are rather resistant to agonist-induced internalization.

Initial evidence for the desensitization and internalization of SSTR2 following agonist treatment *in vivo* came from rat brain slices [Boudin et al., 2000]. Around the same time, it was also observed that SSTR2 internalized when activated in primary cultured hippocampal neurons using fluorescently-labelled SST ligands [Stroh et al., 2000a]. Stereotactic injections of the SST-analog octreotide in the rat parietal cortex [Csaba et al., 2001] and endopiriform nucleus [Csaba and Dournaud, 2001] demonstrated that SSTR2 internalized via a clathrin-mediated pathway. Similar mechanisms were also described for the internalization of SSTR2 *in vivo*, as demonstrated by studies in the rat forebrain [Schreff et al., 2000], dorsolateral septum [Csaba et al., 2002] and arcuate nucleus of the hypothalamus [Csaba et al., 2003]. When transfected in either CHO-K1, HEK-293 or even pancreatic β-cells, human and rat SSTR2 internalize in response to SST stimulation [Cescato et al., 2006; Hukovic et al., 1996; Roosterman et al., 1997; Roth et al., 1997b], via a clathrin-dependent pathway. Furthermore, endocytosis of SSTR2 was also demonstrated in glioma and neuroblastoma cells that endogenously express the receptor [Koenig et al., 1997; Krisch et al., 1998]. In other cell types, the densitization, internalization and phosphorylation of rat SSTR2 was observed [Hipkin et al., 1997; Hipkin et al., 2000; Roosterman et al., 1997]. The phosphorylation of SSTR2 was related to its internalization of clathrin-coated pits and shown to occur at both the C-terminal portion and the intracellular loop of SSTR2. Both protein kinase A and protein kinase C play a role in the phosphorylation and internalization of SSTR2 [Hipkin et al., 2000; Oomen et al., 2001]. Interestingly, although β-arrestin subtype-1 was found to desensitize mouse SSTR2 transfected in CHO-K1 cells, it was not implicated in its internalization. Recently, both GRK2 and β-arrestin subtype-2 were shown to be actively involved in the phosphorylation and clathrin-mediated internalization of the receptor when expressed in HEK-293 cells, respectively [Tulipano et al., 2004]. The same authors also described a

region in the C-terminal portion of the receptor as a recognition site for GRK2 phosphorylation. SSTR2 can therefore be classified a class B receptor, as SSTR2 forms stable associations with β-arrestin throughout its sequestration and localization in endosomes [Tulipano et al., 2004].

The regulation of SSTR3 is very similar to that of SSTR2. Both human and rat forms rapidly internalize following agonist stimulation in various transfected cell lines [Cescato et al., 2006; Hukovic et al., 1996; Roosterman et al., 1997; Roth et al., 1997b]. The receptor is phosphorylated at the C-terminus, a critical determinant for agonist-induced internalization [Roth et al., 1997a; Tulipano et al., 2004]. Internalization follows a clathrin-mediated pathway, a property dependent on the recruitment of β-arrestin [Kreuzer et al., 2001; Tulipano et al., 2004]. Desensitization of the receptor follows a slow recovery rate, as demonstrated by its effector coupling to adenylate cyclase [Roosterman et al., 1997; Roth et al., 1997b]. This could be explained by the high avidity of β-arrestin binding to the receptor, however; both proteins are found colocalized in intracellular endocytic compartments for relatively short time periods [Kreuzer et al., 2001; Tulipano et al., 2004]. Given that the receptor is more prone to degradation unlike SSTR2, it is more probably that sequestration to lysosomes dictates its slow recovery [Tulipano et al., 2004].

The final receptor in the SRIF1 class, SSTR5, undergoes differential regulation in a species-specific manner. For instance, human SSTR5 is rapidly internalized following activation with either SST-14 or SST-28 when expressed in CHO-K1 cells [Cescato et al., 2006; Hukovic et al., 1996; Hukovic et al., 1998]. Desensitization has also been observed as demonstrated by a reduced ability to couple to adenylate cyclase following pre-stimulation, a property highly dependent on the structural domains present at the C-terminus [Hukovic et al., 1998]. The loss of cell surface receptors for rat SSTR5 is rather moderate compared to its human counterpart, as a rapid recycling rate has been described for this difference [Stroh et al., 2000b]. Similar to human SSTR5, the rat homologue also undergoes agonist-regulated desensitization [Roosterman et al., 1997; Roth et al., 1997b; Stroh et al., 2000b]. More recently, the interaction of β-arrestin with SSTR5 has been described [Grant et al., *in revision;* Tulipano et al., 2004], and although rat SSTR5 can be

categorized as a class A receptor as determined by its transient association with β-arrestin [Tulipano et al., 2004], its human homologue does not show any interaction [Grant et al., *in revision*]. The species-related differences in the regulation of human and rat SSTR5 may in part be explained by their differential association with β-arrestin.

As previously mentioned, the SRIF2 class of SSTRs (SSTR1 and SSTR4) are generally resistant to internalization but not desensitization by agonist. For instance, when transfected in CHO-K1 cells, rat SSTR1 is quickly phosphorylated but slowly sequestered within cells [Liu and Schonbrunn, 2001]. Similarly, activation of endogenously expressed SSTR1 in both neurons of the hippocampus and cortex of rat, did not cause its internalization [Stroh et al., 2000a]. The up-regulation of SSTR binding sites in GH4C1 cells was attributed to the presence of SSTR1, as these cells predominantly express this subtype [Presky and Schonbrunn, 1988]. A similar occurrence was observed for hSSTR1 when expressed in CHO-K1 cells, where up-regulation rather than down-regulation predominates followed prolonged agonist exposure [Hukovic et al., 1996]. Further examination revealed that the up-regulation of hSSTR1 was not dependent on *de novo* synthesis, but rather on dephosphorylation of amino acid residues present at the C-terminus and the recruitment of pools of intracellular receptor [Hukovic et al., 1999]. However, when hSSTR1 was expressed in COS-7 cells, only a small fraction of receptor-bound ligand was internalized with the majority of receptor remaining within or just beneath the cell membrane [Nouel et al., 1997].

Contrary to human SSTR1, hSSTR4 does show moderate levels of internalization when expressed in CHO-K1 cells, however; compared to hSSTR1, prolonged treatment with agonist does induce its up-regulation [Hukovic et al., 1996]. The low level of internalized hSSTR4 observed following agonist stimulation was attributed to a rapid recycling rate [Smalley et al., 2001]. Species-related differences have been documented between the regulation of human and rat SSTR4 homologues. For instance, rat SSTR4 does not internalize when transfected in either HEK-293 or rat insulinoma cells following agonist-activation [Smalley et al., 2001]. Interestingly, internalization is apparent when part of the C-terminal portion of the receptor is removed, suggesting a negative-regulatory motif involved in controlling the internalization of rat SSTR4 [Roosterman et

al., 1997; Roth et al., 1997b]. Further investigation using rat SSTR4 mutants, revealed threonine 331 as the residue most accountable for inhibiting internalization [Kreienkamp et al., 1998]. Taken together, the *in vitro* analysis of rat SSTR4 is in good agreement with *in vivo* results, as intracerebroventricular administration of SST-14 does not promote its sequestration [Schreff et al., 2000]. Despite the variability in the trafficking of SSTR1 and SSTR4, it is clear that neither of them depend on interaction with β-arrestin for internalization [Tulipano et al., 2004].

B) GPCR Dimerization and Techniques used in their Investigation

Early evidence for the dimerization of GPCRs

There are various ways in which GPCRs can be regulated, several of them have already been discussed and include desensitization, sequestration, down-regulation or even up-regulation. However, one mode of GPCR regulation that has only recently been recognized is dimerization/oligomerization. It is well known that many different cell surface receptors form oligomeric structures as a prerequisite for signal transduction. The receptor tyrosine kinase superfamily is a prime example. For instance, the inactive state of the epidermal growth factor receptor is a monomer; activation by ligand causes it to stabilize into a dimeric form, a necessary step for signal transmission [Schlessinger, 2002; Ward et al., 2007]. On the other hand, the insulin receptor does not require ligand to dimerize as it is itself, a preformed dimer of two different isoforms linked by disulphide bonds. However, ligand-binding does induce conformational changes that activate its cytoplasmic kinase domain to initiate signal transduction [Ward et al., 2007]. GPCRs were largely accepted to exist as monomeric entities at the cell surface, existing in a 1:1:1 stoichiometric ratio with respect to the ligand and G-protein that they couple to however; initial evidence has suggested a role for dimerization in receptor-function in the early 80's. Using antibodies to crosslink gonadotropin-releasing hormone receptors, Conn et al., converted an antagonist to an agonist [Conn et al., 1982]. This effect was specific to the use of divalent antibodies and not monovalent Fab fragments, implying that receptor-aggregation is necessary for activation [Conn et al., 1982; Hazum and Keinan, 1985]. Similar work on the luteinising hormone-releasing hormone receptor demonstrated dimerization, as induced by antibody crosslinking in pituitary cells, caused their activation [Gregory et al., 1982]. In rat Leydig cells, the same situation arose when using antibodies against the luteinising hormone receptor, as aggregation was suggested to mediate receptor-activation [Podesta et al., 1983; Podesta et al., 1986]. The earliest direct physical evidence for GPCR dimers came from investigation on immunoaffinity

chromatography and Western blotting of lung β_2-adrenergic receptors [Fraser and Venter, 1982] and covalent cross-linking of angiotensin II to its binding sites in rat adrenal membranes [Paglin and Jamieson, 1982]. Additional evidence for the dimerization of GPCRs came from radiation inactivation and photoaffinity labelling experiments, where a number of receptors were demonstrated to be larger than predicted based on simple monomeric structures {*reviewed in* [Hebert and Bouvier, 1998]}. However, not all GPCRs studied gave size estimates corresponding to their dimeric forms and therefore, made conclusions on the functional significance for these higher order species ambiguous.

Development of recombinant DNA expression systems rekindled interest in readdressing the functional significance for GPCR dimers. Various GPCR mutant or chimeric constructs could be reconstituted when co-transfected in cells. For instance, when two functionally inactive GPCR chimeras, one possessing the first five transmembrane domains (TMs) of the α_2-adrenergic receptor and the last two TMs of the muscarinic m3 receptor and vice versa, allowed for restoration of both receptors [Maggio et al., 1993]. Similar results were demonstrated for the angiotensin II receptor however, in this case, trans complementation of two defective binding mutants rescued binding [Monnot et al., 1996]. Several other GPCRs have been reported to behave in a similar fashion, namely the luteinzing hormone [Osuga et al., 1997] and vasopressin V2 [Schoneberg et al., 1997; Schoneberg et al., 1996] receptors. In addition to complementation assays, ligand binding on purified GPCRs has also presented with cooperativity binding data that could easily be explained by formation of dimeric or even oligomeric receptor-complexes {*reviewed in* [Hebert and Bouvier, 1998]}.

Following the development of receptor epitope tagging, the use of highly-specific antibodies targeting the tagged portion of GPCRs was employed, thereby minimizing crossreactivity often seen when using prepared antisera. SDS-resistant receptor species of molecular masses equivalent to dimers or even higher order oligomers have been identified on Western blots for various GPCRs [Alblas et al., 1995; Ali et al., 1994; Debburman et al., 1995; Giannini et al., 1995; Herberg et al., 1984; Ng et al., 1993; Ng et al., 1994a; Ng et al., 1994b; Pickering et al., 1993; Schreurs et al., 1995; Vasudevan et al.,

1995]. Interestingly, many of the GPCRs tested were not dependent on the formation of disulfide bonds, in particular, dimers of the dopamine D2 [Ng et al., 1996], olfactory [Nekrasova et al., 1996] and β_2-adrenergic receptors [Hebert et al., 1996], as their interactions were unaffected by reducing agents. However, disulfide bonding does appear important for the stabilization of the M5 metabotropic glutamate [Kunishima et al., 2000; Romano et al., 1996] and extracellular calcium-sensing receptor-dimers [Bai et al., 1998; Ward et al., 1998].

The first study to provide convincing evidence on the functional significance for GPCR dimers came from experiments on the β_2-adrenergic receptor in the laboratory of M. Bouvier [Hebert et al., 1996]. In this study, Hebert et al. studied the effects of a peptide mimicking TM VI of the β_2-adrenergic receptor. What they found was quite intriguing, as treatment of β_2-adrenergic receptor expressing cells with the peptide, blocked dimerization and agonist-induced signalling. Furthermore, the effect was specific to peptides corresponding to TM VI of the receptor, as other TM peptides had no effect. Ligand also played part in the equilibrium of the complex; treatment with the agonist isoproterenol stabilized the dimers and prevented the TM peptide from interfering whereas inverse agonists were found to favour the stability of monomers. A functional role for the dimerization of δ-opioid receptors was also reported, however, in this case, agonist treatment resulted in the dissociation of pre-existing dimers, a property that when perturbed, disrupted receptor-internalization [Cvejic and Devi, 1997].

The $GABA_B$ receptor story: A common theme in family C GPCRs

Despite these efforts, most attempts to characterize the occurrence of GPCR dimers were criticized as being an artefact of over expression, as hydrophobic proteins such as GPCRs, are prone to aggregation when solubilised from highly expressing cell-expression systems. It wasn't until the cloning and characterization of the $GABA_B$ receptor, a member of the class C superfamily of GPCRs, that the importance of GPCR dimerization began to percolate within the greater scientific community. The first $GABA_B$ cDNA cloned was in 1997, and termed $GABA_BR1$ [Kaupmann et al., 1997].

However, although the receptor was capable of binding GABA agonists when expressed in various cell-types, it was largely non-functional and incapable of efficiently coupling to potassium channels.

In addition, it was not efficiently transported to the cell surface and as a result was largely retained intracellularly. The following year, a second $GABA_B$ subtype was cloned and termed $GABA_BR2$, however; unlike $GABA_BR1$, this receptor-subtype could traffic to the cell surface but did not bind GABA agonists. It was only following the co-expression of both receptor-subtypes did the formation of a fully functional $GABA_B$ receptor emerge that efficiently trafficked to the cell surface [Jones et al., 1998; Kaupmann et al., 1998; Kuner et al., 1999; Martin et al., 1999; Ng et al., 1999; White et al., 1998]. Assembly and cell surface targeting of the $GABA_B$ receptor occurs primarily at its carboxyl-terminus [Kuner et al., 1999; Pagano et al., 2001; White et al., 1998], although it has been demonstrated that heterodimerization can occur through other regions such as their transmembrane domains [Calver et al., 2001; Pagano et al., 2001]. The carboxyl-terminus of $GABA_BR1$ possesses a motif that causes retention in the endoplasmic reticulum, however, this motif is masked by interaction with the C-terminus of $GABA_BR2$ [Kuner et al., 1999; Pagano et al., 2001; White et al., 1998]. These studies were the first to provide strong evidence on the importance of GPCR dimerization in receptor transport and function.

A similar scenario has also been reported for the taste receptors, also members of class C GPCRs, where heterodimerization between receptor-subtypes plays an important part in receptor function. For instance, the two cloned taste receptors, T1R1 and T1R2, were unresponsive to sweet stimuli when expressed alone in heterologous cells [Hoon et al., 1999]. A third taste receptor termed T1R3, was later cloned by six independent groups, yet still unresponsive to sweet stimuli when independently expressed in heterologous cells [Bachmanov et al., 2001; Kitagawa et al., 2001; Max et al., 2001; Montmayeur et al., 2001; Nelson et al., 2001; Sainz et al., 2001]. It was only following the co-expression of both T1R2 and T1R3 that the addition of sweet tastants caused receptor-activation [Nelson et al., 2001], suggesting heterodimerization in the formation of functional sweet taste receptors. Curiosity led to the discovery of yet another

functional heterodimer, T1R1/T1R3, however, in this case the stimulus was not sweeteness but for the sensation known as "umami", a stimulus brought on by the amino acid monosodium glutamate [Zhao et al., 2003]. Although the molecular determinants in the heterodimerization of T1R1/T1R3 and T1R2/T1R3 have not been fully elucidated, the interactions are specific; as no other GPCR investigated to date could form an association, much like the specificity seen in the formation of the $GABA_BR$ heterodimer.

In addition to the $GABA_B$ and taste receptors, other members of the class C family of GPCRs have also been reported to exist as dimers. For instance, western blot analysis of the calcium-sensing receptor and the metabotropic glutamate receptor subtype-5 in whole-cell lysates, demonstrated these receptors to exist as constitutive disulfide-linked dimers [Bai et al., 1998; Bai et al., 1999; Jensen et al., 2002; Pin et al., 2005; Romano et al., 1996]. Furthermore, crystal-structure analysis of the large N-terminal portion of the metabotropic glutamate receptor subtype-1, revealed it to exist as a dimer hinged by disulfide bonding [Kunishima et al., 2000].

Resonance Energy Transfer techniques to study GPCR dimers

Despite the accumulation of evidence on the dimerization of GPCRs, scepticism still lingered on the relevance of these interactions *in vivo*, especially in regards to the class A subfamily of GPCRs, as they do not possess a large extracellular domain to support disulfide linkage. Therefore, a more sensitive and less invasive technique had to be developed in order to monitor GPCR interactions in intact cells. In 2000, the call was answered by three independent groups by adopting techniques of resonance energy transfer (RET) [Angers et al., 2000; Overton and Blumer, 2000; Rocheville et al., 2000b]. The use of fluorescence techniques in examining the properties of proteins in living cells has exploded in the past few years. There have been major advancements in the application of steady-state and time-resolved digital imaging techniques, as well as the development of convenient probes suitable for *in vitro* and *in vivo* labelling [Giepmans et al., 2006]. Fluorescence has become one of the most prominent technologies in biomedicine. In particular, the application of RET techniques has been instrumental in

the study of molecular biology. The potential of RET lies in the fact that it can yield both static information and insight into the internal mobility and flexibility of bimolecular systems. RET is a process of nonradiative energy transfer, the exact theory of which was correctly explained for the first time by Förster over 60 years ago [Forster, 1946; Forster, 1947; Forster, 1948]. The process of RET occurs whenever the emission spectrum of a fluorophore termed the donor, overlaps with the absorptive spectrum of another fluorophore termed the acceptor. It is important to reiterate that the process does not involve emission of light from the donor. The reabsorption process is however dependent on the overall concentration of the acceptor. The extent of the energy transfer is determined by the distance between the donor and acceptor in addition to the spectral overlap of the two fluorophores. The equation for the transfer of energy of a single donor-acceptor pair at a fixed distance is given as follows:

$$E = \frac{R_0^6}{R_0^6 + r^6} \qquad (3.1)$$

where R_0 is the Förster distance and r is the distance between the donor (D) and the acceptor (A). Transfer efficiency is typically measured by the fluorescence intensity of the donor (F_D), in the absence and presence (F_{DA}) of the acceptor:

$$E = \frac{F_D - F_{DA}}{F_D} = \frac{1 - F_{DA}}{F_D} \qquad (3.2)$$

The extent of the energy transfer therefore depends on the sixth power of the distance (r) of the two fluorophores. It is of great avail that the distances between which RET occurs, 10 to 100 Å, happens to be comparable in size to biological macromolecules. Hence, RET can be considered a spectroscopic ruler for measurements of distances between sites

on proteins. The principle forms of RET applied to investigate the dimerization of GPCRs is fluorescence resonance energy transfer (FRET) and bioluminescent resonance energy transfer (BRET). In FRET, the donor molecule needs to be excited by an external light source, contrary to BRET, where the donor molecule is intrinsically luminescent {*reviewed in* [Harrison and van der Graaf, 2006; Milligan, 2004a; Milligan and Bouvier, 2005; Persani et al., 2007; Pfleger and Eidne, 2005]}. In both BRET and FRET, the emission and excitation wavelengths of both the donor and acceptor respectively, must overlap to a certain extent but avoiding excessive overlap to improve signal-to-noise ratios.

Bioluminescence Resonance Energy Transfer (BRET)

One of the more common RET techniques in the study of GPCR dimerization is BRET, partly because it does not require the use of expensive microscopes but rather a spectrophotometer. The donor used in BRET is *Renilla* luciferase (Rluc), an enzyme isolated from the marine sea pansy. Rluc it is not intrinsically fluorescent, but requires the addition of a substrate, colentrazine, that it oxidizes producing light emission in the blue wavelength (395 nm). The acceptor is generally either green fluorescent protein (GFP) or its variant, yellow fluorescent protein (YFP). If the donor is within close proximity to the acceptor, energy transfer occurs exciting the acceptor molecule. There are two versions of BRET; the original version, pioneered by Xu et al. [Xu et al., 1999], utilizes enhanced YFP (eYFP) as the acceptor, and the revised version known as BRET^2. BRET^2 was developed by Perkin Elmer Life Sciences and employs modified variants of GFP and colentrazine, GFP^2 and DeepBlueC respectively, allowing GFP to be excited at 410 nm to give better spectral resolution.

Because it is necessary to produce fusion proteins between the GPCRs of interest and either Rluc, eYFP or GFP^2, the technique can only be performed in recombinant cell systems. The fusion proteins are then transfected into cells, typically by way of transient transfection, where they are then placed in either a cuvette or multiplate reader, and then read at their respective wavelengths following the addition of colentrazine. The first

study to employ the BRET technique in the study of GPCR dimerization, was on the β_2-adreneric receptor, in the lab of M. Bouvier [Angers et al., 2000]. Using first generation BRET, they demonstrated that the β_2-adreneric receptor exists as constitutive dimers in live cells, confirming previous co-immunoprecipitation data, and that agonist binding can increase their RET signal. Furthermore, they also applied the technique to demonstrate the transient agonist-regulated interaction of β-arrestin to the receptor. Although the technique has its advantages, there is one intrinsic disadvantage when studying GPCRs; BRET cannot discriminate between dimers present at the cell surface or those present during synthesis in the endoplasmic reticulum.

Fluorescence Resonance Energy Transfer (FRET)

As previously stated, FRET unlike BRET requires an external light source to excite the donor molecule. There are various forms of FRET, however, all of which apply the same underlying principle: measure the transfer of energy from a donor to an acceptor fluorophore, during its excitation. One form of FRET that is analogous to the BRET technique involves the tagging of GPCRs with GFP variants, usually at the carboxyl-terminus. The commonly used GFP variants in this case are cyan fluorescent protein (CFP) and YFP; however, GFP has been used in place of YFP as they have sufficient spectral overlap [Stanasila et al., 2003]. Cells transfected with the recombinant fusion proteins can either be measured in cuvettes, similar to the BRET technique, or by using confocal or widefield microscopes and analyzed using imaging software. In the lab of K.J. Blumer, application of FRET using CFP and YFP tagged versions of a GPCR was was first described on the α-factor receptor, a product of the STE2 gene from *Saccharomyces cerevisiae* [Overton and Blumer, 2000]. In their study, CFP was excited with a λ_{max} of 440 nm and emission was detected by scanning fluorometry. Fluorescent emission due to FRET was quantified by subtracting the emission spectrum of cells expressing the CFP fusion alone, and the emission spectrum of cells expressing only the YFP fusion protein, from the emission of cells co-expressing CFP and YFP fusion proteins. The efficiency of FRET was quantified by dividing the integrated FRET curve

by the integrated emission curve obtained from direct excitation of YFP at 490 nm. In this fashion, the authors were able to detect a strong FRET signal on the surface of transfected cells, indicative of constitutive dimerization.

Although FRET has its advantages, such as being able to discriminate a FRET signal from the cell surface and intracellular compartments, it does have its disadvantages. One problem associated with direct FRET intensity measurements is the noise or false signals obtained by the autofluorescence of intrinsic cellular proteins. To overcome this problem, variants of FRET have been applied and include time resolved FRET (trFRET), first employed to study the dimerization of GPCRs in 2001 in the lab of G. Milligan, while investigating the human δ-opioid receptor [McVey et al., 2001]. This technique takes advantage of the prolonged fluorescent characteristics of lanthanide compounds, such as europium (donor) and allophycyanin (acceptor), thereby allowing excitation and detection to be temporally separated eliminating the presence of autofluorescence. Unlike the FRET performed using GFP variants, the fluorescent molecules used in trFRET are usually conjugated to antibodies, allowing one to specifically target the receptor at the cell surface.

Photobleaching FRET (pbFRET)

Another technique that also overcomes the problems of direct FRET measurements is photobleaching FRET (pbFRET), which exploits the photobleaching process of fluorophores. The application of pbFRET was originally developed by Jovin et al. in the early 90's [Gadella and Jovin, 1995; Kubitscheck et al., 1991; Young et al., 1994], but only introduced to study the dimerization of GPCRs in the laboratory of Y.C. Patel, in 2000 [Rocheville et al., 2000a; Rocheville et al., 2000b]. Photobleaching is an irreversible process that involves the photochemical destruction of a fluorophore and always occurs in its excited state. Donor photobleaching FRET is the process of photobleaching the donor fluorophore under the intense illumination of its excitation wavelength, while measuring the changes in the intensity of its fluorescence in the absence or presence of the acceptor fluorophore. If the acceptor is in close enough

proximity to the donor, (10-100 Å), FRET occurs and competes with the photobleaching process, decreasing the rate of photobleaching. The FRET efficiency, assuming a single exponential decay, can be calculated as follows:

$$E = 1 - \frac{\tau_D}{\tau_{D+A}} \quad (3.3)$$

where E is the FRET efficiency and τ_D, the photobleaching decay rate of the donor in the absence and τ_{D+A}, presence of the acceptor [Patel et al., 2002b]. One advantage in using this method is that the time constants are measured in the second to minute range unlike regular FRET, which occurs in nanosecond time scale, thereby omitting the need for complex digital imaging instrumentation. The strategy used for detecting the dimerization of hSSTRs by pbFRET is shown in figure 3.5. Cells were stably-transfected to control for receptor expression, with tagged hSSTRs, in this case hemagglutinin (HA) and targeted with anti-HA monoclonal antibodies conjugated to either fluorescein isothiocyanate as the donor or rhodamine as the acceptor. Decreases in the donor fluorescence intensity under prolonged exposure to excitation light are monitored, first in the absence, then in the presence of the acceptor. As mentioned above, any decreases in the fluorescence decay indicates that the receptors were in close enough proximity to allow for FRET. Given the small distance that is needed for FRET to take place, it can be assumed that the receptors are in association. The pbFRET technique is not restricted to the use of conjugated antibodies, as fluorescently labelled ligands [Grant et al., 2004b] and receptors fused with variants of GFP [Dinger et al., 2003] have been used.

Protein Complementation Assays (PCAs)

In addition to the RET techniques aforementioned, protein complementation assays can also be employed to monitor the interaction of GPCRs [Hu et al., 2002; Hu and Kerppola, 2003; Remy and Michnick, 2006; Stefan et al., 2007]. Essentially, PCAs

Figure 3.5.

An example employing pbFRET microscopy to study GPCR dimerization.

Antibodies conjugated to either donor or acceptor fluorophores are targeted towards receptors X and Y respectively. ***A***, If there is no interaction between the two receptors, the donor fluorophore photobleaches at a given rate when under continuous illumination of its excitation wavelength. ***B***, Interaction between receptors X and Y permits the transfer of excitation energy or quenching of the donor fluorophore by the acceptor, reducing the donor photobleaching decay rate.

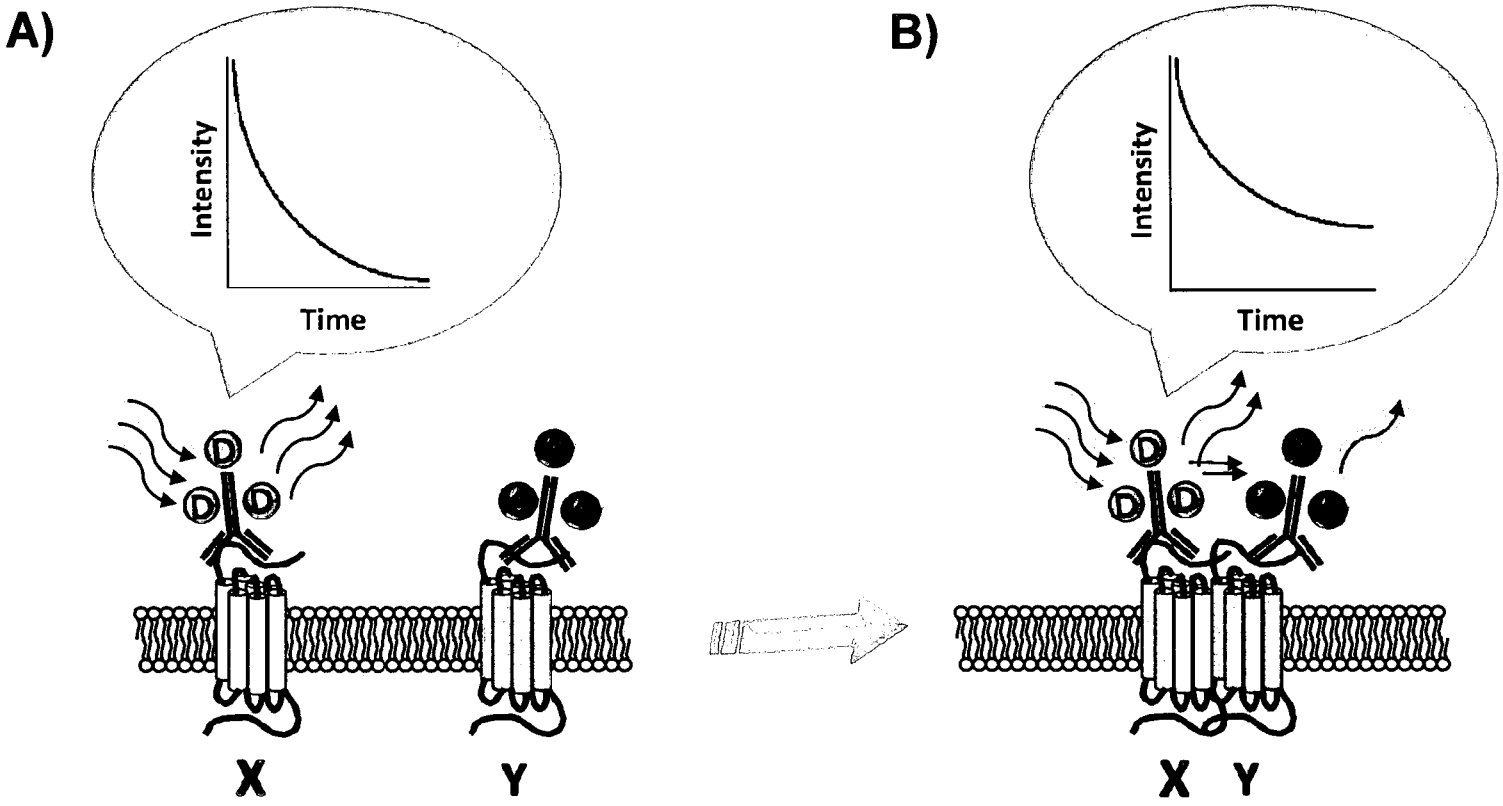
A)
Intensity
Time
D
D
D
X
Y
B)
Intensity
Time
D
D
D
X
Y

involve the reconstitution of a functional protein by the sum of its parts. For instance, both luciferases of the species *Renilla reniformis* and *Gaussia princeps* can be split into two complementary fragments and fused to two proteins that associate. If these proteins interact, a functional luciferase enzyme ensues that can be measured [Remy and Michnick, 2006; Stefan et al., 2007]. In a similar approach, fluorescent proteins such as GFP can be divided into two parts and measured for reconstitution when fused to proteins that associate [Hu et al., 2002; Hu and Kerppola, 2003]. Although considered a type of PCA, the reconstitution of fluorescent proteins is commonly referred to as bimolecular fluorescence complementation (BiFC).

Dimerization of family A GPCRs revisited

Many of the GPCR dimers previously investigated by Western blot have been verified using the newly available RET techniques. It has been determined that GPCR dimerization can occur in live or on the surface of intact cells. However, mechanisms believed to govern the interaction of several of the previously reported GPCRs were reinterpreted based on newly available data. It has been suggested that dimerization may play a role in all stages of the GPCR life cycle, from ontogeny to activation and internalization [Breitwieser, 2004; Bulenger et al., 2005; Hansen and Sheikh, 2004; Milligan, 2004b; Milligan, 2008; Park et al., 2004b; Terrillon and Bouvier, 2004]. Several studies have indicated that dimerization of GPCRs occurs early during synthesis, implying that it might represent a constitutive phenomenon. Furthermore, mutant receptors of vasopressin V2 [Zhu and Wess, 1998], thyroid-stimulating hormone [Calebiro et al., 2005], luteinizing hormone [Tao et al., 2004], gonadotropin-releasing hormone [Brothers et al., 2004], dopamine D3 [Karpa et al., 2000], chemokine CCR5 [Benkirane et al., 1997; Shioda et al., 2001], frizzled 4 [Kaykas et al., 2004], melanocortin-4 [Biebermann et al., 2003] and rhodopsin [Colley et al., 1995], have all been shown to behave in a dominant-negative fashion with respect to their wild-type counterparts by preventing their expression at the cell surface. However, recent studies

have suggested that heterodimerization between the δ-opioid and μ-opioid receptors occurs only after cell-surface delivery [Law et al., 2005].

Several members of the family A superfamily of GPCRs have been shown to form constitutive dimers irrespective and unresponsive to ligand binding [Ayoub et al., 2002; Babcock et al., 2003; Canals et al., 2003; Dinger et al., 2003; Floyd et al., 2003; Issafras et al., 2002; Jensen et al., 2002; Overton and Blumer, 2000; Stanasila et al., 2003; Terrillon et al., 2003; Trettel et al., 2003]. In addition, atomic force microscopy has shown that rhodopsin and opsin form constitutive dimers in dark-adapted native retinal membranes [Fotiadis et al., 2003; Liang et al., 2003]. Although constitutive dimerization may be the general consensus within the family C class of GPCRs, it is not a feature consistent amongst family A receptors, as ligand binding has been shown to promote [AbdAlla et al., 2004; AbdAlla et al., 1999; Angers et al., 2000; Baneres and Parello, 2003; Cornea et al., 2001; Grant et al., *in revision;* Grant et al., 2004b; Hanyaloglu et al., 2002; Horvat et al., 2001; Hunzicker-Dunn et al., 2003; Jiang et al., 2006; Kearn et al., 2005; Mellado et al., 2001b; Patel et al., 2002a; Pello et al., 2008; Rocheville et al., 2000a; Rocheville et al., 2000b; Rodriguez-Frade et al., 2004; Roess and Smith, 2003; Tao et al., 2004; Wurch et al., 2001; Zhu et al., 2002] or even dissociate [Berglund et al., 2003; Cheng and Miller, 2001; Cvejic and Devi, 1997; Devost and Zingg, 2004; Duran-Prado et al., 2007; Gines et al., 2000; Grant et al., 2004a; Latif et al., 2002] GPCR dimers. Additional support for the dynamic nature of GPCR dimers at the cell surface has been noted using synthetic peptides to disrupt their interaction [Hebert et al., 1996; Hernanz-Falcon et al., 2004; Ng et al., 1996; Overton et al., 2003]. Furthermore, selective-internalization of individual protomers of heterodimers have been shown to occur following their activation [Gines et al., 2000; Law et al., 2005; McGraw et al., 2006; Pfeiffer et al., 2001]. For instance, selective activation of SSTR2 in the SSTR2/SSTR3 heterodimer resulted in its internalization, without affecting the cell surface localization of SSTR3 [Pfeiffer et al., 2001]. Similarly, heteromeric complexes between dopamine D1 and adenosine A1 receptors, were found to disappear when treated with D1 receptor agonists by forming intracellular clusters that were devoid of A1 receptors [Gines et al., 2000]. The μ- and δ-opioid receptor heterodimer was also shown not to endocytose as a

complex but yet internalize as monomers when activated by agonists [Law et al., 2005]. Although formation of the prostaglandin-EP_1 and β_2-adrenergic heterodimer directly decreased β_2-adrenergic receptor coupling to $G\alpha_s$; cross-regulation was not involved in attenuating β_2-adrenergic receptor-function, as desensitization and internalization were factors affecting only the activated protomer [McGraw et al., 2006]. Finally, in a recent report, stabilization of the chemokine CXCR4 and δ-opioid receptor occurs following their co-stimulation and not their selective activation, a property that silenced receptor-signalling [Pello et al., 2008]. Taken together, these results provide evidence that GPCR dimers are not necessarily static complexes, in which both protomers are fixed to regulate as a unit. Confounding the issue further is that dimerization itself may not be a property consistent amongst GPCRs, as several receptors including hSSTR1 [Grant et al., 2004b; Patel et al., 2002a], the N-formyl peptide receptor [Gripentrog et al., 2003] and the neurokinin-1 receptor [Meyer et al., 2006] have been shown to exist and function as monomers. Furthermore, contrary of previous reports, employing a more rigorous approach to detecting protein-protein interactions using the BRET technique, revealed the β_2-adrenergic receptor to exist as a monomer [James et al., 2006]. In addition, recent evidence has demonstrated the β_2-adrenergic receptor to efficiently couple with $G\alpha_s$ G-proteins as monomers, when reconstituted in high-density lipoprotein particles [Whorton et al., 2007]. In a similar report, rhodopsin was also demonstrated to efficiently couple to transducin as a monomer [Bayburt et al., 2007; Whorton et al., 2008]. Finally, high-resolution crystallographic analysis of the β_2-adrenergic receptor, the second GPCR to be crystallized since rhodopsin in 2000 [Palczewski et al., 2000], revealed it to exist as a monomer in its inactive state [Rasmussen et al., 2007]. However, in a comparative study by a second group of authors, dimers were present but highly dependent on cholesterol for packing [Cherezov et al., 2007].

Molecular determinants implicated in the dimerization of rhodopsin-like family A GPCRs are variable, as they appear to be specific to the subfamily of GPCRs investigated. Key contributions by transmembrane domains I, IV, V and VI in various GPCRs have been reported [Guo et al., 2005; Hebert et al., 1996; Hernanz-Falcon et al., 2004; Klco et al., 2003; Liang et al., 2003; Ng et al., 1996; Overton et al., 2003; Thevenin

et al., 2005]. Although not exclusive to the transmembrane regions, other determinants have been shown to contribute to dimerization and include the amino-terminal [AbdAlla et al., 1999; Overton and Blumer, 2002] and carboxyl-terminal portions of GPCRs [Cvejic and Devi, 1997; Fan et al., 2005; Grant et al., 2004b; Sarmiento et al., 2004]. Dimerization of the angiotensin II AT1 receptor was shown to occur by the intracellular factor XIII transglutaminase via glutamine residue 315, in the carboxyl-terminal tails of agonist occupied receptors [AbdAlla et al., 2004]. Additionally, high-resolution crystallographic analysis of the β_2-adrenergic receptor, has revealed a single ionic interaction between the amine group of Lys60 of transmembrane domain helix I and the carboxylate of Glu338 in helix VIII at the carboxyl-terminal region of the symmetry-related receptor [Cherezov et al., 2007]. However, as previously mentioned, crystal packing was highly dependent on cholesterol, with over 70% of the contact surface between receptor-monomers being mediated by lipid [Cherezov et al., 2007]. Evidently, cholesterol is known to play a role in β_2-adrenergic receptor signalling; depleting cholesterol from cells increases G-protein coupling. Interestingly, one may speculate dimerization to impart negative cooperativity on β_2-adrenergic receptor signalling.

Epitopes that dictate a heteromeric interaction are often times less apparent. For instance, formation of the human adenosine $A2_A$ and dopamine D2 heterodimer was determined on the basis of electrostatic interactions between an arginine-rich epitope in the third intracellular loop of the D2 receptor and two epitopes in the carboxyl-terminus of the $A2_A$ receptor, one containing adjacent aspartates residues and the other a phosphorylated serine residue [Ciruela et al., 2004]. Interestingly, dephosphorylating the serine residue of the $A2_A$ receptor C-tail epitope prevented the formation of the heterodimer, suggesting phosphorylation/dephosphorylation events as a mechanism of regulation [Ciruela et al., 2004]. Although ligand was not involved in the regulation of the heterodimer, it did however, modulate the extent of co-aggregation, suggesting a role for agonist in the formation of higher order receptor complexes [Hillion et al., 2002]. Surprisingly, in the heterodimerization of μ- and δ-opioid receptors, G-protein itself was identified as a chaperone in stabilizing the interaction. When attempts were made to uncouple $G\alpha_i$ G-proteins using PTX, the heterodimer was abolished [Law et al., 2005].

Furthermore, the receptors internalized as monomers, suggesting that receptor activation by agonist was also capable of disrupting the complex. The importance of G-proteins in the heterodimerization of μ- and δ-opioid receptors is also indirectly supported by findings involving carboxyl-terminal truncations, as removal of the carboxyl-terminus of either receptor impairs their interaction and signalling [Fan et al., 2005].

Pharmacology and signalling of GPCR dimers

The first study to provide strong evidence for the pharmacological diversity of GPCR dimers was in the laboratory of L. Devi, while investigating the δ- and κ-opioid receptor heterodimer [Jordan and Devi, 1999]. Cells co-expressing δ- and κ-opioid receptors exhibited little affinity for receptor-specific agonists but co-administration lead to a synergistic effect on ligand binding. Indeed, this has been demonstrated within the entire opioid receptor-family by co-expressiing various receptor-pairs {*reviewed in* [Jordan et al., 2000; Rios et al., 2001]}. These studies suggested that dimerization, in particular heterodimerization, could provide cooperativity to ligand binding. Notwithstanding, the heterodimerization of other GPCR subtypes have been shown to alter the potency of agonists in signal generation. For instance, the heterodimerization of several other receptor combinations including the dopamine D2 and hSSTR5 [Rocheville et al., 2000a] and the hSSTR1 and hSSTR5 [Rocheville et al., 2000b] heterodimers were also reported to enhance GPCR signalling [AbdAlla et al., 2000; Baragli et al., 2007; Gomes et al., 2004; Scarselli et al., 2001; Waldhoer et al., 2005; Yoshioka et al., 2001; Zhu et al., 2005]. However, not all heterodimers are accompanied by enhanced pharmacology as negative cooperativity has been observed [AbdAlla et al., 2001a; El-Asmar et al., 2005; McGraw et al., 2006; Pello et al., 2008; Pfeiffer et al., 2001; Sohy et al., 2007; Urizar et al., 2005]. For example, McGraw and colleagues demonstrate that activation of the PGE_2 receptor, EP_1, on airway smooth muscle cells, reduced the bronchodilator response to a β_2-adrenergic agonist by uncoupling its interaction with $G\alpha_s$ G-proteins, thereby attenuating the production of cAMP [McGraw et al., 2006]. This cross-talk of the EP_1 receptor on β_2-adrenergic receptor signalling was mediated by

heterodimerization and required both receptors to be activated simultaneously. In a recent report, heterodimerization between the chemokine CXCR4 and the δ-opioid receptors in immune cells suppressed signalling [Pello et al., 2008]. Interestingly, this suppression of signalling occurred following simultaneous addition of their respective ligands and not when the receptors were individually activated.

It has been suggested that a GPCR dimer acts as a footprint suitable for binding a single G-protein α, β, γ-heterotrimer, based on structural analysis of the rhodopsin [Filipek et al., 2004; Fotiadis et al., 2004], the BLT1 leukotriene B4 receptor [Baneres and Parello, 2003], the α_{1b}/α_{1d}-adrenergic receptor [Hague et al., 2004], the metabotropic glutamate receptor [Goudet et al., 2005] and the $GABA_B$ receptor [Galvez et al., 2001; Havlickova et al., 2002] dimers. This holds particular interest for GPCR heterodimers, as they could provide a docking interface with different G-protein selectivity. For instance, the μ-opioid and δ-opioid receptors normally couple to $G\alpha_i$ G-proteins and are therefore sensitive to pertussis toxin treatment, however; when these receptors are co-expressed, the resulting heterodimer is insensitive to pertussis toxin treatment [George et al., 2000]. Similarly, heterodimerization between A1 and P2Y1 receptors results in preferential coupling of $G\alpha_i$ and not $G\alpha_q$, their cognate G-protein [Yoshioka et al., 2001]. Concurrent stimulation of both chemokine receptors CCR2 and CCR5 and not their selective-activation, results in the formation of heterodimers that preferentially couple to $G\alpha_{q/11}$ [Mellado et al., 2001b]. The consequences of this switch in G-protein coupling, from the pertussis toxin sensitive $G\alpha_i$ to $G\alpha_q$, is a delay in phosphatidyl inositol 3-kinase activation and an increased calcium flux, triggering cell adhesion rather than chemotaxis [Mellado et al., 2001b]. The protease-activated receptor-1 (PAR1) and PAR3 heterodimer shows preferential coupling to $G\alpha_{12/13}$, compared to the concomitant activation of $G\alpha_q$ and $G\alpha_{12/13}$ typically seen following activation of PAR1 [McLaughlin et al., 2007]. It was surmised that PAR3 acts as an allosteric modulator of PAR1, selectively increasing its coupling to $G\alpha_{12/13}$, leading to increases in the permeability of endothelial cells [McLaughlin et al., 2007]. These results have particular interest, as targeting PAR3 may alleviate symptoms such as vascular inflammation and lung injury associated with thrombosis. Co-activation of dopamine D1 and D2 receptors results in the generation of a

phospholipase-C-mediated Ca^{2+} signal. Although the D1 receptor is usually associated with $G\alpha_s$ coupling and the D2 receptor with $G\alpha_i$ coupling, co-activation of both subtypes results in coupling to $G\alpha_q$ [Lee et al., 2004]. Recently, the selectivity of the D1-D2 heterodimer to couple to $G\alpha_q$ following co-stimulation of the individual protomers was demonstrated in murine brain, providing physiological evidence for the interaction [Rashid et al., 2007].

Aside from G-protein coupling, other signalling factors such as MAPKs and even cell growth have been shown to be affected by dimerization. Co-expression of the orexin-1 receptor with the cannabinoid CB1 receptor, increased the potency of the peptide orexin-A to phosphorylate MAPKs by 100-fold, an effect that was blocked by the addition of a CB1 antagonist [Hilairet et al., 2003]. These results provide impetus to the development of cannabinoid antagonists for the treatment of obesity, as the orexin-1 receptor is involved in feeding. Heterodimerization between β_1- and β_2-receptors in HEK-293 cells, inhibits MAPK stimulation by the β_2-adrenergic receptor [Lavoie et al., 2002]. Contrarily, heterodimerization between cholecystokinin receptors type A and B enhances signalling and promotes cell growth when expressed in CHO-K1 cells [Cheng et al., 2003].

As previously mentioned, convincing evidence on the importance of GPCR dimerization and signalling, came from the study by Hebert et al., upon investigation of the β_2-adrenergic receptor [Hebert et al., 1996]; addition of a peptide corresponding to the sixth transmembrane domain of the β_2-adrenergic receptor, blocked dimerization and signalling. However, recent evidence has suggested that dimerization of the β_2-adrenergic receptor is not necessary for G-protein coupling and that the minimal functioning unit of the receptor is a monomer [James et al., 2006; Whorton et al., 2007]. Furthermore, the neurotensin NST1 receptor can also function as a monomer at low receptor concentrations and its dimerization at higher receptor levels, results in decreases in nucleotide exchange at the level of the G-protein. Whether or not Family A GPCRs can all function as monomers remains to be determined.

Effects of dimerization on cellular trafficking of GPCRs

A common occurrence following activation of family A GPCRs is their endocytosis or internalization, a well characterized process typically involved in signal attenuation. It has been demonstrated that GPCR dimers internalize as a complex. For instance, studies on the yeast α-factor pheromone receptor have demonstrated it to internalize as a dimer [Yesilaltay and Jenness, 2000]. Contrarily, although both the δ-opioid receptor and hSSTR2 form dimers at the cell surface in the absence of agonist, ligand-binding elicits their dissociation into monomers [Cvejic and Devi, 1997; Grant et al., 2004a]. This property was determined to be important for receptor trafficking, as blocking of which, impedes agonist-induced internalization [Cvejic and Devi, 1997; Grant et al., 2004a]. However, most of the observations documented on the changes in GPCR trafficking by dimerization have been shown for heterodimers. Several heterodimers were demonstrated to co-internalize as a unit following activation of either one or both protomers. These receptor combinations include hSSTR1 and hSSTR5 [Rocheville et al., 2000b], the α_{2A}- and β_1-adrenergic receptors [Xu et al., 2003], the α_{1A} and α_{1b} adrenergic receptors [Stanasila et al., 2003], the β_2-adrenergic and δ-opioid receptors [Jordan et al., 2001] the SSTR2 and μ-opioid receptors [Pfeiffer et al., 2002], and the adenosine A_{2A} and dopamine D_2 receptors [Hillion et al., 2002]. In the case of the β_1- and β_2-adrenergic heterodimer, β_1 prevented the internalization of the β_2-receptor [Lavoie et al., 2002]. Similarly, heterodimerization between the β_2- and the β_3-adrenergic receptors abrogated the sequestration of the β_2-receptor following activation, reflecting a possible dominant effect of the β_3 subtype on β_2, given its resistance to internalization [Breit et al., 2004]. The internalization of the β-alanine-responsive Mas-Related Receptor MrgD, is restricted when it heterodimerize with its closely related family member, MrgE. Reductions in the sequestration of MrgD was associated with an increased potency of ERK1/2 and a maintenance in the capacity of β-alanine to elevate intracellular calcium [Milasta et al., 2006]. The physiological relevance for the effects of dimerization on the desensitization/resensitization cycle remains to be determined. In case of the neurotensin receptors, heterodimerization between NTS1 and NTS2 influenced the subcellular distribution and capacity to down-regulate agonist-stimulated NTS1 [Perron et al., 2007].

In some instances, dimerization alters the association of β-arrestin, a protein intimately involved in coordinating the desensitization and internalization of GPCRs [Claing et al., 2002; Pierce et al., 2002]. Although the vasopressin V1a and V2 receptors form heterodimers that co-internalize upon activation, their endocytic/recycling pathway follows that of V1a, as determined by the association of β-arrestin [Terrillon et al., 2004].

Physiological relevance of GPCR dimers

The physiological relevance of GPCR dimers has always been an underlying issue since most of these studies have been performed in heterologous expression systems. In addition, expression levels of GPCRs in these systems are often times well above the physiological range. For instance, in one study, the β_2-adrenergic and δ-opioid receptors were shown to form heterodimers when co-expressed in HEK-293 cells [Jordan et al., 2001]. These receptors were also found to internalize as a complex following their activation [Jordan et al., 2001]. However, a more recent study failed to show heterodimers between the two receptors, when receptor expression-levels approximated physiological values [Cao et al., 2005]. Random interactions between various GPCRs were also detected in cell-expression systems where over-expression was a factor [Salim et al., 2002]. Because GPCRs are inclined to spuriously interact at higher expression levels, interpretation on their physiological relevance has been questionable. Despite these challenges, there have been notable examples where dimerization of GPCRs has been shown in physiologically relevant cells and tissues. For several years, the dimerization within the opioid receptor family has been recognized as a model to generate novel receptors with distinct signalling capabilities; with particular relevance in improving morphine-based analgesia by limiting tolerance and dependence [Gomes et al., 2004; He et al., 2002; He and Whistler, 2005; Jordan and Devi, 1999]. Recently, these claims have come to fruition, as an agonist with selectivity to an opioid receptor heterodimer has been identified. The ligand 6'-guanidinonaltrindole, is both a spinally selective analgesic and a preferentially agonist to the δ-κ-opioid heterodimer [Waldhoer et al., 2005].

An important receptor in the regulation of hypertension is the AT1 angiotensin II receptor [Schiffrin, 2002]. There has been considerable evidence supporting a role for the homo- and heterodimerization of AT1 receptors in cardiovascular disorders. Heterodimerization between the AT1 and bradykinin B2 receptor provided increases in AT1 receptor signalling and altered its internalization [AbdAlla et al., 2001b; AbdAlla et al., 2000]. Furthermore, heterodimers were found to exist in vessels and platelets in patients with preeclampsia [AbdAlla et al., 2001b; Quitterer et al., 2004]. Recently, AT1/B2 heterodimers were also identified in angiotensin II hypersensitivity in spontaneously hypertensive rats [AbdAlla et al., 2005], providing a mechanism in the pathogenesis of hypertensive renal disease with glomerulosclerosis. In addition to heterodimerizing with the B2 bradykinin receptor, AT1 has also been shown to form constitutive dimers with the β_2-adrenergic receptor in cardiomyocytes [Barki-Harrington et al., 2003]. Dual inhibition of the AT1 and β_2-adrenergic receptors were shown to occur by a single antagonist, involving receptor-G-protein uncoupling. Thus, it is suggested that β-adrenergic antagonists may serve a dual role in the treatment of heart failure by blocking β_2-adrenergic and AT1 receptor signalling. Aside from its suggested role in the pathogenesis of hypertension, AT1 receptors have also been implicated in the onset of atherosclerosis in hypertensive models and patients [AbdAlla et al., 2004]. In these cases, a transglutaminase, Factor XIIIA, was found to crosslink AT1 receptor dimers. It is suggested that elevated levels of cross-linked AT1 receptor dimers present on monocytes of hypertensive patients chronically sensitizes them, thereby sustaining the process of atherogenesis by enhancing their adhesiveness [AbdAlla et al., 2004]. Heterodimerization of the adenosine $A2_A$ and dopamine D2 receptors has been demonstrated to occur in heterologous cell expression systems, neuroblastoma cells and the striatum [Canals et al., 2003; Ciruela et al., 2004; Hillion et al., 2002; Kamiya et al., 2003]. Functional studies have demonstrated a reciprocal inhibitory interaction between $A2_A$ and D2 receptors on adenylate cyclase coupling [Ferre et al., 1997; Kull et al., 1999]. Electrophysiological and behavioural studies have also shown an inhibitory response of $A2_A$ receptor agonists on D2 receptor recognition and signalling [Stromberg et al., 2000; Tanganelli et al., 2004]. Contrarily, $A2_A$ receptor antagonists increase locomotion in reserpinized mice and produce contralateral rotational behaviour in rats following

treatment with sub-threshold doses of L-DOPA or the D2-receptor agonist quinpirole [Tanganelli et al., 2004]. It is of interest that $A2_A$ receptor antagonists have demonstrated antiparkinsonian actions in experimental models [Agnati et al., 2003; Bibbiani et al., 2003; Ferre et al., 1997; Ferre et al., 1992; Fuxe et al., 1998; Fuxe and Ungerstedt, 1974], as blockade of $A2_A$ receptors in the $A2_A$/D2 receptor heteromer may increase the therapeutic index of L-DOPA and D2 receptor agonists, providing novel therapeutics in the treatment of Parkinson's disease.

Dimerization of SSTRs

Physical evidence for the dimerization of SSTRs was first introduced in 2000 by Rocheville et al. using a combination of pharmacological, biochemical and biophysical techniques [Rocheville et al., 2000a; Rocheville et al., 2000b]. In these studies, it was determined that human SSTR5 dimers could be stabilized following agonist treatment in a dose-dependent fashion. Furthermore, using a functional complementation technique with a signalling deficient variant of SSTR5, receptor-activation could be restored when SSTR1 was introduced, presumably due to heterodimerization [Rocheville et al., 2000b]. Heterodimerization was suggested to be a specific process as signalling by the SSTR5 variant could not be reconstituted by SSTR4 expression. Human SSTR1 is known to be resistant to agonist-mediated internalization however, in cells co-expressing both SSTR1 and SSTR5, internalization could be observed [Rocheville et al., 2000b]. In a related study, the homo- and heterodimerization of SSTR1 and SSTR5 were specifically shown in live cells using a combination of RET techniques [Patel et al., 2002a]. In these studies, although SSTR5 was demonstrated to form both homo- and heterodimers with SSTR1 in an agonist-regulated fashion, SSTR1 remained as a monomer when expressed alone despite its activation with agonist. This was the first study to demonstrate using RET techniques that not all GPCRs require dimerization to function, as several other groups would later show [Gripentrog et al., 2003; Meyer et al., 2006; Whorton et al., 2007]. It was also determined that SSTR dimers could be occupied by more than one ligand molecule. In the human pancreas, both SSTR1 and SSTR5 are highly co-expressed in β-

cells suggesting a role for heterodimerization in the control of insulin secretion [Kumar et al., 1999]. Two other members of the SSTR family were shown to dimerize in the laboratory of S. Schulz, namely SSTR2 and SSTR3 [Pfeiffer et al., 2001]. In their investigations, rodent SSTR2 and SSTR3 where demonstrated to form constitutive homodimers and heterodimers when co-expressed in HEK 293 cells. Interestingly, in cells co-expressing SSTR2 and SSTR3, the SSTR3-selective agonist L-796,778 displayed marked reductions in binding affinity, suggesting negative cooperativity of SSTR2 on SSTR3. Furthermore, GTP binding, inhibition of adenylate cyclase and phosphorylation of ERK1/2 by the heterodimer reflected the characteristics of SSTR2 when expressed alone in the same cells. However, unlike SSTR2, the SSTR2/SSTR3 heterodimer displayed a strong resistance to agonist-induced desensitization [Pfeiffer et al., 2001]. The physiological relevance for these observations remains unclear however, both receptors colocalize in tissues such as the pancreas, the anterior lobe of the pituitary [Pfeiffer et al., 2001] and in medullablastoma tumoural cells [Cervera et al., 2002]. The SSTR2-mediated inactivation of SSTR3 may explain the absence of SSTR3 binding sites in the cerebellum of developing rats, as mRNA levels for both SSTR2 and SSTR3 are highly expressed in early development [Viollet et al., 1997].

SSTRs have not only been shown to form dimers within their family but also with other related members, such as the dopamine and opioid receptor families. For instance, when expressed in CHO-K1 cells, human SSTR5 and human dopamine (D2R) could be triggered to heterodimerize when activated by either a dopamine- or a SST-related agonist [Rocheville et al., 2000a]. Furthermore, heterodimerization provided positive cooperativity to SST binding, a property that was also related to enhanced receptor-signalling. Immunohistochemical analysis made evident the possibility of identifying these heterodimers under normal physiological conditions, as colocalization of both SSTR5 and D2R were shown in a subset of neurons from both the cortex and striatum of the rodent [Rocheville et al., 2000a]. Recently, a physical interaction between human SSTR2 and D2R was documented and shown to be regulated by agonist-binding [Baragli et al., 2007]. Interestingly, unlike the SSTR5/D2R heterodimer, positive cooperativity was a property observed for D2R, as the binding affinity of dopamine was markedly

enhanced by agonist-bound SSTR2 [Baragli et al., 2007]. There have been several indications suggesting a functional linkage between the somatostatinergic and dopaminergic systems. For instance, dopamine enhances SSTR-mediated inhibition of adenylate cyclase in rat striatum and hippocampus [Rodriguez-Sanchez et al., 1997]. Additionally, SSTR2 has been shown to mediate striatal dopamine release [Hathway et al., 1999]. Although SSTRs are the primary targets in the medical treatment of acromegaly caused by growth-hormone hyper-secreting pituitary adenomas, the dopamine agonist, cabergoline, provides effective control in 29-39% of patients [Abs et al., 1998; Cozzi et al., 1998]. Incidentally, combination treatment of SST and dopamine agonists has been shown to be more effective than the activation of SST-analogs alone [Marzullo et al., 1999]. The recent development of chimeric molecules that target both SSTR2 and D2R attest to these findings and suggest an interaction between both receptors to account for their behaviour [Jaquet et al., 2005; Saveanu et al., 2006; Saveanu et al., 2002].

Finally, the SST-analog octreotide, has been observed to behave as an antagonist in morphine-dependent individuals [Maurer et al., 1982] and patients undergoing morphine withdrawal have presented with reduced vomiting following octreotide administration [Bell et al., 1999]. Since both receptors, SSTR2 and the μ-opioid receptor, have been shown to be co-localized in neurons of the locus coeruleus [Pfeiffer et al., 2002], a region of the brain implicated in opioid dependency and withdrawal [Gold et al., 2003], it is not unreasonable to assume that heteromeric interactions may exist. Indeed, when expressed in HEK-293 cells, heterodimerization between SSTR2 and the μ-opioid receptor (μOR) could be demonstrated [Pfeiffer et al., 2002]. Although it was determined that ligand binding profiles of either the SST-analog L-779,976 or the μOR agonist DAMGO were unaltered by heterodimerization, receptor regulation such as phosphorylation, desensitization and internalization were affected. For instance, binding of either L-779,976 or DAMGO to the heterodimer resulted in cross-phosphorylation of each receptor-subtype [Pfeiffer et al., 2002]. Furthermore, this form of heterologous desensitization translated into a loss of coupling to adenylate cyclase and a diminished MAPK signalling response. Interestingly, co-internalization of SSTR2 and μOR was only

observed following stimulation of SSTR2 and not by activation of the μOR agonist DAMGO [Pfeiffer et al., 2002]. These results implicate SSTR agonists in the stabilization of this heterodimer. A similar finding was reported for the SSTR2/SSTR3 heterodimer, however, in this case, activation of SSTR2 resulted in its selective-internalization while SSTR3 was maintained at the cell surface [Pfeiffer et al., 2001].

SECTION 4: MANUSCRIPTS

A) Ligand binding and receptor-specificity in the dimerization of human SSTR1 and SSTR5

We had previously described the homo- and heterodimerization of hSSTR1 and hSSTR5, however; it remained unclear as to whether both receptor-subtypes are equally capable of inducing a heteromeric interaction following their selective-activation and as to which molecular determinants may be responsible for mediating their association. In the present manuscript, we report on the specificity of agonist-bound hSSTR5 and not hSSTR1 in orchestrating heterodimerization. Furthermore, we provide additional evidence to the monomeric nature of hSSTR1, a receptor that does not dimerize in monotransfected cells. Finally, the same molecular determinant implicated in resisting the agonist-induced internalization of hSSTR1 also prohibits its dimerization.

Manuscript: Grant, M., Patel, R.C. and Kumar, U. (2004) The role of subtype-specific ligand binding and the C-tail domain in dimer formation of human somatostatin receptors. *J Biol Chem*, **279**, 38636-38643.

The Role of Subtype-Specific Ligand Binding and the C-tail Domain in Dimer Formation of Human Somatostatin Receptors

Michael Grant*,ξ, Ramesh C. Patel§, and Ujendra Kumar*‡

*Fraser Laboratories For Diabetes Research, , Royal Victoria Hospital, Departments of Medicine, and ξPharmacology and Therapeutics, McGill University, Montreal, Quebec, Canada, H3A 1A1; §Department of Chemistry and Physics, Clarkson University, Potsdam, New York 13699-5810, USA.

***Running title**: Dimerization of Somatostatin Receptors*

‡Address for correspondence: Dr. U. Kumar

Room M3.15, Royal Victoria Hospital

687 Pine Avenue West

Montreal, Quebec H3A 1A1, Canada

Phone: (514) 842-1231 ext. 35042

Fax: (514) 843-2819

E-mail: **ujendra.kumar@muhc.mcgill.ca**

SUMMARY

G-protein coupled receptors (GPCRs) represent the largest and most diverse family of cell surface receptors. Several GPCRs have been documented to dimerize with resulting changes in pharmacology. We have previously reported by means of photobleaching fluorescence energy resonance transfer (pbFRET) microscopy and fluorescence correlation spectroscopic (FCS) analysis in live cells, that human somatostatin receptor (hSSTR) 5 could both homodimerize, and heterodimerize with hSSTR1 in the presence of the agonist SST14. In contrast, hSSTR1 remained monomeric when expressed alone regardless of agonist exposure in live cells. In an effort to elucidate the role of ligand and receptor-subtypes in heterodimerization, we have employed both pbFRET microscopy and Western blot on cells stably coexpressing hSSTR1 and hSSTR5 treated with subtype-specific agonists. Here we provide evidence that activation of hSSTR5 but not hSSTR1 is necessary for heterodimeric assembly. This property was also reflected in signalling as shown by increases in adenylyl cyclase coupling efficiencies. Furthermore, receptor c-tail chimeras allowed for the identification of the c-tail as a determinant for dimerization. Finally, we demonstrate that heterodimerization is subtype-selective involving ligand-induced conformational changes in hSSTR5 but not hSSTR1 and could be attributed to molecular events occurring at the c-tail. Understanding the mechanisms by which GPCRs dimerize holds promise for improvements in drug design and efficacy.

[1] **The abbreviations used are:**

GPCR(s), G protein coupled receptor(s); hSSTR, human somatostatin receptor; SST, somatostatin; HA, hemagglutinin; CHO, Chinese hamster ovary; pbFRET, photobleaching fluorescence resonance energy transfer; FITC, fluorescein isothiocyanate; TR, texas red; FCS, fluorescence correlation spectroscopy; TM, transmembrane domain

Φ The terms dimerization and oligomerization are used interchangeably.

INTRODUCTION

In recent years, G-protein coupled receptors (GPCRs) - once believed to exist at the plasma membrane as monomers - have been shown to assemble on the membrane as functional homo- and heterodimers [Agnati et al., 2003; Angers et al., 2002]. Dimerization$^{\Phi}$ of GPCRs has been shown to affect a multitude of receptor functions including ligand binding, signalling, receptor-desensitization and receptor trafficking [Agnati et al., 2003; Angers et al., 2002]. The influence of GPCR dimerization have shown to include cellular immunity, neurotransmission [Agnati et al., 2003], taste [Li et al., 2002; Nelson et al., 2002; Nelson et al., 2001] and disease [AbdAlla et al., 2001b]. Although the mechanism by which GPCR dimerization occurs remains obscure, one model suggests that ligand binding of cell surface receptors induces a conformational change that favours dimer formation; while the other suggests that dimerization is an exclusive event occurring early on during receptor biogenesis most probably in the ER and is a necessary event for proper receptor trafficking and function.

This latter model has been suggested for members of the class C subfamily of GPCRs, which include the GABAergic receptors [Jones et al., 1998; Kaupmann et al., 1998; White et al., 1998], calcium sensing receptor [Bai et al., 1998; Jensen et al., 2002], the metabotropic glutamate receptor [Romano et al., 1996] and the sweet taste receptors [Li et al., 2002; Nelson et al., 2002; Nelson et al., 2001]. However, this paradigm of GPCR assembly is not consistent amongst the class A/rhodopsin-like family of GPCRs. Several reports have shown that agonist plays an active role in GPCR dimerization at the plasma membrane, suggesting an equilibrium between GPCR dimers/monomers that can be regulated by ligand occupancy. These receptors include the human somatostatin receptors (hSSTRs) [Patel et al., 2002a; Rocheville et al., 2000b], dopamine D2 receptor [Wurch et al., 2001], gonadotrophin-releasing hormone receptor [Cornea et al., 2001; Horvat et al., 2001], luteinizing hormone/chorionic gonadotrophin hormone receptor [Roess et al., 2000], bradykinin B_2 receptor [AbdAlla et al., 1999], thyrotropin-releasing hormone receptor [Kroeger et al., 2001], cholecystokinin receptor [Cheng and Miller,

2001], thyrotropin receptor [Latif et al., 2002] and the chemokine receptors [Mellado et al., 2001b; Rodriguez-Frade et al., 1999; Vila-Coro et al., 2000; Vila-Coro et al., 1999].

We have previously reported that hSSTRs, known to modulate neurotransmission, cell secretion, and cell proliferation [Moller et al., 2003; Patel, 1999] are capable of undergoing both homo- and heterodimerization at the cell membrane [Patel et al., 2002a; Rocheville et al., 2000a; Rocheville et al., 2000b]. Recently, we have demonstrated ligand-dependent homo- and heterodimers on the plasma membrane in live cells in both a homogeneous and heterogeneous receptor expressing cell line, using both single- and two-photon dual color fluorescence correlation spectroscopy (FCS) with cross-correlation analysis (a method that discriminates based upon molecular size, number density and average brightness/particle in femtoliter confocal volumes) [Patel et al., 2002a]. One of the receptor sub-types, hSSTR1, did not form homodimers in either the absence or presence of ligand. In contrast, hSSTR5 showed robust dimerization upon agonist exposure. When both receptors were co-expressed in the same cell, we were able to observe two populations of dimers, hSSTR5 homodimers and hSSTR1/hSSTR5 heterodimers [Patel et al., 2002a]. However, it remains unclear as to whether one or both receptor-subtypes are capable of promoting heterodimeration and which receptor motifs may be attributed to this behavior.

In the present study, using subtype-specific agonists and both photobleaching fluorescence resonance energy transfer (pbFRET) and Western blot analysis, we demonstrate that ligand-bound hSSTR5 but not hSSTR1 can promote the heterodimerization of hSSTR1/hSSTR5. Moreover, using receptor c-tail chimeras, we were able to abrogate the homodimerization of hSSTR5 and induce the formation of hSSTR1 homodimers. The hSSTR5 subtype-specific analog of somatostatin, SMS 201-995, displayed a relatively poor signaling profile for hSSTR5 expressed alone despite having nanomolar binding affinity. Accordingly, coexpression with hSSTR1 resulted in a robust signaling efficiency by SMS 201-995 that correlated in part with its ability to induce heterodimerization. Finally, we demonstrate that not all agonists can induce heterodimerization, which was dependent upon ligand-occupancy of a specific receptor-subtype that can lead to alterations in pharmacology.

EXPERIMENTAL PROCEDURES

Materials and Antisera

The peptides SST-14, D-Trp-SST-14, SST-28 and [Leu(8)-D-Trp-22, Tyr-25]-SST-28 (LTT-SST-28) were purchased from Bachem, Torrance, CA; Octreotide [SMS (201-995)] was given by Sandoz, Basel, Switzerland and des-AA^{1,2,5}-[D-Trp^{8}IAmp^{9}]SS (SCH-275) was a gift from Dr. J. Rivier, Salk Institute. Fluorescein-, rhodamine-conjugated and unconjugated mouse monoclonal antibodies against hemagglutinin (HA) (12CA5) were purchased from Roche Molecular Biochemicals, Mannheim, Germany. Anti-c-myc monoclonal antibody was purchased from Sigma-Aldrich, Inc., St. Louis, MO. Rabbit polyclonal antibodies directed against the NH_2-terminal segment of hSSTR1 was generated and characterized as described [Kumar et al., 1999]. Protein A/G-agarose beads were purchased from Oncogene Research Products, La Jolla, CA.

SSTR Constructs and Expressing Cell Lines

Stable transfections of CHO-K1 cells expressing hSSTR5, hSSTR1 and both HA-tagged hSSTR5 and hSSTR1 and c-myc-tagged hSSTR5 were prepared by Lipofectamine transfection reagent as previously described [Rocheville et al., 2000b]. Chimeric receptors R1CR5 and R5CR1 were constructed by interchanging the c-tail of each receptor with one another. R1CR5 was created by adding the c-tail of hSSTR5, the last 46 residues, to hSSTR1 after residue 331. Similarly, R5CR1 includes the remaining 60 residues of hSSTR1 joined to hSSTR5 following residue 318 [Hukovic et al., 1999]. Clones were selected and maintained in CHO-K1 medium containing Hams F12 with 10% fetal bovine serum and 700 μg/ml neomycin. Stable transfections of CHO-K1 and HEK-293 cells co-expressing hSSTR5 and hSSTR1 were made using the vectors pCDNA3.1/Neo (neomycin resistance) and pCDNA3.1/Hygro (hygromycin resistance) such that hSSTR5 was cloned into pCDNA3.1/Hygro and hSSTR1 was cloned into pCDNA3.1/Neo. Stable transfections were selected in CHO-K1 medium containing 700

μg/ml of neomycin with 500 μg/ml of hygromycin or, HEK-293 medium containing 700 μg/ml of neomycin and 400 μg/ml of hygromycin.

Fluorescent SST Ligands

Fluorescent labeled SST ligands were prepared by N-terminal conjugation of D-Trp-SST-14 to fluorescein by use of Fluoroscein Isothiocyanate (SST-FITC) and SST-14 to Texas Red by use of Texas Red succinimidyl ester (SST-TR). The reaction of the dye with the ligand was performed in 0.2 M sodium bicarbonate pH 7.5 for four hours at 4°C in the absence of light. The reaction was stopped with 1.5 M Hydroxylamine followed by HPLC separation as previously described [Nouel et al., 1997].

Binding Assays

Cells were harvested, homogenized using a glass homogenizer and membranes were prepared by centrifugation as previously described [Hukovic et al., 1999; Rocheville et al., 2000b]. Binding studies were performed with 20-40 μg of membrane protein collected from CHO-K1 cells stably expressing the receptor constructs, and ^{125}I-labeled LTT-SST-28 radioligand (~60 pM) in 50 mM HEPES, pH 7.5, 2 mM $CaCl_2$, 5 mM $MgCl_2$, 0.5% bovine serum albumin, 0.02% phenylmethylsulfonyl fluoride, and 0.02% bacitracin (binding buffer) for 30 min at 37°C. Incubations were terminated by the addition of ice cold binding buffer. Membrane pellets were quantified for radioactivity using a LKB gamma counter (LKB-Wallach, Turku, Finland). Binding data were analyzed with Prism 3.0 (Graph Pad Software, San Diego, CA) by non-linear regression analysis.

Coupling to Adenylyl Cyclase

Cells were grown in 6-multiwell plates and tested for receptor coupling to adenylyl cyclase by incubation for 30 min with 20 μM forskolin and 0.5 mM 3-isobutyl-1-methylxanthine with or without agonists (10^{-11} – 10^{-6} M) at 37°C as previously described [Hukovic et al., 1999]. Cells were then scraped in 0.1 N HCl and quantified for cAMP by radioimmunoassay using a cAMP Kit (Inter Medico, Markham, ON) following the manufacturer's guidelines. Data were analyzed by non-linear regression analysis using Prism 3.0 (Graph Pad Software, San Diego, CA). SEMs are representative of at least three independent experiments.

PbFRET Microscopy and Immunocytochemistry

PbFRET experiments were performed on CHO-K1 cells as previously described [Patel et al., 2002a; Patel et al., 2002b; Rocheville et al., 2000a; Rocheville et al., 2000b] stably co-expressing HA-hSSTR5 and hSSTR1, and mono-expressing hSSTR5, hSSTR1 and the receptor chimeras. The effective FRET efficiency (E) was calculated in terms of a percent based upon the photobleaching (pb) time constants of the donor taken in the absence (D – A) and presence (D + A) of acceptor according to $E = 1 - (\tau_{D-A}/ \tau_{D+A}) X 100$. CHO-K1 cells expressing HA-hSSTR5 and hSSTR1 were grown on glass coverslips for 24 hrs, treated with different concentrations of agonist for 15 min at 37°C and fixed with 4% paraformaldehyde for 20 min on ice and processed for immunocytochemistry. Antibodies used were mouse monoclonal anti-HA antibody conjugated to Rhodamine directed to HA-hSSTR5 and rabbit primary antibody followed by secondary anti-rabbit IgG antibody conjugated to fluorescein directed to hSSTR1. PbFRET in CHO-K1 cells expressing hSSTR1, hSSTR5 and the chimera receptors was performed using fluorescently labelled SST ligands. Cells were grown on coverslips as mentioned above, treated with either 20 nM of SST-FITC or 20 nM of SST-FITC and 20 nM SST-TR. Both reactions, either antibody or ligand resulted in specific staining at the plasma membrane. The plasma membrane region was used to analyze the photobleaching decay on a pixel-by-pixel basis as described earlier [Patel et al., 2002b; Rocheville et al., 2000b].

Co-Immunoprecipitation and Western Blot

Membranes from HA-hSSTR1, HA-SSTR5 and HA-hSSTR1/c-myc-hSSTR5 stably transfected in HEK-293 cells were prepared using a glass homogenizer in 20 mM Tris-HCl, 2.5 mM Dithiothreitol (DTT), pH 7.5 as previously described [Rocheville et al., 2000b]. The membrane pellet was washed and resuspended in 20 mM Tris-HCl, pH 7.5 in the absence DTT. Membrane protein (300 μg) was treated with SST-14 (0 and 10^{-6} M) in binding buffer (50 mM Hepes, 2 mM $CaCl_2$, 5 mM $MgCl_2$, pH 7.5) for 30 min at 37 °C. Following treatment membrane protein was solubilized in 1 ml RIPA buffer (150 mM NaCl, 50 mM Tris-HCL, 1% NP-40, 0.1% SDS, 0.5% sodium deoxycholate, pH 8.0) for 1 hour at 4 °C. Samples were centrifuged and lysate was collected and incubated with 1 μg of anti-HA antibody overnight at 4 °C. Antibody was immunoprecipitated with 20 μl of Protein A/G-agarose beads for 2 hours at 4 °C. Beads were then washed three times in RIPA buffer before being solubilized in Laemmli sample buffer containing 62.5 mM Tris-HCl (pH 6.8), 25% glycerol, 2% SDS, 0.01% Bromophenol Blue and 710 mM 2-mercaptoethanol (Bio Rad, Hercules, CA). The sample was heated at 85°C for 5 min before being fractionated by electrophoresis on a 7% SDS polyacrylamide gel. The fractionated proteins were transferred by electrophoresis to a 0.2 μm nitrocellulose membrane (Trans-Blot Transfer Medium, Bio-Rad) in transfer buffer consisting of 25 mM Tris, 192 mM glycine and 20% methanol. Membrane was blotted with anti-HA antibody (dilution 1:5000) for detection of HA-hSSTR1 and HA-hSSTR5 from single expressions, and anti-c-myc antibody (1:5000) for detection of c-myc-hSSTR5 from co-expressions. Blocking of membrane, incubation of primary antibodies, incubation of secondary antibodies and detection by chemiluminescence were performed following WesternBreeze® (Invitrogen Life Technologies) according to manufacturer's instructions. Images were captured using an Alpha Innotech FluorChem 8800 (Alpha Innotech Co., San Leandro, CA) gel box imager and densitometry was carried out using FluorChem software (Alpha Innotech Co.).

RESULTS

Ligand-Dependent Heterodimerization of hSSTR1 and hSSTR5 by pbFRET

To study the heterodimerization of hSSTRs, we stably-expressed hSSTR5 with an N-terminal HA tag and wild-type hSSTR1 in CHO-K1 cells (B_{max} 395 ±12 fmol/mg of protein; K_D 2.3 ±0.1 nM). Cells were treated with various concentrations of the agonists: SST-14, SST-28 – endogenous agonists for both the receptors, SCH-275 (subtype-agonist for hSSTR1) and SMS 201-995 (subtype-agonist for hSSTR5) for 15min. Treatment was terminated by putting the cells on ice, washing once with PBS followed by fixing in 4% paraformaldehyde for 20 min. To determine the physical association between the two receptors, we performed pbFRET microscopy on the cells by using a primary antibody followed by a secondary antibody conjugated with fluorescein (donor) to hSSTR1 and an anti-HA monoclonal antibody conjugated with rhodamine (acceptor) to hSSTR5. A panel of images depicting the co-expression of both receptor-subtypes within the same cell is shown in figure 4A.1. The decrease in donor fluorescence intensity due to photobleaching during prolonged exposure to excitation light was monitored in the absence and presence of acceptor fluorophore. Delays in the photobleaching decay of the donor in the presence of the acceptor related to an increase in FRET efficiency. Because FRET occurs at distances between 10-100 Å, it is a direct measure of protein-protein interaction. By taking a series of digital photographs, we analyzed the photobleaching decay of the donor on the surface of cell membranes on a pixel-by-pixel basis (Figs. 4A.1B and C). Cells were treated with different concentrations of four agonists which displayed differences in their ability to induce heterodimerization. As shown in figure 4A.2, in absence of agonist, a low relative FRET efficiency (<3%) was present in each condition. Treatment of SST-14 resulted in a concentration-dependent increase in heterodimer formation as indicated by increases in FRET efficiency. A maximum of 13.0 ±1.1% at 10^{-6} M was achieved possibly suggesting a saturation in the response (EC_{50} of 3.4 ±2.1 nM) (Fig. 4A.2A). A similar phenomenon was observed for SST-28, which also induced a concentration-dependent increase in FRET efficiency however with greater

efficacy (EC_{50} 0.14 ±0.04 nM) (Fig. 4A.2B). This may indicate that SST-28 is a more potent agonist at inducing heterodimerization than is SST-14. The hSSTR5 subtype-agonist SMS 201-995, although capable of promoting heterodimerization, did so at much higher concentrations as determined by its EC_{50} value (EC_{50} 119 ±16 nM) (Fig. 4A.2C). One possible explanation for this event could be that SMS 201-995 favors the formation of hSSTR5 homodimers than heterodimers, however, further studies are required. In contrast, treatment with the hSSTR1 subtype-agonist SCH-275, did not result in significant increases in FRET efficiency (Fig. 4A.2D). These results demonstrate that hSSTR1 is unable to promote heterodimerization. To further illustrate the active contribution of hSSTR5 in heterodimerization, we performed Western blot and co-immunoprecipitation on membranes prepared from cells either individually or co-expressing the two receptors.

Western blot on ligand-activated hSSTRs

To verify the receptor subtype actively involved in the heteromeric assembly of hSSTR1 and hSSTR5, we performed co-immunoprecipitation and Western blot on membranes from HEK-293 cells mono- and co-expressing the two receptors. In the absence of SST-14, hSSTR5 was found mainly as a monomer (~55 kDa) (Fig. 4A.3). Treatment with SST-14 resulted in the formation of dimers (~110 kDa) including higher order oligomers (Fig. 4A.3). A similar phenomenon was reported for hSSTR5 transfected in CHO-K1 cells, whereby agonist induced the dimerization of the receptor [Rocheville et al., 2000b]. Unlike hSSTR5, hSSTR1 did not form dimers in response to agonist nor was it self-associated under basal conditions (Fig 4A.3). This is in agreement with a previous report on hSSTR1 showing that it remained monomeric even in the presence of agonist in live cells using FCS [Patel et al., 2002a]. Co-immunoprecipitation of membranes expressing both receptor subtypes resulted in the detection of a weak band in the absence of agonist, however, upon agonist stimulation a strong signal was detected (~115 kDa) indicating heterodimeric interaction (Fig. 4A.3). Taken together these results and those

obtained by pbFRET (Fig. 4A.2), suggest that hSSTR1 is not actively involved in heterodimeric assembly.

Membrane Binding Analysis of the hSSTR1 and hSSTR5 Heterodimer

To determine whether heterodimerization altered the binding properties of the receptors, we compared the binding constants for each agonist. Membranes were collected from CHO-K1 cells stably expressing hSSTR1, hSSTR5 and from cells co-expressing the two receptors. Saturation analysis with the radioligand ^{125}I-LTT-SST-28 gave a B_{max} of 415 ±14 fmol/mg of protein and a K_D of 0.49 ±0.08 nM from membranes of the co-transfectants and B_{max} and K_D values of 284 ±5 fmol/mg, 1.4 ±0.05 nM and 231 ±25 fmol/mg, 1.1 ±0.15 nM for membranes transfected with hSSTR5 and hSSTR1 respectively. Binding constants represented as K_i values for each of the four agonists from each receptor species are shown in Table 4A.1. Heteromeric assembly of hSSTR1/hSSTR5 did not result in changes in the K_i values for SST-14 as determined by the lack of statistical significance when compared to the individual receptors. Although the K_i value for SST-28 was lower for the heterodimer than for the individual receptors, indicating a higher affinity, the difference was approximately two fold in comparison to hSSTR5 and four fold to hSSTR1. For the subtype-specific agonists SMS 201-995 and SCH-275, K_i values were slightly higher for the heterodimer than for the individual hSSTRs. Based on our results heterodimerization did not markedly alter the binding properties of the receptors.

Signalling of the Heterodimer

To determine the signalling properties of the heterodimer we measured cAMP accumulation. HSSTRs are well known to inhibit cAMP production through $G\alpha_{i/o}$ coupling [Patel, 1999], we monitored the dose-dependent effect of all four agonists on the inhibition of forskolin-stimulated cAMP production in CHO-K1 cells mono or co-expressing hSSTR1 and hSSTR5. Cells were treated with each of the four agonists with

the indicated concentrations in the presence of forskolin (20 μM) and measured for cAMP. Treatment of cells with SST-14 or SST-28 co-expressing hSSTR1/hSSTR5 resulted in greater signalling efficiencies when compared to treatment of cells expressing either receptor separately (Figs. 4A.4A and B; Table 4A.2). The signalling efficiency of SMS 201-995 in cells expressing hSSTR5 was greatly enhanced upon hSSTR1 co-expression (Fig. 4A.4C). It has been previously reported that SMS 201-995 poorly stimulates hSSTR5 when expressed in CHO-K1 cells contrary to its relatively high binding affinity to the receptor [O'Carroll et al., 1994]. To verify that our results were not dependent on the cell type, we stably-expressed hSSTR5 in HEK-293 cells and performed the same signalling experiments using SMS 201-995. The results were similar to those obtained in CHO-K1 cells therefore indicating that this property was independent of cell type (data not shown). Treatment with the subtype-specific agonist SCH-275 did not demonstrate changes in signalling efficiency for hSSTR1 expressed alone or when co-expressed with hSSTR5 (Fig. 4A.4D).

To determine if heterodimerization resulted in a synergistic effect on adenylyl cyclase coupling efficacy, we compared the total inhibition of forskolin-stimulated cAMP production achieved by saturating concentrations of ligand from both the mono- and coexpressing cell lines. The maximum inhibition achieved in cells expressing hSSTR5 was approximately 85% as determined by treatment with SST-14 and SST-28 (endogenous ligands) using 1 μM concentrations (Figs. 4A.5A and B). The subtype agonist SMS 201-995 did not reach this receptor maximum at 1 μM concentrations (Fig. 4A.5C) despite receptor saturation. The total inhibition reached by cells expressing hSSTR1 was approximately 25%, in agreement with what has been previously reported (Fig. 4A.5D) [Hukovic et al., 1999]. When both receptors were co-expressed the total inhibition achieved was approximately 50% for the agonists SST-14, SST-28 and SMS 201-995 but was unchanged upon treatment with SCH-275 (~25%). These results correlate with our pbFRET and Western blot data indicating that stimulation of hSSTR1 specifically was not sufficient to promote heterodimerization and therefore did not result in changes in signalling. Although the maximum inhibition achievable was lower for the heterodimer, the efficiency for inducing maximum stimulation was higher for agonists

capable of inducing heterodimerization (Fig. 4A.4). This indicates that heterodimerization may not always result in a synergistic effect on coupling efficiency contrary to what we have previously reported for the dopamine receptor 2 and hSSTR5 heterodimer [Rocheville et al., 2000a]. This does not rule out other possible efficacies that may be altered such as MAP kinase activation.

Homo-dimerization of hSSTR1, hSSTR5, hSSTR5-c-tail-R1 and hSSTR1-c-tail-R5 Using Labelled Ligands

To determine the possible molecular determinants involved in the heterodimerization of hSSTR1 and hSSTR5, we compared the pbFRET results using labelled ligands in CHO-K1 cells individually expressing hSSTR1, hSSTR5 and two chimeric receptors: hSSTR5 possessing the c-tail of hSSTR1 (R5CR1) and hSSTR1 possessing the c-tail of hSSTR5 (R1CR5). The R5CR1 chimera was created by replacing c-tail residues 319-363 and swapping them with residues 332-391 of the hSSTR1 c-tail. Similarly, R1CR5 was created by exchanging the same residues. The chimeric receptors were correctly targeted to the plasma membrane as determined by saturation binding analysis and forskolin-stimulated cAMP inhibition analysis [Hukovic et al., 1999]. As previously reported, replacement of the hSSTR5 c-tail with the c-tail of hSSTR1 completely abolishes agonist-mediated internalization [Hukovic et al., 1999]. The R5CR1 chimera mimicked the properties of hSSTR1, suggesting the presence of negative internalization signals in the c-tail of hSSTR1 sufficient to block the internalization of hSSTR5. Similarly, replacement of the hSSTR1 c-tail with that of hSSTR5 not only mimicked that signalling properties of hSSTR5 but also its internalization characteristics [Hukovic et al., 1999]. We have previously reported that hSSTR1 does not undergo homo-dimerization contrary to hSSTR5 which is fully capable of dimerizing [Patel et al., 2002a; Rocheville et al., 2000b]. Therefore, using the chimeric receptors, R5CR1 and R1CR5, we proceeded to determine whether these receptors reflected their wild-type counterparts in undergoing homodimerization. Labelled ligands were generated by conjugation of Fluorescien Isothiocyanate to SST-14-D-Trp8 as the donor, and Texas Red

– succinamidyl ester to SST-14 as the acceptor. In this fashion, the labelled conjugates gave comparable binding affinities, similar to unconjugated SST-14, to be used together in our pbFRET studies (data not shown). CHO-K1 cells stably expressing any of the four receptors were grown on coverslips and then incubated with either the donor ligand alone or the donor ligand with the acceptor ligand, each at a concentration of 20 nM. As shown in figure 4A.6, the FRET efficiencies of hSSTR1 and R5CR1 were comparable suggesting the absence of homodimerization, contrary to the FRET efficiencies obtained for hSSTR5 and R1CR5 (21.5 ±1.7% and 14.9 ±2.8%) indicating homodimer formation. Taken together, these results suggest that the c-tail of hSSTR1 responsible for the inhibition of internalization and upregulation may be also responsible for its inability to homodimerize.

DISCUSSION

There have been several reports documenting GPCR heterodimerization but the mechanism underlying such an event remains largely unknown [Agnati et al., 2003; Angers et al., 2002]. To our knowledge this is the first time that heterodimerization has been shown to be modulated by subtype specific agonists and more specifically through the occupancy of one receptor subtype over another. Using pbFRET microscopy, we were able to demonstrate that both the agonists, SST-14 and SST-28, endogenous ligands for both receptor subtypes, induced a dose-dependent increase in FRET efficiency. These agonists were able to efficiently induce heterodimerization at values corresponding to their binding constants. Co-immunoprecipitation and Western blot also demonstrated increases in heterodimeric interaction when agonist was present. However, this was not the case when specific activation of the individual receptor subtypes was involved. Selective activation of hSSTR1 by SCH-275 did not result in changes in FRET efficiency nor did it present as a dimer or higher order oligomer on immunoblots, an indication that hSSTR1 by itself is monomeric and unable to induce heterodimerizaton. In contrast, selective activation of hSSTR5 resulted in increases in FRET efficiency and therefore could be the active subtype involved in this heterodimeric assembly. Immunoblots of hSSTR5 demonstrated it as being monomeric in basal conditions but displayed profound changes in receptor stoichiometry ranging from receptor dimers to higher order oligomers upon agonist activation. However, for both SST-14 and SST-28, the ligand-induced FRET based efficiency was several fold higher (3.4 ±2.1 nM and 0.14 ±0.04 nM respectively) when compared to SMS 201-995 (119 ±16 nM). This difference could be the result of activation of both receptor subtypes simultaneously that allow conformational changes to better stabilize the heterodimer. Another possibility could be that stimulation of hSSTR5 alone could preferentially form homodimers at lower concentrations of agonist followed by heterodimer formation at higher concentrations. In our previous study using live cells expressing hSSTR1 and hSSTR5 at least three populations of receptors may exist upon stimulation with SST-14; hSSTR1 monomers, hSSTR5 homodimers and hSSTR1/hSSTR5 heterodimers [Patel et al., 2002a]. It would

be interesting if indeed stimulation of hSSTR5 alone preferentially stabilizes homodimers, then one could develop ways of tailoring such processes. A similar scenario has been described for the chemokine receptors CCR2 and CCR5 [Mellado et al., 2001b]. In cells coexpressing the two receptors, selective activation of either receptor alone resulted in homodimerization whereas co-administration of agonist for both receptors induced heterodimerization.

Binding constants for all four agonists for the heterodimer in comparison to the individual receptors did not reveal any marked differences. There was however a small but significant rightward shift in the binding curve for SMS 201-995 towards the heterodimer, indicating a decrease in binding affinity but was less apparent for SCH-275. Finally, the endogenous ligands SST-14 and SST-28 bound to all three receptor combinations (hSSTR1, hSSTR5 and hSSTR1/hSSTR5) with similar affinities. These results indicate that interacting receptor pairs may not always have a profound effect on ligand-binding sites.

Heterodimerization was however, reflected by changes in receptor signalling (Figs. 4A.4 and 4A.5). The maximum coupling efficacy determined by inhibition of forskolin-stimulated cAMP production was approximately 50% for the heterodimer as determined by the agonists SST-14 and SST-28. These results cannot be accounted for by the additive stimulation of both receptor subtypes separately because the maximum stimulation of hSSTR5 and hSSTR1 alone was approximately 80% and 25% respectively. In this context, only SMS 201-995 but not SCH-275 was able to attain this maximum inhibition in cotransfected cells, possibly indicating that SCH-275 was unable to induce heterodimerization. By monitoring coupling efficiency, we determined whether EC_{50} values also contributed to these changes in signalling. Using the subtype-specific agonist for hSSTR1, we were unable to observe alterations in the signalling profiles for hSSTR1 expressed alone or when coexpressed with hSSTR5. In contrast, activation of hSSTR5 by SMS 201-995 resulted in a robust increase in coupling efficiency when both hSSTR5 and hSSTR1 were coexpressed. This property correlated in part with the ability of SMS 201-995 to induce heterodimerization. The alteration in maximum coupling efficacy associated with heterodimerization may have functional implications. One possible

consequence may be associated with the poor response of human prolactinomas to SMS 201-995 treatment. Human prolactinomas are pituitary adenomas that hyper secrete prolactin and predominantly express hSSTR1 and hSSTR5 [Jaquet et al., 1999; Shimon et al., 1997b]. In cultured studies of human excised prolactinomas, tumours that displayed increased expression of hSSTR1 fared poorly to treatment with SMS 201-995 in controlling prolactin release compared to those expressing lower levels of hSSTR1 regardless of hSSTR5 expression [Jaquet et al., 1999]. However, a direct association between heterodimerization and treatment outcome in prolactinomas would be necessary to validate such claims.

HSSTR1 is the only member of the human SSTR family that does not internalize but up-regulates at the cell surface in response to prolonged agonist exposure [Hukovic et al., 1999]. Knowing that the c-tail of hSSTR1 is responsible for its ability to upregulate at the cell surface, we proceeded to determine whether it also mediates its monomeric state. Using receptor c-tail chimeras, whereby the c-tails of both receptors were interchanged, we attempted to characterize a putative interface involved in somatostatin receptor dimerization. Replacement of the c-tail for hSSTR5 with that of hSSTR1 was enough to antagonize homodimerization of hSSTR5. Moreover, when the c-tail of hSSTR5 was in place of the c-tail for hSSTR1, hSSTR1 was capable of forming homodimers. Surprisingly, the molecular determinant responsible for the upregulation of hSSTR1 was also responsible for preventing its homodimerization. Unlike hSSTR1, hSSTR5 does internalize and homodimerize when in the presence of agonist, yet these properties were both inhibited when the c-tail of hSSTR1 was added. It is not the first time that the c-tail has been suggested to be implicated in the heterodimerization of GPCRs. The $GABA_B$ receptor is a heterodimer composed of the subtypes $GABA_BR1$ and $GABA_BR2$ [Jones et al., 1998; Kaupmann et al., 1998; White et al., 1998]. Initial attempts in its cloning have shown that heterologous expression of the individual receptor subtypes were found essentially either retained in the ER ($GABA_BR1$) or expressed at the cell surface but functionally inactive ($GABA_BR2$). When both receptors were co-expressed, a retention sequence found in the c-tail of $GABA_BR1$ was masked through c-tail interaction with $GABA_BR2$. This allowed for proper trafficking and functioning of

the $GABA_B$ receptor. Similarly, the c-tail of the δ-opioid receptor was found necessary for dimerization and when perturbed through c-tail deletion internalization was impaired [Cvejic and Devi, 1997]. However, this does not rule out other possible domains that may also be contributing to dimerization such as the transmembrane region [Hebert et al., 1996; Overton et al., 2003; Pagano et al., 2001].

Although a general mechanism such as preformed or ligand induced dimer formation does not seem to be exclusively valid, our study highlights the importance of ligands, especially receptor specific ligands, in dimer formation. It is noteworthy that hSSTR1 homodimers cannot be formed, yet ligand bound hSSTR5 forms heterodimers with hSSTR1. Indeed, the ligand bound hSSTR1/hSSTR5 heterodimer is more stable as demonstrated by pbFRET and signaling efficiencies of SST-14 and SST-28 suggesting a preferred conformational state resulting from ligand binding. These findings are consistent with earlier results with dopamine 2/hSSTR5 [Rocheville et al., 2000a] and hSSTR1/hSSTR5 [Patel et al., 2002a] heterodimers in which a dimer containing one or two ligands could be established.

In conclusion, we have demonstrated that activation of hSSTR5 but not hSSTR1 was capable of promoting hSSTR1/hSSTR5 heterodimerization. These results also demonstrate that agonist-mediated heterodimerization may occur through ligand occupancy of only one receptor subtype. Furthermore, this process resulted in changes in maximum coupling efficacy and coupling efficiency with little changes in ligand binding. We have also demonstrated that the c-tail of hSSTR1 was responsible for preventing dimerization. However, further studies are required to define any specific residues or motifs that may account for this inhibition of interaction. Our data provide direct biophysical and functional evidence that heterodimerization is a receptor and ligand specific process. We recognize the importance of the c-tail in receptor internalization, G-protein coupling, and dimer formation. A detailed understanding of the significance on the inter relationship(s) among these events are lacking and need to be elucidated.

ACKNOWLEDGEMENTS

This work was supported by Canadian Institute of Health Research (CIHR) grants MT-10411 and MT-6911. We thank M. Correia for her secretarial help and H. Alturaihi and A. Abdallah for their technical assistance. This article has been dedicated to Dr. Yogesh C. Patel.

FIGURE LEGENDS

Figure 4A.1.

Confocal microscope images and a representative histogram time constant plot from pbFRET microscopy from CHO-K1 cells stably expressing HA-hSSTR5 and hSSTR1.

A, confocal photomicrographs illustrating the colocalization of hSSTR1 and HA-SSTR5 in CHO-K1 cells. Cells were incubated with primary rabbit polyclonal anti-hSSTR1 followed by secondary anti-rabbit fluorescein-conjugated antibody shown in green, anti-HA rhodamine-conjugated monoclonal antibody to HA-hSSTR5 shown in red and colocalization of the two images shown in yellow (scale bar 25 μm). ***B***, photobleaching of fluoroscein (donor) in the absence of rhodamine (acceptor), top panel. In this representation, cells were treated with 1 μM of SST14, fixed and followed by donor photobleaching with 488 nm light. A sequence of 20 images was captured, of which only a selected few are shown here. A histogram time constant plot was calculated based on a pixel-by-pixel basis of a selected area on the cell surface. The mean time constant of 21.9 ±0.3s is shown as a black bar taken by averaging the time constants from a Gaussian distribution. ***C***, in this representation, cells treated with 1 μM of SST14 were photobleached in the presence of the acceptor molecule. The top panel shows the visual delay in photobleaching of the donor and below is the histogram time constant bar plot displaying an increase in the mean time constant (25.1 ±0.4 s).

A

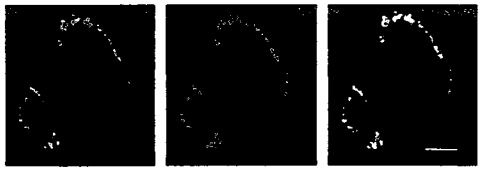
hSSTR1
hSSTR5
Overlay

B


0s
8s
32s
64s
76s

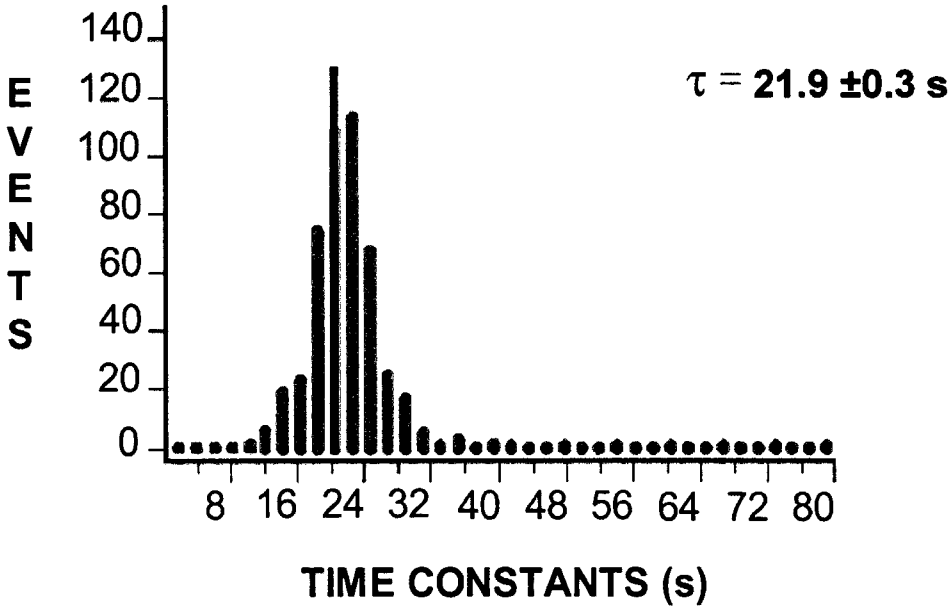
EVENTS
140
120
100
80
60
40
20
0
8 16 24 32 40 48 56 64 72 80
τ = 21.9 ±0.3 s
TIME CONSTANTS (s)

C


0s
8s
32s
64s
76s

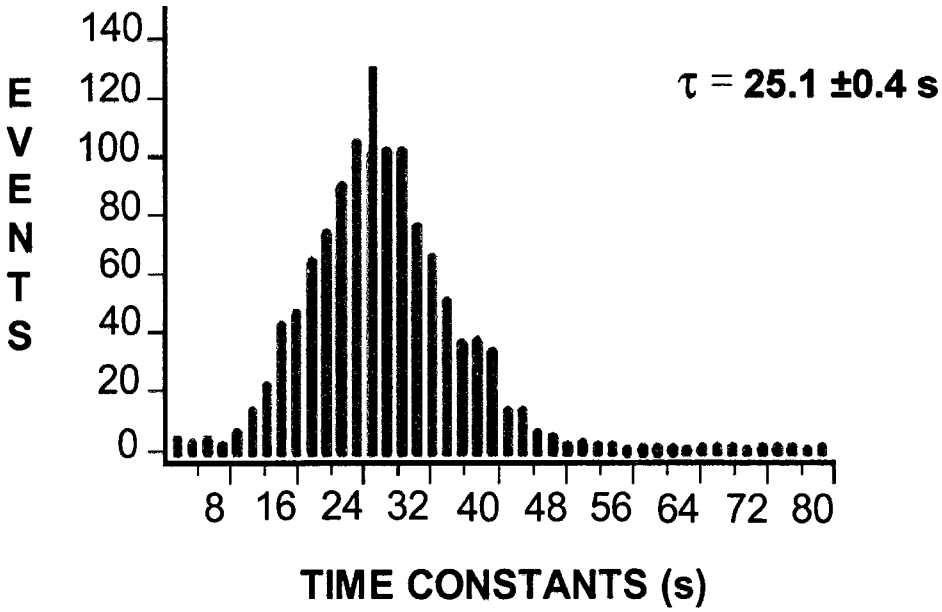
EVENTS
140
120
100
80
60
40
20
0
8 16 24 32 40 48 56 64 72 80
τ = 25.1 ±0.4 s
TIME CONSTANTS (s)

Figure 1

Figure 4A.2.

Concentration-dependent increase in effective FRET efficiencies from CHO-K1 cells stably expressing HA-hSSTR5 and hSSTR1 by different agonists.

Cells were treated with the indicated concentrations of each agonist and analyzed by pbFRET microscopy. The calculated FRET efficiencies (%) and EC_{50} values for each agonist (***A)*** SST-14 (3.4 ± 2.1 nM), (***B)*** SST-28 (0.14 ± 0.04 nM), (***C)*** SMS 201-995 (119 ± 16 nM) were plotted and analyzed by a sigmoidal dose-response equation using Graph Pad Prism 3.0. ***D,*** treatment with SCH-275 did not result in a significant increase in FRET efficiency. Data were analyzed by ANOVA, posthoc Dunnett's and compared with basal conditions without treatment. Means ± SEMs are representative of three independent experiments performed in triplicate; * $p<0.05$, ** $p<0.01$.

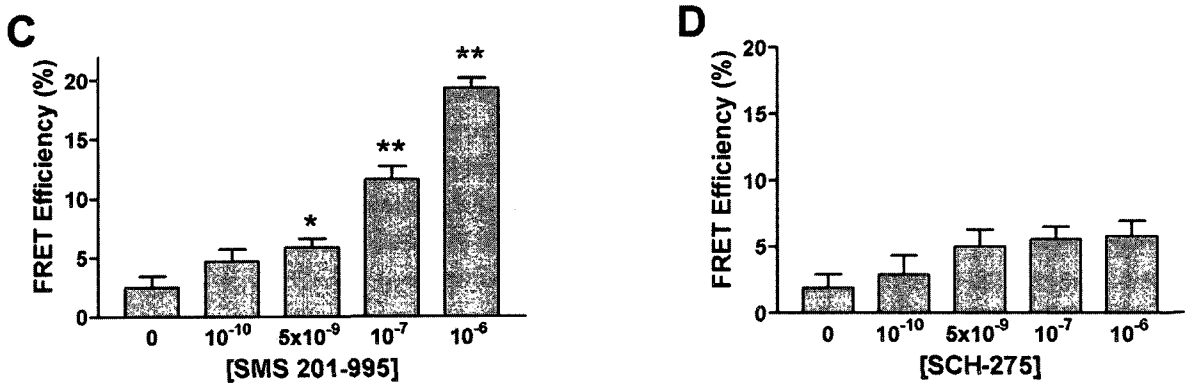
C
FRET Efficiency (%)
0
5
10
15
20
*
**
**
0
10-10
5x10-9
10-7
10-6
[SMS 201-995]
D
FRET Efficiency (%)
0
5
10
15
20
0
10-10
5x10-9
10-7
10-6
[SCH-275]

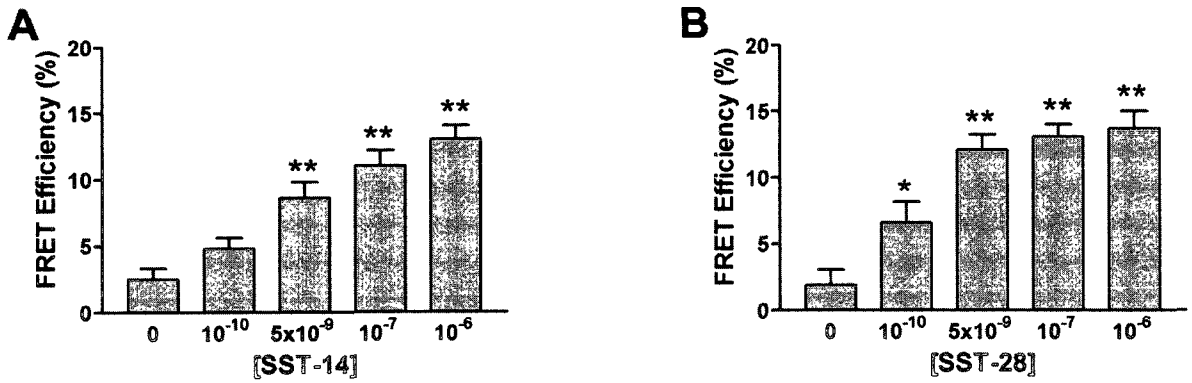
A
FRET Efficiency (%)
20
15
10
5
0
**
**
**
0
10-10
5x10-9
10-7
10-6
[SST-14]
B
FRET Efficiency (%)
20
15
10
5
0
*
**
**
**
0
10-10
5x10-9
10-7
10-6
[SST-28]

Figure 4A.3.

Western blot and co-immunoprecipitation of HEK-293 cells stably expressing HA-hSSTR1, HA-hSSTR5 and co-expressing HA-hSSTR1 and c-myc-hSSTR5.

A, membranes from HEK-293 cells stably expressing HA epitope-tagged hSSTR5 were treated with or without 1 μM SST-14 for 30 min before being separated on a SDS-polyacrylamide gel. HSSTR5 can be seen mainly as a monomer (~55 kDa) but upon treatment with agonist self-associates into dimers (~110 kDa) and higher order oligomers. ***B***, immunoblot of membranes expressing HA epitope-tagged hSSTR1 in the absence or presence of 1 μM SST-14 appearing at ~58 kDa. ***C***, membranes co-expressing HA-hSSTR1 and c-myc-hSSTR5 were incubated with or without SST-14 (1 μM) for 30 min, solubilized and immunoprecipitated with anti-HA antibody against hSSTR1. Immunoblotting was performed with anti-c-myc antibody for detection of hSSTR5. Note the formation of heterodimers upon agonist treatment. Immunoblots are representations of three independent experiments.

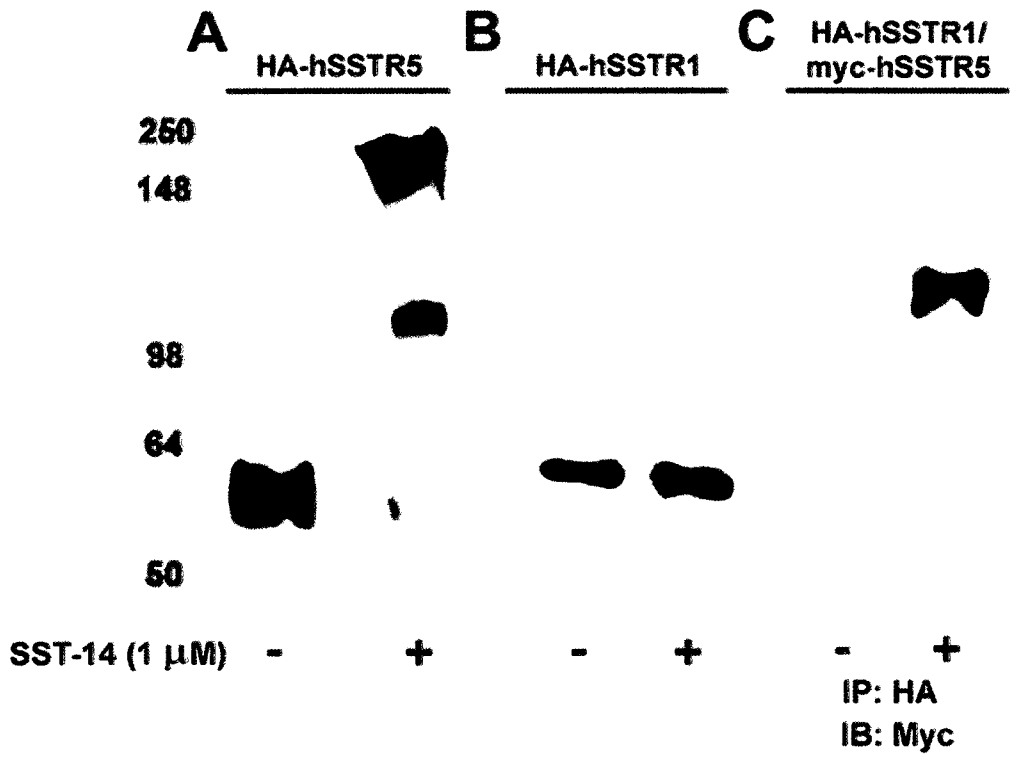
A
HA-hSSTR5
B
HA-hSSTR1
C
HA-hSSTR1/
myc-hSSTR5
250
148
98
64
50
SST-14 (1 μM) - + - + - +
IP: HA
IB: Myc

Figure 4A.4.

Adenylyl cyclase coupling efficiency of the hSSTR1/hSSTR5 heterodimer.

CHO-K1 cells monotransfected with hSSTR1 (▼) and hSSTR5 (■) or cotransfected with both receptors (●) were treated with forskolin (20 μM) alone or in combination with the indicated concentrations of the agonists (***A***) SST-14, (***B***) SST28, (***C***) SMS 201-995 and (***D***) SCH275 for 30 min. Treatment of cells with forskolin alone was taken as 0% inhibition and treatment of forskolin with 1 μM concentrations of agonist was taken as 100% inhibition. The data represent means ± SEM from three independent experiments performed in triplicate.

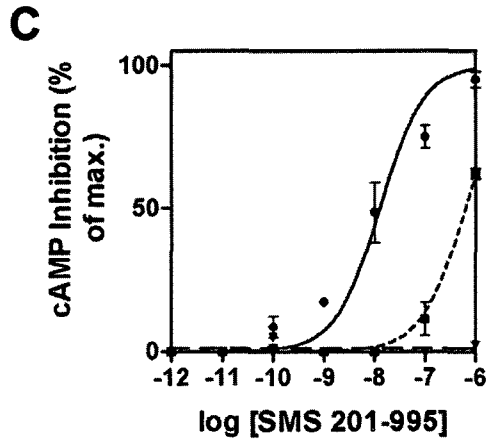
C
cAMP Inhibition (% of max.)
100
50
0
-12 -11 -10 -9 -8 -7 -6
log [SMS 201-995]

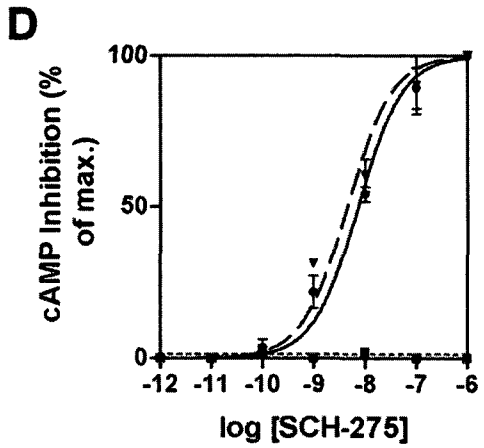
D
cAMP Inhibition (% of max.)
100
50
0
-12 -11 -10 -9 -8 -7 -6
log [SCH-275]

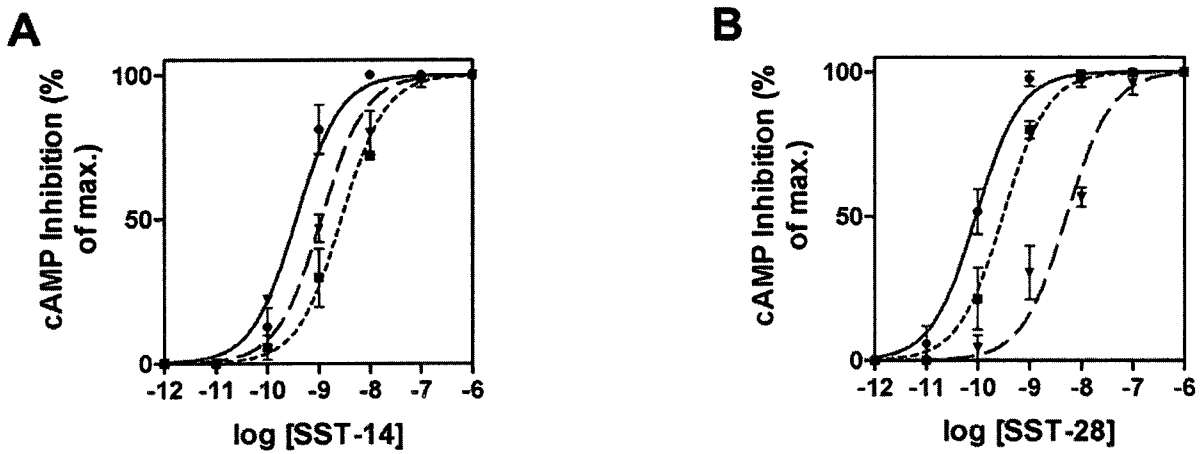
A
cAMP Inhibition (% of max.)
100
50
0
-12 -11 -10 -9 -8 -7 -6
log [SST-14]
B
cAMP Inhibition (% of max.)
100
50
0
-12 -11 -10 -9 -8 -7 -6
log [SST-28]

Figure 4A.5.

Total inhibition of forskolin-stimulated cAMP production.

Maximum coupling efficacy was calculated by treating cells with concentrations of 1 μM of each agonist (***A)*** SST-14, (***B)*** SST-28, (***C)*** SMS 201-995 and (***D)*** SCH-275 in the presence of forskolin for 30 min and compared to cells stimulated with forskolin alone. Treatment of cells monotransfected with hSSTR1 and hSSTR5 were compared statistically to cotransfectants. Statistical significance was determined by ANOVA, posthoc Dunnetts, whereby control was taken as forskolin stimulation alone. There were no statistical differences resulting from treatment with SCH275. Means ± SEMs represent three independent experiments. * $p<0.05$, ** $p<0.01$, compared with cotransfectants.

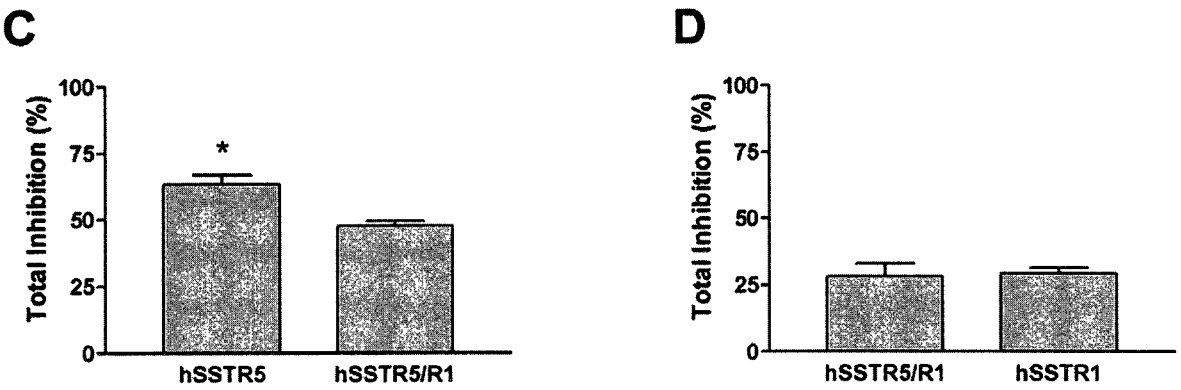
C
Total Inhibition (%)
100
75
50
25
0
*
hSSTR5
hSSTR5/R1
D
Total Inhibition (%)
100
75
50
25
0
hSSTR5/R1
hSSTR1

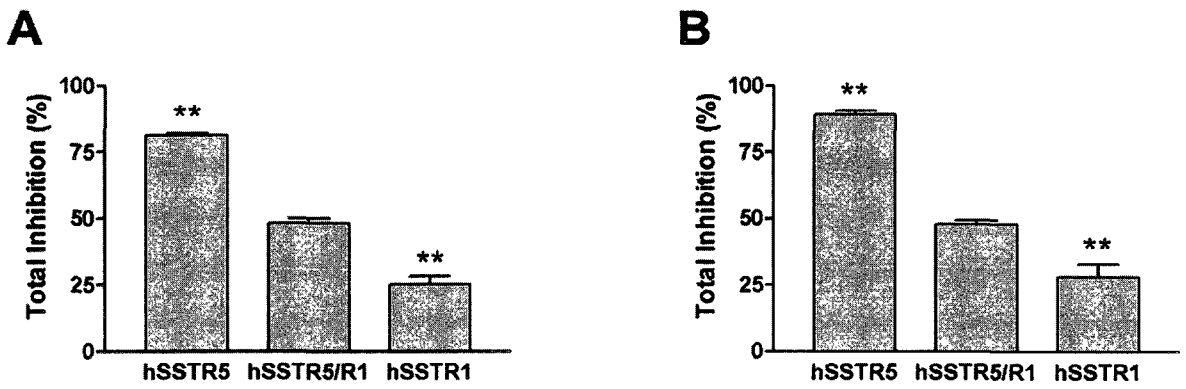
A
Total Inhibition (%)
100
75
50
25
0
**
**
hSSTR5
hSSTR5/R1
hSSTR1
B
Total Inhibition (%)
100
75
50
25
0
**
**
hSSTR5
hSSTR5/R1
hSSTR1

Figure 4A.6.

The characterization of the functional importance of the c-tail in the homodimerization of hSSTR1 and hSSTR5 by pbFRET microscopy.

CHO-K1 cells stably expressing either hSSTR1, hSSTR5, R1CR5 or R5CR1 were treated with 20 nM of SST-FITC (donor) or with 20 nM of SST-FITC and SST-TR (donor + acceptor) and processed for pbFRET microscopy (see text for "Experimental Procedures"). Note the significant changes in FRET efficiencies upon c-tail transposition. Homodimerization of hSSTR1 is promoted through c-tail replacement with hSSTR5.

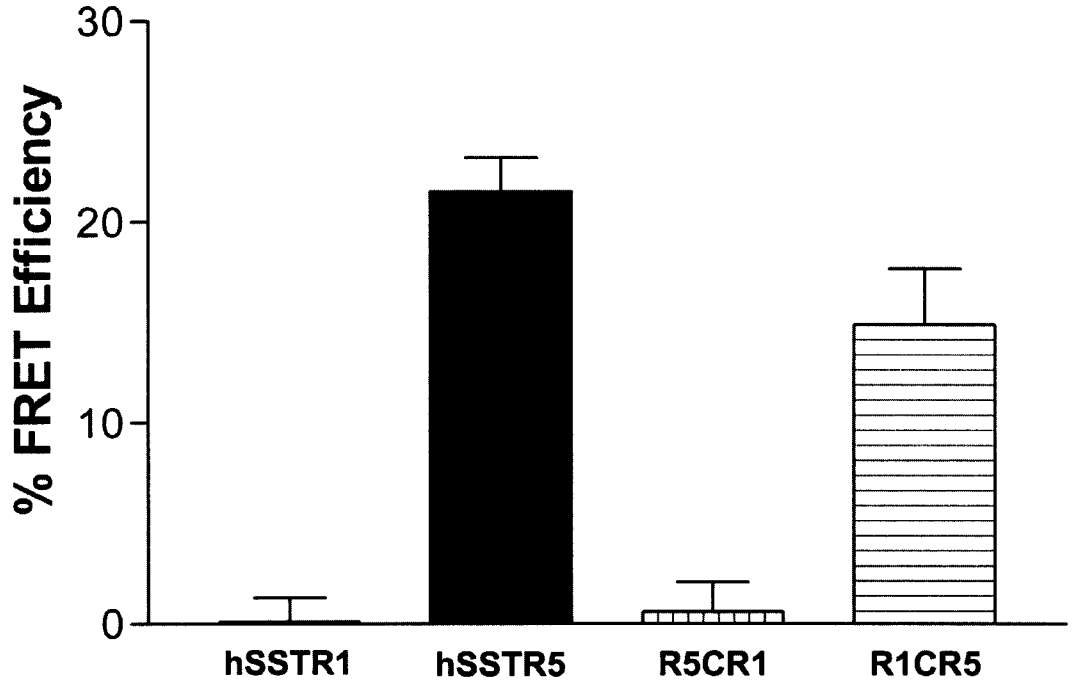
% FRET Efficiency
30
20
10
0
hSSTR1
hSSTR5
R5CR1
R1CR5

Table 4A.1

Comparison of the potencies of SST agonists for binding to membranes expressing hSSTR1, hSSTR5 and hSSTR1/hSSTR5.

Competition analysis on membrane preparations from CHO-K1 cells stably expressing hSSTR1, hSSTR5 and coexpressing the two receptors (hSSTR5/R1). K_i values expressed in nM are the inhibitory concentration required for half-maximal inhibition of ^{125}I-LTT-SST-28 binding. Means ± SEMs represent three independent experiments performed in triplicate.

	Agonists			
Receptors	**SST-14**	**SST-28**	**SMS 201-995**	**SCH-275**
hSSTR1 –	0.20 ± 0.01	2.14 ±0.40	≥1000	4.10 ± 0.56
hSSTR5/R1 –	0.49 ± 0.09	0.50 ± 0.04	45.1 ± 7.4	11.4 ± 0.39
hSSTR5 –	1.25 ± 0.22	0.95 ± 0.11	8.23 ± 0.84	≥1000

Table 4A.2

Comparison of adenylyl cyclase coupling efficiencies by SST agonists.

CHO-K1 cells stably expressing hSSTR1 and hSSTR5 or coexpressing both receptors (hSSTR5/R1) were treated with given concentrations of each agonist in the presence of forskolin and measured for cAMP accumulation. EC_{50} values represented in nM are the half-maximal inhibition of forskolin induced cAMP production. Means ± SEMs represent three independent experiments performed in triplicate.

	Agonists			
Receptors	**SST-14**	**SST-28**	**SMS 201-995**	**SCH-275**
hSSTR1 –	1.21 ± 0.38	5.19 ± 0.23	≥1000	4.93 ± 1.12
hSSTR5/R1 –	0.37 ± 0.05	0.10 ± 0.03	12.8 ± 4.3	7.56 ± 1.50
hSSTR5 –	2.85 ± 1.31	0.32 ± 0.11	643 ± 99	≥1000

B) Ligand binding and receptor-dissociation are implicated in the internalization of hSSTR2

In the previous chapter, the dimerization properties of hSSTR1 and hSSTR5 were described, including the effects of different agonists on regulating their heterodimerization. Our next step was to investigate the dimerization properties of hSSTR2, a receptor-subtype that is frequently expressed in many types of tumours, particularly those of neuroendocrine origin, such as growth hormone-hypersecreting pituitary adenomas. Additionally, it is the primary target of currently available somatostatin analogs. In our investigations, we were surprised to determine that this receptor exists at the plasma membrane as a homodimer in the absence of agonist treatment, a feature unlike the other two receptors that we have studied. Interestingly, hSSTR2 homodimers dissociate into monomers when activated by agonist, a property that when prevented, abrogates agonist-mediated internalization. The dissociation of hSSTR2 dimers is not restricted to human receptors, as a similar observation has recently been reported for porcine SSTR2. These results provide yet another mechanism of protein-protein interaction amongst this family of receptors.

Manuscript: Grant, M., Collier, B. and Kumar, U. (2004) Agonist-dependent dissociation of human somatostatin receptor 2 dimers: a role in receptor trafficking. *J Biol Chem*, **279**, 36179-36183.

Agonist-dependent Dissociation of Human Somatostatin Receptor 2 Dimers: A Role in Receptor Trafficking

Michael Grant[1,2], Brian Collier[2] and Ujendra Kumar[1‡]

[1]Fraser Laboratories For Diabetes Research, Department of Medicine, Royal Victoria Hospital and [2]Department of Pharmacology & Therapeutics, McGill University, Montreal, Quebec, Canada.

Running title: *Dissociation of Somatostatin Receptor Dimers*

‡Address for correspondence: Dr. U. Kumar

Room M3.15, Royal Victoria Hospital

687 Pine Avenue West

Montreal, Quebec H3A 1A1, Canada

Phone: (514) 842-1231 ext. 35042

Fax: (514) 843-2819

E-mail: **ujendra.kumar@muhc.mcgill.ca**

SUMMARY

G-protein coupled receptors (GPCRs) represent the largest and most diverse family of cell surface receptors. Several GPCRs have been documented to dimerize with resulting changes in pharmacology and signaling. We have previously reported by means of photobleaching fluorescence resonance energy transfer (pbFRET) microscopy and fluorescence correlation spectroscopic (FCS) analysis in live cells, that human somatostatin receptor (hSSTR) 5 could both homodimerize, and heterodimerize with hSSTR1 in the presence of the agonist SST-14. By contrast, hSSTR1 remained monomeric when expressed alone regardless of agonist exposure in live cells. However the effect of agonist on other hSSTR members remains unknown. Using pbFRET microscopy and Western blot, we provide evidence for agonist-dependent dissociation of self-associated hSSTR2 stably expressed in CHO-K1 and HEK-293 cells. Furthermore, the dissociation of the hSSTR2 dimer occurred in a concentration-dependent manner. Moreover, blocking receptor dissociation using a cross-linker agent perturbed receptor trafficking. Taken these data together, we suggest that the process of GPCR dimerization may operate differently, even amongst members of the same family, and that receptor dissociation as well as dimerization may be important steps for receptor dynamics.

[2] **The abbreviations used are:**

GPCR(s), G protein coupled receptor(s); hSSTR, human somatostatin receptor; SST, somatostatin; HA, hemagglutinin; CHO, Chinese hamster ovary; HEK, human embryonic kidney cells; pbFRET, photobleaching fluorescence resonance energy transfer; FITC, fluorescein isothiocyanate; Rh, Rhodamine; FCS, fluorescence correlation spectroscopy.

Dimerization and oligomerization are used interchangeably.

INTRODUCTION

G-protein coupled receptors (GPCRs) represent approximately 1% of the human genome, an estimate exceeding 800 genes [Pierce et al., 2002]. The initial notion once stated that GPCRs are present on the membrane as monomeric entities in a 1:1 stoichiometric ratio with their G-protein has been reinterpreted. Several studies have shown using a combination of techniques such as co-immunoprecipitation, bioluminescence resonance energy transfer (BRET) and fluorescence resonance energy transfer (FRET), that at least some GPCRs assemble on the membrane as functional homo- and heterodimers [Agnati et al., 2003; Angers et al., 2002; Bai, 2004]. Dimerization of GPCRs has been shown to affect a multitude of receptor functions including ligand binding, signalling, receptor-desensitization and receptor trafficking [Agnati et al., 2003; Angers et al., 2002; Bai, 2004; Mellado et al., 2001a].

The mechanism by which GPCR dimerization occurs remains obscure and controversial. One model suggests that ligand binding induces a conformational change in the receptor that favours dimer formation. In contrast to this model, the presence of GPCRs which may be assembled as preformed dimers have been shown for members of the class C subfamily, which include the GABAergic receptors [Jones et al., 1998; Kaupmann et al., 1998; White et al., 1998], calcium sensing receptor [Bai et al., 1998; Jensen et al., 2002], the metabotropic glutamate receptor [Romano et al., 1996] and the sweet taste receptors [Li et al., 2002; Nelson et al., 2002; Nelson et al., 2001]. However, this paradigm of GPCR assembly is not consistent amongst the other families of GPCRs [Agnati et al., 2003]. Several reports have shown that agonist plays an active role in GPCR dimerization at the plasma membrane, suggesting equilibrium between GPCR dimers/monomers that can be regulated by ligand occupancy. These receptors include the human somatostatin receptors (hSSTRs) [Patel et al., 2002a; Rocheville et al., 2000b], the dopamine D2 receptor [Wurch et al., 2001], the gonadotrophin-releasing hormone receptor [Cornea et al., 2001; Horvat et al., 2001], the luteinizing hormone/chorionic gonadotrophin hormone receptor [Roess et al., 2000], the bradykinin B_2 receptor [AbdAlla et al., 1999], the thyrotropin-releasing hormone receptor [Kroeger et al., 2001],

the human cholecystokinin receptor (CCKR) [Cheng and Miller, 2001], the human thyrotropin receptor (TSHR) [Latif et al., 2002], the chemokine receptors [Mellado et al., 2001b; Rodriguez-Frade et al., 1999; Vila-Coro et al., 2000; Vila-Coro et al., 1999], the mouse δ-opioid receptor (δ-OR) [Cvejic and Devi, 1997] and the rhesus neuropeptide Y4 receptor (rhY4R) [Berglund et al., 2003].

We have previously reported that hSSTRs are capable of undergoing both homo- and heterodimerization at the cell membrane [Rocheville et al., 2000a; Rocheville et al., 2000b]. Recently, we have demonstrated agonist-dependent homo- and heterodimers on the plasma membrane in live cells using FCS [Patel et al., 2002a]. One of the receptor sub-types, hSSTR1, did not form homodimers in either the absence or presence of agonist in contrast to hSSTR5, which showed robust dimerization upon agonist exposure. When both receptors were co-expressed in the same cell, two populations of dimers were observed, hSSTR5 homodimers and hSSTR1/hSSTR5 heterodimers [Patel et al., 2002a]. The affect of agonist on other members of the hSSTR family is currently unknown.

In the present study using both Western blot and pbFRET analysis, we determined the effect of agonist on hSSTR2 dimerization. We show that agonist induces a dissociation of preassembled hSSTR2 dimers in a concentration-dependent manner. This effect was inhibited when cell membranes were pretreated with a cross-linking agent. hSSTR2 undergoes internalization upon exposure to agonist however; inhibition of dimer dissociation resulted in impaired receptor internalization. Finally, our data provide evidence suggesting that agonist-dependent dissociation of self-associated dimers may be a requirement for proper receptor trafficking.

EXPERIMENTAL PROCEDURES

Materials

The peptides SST-14 and [Leu(8)-D-Trp-22, Tyr-25]-SST-28 (LTT-SST-28) were purchased from Bachem, Torrance, CA. Fluorescein- and rhodamine-conjugated and non-conjugated mouse monoclonal antibodies against hemagglutinin (HA) (12CA5) were purchased from Roche Molecular Biochemicals, Mannheim, Germany. FITC-conjugated goat anti-mouse affinity-purified secondary antibody was purchased from Jackson ImmunoResearch Laboratories, West Grove, PA. The cross-linking agent bis(sulfosuccinimidyl) suberate (BS^3) was purchased from Sigma, St. Louis, MO.

SSTR Constructs and Expressing Cell Lines

Stable CHO-K1 and HEK-293 cells expressing HA-tagged hSSTR2 were prepared by Lipofectamine transfection reagent as previously described [Rocheville et al., 2000b]. Stable transfections were made using the vectors pCDNA3.1/Neo (neomycin resistance), Invitrogen, Carlsbad, CA. Clones from CHO-K1 cells were selected and maintained in medium containing Hams F12 with 10% fetal bovine serum and 700 μg/ml neomycin. Clones from HEK-293 cells were selected in Dulbecco's Modified Eagle Medium containing 10% fetal bovine serum and 700 μg/ml neomycin.

PbFRET Microscopy

PbFRET experiments were performed at the plasma membrane of CHO-K1 cells as previously described [Patel et al., 2002a; Rocheville et al., 2000a; Rocheville et al., 2000b]. In brief, CHO-K1 cells expressing HA-hSSTR2 were treated with different concentrations (0, 10^{-10}, $5x10^{-9}$, 10^{-7} and 10^{-6} M) of agonist for 10 min at 37°C, fixed with 4% paraformaldehyde in PBS for 20 min on ice and processed for immunocytochemistry.

Immunocytochemistry was performed using monoclonal anti-HA antibodies conjugated to FITC and Rhodamine for the donor and acceptor respectively, before being subjected to pbFRET analysis. The effective FRET efficiency (E) was calculated from the average photobleaching time constant of the donor obtained in the absence ($\tau_{ave\ D\text{-}A}$) and presence of the acceptor ($\tau_{ave\ D+A}$) according to $E = 1 - (\tau_{D\text{-}A}/\ \tau_{D+A})$ X 100.

Western Blot Analysis

Membranes from HA-hSSTR2 stably transfected in HEK-293 cells were prepared using a glass homogenizer in 20 mM Tris-HCl, 2.5 mM Dithiothreitol (DTT), pH 7.5 as previously described [Rocheville et al., 2000b]. The membrane pellet was washed and resuspended in 20 mM Tris-HCl, pH 7.5 in the absence DTT. Membrane protein (50 μg) was treated with SST-14 (0, 10^{-10}, 10^{-8} and 10^{-6} M) in binding buffer (50 mM Hepes, 2 mM $CaCl_2$, 5 mM $MgCl_2$, pH 7.5) for 30 min at 37 °C. When the cross-linking agent BS^3 was used, membranes were pretreated with 5 mM BS^3 for 1 hour at 4°C, and this reaction was terminated by the addition of 50 mM Tris-HCl, pH 7.5 for 15 min at 4°C. After treatment with SST-14, membrane protein was solubilized in Laemmli sample buffer containing 62.5 mM Tris-HCl (pH 6.8), 25% glycerol, 2% SDS, 0.01% Bromophenol Blue and 710 mM 2-mercaptoethanol (Bio Rad, Hercules, CA). The sample was heated at 85°C for 5 min before being fractionated by electrophoresis on a 7% SDS polyacrylamide gel. The fractionated proteins were transferred by electrophoresis to a 0.2 μm nitrocellulose membrane (Trans-Blot Transfer Medium, Bio-Rad) in transfer buffer consisting of 25 mM Tris, 192 mM glycine and 20% methanol. Membrane was blotted with anti-HA mouse monoclonal antibody (dilution 1:5000). Blocking of membrane, incubation of primary antibodies, incubation of secondary antibodies and detection by chemiluminescence were performed following WesternBreeze® (Invitrogen Life Technologies) according to manufacturer instructions. Images were captured using an Alpha Innotech FluorChem 8800 (Alpha Innotech Co., San Leandro, CA) gel box imager and densitometry was carried out using FluorChem software (Alpha Innotech Co.).

Internalization by Radioligand and Immunocytochemistry

Receptor internalization was assessed as previously described [Hukovic et al., 1996]. CHO-K1 cells stably expressing HA-hSSTR2 were cultured in 6 well plates to ~90% confluency (~1.5 x 10^6 cells/well). On the day of the experiment, medium was removed and the cells were washed twice with Dulbecco's Phosphate Buffer Salt Solution (D-PBS) and incubated overnight at 4°C in binding buffer (50 mM HEPES, pH 7.5, 2 mM $CaCl_2$, 5 mM $MgCl_2$, 0.5% bovine serum albumin, 0.02% phenylmethylsulfonyl fluoride, and 0.02% bacitracin) with ^{125}I-LTT-SST-28 (200 000 cpm) with or without 1 μM SST-14 to account for non-specific binding. Cells were washed two times in D-PBS and warmed to 37°C for various times (0, 15, 30, 60 min) to initiate internalization. For cross-linking experiments, cells were pretreated with 1 mM BS^3 in D-PBS for 1 hour at 4°C, and this reaction was terminated by washing the cells first with D-PBS followed by the addition of 50 mM Tris-HCl, pH 7.5 for 15 min at 4°C. Surface bound radioligand was removed with 1 ml of acid wash buffer (20 mM Na acetate in 1x Hank's solution, pH 5.0) for 10 min. Internalized radioligand was measured as acid resistant counts taken after removing cells with 1 ml of 1 N NaOH. Radioactive fractions were quantified for radioactivity using a LKB gamma counter (LKB-Wallach, Turku, Finland). Each experiment was performed three times in triplicate.

For internalization by immunocytochemistry CHO-K1 cells stably expressing HA-hSSTR2 were grown on coverslips and treated with SST-14 (1 μM) for 30 min at 37°C. When cross-linker agent was indicated, cells were treated with 1 mM BS^3 for 1 hour at 4°C prior to SST-14 addition. Reaction was terminated with 50 mM Tris-HCl, pH 7.5 for 15 min at 4°C. Cells were washed two times in D-PBS and fixed for 20 min at 4°C with 4% paraformaldehyde. After three subsequent washes in D-PBS cells were incubated in 5% normal goat serum (NGS) in D-PBS for 1 hour followed by incubation with anti-HA monoclonal antibody (1:1000) in 1% NGS overnight at 4°C. Unless indicated, permeablization of cells was performed using 0.2% Triton X100 in D-PBS for 10 min followed by three washes in D-PBS prior to incubation with antibody. Cells were then washed three times in D-PBS followed by incubation with FITC-conjugated goat anti-mouse secondary antibody (1:800) for 1 hour. After two washes in D-PBS cells were

mounted and viewed under a Leica DML microscope attached to a Cool Snap CCD camera.

RESULTS

Ligand-Dependent Dissociation of hSSTR2 Homodimers by pbFRET and Western blot

CHO-K1 cells were stably-expressed with an N-terminal HA-tagged hSSTR2 (B_{max} 435 ±33 fmol/mg of protein; K_D 0.3 ±0.1 nM). Cells were treated with different concentrations of SST-14 and processed for hSSTR2 localization to study pbFRET microscopy. PbFRET microscopy was determined by the photobleaching decay of donor on the cell surface by using monoclonal anti-HA antibodies conjugated with either fluorescein (donor) or rhodamine (acceptor). As shown in figure 3B.1A, in the basal state, the cell surface presented with a high relative FRET efficiency, suggesting the presence of homodimers as compared to SST-14 treated cells. Treatment with SST-14 induced a concentration-dependent decrease in FRET efficiency from a maximum of 11.7 ±1.1% under basal conditions to 2.1 ±0.9% with 1 μM SST-14 (Table 4B.1, Fig. 4B.1A). Our data indicate that unlike the other two hSSTRs, hSSTR1 and hSSTR5, hSSTR2 is self-associated and dissociates upon agonist activation. Since FRET is sensitive to distance, changes in FRET efficiency can be perceived as either dissociation of dimers or changes in receptor conformation. In order to confirm whether ligand activated hSSTR2 is associated with changes in dimer to monomer formation we performed Western blot.

Membranes from HEK-293 cells stably expressing HA-hSSTR2 (B_{max} 2608 ±206 fmol/mg of protein, K_D 0.4 ±0.1 nM), chosen for their higher expression levels, were treated with various concentrations of SST-14 before being processed for Western blot. In the absence of agonist, hSSTR2 was present in both dimeric (120 kDa) and monomeric (60 kDa) forms (Fig. 4B.1B). Treatment of hSSTR2 membrane with SST-14 induced a concentration-dependent decrease in dimer formation (Fig. 4B.1B). Increasing concentrations of SST-14 gradually decreased the ratio of hSSTR2 dimers/monomers (Fig. 4B.1C). Dissociation of the dimeric complex could be prevented when membranes were pretreated with the cross-linking agent BS^3 (Fig. 4B.1D). Western blot in combination with pbFRET analysis support the notion that hSSTR2 is a self-associated

dimer under basal conditions but upon ligand activation preferentially dissociates into monomers. It is unclear as to why there was an appreciable amount of monomeric receptor found by Western blot. One reason could be due to a solubilization artifact, since receptor dimers can be affected by the concentration of detergent used. Another reason could be due to the higher expression levels achieved in HEK-293 cells compared to that in CHO-K1 cells, used in order to perform Western blot. Perhaps the monomeric receptors represent an immature intracellular pool that is only functional when the receptors are in dimeric form present at the cell surface. With the exception of the δ-OR [Cvejic and Devi, 1997], little has been shown to support the functional significance for the dissociation of GPCR dimers. To determine whether dissociation of the dimeric complex is associated with changes in receptor properties, we proceeded to investigate receptor internalization.

Internalization of hSSTR2

CHO-K1 cells stably expressing HA-hSSTR2 were grown on coverslips and treated with 1 μM SST-14 for 30 min with or without prior treatment of BS^3. Since BS^3 is a hydrophilic lipid impermeable cross-linking agent and was shown to inhibit agonist-induced hSSTR2 dissociation (Fig. 4B.1D), only dimeric receptors at the cell surface would be affected upon treatment. Under basal conditions, hSSTR2 was mainly localized at the cell surface with little or no cytoplasmic localization of receptor in permeablized cells (Fig. 4B.2A, left). Treatment with SST-14 (1 μM) resulted in the internalization of hSSTR2 with decreases in cell surface expression (Fig. 4B.2A, middle). Internalization of receptor was appreciably inhibited when cells were treated with cross-linker prior to the exposure of SST-14 (Fig. 4B.2A, right). Thus, we demonstrate that internalization of hSSTR2 can be inhibited when receptor dissociation is blocked. To determine whether receptor internalization was either completely blocked or delayed, we measured internalization kinetics.

Cells expressing hSSTR2 were treated with or without 1 mM cross-linker BS^3 to determine the effect of inhibiting receptor dissociation on the kinetics of internalization.

We used the radioligand ^{125}I-LTT-SST-28, an agonist to hSSTR2, to measure internalization kinetics. Receptor binding was not inhibited upon treatment with BS^3. A maximum internalization was achieved at approximately 30 min when measured up until 1 hour. This internalization rate was significantly altered when cells were pretreated with BS^3, consistent with the immunocytochemistry that inhibition of dimer dissociation impairs receptor trafficking (Fig. 4B.2B).

DISCUSSION

The mechanisms underlying dimerization have become paramount in the elucidation of GPCR function. There are two general models that have been proposed for the dimerization of GPCRs that has resulted in contentious debate (for reviews see [Agnati et al., 2003; Angers et al., 2002; Bai, 2004]). One model states that GPCRs are pre-assembled dimeric complexes occurring earlier on following their synthesis in the ER, without any ensuing effect upon ligand treatment in altering the dimeric state of the receptor. An example that has been well documented in this regard is the $GABA_B$ receptor, a relative of the class C subfamily of GPCRs [Jones et al., 1998; Kaupmann et al., 1998; White et al., 1998]. In this example, the heterodimerization between the $GABA_BR1$ and $GABA_BR2$ receptor subtypes was shown to be a prerequisite for the proper trafficking and functioning at the cell surface [Jones et al., 1998; Kaupmann et al., 1998; White et al., 1998]. The other model states a ligand-dependency for GPCR dimerization and has been documented for several GPCRs; therefore, a ligand-independent constitutive receptor dimerization paradigm cannot be universally accepted for all receptors [Agnati et al., 2003; Angers et al., 2002]. In fact, there have been conflicting reports on the same receptor subtype concerning its dimerization properties, as to whether ligand has a direct effect or not. Cvejic and Devi have reported that ligand-activated mouse δ-OR causes dissociation of receptor dimers to monomers in stably transfected cells using co-immunoprecipitation [Cvejic and Devi, 1997]. On the contrary, Milligan and coworkers found that the human δ-OR displayed constitutive dimerization irrespective of ligand occupancy using both BRET and FRET techniques in transiently transfected cells [McVey et al., 2001]. Whether these discrepancies are due to the types of techniques employed, transfections or species of receptor used is uncertain. In a recent report, transiently transfected cells resulted in the formation of mostly dimeric immature intracellular human lutropin receptors that exhibited no effect upon ligand treatment [Tao et al., 2004]. However, when stably transfected, mature cell surface monomeric receptors were mainly present and displayed ligand-induced increase in dimer formation. Therefore, it was suggested that these promiscuous interactions were occurring at the

level of the ER in transiently transfected cells due to the accumulation of immature receptors [Tao et al., 2004].

We have previously reported that hSSTR5 can both homo- and heterodimerize with hSSTR1 and dopamine 2 receptor, in a ligand-dependent manner in stably transfected cells [Patel et al., 2002a; Rocheville et al., 2000a; Rocheville et al., 2000b]. However, the functional significance for these observations remains unclear. Dimerization of the β_2-adrenergic receptor was suggested to be a requirement for receptor activation [Hebert et al., 1996]. Furthermore, using a coumermycin-gyrase B-induced dimerization system on the platelet-activating factor receptor (PAFR), coumermycin-induced dimerization was sufficient to cause the desensitization and internalization of PAFR in an agonist-independent fashion [Perron et al., 2003]. Taken together this would suggest that dimerization plays a key role in receptor activation and internalization although, this has not been exemplified for all GPCRs.

In the present study, hSSTR2 was found to be a self-associated dimer at the cell surface in stably transfected cells using pbFRET microscopy. This technique was advantageous for probing receptors present only at the cell surface. Furthermore, these observations were also confirmed using Western blot analysis. Ligand activation of hSSTR2 resulted in the dissociation of receptor dimers to monomers as shown using both techniques. Other GPCRs have also been reported to undergo ligand-induced dissociation and include the δ-OR [Cvejic and Devi, 1997], the CCKR [Cheng and Miller, 2001], the TSHR [Latif et al., 2002] and the rhY4R [Berglund et al., 2003]. With the exception of the δ-OR, little has been shown to address the functional significance for the dissociation of receptor dimers. To address this issue for hSSTR2 we monitored the effect of blocking receptor dissociation on internalization kinetics. Using a cell-impermeable cross-linking agent to prevent receptor dissociation, we found that in the presence of agonist, receptor internalization was impaired. Similarly, Cvejic and Devi have also shown impaired receptor trafficking when δ-OR dissociation was not implicated [Cvejic and Devi, 1997].

Whether ligand-dependent receptor dissociation is involved in all SSTR2 species remains obscure. In a report on rat SSTR2, self-associated receptors were shown using

Western blot however, agonist treatment did not have a considerably affect on receptor dimers [Pfeiffer et al., 2001]. Interestingly, the same group also reported on a SSTR2/SSTR3 heterodimer that, when treated with either a selective agonist for SSTR2 or SST-14 (agonist to both receptors), resulted in the dissociation of the heterodimeric complex and selective internalization of SSTR2 [Pfeiffer et al., 2001]. A similar phenomenon was shown for the dopamine D1 and adenosine A1 receptor heterodimer, where treatment with a D1 receptor agonist caused dissociation of the heteromeric complex [Gines et al., 2000].

In conclusion, we show that hSSTR2 preferentially exists as dimers at the basal state but upon stimulation with agonist dissociates into monomeric receptors. Moreover, dissociation of receptor dimers is important for efficient receptor trafficking as inhibiting dimer dissociation alters internalization kinetics. These data provide a new level of understanding in the functioning of hSSTRs and may help elucidate the functional properties of other GPCRs.

ACKNOWLEDGEMENTS

This work was supported by Canadian Institute of Health Research (CIHR) grants MT-10411 and MT-6911. We thank M. Correia for her secretarial help and H. Alturaihi for his technical assistance. This article has been dedicated to Dr. Yogesh C. Patel.

FIGURE LEGENDS

Figure 4B.1.

Agonist-dependent dissociation of the hSSTR2 dimer.

A, CHO-K1 cells stably expressing HA epitope-tagged hSSTR2 were subjected to pbFRET analysis using anti-HA monoclonal antibodies conjugated with either FITC (donor) or Rh (acceptor) as described under "Experimental Procedures". Control represents the FRET efficiency of cells that have not been treated with SST-14. Cells were treated with SST-14 for 10 min before being processed for pbFRET microscopy. Means ±SEMs represent three independent experiments each taken from approximately 40-50 cells. ***B***, HEK-293 cells stably expressing HA epitope-tagged hSSTR2 were treated with the indicated concentrations of SST-14 for 30 min before being processed and separated on a 7% SDS-polyacrylamide gel. Represented blot taken from three independent runs. ***C***, Immunoblots from (***B***) were quantified for changes in the dimeric:monomeric ratio after SST-14 treatment by densitometry using FluorChem software. ***D***, Immunoblot from membranes of HEK-293 cells stably expressing HA-hSSTR2 incubated with 5mM BS^3 prior to treatment with or without 1 μM SST-14. Membranes were separated on a 7% SDS-polyacrylamide gel. Immunoblot is a representation of three independent runs.

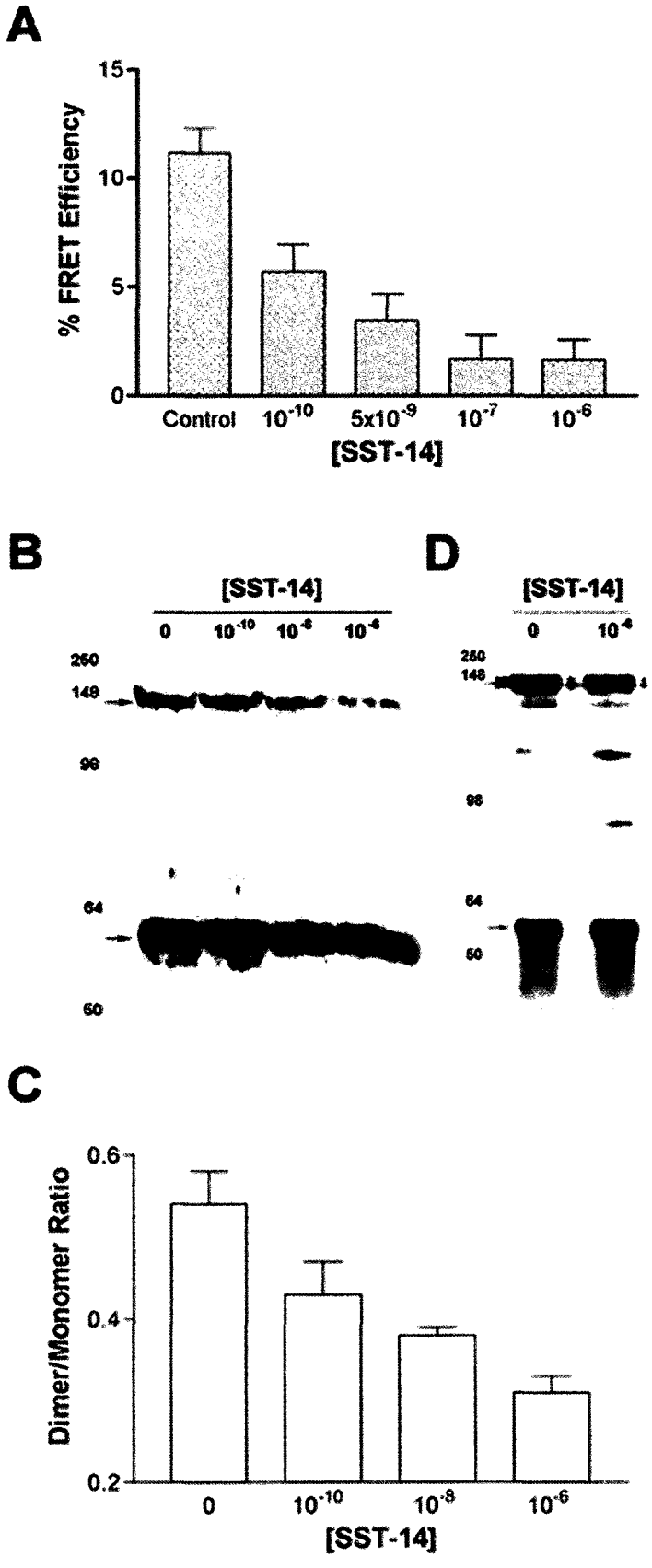
A
% FRET Efficiency
15
10
5
0
Control
10-10
5x10-9
10-7
10-6
[SST-14]
B
[SST-14]
0
10-10
10-8
10-6
250
148
98
64
50
D
[SST-14]
0
10-6
250
148
98
64
50
C
Dimer/Monomer Ratio
0.6
0.4
0.2
0
10-10
10-8
10-6
[SST-14]

Figure 4B.2.

Internalization of hSSTR2.

A, Immunocytochemistry of CHO-K1 cells stably expressing HA-hSSTR2 in the absence (control) or presence of 1 μM SST-14 with or without pretreatment of 1mM BS^3. Non-permeablized cells (NP) represent cell surface distribution of receptor and permeablized cells (P) represent internalized receptor. Arrows indicate both surface and internalized receptors. Magnification 630x. ***B***, Internalization kinetics of HA-hSSTR2 stably expressed in CHO-K1 cells using the radioligand ^{125}I-LTT-SST-28 as described in "Experimental Procedures". Internalization rate of hSSTR2 without (■), or with (◊) pretreatment of 1mM BS^3.

A

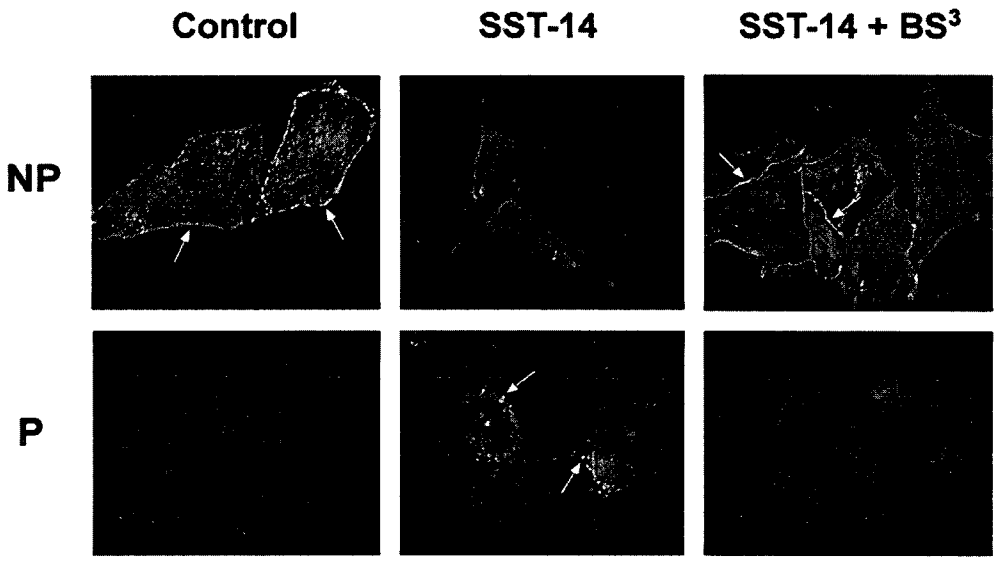
Control
SST-14
SST-14 + BS3
NP
P

B

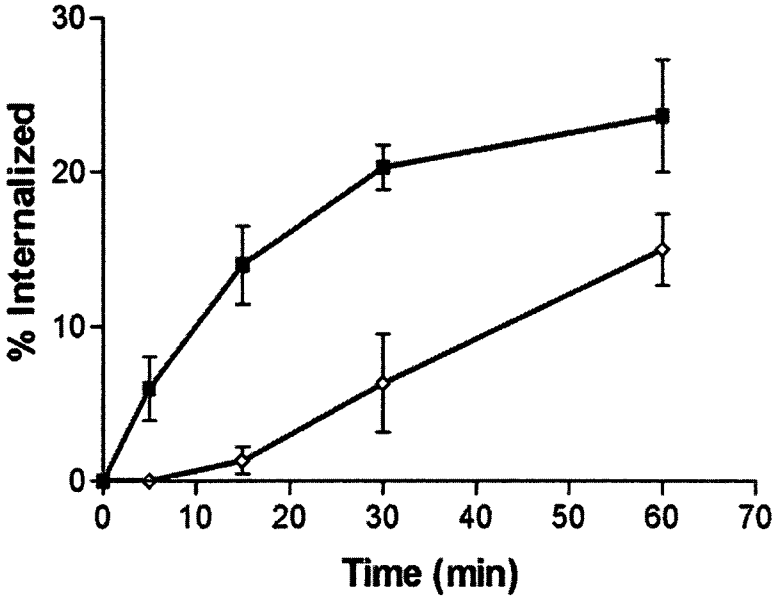
% Internalized
Time (min)
0
10
20
30
40
50
60
70

Table 4B.1.

Concentration-dependent decrease in FRET efficiencies.

CHO-K1 cells expressing HA-hSSTR2 were treated with the indicated concentrations of SST-14 and subjected to pbFRET analysis as described in *"Materials and Methods"*. Symbols are represented as follows: **D-A** and **D+A** correspond to donor in the absence and presence of acceptor respectively; τ_{avg}, mean of ***n*** photobleaching time constants; ***n***, number of cells analyzed; ***E***, average effective FRET efficiency. Means ±SEMs represent three independent experiments.

SST-14 Concentration		τ_{avg}	***n***	***E* (%)**
Control	*D-A*	13.6 ± 0.3	48	
	D+A	15.4 ± 0.3	48	11.7 ± 1.1
10^{-10}	*D-A*	13.2 ± 0.3	48	
	D+A	14.0 ± 0.4	48	5.7 ± 1.3
5×10^{-9}	*D-A*	13.4 ± 0.4	48	
	D+A	13.8 ± 0.2	48	2.9 ± 1.2
10^{-7}	*D-A*	14.1 ± 0.3	48	
	D+A	14.3 ± 0.3	48	1.4 ± 1.1
10^{-6}	*D-A*	14.2 ± 0.4	48	
	D+A	14.5 ± 0.2	48	2.1 ± 0.9

C) Association with hSSTR5 affects the cell signalling, receptor recycling and growth inhibitory properties of hSSTR2

Having identified the dimerization properties of hSSTR2 and hSSTR5, our next inquiry was to investigate whether these two receptors interact and to determine the functional relevance for their heterodimerization. These receptors are predominantly co-expressed in growth hormone-hypersecreting pituitary adenomas and several lines of evidence have already inferred a putative association between these two subtypes [Ben-Shlomo et al., 2005; Ren et al., 2003; Sharif et al., 2007], however; a direct physical interaction remains to be determined. In the final chapter of this section, we describe the hSSTR2/hSSTR5 heterodimer. Interestingly, its regulation is mediated by agonist but in an hSSTR2-selective manner. Furthermore, cell signalling, receptor-recycling and growth inhibition of hSSTR2 are properties affected upon heterodimerization.

Manuscript: Grant, M., Alturaihi, H., Jaquet, P., Collier, B. and Kumar, U. (*in revision*) Cell Growth Inhibition and Functioning of Human Somatostatin Receptor Type 2 are Modulated by Receptor Heterodimerization. *Mol Endocrinol.*

Cell Growth Inhibition and Functioning of Human Somatostatin Receptor Type 2 are Modulated by Receptor Heterodimerization

Michael Grant[1,2], Haydar Alturaihi[1], Philippe Jaquet[3], Brian Collier[2] and Ujendra Kumar[1,4‡]

[1]Fraser Laboratories For Diabetes Research, Department of Medicine, Royal Victoria Hospital, Montreal, Quebec, Canada; [2]Department of Pharmacology & Therapeutics, McGill University, Montreal, Quebec, Canada; [3]Faculty of Medicine, Centre Hospitalier Universitaire Timone, Marseille, France and [4]Faculty of Pharmaceutical Sciences, Division of Pharmacology and Toxicology, University of British Columbia, Vancouver, Canada.

Running Title: Heterodimerization of human somatostatin receptors.

‡Address of correspondence: Dr. Ujendra Kumar

Faculty of Pharmaceutical Sciences

Division of Pharmacology and Toxicology

The University of British Columbia

2146 East Mall

Vancouver, Canada, V6T 1RZ

Tel. 604 827-3660

Fax. 604 822-3035

E-mail:ujkumar@interchange.ubc.ca

SUMMARY

Somatostatin (SST) –analogs have been successfully used in the medical treatment of acromegaly, caused by growth hormone hyper-secreting pituitary adenomas. Patients on SST-analogs rarely develop tachyphylaxis despite years of continuous administration. It has been recently proposed that a functional association between SST receptor (SSTR) subtypes 2 and 5 exists to account for this behaviour, however; a physical interaction has yet to be identified. Using both co-immunoprecipitation and pbFRET microscopy techniques, we determined that SSTR2 and SSTR5 heterodimerize. Surprisingly, selective-activation of SSTR2 and not SSTR5 or their co-stimulation, modulates the association. The SSTR2-selective agonist L-779,976, is more efficacious at inhibiting adenylate cyclase, activating ERK1/2 and inducing the cyclin-dependent kinase inhibitor $p27^{Kip1}$, in cells expressing both SSTR2 and SSTR5, compared to SSTR2 alone. Furthermore, cell growth-inhibition by L-779,976 treatment was markedly extended in co-expressing cells. Trafficking of SSTR2 is also affected upon heterodimerization, an attribute corresponding to modifications in β-arrestin-association kinetics. Activation of SSTR2 results in the recruitment and stable-association of β-arrestin, followed by receptor-internalization and intracellular receptor pooling. Contrarily, heterodimerization increases the recycling rate of internalized SSTR2 by destabilizing its interaction with β-arrestin. Given that SST-analogs show preferential-binding to SSTR2, these data provide a mechanism for their effectiveness in controlling pituitary tumours and the absence of tolerance seen in patients undergoing long-term administration.

[3] **The abbreviations used are:**

GPCR(s), G protein coupled receptor(s); SSTR, human somatostatin receptor; SST, somatostatin; HA, hemagglutinin; HEK, human embryonic kidney; pbFRET, photobleaching fluorescence resonance energy transfer; MAPK, mitogen-activated protein kinase; ERK, extracellular signal-regulated kinase; FBS, foetal bovine serum.

INTRODUCTION

Somatostatin (SST) is a peptide hormone that was originally identified in the hypothalamus and subsequently found throughout the central nervous system and in various peripheral organs [Patel, 1999]. Generally classified as an inhibitory peptide, SST is secreted by endocrine, neuronal and immune cells and acts to regulate cell secretion, neurotransmission and cell proliferation. The physiological role of hypothalamic SST on the pituitary is well established: SST inhibits the basal and stimulated release of growth hormone (GH) and thyroid-stimulating hormone, including the secretions of prolactin and ACTH [Patel, 1999]. SST activity is mediated by five specific receptor subtypes (SSTR1-5) that are differentially expressed in a tissue-specific manner, often with overlapping patterns of distribution [Moller et al., 2003; Patel, 1999]. All SSTRs possess seven-transmembrane spanning domains and are linked to G-proteins; therefore, belonging to the superfamily of G-protein coupled receptors (GPCRs) [Moller et al., 2003; Patel, 1999]. Many tumors have been shown to express SSTRs, the highest density of which is seen in tumors of neuroendocrine origin [Lamberts et al., 2002].

SST-analogs such as lanreotide and octreotide, are frequently administered as first line treatment in acromegaly, caused by growth hormone (GH) hyper-secreting pituitary adenomas to regulate endocrine function [Tichomirowa et al., 2005]. Over 90% of patients on SST-analogs show decreases in circulating GH levels, while approximately 70% of those achieve biochemical normalization. In addition, SST-analog therapy frequently results in tumour shrinkage in roughly 50% of patients [Bevan, 2005; Ferrante et al., 2006; Lamberts et al., 2002; Melmed et al., 2005; Resmini et al., 2007; Zatelli et al., 2006]. Surprisingly, patients rarely show desensitization to treatment despite years of continuous administration, a property not shared upon treatment of other endocrine tumors [Hofland and Lamberts, 2003]. The mechanisms underlying this discrepancy are poorly understood, however; a functional association between SSTR2 and SSTR5, the primary SSTRs expressed in GH secreting pituitary adenomas [Jaquet et al., 2000; Park et

al., 2004a], has been proposed to account for these actions, yet a direct physical interaction remains to be identified [Sharif et al., 2007].

There is a preponderance of evidence suggesting the significance of GPCR dimerization in receptor-biogenesis, regulation and pharmacology [Prinster et al., 2005; Terrillon and Bouvier, 2004]. Moreover, dimerization of GPCRs has been identified in various pathological states, suggesting clinical importance for such protein-protein interactions [AbdAlla et al., 2001b; AbdAlla et al., 2004]. We have previously reported that human SSTRs can form both homo- and heterodimers. In our investigations, SSTR5 was shown to homo- and heterodimerize with SSTR1, a property that regulated receptor internalization and signalling [Grant et al., 2004b; Patel et al., 2002a; Rocheville et al., 2000b]. Furthermore, we have demonstrated that SSTR2 homodimers dissociate into monomers prior to internalization, an aspect that when prevented, altered the internalization rate of the receptor [Grant et al., 2004a].

In the present study, we demonstrate the existence of SSTR2/SSTR5 heterodimers using co-immunoprecipitation and pbFRET microscopy techniques, an occurrence that is further augmented by selective activation of SSTR2 and not SSTR5 or their concurrent stimulation. Heterodimerization alters the association-kinetics of β-arrestin to SSTR2 and augments receptor-recycling. In addition, increases in the efficiency at inhibiting adenylate cyclase, activation of MAP kinases and upregulation of the cyclin-dependent kinase inhibitor $p27^{Kip1}$ are all features observed following heterodimerization. Finally, the enhanced properties of the heterodimer conferred an extended growth inhibitory response. Taken together, these data provide a mechanism for the effectiveness of currently available SST-analogs in treating GH secreting pituitary adenomas, given their preferential-binding to SSTR2.

EXPERIMENTAL PROCEDURES

Materials and Antibodies

The peptides SST-14 and [Leu(8)-D-Trp-22, Tyr-25]-SST-28 (LTT-SST-28) were purchased from Bachem, Torrance, CA. The non-peptide agonists L-779,976 and L-817,818 were provided by Dr. S.P. Rohrer from Merck & Co [Rohrer et al., 1998]. Fluorescein-conjugated mouse monoclonal antibody against hemagglutinin (HA) (12CA5) was purchased from Roche Molecular Biochemicals, Mannheim, Germany. Rhodamine-conjugated and unconjugated anti-c-myc monoclonal antibodies and mouse monoclonal anti-HA antibody were purchased from Sigma-Aldrich, Inc., St. Louis, MO. Monoclonal anti-phospho-ERK1/2 and rabbit polyclonal ERK1/2 antibodies were purchased from Cell Signaling Technology, Danvers, MA and monoclonal anti-β-tubulin antibody from Sigma-Aldrich. Monoclonal anti-$p27^{Kip1}$ antibodies were purchased from Santa Cruz Biotechnology, Santa Cruz, CA. Protein A/G-agarose beads were purchased from Calbiochem, EMD Biosciences, Darmstadt, Germany. DAPI dihydrochloride was purchased from Molecular Probes, Inc., Eugene, OR.

Constructs and Expressing Cell Lines

Stable transfections of HEK 293 cells expressing amino-terminally HA-tagged human SSTR2 (SSTR2), c-Myc-tagged human SSTR5 (SSTR5) or both receptors were prepared by Lipofectamine transfection reagent. Constructs expressing SSTR2 were made from the pCDNA3.1/Neo vector (neomycin resistance) and SSTR5 from the pCDNA3.1/Hygro vector (hygromycin resistance) as previously described [Grant et al., 2004a; Grant et al., 2004b]. Clones were selected and maintained in Dulbecco's DMEM supplemented with 10% fetal bovine serum (FBS) and 700 μg/ml neomycin or 400 μg/ml of hygromycin. Co-transfectants were maintained in medium containing both 700 μg/ml of neomycin and 400 μg/ml of hygromycin as previously described [Grant et al., 2004a; Grant et al., 2004b]. All cells were grown in a 37°C incubator with 5% CO_2. Constructs

for β-arrestin$_2$-GFP and GRK$_2$ were kindly provided by Dr. Stéphane A. Laporte, McGill University.

Saturation Analysis

Cells were harvested, homogenized using a glass homogenizer and membranes were prepared by centrifugation as previously described [Grant et al., 2004a; Grant et al., 2004b]. Saturation binding studies were performed with 20-40 μg of membrane protein collected from HEK 293 cells stably expressing the receptor constructs, and ^{125}I-labeled LTT-SST-28 radioligand (50-2000 pM) in 50 mM HEPES, pH 7.5, 2 mM $CaCl_2$, 5 mM $MgCl_2$, 0.5% bovine serum albumin, 0.02% phenylmethylsulfonyl fluoride, and 0.02% bacitracin (binding buffer) for 30 min at 37°C. Incubations were terminated by the addition of ice cold binding buffer. Membrane pellets were quantified for radioactivity using a LKB gamma counter (LKB-Wallach, Turku, Finland). Binding data were analyzed with Prism 4.0 (Graph Pad Software, San Diego, CA) by non-linear regression analysis.

Coupling to Adenylyl Cyclase and GTP-Binding Assay

Stably transfected HEK 293 cells were grown in 6-multiwell plates and tested for receptor coupling to adenylyl cyclase by incubation for 30 min with 20 μM forskolin and 0.5 mM 3-isobutyl-1-methylxanthine with or without agonists (10^{-11} – 10^{-7} M) at 37°C as previously described [Grant et al., 2004b]. Cells were then scraped in 0.1 N HCl and quantified for cAMP by radioimmunoassay using a cAMP Kit (Inter Medico, Markham, ON) following the manufacturer's guidelines. Samples were measured for radioactivity using a LKB beta scintillation counter (LKB-Wallach). Data were analyzed by non-linear regression analysis using Prism 4.0 (Graph Pad Software, San Diego, CA). SEMs are representative of at least three independent experiments done in duplicate.

The GTP-binding assay was performed by measuring the amount of [^{35}S]GTPγS (GE Healthcare, Waukesha, WI) bound to membranes from HEK 293 cells stably co-expressing SSTR2 and SSTR5. In 100 μL GTP assay buffer (20 mM HEPES, 100 mM NaCl, 10 mM $MgCl_2$, 10 μM GDP), 50 μg membrane protein and 10 pM [^{35}S]GTPγS were added in culture tubes with or without 10 nM agonist (SST-14, L-779,976 and L-817,818). The reaction was incubated in a 30°C water bath shaking for 1 hr. To inactivate $G\alpha_i$ G-proteins, membrane was pretreated with 0.5 μg activated pertussis toxin (PTX) (10 mM DTT, 10 μM ATP, PBS pH 7.4 for 30 min at 30°C) for 1 hr at 30°C prior to GTP binding. The reaction was terminated by the addition of 1 ml ice cold GTP assay buffer. Following centrifugation, membrane pellets were washed thrice in assay buffer before the addition of 7 ml scintillation fluid and counted using a LKB beta scintillation counter (LKB-Wallach).

PbFRET Microscopy and Immunocytochemistry

PbFRET experiments were performed on HEK 293 cells as previously described [Grant et al., 2004a; Grant et al., 2004b; Patel et al., 2002b]. The effective FRET efficiency (E) was calculated in terms of a percent based upon the photobleaching (pb) time constants of the donor taken in the absence (D – A) and presence (D + A) of acceptor according to $E = 1 - (\tau_{D-A}/ \tau_{D+A}) \times 100$. HEK 293 cells were seeded on glass coverslips for 24 hrs, treated with 10 nM of agonist for 10 min at 37°C and fixed with 4% paraformaldehyde for 20 min on ice and processed for immunocytochemistry. Antibodies used were mouse monoclonal anti-HA conjugated to fluorescein directed to SSTR2 as the donor and monoclonal anti-Myc conjugated to rhodamine directed to SSTR5 as the acceptor. The area consisting of the plasma membrane was used to analyze the photobleaching decay rate on a pixel-by-pixel basis as described earlier.

Co-Immunoprecipitation and Western Blot

Membrane protein (500 μg) from stably transfected HEK 293 cells was treated with 10 nM of agonist (SST-14, L-779,976 and L-817,818) in binding buffer (50 mM HEPES, 2 mM $CaCl_2$, 5 mM $MgCl_2$, pH 7.5) for 30 min at 37 °C. Following treatment, membrane protein was solubilized in 1 ml RIPA buffer (150 mM NaCl, 50 mM Tris-HCL, 1% NP-40, 0.1% SDS, 0.5% sodium deoxycholate, pH 8.0) for 1 hour at 4 °C. Samples were incubated with anti-HA antibody for immunoprecipitation and purified with Protein A/G-agarose beads. Purified proteins were fractionated by electrophoresis on a 7% SDS polyacrylamide gel and transferred to PVDF membrane (GE Healthcare) as previously described [Grant et al., 2004a; Grant et al., 2004b]. Immunoblotting for the heterodimer was performed using anti-c-Myc antibody (1:2000). Blocking of membrane, incubation of primary antibodies, incubation of secondary antibodies and detection by chemiluminescence were performed following ECL Western Blotting detection kit (Amersham) according to manufacturer's instructions. Images were captured using an Alpha Innotech FluorChem 8800 (Alpha Innotech Co., San Leandro, CA) gel box imager and densitometry was carried out using FluorChem software (Alpha Innotech Co.).

For MAPK signalling, HEK 293 cells stably co-expressing SSTR2 and SSTR5 were treated with 10 nM of each agonist for the indicated times. The reaction was terminated using ice cold Dulbecco's phosphate buffered saline followed by solubilization in RIPA buffer. Lysate protein was separated on an 8% polyacrylamide gel and transferred to PVDF membranes. Immunoblotting for phosphorylated extracellular signal-regulated kinase (ERK) 1/2 was performed using phospho-specific antibodies. Phosphorylation levels were quantified by densitometry using FluorChem software and normalized for protein loading using β-tubulin. The same procedure was repeated for the expression of $p27^{Kip1}$ however, immunoblotting was performed using monoclonal anti-$p27^{Kip1}$ antibodies. To standardize for protein loading all membranes were reprobed for β-tubulin using Reblot Plus, Chemicon International, Temecula, CA.

Assay of β-arrestin Translocation

HEK 293 cells were seeded in 6-multiwell plates with coverslips for 24 hrs prior to transient transfection with SSTR2, SSTR5 or both receptor subtypes along with *β*-arrestin$_2$-GFP (*β*-arrestin) and GRK$_2$ cDNAs using Lipofectamine transfection reagent. Cells were treated with 10 nM of agonist 48 hrs post-transfection for the indicated times. SSTR2 was localized using an anti-HA antibody and anti-mouse IgG conjugated to cy3 (red) while β-arrestin (green) was identified by direct excitation of the GFP molecule using 488 nm laser light. Cells were fixed in 4% paraformaldehyde before being subjected to immunocytochemistry and imaged using a Zeiss 510 confocal microscope. Cells treated with SST-14 and L-779,976 for 20 min were permeablized using 0.2% Triton X-100 for 10 min prior to immunocytochemistry.

Cell Growth Inhibition

HEK 293 cells stably expressing SSTR2 and SSTR5 were seeded at a density of 5000 cells/well in 96-well plates for 24hrs. Cells were then serum deprived for 24hrs before treatment with 1 nM of either agonist SST-14 or L-779,976 in the presence of 5% FBS for the indicated time periods. As a control, cells were given FBS in the absence of drug to compare for cell growth. Cell viability was measured using a standard MTT assay protocol. Briefly, 10 μL of 5 mg/ml MTT (Thiazolyl Blue Tetrazolium Bromide, Sigma-Aldrich) solution was added and left to incubate for 2 hours at 37°C and 5% CO_2. When the formazan precipitate was formed it was dissolved in 100 μL of detergent solution (*N,N*-Dimethylformamide, 20% SDS solution). The absorbance was measured in a microplate spectrophotometer at 550 nm.

Statistical Analysis

Data were analyzed with the indicated tests using Graph Pad Prism 4.0. Statistical differences were taken at p values < 0.05.

RESULTS

Agonist-bound SSTR2 modulates heterodimerization

To determine whether SSTR2 and SSTR5 interact to form heterodimers, we selected a HEK 293 cell clone stably co-expressing an HA-tagged SSTR2 and a c-Myc-tagged SSTR5 for a total expression of 281 ±12 fmol/mg protein. This clone was chosen for its relatively low expression levels comparable to physiological conditions [Rocheville et al., 2000b] and its approximate 1:1 receptor ratio (SSTR2, 167 ± 3 fmol/mg protein; SSTR5, 115 ± 2 fmol/mg protein). Heterodimerization was verified by co-immunoprecipitating SSTR2 from membrane proteins using an anti-HA antibody and immunoblotting for SSTR5 with an anti-c-Myc antibody. Under these conditions, a band estimated at 105 kDa was observed and could be identified in the absence of agonist treatment (Fig. 4C.1B). The size of the heterodimeric band closely approximated the summation of the molecular weights of the monomeric species of SSTR2 and SSTR5, individually expressed in HEK 293 cells (Fig. 4C.1A). We have previously demonstrated the effect of agonist on the stabilization of the SSTR1 and SSTR5 heterodimer, a property that was associated with enhanced signaling. To ascertain whether a similar mechanism was involved in the formation of the SSTR2/SSTR5 heterodimer, we selectively activated SSTR2, SSTR5 or both receptor-subtypes prior to co-immunoprecipitation. Treatment with the SSTR2-selective agonist L-779,976 but not the SSTR5-selective agonist L-817,818 resulted in a dose-dependent increase in the formation of the heterodimer, a result that was significantly greater than basal as determined by densitometry (Fig. 4C.1, B and C). Surprisingly, stimulation of both receptor-subtypes with the endogenous pan-agonist SST-14, did not reveal increases in heterodimerization despite activation of SSTR2 (Fig. 4C.1B). The specificity of the heterodimeric band upon co-immunoprecipitation was confirmed using the reverse combination of antibodies, whereby SSTR5 was immunoprecipitated followed by immunoblotting of SSTR2 (Fig. 4C.2).

To determine whether heterodimerization of SSTR2 and SSTR5 was an artifact of immunoprecipitation rather than a selective interaction occurring at the cell surface of intact cells, we performed photobleaching fluorescence resonance energy transfer (pbFRET) microscopy [Grant et al., 2004a; Grant et al., 2004b; Patel et al., 2002b]. Using an anti-HA antibody conjugated to fluorescein as the donor and an anti-c-Myc antibody conjugated to rhodamine as the acceptor, we probed the surface of our stable cell line for SSTR2 and SSTR5 respectively (Fig. 4C.3). Under basal conditions, there was a small but sustained FRET efficiency, accordant with the co-immunoprecipitation data, characteristic of pre-assembled receptor complexes. Concordantly, treatment of cells with 10 nM of the SSTR2-selective compound, L-779,976, resulted in a significant increase in FRET efficiency over basal that was not apparent with the addition of SST-14 or the SSTR5-selective compound L-817,818 (Fig. 4C.1D). Although heterodimerization between SSTR2 and SSTR5 was unaltered following stimulation with SST-14, homodimerization of SSTR5 was observed in a dose-dependent manner (Fig. 4C.1E). Taken together, these data indicate the role of ligand-bound SSTR2 in modulating the heterodimer.

Heterodimerization alters the interaction of β-arrestin to SSTR2

A basic tenet following activation of GPCRs is their eventual desensitization and internalization [Tsao et al., 2001]. There have been several instances where the heterodimerization of GPCRs has altered the desensitization and internalization profiles of one or both protomers involved [Prinster et al., 2005]. To determine whether formation of the SSTR2/SSTR5 heterodimer altered receptor-internalization, we first monitored for changes in β-arrestin interaction, a class of proteins known for their involvement in the internalization of GPCRs [Lefkowitz and Shenoy, 2005]. Although both receptors, SSTR2 and SSTR5 internalize following stimulation with agonist, only SSTR2 was found to recruit β-arrestin (green) to the cell surface of HEK 293 cells (Fig. 4C.4A). The high affinity of β-arrestin to SSTR2 was observed subsequent acute treatment with both agonists SST-14 and L-779,976 and persisted in the form of

endosomes following 20 minute stimulation, consistent with previously reported data [Tulipano et al., 2004]. When co-transfected cells were treated with SST-14, β-arrestin translocated from the cytosol to the cell surface within minutes of agonist exposure. However, when the cells were stimulated with agonist for a prolonged period, β-arrestin aggregated in the form of stable endosomal complexes (Fig. 4C.4B). Surprisingly, when co-transfected cells were subjected to L-779,976, β-arrestin did indeed concentrate at the cell surface nevertheless, it did not sequester in the form of endosomes following extended stimulation. This would indicate that heterodimerization interferes with β-arrestin/receptor interaction, causing uncoupling soon after the receptor internalizes.

The transient interaction of β-arrestin on heterodimerization was elaborated further by confocal studies shown in figure 4C.5. When co-transfected cells were treated with L-779,976, β-arrestin and SSTR2 were found to co-localize within five minutes of activation but not following a prolonged stimulus despite SSTR2 internalization. However, β-arrestin was found localized with SSTR2 following its internalization when stimulated with SST-14 (Fig. 4C.5A). Additionally, the transient nature of β-arrestin and SSTR2 on heterodimerization was supported by co-immunoprecipitation studies (Fig. 4C.5, B-D). Stable complexes between SSTR2 and β-arrestin formed following extended treatment with L-779,976 in cells expressing SSTR2 alone; however, the interaction decreased significantly when SSTR5 was co-expressed. This effect was restricted to the SSTR2-specific agonist L-779,976, as treatment with SST-14 in either cell type did not alter the co-immunoprecipitation patterns of β-arrestin (Fig. 4C.5, B-D).

Interestingly, the heterodimer did not internalize as a complex, a fact that has been documented for other GPCR heterodimers [Prinster et al., 2005]. In fact, when co-transfected cells were treated with L-779,976, only SSTR2 was prompted to internalize (Fig. 4C.6). Both SSTR2 and SSTR5 did internalize when stimulated with SST-14, agonist to both receptor subtypes (Fig. 4C.6). Although heterodimerization may affect the sequestration of β-arrestin it did not affect the internalization of SSTR5, possibly implying the absence of heterologous events.

Trafficking of SSTR2 following heterodimerization

GPCR recycling rates have been causally linked to changes in the association of β-arrestin [Lefkowitz and Shenoy, 2005]. Stable associations between β-arrestin and the receptor result in slow recycling rates, contrary to transient interactions, where recycling times are shortened. Furthermore, a greater portion of receptor is sent to lysosomal compartments to be degraded, when β-arrestin is stably associated. Given the effects of heterodimerization on the association of β-arrestin to SSTR2, we sought whether these changes were also reflected in receptor-recycling rates. HEK 293 cells expressing SSTR2 or co-expressing SSTR2 and SSTR5, were treated with agonist and imaged by confocal microscopy to measure receptor trafficking (Fig. 4C.7). When SSTR2-expressing cells were treated with either agonist SST-14 or L-779,976, internalization was evident in permeablized cells following a 20 or 40-minute stimulation, accompanied by decreased cell surface expression levels (Fig. 4C.7). A similar occurrence transpired when HEK 293 cells co-expressing SSTR2 and SSTR5 were treated with SST-14 for either 20 or 40 minutes (Fig. 4C.7). Punctate staining representing internalized receptor was consistently found in perinuclear regions. Similarly, perinuclear staining was also portrayed in cells co-expressing SSTR2 and SSTR5 subsequent SST-14 treatment. A markedly distinct pattern of SSTR2 localization ensued when co-expressing cells were treated with L-779,976 (Fig. 4C.7). Following 20 minutes of activation with L-779,976, SSTR2 was found concentrated intracellularly, however; unlike SSTR2-expressing cells, extended stimulation (40 min) presented with an overall decrease in internalized receptor, with staining primarily localized around the cell periphery and not perinuclear (Fig. 4C.7). Accordingly, co-expressing cells also demonstrated increases in cell surface expression following prolonged activation with L-779,976 (Fig. 4C.7).

Heterodimers potentiate but do not synergize G-protein signalling

There have been several instances where heterodimerization of GPCRs has lead to changes in signalling distinct from that of the individual receptor monomers/homodimers [Prinster et al., 2005]. In fact, most of these changes have been documented within

immediate effector responses such as, changes in adenylyl cyclase activity. However, few reports have shown a physiological implication for GPCR heterodimerization [McGraw et al., 2006; Pello et al., 2008; Prinster et al., 2005; Waldhoer et al., 2005]. To seek a functional relevance for the SSTR2/SSTR5 heterodimer, we began by studying the SSTR-induced inhibition of adenylyl cyclase [Moller et al., 2003; Patel, 1999]. We compared the cAMP efficiency curves of all three agonists from HEK 293 cells stably expressing one or both of the receptor subtypes. The SSTR2 specific agonist, L-779,976, was approximately 20-fold more efficient at inhibiting adenylyl cyclase in co-transfectants then in cells expressing SSTR2 alone (Fig. 4C.8A; Table 4C.1). This increase in potency in co-transfected cells was exclusive to L-779,976 treatment, as the EC_{50} values for either the SSTR5 specific agonist L-817,818 or SST-14 were not significantly altered (Fig. 4C.8, B and C; Table 4C.1). Heterodimerization did not result in a synergistic effect on adenylyl cyclase coupling, as the total inhibition of cAMP synthesis was unchanged (Fig. 4C.8D). Congruently, GTP-coupling as measured from the membranes of co-transfected HEK 293 cells, did not significantly differ amongst the various agonist treatments (Fig. 4C.8E). Binding of GTP was dependent on the coupling of $G\alpha_i$ G-proteins, as the effect was blocked by pre-treatment with pertussis toxin (PTX). Although heterodimerization enhanced adenylyl cyclase coupling efficiency, the effect was not synergistic, as neither the total inhibition of cAMP synthesis nor the binding of GTP were affected.

Heterodimerization enhances ERK1/2 phosphorylation

Phosphorylation of ERK1/2 was shown as a prerequisite to the growth inhibitory effects of somatostatin, a property predominantly associated with SSTR2 activation [Lahlou et al., 2003; Pages et al., 1999]. To determine the effects of SSTR heterodimerization on ERK1/2 activity, we measured its phosphorylation in a time-dependent manner upon activation of SSTR2 in our single and double expressing cell lines. Treatment of HEK 293 cells stably expressing SSTR2 with L-779,976 resulted in a phosphorylation maximum at approximately five minutes, which receded to basal levels

at the end of a forty-minute stimulation period. However, the effect was significantly enhanced and prolonged, an event that persisted beyond forty minutes when SSTR5 was stably present (Fig. 4C.9, A and B). The phosphorylation of ERK1/2 was highly dependent on $G\alpha_i$ G-proteins, as pre-treatment of cells with PTX abrogated the signal (Fig. 4C.9A). Alterations in the phosphorylation profiles of ERK1/2 in co-transfected cells were not apparent when treated with SST-14, agonist to both receptor subtypes, suggesting co-activation is not required to enhance the response (Fig. 4C.9C). Interestingly, selective activation of SSTR5 with L-817,818 did not affect ERK1/2 activation, supporting the importance of SSTR2 in this signaling pathway (Fig. 4C.10).

Upregulation of $p27^{Kip1}$ and cell growth inhibition are increased on heterodimerization

The growth inhibitory effects of somatostatin and its analogs have been characterized on both normal and tumoural cells, a property shown to occur both *in vitro* and *in vivo* [Lamberts et al., 2002]. The intracellular pathway elicited by activation of SSTR2 leading to G_1 cell-cycle arrest, have involved MAP kinases and upregulation of the cyclin-dependent kinase inhibitor $p27^{Kip1}$ [Pages et al., 1999]. Interference of this pathway by the MEK1/2 inhibitor PD98059 abrogates $p27^{Kip1}$ upregulation and growth inhibition [Lahlou et al., 2003]. To determine the effects of heterodimerization on SSTR2 evoked $p27^{Kip1}$ expression, we compared the treatments of SST-14 and L-779,976 on HEK 293 cells stably expressing SSTR2 alone or in combination with SSTR5. Cells were serum deprived for 24hrs prior to incubation with agonist in the presence of foetal bovine serum (FBS) to simulate growth conditions. The addition of FBS significantly decreases the expression of $p27^{Kip1}$, a property associated with the growth promoting effects of the serum (Fig. 4C.11, A and B). Treating co-expressing cells with SST-14 produced a concentration-dependent increase in $p27^{Kip1}$ expression, an effect that reached a maximum at 100 nM. A similar response was procured with as little as 1 nM of L-779,976, a 100-fold increase in potency (Fig. 4C.11A). This potency difference was not apparent when both agonists SST-14 and L-779,976 were used to treat HEK 293 cells

stably-expressing SSTR2 alone (Fig. 4C.11B). As expected, selective stimulation of SSTR5 with L-817,818 in co-expressing cells did not affect $p27^{Kip1}$ induction, given its inability to activate ERK1/2 (Fig. 4C.12).

To determine whether increases in the upregulation of $p27^{Kip1}$ were associated with changes in cell physiology, we monitored the effects of heterodimerization on cell growth. Cell growth was diminished by approximately 50% following a 24-hour incubation period with either agonist SST-14 or L-779,976, in cells stably expressing SSTR2 alone or in combination with SSTR5 (Fig. 4C.13, A and B). The effect was not persistent, as continued treatment with SST-14 resulted in a consistent decline in growth inhibition over the course of a 72-hour period, an indication that cell-cycle arrest was reversed. However, growth inhibition was sustained following treatment of L-779,976 on cells expressing both receptor subtypes, a property associated with the signalling events of SSTR heterodimers (Fig. 4C.13B).

DISCUSSION

Somatostatin analogs are the mainstay in the medical treatment of acromegaly, because they are safe and well tolerated [Tichomirowa et al., 2005]. Their function is highlighted by their effectiveness at normalizing GH and insulin growth factor-1 levels, caused by hyper-secreting pituitary adenomas. In addition, patients on SST-analogs have shown significant reductions in tumor mass; tumor shrinkage of greater than 50% can be seen when SST-analogs are administered as stand-alone therapy, prior to any surgical or radiotherapy procedures [Bevan, 2005; Melmed et al., 2005]. These reports have broadened the potential use of SST-analogs from hormone regulation to tumor control. In addition, GH secreting pituitary adenomas do not undergo desensitization to treatment, as acromegalic patients rarely show any signs of tachyphylaxis despite years of SST-analog therapy. This property is specific to tumors of the pituitary as neither islet cell or carcinoid tumors share this feature; prolonged administration of SST-analogs frequently results in desensitization and relapse, as symptoms invariably return [de Herder et al., 2003; Hofland and Lamberts, 2003; Lamberts et al., 1996].

The mechanisms underlying resistance to desensitization have not been fully elucidated, however; a functional association between SSTR2 and SSTR5, the two primary SSTRs expressed in these tumors [Jaquet et al., 2000; Park et al., 2004a], has been proposed to account for this behavior [Sharif et al., 2007]. This is unlike islet cell tumors or carcinoids of the gut, as SSTR2 expression predominates [de Herder et al., 2003]. In the report by Sharif et al., the internalization and trafficking of murine SSTR2 were modulated by the expression of SSTR5 in both ectopically and endogenously expressing cell systems [Sharif et al., 2007]. Moreover, the effect was dependent on the selective-stimulation of SSTR2 and not both receptor-subtypes. They observed reduced receptor-internalization, increased receptor recycling and a decrease in the desensitization of SSTR2 in co-expressing cells treated with the selective-agonist L-779,976, compared to cells expressing SSTR2 alone or co-expressing cells treated with the pan-agonist SST-14. Additional support on the importance of both SSTR2 and SSTR5 expression on SST-

analog therapy comes from a report by Ballarè et al., describing an acromegalic patient with a tumor harboring a mutant SSTR5 resistant to treatment despite the presence of SSTR2 [Ballare et al., 2001]. These reports and others have suggested the formation of a putative SSTR2/SSTR5 heterodimer however; a physical interaction has yet to be documented [Ben-Shlomo et al., 2005; Ren et al., 2003].

Using both co-immunoprecipitation and pbFRET microscopy techniques, L-779,976 was determined to selectively regulate the SSTR2/SSTR5 heterodimer (Fig. 4C.1). Neither concurrent stimulation nor selective activation of SSTR5 with SST-14 and L-817,818 respectively, stabilized this interaction. Given that SSTR2 exists as a homodimer, which dissociates into monomers following activation with agonist [Duran-Prado et al., 2007; Grant et al., 2004a], it is possible that the uncoupling of the dimer could allow for alternative pairing with SSTR5. This could also explain the lower levels of heteromeric interaction seen under basal conditions and may suggest that SSTR2 has a higher affinity for interacting with itself when inactive. However, this mechanism fails to explain why activation by SST-14 does not regulate the heterodimer. One explanation for this discrepancy could be that although SST-14 binds both SSTR2 and SSTR5 relatively equally, activation of SSTR5 may favor the stabilization of homodimers. Indeed, when cells co-expressing SSTR2 and SSTR5 are treated with SST-14, SSTR5 dimers exhibit dose-dependent formation (Fig. 4C.1D). Furthermore, this could also explain why treatment with the SSTR5-selective compound, L-817,818, does not modulate heterodimerization. Selectivity in the heterodimerization of SSTRs has been reported earlier upon investigation of a SSTR4/SSTR5 heterodimer; co-activation by SST-14 in cells co-expressing both receptor subtypes did not induce an interaction [Rocheville et al., 2000b]. Although co-activation was not favorable for the heterodimerization of SSTR2 and SSTR5, it has been demonstrated as a requirement in the modulation of other GPCR combinations [Gines et al., 2000; Grant et al., 2004b; Jiang et al., 2006; Kearn et al., 2005; Mellado et al., 2001b; Patel et al., 2002a; Pello et al., 2008; Rodriguez-Frade et al., 2004; Yoshioka et al., 2002]. For instance, in the heterodimerization of SSTR1 and SSTR5, concurrent activation was shown to foster an association [Grant et al., 2004b; Patel et al., 2002a]. Heterodimerization between the growth hormone secretagogue and

dopamine D1 receptors was shown to occur by co-activation using both co-immunoprecipitation and bioluminescence resonance energy transfer techniques [Jiang et al., 2006]. Furthermore, the interaction significantly increased dopamine induced cAMP accumulation, a property that is suggested to play an important physiological role given that both receptors are co-expressed in neuronal subpopulations. In a recent report, heterodimerization of the CXCR4 chemokine receptor and the delta opioid receptor in immune cells was stabilized by simultaneous addition of their ligands, whereas individual activation caused dissociation of the complex [Pello et al., 2008]. Interestingly, the heterodimer suppresses signalling, suggesting a dominant negative effect on receptor function [Pello et al., 2008].

Activated GPCRs undergo desensitization followed by internalization in order to terminate signalling; this process usually requires phosphorylation of the receptor by a G-protein coupled receptor kinase, promoting high-affinity binding of β-arrestins [Tsao et al., 2001]. Once bound, β-arrestins prohibit the coupling of G-protein to the receptor and promote internalization by recruiting several factors involved in this machinery [Lefkowitz and Shenoy, 2005]. Only certain members of the somatostatin receptor family exhibit high affinity binding to β-arrestins [Tulipano et al., 2004]. We demonstrate that activated SSTR2 and not SSTR5 are capable of initiating an interaction (Fig. 4C.4A). This may indicate that although SSTR5 internalizes following activation with agonist, it does so without the involvement of β-arrestin. The mechanisms underlying the internalization of SSTR5 are still unclear however, evidence suggests that it may be occurring through clathrin-coated pits [Hukovic et al., 1998; Hukovic et al., 1999; Stroh et al., 2000b]. GPCRs that do interact with β-arrestins are further categorized as class A or class B, depending on their mode of interaction. Although both classes of GPCRs differ in their affinity for β-arrestin subtypes, they are most notably distinguished based on their avidity to β-arrestin: β-arrestin rapidly dissociates from class A receptors during internalization but remains associated with class B receptors, as it is found co-localized in the form of endosomes within cells [Lefkowitz and Shenoy, 2005]. When HEK 293 cells expressing SSTR2 are stimulated with either agonist SST-14 or L-779,976 for an extended period, β-arrestin is prompted to aggregate and remain with the receptor

throughout internalization. Treatment of cells co-expressing both receptor-subtypes with SST-14 results in a similar feature; β-arrestin and SSTR2 co-localize in the form of endosomes. However, when treatment consisted of L-779,976 in lieu of SST-14, SSTR2 internalized without β-arrestin associating. In fact, within minutes of treatment β-arrestin translocates to SSTR2 at the cell surface, but quickly dissociates as there is no co-localization following receptor internalization (Fig. 4C.4B, 4C.5). This is analogous to class A receptors where β-arrestin does not remain as a complex throughout endocytosis.

Changes in the association of β-arrestin to the receptor during internalization are known to directly affect recycling rates: class A receptors recycle to the plasma membrane much quicker than class B receptors and are less likely to be degraded [Lefkowitz and Shenoy, 2005]. Indeed, heterodimerization does affect SSTR2 recycling rates. Following a 20-minute stimulus with L-779,976, SSTR2 internalizes in both single and double expressing cell lines (Fig. 4C.7). However, the striking difference arises when co-expressing cells are treated with L-779,976 for extended periods. Under these conditions, an increase in the cell surface localization of SSTR2 is observed, with a concomitant decrease in intracellular receptor. These results are consistent with those of Sharif et al., where extensive loss of cell surface SSTR2 is seen following stimulation of co-expressing cells with SST-14 and not with the SSTR2-specific agonist L-779,976, which causes SSTR2 to be recycled back to the cell surface [Sharif et al., 2007]. In a report by Terrillon et al., a similar incidence was identified with the vasopressin V1a receptor, where upon heterodimerization with the vasopressin receptor-subtype V2, reverted its pattern of β-arrestin recruitment and endocytic recycling from class A to class B [Terrillon et al., 2004]. In case of the neurotensin receptors, heterodimerization between NTS1 and NTS2 influenced the subcellular distribution and capacity to down-regulate agonist-stimulated NTS1 [Perron et al., 2007]. Similarly, heterodimerization between β-adrenergic receptor subtypes β_1AR and β_2AR and the SSTR1 and SSTR5 subtypes affect ligand-induced receptor-internalization [Lavoie et al., 2002; Rocheville et al., 2000b].

Several lines of evidence implicate SSTRs in tumor regulation, in particular the subtype SSTR2, as it is well documented for its anti-proliferative effects and commonly

expressed in many tumors [Lamberts et al., 2002]. Inhibiting cell proliferation by SSTR2-activation involves the upregulation of the cyclin-dependent kinase inhibitor $p27^{Kip1}$ [Pages et al., 1999], an important factor in pituitary tumorigenesis [Bamberger et al., 1999; Korbonits et al., 2002; Lidhar et al., 1999; Qian et al., 1996; Qian et al., 1998; Takeuchi et al., 1998]. Moreover, a mechanism describing the upregulation of $p27^{Kip1}$ involved an ERK1/2-dependent pathway [Lahlou et al., 2003]. Rapid recycling of SSTR2 could provide a mechanism for the observed increases in ERK1/2 phosphorylation (Fig. 4C.9). This could also explain the increased potency of L-779,976 to upregulate the cyclin-dependent kinase inhibitor $p27^{Kip1}$ and prolong cell growth inhibition (Fig. 4C.11 and 4C.13).

The SSTR2/SSTR5 heterodimer also increased the potency of L-779,976 to inhibit adenylyl cyclase activity by approximately 20-fold (Fig. 4C.8; Table 4C.1). Similar findings were reported for the SSTR1/SSTR5 heterodimer [Grant et al., 2004b] and suggest that heterodimerization may also provide positive cooperativity to receptor function. Indeed, heterodimerization of several other receptor combinations including the dopamine D2 receptor and SSTR5 were also reported to enhance GPCR signaling [AbdAlla et al., 2000; Gomes et al., 2004; Rocheville et al., 2000a; Scarselli et al., 2001; Waldhoer et al., 2005; Yoshioka et al., 2001; Zhu et al., 2005]. Although changes in β-arrestin-association and endocytic recycling following heterodimerization could provide a mechanism for the observed increases in ERK activation and $p27^{Kip1}$ upregulation, positive cooperativity in G-protein signaling may also contribute (Fig. 4C.8; Table 4C.1). A PTX-sensitive $G\alpha_i$ G-protein-mediated signaling complex has been described in orchestrating ERK1/2 activation and cell growth inhibition, following activation of SSTR2 [Lahlou et al., 2003]. Because the carboxy-terminal tail of GPCRs is an important domain with which both G-proteins and β-arrestin interact, it is possible that heterodimerization could alter the properties of this motif, allowing for changes in cooperativity or β-arrestin recruitment. Modifications could arise either by structural changes in the carboxy-terminal tail itself or through its phosphorylation, as both are involved and presumed to affect the avidity of β-arrestin and G-protein to the receptor [Lefkowitz and Shenoy, 2005]. However, despite the possibility that each of the above

mentioned mechanisms may contribute to the enhanced signaling observed following heterodimerization, further investigation is required to mechanistically link the pathways of relevance. Insight on the molecular determinants affected on heterodimerization is required given the emerging roles of GPCR interacting proteins on signal transduction [Bockaert et al., 2004].

It is noteworthy that although SSTR2 heterodimerizes with SSTR5, both protomers did not internalize as a complex and suggests the process is restricted to only the activated protomer (Fig. 4C.6). A similar phenomenon was reported for the SSTR2/SSTR3 heterodimer, where selective activation of SSTR2 resulted in its internalization without affecting the presence of SSTR3 [Pfeiffer et al., 2001]. Furthermore, heteromeric complexes between dopamine D1 and adenosine A1 receptors were shown to disappear when treated with D1 receptor agonists by forming clusters that were devoid of A1 receptors [Gines et al., 2000]. The μ- and δ-opioid receptor heterodimer was also shown not to endocytose as a complex but yet internalize as monomers when activated by agonists [Law et al., 2005]. Although formation of the prostaglandin-EP_1 and β_2-adrenergic heterodimer, directly decreased β_2-adrenergic receptor coupling to $G\alpha_s$; cross-regulation was not involved in attenuating β_2-adrenergic receptor-function as desensitization and internalization were factors affecting only the activated protomer [McGraw et al., 2006]. These results have important meaning as they imply that GPCR heterodimers are not necessarily static complexes, in which both protomers are regulated as a unit.

Since the initial reports providing direct evidence for the heterodimerization of the $GABA_B$ receptor, a requirement for proper receptor trafficking and function [Prinster et al., 2005], the pursuit of other receptor combinations has been sought. Although many such heterodimers have been reported, few have shown functional relevance. This makes their occurrence unclear, as there is no supporting evidence documenting an effect on cell physiology. In this study, we demonstrate that SSTR2 and SSTR5 form heterodimers, a process that leads to alterations in cell growth. Furthermore, agonist and more specifically, subtype-specific activation of SSTR2 modulates the interaction. Heterodimerization between SSTR2 and SSTR5 may provide a mechanism for the lack of

tolerance seen with currently available SST-analogs and their ability in controlling pituitary tumour growth. An understanding on the mechanics involved in GPCR dimerization could offer a rationale in future drug design.

ACKNOWLEDGEMENTS

We thank S.A. Laporte for the β-arrestin-GFP and GRK_2 constructs, A. Abdallah for his technical assistance and G.H. Hendy for his support and critical feedback on the manuscript.

FIGURE LEGENDS

Figure 4C.1.

Modulation of SSTR heterodimerization by agonist.

A, Western blots of membrane proteins (50 μg) from HEK 293 cells stably expressing SSTR5 (lane 1) and SSTR2 (lane 2). B, Co-immunoprecipitation of membranes from HEK 293 cells co-expressing SSTR2 and SSTR5 treated with various concentrations of the indicated agonist prior to immunoprecipitation with anti-HA antibody. Membrane lysates were subjected to Western blotting with anti-c-Myc antibody. A band of approximately 105 kDa appeared as the heterodimer. C, Densotometric analysis on immunoblots in (B) treated with L-779,976 showing significant increases in heterodimerization. Data were analyzed using ANOVA, posthoc Dunnett's to compare against basal. D, PbFRET microscopy on HEK 293 cells stably expressing both SSTR2 and SSTR5 following treatment with 10 nM of the indicated agonists. FRET efficiencies were analyzed using ANOVA, posthoc Dunnett's and compared to control. E, Co-expressing cells treated with various concentrations of SST-14 and processed for pbFRET microscopy using anti-Myc monoclonal antibodies conjugated to either fluorescein (donor) or rhodamine (acceptor), to measure for SSTR5 dimerization only. Data were analyzed using ANOVA, posthoc Dunnett's to compare against basal. Immunoblots and means ± SEMs are representative of at least three independent experiments; *, $p < 0.05$; **, $p < 0.01$; ***, $p < 0.001$.

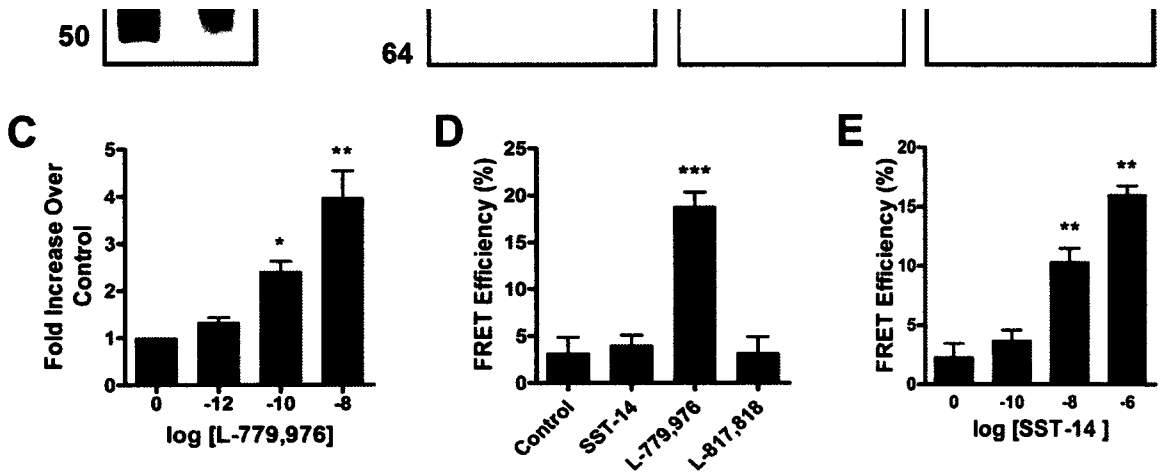
50
64
C
Fold Increase Over Control
0
1
2
3
4
5
*
**
0
-12
-10
-8
log [L-779,976]
D
FRET Efficiency (%)
0
5
10
15
20
25
***
Control
SST-14
L-779,976
L-817,818
E
FRET Efficiency (%)
0
5
10
15
20
**
**
0
-10
-8
-6
log [SST-14]

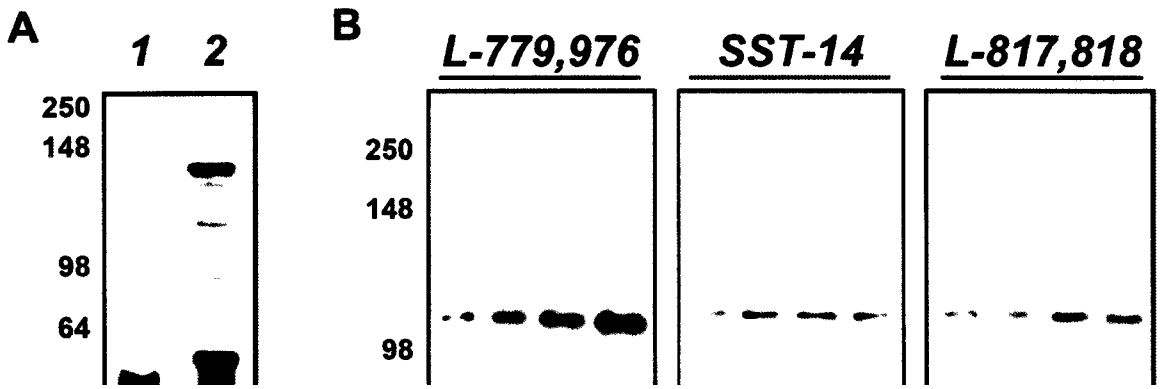
A
1
2
250
148
98
64
B
L-779,976
SST-14
L-817,818
250
148
98

Figure 4C.2

Co-immunoprecipitation of c-Myc-SSTR5 and HA-SSTR2.

Co-immunoprecipitation of membranes from HEK 293 cells co-expressing SSTR2 and SSTR5 treated with 10 nM of the indicated agonist prior to immunoprecipitation with anti-c-Myc antibody. Membrane lysates were subjected to Western blotting with anti-HA antibody. A band of approximately 105 kDa appeared following treatment with L-779,976, representing the heterodimer. Also observed to some extent is the monomeric form of SSTR2, just above the heavy chain of IgG (IgG_H).

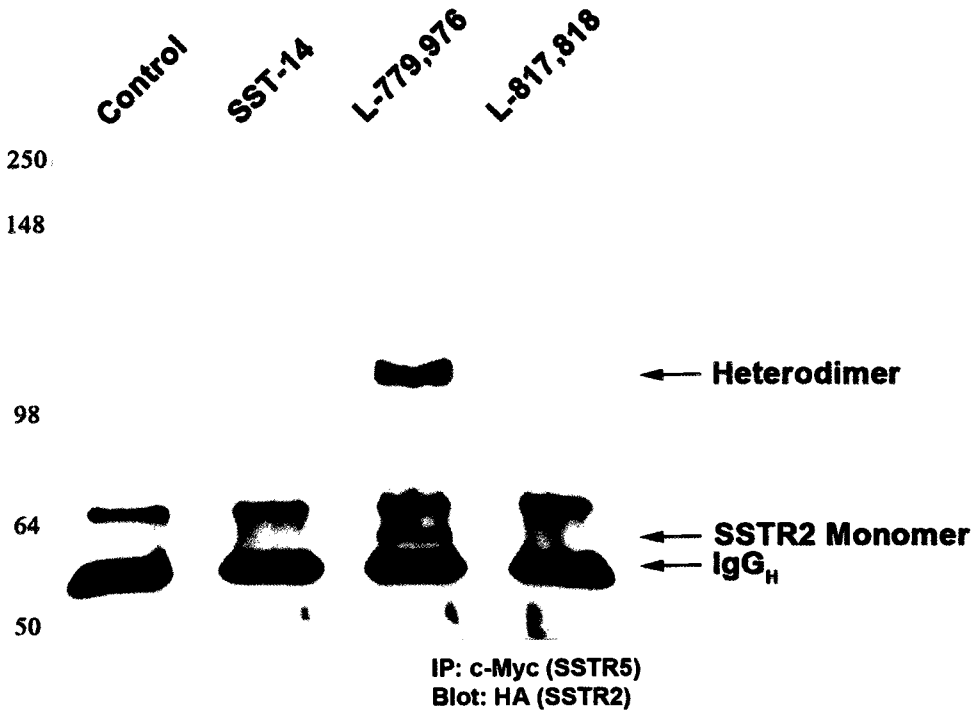
Control
SST-14
L-779,976
L-817,818
250
148
98
64
50
Heterodimer
SSTR2 Monomer
IgG$_H$
IP: c-Myc (SSTR5)
Blot: HA (SSTR2)

Figure 4C.3.

PbFRET microscopy on HEK 293 cells stably co-expressing SSTR2 and SSTR5.

A, Confocal microscopic images illustrating SSTR2 using monoclonal anti-HA antibody conjugated to FITC/donor (green) and SSTR5 using rabbit anti-c-Myc antibody conjugated to rhodamine/acceptor (red) and their colocalization (yellow) in HEK 293 cells. B, A representation of pbFRET microscopy on HEK 293 cells treated with 10 nM L-779,976. A selection of photobleaching micrographs taken from cells incubated with donor antibody alone under constant illumination of 488 nm light. Below, a representative histogram time constant plot calculated from a portion of cell membrane on a pixel-by-pixel basis taken from approximately forty cells. The mean time constant is shown in black calculated from a Gaussian distribution curve (18.5 s). C, Photobleaching micrographs from cells incubated with both donor and acceptor antibodies showing increases in the photobleaching time constant (23.2 s).

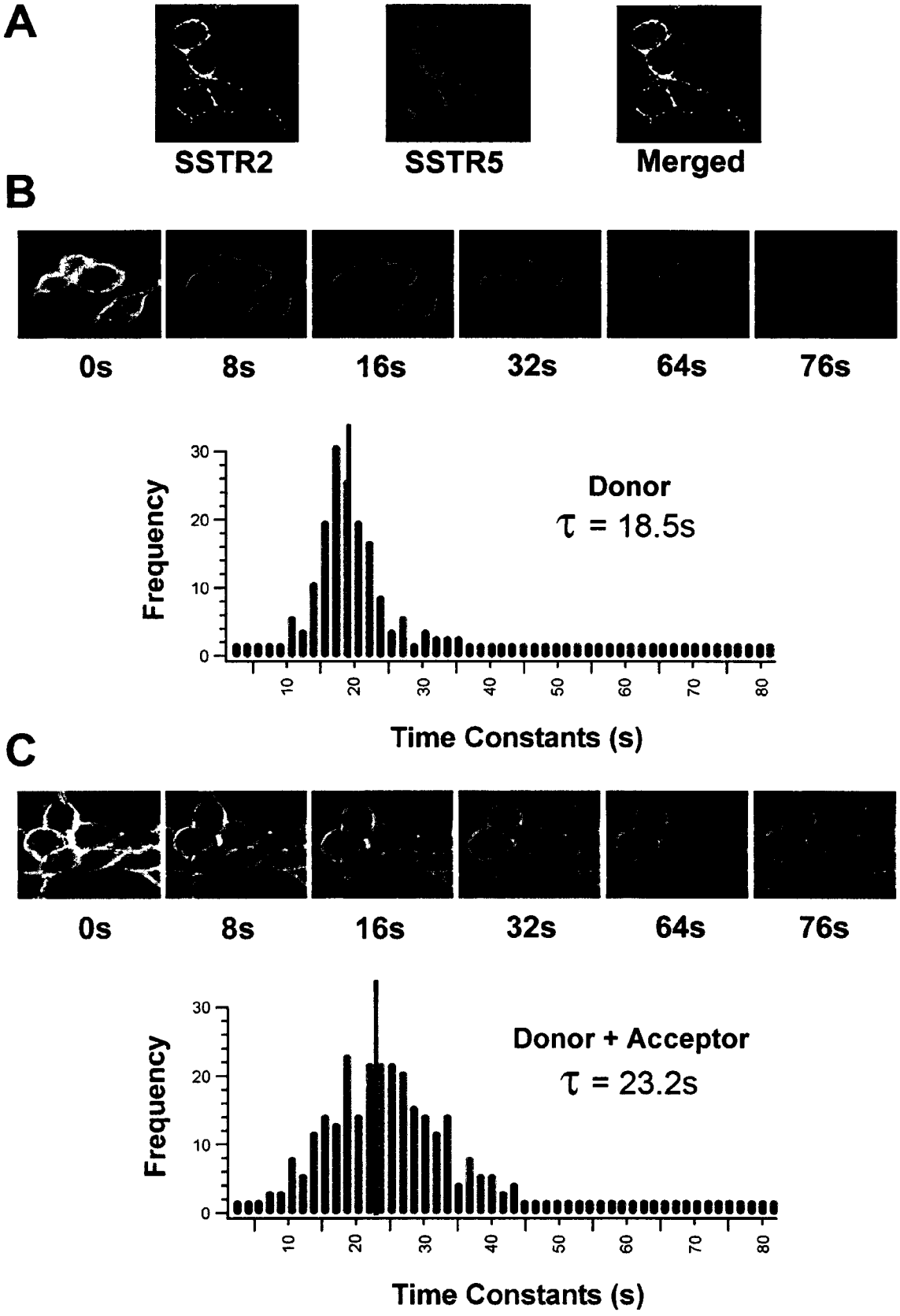
A
SSTR2
SSTR5
Merged
B
0s
8s
16s
32s
64s
76s
Frequency
Donor
τ = 18.5s
Time Constants (s)
C
0s
8s
16s
32s
64s
76s
Frequency
Donor + Acceptor
τ = 23.2s
Time Constants (s)

Figure 4C.4.

Differential trafficking of β-arrestin by SSTR2 and SSTR5.

Confocal microscopy of HEK 293 cells transiently transfected with either 1 μg of (A) SSTR2, SSTR5 or (B) a combination of each receptor, 0.25 μg β-arrestin$_2$-GFP and 0.5 μg GRK_2. Cells were treated with 10 nM of each agonist for the indicated times 48 hrs post-transfection (scale bar, 10 μm).

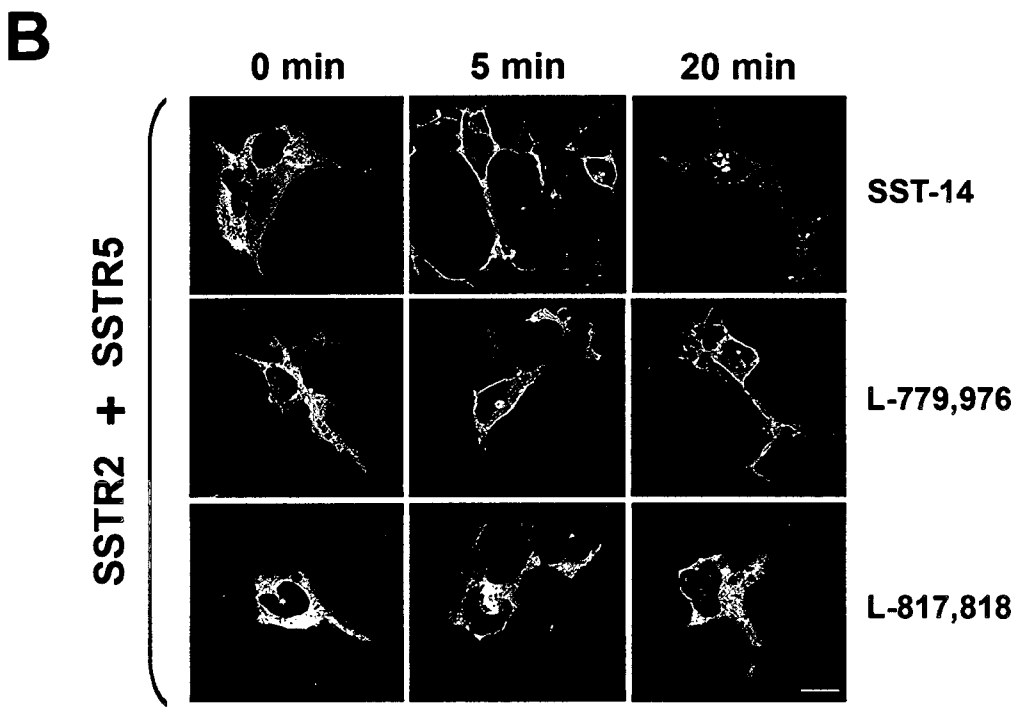
B
0 min
5 min
20 min
SSTR2 + SSTR5
SST-14
L-779,976
L-817,818

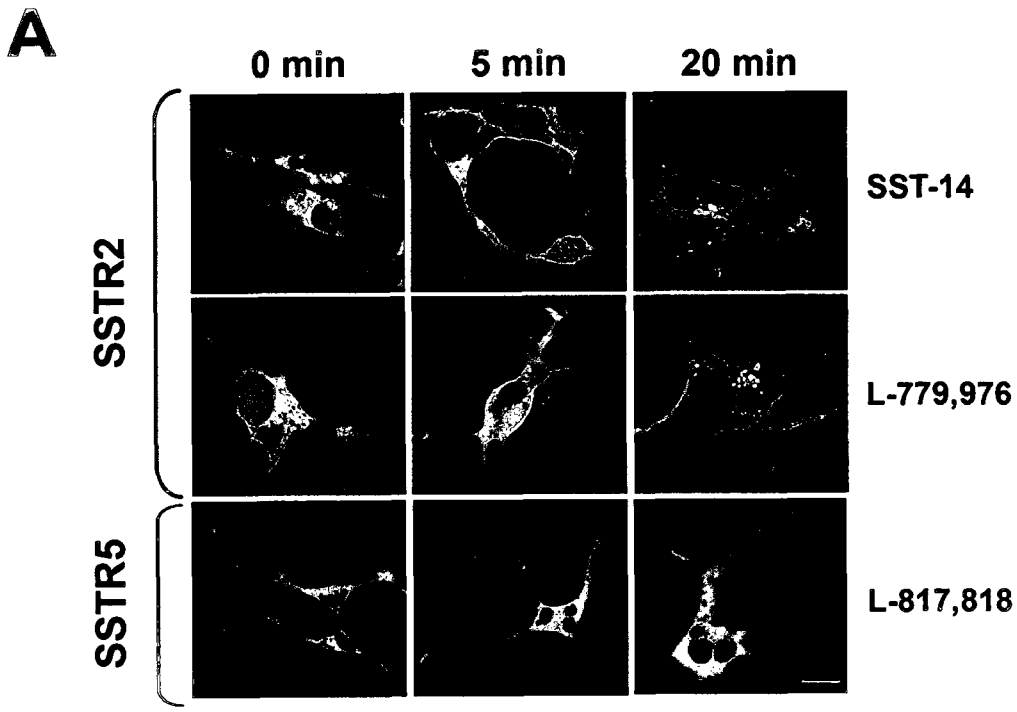
A
0 min
5 min
20 min
SSTR2
SSTR5
SST-14
L-779,976
L-817,818

Figure 4C.5.

Heterodimerization alters the association of *β*-arrestin to SSTR2.

HEK 293 cells were transiently transfected with 1 μg SSTR2, 1 μg SSTR5, 0.25 μg *β*-arrestin$_2$-GFP and 0.50 μg GRK$_2$. Cells were treated 48 hrs post-transfection with 10 nM of the indicated agonist. A, Confocal microscopy of cells treated with agonist showing *β*-arrestin (green) and SSTR2 (red) colocalization. Internalized receptor was imaged following cell permeablization (P). Images represent at least three independent experiments (scale bar, 10μM). B, Co-immunoprecipitation of SSTR2 and *β*-arrestin from HEK 293 cells stably expressing the indicated receptor subtypes. Cells were treated with either SST-14 or L-779,976 for 5 or 20 min. Cell lysate was immunoprecipitated for SSTR2 and immunoblotted against β-arrestin. A band at approximately 50 kDa is represented as *β*-arrestin. C and D, Densitometric analysis on immunoblots presented in (B). Data are represented as fold increase over control (0 min). Statistical analysis to determine significance from control was performed using two-way ANOVA posthoc Bonferroni (***, $p < 0.001$). Means ± SEMs are representative of three independent experiments.

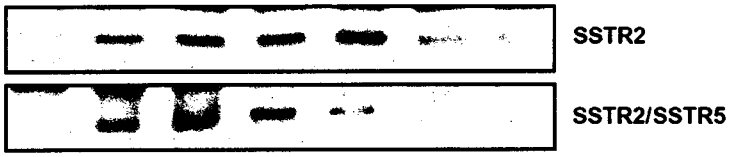
SSTR2
SSTR2/SSTR5

C

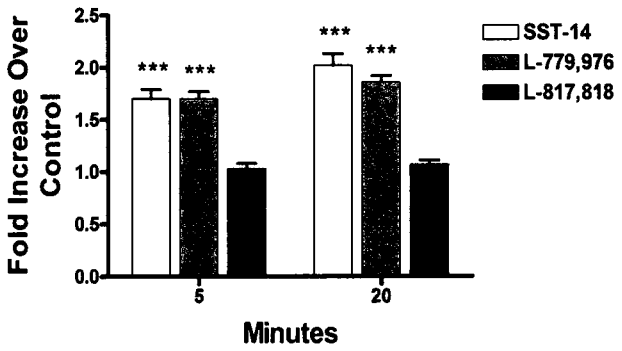
Fold Increase Over Control
2.5
2.0
1.5
1.0
0.5
0.0
***
***
***
***
5
20
Minutes
SST-14
L-779,976
L-817,818

D

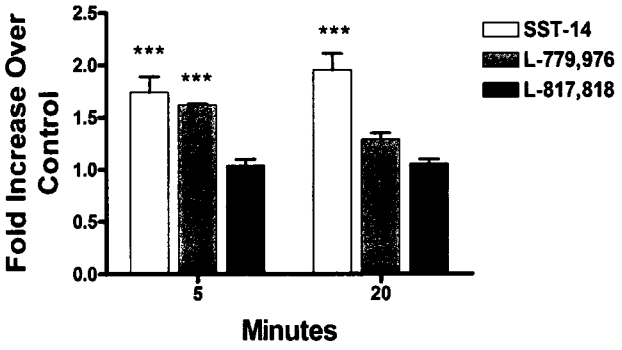
Fold Increase Over Control
2.5
2.0
1.5
1.0
0.5
0.0
***
***
***
5
20
Minutes
SST-14
L-779,976
L-817,818

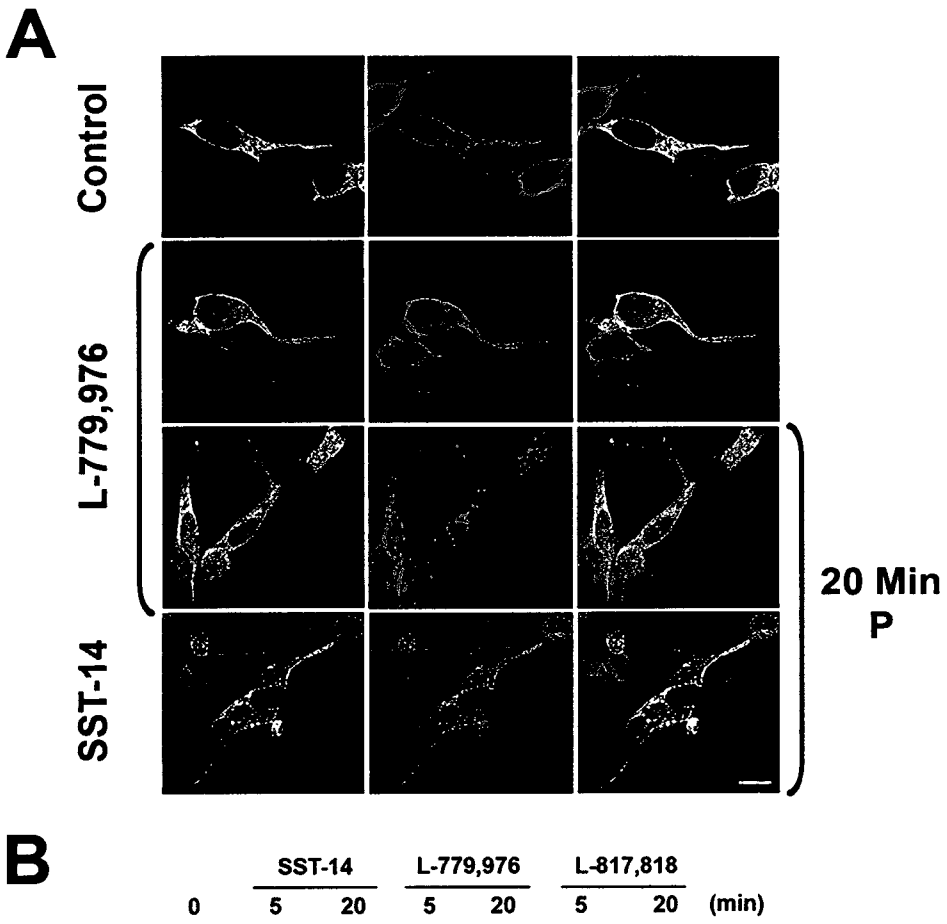
A
Control
L-779,976
SST-14
20 Min
P
B
SST-14
L-779,976
L-817,818
0
5
20
5
20
5
20
(min)

Figure 4C.6.

Agonist-promoted internalization of SSTR2 and SSTR5.

Confocal microscopy of HEK 293 cells stably expressing SSTR2 (red) and SSTR5 (green) following agonist stimulation. Cells were treated with 10 nM of the indicated agonist for 20 min, fixed then permeablized (P) prior to immunocytochemistry. Nuclei were counterstained with DAPI (blue). Images are a representation of at least three independent experiments (scale bar, 10 μm).

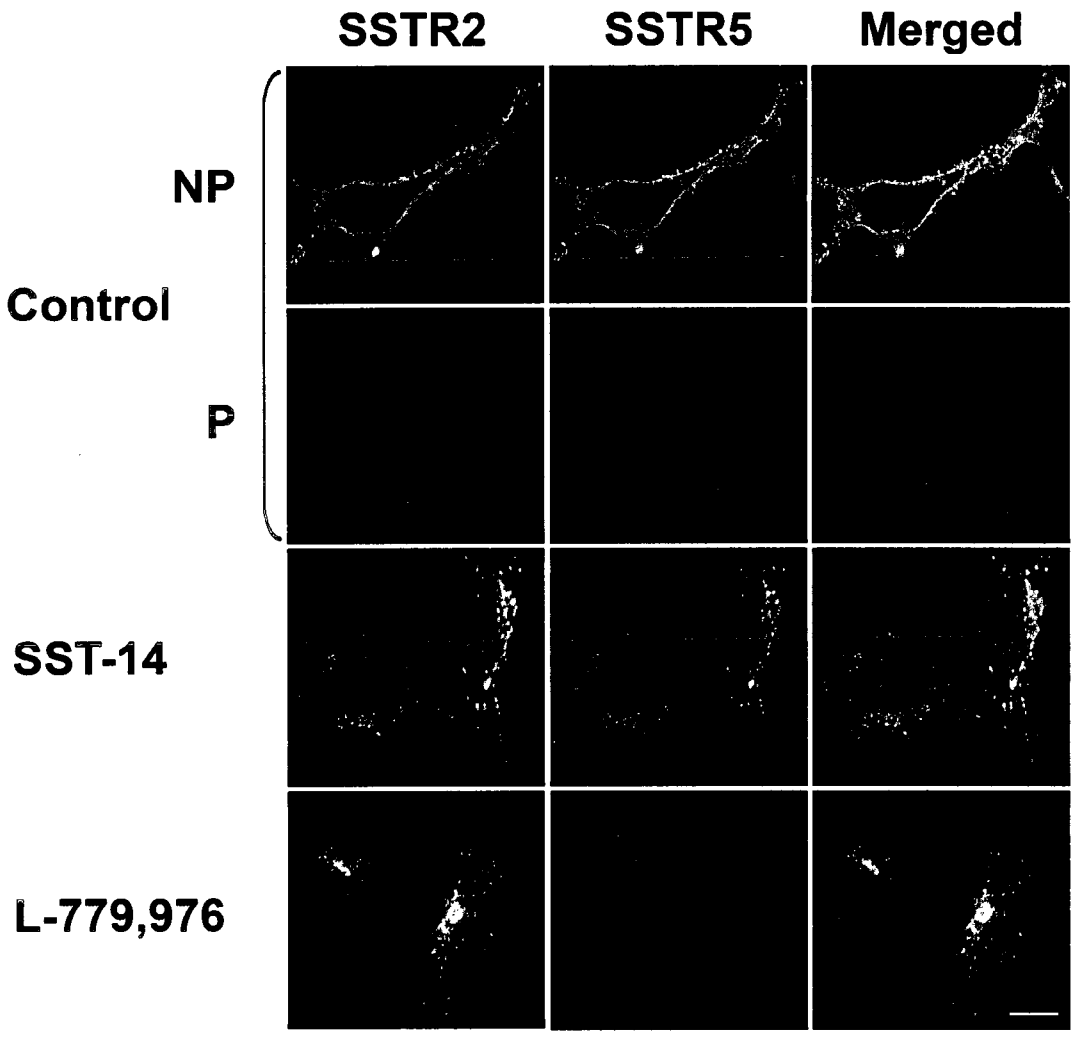
SSTR2
SSTR5
Merged
NP
Control
P
SST-14
L-779,976

Figure 4C.7.

Heterodimerization increases the recycling of SSTR2.

Confocal microscopic images of SSTR2 (red) trafficking following agonist stimulation. HEK 293 cells expressing SSTR2 or SSTR2 and SSTR5 were treated with 10 nM of agonist SST-14 or L-779,976 for 20 or 40 minutes. Immunostaining of SSTR2 was performed using monoclonal anti-HA antibody followed by incubation with anti-mouse IgG antibody conjugated to fluorescein. Internalized receptor was identified by immunocytochemistry in permeablized (P) cells; cell surface localization in non-permeablized (NP) cells. Nuclei were counterstained with DAPI (blue). Images are representative of at least three independent experiments (scale bar, 10 μm).

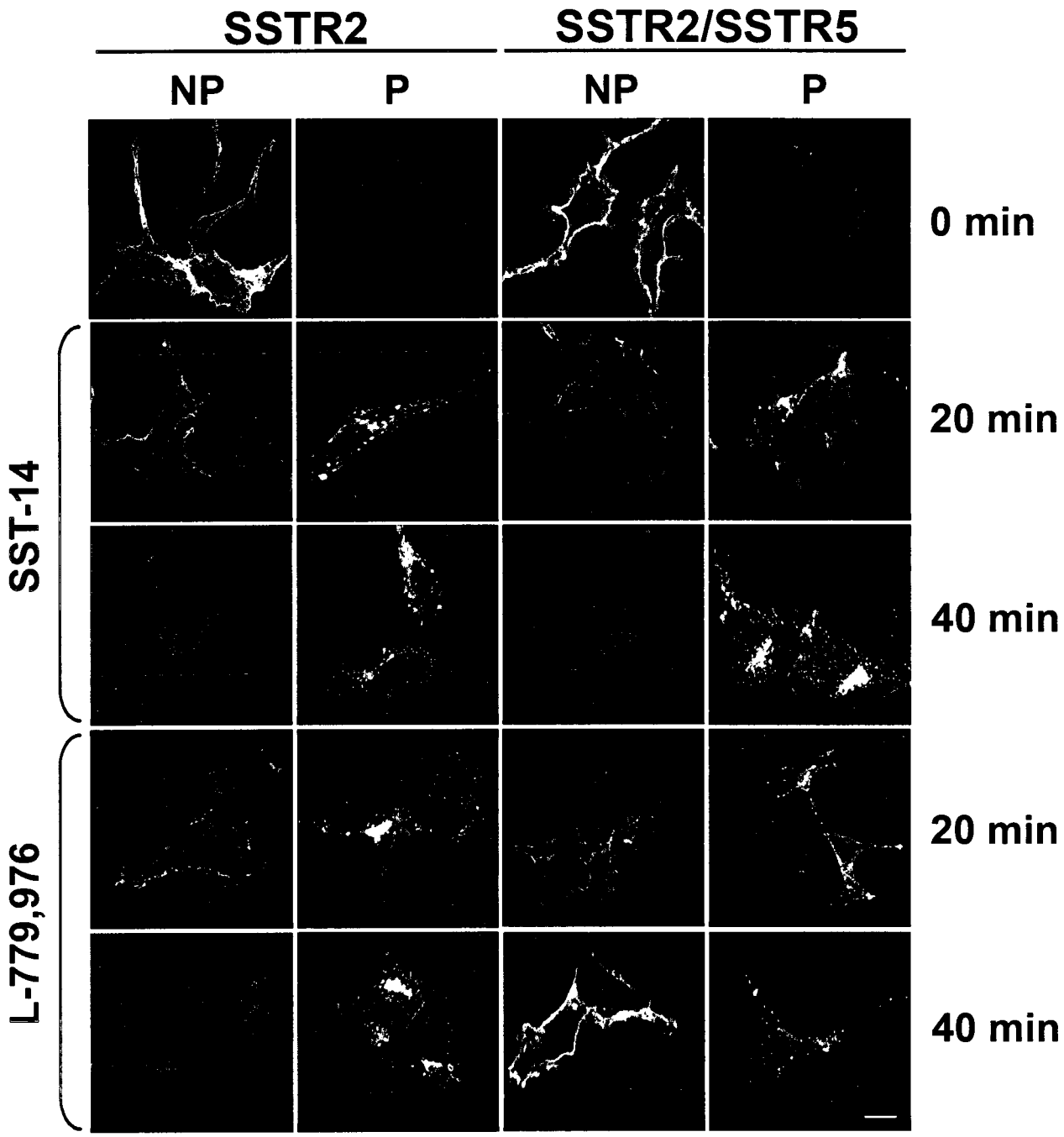
SSTR2
SSTR2/SSTR5
NP
P
NP
P
0 min
20 min
40 min
20 min
40 min
SST-14
L-779,976

Figure 4C.8.

Heterodimerization and effector coupling.

Inhibition of forskolin-stimulated cAMP synthesis in HEK 293 cells stably expressing SSTR2 and SSTR5 individually or in combination and treated with increasing concentrations of (A) L-779,976, (B) SST-14 and (C) L-817,818 calculated as a percent of maximum inhibition. Data were plotted and analyzed following a sigmoidal dose-response equation using Graph Pad Prism 4.0. D, Total inhibition of cAMP production following 10 nM treatment of each agonist in stably transfected cells. E, GTP-binding of membranes extracted from HEK 293 cells stably expressing SSTR2 and SSTR5 treated with 10 nM of the indicated agonists. Binding was inhibited when membranes were pre-treated with PTX. Statistical analysis was performed using ANOVA, posthoc Dunnett's to compare for significance from PTX treated membranes. Means ± SEMs are representative of at least three independent experiments performed in duplicate; ***, $p < 0.001$.

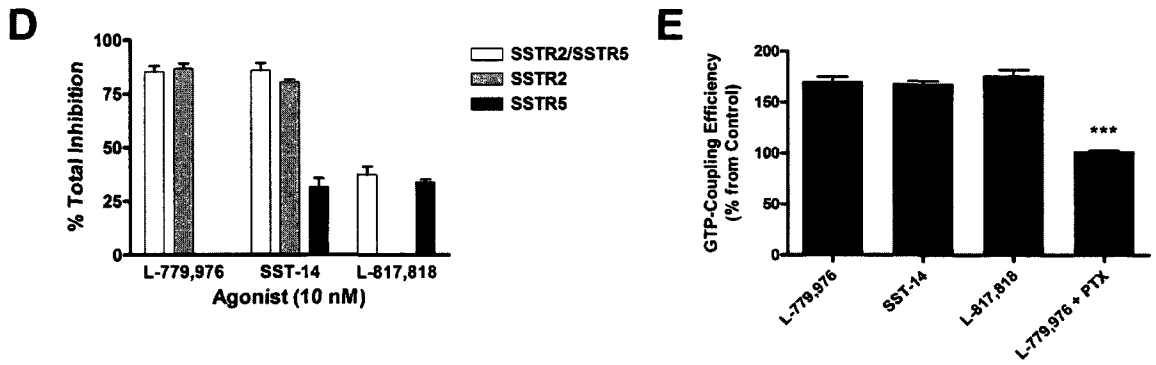
D
100
75
50
25
0
% Total Inhibition
L-779,976
SST-14
L-817,818
Agonist (10 nM)
SSTR2/SSTR5
SSTR2
SSTR5
E
200
150
100
50
0
GTP-Coupling Efficiency
(% from Control)
***
L-779,976
SST-14
L-817,818
L-779,976 + PTX

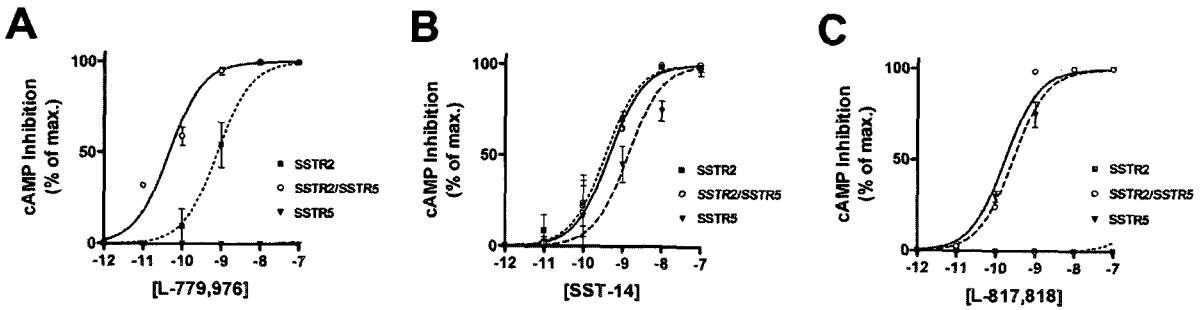
A
B
C
cAMP Inhibition (% of max.)
100
50
0
-12
-11
-10
-9
-8
-7
[L-779,976]
[SST-14]
[L-817,818]
SSTR2
SSTR2/SSTR5
SSTR5

Figure 4C.9.

The effects of heterodimerization on ERK1/2 phosphorylation.

A, HEK 293 cells stably expressing SSTR2 or SSTR2 and SSTR5 were treated with 10 nM of L-779,976 for the indicated times. In case of pertussis toxin (PTX), cells were pretreated 18 hrs prior to agonist stimulation. Cell lysates were subjected to Western blotting and immunoblotted for ERK1/2 proteins. B, Densitometry was performed on phosphorylated ERK1/2 immunoblots in (A). β-tubulin was used to standardize for protein loading. Data were analyzed by ANOVA, posthoc Dunnett's to compare for significance over basal; **, $p < 0.01$. Two-way ANOVA was performed to compare the significance of ERK1/2 phosphorylation between mono-transfected and co-transfected cells; ##, $p < 0.01$; ###, $p < 0.001$. Means ± SEMs are representative of three independent experiments. C, HEK 293 cells stably co-expressing SSTR2 and SSTR5 were treated with 10 nM SST-14 for the indicated times. Cell lysate was collected, subjected to Western blotting and immunoblotted for the designated proteins.

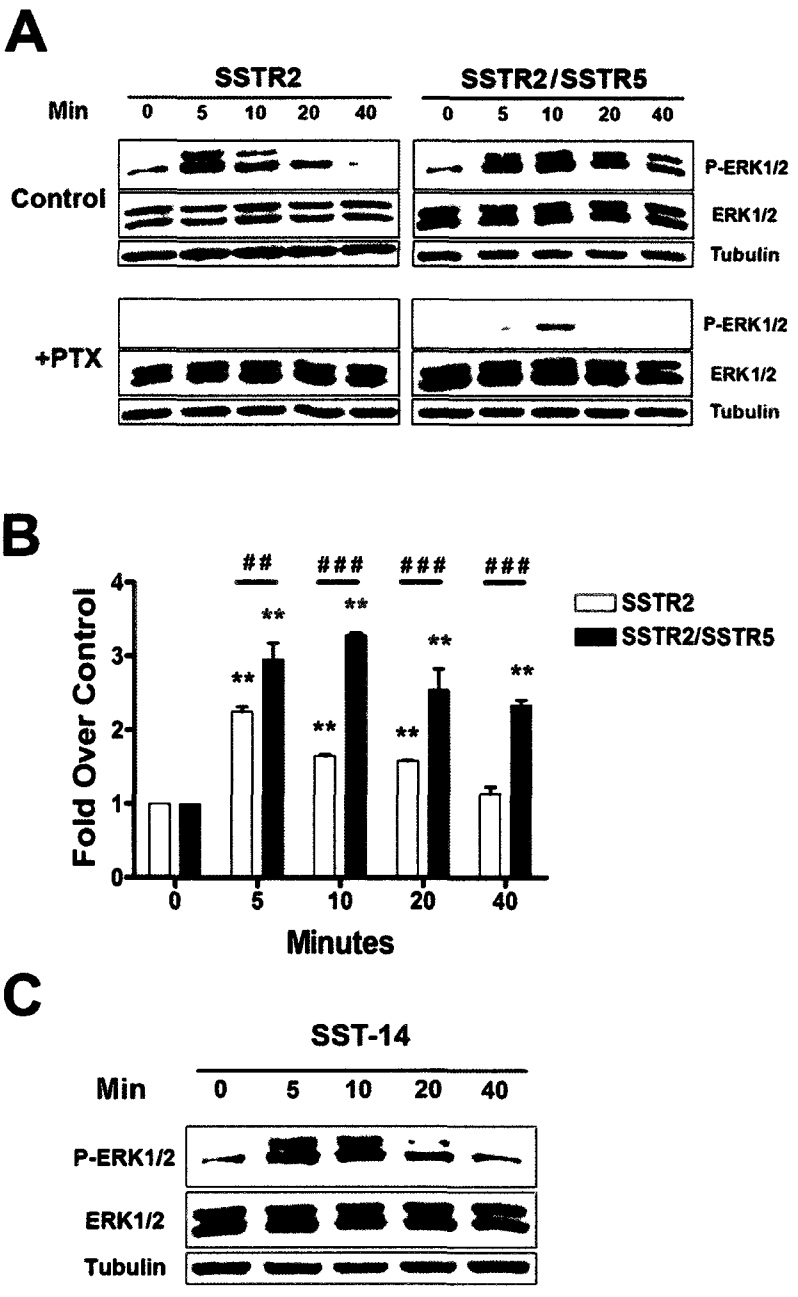
A
SSTR2
SSTR2/SSTR5
Min
0 5 10 20 40
0 5 10 20 40
Control
+PTX
P-ERK1/2
ERK1/2
Tubulin
P-ERK1/2
ERK1/2
Tubulin
B
Fold Over Control
Minutes
SSTR2
SSTR2/SSTR5
C
SST-14
Min
0 5 10 20 40
P-ERK1/2
ERK1/2
Tubulin

Figure 4C.10

The effects of L-817,818 on ERK1/2 phosphorylation in co-expressing cells.

HEK 293 cells stably co-expressing SSTR2 and SSTR5 were treated with 10 nM of L-817,818 for the indicated times. Cell lysates were subjected to Western blotting and immunoblotted for ERK1/2 proteins.

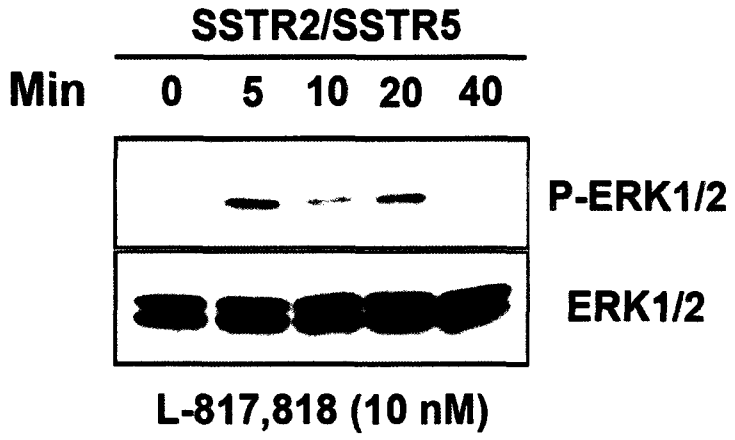
SSTR2/SSTR5
Min
0
5
10
20
40
P-ERK1/2
ERK1/2
L-817,818 (10 nM)

Figure 4C.11.

Heterodimerization potentiates the upregulation of $p27^{Kip1}$.

(A) Upper panel: HEK 293 cells stably expressing SSTR2 and SSTR5 were serum deprived for 24 hrs followed by treatment with the indicated concentrations of each agonist in the presence of 5% FBS, with FBS alone (FBS) or in its absence (Control) for 3 hrs. Cell lysates were subjected to Western blot and probed for $p27^{Kip1}$ expression. Lower panel: Densitometry on $p27^{Kip1}$ immunoblots standardized for protein loading using β-tubulin. Data were analyzed by ANOVA posthoc Dunnett's to determine significance of FBS vs. treated (**, $p < 0.01$). (B) Upper panel: Immunoblot of lysates from HEK 293 cells stably expressing SSTR2 and treated with the indicated concentrations of each agonist and FBS for 3 hrs. Lower panel: Densitometry on $p27^{Kip1}$ immunoblots. Statistical analysis using ANOVA posthoc Dunnett's to determine significance of FBS vs. treated (**, $p < 0.01$).

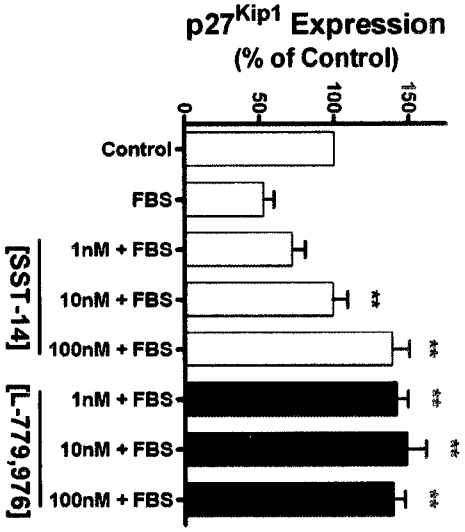
p27Kip1 Expression
(% of Control)
0
50
100
150
Control
FBS
[SST-14]
1nM + FBS
10nM + FBS
100nM + FBS
[L-779,976]
1nM + FBS
10nM + FBS
100nM + FBS
**
**
**
**
**

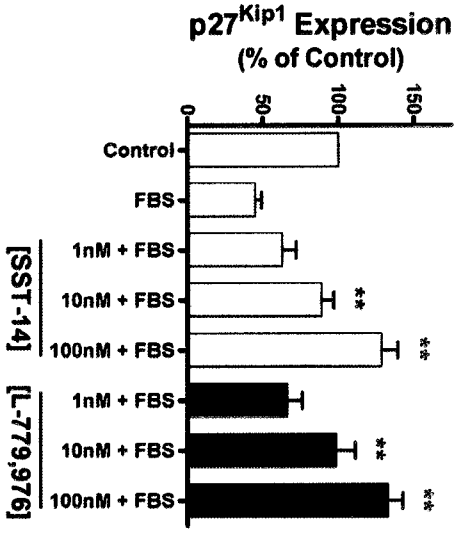
p27Kip1 Expression
(% of Control)
0
50
100
150
Control
FBS
[SST-14]
1nM + FBS
10nM + FBS
100nM + FBS
[L-779,976]
1nM + FBS
10nM + FBS
100nM + FBS
**
**
**
**
**

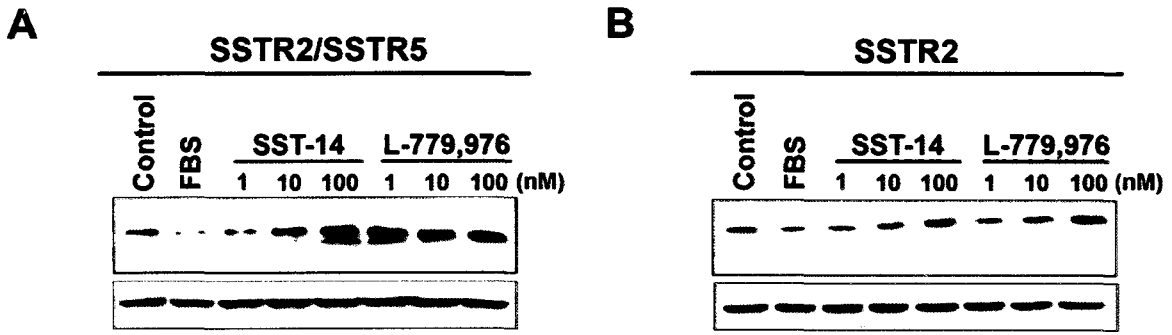
A
SSTR2/SSTR5
Control
FBS
SST-14
L-779,976
1 10 100 1 10 100 (nM)
B
SSTR2
Control
FBS
SST-14
L-779,976
1 10 100 1 10 100 (nM)

Figure 4C.12.

Induction of $p27^{Kip1}$ in cotransfected cells treated with L-817,818.

HEK 293 cells stably expressing SSTR2 and SSTR5 were serum deprived for 24 hrs followed by treatment with 100 nM of L-817,818 in the presence of 5% FBS, with FBS alone (FBS) or in its absence (Control) for 3 hrs. Cell lysates were subjected to Western blot and probed for $p27^{Kip1}$ expression.

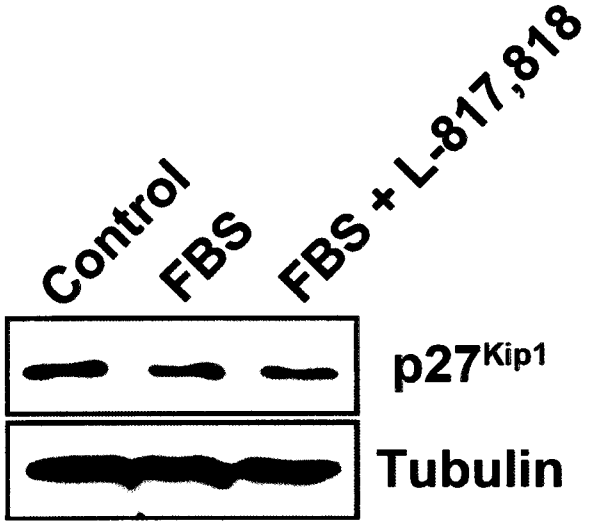
Control
FBS
FBS + L-817,818
p27Kip1
Tubulin

Figure 4C.13.

SSTR heterodimers enhance cell growth inhibition.

A and B, growth inhibition of stably transfected HEK 293 cells treated with 1 nM SST-14 and L-779,976 for 24-72 hrs as a percent of control in the presence of 5% FBS. Two-way ANOVA was used to determine the significance between drug treatments (*, $p < 0.05$). Means ± SEMs are representative of at least four independent experiments.

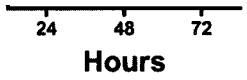
24
48
72
Hours

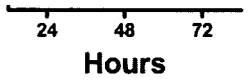
24
48
72
Hours

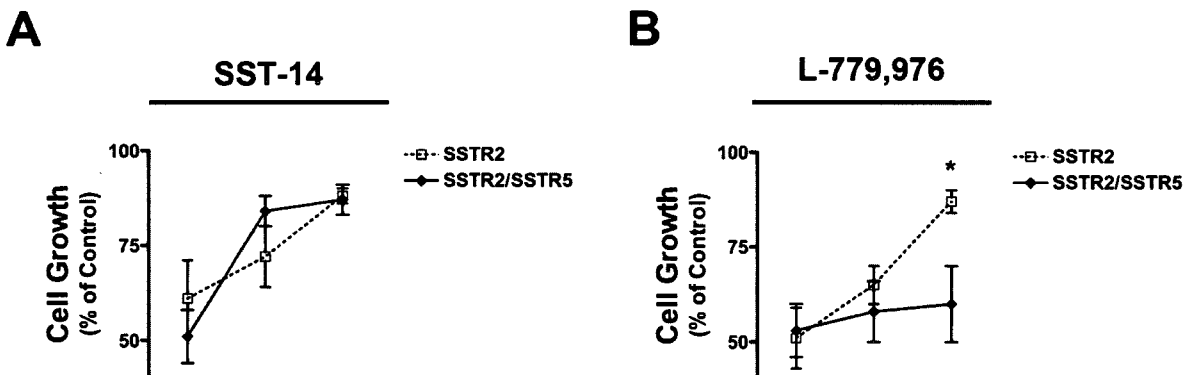
A
SST-14
Cell Growth
(% of Control)
100
75
50
SSTR2
SSTR2/SSTR5
B
L-779,976
Cell Growth
(% of Control)
100
75
50
*
SSTR2
SSTR2/SSTR5

Table 4C.1

Comparison of adenylyl cyclase coupling efficiencies by SSTR agonists.

HEK 293 cells stably expressing SSTR2 and SSTR5 or co-expressing both receptors (SSTR2/R5) were treated with various concentrations of each agonist in the presence of 20 μM forskolin and measured for cAMP accumulation. EC_{50} values represented in nM are the half-maximal inhibition of forskolin induced cAMP production. Means ± SEMs represent three independent experiments performed in duplicate.

	Agonists		
Receptors	**L-779,976**	**SST-14**	**L-817,818**
SSTR2 –	0.84 ± 0.20	0.38 ± 0.10	>1000
SSTR2/R5 –	0.04 ± 0.01	0.46 ± 0.10	0.16 ± 0.03
SSTR5 –	>1000	1.40 ± 0.38	0.25 ± 0.02

SECTION 5: DISCUSSION

Summary

Our laboratory has previously reported on the homodimerization of hSSTR5, a receptor where dimerization is regulated by agonist in a dose-dependent manner [Rocheville et al., 2000b]. It was also demonstrated that hSSTR5 could heterodimerize with hSSTR1, a property that is similarly regulated by the agonist SST-14 [Patel et al., 2002a]. Surprisingly, it was revealed that unlike hSSTR5, hSSTR1 does not homodimerize but remains monomeric regardless of its activation by agonist [Patel et al., 2002a]. However, given this understanding, it remained unclear as to the importance of agonist-activated hSSTR1 in the formation of the hSSTR1/hSSTR5 heterodimer, the possible molecular determinants implicated in the interaction and the significance of heterodimerization on the pharmacology of the receptors. In section 4A, I demonstrate using both co-immunoprecipitation and pbFRET microscopy, that either co-stimulation or selective activation of SSTR5 but not SSTR1 is capable of modulating heterodimerization in stably-co-expressing cells [Grant et al., 2004b]. The intriguing observation that hSSTR1 is incapable of forming homo- or heterodimers in either an active or inactive state (Fig. 4A.2, 4A.3) [Grant et al., 2004b; Patel et al., 2002a] and is the only receptor in the hSSTR family that is resistant to internalization and upregulates following prolonged agonist treatment [Hukovic et al., 1996; Hukovic et al., 1999], prompted us to investigate whether common molecular determinants are involved in these processes. The importance of the carboxyl-terminal tail in GPCR dimerization has been demonstrated earlier: on investigation of the δ-opioid receptor-trafficking [Cvejic and Devi, 1997], in the masking of an ER retention motif on heterodimerization of the γ-aminobutyric acid receptor-subtypes ($GABA_BR$) $GABA_BR1$ and $GABA_BR2$ [Kuner et al., 1999; White et al., 1998] and in generation of the μ- and δ-opioid receptor heterodimer [Fan et al., 2005]. Similarly, in line with the results of Fan et al., the heterodimerization between μ- and δ-opioid receptors could also be modulated by uncoupling of G-protein from the receptors [Law et al., 2005]. Given that the carboxyl-terminal tails of GPCRs are important for G-

protein coupling, a mechanism for the heterodimerization of this receptor pair can be described. Furthermore, a detailed account on the heterodimerization of the adenosine A_{2A} and the dopamine D_2 receptors were shown to occur between the carboxyl-terminal tail of A_{2A} and the third intracellular loop of D_2 [Canals et al., 2003]. More specifically, the interaction was dependent on arginine-rich residues in the intracellular loop of the D_2 receptor with either two aspartate residues or a phosphorylated serine residue in the carboxyl-terminal portion of A_{2A} [Ciruela et al., 2004]. Incidentally, when the carboxyl-terminal tail of hSSTR1 was swapped for that of hSSTR5, not only is homodimerization possible but internalization of the receptor is also permitted following agonist-binding [Grant et al., 2004b; Hukovic et al., 1999].

Although heterodimerization did not significantly alter the binding affinities of the drugs tested (Table 4A.1), it did affect second messenger signalling. The inhibition of adenylate cyclase and cAMP synthesis, a typical hallmark of SSTR activation, is more efficient following heterodimerization. More specifically, an approximate 50-fold increase in signalling efficiency is seen with the drug octreotide (SMS 201-995) in cells co-expressing both hSSTR1 and hSSTR5 compared to hSSTR5 alone (Table 4A.2), despite its very low affinity to hSSTR1 [Patel, 1999]. However, although the signalling efficiency is increased the actual efficacy is not, a property that was instead decreased, suggesting that the formation of the heterodimer results in a new receptor with distinct signalling characteristics (Fig. 4A.5). This alteration in maximum coupling efficacy could have functional implications, as human prolactinomas show poor responses to octreotide treatment. These tumours originate from the pituitary and hyper-secrete the hormone prolactin. Coincidently, prolactinomas predominantly express hSSTR1 and hSSTR5 [Jaquet et al., 1999; Shimon et al., 1997b]. In cultured studies of human excised prolactinomas, tumours that displayed increased expression of hSSTR1 responded poorly to treatment with octreotide in controlling prolactin release, as opposed to those showing lower expression levels regardless of hSSTR5 expression [Jaquet et al., 1999].

In section 4B, I describe the dimerization properties of another member in the human somatostatin receptor family, the subtype hSSTR2. Many tumours often express hSSTR2, especially those of neuroendocrine origin [Lamberts et al., 2002], which is what

made this receptor-subtype an appropriate target to investigate. Using both co-immunoprecipition and pbFRET microscopy techniques, we determined that hSSTR2 exists at the cell surface as a preformed homodimer [Grant et al., 2004a]. To our astonishment, treatment with agonist causes it to dissociate into monomers (Fig. 4B.1). Although ligand-induced dissociation has been reported in the regulation of other GPCR combinations [Berglund et al., 2003; Cheng and Miller, 2001; Cvejic and Devi, 1997; Gines et al., 2000; Latif et al., 2002; Law et al., 2005; Pfeiffer et al., 2001], few have shown functional relevance for their occurrence. In the report by Cvejic and Devi, dissociation of δ-opioid receptor dimers was reported essential for proper receptor-internalization. However, regulated dimerization and not dissociation of the platelet activating factor receptor and the thyrotropin-releasing hormone receptor were shown to increase internalization [Perron et al., 2003; Song and Hinkle, 2005]. Further investigation on the dissociation of hSSTR2 dimers, like the δ-opioid receptor, led us to conclude its importance in receptor-internalization, as crosslinking hSSTR2 dimers to prevent dissociation, drastically impaired its internalization rate (Fig. 4B.2) [Grant et al., 2004a]. Interestingly, in a recent report by Duran-Prado et al., dissociation of porcine SSTR2 dimers was also determined to be a feature occurring prior to its internalization [Duran-Prado et al., 2007], possibly suggesting a common characteristic for this subtype amongst all species.

Lastly, the physiological relevance for SSTR dimerization was put to the test. We focused on the two SSTRs predominantly expressed in GH hyper-secreting pituitary adenomas, hSSTR2 and hSSTR5 [Jaquet et al., 2000; Park et al., 2004a]. SST-analogs are frequently administered as first line treatment in acromegaly, caused by GH hyper-secreting pituitary adenomas to regulate endocrine function [Tichomirowa et al., 2005]. Over 90% of patients on SST-analogs show decreases in circulating GH levels, while approximately 70% of those achieve biochemical normalization. In addition, SST-analog therapy frequently results in tumour shrinkage in roughly 50% of patients [Bevan, 2005; Ferrante et al., 2006; Lamberts et al., 2002; Melmed et al., 2005; Resmini et al., 2007; Zatelli et al., 2006]. It is known that GH secreting pituitary adenomas seldom undergo desensitization to treatment, as acromegalic patients rarely show any signs of

tachyphylaxis despite years of SST-analog therapy. Interestingly, this property is specific to tumours of the pituitary as neither islet cell or carcinoid tumours share this feature; prolonged administration usually results in desensitization and relapse, as symptoms invariably return [de Herder et al., 2003; Hofland and Lamberts, 2003; Lamberts et al., 1996]. Although a mechanism for this resistance to desensitization has not been fully elucidated, a functional association between SSTR2 and SSTR5, the two primary SSTRs expressed in these tumors [Jaquet et al., 2000; Park et al., 2004a], has been proposed to account for this behavior [Sharif et al., 2007]. This is unlike islet cell tumours or carcinoids of the gut, where SSTR2 expression predominates [de Herder et al., 2003]. Additional evidence on the importance of SSTR2 and SSTR5 co-expression on SST-analog therapy comes from a report by Ballarè et al., describing an acromegalic patient with a tumour harbouring a mutant SSTR5 resistant to treatment, despite the expression of SSTR2 [Ballare et al., 2001]. These reports and others, have suggested the formation of a putative SSTR2/SSTR5 heterodimer however, a physical interaction had yet to be documented [Ben-Shlomo et al., 2005; Ren et al., 2003].

In section 4C, our first objective was to demonstrate whether hSSTR2 and hSSTR5 physically interact, and if so, does agonist-binding regulate the interaction. To our surprise, treatment of stably-selected cells, ectopically co-expressing both hSSTR2 and hSSTR5, with the pan-agonist SST-14, did not modulate heterodimer formation (Fig. 4C.1 and 4C.2) [Grant et al., *in revision*]. This is contrary to regulation of the hSSTR1/hSSTR5 heterodimer, where treatment with SST-14 enhances its formation [Grant et al., 2004b; Patel et al., 2002a; Rocheville et al., 2000b]. Similarly, co-stimulation was a requirement in the stabilization of heterodimers between members of other GPCR subfamilies [Gines et al., 2000; Jiang et al., 2006; Kearn et al., 2005; Mellado et al., 2001b; Pello et al., 2008; Rodriguez-Frade et al., 2004; Yoshioka et al., 2002]. However, heterodimerization between dopamine receptor D2 and hSSTR5 [Rocheville et al., 2000a], dopamine receptor D2 and hSSTR2 [Baragli et al., 2007] and prostaglandin-EP1 and β_2-adrenergic receptors [McGraw et al., 2006] were found to be equally fostered following activation of just one of the receptor-protomers. When

hSSTR2 or hSSTR5 were selectively activated in our system, only the hSSTR2-specific agonist induced the formation of heterodimers (Fig. 4C.1) [Grant et al., *in revision*].

Selective activation of SSTR2 and not concurrent stimulation of both SSTR2 and SSTR5, was shown to reduce desensitization and increase the recycling rate of SSTR2 in both ectopically and endogenously expressing cells of murine origin [Sharif et al., 2007]. Indeed, we have also observed a similar characteristic with hSSTR2, as its recycling rate is greatly increased following its selective-activation in co-expressing cells (Fig 4C.7). Although the mechanism contributing to this increased recycling rate of SSTR2 remained unclear, earlier evidence had implicated β-arrestin in altering the endocytic/recycling path of the vasopressin V1a and V2 heterodimer [Terrillon et al., 2004]. Because rSSTR2 is known to interact with β-arrestin during endocytosis [Tulipano et al., 2004], we sought to determine whether there was a link between hSSTR heterodimerization, β-arrestin association and receptor recycling.

GPCRs often require the interaction of β-arrestins to internalize following their stimulation. This process is typically promoted by phosphorylation of the carboxyl-terminal portion of the receptor by a G-protein coupled receptor kinase (GRK). β-arrestins are responsible for the recruitment of several factors implicated in the internalization machinery including clathrin, AP-2 and ARF6, to name a few [Claing et al., 2002; Lefkowitz and Shenoy, 2005; Pierce et al., 2002]. There are two main types of β-arrestin mediated internalization, class A and class B, that are primarily dependent on the avidity of β-arrestin to the receptor. Class A GPCRs form transient interactions with β-arrestin during internalization, whilst class B GPCRs form stable interactions during and following their sequestration. The avidity of β-arrestin to the receptor has direct effects on receptor recycling rates, as class A GPCRs recycle back to the cell surface more efficiently than class B, which is often times sorted to the lysosomal compartment for degradation. Of the SSTRs investigated, only rSSTR2 and rSSTR3 were shown to form stable interactions with β-arrestin, indicative of a class B-dependent subtype [Tulipano et al., 2004]. In a similar vein, we also demonstrate the ability of hSSTR2 to sequester in a complex with β-arrestin following its stimulation with agonist (Fig. 4C.4 and 4C.5). This interaction occurs in a class B-dependent manner, as both the receptor

and β-arrestin remain associated during prolonged stimulation, similar to its rat homologue. Interestingly, β-arrestin does not remain associated with hSSTR2 in cells where hSSTR5 is co-expressed. This phenomenon is specific to the selective-activation of hSSTR2 and not the co-stimulation of both receptor-subtypes, as is the case when the pan-agonist SST-14 is employed (Fig. 4C.4 and 4C.5). Changes in this pattern of β-arrestin association following heterodimerization directly affects the recycling rates of hSSTR2 (Fig. 4C.7), similar to that observed for murine SSTR2 in ectopically and endogenously co-expressing cells [Sharif et al., 2007].

The effects of hSSTR2/hSSTR5 heterodimerization extend beyond receptor recycling to include modifications in cell signalling and cell growth. Firstly, we demonstrate a greater efficiency for G-protein coupling, as the SSTR2-selective agonist, L-779,976, is 10-fold more potent at inhibiting adenylate cyclase in co-expressing cells than in cells expressing hSSTR2 alone (Fig. 4C.8). Secondly, heterodimers enhance and prolong the phosphorylation of MAPKs (Fig. 4C.9), a property that appears to be correlated with the desensitization/resensitization of hSSTR2, given that the receptor is recycled to the cell surface more efficiently (Fig. 4C.7). Thirdly, L-779,976 is more potent at inducing the cyclin-dependent kinase inhibitor $p27^{Kip1}$ in cells where both hSSTR2 and hSSTR5 are co-expressed (Fig. 4C.11). This property is specific to the formation of heterodimers and not the concurrent stimulation of both receptor-subtypes, as is the case with SST-14 treatment. Lastly, heterodimerization demonstrates prolonged growth inhibitory characteristics (Fig. 4C.13), an important aspect in tumour control. We provide a possible mechanism for the lack of tolerance seen with currently available SST-analogs in patients with GH hyper-secreting pituitary adenomas. Therefore, SST-analogs with superior selectivity for SSTR2 could offer greater therapeutic potential.

Conclusions

The concept of GPCR dimerization has come from fable to reality. It is known that GPCRs can dimerize however, the debate continues on their physiological relevance. Notwithstanding, is the controversy surrounding the concept of dynamically regulated

GPCR dimers, most notably by ligand binding. There is, however, little dispute over the issue of dimerization within the class C subfamily of GPCRs, as they represent a well-recognized example of constitutive dimers, where both protomers are linked for the most part by disulfide bridging between their large amino-terminal extracellular domains, with the exception of the $GABA_B$ receptor heterodimer [Bonde et al., 2006; Brauner-Osborne et al., 2007]. Nonetheless, the simplest model describing a GPCR signalling unit has been proposed and consists of one G-protein heterotrimer per receptor dimer [Baneres and Parello, 2003; Filipek et al., 2004; Fotiadis et al., 2004; Galvez et al., 2001; Goudet et al., 2005; Hague et al., 2004; Havlickova et al., 2002]. However, dimerization amongst the class A/Rhodopsin-like family of GPCRs is variable, as several recent reports have questioned their existence, particularly when receptor expression levels are kept to a minimum [Bayburt et al., 2007; Chabre and le Maire, 2005; Gripentrog et al., 2003; James et al., 2006; Meyer et al., 2006; Patel et al., 2002a; Rasmussen et al., 2007; Whorton et al., 2007; Whorton et al., 2008]. A more conservative approach in addressing this issue would be, depending on the receptor-subtype or microenvironment involved, GPCRs could adopt various states, albeit monomer/homodimer/heterodimer. Hence, it can be argued that dimerization is a form of regulation that is important in but not essential to receptor function.

The topic of GPCR heterodimerization holds particular interest in the development of novel therapeutics, as heterodimers have demonstrated changes in cooperativity and allosterism [Franco et al., 2007; Milligan, 2008; Prinster et al., 2005]. Recently, the opioid agonist 6'-guanidinonaltrindole, was shown to be selective for δ-/κ-opioid receptor heterodimers, with functional relevance *in vivo* [Waldhoer et al., 2005]. With respect to hSSTRs, we provide evidence on the unique pharmacological characteristics of the hSSTR1/hSSTR5 heterodimer, an interaction that is mediated by agonist, more specifically, ligand binding of hSSTR5 [Grant et al., 2004b]. Similarly, the hSSTR2/hSSTR5 heterodimer is also modulated by agonist, in this case, the selective-binding of hSSTR2 [Grant et al., *in revision*]. Like the hSSTR1/hSSTR5 heterodimer, the hSSTR2/hSSTR5 heterodimer presented with a pharmacological profile distinct from hSSTR2 and hSSTR5. Moreover, the heterodimer altered downstream signalling

pathways, leading to an extended growth inhibitory response. We also determined the dimerization properties of hSSTR2, a receptor that, unlike the previous hSSTRs investigated, forms constitutive dimers that dissociate following agonist binding [Grant et al., 2004a]. This unique feature of hSSTR2 is important for receptor trafficking, as preventing its dissociation mitigates agonist-mediated internalization. A schematic representing the known hSSTR combinations presented here is shown in figure 5.1.

It is of interest to map out the remaining possible hSSTR dimers, with particular emphasis on the formation of heterodimers. Our investigations on the hSSTR2/hSSTR5 heterodimer have lead to a probable mechanism for the absence of tolerance seen in the treatment of GH hyper-secreting adenomas with clinically available SST-analogs. Future studies should include the validation of hSSTR dimers *in vivo*, as a proof-of-concept, a possible task given the development of highly specific anti-hSSTR antibodies for use in pbFRET microscopy. An understanding on the mechanisms involved in GPCR dimerization could offer a rationale approach in the future design of novel therapeutics.

Figure 5.1

Schematic depicting the known hSSTR dimer pairs.

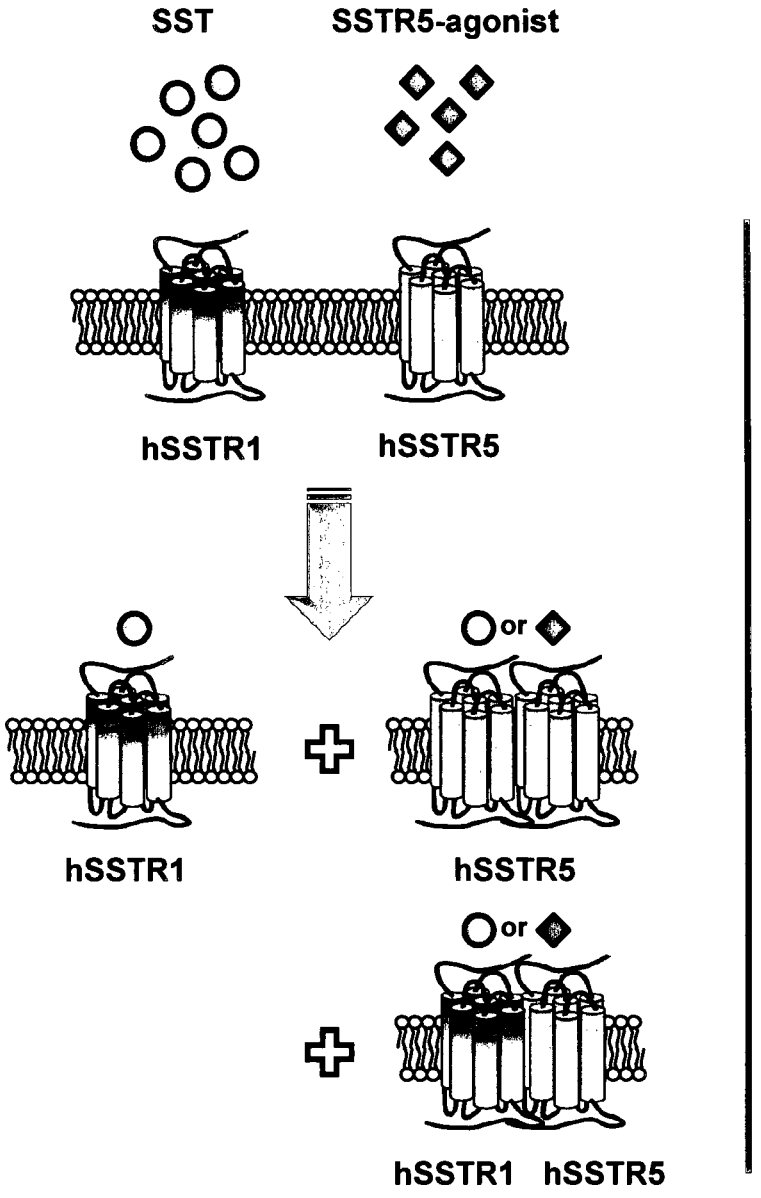
SST
SSTR5-agonist
hSSTR1
hSSTR5
or
hSSTR1
or
hSSTR5
hSSTR1
hSSTR5

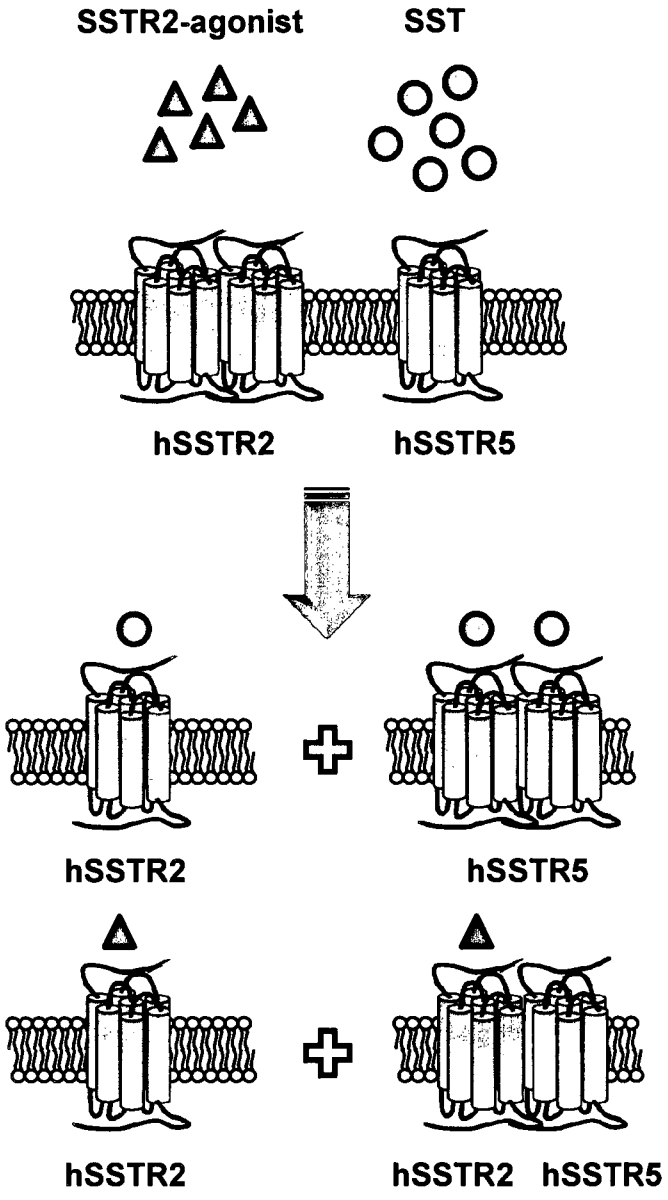
SSTR2-agonist
SST
hSSTR2
hSSTR5
hSSTR2
hSSTR5
hSSTR2
hSSTR2
hSSTR5

REFERENCES

AbdAlla, S., Abdel-Baset, A., Lother, H., el Massiery, A. and Quitterer, U. (2005) Mesangial AT1/B2 receptor heterodimers contribute to angiotensin II hyperresponsiveness in experimental hypertension. *J Mol Neurosci*, **26**, 185-192.

AbdAlla, S., Lother, H., Abdel-tawab, A.M. and Quitterer, U. (2001a) The angiotensin II AT2 receptor is an AT1 receptor antagonist. *J Biol Chem*, **276**, 39721-39726.

AbdAlla, S., Lother, H., el Massiery, A. and Quitterer, U. (2001b) Increased AT(1) receptor heterodimers in preeclampsia mediate enhanced angiotensin II responsiveness. *Nat Med*, **7**, 1003-1009.

AbdAlla, S., Lother, H., Langer, A., el Faramawy, Y. and Quitterer, U. (2004) Factor XIIIA transglutaminase crosslinks AT1 receptor dimers of monocytes at the onset of atherosclerosis. *Cell*, **119**, 343-354.

AbdAlla, S., Lother, H. and Quitterer, U. (2000) AT1-receptor heterodimers show enhanced G-protein activation and altered receptor sequestration. *Nature*, **407**, 94-98.

AbdAlla, S., Zaki, E., Lother, H. and Quitterer, U. (1999) Involvement of the amino terminus of the B(2) receptor in agonist-induced receptor dimerization. *J Biol Chem*, **274**, 26079-26084.

Abs, R., Verhelst, J., Maiter, D., Van Acker, K., Nobels, F., Coolens, J.L., Mahler, C. and Beckers, A. (1998) Cabergoline in the treatment of acromegaly: a study in 64 patients. *J Clin Endocrinol Metab*, **83**, 374-378.

Agnati, L.F., Ferre, S., Lluis, C., Franco, R. and Fuxe, K. (2003) Molecular mechanisms and therapeutical implications of intramembrane receptor/receptor interactions among heptahelical receptors with examples from the striatopallidal GABA neurons. *Pharmacol Rev*, **55**, 509-550.

Aguila, M.C. (1994) Growth hormone-releasing factor increases somatostatin release and mRNA levels in the rat periventricular nucleus via nitric oxide by activation of guanylate cyclase. *Proc Natl Acad Sci U S A*, **91**, 782-786.

Aguila, M.C., Dees, W.L., Haensly, W.E. and McCann, S.M. (1991) Evidence that somatostatin is localized and synthesized in lymphoid organs. *Proc Natl Acad Sci U S A*, **88**, 11485-11489.

Aguila, M.C., Rodriguez, A.M., Aguila-Mansilla, H.N. and Lee, W.T. (1996) Somatostatin antisense oligodeoxynucleotide-mediated stimulation of lymphocyte proliferation in culture. *Endocrinology*, **137**, 1585-1590.

Akopian, A., Johnson, J., Gabriel, R., Brecha, N. and Witkovsky, P. (2000) Somatostatin modulates voltage-gated K(+) and Ca(2+) currents in rod and cone photoreceptors of the salamander retina. *J Neurosci*, **20**, 929-936.

Alberti, K.G., Christensen, N.J., Christensen, S.E., Hansen, A.P., Iversen, J., Lundbaek, K., Seyer-Hansen, K. and Orskov, H. (1973) Inhibition of insulin secretion by somatostatin. *Lancet*, **2**, 1299-1301.

Albini, A., Florio, T., Giunciuglio, D., Masiello, L., Carlone, S., Corsaro, A., Thellung, S., Cai, T., Noonan, D.M. and Schettini, G. (1999) Somatostatin controls Kaposi's sarcoma tumor growth through inhibition of angiogenesis. *FASEB J*, **13**, 647-655.

Alblas, J., van Etten, I., Khanum, A. and Moolenaar, W.H. (1995) C-terminal truncation of the neurokinin-2 receptor causes enhanced and sustained agonist-induced signaling. Role of receptor phosphorylation in signal attenuation. *J Biol Chem*, **270**, 8944-8951.

Alderton, F., Fan, T.P. and Humphrey, P.P. (2001) Somatostatin receptor-mediated arachidonic acid mobilization: evidence for partial agonism of synthetic peptides. *Br J Pharmacol*, **132**, 760-766.

Ali, H., Richardson, R.M., Tomhave, E.D., DuBose, R.A., Haribabu, B. and Snyderman, R. (1994) Regulation of stably transfected platelet activating factor receptor in RBL-2H3 cells. Role of multiple G proteins and receptor phosphorylation. *J Biol Chem*, **269**, 24557-24563.

Altomare, D.A. and Testa, J.R. (2005) Perturbations of the AKT signaling pathway in human cancer. *Oncogene*, **24**, 7455-7464.

Amherdt, M., Patel, Y.C. and Orci, L. (1989) Binding and internalization of somatostatin, insulin, and glucagon by cultured rat islet cells. *J Clin Invest*, **84**, 412-417.

Angers, S., Salahpour, A. and Bouvier, M. (2002) Dimerization: an emerging concept for G protein-coupled receptor ontogeny and function. *Annu Rev Pharmacol Toxicol*, **42**, 409-435.

Angers, S., Salahpour, A., Joly, E., Hilairet, S., Chelsky, D., Dennis, M. and Bouvier, M. (2000) Detection of beta 2-adrenergic receptor dimerization in living cells using bioluminescence resonance energy transfer (BRET). *Proc Natl Acad Sci U S A*, **97**, 3684-3689.

Arena, S., Pattarozzi, A., Massa, A., Esteve, J.P., Iuliano, R., Fusco, A., Susini, C. and Florio, T. (2007) An intracellular multi-effector complex mediates somatostatin receptor 1 activation of phospho-tyrosine phosphatase eta. *Mol Endocrinol*, **21**, 229-246.

Arimura, A., Sato, H., Dupont, A., Nishi, N. and Schally, A.V. (1975) Somatostatin: abundance of immunoreactive hormone in rat stomach and pancreas. *Science*, **189**, 1007-1009.

Arimura, A. and Schally, A.V. (1976) Increase in basal and thyrotropin-releasing hormone (TRH)-stimulated secretion of thyrotropin (TSH) by passive immunization with antiserum to somatostatin in rats. *Endocrinology*, **98**, 1069-1072.

Ayoub, M.A., Couturier, C., Lucas-Meunier, E., Angers, S., Fossier, P., Bouvier, M. and Jockers, R. (2002) Monitoring of ligand-independent dimerization and ligand-induced conformational changes of melatonin receptors in living cells by bioluminescence resonance energy transfer. *J Biol Chem*, **277**, 21522-21528.

Babcock, G.J., Farzan, M. and Sodroski, J. (2003) Ligand-independent dimerization of CXCR4, a principal HIV-1 coreceptor. *J Biol Chem*, **278**, 3378-3385.

Bachmanov, A.A., Li, X., Reed, D.R., Ohmen, J.D., Li, S., Chen, Z., Tordoff, M.G., de Jong, P.J., Wu, C., West, D.B., Chatterjee, A., Ross, D.A. and Beauchamp, G.K. (2001) Positional cloning of the mouse saccharin preference (Sac) locus. *Chem Senses*, **26**, 925-933.

Bai, M. (2004) Dimerization of G-protein-coupled receptors: roles in signal transduction. *Cell Signal*, **16**, 175-186.

Bai, M., Trivedi, S. and Brown, E.M. (1998) Dimerization of the extracellular calcium-sensing receptor (CaR) on the cell surface of CaR-transfected HEK293 cells. *J Biol Chem*, **273**, 23605-23610.

Bai, M., Trivedi, S., Kifor, O., Quinn, S.J. and Brown, E.M. (1999) Intermolecular interactions between dimeric calcium-sensing receptor monomers are important for its normal function. *Proc Natl Acad Sci U S A*, **96**, 2834-2839.

Ballare, E., Persani, L., Lania, A.G., Filopanti, M., Giammona, E., Corbetta, S., Mantovani, S., Arosio, M., Beck-Peccoz, P., Faglia, G. and Spada, A. (2001) Mutation of somatostatin receptor type 5 in an acromegalic patient resistant to somatostatin analog treatment. *J Clin Endocrinol Metab*, **86**, 3809-3814.

Ballian, N., Brunicardi, F.C. and Wang, X.P. (2006) Somatostatin and its receptors in the development of the endocrine pancreas. *Pancreas*, **33**, 1-12.

Bamberger, C.M., Fehn, M., Bamberger, A.M., Ludecke, D.K., Beil, F.U., Saeger, W. and Schulte, H.M. (1999) Reduced expression levels of the cell-cycle inhibitor p27Kip1 in human pituitary adenomas. *Eur J Endocrinol*, **140**, 250-255.

Baneres, J.L. and Parello, J. (2003) Structure-based analysis of GPCR function: evidence for a novel pentameric assembly between the dimeric leukotriene B4 receptor BLT1 and the G-protein. *J Mol Biol*, **329**, 815-829.

Baragli, A., Alturaihi, H., Watt, H.L., Abdallah, A. and Kumar, U. (2007) Heterooligomerization of human dopamine receptor 2 and somatostatin receptor 2 Co-immunoprecipitation and fluorescence resonance energy transfer analysis. *Cell Signal*, **19**, 2304-2316.

Barber, D.L., McGuire, M.E. and Ganz, M.B. (1989) Beta-adrenergic and somatostatin receptors regulate Na-H exchange independent of cAMP. *J Biol Chem*, **264**, 21038-21042.

Barinaga, M., Bilezikjian, L.M., Vale, W.W., Rosenfeld, M.G. and Evans, R.M. (1985) Independent effects of growth hormone releasing factor on growth hormone release and gene transcription. *Nature*, **314**, 279-281.

Barkan, A.L., Dimaraki, E.V., Jessup, S.K., Symons, K.V., Ermolenko, M. and Jaffe, C.A. (2003) Ghrelin secretion in humans is sexually dimorphic, suppressed by somatostatin, and not affected by the ambient growth hormone levels. *J Clin Endocrinol Metab*, **88**, 2180-2184.

Barki-Harrington, L., Luttrell, L.M. and Rockman, H.A. (2003) Dual inhibition of beta-adrenergic and angiotensin II receptors by a single antagonist: a functional role for receptor-receptor interaction in vivo. *Circulation*, **108**, 1611-1618.

Barnett, P. (2003) Somatostatin and somatostatin receptor physiology. *Endocrine*, **20**, 255-264.

Barrie, R., Woltering, E.A., Hajarizadeh, H., Mueller, C., Ure, T. and Fletcher, W.S. (1993) Inhibition of angiogenesis by somatostatin and somatostatin-like compounds is structurally dependent. *J Surg Res*, **55**, 446-450.

Baskin, D.G. and Ensinck, J.W. (1984) Somatostatin in epithelial cells of intestinal mucosa is present primarily as somatostatin 28. *Peptides*, **5**, 615-621.

Bass, R.T., Buckwalter, B.L., Patel, B.P., Pausch, M.H., Price, L.A., Strnad, J. and Hadcock, J.R. (1996) Identification and characterization of novel somatostatin antagonists. *Mol Pharmacol*, **50**, 709-715.

Bauer, W., Briner, U., Doepfner, W., Haller, R., Huguenin, R., Marbach, P., Petcher, T.J. and Pless. (1982) SMS 201-995: a very potent and selective octapeptide analogue of somatostatin with prolonged action. *Life Sci*, **31**, 1133-1140.

Bayburt, T.H., Leitz, A.J., Xie, G., Oprian, D.D. and Sligar, S.G. (2007) Transducin activation by nanoscale lipid bilayers containing one and two rhodopsins. *J Biol Chem*, **282**, 14875-14881.

Bell, J.R., Young, M.R., Masterman, S.C., Morris, A., Mattick, R.P. and Bammer, G. (1999) A pilot study of naltrexone-accelerated detoxification in opioid dependence. *Med J Aust*, **171**, 26-30.

Ben-Shlomo, A., Wawrowsky, K.A., Proekt, I., Wolkenfeld, N.M., Ren, S.G., Taylor, J., Culler, M.D. and Melmed, S. (2005) Somatostatin receptor type 5 modulates somatostatin receptor type 2 regulation of adrenocorticotropin secretion. *J Biol Chem*, **280**, 24011-24021.

Benkirane, M., Jin, D.Y., Chun, R.F., Koup, R.A. and Jeang, K.T. (1997) Mechanism of transdominant inhibition of CCR5-mediated HIV-1 infection by ccr5delta32. *J Biol Chem*, **272**, 30603-30606.

Benoit, R., Ling, N. and Esch, F. (1987) A new prosomatostatin-derived peptide reveals a pattern for prohormone cleavage at monobasic sites. *Science*, **238**, 1126-1129.

Benuck, M. and Marks, N. (1976) Differences in the degradation of hypothalamic releasing factors by rat and human serum. *Life Sci*, **19**, 1271-1276.

Berelowitz, M., Dudlak, D. and Frohman, L.A. (1982) Release of somatostatin-like immunoreactivity from incubated rat hypothalamus and cerebral cortex. Effects of glucose and glucoregulatory hormones. *J Clin Invest*, **69**, 1293-1301.

Berelowitz, M., Firestone, S.L. and Frohman, L.A. (1981a) Effects of growth hormone excess and deficiency on hypothalamic somatostatin content and release and on tissue somatostatin distribution. *Endocrinology*, **109**, 714-719.

Berelowitz, M., Szabo, M., Frohman, L.A., Firestone, S., Chu, L. and Hintz, R.L. (1981b) Somatomedin-C mediates growth hormone negative feedback by effects on both the hypothalamus and the pituitary. *Science*, **212**, 1279-1281.

Berglund, M.M., Schober, D.A., Esterman, M.A. and Gehlert, D.R. (2003) Neuropeptide Y Y4 receptor homodimers dissociate upon agonist stimulation. *J Pharmacol Exp Ther*, **307**, 1120-1126.

Bersani, M., Thim, L., Baldissera, F.G. and Holst, J.J. (1989) Prosomatostatin 1-64 is a major product of somatostatin gene expression in pancreas and gut. *J Biol Chem*, **264**, 10633-10636.

Bevan, J.S. (2005) Clinical review: The antitumoral effects of somatostatin analog therapy in acromegaly. *J Clin Endocrinol Metab*, **90**, 1856-1863.

Bibbiani, F., Oh, J.D., Petzer, J.P., Castagnoli, N., Jr., Chen, J.F., Schwarzschild, M.A. and Chase, T.N. (2003) A2A antagonist prevents dopamine agonist-induced motor complications in animal models of Parkinson's disease. *Exp Neurol*, **184**, 285-294.

Biebermann, H., Krude, H., Elsner, A., Chubanov, V., Gudermann, T. and Gruters, A. (2003) Autosomal-dominant mode of inheritance of a melanocortin-4 receptor

mutation in a patient with severe early-onset obesity is due to a dominant-negative effect caused by receptor dimerization. *Diabetes*, **52**, 2984-2988.

Blum, A.M., Metwali, A., Mathew, R.C., Cook, G., Elliott, D. and Weinstock, J.V. (1992) Granuloma T lymphocytes in murine schistosomiasis mansoni have somatostatin receptors and respond to somatostatin with decreased IFN-gamma secretion. *J Immunol*, **149**, 3621-3626.

Bockaert, J., Fagni, L., Dumuis, A. and Marin, P. (2004) GPCR interacting proteins (GIP). *Pharmacol Ther*, **103**, 203-221.

Bonde, M.M., Sheikh, S.P. and Hansen, J.L. (2006) Family C 7TM receptor dimerization and activation. *Endocr Metab Immune Disord Drug Targets*, **6**, 7-16.

Boudin, H., Sarret, P., Mazella, J., Schonbrunn, A. and Beaudet, A. (2000) Somatostatin-induced regulation of SST(2A) receptor expression and cellsurface availability in central neurons: role of receptor internalization. *J Neurosci*, **20**, 5932-5939.

Bousquet, C., Delesque, N., Lopez, F., Saint-Laurent, N., Esteve, J.P., Bedecs, K., Buscail, L., Vaysse, N. and Susini, C. (1998) sst2 somatostatin receptor mediates negative regulation of insulin receptor signaling through the tyrosine phosphatase SHP-1. *J Biol Chem*, **273**, 7099-7106.

Bousquet, C., Puente, E., Buscail, L., Vaysse, N. and Susini, C. (2001) Antiproliferative effect of somatostatin and analogs. *Chemotherapy*, **47 Suppl 2**, 30-39.

Brauner-Osborne, H., Wellendorph, P. and Jensen, A.A. (2007) Structure, pharmacology and therapeutic prospects of family C G-protein coupled receptors. *Curr Drug Targets*, **8**, 169-184.

Brazeau, P., Vale, W., Burgus, R., Ling, N., Butcher, M., Rivier, J. and Guillemin, R. (1973) Hypothalamic polypeptide that inhibits the secretion of immunoreactive pituitary growth hormone. *Science*, **179**, 77-79.

Breit, A., Lagace, M. and Bouvier, M. (2004) Hetero-oligomerization between beta2- and beta3-adrenergic receptors generates a beta-adrenergic signaling unit with distinct functional properties. *J Biol Chem*, **279**, 28756-28765.

Breitwieser, G.E. (2004) G protein-coupled receptor oligomerization: implications for G protein activation and cell signaling. *Circ Res*, **94**, 17-27.

Bresson, J.L., Clavequin, M.C., Fellmann, D. and Bugnon, C. (1984) Ontogeny of the neuroglandular system revealed with HPGRF 44 antibodies in human hypothalamus. *Neuroendocrinology*, **39**, 68-73.

Brothers, S.P., Cornea, A., Janovick, J.A. and Conn, P.M. (2004) Human loss-of-function gonadotropin-releasing hormone receptor mutants retain wild-type receptors in the endoplasmic reticulum: molecular basis of the dominant-negative effect. *Mol Endocrinol*, **18**, 1787-1797.

Bruno, J.F., Xu, Y. and Berelowitz, M. (1994a) Somatostatin regulates somatostatin receptor subtype mRNA expression in GH3 cells. *Biochem Biophys Res Commun*, **202**, 1738-1743.

Bruno, J.F., Xu, Y., Song, J. and Berelowitz, M. (1993) Tissue distribution of somatostatin receptor subtype messenger ribonucleic acid in the rat. *Endocrinology*, **133**, 2561-2567.

Bruno, J.F., Xu, Y., Song, J. and Berelowitz, M. (1994b) Pituitary and hypothalamic somatostatin receptor subtype messenger ribonucleic acid expression in the food-deprived and diabetic rat. *Endocrinology*, **135**, 1787-1792.

Bruns, C., Lewis, I., Briner, U., Meno-Tetang, G. and Weckbecker, G. (2002) SOM230: a novel somatostatin peptidomimetic with broad somatotropin release inhibiting factor (SRIF) receptor binding and a unique antisecretory profile. *Eur J Endocrinol*, **146**, 707-716.

Bugnon, C., Fellmann, D. and Bloch, B. (1978) Immunocytochemical study of the ontogenesis of the hypothalamic somatostatin-containing neurons in the human fetus. *Metabolism*, **27**, 1161-1165.

Bulenger, S., Marullo, S. and Bouvier, M. (2005) Emerging role of homo- and heterodimerization in G-protein-coupled receptor biosynthesis and maturation. *Trends Pharmacol Sci*, **26**, 131-137.

Buscail, L., Delesque, N., Esteve, J.P., Saint-Laurent, N., Prats, H., Clerc, P., Robberecht, P., Bell, G.I., Liebow, C., Schally, A.V. and et al. (1994) Stimulation of tyrosine phosphatase and inhibition of cell proliferation by somatostatin analogues: mediation by human somatostatin receptor subtypes SSTR1 and SSTR2. *Proc Natl Acad Sci U S A*, **91**, 2315-2319.

Buscail, L., Esteve, J.P., Saint-Laurent, N., Bertrand, V., Reisine, T., O'Carroll, A.M., Bell, G.I., Schally, A.V., Vaysse, N. and Susini, C. (1995) Inhibition of cell proliferation by the somatostatin analogue RC-160 is mediated by somatostatin receptor subtypes SSTR2 and SSTR5 through different mechanisms. *Proc Natl Acad Sci U S A*, **92**, 1580-1584.

Calebiro, D., de Filippis, T., Lucchi, S., Covino, C., Panigone, S., Beck-Peccoz, P., Dunlap, D. and Persani, L. (2005) Intracellular entrapment of wild-type TSH receptor by oligomerization with mutants linked to dominant TSH resistance. *Hum Mol Genet*, **14**, 2991-3002.

Calver, A.R., Robbins, M.J., Cosio, C., Rice, S.Q., Babbs, A.J., Hirst, W.D., Boyfield, I., Wood, M.D., Russell, R.B., Price, G.W., Couve, A., Moss, S.J. and Pangalos, M.N. (2001) The C-terminal domains of the GABA(b) receptor subunits mediate intracellular trafficking but are not required for receptor signaling. *J Neurosci*, **21**, 1203-1210.

Canals, M., Marcellino, D., Fanelli, F., Ciruela, F., de Benedetti, P., Goldberg, S.R., Neve, K., Fuxe, K., Agnati, L.F., Woods, A.S., Ferre, S., Lluis, C., Bouvier, M. and Franco, R. (2003) Adenosine A2A-dopamine D2 receptor-receptor heteromerization: qualitative and quantitative assessment by fluorescence and bioluminescence energy transfer. *J Biol Chem*, **278**, 46741-46749.

Cao, T.T., Brelot, A. and von Zastrow, M. (2005) The composition of the beta-2 adrenergic receptor oligomer affects its membrane trafficking after ligand-induced endocytosis. *Mol Pharmacol*, **67**, 288-297.

Cattaneo, M.G., Scita, G. and Vicentini, L.M. (1999) Somatostatin inhibits PDGF-stimulated Ras activation in human neuroblastoma cells. *FEBS Lett*, **459**, 64-68.

Cattaneo, M.G., Taylor, J.E., Culler, M.D., Nisoli, E. and Vicentini, L.M. (2000) Selective stimulation of somatostatin receptor subtypes: differential effects on Ras/MAP kinase pathway and cell proliferation in human neuroblastoma cells. *FEBS Lett*, **481**, 271-276.

Cervera, P., Videau, C., Viollet, C., Petrucci, C., Lacombe, J., Winsky-Sommerer, R., Csaba, Z., Helboe, L., Daumas-Duport, C., Reubi, J.C. and Epelbaum, J. (2002)

Comparison of somatostatin receptor expression in human gliomas and medulloblastomas. *J Neuroendocrinol*, **14**, 458-471.

Cescato, R., Schulz, S., Waser, B., Eltschinger, V., Rivier, J.E., Wester, H.J., Culler, M., Ginj, M., Liu, Q., Schonbrunn, A. and Reubi, J.C. (2006) Internalization of sst2, sst3, and sst5 receptors: effects of somatostatin agonists and antagonists. *J Nucl Med*, **47**, 502-511.

Chabre, M. and le Maire, M. (2005) Monomeric G-protein-coupled receptor as a functional unit. *Biochemistry*, **44**, 9395-9403.

Cheng, Z.J., Harikumar, K.G., Holicky, E.L. and Miller, L.J. (2003) Heterodimerization of type A and B cholecystokinin receptors enhance signaling and promote cell growth. *J Biol Chem*, **278**, 52972-52979.

Cheng, Z.J. and Miller, L.J. (2001) Agonist-dependent dissociation of oligomeric complexes of G protein-coupled cholecystokinin receptors demonstrated in living cells using bioluminescence resonance energy transfer. *J Biol Chem*, **276**, 48040-48047.

Cherezov, V., Rosenbaum, D.M., Hanson, M.A., Rasmussen, S.G., Thian, F.S., Kobilka, T.S., Choi, H.J., Kuhn, P., Weis, W.I., Kobilka, B.K. and Stevens, R.C. (2007) High-resolution crystal structure of an engineered human beta2-adrenergic G protein-coupled receptor. *Science*, **318**, 1258-1265.

Chihara, K., Arimura, A. and Schally, A.V. (1979) Effect of intraventricular injection of dopamine, noreprinephrine, acetylcholine, and 5-hydroxytryptamine on immunoreactive somatostatin release into rat hypophyseal portal blood. *Endocrinology*, **104**, 1656-1662.

Ciruela, F., Burgueno, J., Casado, V., Canals, M., Marcellino, D., Goldberg, S.R., Bader, M., Fuxe, K., Agnati, L.F., Lluis, C., Franco, R., Ferre, S. and Woods, A.S. (2004) Combining mass spectrometry and pull-down techniques for the study of receptor heteromerization. Direct epitope-epitope electrostatic interactions between adenosine A2A and dopamine D2 receptors. *Anal Chem*, **76**, 5354-5363.

Claing, A., Laporte, S.A., Caron, M.G. and Lefkowitz, R.J. (2002) Endocytosis of G protein-coupled receptors: roles of G protein-coupled receptor kinases and beta-arrestin proteins. *Prog Neurobiol*, **66**, 61-79.

Claing, A., Perry, S.J., Achiriloaie, M., Walker, J.K., Albanesi, J.P., Lefkowitz, R.J. and Premont, R.T. (2000) Multiple endocytic pathways of G protein-coupled receptors delineated by GIT1 sensitivity. *Proc Natl Acad Sci U S A*, **97**, 1119-1124.

Colley, N.J., Cassill, J.A., Baker, E.K. and Zuker, C.S. (1995) Defective intracellular transport is the molecular basis of rhodopsin-dependent dominant retinal degeneration. *Proc Natl Acad Sci U S A*, **92**, 3070-3074.

Conn, P.M., Rogers, D.C., Stewart, J.M., Niedel, J. and Sheffield, T. (1982) Conversion of a gonadotropin-releasing hormone antagonist to an agonist. *Nature*, **296**, 653-655.

Cordelier, P., Esteve, J.P., Bousquet, C., Delesque, N., O'Carroll, A.M., Schally, A.V., Vaysse, N., Susini, C. and Buscail, L. (1997) Characterization of the antiproliferative signal mediated by the somatostatin receptor subtype sst5. *Proc Natl Acad Sci U S A*, **94**, 9343-9348.

Cornea, A., Janovick, J.A., Maya-Nunez, G. and Conn, P.M. (2001) Gonadotropin-releasing hormone receptor microaggregation. Rate monitored by fluorescence resonance energy transfer. *J Biol Chem*, **276**, 2153-2158.

Cox, B.A., Rosser, M.P., Kozlowski, M.R., Duwe, K.M., Neve, R.L. and Neve, K.A. (1995) Regulation and functional characterization of a rat recombinant dopamine D3 receptor. *Synapse*, **21**, 1-9.

Cozzi, R., Attanasio, R., Barausse, M., Dallabonzana, D., Orlandi, P., Da Re, N., Branca, V., Oppizzi, G. and Gelli, D. (1998) Cabergoline in acromegaly: a renewed role for dopamine agonist treatment? *Eur J Endocrinol*, **139**, 516-521.

Csaba, Z., Bernard, V., Helboe, L., Bluet-Pajot, M.T., Bloch, B., Epelbaum, J. and Dournaud, P. (2001) In vivo internalization of the somatostatin sst2A receptor in rat brain: evidence for translocation of cell-surface receptors into the endosomal recycling pathway. *Mol Cell Neurosci*, **17**, 646-661.

Csaba, Z. and Dournaud, P. (2001) Cellular biology of somatostatin receptors. *Neuropeptides*, **35**, 1-23.

Csaba, Z., Simon, A., Helboe, L., Epelbaum, J. and Dournaud, P. (2002) Neurochemical characterization of receptor-expressing cell populations by in vivo agonist-induced internalization: insights from the somatostatin sst2A receptor. *J Comp Neurol*, **454**, 192-199.

Csaba, Z., Simon, A., Helboe, L., Epelbaum, J. and Dournaud, P. (2003) Targeting sst2A receptor-expressing cells in the rat hypothalamus through in vivo agonist stimulation: neuroanatomical evidence for a major role of this subtype in mediating somatostatin functions. *Endocrinology*, **144**, 1564-1573.

Cvejic, S. and Devi, L.A. (1997) Dimerization of the delta opioid receptor: implication for a role in receptor internalization. *J Biol Chem*, **272**, 26959-26964.

Dalm, V.A., Van Hagen, P.M., de Krijger, R.R., Kros, J.M., Van Koetsveld, P.M., Van Der Lely, A.J., Lamberts, S.W. and Hofland, L.J. (2004) Distribution pattern of somatostatin and cortistatin mRNA in human central and peripheral tissues. *Clin Endocrinol (Oxf)*, **60**, 625-629.

Danesi, R., Agen, C., Benelli, U., Paolo, A.D., Nardini, D., Bocci, G., Basolo, F., Campagni, A. and Tacca, M.D. (1997) Inhibition of experimental angiogenesis by the somatostatin analogue octreotide acetate (SMS 201-995). *Clin Cancer Res*, **3**, 265-272.

Danesi, R. and Del Tacca, M. (1996) The effects of the somatostatin analog octreotide on angiogenesis in vitro. *Metabolism*, **45**, 49-50.

Danila, D.C., Haidar, J.N., Zhang, X., Katznelson, L., Culler, M.D. and Klibanski, A. (2001) Somatostatin receptor-specific analogs: effects on cell proliferation and growth hormone secretion in human somatotroph tumors. *J Clin Endocrinol Metab*, **86**, 2976-2981.

Dasgupta, P. and Mukherjee, R. (2000) Lipophilization of somatostatin analog RC-160 with long chain fatty acid improves its antiproliferative and antiangiogenic activity in vitro. *Br J Pharmacol*, **129**, 101-109.

Day, R., Dong, W., Panetta, R., Kraicer, J., Greenwood, M.T. and Patel, Y.C. (1995) Expression of mRNA for somatostatin receptor (sstr) types 2 and 5 in individual rat pituitary cells. A double labeling in situ hybridization analysis. *Endocrinology*, **136**, 5232-5235.

de Herder, W.W., Hofland, L.J., van der Lely, A.J. and Lamberts, S.W. (2003) Somatostatin receptors in gastroentero-pancreatic neuroendocrine tumours. *Endocr Relat Cancer*, **10**, 451-458.

de Lecea, L., Criado, J.R., Prospero-Garcia, O., Gautvik, K.M., Schweitzer, P., Danielson, P.E., Dunlop, C.L., Siggins, G.R., Henriksen, S.J. and Sutcliffe, J.G. (1996) A cortical neuropeptide with neuronal depressant and sleep-modulating properties. *Nature*, **381**, 242-245.

de Weille, J.R., Schmid-Antomarchi, H., Fosset, M. and Lazdunski, M. (1989) Regulation of ATP-sensitive K+ channels in insulinoma cells: activation by somatostatin and protein kinase C and the role of cAMP. *Proc Natl Acad Sci U S A*, **86**, 2971-2975.

Debburman, S.K., Kunapuli, P., Benovic, J.L. and Hosey, M.M. (1995) Agonist-dependent phosphorylation of human muscarinic receptors in Spodoptera frugiperda insect cell membranes by G protein-coupled receptor kinases. *Mol Pharmacol*, **47**, 224-233.

Dent, P., Wang, Y., Gu, Y.Z., Wood, S.L., Reardon, D.B., Mangues, R., Pellicer, A., Schonbrunn, A. and Sturgill, T.W. (1997) S49 cells endogenously express subtype 2 somatostatin receptors which couple to increase protein tyrosine phosphatase activity in membranes and down-regulate Raf-1 activity in situ. *Cell Signal*, **9**, 539-549.

Devost, D. and Zingg, H.H. (2004) Homo- and hetero-dimeric complex formations of the human oxytocin receptor. *J Neuroendocrinol*, **16**, 372-377.

Dhanasekaran, N., Heasley, L.E. and Johnson, G.L. (1995) G protein-coupled receptor systems involved in cell growth and oncogenesis. *Endocr Rev*, **16**, 259-270.

Dinger, M.C., Bader, J.E., Kobor, A.D., Kretzschmar, A.K. and Beck-Sickinger, A.G. (2003) Homodimerization of neuropeptide y receptors investigated by fluorescence resonance energy transfer in living cells. *J Biol Chem*, **278**, 10562-10571.

Djordjijevic, D., Zhang, J., Priam, M., Viollet, C., Gourdji, D., Kordon, C. and Epelbaum, J. (1998) Effect of 17beta-estradiol on somatostatin receptor expression and inhibitory effects on growth hormone and prolactin release in rat pituitary cell cultures. *Endocrinology*, **139**, 2272-2277.

Douziech, N., Calvo, E., Coulombe, Z., Muradia, G., Bastien, J., Aubin, R.A., Lajas, A. and Morisset, J. (1999) Inhibitory and stimulatory effects of somatostatin on two human pancreatic cancer cell lines: a primary role for tyrosine phosphatase SHP-1. *Endocrinology*, **140**, 765-777.

Dubois, M.P. (1975) Immunoreactive somatostatin is present in discrete cells of the endocrine pancreas. *Proc Natl Acad Sci U S A*, **72**, 1340-1343.

Duran-Prado, M., Bucharles, C., Gonzalez, B.J., Vazquez-Martinez, R., Martinez-Fuentes, A.J., Garcia-Navarro, S., Rhodes, S.J., Vaudry, H., Malagon, M.M. and Castano, J.P. (2007) Porcine somatostatin receptor 2 displays typical pharmacological sst2 features but unique dynamics of homodimerization and internalization. *Endocrinology*, **148**, 411-421.

El-Asmar, L., Springael, J.Y., Ballet, S., Andrieu, E.U., Vassart, G. and Parmentier, M. (2005) Evidence for negative binding cooperativity within CCR5-CCR2b heterodimers. *Mol Pharmacol*, **67**, 460-469.

Elliott, D.E. (2004) Expression and function of somatostatin and its receptors in immune cells. In Srikant, C.B. (ed.), *Somatostatin*. Kluwer Academic Publishers, Norwell, pp. 169-184.

Elliott, D.E., Metwali, A., Blum, A.M., Sandor, M., Lynch, R. and Weinstock, J.V. (1994) T lymphocytes isolated from the hepatic granulomas of schistosome-infected mice express somatostatin receptor subtype II (SSTR2) messenger RNA. *J Immunol*, **153**, 1180-1186.

Ensinck, J.W., Laschansky, E.C., Vogel, R.E., Simonowitz, D.A., Roos, B.A. and Francis, B.H. (1989) Circulating prosomatostatin-derived peptides. Differential responses to food ingestion. *J Clin Invest*, **83**, 1580-1589.

Epelbaum, J., Dournaud, P., Fodor, M. and Viollet, C. (1994) The neurobiology of somatostatin. *Crit Rev Neurobiol*, **8**, 25-44.

Eriksson, B. and Oberg, K. (1999) Summing up 15 years of somatostatin analog therapy in neuroendocrine tumors: future outlook. *Ann Oncol*, **10 Suppl 2**, S31-38.

Fan, T., Varghese, G., Nguyen, T., Tse, R., O'Dowd, B.F. and George, S.R. (2005) A role for the distal carboxyl tails in generating the novel pharmacology and G protein activation profile of mu and delta opioid receptor hetero-oligomers. *J Biol Chem*, **280**, 38478-38488.

Fedele, M., De Martino, I., Pivonello, R., Ciarmiello, A., Del Basso De Caro, M.L., Visone, R., Palmieri, D., Pierantoni, G.M., Arra, C., Schmid, H.A., Hofland, L., Lombardi, G., Colao, A. and Fusco, A. (2007) SOM230, a new somatostatin analogue, is highly effective in the therapy of growth hormone/prolactin-secreting pituitary adenomas. *Clin Cancer Res*, **13**, 2738-2744.

Feniuk, W., Jarvie, E., Luo, J. and Humphrey, P.P. (2000) Selective somatostatin sst(2) receptor blockade with the novel cyclic octapeptide, CYN-154806. *Neuropharmacology*, **39**, 1443-1450.

Ferjoux, G., Bousquet, C., Cordelier, P., Benali, N., Lopez, F., Rochaix, P., Buscail, L. and Susini, C. (2000) Signal transduction of somatostatin receptors negatively controlling cell proliferation. *J Physiol Paris*, **94**, 205-210.

Ferjoux, G., Lopez, F., Esteve, J.P., Ferrand, A., Vivier, E., Vely, F., Saint-Laurent, N., Pradayrol, L., Buscail, L. and Susini, C. (2003) Critical role of Src and SHP-2 in sst2 somatostatin receptor-mediated activation of SHP-1 and inhibition of cell proliferation. *Mol Biol Cell*, **14**, 3911-3928.

Ferland, L., Labrie, F., Jobin, M., Arimura, A. and Schally, A.V. (1976) Physiological role of somatostatin in the control of growth hormone and thyrotropin secretion. *Biochem Biophys Res Commun*, **68**, 149-156.

Ferrante, E., Pellegrini, C., Bondioni, S., Peverelli, E., Locatelli, M., Gelmini, P., Luciani, P., Peri, A., Mantovani, G., Bosari, S., Beck-Peccoz, P., Spada, A. and Lania, A. (2006) Octreotide promotes apoptosis in human somatotroph tumor cells by activating somatostatin receptor type 2. *Endocr Relat Cancer*, **13**, 955-962.

Ferre, S., Fredholm, B.B., Morelli, M., Popoli, P. and Fuxe, K. (1997) Adenosine-dopamine receptor-receptor interactions as an integrative mechanism in the basal ganglia. *Trends Neurosci*, **20**, 482-487.

Ferre, S., Fuxe, K., von Euler, G., Johansson, B. and Fredholm, B.B. (1992) Adenosine-dopamine interactions in the brain. *Neuroscience*, **51**, 501-512.

Filipek, S., Krzysko, K.A., Fotiadis, D., Liang, Y., Saperstein, D.A., Engel, A. and Palczewski, K. (2004) A concept for G protein activation by G protein-coupled receptor dimers: the transducin/rhodopsin interface. *Photochem Photobiol Sci*, **3**, 628-638.

Finley, J.C., Maderdrut, J.L., Roger, L.J. and Petrusz, P. (1981) The immunocytochemical localization of somatostatin-containing neurons in the rat central nervous system. *Neuroscience*, **6**, 2173-2192.

Florio, T. (2008) Molecular mechanisms of the antiproliferative activity of somatostatin receptors (SSTRs) in neuroendocrine tumors. *Front Biosci*, **13**, 822-840.

Florio, T., Arena, S., Thellung, S., Iuliano, R., Corsaro, A., Massa, A., Pattarozzi, A., Bajetto, A., Trapasso, F., Fusco, A. and Schettini, G. (2001) The activation of the phosphotyrosine phosphatase eta (r-PTP eta) is responsible for the somatostatin inhibition of PC Cl3 thyroid cell proliferation. *Mol Endocrinol*, **15**, 1838-1852.

Florio, T., Morini, M., Villa, V., Arena, S., Corsaro, A., Thellung, S., Culler, M.D., Pfeffer, U., Noonan, D.M., Schettini, G. and Albini, A. (2003a) Somatostatin inhibits tumor angiogenesis and growth via somatostatin receptor-3-mediated regulation of endothelial nitric oxide synthase and mitogen-activated protein kinase activities. *Endocrinology*, **144**, 1574-1584.

Florio, T., Rim, C., Hershberger, R.E., Loda, M. and Stork, P.J. (1994) The somatostatin receptor SSTR1 is coupled to phosphotyrosine phosphatase activity in CHO-K1 cells. *Mol Endocrinol*, **8**, 1289-1297.

Florio, T., Scorziello, A., Thellung, S., Salzano, S., Berlingieri, M.T., Fusco, A. and Schettini, G. (1997) Oncogene transformation of PC Cl3 clonal thyroid cell line induces an autonomous pattern of proliferation that correlates with a loss of basal and stimulated phosphotyrosine phosphatase activity. *Endocrinology*, **138**, 3756-3763.

Florio, T., Thellung, S., Arena, S., Corsaro, A., Bajetto, A., Schettini, G. and Stork, P.J. (2000) Somatostatin receptor 1 (SSTR1)-mediated inhibition of cell proliferation correlates with the activation of the MAP kinase cascade: role of the phosphotyrosine phosphatase SHP-2. *J Physiol Paris*, **94**, 239-250.

Florio, T., Thellung, S., Corsaro, A., Bocca, L., Arena, S., Pattarozzi, A., Villa, V., Massa, A., Diana, F., Schettini, D., Barbieri, F., Ravetti, J.L., Spaziante, R., Giusti, M. and Schettini, G. (2003b) Characterization of the intracellular mechanisms mediating somatostatin and lanreotide inhibition of DNA synthesis and growth hormone release from dispersed human GH-secreting pituitary adenoma cells in vitro. *Clin Endocrinol (Oxf)*, **59**, 115-128.

Florio, T., Yao, H., Carey, K.D., Dillon, T.J. and Stork, P.J. (1999) Somatostatin activation of mitogen-activated protein kinase via somatostatin receptor 1 (SSTR1). *Mol Endocrinol*, **13**, 24-37.

Floyd, D.H., Geva, A., Bruinsma, S.P., Overton, M.C., Blumer, K.J. and Baranski, T.J. (2003) C5a receptor oligomerization. II. Fluorescence resonance energy transfer studies of a human G protein-coupled receptor expressed in yeast. *J Biol Chem*, **278**, 35354-35361.

Forster, T. (1946) Energiewanderung und fluoreszenz. *Naturwissenschaften*, **6**, 166-175.

Forster, T. (1947) Fluoreszenzversuche an farbstoffmischungen. *Angew. Chem. A*, **59**, 181-187.

Forster, T. (1948) Zwischenmolekulare energiewanderung und fluoreszenz. *Ann. Phys.*, **2**, 55-75.

Fotiadis, D., Liang, Y., Filipek, S., Saperstein, D.A., Engel, A. and Palczewski, K. (2003) Atomic-force microscopy: Rhodopsin dimers in native disc membranes. *Nature*, **421**, 127-128.

Fotiadis, D., Liang, Y., Filipek, S., Saperstein, D.A., Engel, A. and Palczewski, K. (2004) The G protein-coupled receptor rhodopsin in the native membrane. *FEBS Lett*, **564**, 281-288.

Franco, R., Canals, M., Marcellino, D., Ferre, S., Agnati, L., Mallol, J., Casado, V., Ciruela, F., Fuxe, K., Lluis, C. and Canela, E.I. (2003) Regulation of heptaspanning-membrane-receptor function by dimerization and clustering. *Trends Biochem Sci*, **28**, 238-243.

Franco, R., Casado, V., Cortes, A., Ferrada, C., Mallol, J., Woods, A., Lluis, C., Canela, E.I. and Ferre, S. (2007) Basic concepts in G-protein-coupled receptor homo- and heterodimerization. *ScientificWorldJournal*, **7**, 48-57.

Frankel, B.J., Heldt, A.M. and Grodsky, G.M. (1982) Effects of K+ and arginine on insulin, glucagon, and somatostatin release from the in vitro perfused rat pancreas. *Endocrinology*, **110**, 428-431.

Fraser, C.M. and Venter, J.C. (1982) The size of the mammalian lung beta 2-adrenergic receptor as determined by target size analysis and immunoaffinity chromatography. *Biochem Biophys Res Commun*, **109**, 21-29.

Fukusumi, S., Kitada, C., Takekawa, S., Kizawa, H., Sakamoto, J., Miyamoto, M., Hinuma, S., Kitano, K. and Fujino, M. (1997) Identification and characterization of a novel human cortistatin-like peptide. *Biochem Biophys Res Commun*, **232**, 157-163.

Fuller, P.J. and Verity, K. (1989) Somatostatin gene expression in the thymus gland. *J Immunol*, **143**, 1015-1017.

Funckes, C.L., Minth, C.D., Deschenes, R., Magazin, M., Tavianini, M.A., Sheets, M., Collier, K., Weith, H.L., Aron, D.C., Roos, B.A. and Dixon, J.E. (1983) Cloning and characterization of a mRNA-encoding rat preprosomatostatin. *J Biol Chem*, **258**, 8781-8787.

Fuxe, K., Ferre, S., Zoli, M. and Agnati, L.F. (1998) Integrated events in central dopamine transmission as analyzed at multiple levels. Evidence for intramembrane adenosine A2A/dopamine D2 and adenosine A1/dopamine D1 receptor interactions in the basal ganglia. *Brain Res Brain Res Rev*, **26**, 258-273.

Fuxe, K. and Ungerstedt, U. (1974) Action of caffeine and theophyllamine on supersensitive dopamine receptors: considerable enhancement of receptor response to treatment with DOPA and dopamine receptor agonists. *Med Biol*, **52**, 48-54.

Gadella, T.W., Jr. and Jovin, T.M. (1995) Oligomerization of epidermal growth factor receptors on A431 cells studied by time-resolved fluorescence imaging microscopy. A stereochemical model for tyrosine kinase receptor activation. *J Cell Biol*, **129**, 1543-1558.

Galvez, T., Duthey, B., Kniazeff, J., Blahos, J., Rovelli, G., Bettler, B., Prezeau, L. and Pin, J.P. (2001) Allosteric interactions between GB1 and GB2 subunits are required for optimal GABA(B) receptor function. *EMBO J*, **20**, 2152-2159.

Garcia de la Torre, N., Wass, J.A. and Turner, H.E. (2002) Antiangiogenic effects of somatostatin analogues. *Clin Endocrinol (Oxf)*, **57**, 425-441.

Gardette, R., Petit, F., Peineau, S., Lanneau, C. and Epelbaum, J. (2004) Molecular evolution of somatostatin genes. In Srikant, C.B. (ed.), *Somatostatin*. Kluwer Academic Publishers, Norwell, pp. 123-142.

George, S.R., Fan, T., Xie, Z., Tse, R., Tam, V., Varghese, G. and O'Dowd, B.F. (2000) Oligomerization of mu- and delta-opioid receptors. Generation of novel functional properties. *J Biol Chem*, **275**, 26128-26135.

German, M.S., Moss, L.G. and Rutter, W.J. (1990) Regulation of insulin gene expression by glucose and calcium in transfected primary islet cultures. *J Biol Chem*, **265**, 22063-22066.

Giannini, E., Brouchon, L. and Boulay, F. (1995) Identification of the major phosphorylation sites in human C5a anaphylatoxin receptor in vivo. *J Biol Chem*, **270**, 19166-19172.

Giepmans, B.N., Adams, S.R., Ellisman, M.H. and Tsien, R.Y. (2006) The fluorescent toolbox for assessing protein location and function. *Science*, **312**, 217-224.

Gines, S., Hillion, J., Torvinen, M., Le Crom, S., Casado, V., Canela, E.I., Rondin, S., Lew, J.Y., Watson, S., Zoli, M., Agnati, L.F., Verniera, P., Lluis, C., Ferre, S., Fuxe, K. and Franco, R. (2000) Dopamine D1 and adenosine A1 receptors form functionally interacting heteromeric complexes. *Proc Natl Acad Sci U S A*, **97**, 8606-8611.

Gold, S.J., Han, M.H., Herman, A.E., Ni, Y.G., Pudiak, C.M., Aghajanian, G.K., Liu, R.J., Potts, B.W., Mumby, S.M. and Nestler, E.J. (2003) Regulation of RGS proteins by chronic morphine in rat locus coeruleus. *Eur J Neurosci*, **17**, 971-980.

Gomes, I., Gupta, A., Filipovska, J., Szeto, H.H., Pintar, J.E. and Devi, L.A. (2004) A role for heterodimerization of mu and delta opiate receptors in enhancing morphine analgesia. *Proc Natl Acad Sci U S A*, **101**, 5135-5139.

Goodman, R.H., Jacobs, J.W., Dee, P.C. and Habener, J.F. (1982) Somatostatin-28 encoded in a cloned cDNA obtained from a rat medullary thyroid carcinoma. *J Biol Chem*, **257**, 1156-1159.

Goodman, R.H., Lund, P.K., Barnett, F.H. and Habener, J.F. (1981) Intestinal pre-prosomatostatin. Identification of mRNA coding for a precursor by cell-free translations and hybridization with a cloned islet cDNA. *J Biol Chem*, **256**, 1499-1501.

Goodman, R.H., Lund, P.K., Jacobs, J.W. and Habener, J.F. (1980) Pre-prosomatostatins. Products of cell-free translations of messenger RNAs from anglerfish islets. *J Biol Chem*, **255**, 6549-6552.

Gottero, C., Prodam, F., Destefanis, S., Benso, A., Gauna, C., Me, E., Filtri, L., Riganti, F., Van Der Lely, A.J., Ghigo, E. and Broglio, F. (2004) Cortistatin-17 and -14 exert the same endocrine activities as somatostatin in humans. *Growth Horm IGF Res*, **14**, 382-387.

Goudet, C., Kniazeff, J., Hlavackova, V., Malhaire, F., Maurel, D., Acher, F., Blahos, J., Prezeau, L. and Pin, J.P. (2005) Asymmetric functioning of dimeric metabotropic glutamate receptors disclosed by positive allosteric modulators. *J Biol Chem*, **280**, 24380-24385.

Grant, M., Alturaihi, H., Jaquet, P., Collier, B. and Kumar, U. (*in revision*) Cell Growth Inhibition and Functioning of Human Somatostatin Receptor Type 2 are Modulated by Receptor Heterodimerization. *Mol Endocrinol.*

Grant, M., Collier, B. and Kumar, U. (2004a) Agonist-dependent dissociation of human somatostatin receptor 2 dimers: a role in receptor trafficking. *J Biol Chem*, **279**, 36179-36183.

Grant, M., Patel, R.C. and Kumar, U. (2004b) The role of subtype-specific ligand binding and the C-tail domain in dimer formation of human somatostatin receptors. *J Biol Chem*, **279**, 38636-38643.

Greenman, Y. and Melmed, S. (1994a) Expression of three somatostatin receptor subtypes in pituitary adenomas: evidence for preferential SSTR5 expression in the mammosomatotroph lineage. *J Clin Endocrinol Metab*, **79**, 724-729.

Greenman, Y. and Melmed, S. (1994b) Heterogeneous expression of two somatostatin receptor subtypes in pituitary tumors. *J Clin Endocrinol Metab*, **78**, 398-403.

Gregory, H., Taylor, C.L. and Hopkins, C.R. (1982) Luteinizing hormone release from dissociated pituitary cells by dimerization of occupied LHRH receptors. *Nature*, **300**, 269-271.

Gripentrog, J.M., Kantele, K.P., Jesaitis, A.J. and Miettinen, H.M. (2003) Experimental evidence for lack of homodimerization of the G protein-coupled human N-formyl peptide receptor. *J Immunol*, **171**, 3187-3193.

Gromada, J., Hoy, M., Buschard, K., Salehi, A. and Rorsman, P. (2001) Somatostatin inhibits exocytosis in rat pancreatic alpha-cells by G(i2)-dependent activation of calcineurin and depriming of secretory granules. *J Physiol*, **535**, 519-532.

Grozinsky-Glasberg, S., Franchi, G., Teng, M., Leontiou, C.A., Ribeiro de Oliveira, A., Jr., Dalino, P., Salahuddin, N., Korbonits, M. and Grossman, A.B. (2008a) Octreotide and the mTOR inhibitor RAD001 (everolimus) block proliferation and interact with the Akt-mTOR-p70S6K pathway in a neuro-endocrine tumour cell Line. *Neuroendocrinology*, **87**, 168-181.

Grozinsky-Glasberg, S., Grossman, A.B. and Korbonits, M. (2008b) The role of somatostatin analogues in the treatment of neuroendocrine tumours. *Mol Cell Endocrinol*, **286**, 238-250.

Grozinsky-Glasberg, S., Shimon, I., Korbonits, M. and Grossman, A.B. (2008c) Somatostatin analogues in the control of neuroendocrine tumours: efficacy and mechanisms. *Endocr Relat Cancer*, **15**, 701-720.

Gu, Y.Z. and Schonbrunn, A. (1997) Coupling specificity between somatostatin receptor sst2A and G proteins: isolation of the receptor-G protein complex with a receptor antibody. *Mol Endocrinol*, **11**, 527-537.

Guillermet, J., Saint-Laurent, N., Rochaix, P., Cuvillier, O., Levade, T., Schally, A.V., Pradayrol, L., Buscail, L., Susini, C. and Bousquet, C. (2003) Somatostatin receptor subtype 2 sensitizes human pancreatic cancer cells to death ligand-induced apoptosis. *Proc Natl Acad Sci U S A*, **100**, 155-160.

Guo, W., Shi, L., Filizola, M., Weinstein, H. and Javitch, J.A. (2005) Crosstalk in G protein-coupled receptors: changes at the transmembrane homodimer interface determine activation. *Proc Natl Acad Sci U S A*, **102**, 17495-17500.

Gyr, K., Beglinger, C., Kohler, E., Trautzl, U., Keller, U. and Bloom, S.R. (1987) Circulating somatostatin. Physiological regulator of pancreatic function? *J Clin Invest*, **79**, 1595-1600.

Hague, C., Uberti, M.A., Chen, Z., Hall, R.A. and Minneman, K.P. (2004) Cell surface expression of alpha1D-adrenergic receptors is controlled by heterodimerization with alpha1B-adrenergic receptors. *J Biol Chem*, **279**, 15541-15549.

Hansen, J.L. and Sheikh, S.P. (2004) Functional consequences of 7TM receptor dimerization. *Eur J Pharm Sci*, **23**, 301-317.

Hanyaloglu, A.C., Seeber, R.M., Kohout, T.A., Lefkowitz, R.J. and Eidne, K.A. (2002) Homo- and hetero-oligomerization of thyrotropin-releasing hormone (TRH) receptor subtypes. Differential regulation of beta-arrestins 1 and 2. *J Biol Chem*, **277**, 50422-50430.

Harrison, C. and van der Graaf, P.H. (2006) Current methods used to investigate G protein coupled receptor oligomerisation. *J Pharmacol Toxicol Methods*, **54**, 26-35.

Hathway, G.J., Humphrey, P.P. and Kendrick, K.M. (1999) Evidence that somatostatin sst2 receptors mediate striatal dopamine release. *Br J Pharmacol*, **128**, 1346-1352.

Havlickova, M., Prezeau, L., Duthey, B., Bettler, B., Pin, J.P. and Blahos, J. (2002) The intracellular loops of the GB2 subunit are crucial for G-protein coupling of the heteromeric gamma-aminobutyrate B receptor. *Mol Pharmacol*, **62**, 343-350.

Hayry, P., Raisanen, A., Ustinov, J., Mennander, A. and Paavonen, T. (1993) Somatostatin analog lanreotide inhibits myocyte replication and several growth factors in allograft arteriosclerosis. *Faseb J*, **7**, 1055-1060.

Hazum, E. and Keinan, D. (1985) Gonadotropin releasing hormone activation is mediated by dimerization of occupied receptors. *Biochem Biophys Res Commun*, **133**, 449-456.

He, L., Fong, J., von Zastrow, M. and Whistler, J.L. (2002) Regulation of opioid receptor trafficking and morphine tolerance by receptor oligomerization. *Cell*, **108**, 271-282.

He, L. and Whistler, J.L. (2005) An opiate cocktail that reduces morphine tolerance and dependence. *Curr Biol*, **15**, 1028-1033.

Hebert, T.E. and Bouvier, M. (1998) Structural and functional aspects of G protein-coupled receptor oligomerization. *Biochem Cell Biol*, **76**, 1-11.

Hebert, T.E., Moffett, S., Morello, J.P., Loisel, T.P., Bichet, D.G., Barret, C. and Bouvier, M. (1996) A peptide derived from a beta2-adrenergic receptor transmembrane domain inhibits both receptor dimerization and activation. *J Biol Chem*, **271**, 16384-16392.

Hellman, B. and Lernmark, A. (1969) Inhibition of the in vitro secretion of insulin by an extract of pancreatic alpha-1 cells. *Endocrinology*, **84**, 1484-1488.

Herberg, J.T., Codina, J., Rich, K.A., Rojas, F.J. and Iyengar, R. (1984) The hepatic glucagon receptor. Solubilization, characterization, and development of an affinity adsorption assay for the soluble receptor. *J Biol Chem*, **259**, 9285-9294.

Hernanz-Falcon, P., Rodriguez-Frade, J.M., Serrano, A., Juan, D., del Sol, A., Soriano, S.F., Roncal, F., Gomez, L., Valencia, A., Martinez, A.C. and Mellado, M. (2004) Identification of amino acid residues crucial for chemokine receptor dimerization. *Nat Immunol*, **5**, 216-223.

Hierowski, M.T., Liebow, C., du Sapin, K. and Schally, A.V. (1985) Stimulation by somatostatin of dephosphorylation of membrane proteins in pancreatic cancer MIA PaCa-2 cell line. *FEBS Lett*, **179**, 252-256.

Hilairet, S., Bouaboula, M., Carriere, D., Le Fur, G. and Casellas, P. (2003) Hypersensitization of the Orexin 1 receptor by the CB1 receptor: evidence for cross-talk blocked by the specific CB1 antagonist, SR141716. *J Biol Chem*, **278**, 23731-23737.

Hillion, J., Canals, M., Torvinen, M., Casado, V., Scott, R., Terasmaa, A., Hansson, A., Watson, S., Olah, M.E., Mallol, J., Canela, E.I., Zoli, M., Agnati, L.F., Ibanez, C.F., Lluis, C., Franco, R., Ferre, S. and Fuxe, K. (2002) Coaggregation, cointernalization, and codesensitization of adenosine A2A receptors and dopamine D2 receptors. *J Biol Chem*, **277**, 18091-18097.

Hipkin, R.W., Friedman, J., Clark, R.B., Eppler, C.M. and Schonbrunn, A. (1997) Agonist-induced desensitization, internalization, and phosphorylation of the sst2A somatostatin receptor. *J Biol Chem*, **272**, 13869-13876.

Hipkin, R.W., Wang, Y. and Schonbrunn, A. (2000) Protein kinase C activation stimulates the phosphorylation and internalization of the sst2A somatostatin receptor. *J Biol Chem*, **275**, 5591-5599.

Hofland, L.J., Breeman, W.A., Krenning, E.P., de Jong, M., Waaijers, M., van Koetsveld, P.M., Macke, H.R. and Lamberts, S.W. (1999) Internalization of [DOTA degrees,125I-Tyr3]Octreotide by somatostatin receptor-positive cells in vitro and in vivo: implications for somatostatin receptor-targeted radio-guided surgery. *Proc Assoc Am Physicians*, **111**, 63-69.

Hofland, L.J. and Lamberts, S.W. (2003) The pathophysiological consequences of somatostatin receptor internalization and resistance. *Endocr Rev*, **24**, 28-47.

Hofland, L.J., van Koetsveld, P.M., Waaijers, M., Zuyderwijk, J., Breeman, W.A. and Lamberts, S.W. (1995) Internalization of the radioiodinated somatostatin analog [125I-Tyr3]octreotide by mouse and human pituitary tumor cells: increase by unlabeled octreotide. *Endocrinology*, **136**, 3698-3706.

Hokfelt, T., Efendic, S., Hellerstrom, C., Johansson, O., Luft, R. and Arimura, A. (1975) Cellular localization of somatostatin in endocrine-like cells and neurons of the rat with special references to the A1-cells of the pancreatic islets and to the hypothalamus. *Acta Endocrinol Suppl (Copenh)*, **200**, 5-41.

Hook, V.Y., Azaryan, A.V., Hwang, S.R. and Tezapsidis, N. (1994) Proteases and the emerging role of protease inhibitors in prohormone processing. *Faseb J*, **8**, 1269-1278.

Hoon, M.A., Adler, E., Lindemeier, J., Battey, J.F., Ryba, N.J. and Zuker, C.S. (1999) Putative mammalian taste receptors: a class of taste-specific GPCRs with distinct topographic selectivity. *Cell*, **96**, 541-551.

Hortala, M., Ferjoux, G., Estival, A., Bertrand, C., Schulz, S., Pradayrol, L., Susini, C. and Clemente, F. (2003) Inhibitory role of the somatostatin receptor SST2 on the intracrine-regulated cell proliferation induced by the 210-amino acid fibroblast growth factor-2 isoform: implication of JAK2. *J Biol Chem*, **278**, 20574-20581.

Horvat, R.D., Roess, D.A., Nelson, S.E., Barisas, B.G. and Clay, C.M. (2001) Binding of agonist but not antagonist leads to fluorescence resonance energy transfer between

intrinsically fluorescent gonadotropin-releasing hormone receptors. *Mol Endocrinol*, **15**, 695-703.

Horvath, S., Palkovits, M., Gorcs, T. and Arimura, A. (1989) Electron microscopic immunocytochemical evidence for the existence of bidirectional synaptic connections between growth hormone-releasing hormone- and somatostatin-containing neurons in the hypothalamus of the rat. *Brain Res*, **481**, 8-15.

Hou, C., Gilbert, R.L. and Barber, D.L. (1994) Subtype-specific signaling mechanisms of somatostatin receptors SSTR1 and SSTR2. *J Biol Chem*, **269**, 10357-10362.

Hoyer, D., Nunn, C., Hannon, J., Schoeffter, P., Feuerbach, D., Schuepbach, E., Langenegger, D., Bouhelal, R., Hurth, K., Neumann, P., Troxler, T. and Pfaeffli, P. (2004) SRA880, in vitro characterization of the first non-peptide somatostatin sst(1) receptor antagonist. *Neurosci Lett*, **361**, 132-135.

Hu, C.D., Chinenov, Y. and Kerppola, T.K. (2002) Visualization of interactions among bZIP and Rel family proteins in living cells using bimolecular fluorescence complementation. *Mol Cell*, **9**, 789-798.

Hu, C.D. and Kerppola, T.K. (2003) Simultaneous visualization of multiple protein interactions in living cells using multicolor fluorescence complementation analysis. *Nat Biotechnol*, **21**, 539-545.

Hukovic, N., Panetta, R., Kumar, U. and Patel, Y.C. (1996) Agonist-dependent regulation of cloned human somatostatin receptor types 1-5 (hSSTR1-5): subtype selective internalization or upregulation. *Endocrinology*, **137**, 4046-4049.

Hukovic, N., Panetta, R., Kumar, U., Rocheville, M. and Patel, Y.C. (1998) The cytoplasmic tail of the human somatostatin receptor type 5 is crucial for interaction with adenylyl cyclase and in mediating desensitization and internalization. *J Biol Chem*, **273**, 21416-21422.

Hukovic, N., Rocheville, M., Kumar, U., Sasi, R., Khare, S. and Patel, Y.C. (1999) Agonist-dependent up-regulation of human somatostatin receptor type 1 requires molecular signals in the cytoplasmic C-tail. *J Biol Chem*, **274**, 24550-24558.

Hunzicker-Dunn, M., Barisas, G., Song, J. and Roess, D.A. (2003) Membrane organization of luteinizing hormone receptors differs between actively signaling and desensitized receptors. *J Biol Chem*, **278**, 42744-42749.

Ikeda, S.R. and Schofield, G.G. (1989) Somatostatin blocks a calcium current in rat sympathetic ganglion neurones. *J Physiol*, **409**, 221-240.

Issafras, H., Angers, S., Bulenger, S., Blanpain, C., Parmentier, M., Labbe-Jullie, C., Bouvier, M. and Marullo, S. (2002) Constitutive agonist-independent CCR5 oligomerization and antibody-mediated clustering occurring at physiological levels of receptors. *J Biol Chem*, **277**, 34666-34673.

Jais, P., Terris, B., Ruszniewski, P., LeRomancer, M., Reyl-Desmars, F., Vissuzaine, C., Cadiot, G., Mignon, M. and Lewin, M.J. (1997) Somatostatin receptor subtype gene expression in human endocrine gastroentero-pancreatic tumours. *Eur J Clin Invest*, **27**, 639-644.

James, J.R., Oliveira, M.I., Carmo, A.M., Iaboni, A. and Davis, S.J. (2006) A rigorous experimental framework for detecting protein oligomerization using bioluminescence resonance energy transfer. *Nat Methods*, **3**, 1001-1006.

James, R.A., Sarapura, V.D., Bruns, C., Raulf, F., Dowding, J.M., Gordon, D.F., Wood, W.M. and Ridgway, E.C. (1997) Thyroid hormone-induced expression of specific

somatostatin receptor subtypes correlates with involution of the TtT-97 murine thyrotrope tumor. *Endocrinology*, **138**, 719-724.

Jaquet, P., Gunz, G., Saveanu, A., Dufour, H., Taylor, J., Dong, J., Kim, S., Moreau, J.P., Enjalbert, A. and Culler, M.D. (2005) Efficacy of chimeric molecules directed towards multiple somatostatin and dopamine receptors on inhibition of GH and prolactin secretion from GH-secreting pituitary adenomas classified as partially responsive to somatostatin analog therapy. *Eur J Endocrinol*, **153**, 135-141.

Jaquet, P., Ouafik, L., Saveanu, A., Gunz, G., Fina, F., Dufour, H., Culler, M.D., Moreau, J.P. and Enjalbert, A. (1999) Quantitative and functional expression of somatostatin receptor subtypes in human prolactinomas. *J Clin Endocrinol Metab*, **84**, 3268-3276.

Jaquet, P., Saveanu, A., Gunz, G., Fina, F., Zamora, A.J., Grino, M., Culler, M.D., Moreau, J.P., Enjalbert, A. and Ouafik, L.H. (2000) Human somatostatin receptor subtypes in acromegaly: distinct patterns of messenger ribonucleic acid expression and hormone suppression identify different tumoral phenotypes. *J Clin Endocrinol Metab*, **85**, 781-792.

Jensen, A.A., Hansen, J.L., Sheikh, S.P. and Brauner-Osborne, H. (2002) Probing intermolecular protein-protein interactions in the calcium-sensing receptor homodimer using bioluminescence resonance energy transfer (BRET). *Eur J Biochem*, **269**, 5076-5087.

Jiang, H., Betancourt, L. and Smith, R.G. (2006) Ghrelin amplifies dopamine signaling by cross talk involving formation of growth hormone secretagogue receptor/dopamine receptor subtype 1 heterodimers. *Mol Endocrinol*, **20**, 1772-1785.

Johansson, O., Hokfelt, T. and Elde, R.P. (1984) Immunohistochemical distribution of somatostatin-like immunoreactivity in the central nervous system of the adult rat. *Neuroscience*, **13**, 265-339.

Jones, K.A., Borowsky, B., Tamm, J.A., Craig, D.A., Durkin, M.M., Dai, M., Yao, W.J., Johnson, M., Gunwaldsen, C., Huang, L.Y., Tang, C., Shen, Q., Salon, J.A., Morse, K., Laz, T., Smith, K.E., Nagarathnam, D., Noble, S.A., Branchek, T.A. and Gerald, C. (1998) GABA(B) receptors function as a heteromeric assembly of the subunits GABA(B)R1 and GABA(B)R2. *Nature*, **396**, 674-679.

Jordan, B.A., Cvejic, S. and Devi, L.A. (2000) Opioids and their complicated receptor complexes. *Neuropsychopharmacology*, **23**, S5-S18.

Jordan, B.A. and Devi, L.A. (1999) G-protein-coupled receptor heterodimerization modulates receptor function. *Nature*, **399**, 697-700.

Jordan, B.A., Trapaidze, N., Gomes, I., Nivarthi, R. and Devi, L.A. (2001) Oligomerization of opioid receptors with beta 2-adrenergic receptors: a role in trafficking and mitogen-activated protein kinase activation. *Proc Natl Acad Sci U S A*, **98**, 343-348.

Joseph-Bravo, P., Charli, J.L., Sherman, T., Boyer, H., Bolivar, F. and McKelvy, J.F. (1980) Identification of a putative hypothalamic mRNA coding for somatostatin and of its product in cell-free translation. *Biochem Biophys Res Commun*, **94**, 1004-1012.

Kamiya, T., Saitoh, O., Yoshioka, K. and Nakata, H. (2003) Oligomerization of adenosine A2A and dopamine D2 receptors in living cells. *Biochem Biophys Res Commun*, **306**, 544-549.

Kanatsuka, A., Makino, H., Matsushima, Y., Kasanuki, J., Osegawa, M. and Kumagai, A. (1981) Effect of calcium on the secretion of somatostatin and insulin from pancreatic islets. *Endocrinology*, **108**, 2254-2257.

Karalis, K., Mastorakos, G., Chrousos, G.P. and Tolis, G. (1994) Somatostatin analogues suppress the inflammatory reaction in vivo. *J Clin Invest*, **93**, 2000-2006.

Karpa, K.D., Lin, R., Kabbani, N. and Levenson, R. (2000) The dopamine D3 receptor interacts with itself and the truncated D3 splice variant d3nf: D3-D3nf interaction causes mislocalization of D3 receptors. *Mol Pharmacol*, **58**, 677-683.

Katakami, H., Downs, T.R. and Frohman, L.A. (1988) Inhibitory effect of hypothalamic medial preoptic area somatostatin on growth hormone-releasing factor in the rat. *Endocrinology*, **123**, 1103-1109.

Kaupmann, K., Huggel, K., Heid, J., Flor, P.J., Bischoff, S., Mickel, S.J., McMaster, G., Angst, C., Bittiger, H., Froestl, W. and Bettler, B. (1997) Expression cloning of GABA(B) receptors uncovers similarity to metabotropic glutamate receptors. *Nature*, **386**, 239-246.

Kaupmann, K., Malitschek, B., Schuler, V., Heid, J., Froestl, W., Beck, P., Mosbacher, J., Bischoff, S., Kulik, A., Shigemoto, R., Karschin, A. and Bettler, B. (1998) GABA(B)-receptor subtypes assemble into functional heteromeric complexes. *Nature*, **396**, 683-687.

Kaykas, A., Yang-Snyder, J., Heroux, M., Shah, K.V., Bouvier, M. and Moon, R.T. (2004) Mutant Frizzled 4 associated with vitreoretinopathy traps wild-type Frizzled in the endoplasmic reticulum by oligomerization. *Nat Cell Biol*, **6**, 52-58.

Kearn, C.S., Blake-Palmer, K., Daniel, E., Mackie, K. and Glass, M. (2005) Concurrent stimulation of cannabinoid CB1 and dopamine D2 receptors enhances heterodimer formation: a mechanism for receptor cross-talk? *Mol Pharmacol*, **67**, 1697-1704.

Kendall, D.M., Poitout, V., Olson, L.K., Sorenson, R.L. and Robertson, R.P. (1995) Somatostatin coordinately regulates glucagon gene expression and exocytosis in HIT-T15 cells. *J Clin Invest*, **96**, 2496-2502.

Kimura, N., Tomizawa, S., Arai, K.N. and Kimura, N. (1998) Chronic treatment with estrogen up-regulates expression of sst2 messenger ribonucleic acid (mRNA) but down-regulates expression of sst5 mRNA in rat pituitaries. *Endocrinology*, **139**, 1573-1580.

Kitagawa, M., Kusakabe, Y., Miura, H., Ninomiya, Y. and Hino, A. (2001) Molecular genetic identification of a candidate receptor gene for sweet taste. *Biochem Biophys Res Commun*, **283**, 236-242.

Klco, J.M., Lassere, T.B. and Baranski, T.J. (2003) C5a receptor oligomerization. I. Disulfide trapping reveals oligomers and potential contact surfaces in a G protein-coupled receptor. *J Biol Chem*, **278**, 35345-35353.

Kleinman, R., Gingerich, R., Ohning, G., Wong, H., Olthoff, K., Walsh, J. and Brunicardi, F.C. (1995) The influence of somatostatin on glucagon and pancreatic polypeptide secretion in the isolated perfused human pancreas. *Int J Pancreatol*, **18**, 51-57.

Kleuss, C., Hescheler, J., Ewel, C., Rosenthal, W., Schultz, G. and Wittig, B. (1991) Assignment of G-protein subtypes to specific receptors inducing inhibition of calcium currents. *Nature*, **353**, 43-48.

Koenig, J.A., Edwardson, J.M. and Humphrey, P.P. (1997) Somatostatin receptors in Neuro2A neuroblastoma cells: ligand internalization. *Br J Pharmacol*, **120**, 52-59.

Koerker, D.J., Ruch, W., Chideckel, E., Palmer, J., Goodner, C.J., Ensinck, J. and Gale, C.C. (1974) Somatostatin: hypothalamic inhibitor of the endocrine pancreas. *Science*, **184**, 482-484.

Koizumi, M., Onda, M., Tanaka, N., Seya, T., Yamada, T. and Takahashi, Y. (2002) Antiangiogenic effect of octreotide inhibits the growth of human rectal neuroendocrine carcinoma. *Digestion*, **65**, 200-206.

Korbonits, M., Chahal, H.S., Kaltsas, G., Jordan, S., Urmanova, Y., Khalimova, Z., Harris, P.E., Farrell, W.E., Claret, F.X. and Grossman, A.B. (2002) Expression of phosphorylated p27(Kip1) protein and Jun activation domain-binding protein 1 in human pituitary tumors. *J Clin Endocrinol Metab*, **87**, 2635-2643.

Kreienkamp, H.J., Liew, C.W., Bachner, D., Mameza, M.G., Soltau, M., Quitsch, A., Christenn, M., Wente, W. and Richter, D. (2004) Physiology of somatostatin receptors: From genetics to molecular analysis. In Srikant, C.B. (ed.), *Somatostatin*. Kluwer Academic Publishers, Norwell, pp. 185-202.

Kreienkamp, H.J., Roth, A. and Richter, D. (1998) Rat somatostatin receptor subtype 4 can be made sensitive to agonist-induced internalization by mutation of a single threonine (residue 331). *DNA Cell Biol*, **17**, 869-878.

Kreuzer, O.J., Krisch, B., Dery, O., Bunnett, N.W. and Meyerhof, W. (2001) Agonist-mediated endocytosis of rat somatostatin receptor subtype 3 involves beta-arrestin and clathrin coated vesicles. *J Neuroendocrinol*, **13**, 279-287.

Krisch, B., Feindt, J. and Mentlein, R. (1998) Immunoelectronmicroscopic analysis of the ligand-induced internalization of the somatostatin receptor subtype 2 in cultured human glioma cells. *J Histochem Cytochem*, **46**, 1233-1242.

Kroeger, K.M., Hanyaloglu, A.C., Seeber, R.M., Miles, L.E. and Eidne, K.A. (2001) Constitutive and agonist-dependent homo-oligomerization of the thyrotropin-releasing hormone receptor. Detection in living cells using bioluminescence resonance energy transfer. *J Biol Chem*, **276**, 12736-12743.

Kroeger, K.M., Pfleger, K.D. and Eidne, K.A. (2003) G-protein coupled receptor oligomerization in neuroendocrine pathways. *Front Neuroendocrinol*, **24**, 254-278.

Krulich, L., Dhariwal, A.P. and McCann, S.M. (1968) Stimulatory and inhibitory effects of purified hypothalamic extracts on growth hormone release from rat pituitary in vitro. *Endocrinology*, **83**, 783-790.

Kubitscheck, U., Kircheis, M., Schweitzer-Stenner, R., Dreybrodt, W., Jovin, T.M. and Pecht, I. (1991) Fluorescence resonance energy transfer on single living cells. Application to binding of monovalent haptens to cell-bound immunoglobulin E. *Biophys J*, **60**, 307-318.

Kull, B., Ferre, S., Arslan, G., Svenningsson, P., Fuxe, K., Owman, C. and Fredholm, B.B. (1999) Reciprocal interactions between adenosine A2A and dopamine D2 receptors in Chinese hamster ovary cells co-transfected with the two receptors. *Biochem Pharmacol*, **58**, 1035-1045.

Kumar, U., Sasi, R., Suresh, S., Patel, A., Thangaraju, M., Metrakos, P., Patel, S.C. and Patel, Y.C. (1999) Subtype-selective expression of the five somatostatin receptors (hSSTR1-5) in human pancreatic islet cells: a quantitative double-label immunohistochemical analysis. *Diabetes*, **48**, 77-85.

Kuner, R., Kohr, G., Grunewald, S., Eisenhardt, G., Bach, A. and Kornau, H.C. (1999) Role of heteromer formation in GABAB receptor function. *Science*, **283**, 74-77.

Kunishima, N., Shimada, Y., Tsuji, Y., Sato, T., Yamamoto, M., Kumasaka, T., Nakanishi, S., Jingami, H. and Morikawa, K. (2000) Structural basis of glutamate recognition by a dimeric metabotropic glutamate receptor. *Nature*, **407**, 971-977.

Kwekkeboom, D.J., de Jong, M. and Krenning, E.P. (2004) Somatostatin receptor imaging. In Srikant, C.B. (ed.), *Somatostatin*. Kluwer Academic Publishers, Norwell, pp. 203-214.

Labeur, M., Theodoropoulou, M., Sievers, C., Paez-Pereda, M., Castillo, V., Arzt, E. and Stalla, G.K. (2006) New aspects in the diagnosis and treatment of Cushing disease. *Front Horm Res*, **35**, 169-178.

Lahlou, H., Saint-Laurent, N., Esteve, J.P., Eychene, A., Pradayrol, L., Pyronnet, S. and Susini, C. (2003) sst2 Somatostatin receptor inhibits cell proliferation through Ras-, Rap1-, and B-Raf-dependent ERK2 activation. *J Biol Chem*, **278**, 39356-39371.

Lamberts, S.W., de Herder, W.W. and Hofland, L.J. (2002) Somatostatin analogs in the diagnosis and treatment of cancer. *Trends Endocrinol Metab*, **13**, 451-457.

Lamberts, S.W., Krenning, E.P. and Reubi, J.C. (1991) The role of somatostatin and its analogs in the diagnosis and treatment of tumors. *Endocr Rev*, **12**, 450-482.

Lamberts, S.W., van der Lely, A.J., de Herder, W.W. and Hofland, L.J. (1996) Octreotide. *N Engl J Med*, **334**, 246-254.

Latif, R., Graves, P. and Davies, T.F. (2002) Ligand-dependent inhibition of oligomerization at the human thyrotropin receptor. *J Biol Chem*, **277**, 45059-45067.

Lavoie, C., Mercier, J.F., Salahpour, A., Umapathy, D., Breit, A., Villeneuve, L.R., Zhu, W.Z., Xiao, R.P., Lakatta, E.G., Bouvier, M. and Hebert, T.E. (2002) Beta 1/beta 2-adrenergic receptor heterodimerization regulates beta 2-adrenergic receptor internalization and ERK signaling efficacy. *J Biol Chem*, **277**, 35402-35410.

Law, P.Y., Erickson-Herbrandson, L.J., Zha, Q.Q., Solberg, J., Chu, J., Sarre, A. and Loh, H.H. (2005) Heterodimerization of mu- and delta-opioid receptors occurs at the cell surface only and requires receptor-G protein interactions. *J Biol Chem*, **280**, 11152-11164.

Lee, S.P., So, C.H., Rashid, A.J., Varghese, G., Cheng, R., Lanca, A.J., O'Dowd, B.F. and George, S.R. (2004) Dopamine D1 and D2 receptor Co-activation generates a novel phospholipase C-mediated calcium signal. *J Biol Chem*, **279**, 35671-35678.

Lefkowitz, R.J. (2004) Historical review: a brief history and personal retrospective of seven-transmembrane receptors. *Trends Pharmacol Sci*, **25**, 413-422.

Lefkowitz, R.J. and Shenoy, S.K. (2005) Transduction of receptor signals by beta-arrestins. *Science*, **308**, 512-517.

Li, X., Staszewski, L., Xu, H., Durick, K., Zoller, M. and Adler, E. (2002) Human receptors for sweet and umami taste. *Proc Natl Acad Sci U S A*, **99**, 4692-4696.

Liang, Y., Fotiadis, D., Filipek, S., Saperstein, D.A., Palczewski, K. and Engel, A. (2003) Organization of the G protein-coupled receptors rhodopsin and opsin in native membranes. *J Biol Chem*, **278**, 21655-21662.

Liapakis, G., Hoeger, C., Rivier, J. and Reisine, T. (1996) Development of a selective agonist at the somatostatin receptor subtype sstr1. *J Pharmacol Exp Ther*, **276**, 1089-1094.

Lidhar, K., Korbonits, M., Jordan, S., Khalimova, Z., Kaltsas, G., Lu, X., Clayton, R.N., Jenkins, P.J., Monson, J.P., Besser, G.M., Lowe, D.G. and Grossman, A.B. (1999) Low expression of the cell cycle inhibitor p27Kip1 in normal corticotroph cells, corticotroph tumors, and malignant pituitary tumors. *J Clin Endocrinol Metab*, **84**, 3823-3830.

Lin, C.Y., Varma, M.G., Joubel, A., Madabushi, S., Lichtarge, O. and Barber, D.L. (2003) Conserved motifs in somatostatin, D2-dopamine, and alpha 2B-adrenergic receptors for inhibiting the Na-H exchanger, NHE1. *J Biol Chem*, **278**, 15128-15135.

Liu, D., Martino, G., Thangaraju, M., Sharma, M., Halwani, F., Shen, S.H., Patel, Y.C. and Srikant, C.B. (2000) Caspase-8-mediated intracellular acidification precedes mitochondrial dysfunction in somatostatin-induced apoptosis. *J Biol Chem*, **275**, 9244-9250.

Liu, Q. and Schonbrunn, A. (2001) Agonist-induced phosphorylation of somatostatin receptor subtype 1 (sst1). Relationship to desensitization and internalization. *J Biol Chem*, **276**, 3709-3717.

Liu, Y.F., Jakobs, K.H., Rasenick, M.M. and Albert, P.R. (1994) G protein specificity in receptor-effector coupling. Analysis of the roles of G0 and Gi2 in GH4C1 pituitary cells. *J Biol Chem*, **269**, 13880-13886.

Lohse, M.J., Benovic, J.L., Codina, J., Caron, M.G. and Lefkowitz, R.J. (1990) beta-Arrestin: a protein that regulates beta-adrenergic receptor function. *Science*, **248**, 1547-1550.

Lopez, F., Esteve, J.P., Buscail, L., Delesque, N., Saint-Laurent, N., Theveniau, M., Nahmias, C., Vaysse, N. and Susini, C. (1997) The tyrosine phosphatase SHP-1 associates with the sst2 somatostatin receptor and is an essential component of sst2-mediated inhibitory growth signaling. *J Biol Chem*, **272**, 24448-24454.

Lopez, F., Ferjoux, G., Cordelier, P., Saint-Laurent, N., Esteve, J.P., Vaysse, N., Buscail, L. and Susini, C. (2001) Neuronal nitric oxide synthase: a substrate for SHP-1 involved in sst2 somatostatin receptor growth inhibitory signaling. *FASEB J*, **15**, 2300-2302.

Losa, M., Ciccarelli, E., Mortini, P., Barzaghi, R., Gaia, D., Faccani, G., Papotti, M., Mangili, F., Terreni, M.R., Camanni, F. and Giovanelli, M. (2001) Effects of octreotide treatment on the proliferation and apoptotic index of GH-secreting pituitary adenomas. *J Clin Endocrinol Metab*, **86**, 5194-5200.

Low, M.J., Otero-Corchon, V., Parlow, A.F., Ramirez, J.L., Kumar, U., Patel, Y.C. and Rubinstein, M. (2001) Somatostatin is required for masculinization of growth hormone-regulated hepatic gene expression but not of somatic growth. *J Clin Invest*, **107**, 1571-1580.

Luft, R., Efendic, S., Hokfelt, T., Johansson, O. and Arimura, A. (1974) Immunohistochemical evidence for the localization of somatostatin--like

immunoreactivity in a cell population of the pancreatic islets. *Med Biol*, **52**, 428-430.

Maggio, R., Vogel, Z. and Wess, J. (1993) Coexpression studies with mutant muscarinic/adrenergic receptors provide evidence for intermolecular "cross-talk" between G-protein-linked receptors. *Proc Natl Acad Sci U S A*, **90**, 3103-3107.

Mandarino, L., Stenner, D., Blanchard, W., Nissen, S., Gerich, J., Ling, N., Brazeau, P., Bohlen, P., Esch, F. and Guillemin, R. (1981) Selective effects of somatostatin-14, -25 and -28 on in vitro insulin and glucagon secretion. *Nature*, **291**, 76-77.

Marks, N., Stern, F. and Benuck, M. (1976) Correlation between biological potency and biodegradation of a somatostatin analogue. *Nature*, **261**, 511-512.

Martin, S.C., Russek, S.J. and Farb, D.H. (1999) Molecular identification of the human GABABR2: cell surface expression and coupling to adenylyl cyclase in the absence of GABABR1. *Mol Cell Neurosci*, **13**, 180-191.

Marzullo, P., Ferone, D., Di Somma, C., Pivonello, R., Filippella, M., Lombardi, G. and Colao, A. (1999) Efficacy of combined treatment with lanreotide and cabergoline in selected therapy-resistant acromegalic patients. *Pituitary*, **1**, 115-120.

Massa, A., Barbieri, F., Aiello, C., Arena, S., Pattarozzi, A., Pirani, P., Corsaro, A., Iuliano, R., Fusco, A., Zona, G., Spaziante, R., Florio, T. and Schettini, G. (2004a) The expression of the phosphotyrosine phosphatase DEP-1/PTPeta dictates the responsivity of glioma cells to somatostatin inhibition of cell proliferation. *J Biol Chem*, **279**, 29004-29012.

Massa, A., Barbieri, F., Aiello, C., Iuliano, R., Arena, S., Pattarozzi, A., Corsaro, A., Villa, V., Fusco, A., Zona, G., Spaziante, R., Schettini, G. and Florio, T. (2004b) The phosphotyrosine phosphatase eta mediates somatostatin inhibition of glioma proliferation via the dephosphorylation of ERK1/2. *Ann N Y Acad Sci*, **1030**, 264-274.

Maurer, R., Gaehwiler, B.H., Buescher, H.H., Hill, R.C. and Roemer, D. (1982) Opiate antagonistic properties of an octapeptide somatostatin analog. *Proc Natl Acad Sci U S A*, **79**, 4815-4817.

Max, M., Shanker, Y.G., Huang, L., Rong, M., Liu, Z., Campagne, F., Weinstein, H., Damak, S. and Margolskee, R.F. (2001) Tas1r3, encoding a new candidate taste receptor, is allelic to the sweet responsiveness locus Sac. *Nat Genet*, **28**, 58-63.

McGraw, D.W., Mihlbachler, K.A., Schwarb, M.R., Rahman, F.F., Small, K.M., Almoosa, K.F. and Liggett, S.B. (2006) Airway smooth muscle prostaglandin-EP1 receptors directly modulate beta2-adrenergic receptors within a unique heterodimeric complex. *J Clin Invest*, **116**, 1400-1409.

McLaughlin, J.N., Patterson, M.M. and Malik, A.B. (2007) Protease-activated receptor-3 (PAR3) regulates PAR1 signaling by receptor dimerization. *Proc Natl Acad Sci U S A*, **104**, 5662-5667.

McVey, M., Ramsay, D., Kellett, E., Rees, S., Wilson, S., Pope, A.J. and Milligan, G. (2001) Monitoring receptor oligomerization using time-resolved fluorescence resonance energy transfer and bioluminescence resonance energy transfer. The human delta -opioid receptor displays constitutive oligomerization at the cell surface, which is not regulated by receptor occupancy. *J Biol Chem*, **276**, 14092-14099.

Mellado, M., Rodriguez-Frade, J.M., Manes, S. and Martinez, A.C. (2001a) Chemokine signaling and functional responses: the role of receptor dimerization and TK pathway activation. *Annu Rev Immunol*, **19**, 397-421.

Mellado, M., Rodriguez-Frade, J.M., Vila-Coro, A.J., Fernandez, S., Martin de Ana, A., Jones, D.R., Toran, J.L. and Martinez, A.C. (2001b) Chemokine receptor homo- or heterodimerization activates distinct signaling pathways. *Embo J*, **20**, 2497-2507.

Melmed, S., Sternberg, R., Cook, D., Klibanski, A., Chanson, P., Bonert, V., Vance, M.L., Rhew, D., Kleinberg, D. and Barkan, A. (2005) A critical analysis of pituitary tumor shrinkage during primary medical therapy in acromegaly. *J Clin Endocrinol Metab*, **90**, 4405-4410.

Meriney, S.D., Gray, D.B. and Pilar, G.R. (1994) Somatostatin-induced inhibition of neuronal Ca2+ current modulated by cGMP-dependent protein kinase. *Nature*, **369**, 336-339.

Meyer, B.H., Segura, J.M., Martinez, K.L., Hovius, R., George, N., Johnsson, K. and Vogel, H. (2006) FRET imaging reveals that functional neurokinin-1 receptors are monomeric and reside in membrane microdomains of live cells. *Proc Natl Acad Sci U S A*, **103**, 2138-2143.

Meyerhof, W. (1998) The elucidation of somatostatin receptor functions: a current view. *Rev Physiol Biochem Pharmacol*, **133**, 55-108.

Milasta, S., Pediani, J., Appelbe, S., Trim, S., Wyatt, M., Cox, P., Fidock, M. and Milligan, G. (2006) Interactions between the Mas-related receptors MrgD and MrgE alter signalling and trafficking of MrgD. *Mol Pharmacol*, **69**, 479-491.

Miller, G.M., Alexander, J.M., Bikkal, H.A., Katznelson, L., Zervas, N.T. and Klibanski, A. (1995) Somatostatin receptor subtype gene expression in pituitary adenomas. *J Clin Endocrinol Metab*, **80**, 1386-1392.

Milligan, G. (2004a) Applications of bioluminescence- and fluorescence resonance energy transfer to drug discovery at G protein-coupled receptors. *Eur J Pharm Sci*, **21**, 397-405.

Milligan, G. (2004b) G protein-coupled receptor dimerization: function and ligand pharmacology. *Mol Pharmacol*, **66**, 1-7.

Milligan, G. (2008) A day in the life of a G protein-coupled receptor: the contribution to function of G protein-coupled receptor dimerization. *Br J Pharmacol*, **153 Suppl 1**, S216-229.

Milligan, G. and Bouvier, M. (2005) Methods to monitor the quaternary structure of G protein-coupled receptors. *Febs J*, **272**, 2914-2925.

Moller, L.N., Stidsen, C.E., Hartmann, B. and Holst, J.J. (2003) Somatostatin receptors. *Biochim Biophys Acta*, **1616**, 1-84.

Monnot, C., Bihoreau, C., Conchon, S., Curnow, K.M., Corvol, P. and Clauser, E. (1996) Polar residues in the transmembrane domains of the type 1 angiotensin II receptor are required for binding and coupling. Reconstitution of the binding site by co-expression of two deficient mutants. *J Biol Chem*, **271**, 1507-1513.

Montmayeur, J.P., Liberles, S.D., Matsunami, H. and Buck, L.B. (2001) A candidate taste receptor gene near a sweet taste locus. *Nat Neurosci*, **4**, 492-498.

Montminy, M.R., Low, M.J., Tapia-Arancibia, L., Reichlin, S., Mandel, G. and Goodman, R.H. (1986) Cyclic AMP regulates somatostatin mRNA accumulation

in primary diencephalic cultures and in transfected fibroblast cells. *J Neurosci*, **6**, 1171-1176.

Morel, G., Leroux, P. and Pelletier, G. (1985) Ultrastructural autoradiographic localization of somatostatin-28 in the rat pituitary gland. *Endocrinology*, **116**, 1615-1620.

Mouchantaf, R., Patel, Y.C. and Kumar, U. (2004) Processing and intracellular targeting of somatostatin. In Srikant, C.B. (ed.), *Somatostatin*. Kluwer Academic Publishers, Norwell, pp. 16-27.

Murray, R.D., Kim, K., Ren, S.G., Chelly, M., Umehara, Y. and Melmed, S. (2004) Central and peripheral actions of somatostatin on the growth hormone-IGF-I axis. *J Clin Invest*, **114**, 349-356.

Neel, N.F., Schutyser, E., Sai, J., Fan, G.H. and Richmond, A. (2005) Chemokine receptor internalization and intracellular trafficking. *Cytokine Growth Factor Rev*, **16**, 637-658.

Nekrasova, E., Sosinskaya, A., Natochin, M., Lancet, D. and Gat, U. (1996) Overexpression, solubilization and purification of rat and human olfactory receptors. *Eur J Biochem*, **238**, 28-37.

Nelson-Piercy, C., Hammond, P.J., Gwilliam, M.E., Khandan-Nia, N., Myers, M.J., Ghatei, M.A. and Bloom, S.R. (1994) Effect of a new oral somatostatin analog (SDZ CO 611) on gastric emptying, mouth to cecum transit time, and pancreatic and gut hormone release in normal male subjects. *J Clin Endocrinol Metab*, **78**, 329-336.

Nelson, G., Chandrashekar, J., Hoon, M.A., Feng, L., Zhao, G., Ryba, N.J. and Zuker, C.S. (2002) An amino-acid taste receptor. *Nature*, **416**, 199-202.

Nelson, G., Hoon, M.A., Chandrashekar, J., Zhang, Y., Ryba, N.J. and Zuker, C.S. (2001) Mammalian sweet taste receptors. *Cell*, **106**, 381-390.

Ng, G.Y., Clark, J., Coulombe, N., Ethier, N., Hebert, T.E., Sullivan, R., Kargman, S., Chateauneuf, A., Tsukamoto, N., McDonald, T., Whiting, P., Mezey, E., Johnson, M.P., Liu, Q., Kolakowski, L.F., Jr., Evans, J.F., Bonner, T.I. and O'Neill, G.P. (1999) Identification of a GABAB receptor subunit, gb2, required for functional GABAB receptor activity. *J Biol Chem*, **274**, 7607-7610.

Ng, G.Y., George, S.R., Zastawny, R.L., Caron, M., Bouvier, M., Dennis, M. and O'Dowd, B.F. (1993) Human serotonin1B receptor expression in Sf9 cells: phosphorylation, palmitoylation, and adenylyl cyclase inhibition. *Biochemistry*, **32**, 11727-11733.

Ng, G.Y., Mouillac, B., George, S.R., Caron, M., Dennis, M., Bouvier, M. and O'Dowd, B.F. (1994a) Desensitization, phosphorylation and palmitoylation of the human dopamine D1 receptor. *Eur J Pharmacol*, **267**, 7-19.

Ng, G.Y., O'Dowd, B.F., Caron, M., Dennis, M., Brann, M.R. and George, S.R. (1994b) Phosphorylation and palmitoylation of the human D2L dopamine receptor in Sf9 cells. *J Neurochem*, **63**, 1589-1595.

Ng, G.Y., O'Dowd, B.F., Lee, S.P., Chung, H.T., Brann, M.R., Seeman, P. and George, S.R. (1996) Dopamine D2 receptor dimers and receptor-blocking peptides. *Biochem Biophys Res Commun*, **227**, 200-204.

Ng, G.Y., Varghese, G., Chung, H.T., Trogadis, J., Seeman, P., O'Dowd, B.F. and George, S.R. (1997) Resistance of the dopamine D2L receptor to desensitization

accompanies the up-regulation of receptors on to the surface of Sf9 cells. *Endocrinology*, **138**, 4199-4206.

Nichols, B. (2003) Caveosomes and endocytosis of lipid rafts. *J Cell Sci*, **116**, 4707-4714.

Nouel, D., Gaudriault, G., Houle, M., Reisine, T., Vincent, J.P., Mazella, J. and Beaudet, A. (1997) Differential internalization of somatostatin in COS-7 cells transfected with SST1 and SST2 receptor subtypes: a confocal microscopic study using novel fluorescent somatostatin derivatives. *Endocrinology*, **138**, 296-306.

Nunn, C., Langenegger, D., Hurth, K., Schmidt, K., Fehlmann, D. and Hoyer, D. (2003) Agonist properties of putative small-molecule somatostatin sst2 receptor-selective antagonists. *Eur J Pharmacol*, **465**, 211-218.

O'Carroll, A.M. and Krempels, K. (1995) Widespread distribution of somatostatin receptor messenger ribonucleic acids in rat pituitary. *Endocrinology*, **136**, 5224-5227.

O'Carroll, A.M., Raynor, K., Lolait, S.J. and Reisine, T. (1994) Characterization of cloned human somatostatin receptor SSTR5. *Mol Pharmacol*, **46**, 291-298.

Olias, G., Viollet, C., Kusserow, H., Epelbaum, J. and Meyerhof, W. (2004) Regulation and function of somatostatin receptors. *J Neurochem*, **89**, 1057-1091.

Oomen, S.P., Hofland, L.J., Lamberts, S.W., Lowenberg, B. and Touw, I.P. (2001) Internalization-defective mutants of somatostatin receptor subtype 2 exert normal signaling functions in hematopoietic cells. *FEBS Lett*, **503**, 163-167.

Orci, L., Baetens, D., Dubois, M.P. and Rufener, C. (1975) Evidence for the D-cell of the pancreas secreting somatostatin. *Horm Metab Res*, **7**, 400-402.

Osuga, Y., Hayashi, M., Kudo, M., Conti, M., Kobilka, B. and Hsueh, A.J. (1997) Co-expression of defective luteinizing hormone receptor fragments partially reconstitutes ligand-induced signal generation. *J Biol Chem*, **272**, 25006-25012.

Overton, M.C. and Blumer, K.J. (2000) G-protein-coupled receptors function as oligomers in vivo. *Curr Biol*, **10**, 341-344.

Overton, M.C. and Blumer, K.J. (2002) The extracellular N-terminal domain and transmembrane domains 1 and 2 mediate oligomerization of a yeast G protein-coupled receptor. *J Biol Chem*, **277**, 41463-41472.

Overton, M.C., Chinault, S.L. and Blumer, K.J. (2003) Oligomerization, biogenesis, and signaling is promoted by a glycophorin A-like dimerization motif in transmembrane domain 1 of a yeast G protein-coupled receptor. *J Biol Chem*, **278**, 49369-49377.

Oyama, H., O'Connell, K. and Permutt, A. (1980) Cell-mediated synthesis of somatostatin. *Endocrinology*, **107**, 845-847.

Pagano, A., Rovelli, G., Mosbacher, J., Lohmann, T., Duthey, B., Stauffer, D., Ristig, D., Schuler, V., Meigel, I., Lampert, C., Stein, T., Prezeau, L., Blahos, J., Pin, J., Froestl, W., Kuhn, R., Heid, J., Kaupmann, K. and Bettler, B. (2001) C-terminal interaction is essential for surface trafficking but not for heteromeric assembly of GABA(b) receptors. *J Neurosci*, **21**, 1189-1202.

Pages, P., Benali, N., Saint-Laurent, N., Esteve, J.P., Schally, A.V., Tkaczuk, J., Vaysse, N., Susini, C. and Buscail, L. (1999) sst2 somatostatin receptor mediates cell cycle arrest and induction of p27(Kip1). Evidence for the role of SHP-1. *J Biol Chem*, **274**, 15186-15193.

Pagliacci, M.C., Tognellini, R., Grignani, F. and Nicoletti, I. (1991) Inhibition of human breast cancer cell (MCF-7) growth in vitro by the somatostatin analog SMS 201-995: effects on cell cycle parameters and apoptotic cell death. *Endocrinology*, **129**, 2555-2562.

Paglin, S. and Jamieson, J.D. (1982) Covalent crosslinking of angiotensin II to its binding sites in rat adrenal membranes. *Proc Natl Acad Sci U S A*, **79**, 3739-3743.

Palczewski, K., Kumasaka, T., Hori, T., Behnke, C.A., Motoshima, H., Fox, B.A., Le Trong, I., Teller, D.C., Okada, T., Stenkamp, R.E., Yamamoto, M. and Miyano, M. (2000) Crystal structure of rhodopsin: A G protein-coupled receptor. *Science*, **289**, 739-745.

Panetta, R. and Patel, Y.C. (1995) Expression of mRNA for all five human somatostatin receptors (hSSTR1-5) in pituitary tumors. *Life Sci*, **56**, 333-342.

Papotti, M., Tarabra, E., Allia, E., Bozzalla-Cassione, F., Broglio, F., Deghenghi, R., Ghigo, E. and Muccioli, G. (2003) Presence of cortistatin in the human pancreas. *J Endocrinol Invest*, **26**, RC15-18.

Park, C., Yang, I., Woo, J., Kim, S., Kim, J., Kim, Y., Sohn, S., Kim, E., Lee, M., Park, H., Jung, J. and Park, S. (2004a) Somatostatin (SRIF) receptor subtype 2 and 5 gene expression in growth hormone-secreting pituitary adenomas: the relationship with endogenous srif activity and response to octreotide. *Endocr J*, **51**, 227-236.

Park, P.S., Filipek, S., Wells, J.W. and Palczewski, K. (2004b) Oligomerization of G protein-coupled receptors: past, present, and future. *Biochemistry*, **43**, 15643-15656.

Patch, D. and Burroughs, A. (2002) Vapreotide in variceal bleeding. *J Hepatol*, **37**, 167-168.

Patel, R.C., Kumar, U., Lamb, D.C., Eid, J.S., Rocheville, M., Grant, M., Rani, A., Hazlett, T., Patel, S.C., Gratton, E. and Patel, Y.C. (2002a) Ligand binding to somatostatin receptors induces receptor-specific oligomer formation in live cells. *Proc Natl Acad Sci U S A*, **99**, 3294-3299.

Patel, R.C., Lange, D.C. and Patel, Y.C. (2002b) Photobleaching fluorescence resonance energy transfer reveals ligand-induced oligomer formation of human somatostatin receptor subtypes. *Methods*, **27**, 340-348.

Patel, Y.C. (1992) General aspects of the biology and function of somatostatin. In Y.C. Patel, W.E.E.M.a.M.O.T. (ed.), *Basic and Clinical Aspects of Neuroscience*. Springer-Verlag, Berlin, Vol. 4, pp. 1-16.

Patel, Y.C. (1997) Molecular pharmacology of somatostatin receptor subtypes. *J Endocrinol Invest*, **20**, 348-367.

Patel, Y.C. (1999) Somatostatin and its receptor family. *Front Neuroendocrinol*, **20**, 157-198.

Patel, Y.C., Greenwood, M., Kent, G., Panetta, R. and Srikant, C.B. (1993) Multiple gene transcripts of the somatostatin receptor SSTR2: tissue selective distribution and cAMP regulation. *Biochem Biophys Res Commun*, **192**, 288-294.

Patel, Y.C., Greenwood, M., Panetta, R., Hukovic, N., Grigorakis, S., Robertson, L.A. and Srikant, C.B. (1996) Molecular biology of somatostatin receptor subtypes. *Metabolism*, **45**, 31-38.

Patel, Y.C., Greenwood, M.T., Panetta, R., Demchyshyn, L., Niznik, H. and Srikant, C.B. (1995) The somatostatin receptor family. *Life Sci*, **57**, 1249-1265.

Patel, Y.C., Greenwood, M.T., Warszynska, A., Panetta, R. and Srikant, C.B. (1994) All five cloned human somatostatin receptors (hSSTR1-5) are functionally coupled to adenylyl cyclase. *Biochem Biophys Res Commun*, **198**, 605-612.

Patel, Y.C., Liu, J.L., Galanopoulou, A.S. and Papachristou, D.N. (2001) Production, action, and degradation of somatostatin. In Jefferson, L.S. and Cherrington, A.D. (eds.), *Handbook of Physiology, The Endocrine Pancreas and Regulation of Metabolism*. Oxford University Press, New York, Vol. II.

Patel, Y.C., Murthy, K.K., Escher, E.E., Banville, D., Spiess, J. and Srikant, C.B. (1990) Mechanism of action of somatostatin: an overview of receptor function and studies of the molecular characterization and purification of somatostatin receptor proteins. *Metabolism*, **39**, 63-69.

Patel, Y.C. and O'Neil, W. (1988) Peptides derived from cleavage of prosomatostatin at carboxyl- and amino-terminal segments. Characterization of tissue and secreted forms in the rat. *J Biol Chem*, **263**, 745-751.

Patel, Y.C., Papachristou, D.N., Zingg, H.H. and Farkas, E.M. (1991) Regulation of islet somatostatin secretion and gene expression: selective effects of adenosine 3',5'-monophosphate and phorbol esters in normal islets of Langerhans and in a somatostatin-producing rat islet clonal cell line 1027 B2. *Endocrinology*, **128**, 1754-1762.

Patel, Y.C. and Reichlin, S. (1978) Somatostatin in hypothalamus, extrahypothalamic brain, and peripheral tissues of the rat. *Endocrinology*, **102**, 523-530.

Patel, Y.C., Wheatley, T. and Ning, C. (1981) Multiple forms of immunoreactive somatostatin: comparison of distribution in neural and nonneural tissues and portal plasma of the rat. *Endocrinology*, **109**, 1943-1949.

Patzelt, C., Tager, H.S., Carroll, R.J. and Steiner, D.F. (1980) Identification of prosomatostatin in pancreatic islets. *Proc Natl Acad Sci U S A*, **77**, 2410-2414.

Peeters, T.L., Depraetere, Y. and Vantrappen, G.R. (1981) Simple extraction method and radioimmunoassay for somatostatin in human plasma. *Clin Chem*, **27**, 888-891.

Pelletier, G., Leclerc, R., Arimura, A. and Schally, A.V. (1975) Letter: Immunohistochemical localization of somatostatin in the rat pancreas. *J Histochem Cytochem*, **23**, 699-702.

Pello, O.M., Martinez-Munoz, L., Parrillas, V., Serrano, A., Rodriguez-Frade, J.M., Toro, M.J., Lucas, P., Monterrubio, M., Martinez, A.C. and Mellado, M. (2008) Ligand stabilization of CXCR4/delta-opioid receptor heterodimers reveals a mechanism for immune response regulation. *Eur J Immunol*, **38**, 537-549.

Penman, E., Wass, J.A., Medbak, S., Morgan, L., Lewis, J.M., Besser, G.M. and Rees, L.H. (1981) Response of circulating immunoreactive somatostatin to nutritional stimuli in normal subjects. *Gastroenterology*, **81**, 692-699.

Perron, A., Chen, Z.G., Gingras, D., Dupre, D.J., Stankova, J. and Rola-Pleszczynski, M. (2003) Agonist-independent desensitization and internalization of the human platelet-activating factor receptor by coumermycin-gyrase B-induced dimerization. *J Biol Chem*, **278**, 27956-27965.

Perron, A., Sharif, N., Sarret, P., Stroh, T. and Beaudet, A. (2007) NTS2 modulates the intracellular distribution and trafficking of NTS1 via heterodimerization. *Biochem Biophys Res Commun*, **353**, 582-590.

Persani, L., Calebiro, D. and Bonomi, M. (2007) Technology Insight: modern methods to monitor protein-protein interactions reveal functional TSH receptor oligomerization. *Nat Clin Pract Endocrinol Metab*, **3**, 180-190.

Pfeiffer, M., Koch, T., Schroder, H., Klutzny, M., Kirscht, S., Kreienkamp, H.J., Hollt, V. and Schulz, S. (2001) Homo- and heterodimerization of somatostatin receptor subtypes. Inactivation of sst(3) receptor function by heterodimerization with sst(2A). *J Biol Chem*, **276**, 14027-14036.

Pfeiffer, M., Koch, T., Schroder, H., Laugsch, M., Hollt, V. and Schulz, S. (2002) Heterodimerization of somatostatin and opioid receptors cross-modulates phosphorylation, internalization, and desensitization. *J Biol Chem*, **277**, 19762-19772.

Pfleger, K.D. and Eidne, K.A. (2005) Monitoring the formation of dynamic G-protein-coupled receptor-protein complexes in living cells. *Biochem J*, **385**, 625-637.

Philippe, J. (1993) Somatostatin inhibits insulin-gene expression through a posttranscriptional mechanism in a hamster islet cell line. *Diabetes*, **42**, 244-249.

Pickering, D.S., Thomsen, C., Suzdak, P.D., Fletcher, E.J., Robitaille, R., Salter, M.W., MacDonald, J.F., Huang, X.P. and Hampson, D.R. (1993) A comparison of two alternatively spliced forms of a metabotropic glutamate receptor coupled to phosphoinositide turnover. *J Neurochem*, **61**, 85-92.

Pierce, K.L., Premont, R.T. and Lefkowitz, R.J. (2002) Seven-transmembrane receptors. *Nat Rev Mol Cell Biol*, **3**, 639-650.

Pin, J.P., Kniazeff, J., Liu, J., Binet, V., Goudet, C., Rondard, P. and Prezeau, L. (2005) Allosteric functioning of dimeric class C G-protein-coupled receptors. *Febs J*, **272**, 2947-2955.

Podesta, E.J., Solano, A.R., Attar, R., Sanchez, M.L. and Molina y Vedia, L. (1983) Receptor aggregation induced by antilutropin receptor antibody and biological response in rat testis Leydig cells. *Proc Natl Acad Sci U S A*, **80**, 3986-3990.

Podesta, E.J., Solano, A.R. and Sanchez, M.L. (1986) Luteinizing hormone triggers two opposite regulatory pathways through an initial common event, receptor aggregation. *Endocrinology*, **119**, 989-997.

Poitout, L., Roubert, P., Contour-Galcera, M.O., Moinet, C., Lannoy, J., Pommier, J., Plas, P., Bigg, D. and Thurieau, C. (2001) Identification of potent non-peptide somatostatin antagonists with sst(3) selectivity. *J Med Chem*, **44**, 2990-3000.

Polak, J.M., Pearse, A.G., Grimelius, L. and Bloom, S.R. (1975) Growth-hormone release-inhibiting hormone in gastrointestinal and pancreatic D cells. *Lancet*, **1**, 1220-1222.

Pradayrol, L., Jornvall, H., Mutt, V. and Ribet, A. (1980) N-terminally extended somatostatin: the primary structure of somatostatin-28. *FEBS Lett*, **109**, 55-58.

Premont, R.T. and Gainetdinov, R.R. (2007) Physiological roles of G protein-coupled receptor kinases and arrestins. *Annu Rev Physiol*, **69**, 511-534.

Presky, D.H. and Schonbrunn, A. (1988) Somatostatin pretreatment increases the number of somatostatin receptors in GH4C1 pituitary cells and does not reduce cellular responsiveness to somatostatin. *J Biol Chem*, **263**, 714-721.

Prinster, S.C., Hague, C. and Hall, R.A. (2005) Heterodimerization of g protein-coupled receptors: specificity and functional significance. *Pharmacol Rev*, **57**, 289-298.

Putney, L.K., Denker, S.P. and Barber, D.L. (2002) The changing face of the Na+/H+ exchanger, NHE1: structure, regulation, and cellular actions. *Annu Rev Pharmacol Toxicol*, **42**, 527-552.

Qanbar, R. and Bouvier, M. (2003) Role of palmitoylation/depalmitoylation reactions in G-protein-coupled receptor function. *Pharmacol Ther*, **97**, 1-33.

Qian, X., Jin, L., Grande, J.P. and Lloyd, R.V. (1996) Transforming growth factor-beta and p27 expression in pituitary cells. *Endocrinology*, **137**, 3051-3060.

Qian, X., Jin, L., Kulig, E. and Lloyd, R.V. (1998) DNA methylation regulates p27kip1 expression in rodent pituitary cell lines. *Am J Pathol*, **153**, 1475-1482.

Quintela, M., Senaris, R.M. and Dieguez, C. (1997) Transforming growth factor-betas inhibit somatostatin messenger ribonucleic acid levels and somatostatin secretion in hypothalamic cells in culture. *Endocrinology*, **138**, 4401-4409.

Quitterer, U., Lother, H. and Abdalla, S. (2004) AT1 receptor heterodimers and angiotensin II responsiveness in preeclampsia. *Semin Nephrol*, **24**, 115-119.

Rabbani, S.N. and Patel, Y.C. (1990) Peptides derived by processing of rat prosomatostatin near the amino-terminus: characterization, tissue distribution, and release. *Endocrinology*, **126**, 2054-2061.

Rashid, A.J., So, C.H., Kong, M.M., Furtak, T., El-Ghundi, M., Cheng, R., O'Dowd, B.F. and George, S.R. (2007) D1-D2 dopamine receptor heterooligomers with unique pharmacology are coupled to rapid activation of Gq/11 in the striatum. *Proc Natl Acad Sci U S A*, **104**, 654-659.

Rasmussen, S.G., Choi, H.J., Rosenbaum, D.M., Kobilka, T.S., Thian, F.S., Edwards, P.C., Burghammer, M., Ratnala, V.R., Sanishvili, R., Fischetti, R.F., Schertler, G.F., Weis, W.I. and Kobilka, B.K. (2007) Crystal structure of the human beta2 adrenergic G-protein-coupled receptor. *Nature*, **450**, 383-387.

Ravazzola, M., Benoit, R., Ling, N. and Orci, L. (1989) Prosomatostatin-derived antrin is present in gastric D cells and in portal blood. *J Clin Invest*, **83**, 362-366.

Reardon, D.B., Dent, P., Wood, S.L., Kong, T. and Sturgill, T.W. (1997) Activation in vitro of somatostatin receptor subtypes 2, 3, or 4 stimulates protein tyrosine phosphatase activity in membranes from transfected Ras-transformed NIH 3T3 cells: coexpression with catalytically inactive SHP-2 blocks responsiveness. *Mol Endocrinol*, **11**, 1062-1069.

Redmon, J.B., Towle, H.C. and Robertson, R.P. (1994) Regulation of human insulin gene transcription by glucose, epinephrine, and somatostatin. *Diabetes*, **43**, 546-551.

Reichlin, S. (1983a) Somatostatin. *N Engl J Med*, **309**, 1495-1501.

Reichlin, S. (1983b) Somatostatin (second of two parts). *N Engl J Med*, **309**, 1556-1563.

Reisine, T. and Axelrod, J. (1983) Prolonged somatostatin pretreatment desensitizes somatostatin's inhibition of receptor-mediated release of adrenocorticotropin hormone and sensitizes adenylate cyclase. *Endocrinology*, **113**, 811-813.

Reisine, T. and Bell, G.I. (1995) Molecular biology of somatostatin receptors. *Endocr Rev*, **16**, 427-442.

Remy, I. and Michnick, S.W. (2006) A highly sensitive protein-protein interaction assay based on Gaussia luciferase. *Nat Methods*, **3**, 977-979.

Ren, S.G., Taylor, J., Dong, J., Yu, R., Culler, M.D. and Melmed, S. (2003) Functional association of somatostatin receptor subtypes 2 and 5 in inhibiting human growth hormone secretion. *J Clin Endocrinol Metab*, **88**, 4239-4245.

Resmini, E., Dadati, P., Ravetti, J.L., Zona, G., Spaziante, R., Saveanu, A., Jaquet, P., Culler, M.D., Bianchi, F., Rebora, A., Minuto, F. and Ferone, D. (2007) Rapid pituitary tumor shrinkage with dissociation between antiproliferative and antisecretory effects of a long-acting octreotide in an acromegalic patient. *J Clin Endocrinol Metab*, **92**, 1592-1599.

Reubi, J.C., Hacki, W.H. and Lamberts, S.W. (1987) Hormone-producing gastrointestinal tumors contain a high density of somatostatin receptors. *J Clin Endocrinol Metab*, **65**, 1127-1134.

Reubi, J.C. and Landolt, A.M. (1984) High density of somatostatin receptors in pituitary tumors from acromegalic patients. *J Clin Endocrinol Metab*, **59**, 1148-1151.

Reubi, J.C., Schaer, J.C., Wenger, S., Hoeger, C., Erchegyi, J., Waser, B. and Rivier, J. (2000) SST3-selective potent peptidic somatostatin receptor antagonists. *Proc Natl Acad Sci U S A*, **97**, 13973-13978.

Reubi, J.C., Waser, B. and Schaer, J.C. (2004) Expression of somatostatin receptors in human tissue in health and disease. In Srikant, C.B. (ed.), *Somatostatin*. Kluwer Academic Publishers, Norwell, pp. 107-121.

Rios, C.D., Jordan, B.A., Gomes, I. and Devi, L.A. (2001) G-protein-coupled receptor dimerization: modulation of receptor function. *Pharmacol Ther*, **92**, 71-87.

Rocheville, M., Lange, D.C., Kumar, U., Patel, S.C., Patel, R.C. and Patel, Y.C. (2000a) Receptors for dopamine and somatostatin: formation of hetero-oligomers with enhanced functional activity. *Science*, **288**, 154-157.

Rocheville, M., Lange, D.C., Kumar, U., Sasi, R., Patel, R.C. and Patel, Y.C. (2000b) Subtypes of the somatostatin receptor assemble as functional homo- and heterodimers. *J Biol Chem*, **275**, 7862-7869.

Rodriguez-Arnao, M.D., Gomez-Pan, A., Rainbow, S.J., Woodhead, S., Comaru-Schally, A.M., Schally, A.V., Meyers, C.A., Coy, D.H. and Hall, R. (1981) Effects of prosomatostatin on growth hormone and prolactin response to arginine in man. Comparison with somatostatin. *Lancet*, **1**, 353-356.

Rodriguez-Frade, J.M., del Real, G., Serrano, A., Hernanz-Falcon, P., Soriano, S.F., Vila-Coro, A.J., de Ana, A.M., Lucas, P., Prieto, I., Martinez, A.C. and Mellado, M. (2004) Blocking HIV-1 infection via CCR5 and CXCR4 receptors by acting in trans on the CCR2 chemokine receptor. *Embo J*, **23**, 66-76.

Rodriguez-Frade, J.M., Vila-Coro, A.J., de Ana, A.M., Albar, J.P., Martinez, A.C. and Mellado, M. (1999) The chemokine monocyte chemoattractant protein-1 induces functional responses through dimerization of its receptor CCR2. *Proc Natl Acad Sci U S A*, **96**, 3628-3633.

Rodriguez-Sanchez, M.N., Puebla, L., Lopez-Sanudo, S., Rodriguez-Martin, E., Martin-Espinosa, A., Rodriguez-Pena, M.S., Juarranz, M.G. and Arilla, E. (1997) Dopamine enhances somatostatin receptor-mediated inhibition of adenylate cyclase in rat striatum and hippocampus. *J Neurosci Res*, **48**, 238-248.

Roess, D.A., Horvat, R.D., Munnelly, H. and Barisas, B.G. (2000) Luteinizing hormone receptors are self-associated in the plasma membrane. *Endocrinology*, **141**, 4518-4523.

Roess, D.A. and Smith, S.M. (2003) Self-association and raft localization of functional luteinizing hormone receptors. *Biol Reprod*, **69**, 1765-1770.

Rohrer, S.P., Birzin, E.T., Mosley, R.T., Berk, S.C., Hutchins, S.M., Shen, D.M., Xiong, Y., Hayes, E.C., Parmar, R.M., Foor, F., Mitra, S.W., Degrado, S.J., Shu, M., Klopp, J.M., Cai, S.J., Blake, A., Chan, W.W., Pasternak, A., Yang, L., Patchett, A.A., Smith, R.G., Chapman, K.T. and Schaeffer, J.M. (1998) Rapid identification of subtype-selective agonists of the somatostatin receptor through combinatorial chemistry. *Science*, **282**, 737-740.

Romano, C., Yang, W.L. and O'Malley, K.L. (1996) Metabotropic glutamate receptor 5 is a disulfide-linked dimer. *J Biol Chem*, **271**, 28612-28616.

Roosterman, D., Roth, A., Kreienkamp, H.J., Richter, D. and Meyerhof, W. (1997) Distinct agonist-mediated endocytosis of cloned rat somatostatin receptor subtypes expressed in insulinoma cells. *J Neuroendocrinol*, **9**, 741-751.

Roth, A., Kreienkamp, H.J., Meyerhof, W. and Richter, D. (1997a) Phosphorylation of four amino acid residues in the carboxyl terminus of the rat somatostatin receptor subtype 3 is crucial for its desensitization and internalization. *J Biol Chem*, **272**, 23769-23774.

Roth, A., Kreienkamp, H.J., Nehring, R.B., Roosterman, D., Meyerhof, W. and Richter, D. (1997b) Endocytosis of the rat somatostatin receptors: subtype discrimination, ligand specificity, and delineation of carboxy-terminal positive and negative sequence motifs. *DNA Cell Biol*, **16**, 111-119.

Sainz, E., Korley, J.N., Battey, J.F. and Sullivan, S.L. (2001) Identification of a novel member of the T1R family of putative taste receptors. *J Neurochem*, **77**, 896-903.

Saito, T., Iwata, N., Tsubuki, S., Takaki, Y., Takano, J., Huang, S.M., Suemoto, T., Higuchi, M. and Saido, T.C. (2005) Somatostatin regulates brain amyloid beta peptide Abeta42 through modulation of proteolytic degradation. *Nat Med*, **11**, 434-439.

Salim, K., Fenton, T., Bacha, J., Urien-Rodriguez, H., Bonnert, T., Skynner, H.A., Watts, E., Kerby, J., Heald, A., Beer, M., McAllister, G. and Guest, P.C. (2002) Oligomerization of G-protein-coupled receptors shown by selective co-immunoprecipitation. *J Biol Chem*, **277**, 15482-15485.

Samuels, M.H., Henry, P. and Ridgway, E.C. (1992) Effects of dopamine and somatostatin on pulsatile pituitary glycoprotein secretion. *J Clin Endocrinol Metab*, **74**, 217-222.

Sarmiento, J.M., Anazco, C.C., Campos, D.M., Prado, G.N., Navarro, J. and Gonzalez, C.B. (2004) Novel down-regulatory mechanism of the surface expression of the vasopressin V2 receptor by an alternative splice receptor variant. *J Biol Chem*, **279**, 47017-47023.

Saveanu, A., Gunz, G., Dufour, H., Caron, P., Fina, F., Ouafik, L., Culler, M.D., Moreau, J.P., Enjalbert, A. and Jaquet, P. (2001) Bim-23244, a somatostatin receptor subtype 2- and 5-selective analog with enhanced efficacy in suppressing growth hormone (GH) from octreotide-resistant human GH-secreting adenomas. *J Clin Endocrinol Metab*, **86**, 140-145.

Saveanu, A., Gunz, G., Guillen, S., Dufour, H., Culler, M.D. and Jaquet, P. (2006) Somatostatin and dopamine-somatostatin multiple ligands directed towards somatostatin and dopamine receptors in pituitary adenomas. *Neuroendocrinology*, **83**, 258-263.

Saveanu, A., Lavaque, E., Gunz, G., Barlier, A., Kim, S., Taylor, J.E., Culler, M.D., Enjalbert, A. and Jaquet, P. (2002) Demonstration of enhanced potency of a chimeric somatostatin-dopamine molecule, BIM-23A387, in suppressing growth hormone and prolactin secretion from human pituitary somatotroph adenoma cells. *J Clin Endocrinol Metab*, **87**, 5545-5552.

Scarborough, D.E., Lee, S.L., Dinarello, C.A. and Reichlin, S. (1989) Interleukin-1 beta stimulates somatostatin biosynthesis in primary cultures of fetal rat brain. *Endocrinology*, **124**, 549-551.

Scarselli, M., Novi, F., Schallmach, E., Lin, R., Baragli, A., Colzi, A., Griffon, N., Corsini, G.U., Sokoloff, P., Levenson, R., Vogel, Z. and Maggio, R. (2001) D2/D3 dopamine receptor heterodimers exhibit unique functional properties. *J Biol Chem*, **276**, 30308-30314.

Schaer, J.C., Waser, B., Mengod, G. and Reubi, J.C. (1997) Somatostatin receptor subtypes sst1, sst2, sst3 and sst5 expression in human pituitary, gastroentero-pancreatic and mammary tumors: comparison of mRNA analysis with receptor autoradiography. *Int J Cancer*, **70**, 530-537.

Schiffrin, E.L. (2002) Beyond blood pressure: the endothelium and atherosclerosis progression. *Am J Hypertens*, **15**, 115S-122S.

Schlessinger, J. (2002) Ligand-induced, receptor-mediated dimerization and activation of EGF receptor. *Cell*, **110**, 669-672.

Schonbrunn, A. and Tashjian, H., Jr. (1978) Characterization of functional receptors for somatostatin in rat pituitary cells in culture. *J Biol Chem*, **253**, 6473-6483.

Schoneberg, T., Sandig, V., Wess, J., Gudermann, T. and Schultz, G. (1997) Reconstitution of mutant V2 vasopressin receptors by adenovirus-mediated gene transfer. Molecular basis and clinical implication. *J Clin Invest*, **100**, 1547-1556.

Schoneberg, T., Yun, J., Wenkert, D. and Wess, J. (1996) Functional rescue of mutant V2 vasopressin receptors causing nephrogenic diabetes insipidus by a co-expressed receptor polypeptide. *Embo J*, **15**, 1283-1291.

Schreff, M., Schulz, S., Handel, M., Keilhoff, G., Braun, H., Pereira, G., Klutzny, M., Schmidt, H., Wolf, G. and Hollt, V. (2000) Distribution, targeting, and internalization of the sst4 somatostatin receptor in rat brain. *J Neurosci*, **20**, 3785-3797.

Schreurs, J., Yamamoto, R., Lyons, J., Munemitsu, S., Conroy, L., Clark, R., Takeda, Y., Krause, J.E. and Innis, M. (1995) Functional wild-type and carboxyl-terminal-tagged rat substance P receptors expressed in baculovirus-infected insect Sf9 cells. *J Neurochem*, **64**, 1622-1631.

Schusdziarra, V., Dobbs, R.E., Harris, V. and Unger, R.H. (1977) Immunoreactive somatostatin levels in plasma of normal and alloxan diabetic dogs. *FEBS Lett*, **81**, 69-72.

Seidah, N.G. and Chretien, M. (1999) Proprotein and prohormone convertases: a family of subtilases generating diverse bioactive polypeptides. *Brain Res*, **848**, 45-62.

Sellers, L.A., Alderton, F., Carruthers, A.M., Schindler, M. and Humphrey, P.P. (2000) Receptor isoforms mediate opposing proliferative effects through gbetagamma-activated p38 or Akt pathways. *Mol Cell Biol*, **20**, 5974-5985.

Senaris, R.M., Lago, F. and Dieguez, C. (1996) Gonadal regulation of somatostatin receptor 1, 2 and 3 mRNA levels in the rat anterior pituitary. *Brain Res Mol Brain Res*, **38**, 171-175.

Sharif, N., Gendron, L., Wowchuk, J., Sarret, P., Mazella, J., Beaudet, A. and Stroh, T. (2007) Coexpression of somatostatin receptor subtype 5 affects internalization and trafficking of somatostatin receptor subtype 2. *Endocrinology*, **148**, 2095-2105.

Sharma, K., Patel, Y.C. and Srikant, C.B. (1996) Subtype-selective induction of wild-type p53 and apoptosis, but not cell cycle arrest, by human somatostatin receptor 3. *Mol Endocrinol*, **10**, 1688-1696.

Sharma, K., Patel, Y.C. and Srikant, C.B. (1999) C-terminal region of human somatostatin receptor 5 is required for induction of Rb and G1 cell cycle arrest. *Mol Endocrinol*, **13**, 82-90.

Sharma, K. and Srikant, C.B. (1998a) G protein coupled receptor signaled apoptosis is associated with activation of a cation insensitive acidic endonuclease and intracellular acidification. *Biochem Biophys Res Commun*, **242**, 134-140.

Sharma, K. and Srikant, C.B. (1998b) Induction of wild-type p53, Bax, and acidic endonuclease during somatostatin-signaled apoptosis in MCF-7 human breast cancer cells. *Int J Cancer*, **76**, 259-266.

Shen, L.P., Pictet, R.L. and Rutter, W.J. (1982) Human somatostatin I: sequence of the cDNA. *Proc Natl Acad Sci U S A*, **79**, 4575-4579.

Shields, D. (1980) In vitro biosynthesis of somatostatin. Evidence for two distinct preprosomatostatin molecules. *J Biol Chem*, **255**, 11625-11628.

Shimon, I., Taylor, J.E., Dong, J.Z., Bitonte, R.A., Kim, S., Morgan, B., Coy, D.H., Culler, M.D. and Melmed, S. (1997a) Somatostatin receptor subtype specificity in human fetal pituitary cultures. Differential role of SSTR2 and SSTR5 for growth hormone, thyroid-stimulating hormone, and prolactin regulation. *J Clin Invest*, **99**, 789-798.

Shimon, I., Yan, X., Taylor, J.E., Weiss, M.H., Culler, M.D. and Melmed, S. (1997b) Somatostatin receptor (SSTR) subtype-selective analogues differentially suppress in vitro growth hormone and prolactin in human pituitary adenomas. Novel potential therapy for functional pituitary tumors. *J Clin Invest*, **100**, 2386-2392.

Shioda, T., Nakayama, E.E., Tanaka, Y., Xin, X., Liu, H., Kawana-Tachikawa, A., Kato, A., Sakai, Y., Nagai, Y. and Iwamoto, A. (2001) Naturally occurring deletional mutation in the C-terminal cytoplasmic tail of CCR5 affects surface trafficking of CCR5. *J Virol*, **75**, 3462-3468.

Shoelson, S.E., Polonsky, K.S., Nakabayashi, T., Jaspan, J.B. and Tager, H.S. (1986) Circulating forms of somatostatinlike immunoreactivity in human plasma. *Am J Physiol*, **250**, E428-434.

Shojamanesh, H., Gibril, F., Louie, A., Ojeaburu, J.V., Bashir, S., Abou-Saif, A. and Jensen, R.T. (2002) Prospective study of the antitumor efficacy of long-term octreotide treatment in patients with progressive metastatic gastrinoma. *Cancer*, **94**, 331-343.

Siler, T.M., Yen, S.C., Vale, W. and Guillemin, R. (1974) Inhibition by somatostatin on the release of TSH induced in man by thyrotropin-releasing factor. *J Clin Endocrinol Metab*, **38**, 742-745.

Sims, S.M., Lussier, B.T. and Kraicer, J. (1991) Somatostatin activates an inwardly rectifying K+ conductance in freshly dispersed rat somatotrophs. *J Physiol*, **441**, 615-637.

Skamene, A. and Patel, Y.C. (1984) Infusion of graded concentrations of somatostatin in man: pharmacokinetics and differential inhibitory effects on pituitary and islet hormones. *Clin Endocrinol (Oxf)*, **20**, 555-564.

Smalley, K.S., Feniuk, W. and Humphrey, P.P. (1998) Differential agonist activity of somatostatin and L-362855 at human recombinant sst4 receptors. *Br J Pharmacol*, **125**, 833-841.

Smalley, K.S., Feniuk, W., Sellers, L.A. and Humphrey, P.P. (1999) The pivotal role of phosphoinositide-3 kinase in the human somatostatin sst(4) receptor-mediated stimulation of p44/p42 mitogen-activated protein kinase and extracellular acidification. *Biochem Biophys Res Commun*, **263**, 239-243.

Smalley, K.S., Koenig, J.A., Feniuk, W. and Humphrey, P.P. (2001) Ligand internalization and recycling by human recombinant somatostatin type 4 (h sst(4)) receptors expressed in CHO-K1 cells. *Br J Pharmacol*, **132**, 1102-1110.

Sohy, D., Parmentier, M. and Springael, J.Y. (2007) Allosteric transinhibition by specific antagonists in CCR2/CXCR4 heterodimers. *J Biol Chem*, **282**, 30062-30069.

Song, G.J. and Hinkle, P.M. (2005) Regulated dimerization of the thyrotropin-releasing hormone receptor affects receptor trafficking but not signaling. *Mol Endocrinol*, **19**, 2859-2870.

Spier, A.D. and de Lecea, L. (2000) Cortistatin: a member of the somatostatin neuropeptide family with distinct physiological functions. *Brain Res Brain Res Rev*, **33**, 228-241.

Srikant, C.B. (1995) Cell cycle dependent induction of apoptosis by somatostatin analog SMS 201-995 in AtT-20 mouse pituitary cells. *Biochem Biophys Res Commun*, **209**, 400-406.

Srikant, C.B. and Patel, Y.C. (1981) Receptor binding of somatostatin-28 is tissue specific. *Nature*, **294**, 259-260.

Srikant, C.B. and Shen, S.H. (1996) Octapeptide somatostatin analog SMS 201-995 induces translocation of intracellular PTP1C to membranes in MCF-7 human breast adenocarcinoma cells. *Endocrinology*, **137**, 3461-3468.

Stanasila, L., Perez, J.B., Vogel, H. and Cotecchia, S. (2003) Oligomerization of the alpha 1a- and alpha 1b-adrenergic receptor subtypes. Potential implications in receptor internalization. *J Biol Chem*, **278**, 40239-40251.

Stefan, E., Aquin, S., Berger, N., Landry, C.R., Nyfeler, B., Bouvier, M. and Michnick, S.W. (2007) Quantification of dynamic protein complexes using Renilla luciferase fragment complementation applied to protein kinase A activities in vivo. *Proc Natl Acad Sci U S A*, **104**, 16916-16921.

Stroh, T., Jackson, A.C., Dal Farra, C., Schonbrunn, A., Vincent, J.P. and Beaudet, A. (2000a) Receptor-mediated internalization of somatostatin in rat cortical and hippocampal neurons. *Synapse*, **38**, 177-186.

Stroh, T., Jackson, A.C., Sarret, P., Dal Farra, C., Vincent, J.P., Kreienkamp, H.J., Mazella, J. and Beaudet, A. (2000b) Intracellular dynamics of sst5 receptors in transfected COS-7 cells: maintenance of cell surface receptors during ligand-induced endocytosis. *Endocrinology*, **141**, 354-365.

Stromberg, I., Popoli, P., Muller, C.E., Ferre, S. and Fuxe, K. (2000) Electrophysiological and behavioural evidence for an antagonistic modulatory role of adenosine A2A receptors in dopamine D2 receptor regulation in the rat dopamine-denervated striatum. *Eur J Neurosci*, **12**, 4033-4037.

Sullivan, S.J. and Schonbrunn, A. (1988) Distribution of somatostatin receptors in RINm5F insulinoma cells. *Endocrinology*, **122**, 1137-1145.

Susini, C. and Buscail, L. (2006) Rationale for the use of somatostatin analogs as antitumor agents. *Ann Oncol*, **17**, 1733-1742.

Takano, K., Yasufuku-Takano, J., Teramoto, A. and Fujita, T. (1997) Gi3 mediates somatostatin-induced activation of an inwardly rectifying K+ current in human growth hormone-secreting adenoma cells. *Endocrinology*, **138**, 2405-2409.

Takeba, Y., Suzuki, N., Takeno, M., Asai, T., Tsuboi, S., Hoshino, T. and Sakane, T. (1997) Modulation of synovial cell function by somatostatin in patients with rheumatoid arthritis. *Arthritis Rheum*, **40**, 2128-2138.

Takeuchi, S., Koeffler, H.P., Hinton, D.R., Miyoshi, I., Melmed, S. and Shimon, I. (1998) Mutation and expression analysis of the cyclin-dependent kinase inhibitor gene p27/Kip1 in pituitary tumors. *J Endocrinol*, **157**, 337-341.

Tallent, M. and Reisine, T. (1992) Gi alpha 1 selectively couples somatostatin receptors to adenylyl cyclase in pituitary-derived AtT-20 cells. *Mol Pharmacol*, **41**, 452-455.

Tanganelli, S., Sandager Nielsen, K., Ferraro, L., Antonelli, T., Kehr, J., Franco, R., Ferre, S., Agnati, L.F., Fuxe, K. and Scheel-Kruger, J. (2004) Striatal plasticity at the network level. Focus on adenosine A2A and D2 interactions in models of Parkinson's Disease. *Parkinsonism Relat Disord*, **10**, 273-280.

Tanjasiri, P., Kozbur, X. and Florsheim, W.H. (1976) Somatostatin in the physiologic feedback control of thyrotropin secretion. *Life Sci*, **19**, 657-660.

Tannenbaum, G.S., McCarthy, G.F., Zeitler, P. and Beaudet, A. (1990) Cysteamine-induced enhancement of growth hormone-releasing factor (GRF) immunoreactivity in arcuate neurons: morphological evidence for putative somatostatin/GRF interactions within hypothalamus. *Endocrinology*, **127**, 2551-2560.

Tannenbaum, G.S., Turner, J., Guo, F., Videau, C., Epelbaum, J. and Beaudet, A. (2001) Homologous upregulation of sst2 somatostatin receptor expression in the rat arcuate nucleus in vivo. *Neuroendocrinology*, **74**, 33-42.

Tannenbaum, G.S., Zhang, W.H., Lapointe, M., Zeitler, P. and Beaudet, A. (1998) Growth hormone-releasing hormone neurons in the arcuate nucleus express both Sst1 and Sst2 somatostatin receptor genes. *Endocrinology*, **139**, 1450-1453.

Tao, Y.X., Johnson, N.B. and Segaloff, D.L. (2004) Constitutive and agonist-dependent self-association of the cell surface human lutropin receptor. *J Biol Chem*, **279**, 5904-5914.

Teijeiro, R., Rios, R., Costoya, J.A., Castro, R., Bello, J.L., Devesa, J. and Arce, V.M. (2002) Activation of human somatostatin receptor 2 promotes apoptosis through a mechanism that is independent from induction of p53. *Cell Physiol Biochem*, **12**, 31-38.

Terrillon, S., Barberis, C. and Bouvier, M. (2004) Heterodimerization of V1a and V2 vasopressin receptors determines the interaction with beta-arrestin and their trafficking patterns. *Proc Natl Acad Sci U S A*, **101**, 1548-1553.

Terrillon, S. and Bouvier, M. (2004) Roles of G-protein-coupled receptor dimerization. *EMBO Rep*, **5**, 30-34.

Terrillon, S., Durroux, T., Mouillac, B., Breit, A., Ayoub, M.A., Taulan, M., Jockers, R., Barberis, C. and Bouvier, M. (2003) Oxytocin and vasopressin V1a and V2 receptors form constitutive homo- and heterodimers during biosynthesis. *Mol Endocrinol*, **17**, 677-691.

Thangaraju, M., Sharma, K., Liu, D., Shen, S.H. and Srikant, C.B. (1999) Interdependent regulation of intracellular acidification and SHP-1 in apoptosis. *Cancer Res*, **59**, 1649-1654.

Thapar, K., Kovacs, K.T., Stefaneanu, L., Scheithauer, B.W., Horvath, E., Lloyd, R.V., Li, J. and Laws, E.R., Jr. (1997) Antiproliferative effect of the somatostatin analogue octreotide on growth hormone-producing pituitary tumors: results of a multicenter randomized trial. *Mayo Clin Proc*, **72**, 893-900.

Theodoropoulou, M., Zhang, J., Laupheimer, S., Paez-Pereda, M., Erneux, C., Florio, T., Pagotto, U. and Stalla, G.K. (2006) Octreotide, a somatostatin analogue, mediates its antiproliferative action in pituitary tumor cells by altering phosphatidylinositol 3-kinase signaling and inducing Zac1 expression. *Cancer Res*, **66**, 1576-1582.

Thevenin, D., Lazarova, T., Roberts, M.F. and Robinson, C.R. (2005) Oligomerization of the fifth transmembrane domain from the adenosine A2A receptor. *Protein Sci*, **14**, 2177-2186.

Tichomirowa, M.A., Daly, A.F. and Beckers, A. (2005) Treatment of pituitary tumors: somatostatin. *Endocrine*, **28**, 93-100.

Tostivint, H., Lihrmann, I., Bucharles, C., Vieau, D., Coulouarn, Y., Fournier, A., Conlon, J.M. and Vaudry, H. (1996) Occurrence of two somatostatin variants in the frog brain: characterization of the cDNAs, distribution of the mRNAs, and receptor-binding affinities of the peptides. *Proc Natl Acad Sci U S A*, **93**, 12605-12610.

Tostivint, H., Trabucchi, M., Vallarino, M., Conlon, J.M., Lihrmann, I. and Vaudry, H. (2004) Molecular evolution of somatostatin genes. In Srikant, C.B. (ed.), *Somatostatin*. Kluwer Academic Publishers, Norwell, pp. 47-64.

Tran, V.T., Beal, M.F. and Martin, J.B. (1985) Two types of somatostatin receptors differentiated by cyclic somatostatin analogs. *Science*, **228**, 492-495.

Trettel, F., Di Bartolomeo, S., Lauro, C., Catalano, M., Ciotti, M.T. and Limatola, C. (2003) Ligand-independent CXCR2 dimerization. *J Biol Chem*, **278**, 40980-40988.

Tsao, P., Cao, T. and von Zastrow, M. (2001) Role of endocytosis in mediating downregulation of G-protein-coupled receptors. *Trends Pharmacol Sci*, **22**, 91-96.

Tsuda, K., Sakurai, H., Seino, Y., Seino, S., Tanigawa, K., Kuzuya, H. and Imura, H. (1981) Somatostatin-like immunoreactivity in human peripheral plasma measured by radioimmunoassay following affinity chromatography. *Diabetes*, **30**, 471-474.

Tulipano, G., Bonfanti, C., Milani, G., Billeci, B., Bollati, A., Cozzi, R., Maira, G., Murphy, W.A., Poiesi, C., Turazzi, S. and Giustina, A. (2001) Differential inhibition of growth hormone secretion by analogs selective for somatostatin

receptor subtypes 2 and 5 in human growth-hormone-secreting adenoma cells in vitro. *Neuroendocrinology*, **73**, 344-351.

Tulipano, G., Soldi, D., Bagnasco, M., Culler, M.D., Taylor, J.E., Cocchi, D. and Giustina, A. (2002) Characterization of new selective somatostatin receptor subtype-2 (sst2) antagonists, BIM-23627 and BIM-23454. Effects of BIM-23627 on GH release in anesthetized male rats after short-term high-dose dexamethasone treatment. *Endocrinology*, **143**, 1218-1224.

Tulipano, G., Stumm, R., Pfeiffer, M., Kreienkamp, H.J., Hollt, V. and Schulz, S. (2004) Differential beta-arrestin trafficking and endosomal sorting of somatostatin receptor subtypes. *J Biol Chem*, **279**, 21374-21382.

Urizar, E., Montanelli, L., Loy, T., Bonomi, M., Swillens, S., Gales, C., Bouvier, M., Smits, G., Vassart, G. and Costagliola, S. (2005) Glycoprotein hormone receptors: link between receptor homodimerization and negative cooperativity. *Embo J*, **24**, 1954-1964.

Vale, W., Brazeau, P., Rivier, C., Brown, M., Boss, B., Rivier, J., Burgus, R., Ling, N. and Guillemin, R. (1975) Somatostatin. *Recent Prog Horm Res*, **31**, 365-397.

Vale, W., Rivier, J., Ling, N. and Brown, M. (1978) Biologic and immunologic activities and applications of somatostatin analogs. *Metabolism*, **27**, 1391-1401.

Vallejo, M. (2004) Somatostatin gene structure and regulation. In Srikant, C.B. (ed.), *Somatostatin*. Kluwer Academic Publishers, Norwell, pp. 1-16.

Van Den Bossche, B., D'Haeninck, E., De Vos, F., Dierckx, R.A., Van Belle, S., Bracke, M. and Van de Wiele, C. (2004) Oestrogen-mediated regulation of somatostatin receptor expression in human breast cancer cell lines assessed with 99mTc-depreotide. *Eur J Nucl Med Mol Imaging*, **31**, 1022-1030.

Vasquez, B., Harris, V. and Unger, R.H. (1982) Extraction of somatostatin from human plasma on octadecylsilyl silica. *J Clin Endocrinol Metab*, **55**, 807-809.

Vasudevan, S., Hulme, E.C., Bach, M., Haase, W., Pavia, J. and Reilander, H. (1995) Characterization of the rat m3 muscarinic acetylcholine receptor produced in insect cells infected with recombinant baculovirus. *Eur J Biochem*, **227**, 466-475.

Vidal, C., Rauly, I., Zeggari, M., Delesque, N., Esteve, J.P., Saint-Laurent, N., Vaysse, N. and Susini, C. (1994) Up-regulation of somatostatin receptors by epidermal growth factor and gastrin in pancreatic cancer cells. *Mol Pharmacol*, **46**, 97-104.

Vila-Coro, A.J., Mellado, M., Martin de Ana, A., Lucas, P., del Real, G., Martinez, A.C. and Rodriguez-Frade, J.M. (2000) HIV-1 infection through the CCR5 receptor is blocked by receptor dimerization. *Proc Natl Acad Sci U S A*, **97**, 3388-3393.

Vila-Coro, A.J., Rodriguez-Frade, J.M., Martin De Ana, A., Moreno-Ortiz, M.C., Martinez, A.C. and Mellado, M. (1999) The chemokine SDF-1alpha triggers CXCR4 receptor dimerization and activates the JAK/STAT pathway. *Faseb J*, **13**, 1699-1710.

Viollet, C., Bodenant, C., Prunotto, C., Roosterman, D., Schaefer, J., Meyerhof, W., Epelbaum, J., Vaudry, H. and Leroux, P. (1997) Differential expression of multiple somatostatin receptors in the rat cerebellum during development. *J Neurochem*, **68**, 2263-2272.

Visser-Wisselaar, H.A., Van Uffelen, C.J., Van Koetsveld, P.M., Lichtenauer-Kaligis, E.G., Waaijers, A.M., Uitterlinden, P., Mooy, D.M., Lamberts, S.W. and Hofland, L.J. (1997) 17-beta-estradiol-dependent regulation of somatostatin receptor

subtype expression in the 7315b prolactin secreting rat pituitary tumor in vitro and in vivo. *Endocrinology*, **138**, 1180-1189.

Waldhoer, M., Fong, J., Jones, R.M., Lunzer, M.M., Sharma, S.K., Kostenis, E., Portoghese, P.S. and Whistler, J.L. (2005) A heterodimer-selective agonist shows in vivo relevance of G protein-coupled receptor dimers. *Proc Natl Acad Sci U S A*, **102**, 9050-9055.

Wang, H.L., Bogen, C., Reisine, T. and Dichter, M. (1989) Somatostatin-14 and somatostatin-28 induce opposite effects on potassium currents in rat neocortical neurons. *Proc Natl Acad Sci U S A*, **86**, 9616-9620.

Ward, C.W., Lawrence, M.C., Streltsov, V.A., Adams, T.E. and McKern, N.M. (2007) The insulin and EGF receptor structures: new insights into ligand-induced receptor activation. *Trends Biochem Sci*, **32**, 129-137.

Ward, D.T., Brown, E.M. and Harris, H.W. (1998) Disulfide bonds in the extracellular calcium-polyvalent cation-sensing receptor correlate with dimer formation and its response to divalent cations in vitro. *J Biol Chem*, **273**, 14476-14483.

Weckbecker, G., Briner, U., Lewis, I. and Bruns, C. (2002) SOM230: a new somatostatin peptidomimetic with potent inhibitory effects on the growth hormone/insulin-like growth factor-I axis in rats, primates, and dogs. *Endocrinology*, **143**, 4123-4130.

Weckbecker, G., Lewis, I., Albert, R., Schmid, H.A., Hoyer, D. and Bruns, C. (2003) Opportunities in somatostatin research: biological, chemical and therapeutic aspects. *Nat Rev Drug Discov*, **2**, 999-1017.

Weckbecker, G., Raulf, F., Stolz, B. and Bruns, C. (1993) Somatostatin analogs for diagnosis and treatment of cancer. *Pharmacol Ther*, **60**, 245-264.

Weiss, R.E., Reddi, A.H. and Nimni, M.E. (1981) Somatostatin can locally inhibit proliferation and differentiation of cartilage and bone precursor cells. *Calcif Tissue Int*, **33**, 425-430.

White, J.H., Wise, A., Main, M.J., Green, A., Fraser, N.J., Disney, G.H., Barnes, A.A., Emson, P., Foord, S.M. and Marshall, F.H. (1998) Heterodimerization is required for the formation of a functional GABA(B) receptor. *Nature*, **396**, 679-682.

White, R.E., Schonbrunn, A. and Armstrong, D.L. (1991) Somatostatin stimulates Ca(2+)-activated K+ channels through protein dephosphorylation. *Nature*, **351**, 570-573.

Whorton, M.R., Bokoch, M.P., Rasmussen, S.G., Huang, B., Zare, R.N., Kobilka, B. and Sunahara, R.K. (2007) A monomeric G protein-coupled receptor isolated in a high-density lipoprotein particle efficiently activates its G protein. *Proc Natl Acad Sci U S A*, **104**, 7682-7687.

Whorton, M.R., Jastrzebska, B., Park, P.S., Fotiadis, D., Engel, A., Palczewski, K. and Sunahara, R.K. (2008) Efficient coupling of transducin to monomeric rhodopsin in a phospholipid bilayer. *J Biol Chem*, **283**, 4387-4394.

Wulbrand, U., Wied, M., Zofel, P., Goke, B., Arnold, R. and Fehmann, H. (1998) Growth factor receptor expression in human gastroenteropancreatic neuroendocrine tumours. *Eur J Clin Invest*, **28**, 1038-1049.

Wurch, T., Matsumoto, A. and Pauwels, P.J. (2001) Agonist-independent and -dependent oligomerization of dopamine D(2) receptors by fusion to fluorescent proteins. *FEBS Lett*, **507**, 109-113.

Xidakis, C., Mastrodimou, N., Notas, G., Renieri, E., Kolios, G., Kouroumalis, E. and Thermos, K. (2007) RT-PCR and immunocytochemistry studies support the presence of somatostatin, cortistatin and somatostatin receptor subtypes in rat Kupffer cells. *Regul Pept*, **143**, 76-82.

Xu, J., He, J., Castleberry, A.M., Balasubramanian, S., Lau, A.G. and Hall, R.A. (2003) Heterodimerization of alpha 2A- and beta 1-adrenergic receptors. *J Biol Chem*, **278**, 10770-10777.

Xu, Y., Berelowitz, M. and Bruno, J.F. (1995) Dexamethasone regulates somatostatin receptor subtype messenger ribonucleic acid expression in rat pituitary GH4C1 cells. *Endocrinology*, **136**, 5070-5075.

Xu, Y., Piston, D.W. and Johnson, C.H. (1999) A bioluminescence resonance energy transfer (BRET) system: application to interacting circadian clock proteins. *Proc Natl Acad Sci U S A*, **96**, 151-156.

Xu, Y., Song, J., Berelowitz, M. and Bruno, J.F. (1996) Estrogen regulates somatostatin receptor subtype 2 messenger ribonucleic acid expression in human breast cancer cells. *Endocrinology*, **137**, 5634-5640.

Yamada, Y., Post, S.R., Wang, K., Tager, H.S., Bell, G.I. and Seino, S. (1992) Cloning and functional characterization of a family of human and mouse somatostatin receptors expressed in brain, gastrointestinal tract, and kidney. *Proc Natl Acad Sci U S A*, **89**, 251-255.

Ye, W.Z., Mathieu, S. and Marteau, C. (1999) Somatostatin inhibits the Na+/H+ exchange activity of rat hepatocytes in short term primary culture. *Cell Mol Biol (Noisy-le-grand)*, **45**, 1183-1189.

Yesilaltay, A. and Jenness, D.D. (2000) Homo-oligomeric complexes of the yeast alpha-factor pheromone receptor are functional units of endocytosis. *Mol Biol Cell*, **11**, 2873-2884.

Yoshioka, K., Saitoh, O. and Nakata, H. (2001) Heteromeric association creates a P2Y-like adenosine receptor. *Proc Natl Acad Sci U S A*, **98**, 7617-7622.

Yoshioka, K., Saitoh, O. and Nakata, H. (2002) Agonist-promoted heteromeric oligomerization between adenosine A(1) and P2Y(1) receptors in living cells. *FEBS Lett*, **523**, 147-151.

Young, R.M., Arnette, J.K., Roess, D.A. and Barisas, B.G. (1994) Quantitation of fluorescence energy transfer between cell surface proteins via fluorescence donor photobleaching kinetics. *Biophys J*, **67**, 881-888.

Zalatnai, A. and Timar, F. (2002) In vitro antiangiogenic effect of sandostatin (octreotide) on the proliferation of the placental vessels. *Anticancer Res*, **22**, 4225-4227.

Zapata, P.D., Ropero, R.M., Valencia, A.M., Buscail, L., Lopez, J.I., Martin-Orozco, R.M., Prieto, J.C., Angulo, J., Susini, C., Lopez-Ruiz, P. and Colas, B. (2002) Autocrine regulation of human prostate carcinoma cell proliferation by somatostatin through the modulation of the SH2 domain containing protein tyrosine phosphatase (SHP)-1. *J Clin Endocrinol Metab*, **87**, 915-926.

Zatelli, M.C., Piccin, D., Ambrosio, M.R., Bondanelli, M. and degli Uberti, E.C. (2006) Antiproliferative effects of somatostatin analogs in pituitary adenomas. *Pituitary*, **9**, 27-34.

Zatelli, M.C., Piccin, D., Bottoni, A., Ambrosio, M.R., Margutti, A., Padovani, R., Scanarini, M., Taylor, J.E., Culler, M.D., Cavazzini, L. and degli Uberti, E.C.

(2004) Evidence for differential effects of selective somatostatin receptor subtype agonists on alpha-subunit and chromogranin a secretion and on cell viability in human nonfunctioning pituitary adenomas in vitro. *J Clin Endocrinol Metab*, **89**, 5181-5188.

Zatelli, M.C., Piccin, D., Tagliati, F., Bottoni, A., Ambrosio, M.R., Margutti, A., Scanarini, M., Bondanelli, M., Culler, M.D. and degli Uberti, E.C. (2005a) Dopamine receptor subtype 2 and somatostatin receptor subtype 5 expression influences somatostatin analogs effects on human somatotroph pituitary adenomas in vitro. *J Mol Endocrinol*, **35**, 333-341.

Zatelli, M.C., Piccin, D., Tagliati, F., Bottoni, A., Luchin, A. and degli Uberti, E.C. (2005b) SRC homology-2-containing protein tyrosine phosphatase-1 restrains cell proliferation in human medullary thyroid carcinoma. *Endocrinology*, **146**, 2692-2698.

Zhang, H.J., Redmon, J.B., Andresen, J.M. and Robertson, R.P. (1991) Somatostatin and epinephrine decrease insulin messenger ribonucleic acid in HIT cells through a pertussis toxin-sensitive mechanism. *Endocrinology*, **129**, 2409-2414.

Zhao, G.Q., Zhang, Y., Hoon, M.A., Chandrashekar, J., Erlenbach, I., Ryba, N.J. and Zuker, C.S. (2003) The receptors for mammalian sweet and umami taste. *Cell*, **115**, 255-266.

Zhou, A., Webb, G., Zhu, X. and Steiner, D.F. (1999) Proteolytic processing in the secretory pathway. *J Biol Chem*, **274**, 20745-20748.

Zhu, C.C., Cook, L.B. and Hinkle, P.M. (2002) Dimerization and phosphorylation of thyrotropin-releasing hormone receptors are modulated by agonist stimulation. *J Biol Chem*, **277**, 28228-28237.

Zhu, L.J., Krempels, K., Bardin, C.W., O'Carroll, A.M. and Mezey, E. (1998) The localization of messenger ribonucleic acids for somatostatin receptors 1, 2, and 3 in rat testis. *Endocrinology*, **139**, 350-357.

Zhu, W.Z., Chakir, K., Zhang, S., Yang, D., Lavoie, C., Bouvier, M., Hebert, T.E., Lakatta, E.G., Cheng, H. and Xiao, R.P. (2005) Heterodimerization of beta1- and beta2-adrenergic receptor subtypes optimizes beta-adrenergic modulation of cardiac contractility. *Circ Res*, **97**, 244-251.

Zhu, X. and Wess, J. (1998) Truncated V2 vasopressin receptors as negative regulators of wild-type V2 receptor function. *Biochemistry*, **37**, 15773-15784.

Zhu, Y. and Yakel, J.L. (1997) Calcineurin modulates G protein-mediated inhibition of N-type calcium channels in rat sympathetic neurons. *J Neurophysiol*, **78**, 1161-1165.

Zingg, H.H. and Patel, Y.C. (1982) Biosynthesis of immunoreactive somatostatin by hypothalamic neurons in culture. *J Clin Invest*, **70**, 1101-1109.

[1] The abbreviations used are:

GPCR(s), G protein coupled receptor(s); hSSTR, human somatostatin receptor; SST, somatostatin; HA, hemagglutinin; CHO, Chinese hamster ovary; pbFRET, photobleaching fluorescence resonance energy transfer; FITC, fluorescein isothiocyanate; TR, texas red; FCS, fluorescence correlation spectroscopy; TM, transmembrane domain

Φ The terms dimerization and oligomerization are used interchangeably.

[2] The abbreviations used are:

GPCR(s), G protein coupled receptor(s); hSSTR, human somatostatin receptor; SST, somatostatin; HA, hemagglutinin; CHO, Chinese hamster ovary; HEK, human embryonic kidney cells; pbFRET, photobleaching fluorescence resonance energy transfer; FITC, fluorescein isothiocyanate; Rh, Rhodamine; FCS, fluorescence correlation spectroscopy.

Dimerization and oligomerization are used interchangeably.

[3] The abbreviations used are:

GPCR(s), G protein coupled receptor(s); SSTR, human somatostatin receptor; SST, somatostatin; HA, hemagglutinin; HEK, human embryonic kidney; pbFRET, photobleaching fluorescence resonance energy transfer; MAPK, mitogen-activated protein kinase; ERK, extracellular signal-regulated kinase; FBS, fetal bovine serum.

APPENDIX

Abstracts

1) Grant, M., Alturaihi, H and Kumar, U.

Heterodimerization of Human Somatostatin Receptors Enhances Cell Signalling and Potentiates Anti-Proliferation.

Program Pharmacology Research Day, McGill University, Montreal, Quebec, June 8, 2006.

2) Grant, M., Alturaihi, H and Kumar, U.

Heterodimerization of Human Somatostatin Receptors Enhances Receptor Signaling and Potentiates Anti-Proliferation.

Program Annual McGill Biomedical Graduate Conference, McGill University, Montreal, Canada, February 22, 2006.

3) Grant, M., Alturaihi H. and Kumar, U.

Heterodimerization Of Human Somatostatin Receptor 2 And 5 Is Ligand-Specific Resulting In Enhanced Receptor Function.

Program Annual Meeting US Endocrine Society, San Diego, USA, June 4-7, 2005.

4) Grant, M., Alturaihi, H. and Kumar, U.

Heterodimerization Of Human Somatostatin Receptor 2 And 5 Is Ligand-Specific Resulting In Enhanced Receptor Function.

Program Annual McGill Novartis Endocrine Retreat, McGill University, Montreal, Quebec, *May 12, 2005.*

5) Pidasheva, S., Grant, M., Canaff, L., Kumar, U. and Hendy, G.N.

The Calcium-sensing Receptor (CASR) Dimerizes in the Endoplasmic Reticulum: Biochemical and Biophysical Characterization of CASR Mutants Retained Intracellularly.

Program Annual Meeting of the American Society for Bone and Mineral Research, Nashville, Tennessee, USA, September 23-27, 2005.

6) Kelleman, A., Huang, H., Melacini, G., Grant, M., Kumar, U., VanNieuwenhze, M.S. and Goodman, M.

Design and synthesis of type-II' β-turn constrained somatostatin analogues selective for receptor subtype hsst2.

Program American Chemical Society, San Diego, USA, Mar. 13-17, 2005.

7) Kumar, U., Ong, W.Y., Alturaihi, H., Watt, H.L., Grant, M., and Patel, S.C.

Concentration and time dependent effects of NMDA and β-amyloid on the release of cytokines in cultured cortical neurons.

Program Society for Neuroscience, New Orleans, USA, Oct. 23-27, 2004.

8) Grant, M. and Kumar U.

Ligand-dependent dissociation of human somatostatin receptor 2 dimers: A role in receptor trafficking.

Program International Multidisciplinary Symposium Peptide Receptors, Montreal, Canada, July 31-Aug. 4, 2004.

9) Grant, M. and Kumar, U.

Ligand-dependent dissociation of human somatostatin receptor 2 dimers: A role in receptor trafficking.

Program Pharmacology Research Day, McGill University, Montreal, Quebec, 2004.

10) Kumar, U., Baragli, A., Alturaihi, H., Grant, M., Patel, R.C. and Patel, S.C.

Hetero-oligomerization of NMDA receptors and dopamine receptor subtypes in striatal cultured neurons.

Program Society for Neuroscience, New Orleans, USA, 2003.

11) Grant, M., Kumar, U., Patel, R.C. and Patel, Y.C.

Hetero-oligomerization of somatostatin receptor 1 and 5 is receptor-specific and exhibits altered signaling properties.

Program Annual Meeting US Endocrine Society, Philadelphia, USA, June 19-22, 2003.

12) Grant, M., Kumar, U., Patel, R.C. and Patel, Y.C.

Hetero-oligomerization of somatostatin receptors is receptor-specific and displays altered signaling properties.

Program Annual McGill Biomedical Graduate Conference, McGill University, Montreal, Canada, February 26, 2003.

13) Patel, Y.C., Rocheville, M., Kumar, U., Lamb, D.C., Eid, J., Grant, M., Rani, A., Hazlett, T., Gratton, E. and Patel, R.C.

Oligomerization of somatostatin receptors: implications for function.

Program Inaugural James Black Conference, Churchill College, Cambridge, UK, July 22-25, 2002.

14) Patel, Y.C., Rocheville, M., Kumar, U., Lamb, D.C., Eid, J., Grant, M., Rani, A., Hazlett, T., Gratton, E. and Patel, R.C.

Oligomerization of somatostatin receptors: implications for function.

Program 5th International Congress of Neuroendocrinology, Bristol, UK, August 31-September 4, 2002.

15) Patel, Y.C., Rocheville, M., Kumar, U., Lamb, D.C., Grant, M., Rani, A., Hazlett, T., Gratton, E. and Patel, R.C.

Molecular cross-talk between somatostatin and dopamine receptors.

Program 10th Meeting of the European Neuroendocrine Association, Munich, Germany, September 12-14, 2002.

16) Grant, M., Venkateswaran, A.V., Kumar, U., Patel, R.C. and Patel, Y.C.

Hetero-oligomerization of somatostatin receptor 1 and 5: Pharmacological and physical characterization.

Program Annual McGill Novartis Endocrine Retreat, McGill University, Montreal, Quebec, *May 23, 2002.*

17) Patel, Y.C., Rocheville, M., Kumar, U., Lamb, D.C., Eid, J., Grant, M., Aruna R.V., Hazlett, T., Gratton, E. and Patel, R.C.

Oligomerization of G protein coupled receptors.

Program International Multidisciplinary Symposium Peptide Receptors, Montreal, Canada, July 29-August 2, 2001.

18) Grant, M., Rocheville, M., Kumar, U., Venkateswaran, A.R., Patel, R.C., Patel Y.C.

Pharmacology and physical characterization of the somatostatin receptor 1 and 5 heterodimer.

Program Pharmacology Research Day, McGill University, Montreal, Quebec, May 16, 2001.

19) Kumar, U., Lamb, D.C., Hazlett, T., Eid, J., Rocheville, M., Grant, M., Aruna R.V., Gratton, E., Patel, R.C. and Patel, Y.C.

FRET analysis by multi-photon excitation spectroscopy in living cells reveals interaction of somatostatin receptor homo- and heterodimers with two ligand molecules.

Program Annual McGill Novartis Endocrine Retreat, McGill University, Montreal, Quebec, May 10, 2001.

20) Kumar, U., Lange, D., Lamb, D.C., Grant, M., Aruna RV., Kothari, R., Hazlett, T., Eid, J., Gratton, E. and Patel, R.C.

Hetero-oligomerization as a molecular basis for membrane interaction between subtypes of the somatostatin and dopamine receptors.

Program 2ND Annual Great Lakes GPCR Retreat, London, Ontario, October 20-22, 2000.

Paper Reprints (published materials)

1) Pidasheva S., Grant M., Canaff L., Ercan O., Kumar U. and Hendy G.N.

Calcium-sensing receptor dimerizes in the endoplasmic reticulum: biochemical and biophysical characterization of CASR mutants retained intracellularly.

Human Molecular Genetics **15**: 2200-2209, 2006.

2) Moore S.B., Grant M., Rew Y., Bosa E., Fabbri M., Kumar U. and Goodman M.

Synthesis and biologic activity of conformationally constrained analogs of L-363,301.

Journal of Peptide Research **66**:404-422, 2005.

3) Grant M., Patel R.C. and Kumar U.

The role of subtype-specific ligand binding and the C-tail domain in dimer formation of human somatostatin receptors.

Journal of Biological Chemistry **279**:38636-38643, 2004.

4) Grant M., Collier B. and Kumar U.

Agonist-dependent dissociation of human somatostatin receptor 2 dimers: A role in receptor trafficking.

Journal of Biological Chemistry **279**:36179-36183, 2004.

5) Ramírez J.L., Grant M., Norman M., Moldovan S., de Mayo F.J., Brunicardi C. and Kumar U.

Deficiency of somatostatin (SST) receptor 5 (SSTR5) is associated with sexually dimorphic changes in the expression of SST and SST receptors in brain and pancreas.

Molecular and Cellular Endocrinology **221**:105-119, 2004.

6) Patel R.C., Kumar U., Lamb D.C., Eid J.S., Rocheville M., Grant M., Rani A., Hazlett T., Patel S.C., Gratton E. and Patel Y.C.

Ligand binding to somatostatin receptors induces receptor-specific oligomer formation in live cells.

Proceedings of the National Academy of Sciences (USA). **99**: 3294-3299, 2002.

Human Molecular Genetics, 2006, Vol. 15, No. 14 **2200–2209**
doi:10.1093/hmg/ddl145
Advance Access published on June 1, 2006

Calcium-sensing receptor dimerizes in the endoplasmic reticulum: biochemical and biophysical characterization of CASR mutants retained intracellularly

Svetlana Pidasheva[1,4], Michael Grant[1,5], Lucie Canaff[1,4], Oya Ercan[7], Ujendra Kumar[1,5,†] and Geoffrey N. Hendy[1,2,3,4,6,*]

[1]Department of Medicine, [2]Department of Physiology, [3]Department of Human Genetics, [4]Calcium Research Laboratory, [5]Fraser Laboratories and [6]Hormones and Cancer Research Unit, Royal Victoria Hospital, McGill University, Montreal, Canada QC H3A 1A1 and [7]Cerrahpasa Medical Faculty, Department of Paediatrics, Istanbul University, Istanbul, Turkey

Received April 6, 2006; Revised and Accepted May 30, 2006

Calcium-sensing receptor (CASR), expressed in parathyroid gland and kidney, is a critical regulator of extracellular calcium homeostasis. This G protein-coupled receptor exists at the plasma membrane as a homodimer, although it is unclear at which point in the biosynthetic pathway dimerization occurs. To address this issue, we have analyzed wild-type and mutant CASRs harboring R66H, R66C or N583X-inactivating mutations identified in familial hypocalciuric hypercalcemia/neonatal severe hyperparathyroid patients, which were transiently expressed in kidney cells. All mutants were deficient in cell signaling responses to extracellular CASR ligands relative to wild-type. All mutants, although as well expressed as wild-type, lacked mature glycosylation, indicating impaired trafficking from the endoplasmic reticulum (ER). Dimerized forms of wild-type, R66H and R66C mutants were present, but not of the N583X mutant. By immunofluorescence confocal microscopy of non-permeabilized cells, although cell surface expression was observed for the wild-type, little or none was seen for the mutants. In permeabilized cells, perinuclear staining was observed for both wild-type and mutants. By colocalization fluorescence confocal microscopy, the mutant CASRs were localized within the ER but not within the Golgi apparatus. By the use of photobleaching fluorescence resonance energy transfer microscopy, it was demonstrated that the wild-type, R66H and R66C mutants were dimerized in the ER, whereas the N583X mutant was not. Hence, constitutive CASR dimerization occurs in the ER and is likely to be necessary, but is not sufficient, for exit of the receptor from the ER and trafficking to the cell surface.

INTRODUCTION

Calcium-sensing receptor (CASR) is a plasma membrane G protein-coupled receptor (GPCR) that plays a central role in regulating extracellular calcium ion concentrations. The CASR is expressed abundantly in the tissues and cells involved in calcium homeostasis, such as the parathyroid glands and in the cells lining the kidney tubule (1). This receptor is responsive to small changes in the circulating calcium concentration, and once activated, it inhibits parathyroid hormone (PTH) secretion and renal tubule calcium reabsorption.

The key role of this receptor as a 'calciostat' has been emphasized by the identification of naturally occurring

*To whom correspondence should be addressed at: Calcium Research Laboratory, Royal Victoria Hospital, 687 Pine Avenue West, Room H4.67, Montreal, QC, Canada H3A 1A1. Tel: +1 5148431632; Fax: +1 5148431712; Email: geoffrey.hendy@mcgill.ca
†Present address: Faculty of Pharmaceutical Sciences, Department of Pharmacology and Toxicology, University of British Columbia, Vancouver, BC, Canada V6T 1Z3.

inactivating or activating mutations in the CASR gene causing hypercalcemic or hypocalcemic disorders, respectively (2–4). Familial (benign) hypocalciuric hypercalcemia (FHH) is caused by heterozygous loss-of-function mutations, an asymptomatic condition in most cases (5,6). However, the homozygous form of such mutations causes neonatal severe hyperparathyroidism (NSHPT), a rare disorder characterized by extreme hypercalcemia and the bony changes of hyperparathyroidism which occur within the first 6 months of life (7). So far, over 70 naturally occurring loss-of-function mutations have been reported (see the online database at http://www.casrdb.mcgill.ca) (8). Identification and analysis of these mutations has helped to better understand the structure and function of the receptor.

It has been known for some time that growth factor receptors of the tyrosine kinase type undergo ligand-induced dimerization at the cell surface. More recently, it has been appreciated that several GPCRs dimerize and it has been demonstrated that the CASR exists as a homodimer on the cell surface and that this is not ligand-induced (9). However, it is not clear where precisely dimerization of this receptor occurs.

In the present study, we describe the identification of novel mutations in the CASR in individuals with FHH or NSHPT. These two mutants (in addition to a previously described mutant) were analyzed with respect to cellular and plasma membrane expression, cell signaling, colocalization with endoplasmic reticulum (ER) and Golgi markers and dimerization status as assessed by photobleaching fluorescence resonance energy transfer (pbFRET). In this way, we showed that dimers of the CASR are already present in the ER and implicate dimerization as an important early event in the life history of this GPCR.

RESULTS

Case 1

This family (Fig. 1) came to attention when the first child, a boy (VI-1), of related parents was admitted at 3 months of age with complaints of dyspnea, hypotonia, constipation, vomiting and failure to thrive. He was hypercalcemic (Table 1). This patient had hyperparathyroid bone disease and underwent total parathyroidectomy. He died from respiratory failure a month later, despite being normocalcemic. The second child (VI-2), a girl, was born a year later. She was admitted at 2.5 months of age and immediately underwent total parathyroidectomy and heterotopic autotransplantation. She had medical treatment for hypocalcemia and later hypercalcemia and became normocalcemic 4 months later. The parents (V-2 and V-6) are mildly hypercalcemic (Table 1) with low urinary calcium/creatinine clearance ratios (data not shown).

Case 2

An individual who was diagnosed with FHH on the basis of modest hypercalcemia, inappropriately normal serum PTH levels and a low urinary calcium to creatinine clearance ratio.

Case 3

The proband of this family was diagnosed with NSHPT at birth (10). Before parathyroidectomy, his serum calcium level was 19 mg/dl and PTH concentration was >800 pg/ml (normal range 10–65). He is homozygous, and his parents heterozygous, for an R66C mutation in the CASR (11).

Identification of CASR mutations

Case 1. Direct sequence analysis of PCR-amplified CASR exons identified a homozygous mutation (R66H, CGT-CAT) encoded by exon 3 of the gene in the proband (VI-1) of the family. The sister (VI-2) was homozygous and both parents (V-2 and V-6) were heterozygous for the mutation that introduced an *Nco*I enzyme restriction site, not present in wild-type DNA, which was useful for mutation confirmation in the proband and analysis of family members. This change was not found in 100 CASR gene alleles from 50 unrelated normal individuals.

Case 2. Direct sequence analysis of PCR-amplified CASR exons in the FHH patient identified a heterozygous mutation in exon 7 such that an additional 'T' was inserted between codons 582 and 583, causing a frame shift and introduction of a stop codon at position 583 (N583X). This change was not found in 100 CASR gene alleles from 50 unrelated normal individuals.

Transfected R66H and N583X mutants demonstrate impaired cell signaling in response to extracellular increases in CASR agonists in HEK293 cells

The ability of the mutant receptors to respond to extracellular increases in CASR ligands relative to wild-type receptor was assessed in different systems. To test mitogen-activated protein kinase (MAPK) activity, two different assays were used. In a trans-reporting system that measures the activity of Elk-1, a transcription factor targeted by MAPK pathways, the wild-type CASR, when transiently expressed in HEK293 cells, exhibited a half-maximal response (EC_{50}) of 3.9 ± 0.15 mM (mean $\pm$ SE) (Fig. 2A) to increasing calcium concentrations. In contrast, both the R66H and N583X mutants were unresponsive and the R66C mutant was poorly responsive even to very high calcium levels (Fig. 2A).

Also, changes in the activation status of endogenous extracellular kinases 1 and 2 (ERK 1/2) in response to increasing extracellular calcium concentrations in HEK293 cells that had been transfected with the CASR cDNAs were assessed by a western blot assay of the phosphorylated and total ERK 1/2. This indicated that for the wild-type CASR, increasing the extracellular calcium concentration stimulated phosphorylation of ERK 1/2 with no change in total ERK 1/2 and tubulin. However, little or no activation of ERK 1/2 was found for the R66C, R66H or N583X mutants (data not shown).

In addition, increases in intracellular calcium transients in response to changes in the extracellular concentration of the CASR ligand, gadolinium (Gd^{3+}), were monitored in HEK293 cells stably expressing apoaequorin that were then charged with coelenterazine to form holoaequorin. In cells transiently expressing the wild-type receptor, increases in luminescence occurred with increasing extracellular Gd^{3+} concentrations (EC_{50}, 70 ± 3.0 μM; mean $\pm$ SE). However, the R66H and N583X mutants were completely unresponsive

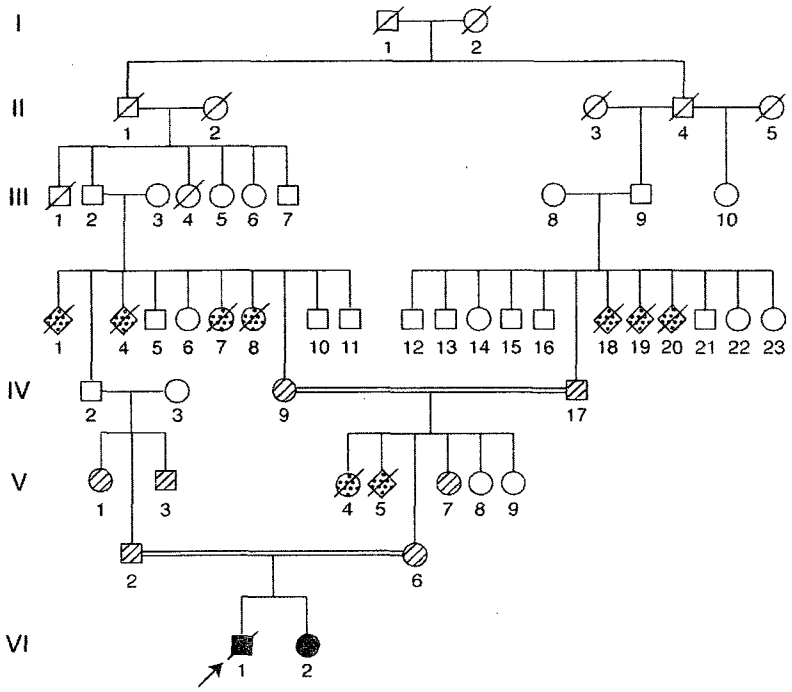

Figure 1. Pedigree of family 1 with FHH/NSHPT. Clinical status is indicated by open symbols (unaffected or status not known), hatched symbols (FHH) and solid symbols (NSHPT). Further clinical details are given in Table 1. Dotted symbols indicate neonatal death (with unknown serum calcium level). The proband is indicated by the arrow.

Table 1. Biochemical characteristics of FHH/NSHPT family 1 members

Pedigree number	Serum total calcium (8.8–10.4 mg/dl)[a]	Serum phosphate (3.72–5.36 mg/dl)	Serum magnesium (1.46–2.4 mg/dl)	Serum PTH (10–62 pg/ml)	Serum alkaline phosphatase (30–130 U/l)
IV-9	10.6	ND[b]	ND	ND	73
IV-17	10.4	ND	ND	ND	94
V-1	11.0	2.1	ND	ND	ND
V-2	11.3	3.0	2.48	36.8	ND
V-3	10.9	1.9	ND	21.2	ND
V-6	11.2	3.4	2.42	26.3	ND
V-7	10.8	ND	ND	ND	80
V-8	9.8	ND	ND	ND	64
VI-1	26.5	1.8	ND	64.1	1023
VI-2	22.5	2.0	ND	>2500	1399

[a]Normal ranges are in parentheses.
[b]Not done.

and the R66C mutant had much reduced responsiveness to Gd^{3+} (Fig. 2B).

Transfected R66H and N583X mutants demonstrate little cell-surface expression in HEK293 cells

To examine whether the mutant CASRs were expressed on the cell surface, fluorescence immunocytochemistry was performed on HEK293 cells transiently transfected with c-Myc-tagged wild-type and mutant CASR cDNAs and then permeabilized or not. Cells mock-transfected or transfected with empty vector or untagged CASR cDNA showed no specific staining with the c-Myc antibody (data not shown). Strong cell-surface staining was present in non-permeabilized HEK293 cells transfected with the epitope-tagged wild-type receptor (Fig. 3A). Permeabilization of such cells revealed

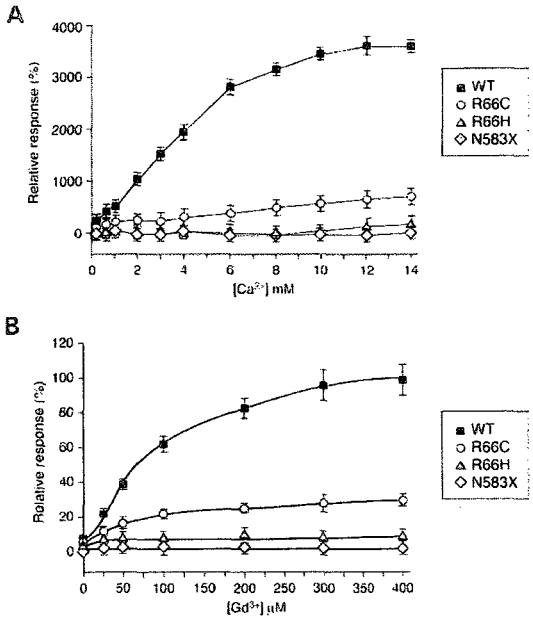

Figure 2. (A) Extracellular Ca^{2+}-evoked increases in MAPK activity in HEK293 cells transiently transfected with either wild-type (WT) or mutant (R66C, R66H or N583X) CASR cDNA and a MAPK trans-reporting system. Values shown are the mean ± SE of four estimations. (B) Extracellular Gd^{3+}-evoked increases in intracellular Ca^{2+} in HEK293 cells (stably expressing apoaequorin) that were transiently transfected with either wild-type (WT) or mutant (R66C, R66H or N583X) CASR cDNA and the day after charged with coelenterazine-cp to generate holoaequorin. Luminescence values shown are the mean ± SE of eight estimations.

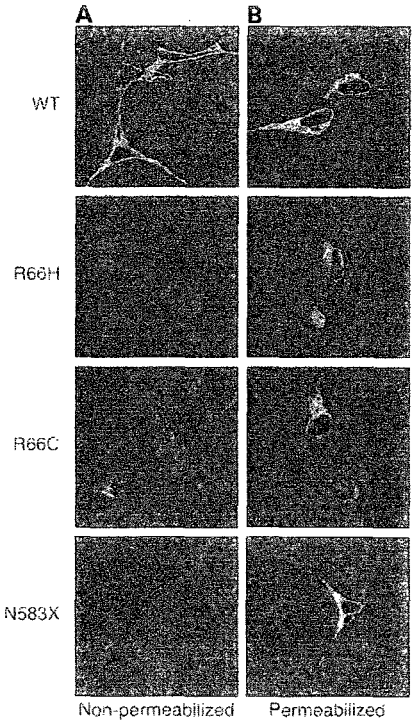

Figure 3. Plasma membrane and intracellular expression of wild-type and mutant CASRs in transfected HEK293 cells. Fluorescence immunocytochemistry and confocal microscopy were performed on HEK293 cells transiently transfected with wild-type (WT) or mutant (R66H, R66C, N583X) c-Myc-tagged CASR cDNA. Immunostaining was done with c-Myc monoclonal antibody 9E10, and detection was made with goat anti-mouse FITC-conjugated secondary antibody. Examples of fields of non-permeabilized (**A**) and permeabilized (**B**) cells are shown.

further intracellular perinuclear staining associated with the ER and Golgi apparatus (Fig. 3B). In contrast, non-permeabilized cells that had been transfected with mutant CASR cDNAs demonstrated either no (R66H, N583X) or very little (R66C) cell-surface staining, respectively (Fig. 3A). However, permeabilized cells transfected with these mutants demonstrated intracellular perinuclear staining similar in amount to cells transfected with the wild-type (Fig. 3B). The HEK293 cell transfection and fluorescence immunocytochemistry analysis showed that although all the CASR mutants were deficient with respect to cell surface expression, they were present intracellularly.

CASR mutants are found in the ER but not in the Golgi apparatus

To identify where the CASR mutants are present intracellularly, colocalization studies were carried out with specific markers for the ER (anti-calnexin antibody) or the Golgi apparatus (wheat germ agglutinin conjugated to fluorescein) and the CASR (anti-c-Myc antibody conjugated to Cy3) in HEK293 cells transiently transfected with either wild-type CASR or one of the mutant CASR cDNAs. In the cells expressing the wild-type CASR, localization of the CASR to both organelles was demonstrated (Fig. 4A); however, the CASR mutant, R66H, although being present in the ER was not found in the Golgi apparatus (Fig. 4B). A similar observation was made for the other CASR mutant, R66C (data not shown).

Transfected R66H and R66C mutants demonstrate no or little of the mature (160 kDa) glycosylated form although dimerization is unimpaired

To examine whether the mutant CASRs are expressed normally and exhibit similar molecular species as wild-type CASR, western blot analysis of extracts of HEK293 cells transiently transfected with either the c-Myc-tagged wild-type (positive control) or mutant CASR cDNAs or empty vector (negative control) was carried out. The CASR molecular species were revealed on immunoblots with an antibody

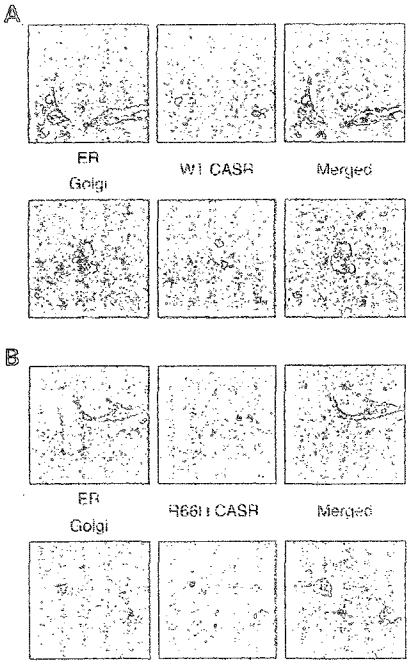

Figure 4. CASR and ER and Golgi apparatus colocalization. Fluorescence immunocytochemistry and confocal microscopy were performed on HEK293 cells transiently transfected with (A) wild-type (WT) or (B) R66H mutant c-Myc-tagged CASR cDNA. Representative fields are shown for cells incubated with (left panels) anti-calnexin antibody followed by FITC-labeled IgG for ER staining (green) or wheat germ agglutinin conjugated to fluorescein for Golgi apparatus staining (green). Middle panels: c-Myc-Cy3-conjugated monoclonal antibody was added to visualize the CASR (red). Merging of the right and middle panels is shown in the right panels (yellow indicates colocalization).

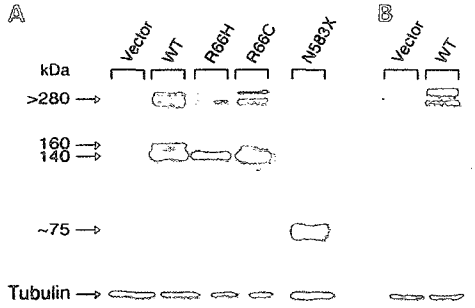

Figure 5. (A) Expression levels of wild-type and mutant CASRs in HEK293 cells. Western blot analysis was performed on extracts of HEK293 cells either empty-vector transfected (vector) or transiently transfected with wild-type (WT) or mutant (R66H, R66C, N583X) c-Myc-tagged CASR cDNA. CASR proteins were stained with c-Myc monoclonal antibody 9E10 and endogenous proteins (for loading control) were stained with β-tubulin antibody. (B) HEK293 cells stably expressing c-Myc-tagged wild-type CASR were subjected to cell-surface biotin labeling followed by immunoprecipitation and western blotting with the c-Myc monoclonal antibody and β-tubulin antibody.

against the c-Myc epitope tag. Under the particular western blotting conditions used, the wild-type CASR exists in both monomeric and dimeric forms: the monomeric non-glycosylated species is 120 kDa (but is not present in sufficient amount to be revealed on the immunoblot), the core glycosylated (immature) species is 140 kDa and the mature, fully glycosylated species, is 160 kDa (Fig. 5A). Immature glycosylation occurs early in the ER, whereas mature glycosylation occurs only later after trafficking to the Golgi apparatus. Dimeric (or oligomeric) forms of the receptor migrate at a size of >280 kDa on the immunoblot (Fig. 5A). Both monomeric and dimeric species were present in the R66H and R66C mutant-transfected cells; however, virtually none or little of the 160 kDa species was evident for the R66H or R66C mutants, respectively (Fig. 5A). For the N583X mutant, a single monomeric species of ~75 kDa was observed with no dimers present (Fig. 5A). The ~75 kDa species was reduced to ~65 kDa by endoglycosidase H (Endo H) treatment revealing it to represent an immature core-glycosylated form (data not shown). Under these conditions, no mature glycosylated species was detected indicating that, if occurring, appropriate trafficking of any N583X mutant protein to the *cis*-Golgi and release into the medium was only taking place at an extremely low level. Consistent with this hypothesis, although western blot analysis of conditioned medium of N583X-transfected cells did identify a single ~85 kDa Endo H-resistant species (therefore representing a mature glycosylated form), it was present in an amount some 200-fold less than a control of exogenously expressed progranulin representing a known constitutively secreted glycoprotein of similar size to the CASR N583X mutant (data not shown). Hence, the N583X protein appearing in the medium likely represented a very minor fraction of the total that had escaped the quality control mechanisms that retained the vast majority of the N583X mutant within the cell. By biotin cell surface labeling of HEK293 cells stably expressing the wild-type CASR, followed by immunoprecipitation and western blotting, CASR dimers (oligomers) were identified as the molecular species present on the cell surface (Fig. 5B).

pbFRET microscopy

To further characterize the dimerization status of the wild-type and mutant CASRs, pbFRET microscopy was used. The FRET technique is a spectroscopic method for monitoring the energy transfer from an excited molecule (the donor) to another molecule (the acceptor) and it occurs when the absorption spectrum of the acceptor overlaps with the emission spectrum of the donor. When used for measuring GPCR protein–protein interactions, the technique can discriminate between receptors localized intracellularly as opposed to those that are cell-surface associated. The competitive nature of FRET and photobleaching (irreversible loss of a fluorophore's capacity to fluoresce) allows indirect measurement of FRET via its effect on donor photobleaching. In HEK293 cells transfected with the c-Myc-tagged CASR

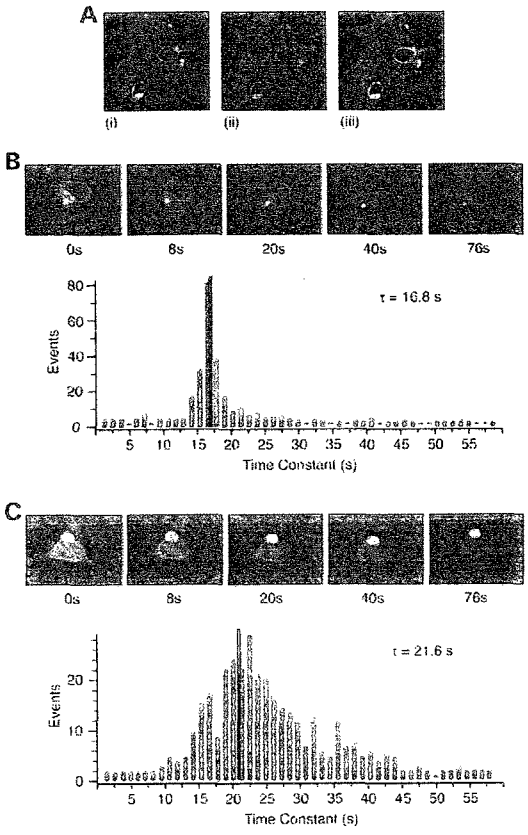

Figure 6. Confocal microscope images and representative histogram time constant plots from pbFRET microscopy of HEK293 cells transiently expressing the c-Myc-tagged CASR R66H mutant. **(A)** Cells were incubated with primary anti-c-Myc mouse monoclonal antibody followed by (i) secondary anti-mouse fluorescein-conjugated antibody shown in green or (ii) anti-mouse Cy3-conjugated antibody shown in red and (iii) colocalization of the two images shown in yellow. **(B)** Photobleaching of fluorescein (donor) in the absence of Cy3 (acceptor). *Top*: cells were treated with the appropriate antibodies, fixed and followed by donor photobleaching with 488 nm light. A sequence of 20 timed images was captured (one image every 4 s with exposure time of 3 s), and a subset is shown. *Bottom*: the time constants displayed in the histogram bar plot were calculated on the basis of a pixel-by-pixel analysis of a selected intracellular area. The mean time constant of 16.8 s is shown as a black bar calculated by averaging the time constants from a Gaussian distribution. **(C)** As in (B), but with photobleaching of fluorescein (donor) in the presence of Cy3 (acceptor). *Top*: there is an obvious visual delay in photobleaching of the donor in the presence of the acceptor. *Bottom*: the histogram time constant bar plot displays the increased mean time constant (21.6 s).

R66H mutant, the staining patterns obtained with anti-c-Myc antibodies conjugated to either donor (FITC) or acceptor (Cy3) fluorophores colocalized in intracellular compartments (Fig. 6A). The photobleaching decay and the associated time constants of the donor molecule were calculated from

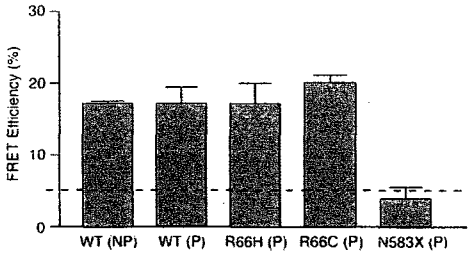

Figure 7. *Effective FRET efficiencies were determined as described in the* legend to Fig. 6 and in Materials and Methods in HEK293 cells transiently transfected with wild-type CASR (wt) or CASR mutants (R66H, R66C, N583X) and permeabilized (P) or not (NP).

experiments in the absence and presence of the acceptor molecule, respectively (Fig. 6B and C). Any retardation in photobleaching on exposure to light indicates that the acceptor molecules are in sufficient proximity to donor molecules to act as acceptors for energy transfer. Given that the two fluorophores are associated with different receptor molecules, receptor association is indicated. A decrease in photobleaching decay rate was observed in the presence of the acceptor molecule (Fig. 6C), showing that the donor and acceptor molecules were within 100 Å of each other, indicative of protein–protein interaction. Similar experiments were conducted with HEK293 cells transfected with either wild-type CASR or the R66C and N583X mutants. The time constants for each condition were averaged over many cells and converted into FRET efficiencies (Fig. 7). Both cell-surface and intracellular wild-type CASR and intracellular CASR R66H and R66C mutants exhibited relatively high FRET efficiencies (~17–20%), an indication that these receptors all exist as dimers. The exception was the CASR truncation mutant N583X, with a relatively low FRET efficiency (~3%), inconsistent with this receptor molecule existing in a dimeric form.

DISCUSSION

The fact of dimerization of GPCRs has only been appreciated relatively recently, and the mechanisms underlying the process of dimerization and its underlying functional significance are still being worked out for the different subgroups within the GPCR superfamily. GPCR dimerization could potentially affect trafficking to the plasma membrane, ligand binding, activation, signaling and desensitization and internalization. Some GPCRs dimerize only on the cell surface upon ligand activation, whereas others dimerize intracellularly prior to reaching the cell surface. Agonist-induced oligomerization has been shown for receptors such as those for somatostatin (12,13), thyrotropin-releasing hormone and gonadotropin-releasing hormone (14). For the CASR, evidence has been presented that it is present as a dimer on the cell surface, but that the calcium ligand does not affect the dimerization status (9).

In the present study, we identified two novel inactivating CASR mutations R66H and N583X in FHH and/or NSHPT

patients. CASR mutants harboring these mutations along with another one representing the previously identified R66C mutation were characterized functionally and compared with the wild-type CASR in a number of ways. The CASR can couple to different types of G protein and activate multiple signaling pathways. Coupling to the pertussis, toxin-insensitive $G_{q/11}$ stimulates phospholipase C-mediated inositol trisphosphate (IP_3) formation with intracellular Ca^{2+} mobilization and PKC activation, which contributes to stimulation of the MAPK cascade (15). Some evidence has been presented that activation of the MAPK pathway is relevant to the control of parathyroid secretory function by the CASR (16,17). In the present study, changes in intracellular Ca^{2+} (using an aequorin assay) and MAPK activation (both exogenous and endogenous) were measured in response to increases in the CASR agonists Gd^{3+} or Ca^{2+}. All three CASR mutants were defective with respect to cell signaling when compared with the wild-type. The complete lack of activity would be expected in the case of the N583X truncation mutant. The absent or markedly reduced activity of the R66H and R66C mutants, respectively, is consistent with the fluorescence immunocytochemical analysis of non-permeabilized cells that showed no or little cell-surface staining for all the mutants compared with the wild-type CASR.

However, the immunocytochemistry confocal microscopy of permeabilized cells did show that all three mutants were well expressed intracellularly similar to the wild-type. Therefore, these particular mutants belong to a class of CASR mutants that are retained within the cell and are unable to traffic normally to the cell surface. Previously, we had shown that other inactivating mutations, G549R and C850_851ins/fs, were only present intracellularly and not at the cell surface (18).

The CASR undergoes core (immature) N-linked glycosylation in the ER. Once properly folded, the core-glycosylated receptor transits to the Golgi apparatus where it undergoes mature glycosylation and is then expressed at the cell surface. The N-glycosylation with complex carbohydrates is important for cell-surface expression of the CASR but is not critical for signal transduction (19). Enzymatic deglycosylation experiments on extracts of HEK293 cells transfected with wild-type or mutant CASRs have defined the molecular species observed by immunoblotting analysis (18,20). The 160 kDa species is the fully glycosylated (mature) form, whereas the 140 kDa species is the immature core-glycosylated form. From the immunoblot analyses of the present studies, it is clear that the N583X truncation mutant does not achieve mature glycosylation essentially at all and that the R66H and R66C mutants undergo either no or little mature glycosylation, respectively. This is consistent with the results of the fluorescence immunocytochemistry and indicate that the mutants were all defective in trafficking to the plasma membrane.

Colocalization experiments were performed with the wild-type CASR and the mutants with markers specific for the ER and Golgi apparatus. Although the wild-type CASR was clearly localized to both organelles, none of the mutants was found in the Golgi, but only in the ER, indicating an impairment in their cellular trafficking.

Many studies have documented, by immunoblot analysis of parathyroid or kidney tissues or HEK293 cells transfected with the wild-type CASR cDNA, molecular species of >280 kDa. These represent dimers (or higher order oligomers) that are resistant to complete denaturation under the conventional SDS–PAGE conditions used. The CASR dimerizes through multiple types of intermolecular interactions including disulfide linkages involving C129 and C131 (21,22) and non-covalent interactions between L112 and L156 on each protomer, all within the extracellular domains (23). Mutation of some but not all of these interacting sites does not disrupt dimer formation but may lead in some cases to enhanced cell-signaling activity (23). In the present study, by immunoblot analysis of extracts of HEK293 cells transfected with the N583X truncation mutant cDNA, no dimeric form of the receptor was evident, only a monomeric species of ~75 kDa. This would be consistent with the view that, in addition to the interactions between the dimer interface in the extracellular domains (~600 amino acids) of the two protomers, non-covalent interactions involving other parts of the molecule are likely to be important (24,25). In contrast, the R66H and R66C mutants, although having almost no mature monomeric forms, had significant amounts of SDS-resistant dimeric forms similar to wild-type. By biotin cell-surface labeling of HEK293 cells that stably express the c-Myc-tagged CASR followed by immunoprecipitation with c-Myc antibody and immunoblot with streptavidin, it was confirmed that the CASR is present predominantly at the cell surface as a dimer.

With the naturally occurring CASR mutants that are retained intracellularly, two of which (R66H and R66C) that could dimerize and one (N583X) that could not, the issue of intracellular dimerization of the CASR was explored further by using the biophysical pbFRET method. In this context, the N583X mutant is valuable as a negative control. The FRET efficiency (E) depends on the distance between and the orientation of the chromophores, with enhanced resolution up to 100 Å. Hence, E is related to the level of dimerization. A two-state model is assumed in which receptors exist in one of two populations in either a monomeric or a dimeric state. FRET occurs only in a receptor dimer composed of one donor and one acceptor-labeled receptor. When donor and acceptor molecules are close enough, the acceptor fluorophore offers an alternate route for the deactivation of the energetically excited state of the fluorophore, which leads to slower photobleaching, an intrinsic property of a fluorophore characterized by the fading of the fluorescent signal when continuously exposed to excitation light of the donor molecule (13).

In the present study, a c-Myc epitope-tagged CASR was used. Only one monoclonal anti-Myc monoclonal antibody molecule can be bound per receptor molecule. If when receptors are incubated with both FITC- and Cy3-conjugated monoclonal antibodies, donor and acceptor, respectively, and a slower rate of photobleaching is observed in comparison to when only the donor FITC-conjugated antibody is used, then dimerization is indicated. The present experiments demonstrated that R66H and R66C mutants present in the ER, exist, like wild-type CASR, as dimers.

Dimers of the CASR have been identified in detergent extracts of rat kidney medulla (26), and the use of the bioluminescence resonance energy transfer technique in cells expressing GFP-tagged CASR has indicated the presence of dimers (27). In the present study, we provide firm evidence

of constitutive dimerization of the CASR in the ER. In addition, the finding of dimerization of mutant CASRs that are retained in this organelle suggests that although dimerization of the CASR may be necessary, it is not sufficient for the exit of the receptor from the ER and trafficking to the cell surface.

MATERIALS AND METHODS

Subjects

All subjects gave informed consent for the study that was approved by the respective institutional Ethics Committees.

Reagents

The c-Myc 9E10 mouse monoclonal antibody was from Santa Cruz Biotechnologies, the calnexin antibody (28) was kindly provided by Dr Eric Chevet (McGill University), the wheat germ agglutinin conjugated to fluorescein was as described (29), PhosphoPlus p44/42 MAP Kinase (Thr202/Tyr204) antibody kits were from Cell Signaling Technology, Beverly, MA, USA, the HA-tagged progranulin expression vector was kindly provided by David Baranowski and Dr Hugh P.J. Bennett (McGill University) and the pGL3 promoter plasmid was from Promega.

Sequence analysis of the *CASR* gene

Leukocyte DNA was isolated using standard methods. Exons 2–7 of the *CASR* gene were amplified as described (18). Gel purified PCR products were directly sequenced.

Site-directed mutagenesis

The Quick Change Site-Directed Mutagenesis kit (Stratagene, La Jolla, CA, USA) was used. For each mutation, the primers were complementary with the mutant sequence placed in the middle. The primers were annealed to the template (c-Myc-tagged human CASR cDNA in pcDNA3.1), and 12 rounds of extension were performed with Pfu Turbo DNA polymerase, followed by digestion of the template with *Dpn*I enzyme. The reaction was used to transform an *Escherichia coli* strain (XLI-Blue) that can incorporate nicked DNA and repair it, and colonies were screened by restriction enzyme digestion for the presence of the mutation. The correctness of all constructs was confirmed by sequencing.

Transient transfection of human CASR cDNA

Human embryonic kidney (HEK293) cells (provided by NPS Pharmaceuticals Inc., Salt Lake City, UT, USA) were cultured in 100 mM plates and transfected with human CASR cDNA (8 μg) using PolyFect transfection reagent. Forty-eight hours after transfection, cells were harvested for total cellular protein extraction and western blot analysis of total cell extracts was performed with the c-Myc 9E10 monoclonal antibody (18). All experiments were repeated at least three times and membranes were stripped and re-probed with β-tubulin mouse monoclonal antibody as a loading control.

Stable HEK293 cell lines expressing cDNA for wild-type CASR, empty vector and/or apoaequorin

HEK293 cells (that do not express CASR) were cultured in DMEM growth medium containing 10% fetal bovine serum. Cells were transfected with plasmid pcAEQ (30) that has the apoaequorin gene inserted in pcDNA3.1 (kindly provided by Drs A.D. Conigrave and A.H. Franks, University of Sydney, Australia), wild-type CASR or empty vector pcDNA3.1. Seventy-two hours after transfection, a medium containing 500 μg/ml of G418 was used to select only plasmid expressing cells. Non-transfected cells were used as a control. The selection medium was changed every 3 days and resistant colonies were maintained for 2 weeks. Several G418-resistant well-isolated colonies were selected for each cell line. The expression of apoaequorin, CASR and GAPDH was assessed by RT–PCR, in the case of the CASR, using primers located in different exons (4 and 6), and western blot analysis (data not shown). Mock-transfected or empty vector-transfected HEK293 cells were used as a control.

Cytoplasmic-free Ca^{2+} changes measured by aequorin luminescence assay

HEK-293 cells stably expressing aequorin were transiently transfected with wild-type or mutant CASR cDNA and pGL3 promoter plasmid and aliquoted into 96-well plates 24 h later. The next day, cells were rinsed once and charged for 1 h at 37°C in a buffer [20 mM HEPES, pH 7.4, 125 mM NaCl, 4 mM KCl, 1.25 mM $CaCl_2$, 1 mM $MgSO_4$, 1 mM NaH_2PO_4, 0.1% bovine serum albumin (BSA), 0.1% dextrose] containing 5 μM coelenterazine (cp form, Molecular Probes, Inc., Eugene, OR, USA) to form holoaequorin (30). The charging solution was then replaced with solution containing a low calcium concentration (20 mM HEPES, pH 7.4, 125 mM NaCl, 4 mM KCl, 0.5 mM $CaCl_2$, 0.5 mM $MgCl_2$, 0.1% dextrose, 0.1% BSA). Transfected cells were exposed to increasing Gd^{3+} concentrations (25–400 μM) and luminescence measurements were made (Fluostar Optima; BMG Labtech). Light emission was recorded at 0.5 s intervals for 30 s. The maximum response (for either wild-type or mutant CASR cDNA) was normalized to that with the empty vector pcDNA3.1. All the experiments were done with eight replicates per sample and repeated three times. Normalization for transfection efficiency was made to luciferase activity (pGL3) assay.

MAPK assays

MAPK activity induced by activation of the CASR was assessed in two ways. Amounts of endogenous phosphorylated extracellular signal-regulated kinases 1 and 2 (ERK 1/2) were assessed as described (31). In brief, HEK293 cells were transiently transfected with wild-type or mutant CASR cDNAs in six well plates. Forty-eight hours later, cells were serum-starved for 18 h and the medium was renewed for 2 h before cells were treated with various $CaCl_2$ concentrations (0.5–10 mM) for 5 min. Cells were lysed with a buffer containing sodium ortho-vanadate and complete protease inhibitor tablets. Whole cell extract proteins were separated by 10%

SDS–PAGE and phosphorylated and total ERK 1/2 were detected using the PhosphoPlus p44/42 MAP Kinase (Thr202/Tyr204) antibody Kit (Cell Signaling Technology) according to manufacturer's instructions.

Exogenous MAPK activity was assessed as described (32). In brief, a trans-reporting system (Stratagene) was used to measure the activity of Elk-1, an ETS domain transcription factor targeted by MAPK pathways. HEK293 cells were transiently cotransfected with vectors expressing wild-type (0.5 μg) or mutant receptor (0.5 μg) plus Elk-1 reporter constructs. The next day, cells were serum starved in DMEM containing 0.5 mM $CaCl_2$ for 8 h and cultured in various concentrations of $CaCl_2$ ranging from 0.25–15 mM for 16 h. The cells were washed in phosphate-buffered saline (PBS) and lysed on ice. Luciferase activity was measured using 45 μl cell lysate and D-luciferin using a Fluostar Optima. Luciferase activity was normalized to β-galactosidase activity.

Fluorescence immunocytochemistry and confocal microscopy

HEK293 cells were transiently transfected with either c-Myc-tagged wild-type or mutant CASR cDNA as described (33). Forty-eight hours after transfection, the PBS-washed cells were fixed in 4% paraformaldehyde. Cells were permeabilized with 0.1% Triton X-100 in PBS for 15 min if required. Washed cells were incubated in 5% goat serum for 1 h and then at 4 C overnight with 9E10 c-Myc monoclonal antibody at a 1:250 dilution. Washed cells were incubated for 1 h with a goat anti-mouse FITC-conjugated antibody (Molecular Probes, Inc.). Slides were mounted with mount medium and dried overnight at room temperature. Confocal images of labeled cells were acquired with a Zeiss LSM 510 META laser-scanning microscope (Carl Zeiss, Jena, Germany) using a 60× oil immersion lens. FITC fluorescence was visualized using a singletrack mode with laser excitation (488 nm) and emission (LP 505) filter sets.

For the ER and Golgi colocalization studies, the protocol was similar to that described above except, after permeabilization, cells were washed and incubated in 10% goat serum for 1 h and then incubated either with affinity-purified anti-calnexin antibody (αC4) (28), followed by FITC-labeled donkey anti-rabbit IgG for ER staining, or with wheat germ agglutinin conjugated to fluorescein for Golgi apparatus staining (29). In both cases, c-Myc-Cy3-conjugated monoclonal antibody was added to visualize the CASR. For ER staining, cells were washed and then incubated with secondary antibody for 1 h and mounted and visualized by confocal microscopy.

Biotinylation of cell surface CASR and immunoprecipitation

HEK293 cells stably transfected with either the c-Myc-tagged wild-type CASR construct or the empty vector were treated as described (34). Cell-surface proteins of the intact cells were labeled with membrane-impermeant Biotin-7-NHS using a Cellular Labeling Kit (Roche Molecular Biochemicals). Cells were washed once with PBS and treated with 50 μg/ml Biotin-7-NHS in biotinylation buffer for 15 min at room temperature. Reactions were stopped by adding 50 mM NH_4Cl and incubating on ice. The cells were washed twice with PBS and solubilized with 1 ml of lysis buffer per well containing 50 mM iodoacetamide and protease inhibitor mixture.

For immunoprecipitation, total protein of the whole cell lysate was incubated with a protein A-agarose suspension for 3 h at 4°C. Beads were pelleted by gravity centrifugation and supernatants were transferred to fresh tubes. After adding c-Myc 9E10 monoclonal antibody, the mixtures were incubated for 1 hour at 4°C. Protein A-agarose was added and incubation continued overnight at 4°C. Complexes were centrifuged and supernatants removed. The beads were washed three times and gel-loading buffer was added and proteins denatured at 100°C for 3 min. After centrifugation, aliquots of the supernatants were analyzed by electrophoresis through SDS 4–12% gradient gels. Gels were blotted onto PVDF membranes, incubated with blocking buffer to prevent non-specific binding of conjugate or substrate. The biotin-labeled proteins were reacted with a streptavidin-POD enzyme conjugate and visualized with a western blotting chemiluminescent reagent.

Immunocytochemistry and pbFRET microscopy

For pbFRET microscopy, HEK293 cells were transiently transfected with either c-Myc-tagged wild-type or mutant CASR cDNAs. Forty-eight hours later, cells were fixed with 4% paraformaldehyde in PBS on ice for 20 min. Cells were permeabilized with 0.2% Triton X-100 for intracellular localization of the receptors. Immunocytochemistry was performed with monoclonal anti-c-Myc antibody conjugated to either FITC or Cy3 corresponding to donor or acceptor, respectively, before being subjected to pbFRET analysis (12,35). The effective FRET efficiencies (E) were calculated according to the average photobleaching time constant of the donor obtained in the absence ($\tau_{ave\ D-A}$) and presence of the acceptor ($\tau_{ave\ D+A}$) using the equation $E = 1 - (\tau_{D-A}/\tau_{D+A}) \times 100$ (12).

ACKNOWLEDGEMENTS

We thank all family members for their participation, Drs S. Hatemi, E. Adal, D. Yardimci, E. Savgan, R. Kodakoglu, M. Karperien and S.E. Papapoulos for providing patient samples and/or clinical details, Dr E.M. Brown for help with the clinical evaluation of Case 1, Bing Yang and Irina Mosesova for technical support, Dr Stephane A. Laporte and Delphine Fessart for facilitating the confocal microscopy studies, Drs A.D. Conigrave and A.H. Franks for providing the apoaequorin plasmid and Drs Eric Chevet and Eric A. Shoubridge for critical review of the manuscript. This work was supported by the Canadian Institutes of Health Research (CIHR) Grants MOP-57730 (to G.N.H.) and MOP-74465 (to U.K.). S.P. was a recipient of a studentship from the McGill University Hospital Centre Research Institute and a scholarship from the CIHR Strategic Training Program in Skeletal Health. L.C. was the recipient of a postdoctoral fellowship from the Kidney Foundation of Canada.

Conflict of Interest statement. None declared.

REFERENCES

1. Brown, E.M., Gamba, G., Riccardi, D., Lombardi, M., Butters, R., Kifor, O., Sun, A., Hediger, M.A., Lytton, J. and Hebert, S.C. (1993) Cloning and characterization of an extracellular Ca(2+)-sensing receptor from bovine parathyroid. *Nature*, **366**, 575–580.
2. Pollak, M.R., Brown, E.M., Chou, Y.H., Hebert, S.C., Marx, S.J., Steinmann, B., Levi, T., Seidman, C.E. and Seidman, J.G. (1993) Mutations in the human Ca^{2+}-sensing receptor gene cause familial hypocalciuric hypercalcemia and neonatal severe hyperparathyroidism. *Cell*, **75**, 1297–1303.
3. Pollak, M.R., Brown, E.M., Estep, H.L., McLaine, P.N., Kifor, O., Park, J., Hebert, S.C., Seidman, C.E. and Seidman, J.G. (1994) Autosomal dominant hypocalcaemia caused by a Ca(2+)-sensing receptor gene mutation. *Nat. Genet.*, **8**, 303–307.
4. Hendy, G.N., D'Souza-Li, L., Yang, B., Canaff, L. and Cole, D.E.C. (2000) Mutations of the calcium-sensing receptor (CASR) in familial hypocalciuric hypercalcemia, neonatal severe hyperparathyroidism, and autosomal dominant hypocalcemia. *Hum. Mutat.*, **16**, 281–296.
5. Marx, S.J., Attie, M.F., Levine, M.A., Spiegel, A.M., Downs, R.W.J. and Lasker, R.D. (1981) The hypocalciuric or benign variant of familial hypercalcemia: clinical and biochemical features of fifteen families. *Medicine (Baltimore)*, **60**, 397–412.
6. Law, W.M., Jr. and Heath, H., III. (1985) Familial benign hypercalcemia (hypocalciuric hypercalcemia): clinical and pathogenetic study of 21 families. *Ann. Intern. Med.*, **102**, 511–519.
7. Cole, D.E.C., Forsythe, C.R., Dooley, J.M., Grantmyre, E.B. and Salisbury, S.R. (1990) Primary neonatal hyperparathyroidism: a devastating neurodevelopmental disorder if left untreated. *J. Craniofac. Genet. Dev. Biol.*, **10**, 205–214.
8. Pidasheva, S., D'Souza-Li, L., Canaff, L., Cole, D.E.C. and Hendy, G.N. (2004) CASRdb: calcium-sensing receptor locus-specific database for mutations causing familial (benign) hypocalciuric hypercalcemia, neonatal severe hyperparathyroidism, and autosomal dominant hypocalcemia. *Hum. Mutat.*, **24**, 107–111.
9. Bai, M., Trivedi, S. and Brown, E.M. (1998) Dimerization of the extracellular calcium-sensing receptor (CaR) on the cell surface of CaR-transfected HEK293 cells. *J. Biol. Chem.*, **273**, 23605–23610.
10. Pollak, M.R., Chou, Y-H.W., Marx, S.J., Steinmann, B., Cole, D.E.C., Brandi, M.L., Papapoulos, S.E., Menko, F.H., Hendy, G.N., Brown, E.M. *et al.* (1994) Familial hypocalciuric hypercalcemia and neonatal severe hyperparathyroidism. Effects of mutant gene dosage on phenotype. *J. Clin. Invest.*, **93**, 1108–1112.
11. Chou, Y.-H.W., Pollak, M.R., Brandi, M.L., Toss, G., Arnqvist, H., Atkinson, A.B., Papapoulos, S.E., Marx, S.J., Brown, E.M., Seidman, J.G. and Seidman, C.E. (1995) Mutations in the human Ca^{2+}sensing receptor gene that cause familial hypocalciuric hypercalcemia. *Am. J. Hum. Genet.*, **56**, 1075–1079.
12. Patel, R.C., Lange, D.C. and Patel, Y.C. (2002) Photobleaching fluorescence resonance energy transfer reveals ligand-induced oligomer formation of human somatostatin receptor subtypes. *Methods*, **27**, 340–348.
13. Rocheville, M., Lange, D.C., Kumar, U., Sasi, R., Patel, R.C. and Patel, Y.C. (2000) Subtypes of the somatostatin receptor assemble as functional homo- and heterodimers. *J. Biol. Chem.*, **275**, 7862–7869.
14. Kroeger, K.M., Pfleger, K.D.G. and Eidne, K.A. (2003) G-protein coupled receptor oligomerization in neuroendocrine pathways. *Front. Neuroendocrinol.*, **24**, 254–278.
15. Ward, D.T. (2004) Calcium receptor-mediated intracellular signaling. *Cell Calcium*, **35**, 217–228.
16. Kifor, O., MacLeod, R.J., Diaz, R., Bai, M., Yamaguchi, T., Yao, T., Kifor, I. and Brown, E.M. (2001) Regulation of MAP kinase by calcium-sensing receptor in bovine parathyroid and CaR-transfected HEK293 cells. *Am. J. Physiol.*, **280**, F291–F302.
17. Corbetta, S., Lania, A., Filopanti, M., Vicentini, L., Ballare, E. and Spada, A. (2002) Mitogen-activated protein kinase cascade in human normal and tumoral parathyroid cells. *J. Clin. Endocrinol. Metab.*, **87**, 2201–2205.
18. D'Souza-Li, L., Yang, B., Canaff, L., Bai, M., Hanley, D.A., Bastepe, M., Salisbury, S.R., Brown, E.M., Cole, D.E.C. and Hendy, G.N. (2002) Identification and functional characterization of novel calcium-sensing receptor mutations in familial hypocalciuric hypercalcemia and autosomal dominant hypocalcemia. *J. Clin. Endocrinol. Metab.*, **87**, 1309–1318.
19. Ray, K., Clapp, P., Goldsmith, P.K. and Spiegel, A.M. (1998) Identification of the sites of N-linked glycosylation on the human calcium receptor and assessment of their role in cell surface expression and signal transduction. *J. Biol. Chem.*, **273**, 34558–34567.
20. Bai, M., Quinn, S., Trivedi, S., Kifor, O., Pearce, S.H., Pollak, M.R., Krapcho, K., Hebert, S.C. and Brown, E.M. (1996) Expression and characterization of inactivating and activating mutations in the human Ca2 + o-sensing receptor. *J. Biol. Chem.*, **271**, 19537–19545.
21. Ray, K., Hauschild, B.C., Steinbach, P.J., Goldsmith, P.K., Hauache, O. and Spiegel, A.M. (1999) Identification of the cysteine residues in the amino-terminal extracellular domain of the human Ca^{2+} receptor critical for dimerization. Implications for the function of monomeric Ca^{2+} receptor. *J. Biol. Chem.*, **274**, 27642–27650.
22. Zhang, Z., Sun, S., Quinn, S.J., Brown, E.M. and Bai, M. (2001) The extracellular calcium-sensing receptor dimerizes through multiple types of intermolecular interactions. *J. Biol. Chem.*, **276**, 5316–5322.
23. Jiang, Y., Minet, E., Zhang, Z., Silver, P.A. and Bai, M. (2004) Modulation of interprotomer relationships is important for activation of dimeric calcium-sensing receptor. *J. Biol. Chem.*, **279**, 14147–14156.
24. Pace, A.J., Gama, L. and Breitwieser, G.E. (1999) Dimerization of the calcium-sensing receptor occurs within the extracellular domain and is eliminated by Cys −> Ser mutations at Cys^{101} and Cys^{236}. *J. Biol. Chem.*, **274**, 11629–11634.
25. Hu, J. and Spiegel, A.M. (2003) Naturally occurring mutations of the extracellular Ca^{2+}-sensing receptor: implications for its structure and function. *Trends Endocrinol. Metab.*, **14**, 282–288.
26. Ward, D.T., Brown, E.M. and Harris, H.W. (1998) Disulfide bonds in the extracellular calcium-polyvalent cation-sensing receptor correlate with dimer formation and its response to divalent cations *in vitro*. *J. Biol. Chem.*, **273**, 14476–14453.
27. Jensen, A.A., Hansen, J.L., Sheikh, S.P. and Brauner-Osborne, H. (2002) Probing intermolecular protein–protein interactions in the calcium-sensing receptor homodimer using bioluminescence resonance energy transfer (BRET). *Eur. J. Biochem.*, **269**, 5076–5087.
28. Dickson, K.M., Bergeron, J.J., Shames, I., Colby, J., Nguyen, D.T., Chevet, E., Thomas, D.Y. and Snipes, G.J. (2002) Association of calnexin with mutant peripheral myelin protein-22 *ex vivo*: a basis for 'gain-of-function' ER diseases. *Proc. Natl Acad. Sci. USA*, **99**, 9852–9857.
29. Mouchantaf, R., Kumar, U., Sulea, T. and Patel, Y.C. (2001) A conserved alpha-helix at the amino terminus of prosomatostatin serves as a sorting signal for the regulated secretory pathway. *J. Biol. Chem.*, **276**, 26308–26316.
30. Tan, Y.M., Cardinal, J., Franks, A.H., Mun, H.C., Lewis, N., Harris, L.B., Prins, J.B. and Conigrave, A.D. (2003) Autosomal dominant hypocalcemia: a novel activating mutation (E604K) in the cysteine-rich domain of the calcium-sensing receptor. *J. Clin. Endocrinol. Metab.*, **88**, 605–610.
31. Loretz, C.A., Pollina, C., Hyodo, S., Takei, Y., Chang, W. and Shoback, D. (2004) cDNA cloning and functional expression of a Ca2+-sensing receptor with truncated carboxyterminal tail from the mozambique tilapia (*Oreochromis mossambicus*). *J. Biol. Chem.*, **279**, 53288–53287.
32. Hendy, G.N., Minutti, C., Canaff, L., Pidasheva, S., Yang, B., Nouhi, Z., Zimmerman, D., Wei, C. and Cole, D.E.C. (2003) Recurrent familial hypocalcemia due to germline mosaicism for an activating mutation of the calcium-sensing receptor gene. *J. Clin. Endocrinol. Metab.*, **88**, 3674–3681.
33. Pidasheva, S., Canaff, L., Simonds, W.F., Marx, S.J. and Hendy, G.N. (2005) Impaired cotranslational processing of the calcium-sensing receptor due to signal peptide missense mutations in familial hypocalciuric hypercalcemia. *Hum. Mol. Genet.*, **14**, 1679–1690.
34. Hu, J., Hauache, O. and Spiegel, A.M. (2000) Human Ca2+ receptor cysteine-rich domain. Analysis of function of mutant and chimeric receptors. *J. Biol. Chem.*, **275**, 16382–16389.
35. Grant, M., Patel, R.C. and Kumar, U. (2004) The role of subtype-specific ligand binding and the C-tail domain in dimer formation of human somatostatin receptors. *J. Biol. Chem.*, **279**, 38636–38643.

S.B. Moore
M. Grant
Y. Rew
E. Bosa
M. Fabbri
U. Kumar
M. Goodman†

Synthesis and biologic activity of conformationally constrained analogs of L-363,301

Authors' affiliations:
S.B. Moore, Y. Rew, E. Bosa, M. Fabbri and M. Goodman, Department of Chemistry and Biochemistry, University of California, San Diego, 9500 Gilman Dr, La Jolla, CA 92093-0343, USA

M. Grant and U. Kumar, Fraser Laboratories for Diabetes Research, Royal Victoria Hospital, Department of Medicine, McGill University, Montreal, Quebec H3A 1A1, Canada

Correspondence to:
S.B. Moore
Department of Chemistry and Biochemistry
University of California, San Diego
9500 Gilman Dr
La Jolla
CA 92093-0343
USA
Tel.: 858 534 4801
Fax: 858 534 0202
E-mail: jpt@chem.ucsd.edu

Dates:
Received 6 May 2005
Accepted 11 September 2005

†This article is dedicated to the memory of Professor Murray Goodman.

To cite this article:
Moore, S.B., Grant, M., Rew, Y., Bosa, E., Fabbri, M., Kumar, U. & Goodman, M. Synthesis and biologic activity of conformationally constrained analogs of L-363,301. *J. Peptide Res.*, 2005, 66, 404–422.
DOI 10.1111/j.1399-3011.2005.00309.x

Key words: binding affinity; biological activity; chiral β-methylated amino acids; hsst receptors; organic synthesis; peptide synthesis; peptidomimetic; selectivity; solid phase peptide synthesis; somatostatin analogs

Abstract: We report the synthesis, biological activity and conformational analysis of analogs of the cyclic hexapeptide L-363,301, c[Pro^6-Phe^7-D-Trp^8-Lys^9-Thr^{10}-Phe^{11}] (numbering as in the native hormone somatostatin-14). The D-Trp in position 8 was replaced with (2R,3S)- and (2R,3R)-β-MeTrp respectively, with an added methyl group in the beta position of Trp. The objective of our study was to determine the potency and selectivity generated by the added constraint in the beta position of the D-Trp upon binding to human somatostatin receptors hsst1-5. We synthesized the building blocks enantioselectively and incorporated them into the peptides by SPPS. Competition binding assays revealed that both compounds **2** and **3** were selective for hsst2 over hsst5. The (2R,3S) analog **2** was approximately 30 times more potent at hsst2 than the (2R,3R) analog **3**. Interestingly, the (2R,3R) compound showed no binding affinity at hsst5.

Abbreviations: AcCN, acetonitrile; AcOH, acetic acid; Boc, *tert*-butyloxycarbonyl; DMAP, *N,N'*-dimethylaminopyridine; DPPA, diphenylphosphoryl azide; EtOAc, ethyl acetate; Fmoc, fluorenylmethoxycarbonyl; HOBt, 1-hydroxybenzotriazole; KHMDS, potassium bis(trimethylsilyl) amide; NBS, *n*-bromosuccinimide; PyBOP, benzotriazol-1-yl-oxytripyrrolidinophosphonium hexafluorophosphate; TFA, trifluoroacetic acid; $TIPSN_3$, triisopropylbenzenesulfonyl azide.

Introduction

Somatostatin, a peptide that regulates many physiologic functions, was discovered in 1973 as the factor responsible

for inhibition of growth hormone (GH) from the pituitary (1). In humans, it is found in two forms: somatostatin-14 (SS-14), with 14 amino acids, and SS-28, extended at the N-terminus (2). The hormone inhibits endocrine and exocrine secretions of GH, insulin, glucagon, amylase, and others. It is involved in neurotransmission, neuromodulation, inhibition of gastric acid, and other hormones from the gut (3).

The biologic effects of somatostatin follow from the interaction with G protein-coupled receptors in the gastrointestinal tract, the pancreas, the pituitary, and the brain (4). Various tumors also express somatostatin receptors (5). Five receptor subtypes have been cloned and characterized: sst1 and sst2 (6), sst3 (7,8), sst4 (9), and sst5 (10,11). It has been a priority to identify the functions of each receptor (3). The receptor subtypes have been classified into two subfamilies according to their structure and pharmacology (12). The first subfamily, denoted $SRIF_1$, includes sst2, sst3, and sst5. In general, synthetic octapeptide and hexapeptide analogs of somatostatin (e.g. octreotide, L-363,301) bind to this subfamily of receptors with high affinity. The other subfamily, $SRIF_2$, includes receptors sst1 and sst4, whose functions are less well known. Octapeptide and hexapeptide analogs such as octreotide and L-363,301 do not bind significantly to the $SRIF_2$ subfamily. The receptors in each subfamily show marked sequence similarities within the subfamily, especially within the transmembrane regions [sequence homologies of 90% for sst2/sst3/sst5 and 80% for sst1/sst4; sequence homology between the two groups of receptors were only 50–70% within the transmembrane regions (12)].

Many analogs which are smaller and long-acting compared with the native peptide have been synthesized and reviewed (13,14). An issue that received constant attention was the elucidation of the 'bioactive conformation' of the hormone and its analogs. The 'bioactive conformation' was defined by Veber (15) as 'the conformation of the peptide which interacts with the receptors to produce the effects characteristic to the peptide'. Because the native peptide is large and flexible, its study by nuclear magnetic resonance (NMR) methods is very difficult. To circumvent the flexibility problem, the structure was constrained through synthesis of cyclic analogs with smaller ring sizes and/or the incorporation of side chain-modified amino acids (smaller modified peptides may have better pharmacokinetic properties as well). Several publications by the Goodman group (16,17), as well as the novel scaffold approach of Hirschmann *et al.* (18,19), have demonstrated that the backbone of L-363,301, a highly potent cyclic hexapeptide analog of somatostatin c[Pro^6-Phe^7-D-Trp^8-Lys^9-Thr^{10}-Phe^{11}] **1** (Table 1; numbering refers to the order of amino acids in native somatostatin), is not in itself important for binding to receptors, but rather serves as a scaffold to maintain the side chains in the 'correct' three-dimensional array. The role of the side chains for binding to somatostatin receptors is crucial. To obtain information on the bioactive conformation of the side chains, Huang *et al.* from our group (17) have synthesized analogs of L-363,301 incorporating α- and β-methylated residues at positions 7, 8, and 11. These analogs displayed very different in vitro-binding affinities. Other groups, such as the Hruby group, have successfully and extensively applied the β-methylation approach (20–23). The amino acid β-Me-Trp was also used by Merck to obtain potent peptidomimetic and nonpeptide, subtype-selective analogs (24–26), and by the Ellman group in the synthesis of interesting scaffold-based β-turn mimetics (27,28). Other amino acids with modified side chains, such as 4-(*N*-isopropyl)-aminomethylphenylalanine (IAmp) and β-Me-naphthylalanine (β-Me-Nal) were used by the Rivier group to obtain hsst1- (29–32), hsst3- (33), and hsst4-selective somatostatin analogs (34–36). Researchers at Novartis recently used several side chain-modified amino acids to synthesize a 'universal' analog, SOM 230, which was more stable and more potent at receptors hsst1 and hsst5 than octreotide (37,38).

Table 1. **Binding constants[a] for β-methylated analogs (17)**

Number	Analog	IC_{50} (nM)
1	c[Pro-Phe-D-Trp-Lys-Thr-Phe], L-363,301	1
2	c[Pro-Phe-(*2R,3S*)-β-Me-Trp-Lys-Thr-Phe]	<1
3	c[Pro-Phe-(*2R,3R*)-β-Me-Trp-Lys-Thr-Phe]	>1000
4	c[Pro-Phe-(*2S,3R*)-β-Me-Trp-Lys-Thr-Phe]	10
5	c[Pro-Phe-(*2S,3S*)-β-Me-Trp-Lys-Thr-Phe]	>1000

a. Assays were carried out on membranes of mouse of AtT-20 cells, containing mixtures of receptors.

Huang *et al.* (17) studied the above methylated compounds incorporating constrained side chain conformations. These studies were based on the premise that direct information on the possible 'bioactive conformation' can be obtained from the constrained side chains. Also, analogs with increased potency and selectivity are likely to result by constraining the side chains to adopt a structure close to the 'bioactive conformation'. The design rationale for the β-methylated residues was inspired from the point of view of both the ligand and the receptor. The β-methyl group introduces a topologic effect, reducing the flexibility of the side chain, specifically constraining it to prefer a particular rotamer. The β-methyl group also introduces a chiral effect.

There are different steric effects on a receptor surface, depending on the configuration of the β-carbon atom. The added steric bulk will affect binding to the receptor favorably or not, depending on configuration.

The most interesting effects on binding were observed for the compounds containing β-Me-Trp (Table 1). Compound 2, with (2R,3S)-β-Me-Trp^8, had a higher binding affinity than the standard compound 1. Compound 3, with (2R,3R)-β-Me-Trp^8, displayed a binding affinity about an order of magnitude lower than 1. Compound 4 was less potent than the standard compound, while compound 5 was much weaker. These significant changes in binding affinity suggested critical topochemical requirements for the side chain groups. The conformations of these compounds were studied by one-dimensional (1D) and two-dimensional (2D) NMR. Conclusions regarding the bioactive conformations of these compounds were drawn, and a model for the 'bioactive conformation' of the main chain and side chains was generated. The most active peptidomimetic was compound 2 incorporating (2R,3S)-β-methyltryptophan. It was found that the backbone conformation was not disturbed by the β-methylation. However, β-methylation strongly affected the conformational preferences of the side chains. The 'bioactive conformations' of the side chains Phe^7, Trp^8, Lys^9, and Phe^{11} (which constitute the pharmacophore) were determined by conformational analysis. It was concluded that the analogs had two possible conformations available: a 'folded' and a 'flat' topology. It was shown that the 'folded' conformation is the bioactive one. Other features of the bioactive conformation include the side chains of β-Me-Trp^8 and Lys^9 in close proximity. The side chain of Phe^{11} is also close to the Trp-Lys side chains, facilitated by the 'folded' (or 'cup-shaped') backbone structure. There is a βII' turn about Trp^8-Lys^9 and a βVI turn around Phe^{11}-Pro^6.

The above study was a significant contribution in the field of somatostatin research. However, at the time the study was carried out, the five subtypes of somatostatin receptors were not readily available. The authors of that paper refer to a 'somatostatin receptor'. The biologic testing was performed on membranes of AtT-20 cells, which were shown to express several somatostatin and β-adrenergic receptors (19,39).

In the present study, we desired to establish the binding profile of ligands 2 and 3 at each individual receptor subtype, in particular hsst2 and hsst5, to better understand the conformational requirements at each receptor subtype. We chose to study the (2R,3S) analog as it appeared to be more potent than the reference compound L-363,301. We also studied the (2R,3R) analog as a negative control. This knowledge in turn can lead to the synthesis of more selective and potent analogs, with increased activity and reduced side effects.

Amino acid and peptide synthesis

The building blocks, Fmoc-(2R,3S)-β-Me-Trp(N^{in}-Boc)-OH and Fmoc-(2R,3R)-β-Me-Trp(N^{in}-Boc)-OH were synthesized according to a procedure elaborated by Hruby and co-workers (40) and revised for the synthesis of Fmoc-(2S,3S)-β-Me-Trp(N^{in}-Boc)-OH (41). We combined and adapted the two methods to obtain the (2R,3S)- and (2R,3R)-β-Me-Trp diastereomers. The synthesis of the two amino acids, based on a chiral auxiliary approach, is illustrated in Figs 1 and 2. This synthesis method is enantioselective, different from the one used by Huang *et al.* (17). Indeed, the previous synthesis used the method of Snyder (42), resulting in two pairs of diastereomers: the *threo* pair [(2R,3S) + (2S,3R)] and the *erythro* pair [(2R,3R) + (2S,3S)]. Each pair was used in the construction of the peptides, and the absolute stereochemistry of each individual building block elucidated at the end of the synthesis. Mixtures of linear peptides, partially deprotected, had to be separated by high-performance liquid chromatography (HPLC), followed by cyclization in solution, followed by another deprotection, and finally another HPLC purification to obtain the desired peptides. The building blocks were added third in the peptide sequence. This strategy exposed the acid-sensitive Trp side chain to a few acid deprotection steps during the solid phase peptide synthesis (SPPS) using Boc-protocols.

In the present strategy, we synthesized each β-Me-Trp building block separately, then incorporated them as the last amino acid in the sequence on a simply constructed peptide chain (we are indebted to the Hruby group for their efforts to accomplish the synthesis of enantiomerically pure β-methylated amino acids, which were very useful to adopt for this project's goals). We did this to take advantage of the observation that having a D-Trp as a 'head' amino acid provided the best cyclization yield in a hexapeptide somatostatin analog sequence (43). Also, adding the synthesized building block last was hoped to minimize side reactions on the indole ring or loss of material because of loss of peptide from the resin. We used a Rink acid resin, requiring Fmoc protocols. This resin provided the added advantage that the linear peptides could be cleaved off easily with dilute acid [10% AcOH/dichloromethane (DCM)] as opposed to HF, and the side chains remained protected. The cyclization reactions were carried out in

Figure 1. Synthesis of Fmoc-(2R,3S)-β-Me-Trp(Boc)-OH.

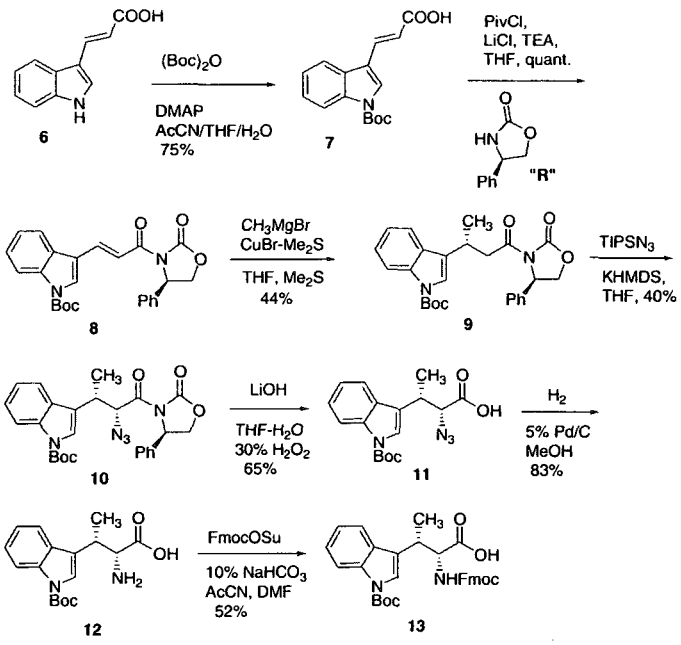

Figure 2. Synthesis of Fmoc-(2R,3R)-β-Me-Trp(Boc)-OH.

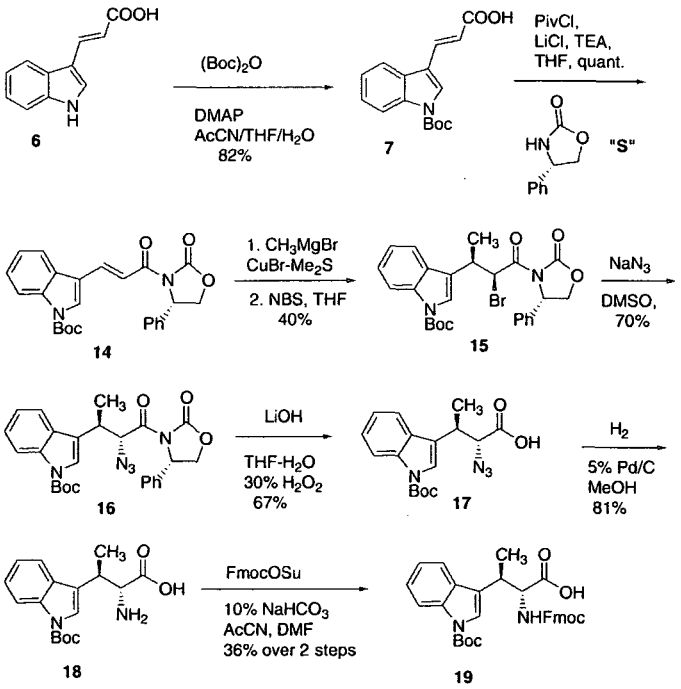

solution, but with linear peptides with protected side chains, which gave excellent cyclization yields (e.g. 74% for 2R,3R). Finally, only one HPLC purification was required.

The indole nitrogen of *trans*-3-indole-acrylic acid was protected under mild conditions with Boc, which prevents side reactions on the indole ring during the synthesis. The

Boc-protecting group also presents the advantage that it is compatible with peptide synthesis by Fmoc strategy. The chiral oxazolidinone, *R*-(−)-4-phenyl-2-oxazolidinone or *S*-(+)-4-phenyl-2-oxazolidinone, was coupled to the carboxylic acid by the mixed anhydride route using pivaloyl chloride and LiCl as a promoter. To obtain the (2R,3S) isomer, the β-methyl was introduced by an asymmetric Michael conjugate addition in the presence of a methylcopper organometallic reagent generated by the reaction of methylmagnesium bromide and CuBr–dimethylsulfide complex. The amino group in the α-position was introduced via a potassium imide-enolate azide formation reaction, in the presence of KHMDS and triisopropylbenzenesulfonyl azide ($TIPSN_3$; 44). To obtain the (2R,3R) isomer, the stereochemistry at the α- and β-positions was set in a one-pot fashion as follows. The addition of the methylcuprate to the enone-imides generated an α-methylated metal enolate intermediate stabilized by chelation. The enolate was trapped with NBS as the bromine electrophile, thus functionalizing the β-position. In the next step, the bromine was displaced with the azide group using NaN_3. The removal of the chiral auxiliary was achieved by basic hydrolysis with LiOH in tetrahydrofuran (THF)/H_2O and 30% hydrogen peroxide. For both enantiomers, the azido acids were reduced by hydrogenation over 5% Pd/C. The amino groups of both amino acids were Fmoc-protected. It has been established previously that these reactions occurred with high stereoselectivity in favor of the desired products. Therefore, we did not determine the diastereomeric excess for each step. In all cases, the optical rotation values of the purified intermediates were in the range of the published data.

The peptides were synthesized by solid phase techniques, using the Fmoc strategy as illustrated in Fig. 3.

The side chain-protected linear peptides were cleaved from the resin by treatment with 10% AcOH/DCM, to produce the free carboxylic acid-terminus. The cyclization took place in solution, in the presence of DPPA/$NaHCO_3$. The cyclic peptides were deprotected with trifluoroacetic acid (TFA) and purified by reverse phase (RP)-HPLC.

Conformational studies

The 1D and 2D NMR measurements were carried out by Elisabetta Bosa on a 500 MHz Bruker (Billerica, MA, USA) AMX 500 (500 MHz) machine. The chemical shifts for the peptides are shown in Tables 2 and 3. Mara Fabbri carried out computer simulations on an SGI IRIX 6.5 workstation, using the INSIGHT II and DISCOVER programs for the energy minimization, dynamics calculations and visualization. The details of this study are presented in the Experimental Section.

Results

Biologic activity

The peptides were subjected to competitive-binding assays at cloned receptors hsst1–5 using ^{125}I-LTT-SST28 as the radioligand. The data are given in Table 4. We report binding affinity results at receptor subtypes hsst1–5.

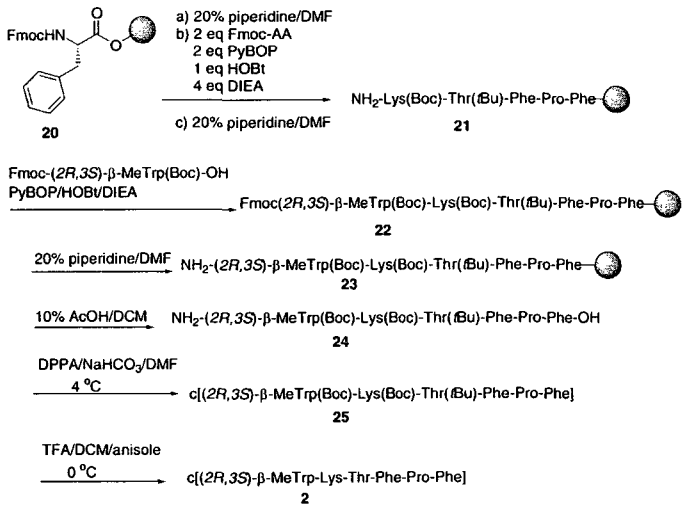

Figure 3. Synthesis of c[(2R,3S)-β-Me-Trp-Lys-Thr-Phe-Pro-Phe] **2**. The (2R,3R) building block was attached following a similar procedure, to obtain **3**.

Table 2. Chemical shifts for (*2R,3S*)-β-Me-Trp-containing peptide 2 (dimethyl sulfoxide, DMSO; 500 MHz)

Residue	p.p.m.
Pro[6]	
α	3.74
β	1.75, 1.08
γ	1.54, 1.35
δ	3.24, 3.15
Phe[7]	
NH	7.43
α	4.73
β	2.97, 2.89
β-Me-Trp[8]	
NH	8.53
α	4.43
β	3.21
β-Me	0.94
Lys[9]	
NH	8.22
α	3.38
β	1.36, 1.14
γ	0.36, 0.31
δ	1.14
ε	2.48, 2.41
Thr[10]	
NH	6.94
α	4.13
β	3.88
γ	0.98
Phe[11]	
NH	8.31
α	4.24
β	2.86

Table 3. Chemical shifts for (*2R,3R*)-β-Me-Trp-containing peptide 3 (dimethyl sulfoxide, DMSO; 500 MHz)

Residue	p.p.m.
Pro[6]	
α	3.67
β	1.65, 1.27
γ	1.49, 1.29
δ	3.19, 3.06
Phe[7]	
NH	6.73
α	4.44
β	2.69, 2.29
β-Me-Trp[8]	
NH	8.37
α	4.73
β	3.26
β-Me	1.30
Lys[9]	
NH	9.00
α	4.05
β	1.83, 1.58
γ	1.45, 1.38
δ	1.54
ε	2.76
Thr[10]	
NH	7.05
α	4.15
β	4.04
γ	0.98
Phe[11]	
NH	8.13
α	4.22
β	2.85

The data (Table 4) reveal that both the (2R,3S) **2** and (2R,3R) **3** analogs are selective at hsst2.

The (2R,3S) compound **2** has about the same potency as compound **1**, and similar selectivity as compound **1** at hsst2 compared with hsst5. Compound **3** is 31 times less potent than compound **2** at hsst2, and 45 times less potent than compound **1**. However, compound **3** maintains nanomolar-binding affinity at hsst2, and thus is hsst2-selective. Interestingly, compound **2** showed an increase in binding affinity at hsst4 compared with **1**.

In summary, we obtained analogs that are potent and selective at hsst2, with an order of magnitude difference in binding affinity between the (2R,3S) and (2R,3R) analogs.

Molecular dynamics simulations

We were interested in correlating the biologic activities with conformations. We subjected the compounds to a 10 ns-long free dynamics simulation. The simulation revealed that in the (2R,3S) analog **2**, the pharmacophoric side chains of β-Me-Trp and -Lys remained in close proximity and parallel (average distance of 5 Å between the center of mass of Trp and the γ-proton of the Lys) throughout the 10 ns simulation (Fig. 4), while in the (2R,3R) compound they were extended away from each other (average distance between the center of mass of Trp and the γ-proton of Lys of 9–10 Å; Fig. 5). There were a

Table 4. **Binding affinity data to cloned somatostatin receptors hsst1–5**

	IC_{50} (nM)				
Compound	hsst1	hsst2	hsst3	hsst4	hsst5
SS-14	0.17 ± 0.1	1.2 ± 0.4	0.11 ± 0.1	0.14 ± 0.1	0.53 ± 0.2
L-363,301, 1	897 ± 97	0.16 ± 0.1	917 ± 131	756 ± 6	39 ± 6
(*2R,3S*) analog, 2	969 ± 18	0.23 ± 0.1	>1000	242 ± 6	68 ± 13
(*2R,3R*) analog, 3	915 ± 69	7.2 ± 1.5	>1000	936 ± 155	>1000

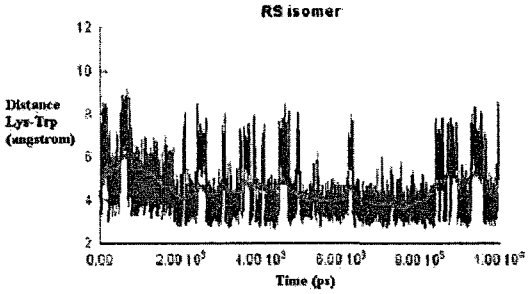

Figure 4. Distance between the center of mass of Trp and the γ-proton of the Lys during the 10 ns simulation of the (2R,3S) peptide 2.

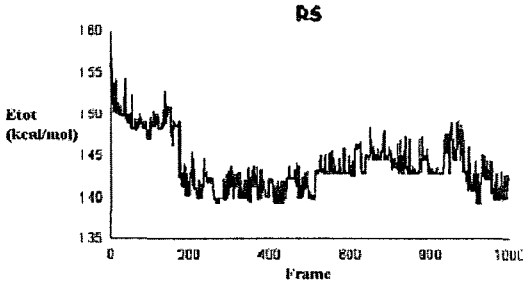

Figure 6. Total energy of the (2R,3S) peptide 2 sampled and minimized every 10 ps.

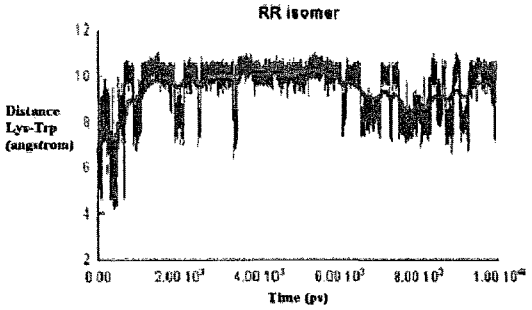

Figure 5. Distance between the Trp center of mass and the γ-proton of the Lys side chain during 10 ns simulation of the (2R,3R) peptide 3.

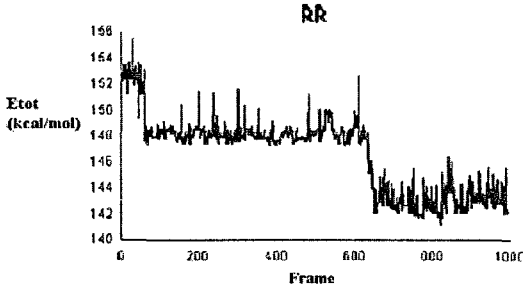

Figure 7. Total energy of the (2R,3R) peptide 3 sampled and minimized every 10 ps.

few low-energy conformations available to the (2R,3S) analog (Fig. 6). The (2R,3R) analog evolved in a stepwise fashion from a high-energy state to a lower energy conformation, which was preferred for the rest of the simulation (Fig. 7). This showed that the (2R,3S) analog 2 is more flexible than the (2R,3R) analog 3. The lowest energy conformations for the (2R,3S) compound 2 corresponded to an average distance of 5 Å between the center of mass of Trp and the γ-proton of the Lys. The results of this study are in accord with our previous model of the 'bioactive conformation' of L-363,301 analogs (17,45), described recently as the sst2/sst5-binding model (32).

Discussion

We synthesized β-methylated analogs of Trp enantioselectively and incorporated them into the cyclic hexapeptide L-363,301. The binding potencies and selectivities of c[Pro-Phe-(2R,3S)-β-Me-Trp-Lys-Thr-Phe] (2) and c[Pro-Phe-

(2R,3R)-β-Me-Trp-Lys-Thr-Phe) (3) at somatostatin receptors hsst1–5 were determined, to re-examine the intriguing results we obtained when the individual receptors were not available. In those studies, the (2R,3S) analog 2 was more potent than the parent peptide 1, while the (2R,3R) analog 3 was much less active. We hoped to establish the role of the added β-methyl group upon binding. In the present tests, both compounds bound to receptor hsst2 in nanomolar range. There was, however, a 31-fold difference in binding potency at hsst2, in favor of the (2R,3S) compound 2. The analogs proved selective for hsst2 over hsst5 (1), whereas compound 3 was about twice less selective than L-363,301. Standard compound L-363,301, binds well to both receptors hsst2 and hsst5 (46). Compound 3 lost binding affinity at hsst5.

Through molecular dynamics simulations we observed that the (2R,3S) analog is more flexible than the (2R,3R), but keeps its pharmacophoric side chains of D-Trp and Lys in a close spatial array. In contrast, the (2R,3R) analog evolves to a stable low-energy conformation in which the pharmacophoric side chains are not close to each other. These characteristics probably account for the observation that the binding affinity of the (2R,3S) molecule is higher. Statistically, the (2R,3S) molecule adopts the 'bioactive conformation' most of the time, being constrained with the pharmacophoric side chains close to each other. The NMR data supports the findings related to the proximity of the side chains (Tables 2 and 3). There is an upfield shift for the γ-proton of Lys in the (2R,3S) compound 2, indicating a shielding effect of the aromatic ring of Trp in close proximity to the Lys. There is a downfield shift of the same proton in the (2R,3R) analog 3 showing the aromatic ring does not exert an influence and must be far from the Lys side chain. In the (2R,3S) analog 2, there are NOEs between the protons of the Lys side chain and the D-Trp side chain. These NOEs are absent in the case of the (2R,3R) compound (see Supplementary material).

Thus, synthesis, binding affinity data, NMR, and molecular modeling studies have shown that the difference in one chiral center at the D-Trp side chain has a marked effect on the behavior of L-363,301 analogs. The compounds were observed during a 10 ns dynamics simulation. The (2R,3S) compound appeared to be more flexible, converting back and forth between a few low-energy conformations. All throughout the simulation, the side chains of β-Me-Trp and -Lys stayed and in close proximity. It has been accepted that these two side chains in proximity constitute part of the 'bioactive conformation', which is found in all cyclic peptide analogs of somatostatin active at hsst2 and hsst5 (17,45,47). In contrast, the (2R,3R) molecule is more rigid in the sense that it prefers a low-energy conformation where the β-Me-Trp and -Lys side chains are situated far from each other. The 31-fold difference in activity at hsst2 may arise because energy is required to force the side chains in the (2R,3R) molecule to be parallel and in close proximity. Therefore, this molecule is less active than the (2R,3S) molecule, showing only approximately 10-nm affinity at hsst2 and no affinity at hsst5. It appears that a deviation from the conformation with the pharmacophoric side chains being close together has a lowering effect on binding at hsst5. The change in chirality at the Cβ from *S* to *R* brought with it a change in the preferred lowest energy conformation, which caused an order of magnitude loss of binding at receptor hsst2 and a loss of binding at all receptors in general. This rather small structural change had a significant effect upon somatostatin receptor affinity.

It is difficult to compare the present biologic results with results obtained in the past paper that generated this study (17), because the past biologic tests were carried out with a mixture of receptors. While compound 2 maintained high potency at hsst2 and hsst5, it was not more potent than L-363,301 as before. Compound 3 was not active at receptors hsst1, 3, 4, and 5, but still maintained binding affinity at hsst2. The present result confirmed that 2 was more active than 3 at hsst2, and showed that 3 was inactive at hsst5. Our previous 'bioactive conformation' model is confirmed. In the past paper, it was not possible to explain why certain compounds could theoretically attain the 'bioactive conformation' and yet to be completely inactive. The present results show that some binding affinity remained at hsst2 for the compound with the unfavorable chirality at the β-position of Trp, which indicates the role of the added methyl group in modulating the binding potency to hsst2 and hsst5. A comparison between our previous sst2/sst5 pharmacophore model and the models for sst1 and sst4 selectivity of octapeptides can be found in a recent publication of the Rivier group (32).

In conclusion, the peptidomimetic analog of L-363,301 containing the (2R,3S)-β-Me-Trp diastereomer 2 possesses the 'correct' combination of features that allow it to bind to the hsst2 receptor subtype in subnanomolar range. These features include a 'folded' backbone, with side chains of β-Me-Trp^{8} and Lys^{9} close to each other and to Phe^{11}. The methyl group modulates binding affinity by influencing the orientation of the pharmacophore side chains. This finding has consequences for the future design of hsst2-selective somatostatin analogs.

Experimental Section

General procedures and notes

Reagents were purchased from Sigma-Aldrich (St Louis, MO, USA) and Acros Organics (Pittsburgh, PA, USA) and used without further purification. Tetrahydrofuran was dried by refluxing over sodium/benzophenone. DCM was dried by refluxing over CaH_2. Triethylamine (TEA) was refluxed over CaH_2. Reactions were carried out under an inert atmosphere (N_2). The *N,N*-dimethylformamide (DMF) was purchased from Fisher Scientific (Pittsburgh, PA, USA) and treated with sodium aluminosilicate molecular sieves (4 Å pore diameter) obtained from Sigma and Amberlite (Bio Rad, Hercules, CA, USA) IR120 (plus) cation-exchange resin, strongly acidic. Protected amino acids, Rink acid resin and PyBOP were purchased from Calbiochem-Novabiochem AG (San Diego, CA, USA). The reactions were monitored by TLC carried out on EM Science Merck (San Diego, CA, USA) silica gel coated on aluminum plates (0.2 mm thickness, 60 F_{254}) using UV light (254 nm) as the visualizing agent and 10% ninhydrin in ethanol, bromocresol green in ethanol, 7% ethanolic phosphomolybdic acid and a solution of 1 g vanillin in 10 mL EtOH with 10 mL H_2SO_4 ('vanillin stain') and heat as developing agents. Silica gel 60 (230–400 mesh) purchased from EM Science was used for column chromatography. The Kaiser test (48) was used as a qualitative assay for the presence or absence of free amino groups during reactions on solid phase.

The NMR spectra were obtained on a Varian HG-400 (400 MHz) and a Bruker AMX 500 (500 MHz) spectrometers. Chemical shifts (δ) are reported in parts per million (p.p.m.) relative to residual undeuterated solvent as an internal reference. The following abbreviations were used to explain multiplicities: s, singlet; d, doublet; t, triplet; q, quartet; dd, doublet of doublets; m, multiplet; b, broad.

Optical rotations were measured using a Perkin-Elmer (Wellesley, MA, USA) 241 polarimeter. Infrared (IR) spectra were obtained with a Nicolet-Magna-IR (Madison, WI, USA) 550 Series II spectrometer. Mass spectroscopic (MS) analyses (ESI, MALDI-FTMS) were carried out by the MS laboratory at The Scripps Research Institute, La Jolla, CA, USA.

The final products were purified and analyzed by RP-HPLC using Vydac Protein Peptide C_{18} columns. Column dimensions were 4.5 × 250 mm (90 Å silica, 5 μm) for analytical and 22 × 250 mm (90 Å silica, 10 μm) for preparative HPLC, and UV absorbance was monitored at 220 nm or 280 nm. A binary system of water with 0.1% TFA (A) and acetonitrile with 0.1% TFA (B), was used throughout. Preparative HPLC was carried out at 10 mL/min flow rate, on two different instruments. One instrument was a system composed of two Waters (Milford, MA, USA) 510 pumps and a dual wavelength UV absorbance detector. The other instrument, which was also used for analytical purposes as described below, was a Waters Millenium 2010 system, composed of two Waters 510 pumps, a 715 Ultra WISP sample injector, and a Waters TM 996 photodiode array detector (PDA), operated by a NecPower Mate (NEC USA, Inc., Melville, NY, USA) 485/331 PC compatible computer. Two analytical HPLC profiles of the pure compounds were obtained on the Waters Millenium PDA system, using a linear gradient of 10–90% acetonitrile (B) in water (A) over 40 min and an isocratic elution at 1 mL/min flow rate.

The $TIPSN_3$ was prepared from triisopropylbenzenesulfonyl chloride and sodium azide (49,50). The nomenclature of the compounds was established with the Beilstein AutoNom feature.

Synthesis

Synthesis of Fmoc-(*2R,3S*)-β-Me-Trp(Boc)-OH (13)

(1-*t*-butyloxycarbonyl)indole-3-acrylic acid (7)

Trans-3-indoleacrylic acid 6 (10.0 g, 53.42 mmol) was suspended in AcCN (250 mL), THF (10 mL) and H_2O (10 mL; Fig. 1). The suspension was cooled in an ice bath and TEA (15 mL, 106.84 mmol) was added dropwise. The solution turned clear yellow upon the addition of base. Solid DMAP (1.31 g, 10.68 mmol) was added, followed by solid $(Boc)_2O$ (23.32 g, 106.84 mmol) in one portion. The reaction mixture was allowed to stir in the ice bath, under a N_2 atmosphere, slowly equilibrating to room temperature, for a total of 4 h. The solvent was removed under reduced pressure until a thick yellowish oil remained. Water (250 mL) was added, followed by extraction with EtOAc (3 × 50 mL). The organic extract was discarded. The aqueous layer was acidified in an ice bath with 6 N HCl, and the resulting yellow precipitate filtered through a Buchner funnel and rapidly washed with water. The precipitate was dried under high vacuum overnight, yielding 10.4 g. To obtain additional product, the aqueous filtrate was re-extracted with EtOAc

(3 × 50 mL). The organic layer was dried over Na_2SO_4, filtered and concentrated to yield a yellow foam, which was dried overnight on a vacuum manifold to yield another 1.0 g of product. Therefore, the total yield of product was 11.4 g (75%).

^{1}H-NMR (dimethyl sulfoxide, DMSO) δ (p.p.m.) 8.26 (s, 1H), 8.12 (d, J = 8.4 Hz, 1H), 7.95 (d, J = 8 MHz, 1H), 7.80 (d, J = 16.8 Hz, 1H), 7.41 (t, J = 7.2 Hz, 1H), 7.34 (t, J = 7.6 Hz, 1H), 6.56 (d, J = 17.2 Hz, 1H), 1.63 (s, 9H); ESI (m/z): $[M + H]^+$ calcd for $C_{16}H_{17}NO_4$, expected 288, found 288, $[M + Na]^+$ expected 310, found 310, $[M - H]^-$ expected 286, found 286. TLC ($CHCl_3$: MeOH : CH_3COOH 98 : 2 : 1, bromocresol green), R_f = 0.36.

[3(2*E*), 4*R*]-3-[3-(*N*-(2-*t*-butyloxycarbonyl)-3-indolyl-1-oxopropenyl]-4-phenyl-2-oxazolidinone (8)

An oven-dried, three-necked 500 mL round-bottomed flask set up with a thermometer adapter and thermometer, was cooled under N_2. The starting material, carboxylic acid 7 (8.60 g, 29.93 mmol) was rapidly added as a solid, then 115 mL dry THF were added via syringe and the solution cooled to −78 °C. Freshly distilled TEA (13 mL, 92.08 mmol) was added dropwise (internal temperature −60 °C), then pivaloyl chloride (4.5 mL, 34.53 mmol), dropwise. The suspension was allowed to stir, warming slowly, for 2 h and 30 min (initial temperature −40 °C, final temperature −20 °C). Lithium chloride was added (1.46 g, 34.53 mmol), followed by (*R*)-(−)-4-phenyl-2-oxazolidinone (3.76 g, 23.02 mmol). The reaction mixture was allowed to warm to room temperature, overnight, under N_2. The reaction was quenched by addition of 50 mL 0.2 M HCl. The solvent was removed under reduced pressure until only the aqueous layer remained, followed by addition of EtOAc (50 mL). The aqueous layer was extracted with EtOAc (3 × 20 mL), and the combined organic layer re-extracted with 0.2 M HCl (5 × 15 mL), $NaHCO_3$ (3 × 20 mL) and sat. NaCl (2 × 20 mL). After drying over Na_2SO_4, the solvent was removed under reduced pressure and the residue dried on a vacuum manifold overnight to yield 11.1 g crude product. The crude product was sufficiently pure to be used for the next reaction, alkylation at the β-position. To characterize the material, a portion was purified by column chromatography using 10% EtOAc/hexanes, followed by 50% EtOAc/hexanes.

^{1}H-NMR ($CDCl_3$) δ (p.p.m.) 8.18–7.24 (arom, 10H and 2H, olefinic), 5.575 (dd, J_1 = 8 Hz, J_2 = 4 Hz, 1H), 4.74 (t, J = 8 Hz), 4.32 (dd, 1H, J_1 = 8 Hz, J_2 = 4 Hz), 1.66 (s, 9H); ESI (m/z): calcd for $C_{25}H_{24}N_2O_5$, $[M + H]^+$ expected 433, found 433, $[M + Na]^+$ expected 455, found 455, $[M - H]^-$ expected 431, found 431, $[M + Cl]^-$ expected 467, found 467. TLC (EtOAc : hexanes 1 : 1, vanillin), R_f = 0.66.

[3(3*R*), 4*R*]-3-[3-(*N*-(2-*t*-butyloxycarbonyl)-3-indolyl)-1-oxobutyl]-4-phenyl-2-oxazolidinone (9)

In an oven-dried, three-necked 500 mL round-bottomed flask was added CuBr–Me_2S complex (7.64 g, 37.14 mmol) followed by Me_2S (37 mL) and THF (100 mL) and the resulting clear brown solution was cooled to 0 °C. After stirring for about 10 min, a solution of CH_3MgBr (3 M in ether, 16 mL) was added dropwise. Stirring at 0 °C was continued for 40 min. A solution of starting material 8 (10.70 g, 24.76 mmol) was dissolved in THF (50 mL), stored under N_2 and cooled to 0 °C. The cooled starting material solution was cannulated into the slurry of the copper complex and the mixture stirred at 0 °C for 2 h, then overnight, slowly equilibrating to room temperature. The reaction was quenched by the slow addition of excess sat. NH_4Cl, and stirred for 30 min.

The layers were separated and the organic layer washed with sat. NH_4Cl (6 × 25 mL) until the blue aqueous layer turned clear, followed by washing with sat. NaCl (2 × 25 mL). The organic layer was dried over Na_2SO_4, filtered, concentrated and dried overnight on a vacuum manifold to yield 10.3 g of crude yellow oil. This was purified by column chromatography using 15% EtOAc/hexanes, to yield 4.84 g (44%) white foamy solid.

^{1}H-NMR ($CDCl_3$) δ (p.p.m.) 8.10 (bs, 1H), 7.59 (d, J = 4 Hz, 1H), 7.34–7.19 (m, 8H), 5.30 (dd, J_1 = 8 Hz, J_2 = 4 Hz, 1H), 4.56 (t, J = 8 Hz, 1H), 4.22 (dd, J_1 = 8 Hz, J_2 = 4 Hz, 1H), 3.58 (m, 1H), 3.44 (dd, J_1 = 16 Hz, J_2 = 8 Hz, 1H), 3.22 (dd, J_1 = 16 Hz, J_2 = 8 Hz, 1H), 1.64 (s, 9H), 1.32 (d, J = 8 Hz, 3H); MALDI-FTMS calcd for $C_{26}H_{28}N_2O_5$ $[M + Na]^+$ expected 471.189, found 471.1870, exact mass error 2.0 mμ, 4.2 p.p.m.; TLC (EtOAc : hexanes 3 : 7), R_f = 0.54; $[\alpha]_D^{25}$: −51.7° (c = 1, $CHCl_3$).

[3(2*R*, 3*S*), 4*R*]-3-[2-azido-3-(*N*-(2-*t*-butyloxycarbonyl)-3-indolyl)-1-oxobutyl]-4-phenyl-2-oxazolidinone (10)

A solution of β-methylated *N*-acyl-oxazolidinone 9 (2.11 g, 4.72 mmol) in THF (20 mL) was cooled to −78 °C, under N_2. In a 250 mL oven-dried round-bottomed flask was added THF (20 mL), and after cooling to −78 °C, KHMDS (0.5 M in toluene, 1.5 mL, 7.08 mmol) was added dropwise. The solution was stirred at this temperature for 5 min, and the cooled starting material solution was carefully cannulated into it while monitoring the temperature. This mixture (A) was stirred for 30 min at −78 °C. Separately, a solution of $TIPSN_3$ (2.04 g, 6.61 mmol) was prepared in

THF (20 mL) and cooled to −78 °C (B). After 30 min, the $TIPSN_3$ solution (B) was added to the starting material enolate solution (A), by cannulation. The reaction was allowed to proceed for 5 min after complete addition and was quenched with glacial acetic acid (1.7 mL, 29.72 mmol). The reaction mixture was stirred under N_2, overnight. To isolate the product, 15 mL of ether and 15 mL sat. NaCl were added. The layers were separated and the aqueous layer was extracted with 1 : 1 ether : THF (3 × 15 mL). The combined organic layer was carefully washed with sat. $NaHCO_3$ (6 × 15 mL), sat. NaCl (2 × 15 mL), dried over Na_2SO_4 and filtered. The solvent was removed under reduced pressure and the residue dried on a vacuum manifold overnight to yield 3.61 g crude yellow oil. The material was purified by column chromatography with 10–15% EtOAc/hexanes, resulting in 0.89 g pure product (40%, white foam), and 0.54 g mixture.

^{1}H-NMR ($CDCl_3$) δ (p.p.m.) 8.16 (d, J = 8 Hz, 1H), 7.62 (d, J = 8 Hz, 1H), 7.50 (s, 1H), 7.35–7.14 (m, arom, 10H), 5.32 (d, J = 9.2 Hz, 1H), 4.76 (dd, J_1 = 8 Hz, J_2 = 4 Hz, 1H), 3.99 (dd, J_1 = 8 Hz, J_2 = 4 Hz, 1H), 3.82 (t, J = 8 Hz, 1H), 3.60 (m, 1H), 1.65 (s, 9H), 1.54 (d, J = 8 Hz, 3H); ESI (m/z): $[M + Na]^+$ calcd for $C_{26}H_{27}N_5O_5$ expected 512, found 512; $[\alpha]_D^{25}$: −161° (c = 1, $CHCl_3$); IR (film on NaCl plate, per cm) 2107, 1782, 1733, 1451, 1369, 1155. TLC (EtOAc : hexanes 3 : 7, vanillin), R_f = 0.66.

(2*R*,3*S*)-2-azido-3-[*N*-(2-*t*-butyloxycarbonyl))-3-indolyl]butanoic acid (11)

The α-azido-β-methylated *N*-acyloxazolidinone 10 (0.71 g, 1.46 mmol) was dissolved in THF (22 mL). Water (8 mL) was added and the solution cooled to 0 °C under N_2. A solution of 30% hydrogen peroxide (1.32 mL, 11.68 mmol) was added dropwise, followed by a solution of LiOH (0.25 g, 5.84 mmol) in H_2O (4 mL). The mixture was allowed to react for 5 h, under N_2, slowly equilibrating to room temperature. The reaction was quenched by addition of solid Na_2SO_3. After stirring for 30 min, the THF was removed under reduced pressure. The remaining aqueous layer was cooled in an ice bath and carefully acidified with 6 N HCl. The product was extracted into EtOAc (5 × 20 mL). The organic layer was washed with sat. NaCl (2 × 25 mL), dried over Na_2SO_4 and filtered. The solvent was removed under reduced pressure until a white oil remained, 0.77 g. The crude product was purified by column chromatography with 1 : 1 EtOAc : hexanes, followed by 100% EtOAc, then 0.1% CH_3COOH in EtOAc. After purification the product was obtained as white oil, 0.31 g (65%).

^{1}H-NMR ($CDCl_3$) δ (p.p.m.) 8.11 (bs, 1H), 7.57–7.22 (m, arom, 4H), 4.37 (bs, 1H), 3.37 (m, 1H), 1.65 (s, 9H), 1.4 (d, J = 8 Hz, 3H); ESI (m/z): calcd for $C_{17}H_{20}N_4O_4$ $[M + Na]^+$ expected 367, found 367, $[M - H]^-$ expected 343, found 343; $[\alpha]_D^{25}$: −4.4° (c = 0.33, $CHCl_3$). TLC (EtOAc : hexanes 1 : 1, bromocresol green), R_f = 0.25.

(2*R*,3*S*)-2-amino-3-[*N*-(2-*t*-butyloxycarbonyl)-3-indolyl]butanoic acid (12)

The α-azido-β-methylated carboxylic acid 11 (0.30 g, 0.87 mmol) was dissolved in MeOH (8 mL), and 5% Pd/C (0.020 g) was added. The flask was evacuated, filled with H_2 and the suspension stirred at room temperature for 4 h. The suspension was filtered through Celite, which was washed extensively with MeOH (10 × 5 mL). After removal of the solvent under reduced pressure, 0.27 g of white solid was obtained. This was purified by column chromatography using as eluent $CHCl_3$: MeOH : CH_3COOH 7 : 1 : 0.1. After removal of the solvent on a rotary evaporator and drying overnight, the product resulted as a white solid (0.23 g, 83%).

^{1}H-NMR (CD_3OD) δ (p.p.m.) 8.07 (d, J = 8 Hz, 1H), 7.72 (d, J = 8 Hz, 1H), 7.49 (s, 1H), 7.30–7.20 (two triplets, arom, 2H), 3.89 (bs, 2H), 3.25 (q, 1H), 1.62 (s, 9H), 1.34 (d, 3H, poorly resolved); ^{13}C-NMR (DMSO) 176.2, 148.9, 134.8, 129.3, 124.1, 123.3, 122.8, 122.2, 119.0, 114.7, 83.3, 57.7, 31.9, 27.7, 12.5. ESI (m/z) calcd for $C_{17}H_{22}N_2O_4$, $[M + H]^+$ expected 319, found 319, $[M + Na]^+$ expected 341, found 341, $[M - H]^-$ expected 317, found 317. $[\alpha]_D^{25}$: −7.6° (c = 1, MeOH); IR (film, NaCl plate): 3443, 2249, 2126, 1723, 1659, 1579, 1371, 1162, 1040. TLC: ($CHCl_3$: MeOH : AcOH 7 : 1 : 0.1, bromocresol green), R_f = 0.18.

(2*R*,3*S*)-2-(9*H*-fluoren-9-yl-methoxycarbonylamino)-3-[*N*-(2-tertbutyloxycarbonyl)-3-indolyl]butanoic acid, i.e. N^{α}(Fmoc)-(2*R*,3*S*)-β-methyl-(N^{in}-Boc)-tryptophan (13)

The amino acid 12 (0.13 g, 0.41 mmol) in DMSO (1 mL) and 9 mL AcCN was cooled to 0 °C. A solution of 10% $NaHCO_3$ (1.85 mL, 2.21 mmol) was added dropwise, followed by solid FmocOSu (0.26 g, 0.76 mmol). The flask was evacuated and filled with N_2 and the reaction carried out for 4 h, slowly equilibrating to room temperature. The solvent was removed under reduced pressure, then H_2O was added. After cooling in an ice bath, the mixture was acidified with 0.2 M HCl. The resulting white precipitate was extracted with EtOAc (10 × 10 mL). The organic layer was washed with sat. NaCl (3 × 20 mL), dried over Na_2SO_4 and overnight on a vacuum manifold to result in 0.32 g crude product. This material was purified by column chroma-

tography with 1 : 1 EtOAc : hexanes, then 1% CH_3COOH/EtOAc, to provide 0.11 g clear oil (52%).

^{1}H-NMR (DMSO) δ (p.p.m.) 8.00 (d, J = 8 Hz, 1H) and 7.81 (d, J = 8 Hz, 3H), 7.66 (d, J = 8 Hz) and 7.60 (d, J = 8 Hz), 3H together, 7.51 (s, 1H), 7.37–7.19 (m, arom, 7H), 4.43 (dd, J_1 = 8.8 Hz, J_2 = 4.8 Hz, 1H), 4.13 (m, 3H), 3.59 (m, 1H), 1.52 (s, 9H), 1.33 (d, J = 8 Hz, 3H); MALDI-FTMS (m/z) calcd for $C_{32}H_{32}N_2O_6$, $[M + Na]^+$ expected 563.2152, found 563.2170, exact mass error 1.8 mμ, 3.2 p.p.m.; ^{13}C-NMR (DMSO) δ (p.p.m.) 172.5, 156.1, 148.8, 143.5, 140.4, 134.5, 129.2, 127.4, 126.8, 125.2, 125.0, 124.1, 122.7, 122.3, 121.9, 119.9, 119, 114.7, 83.5, 65.8, 58.0, 46.7, 31.8, 27.7, 15.4; $[\alpha]_D^{25}$: −4.19° (c = 1, MeOH); TLC (EtOAc : hexanes 7 : 3, bromocresol green) R_f = 0.33; ($CHCl_3$: MeOH : AcOH 95 : 5 : 1), R_f = 0.33.

Synthesis of Fmoc-(*2R,3R*)-β-Me-Trp(Boc)-OH (19)

(1-*t*-butyloxycarbonyl)indole-3-acrylic acid (7)

Trans-3-indoleacrylic acid (10.0 g, 53.42 mmol) was suspended in AcCN (250 mL), THF (10 mL), and H_2O (10 mL; Fig. 2). The suspension was cooled in an ice bath and TEA (15 mL, 106.84 mmol) was added dropwise. The solution turned clear yellow upon the addition of base. Solid DMAP (1. 31 g, 10.68 mmol) was added, followed by solid $(Boc)_2O$ (23.32 g, 106.84 mmol) in one portion. The reaction mixture was allowed to stir in the ice bath, slowly equilibrating to room temperature, for a total of 4 h. The solvent was removed under reduced pressure until a thick yellowish oil remained. Water (250 mL) was added, followed by extraction with EtOAc (3 × 50 mL). The organic extract was discarded. The aqueous layer was acidified in an ice bath with 6 N HCl, and the resulting yellow precipitate filtered through a Buchner funnel and rapidly washed with water. The precipitate was dried under high vacuum overnight, yielding 9.4 g. To obtain additional product, the aqueous filtrate was re-extracted with EtOAc (3 × 50 mL). The organic layer was dried over Na_2SO_4, filtered and concentrated to yield a yellow foam, which was dried overnight on a vacuum manifold to yield 3.1 g of product. The combined products 9.4 and 3.1 g afforded a total yield of 12.5 g (82%).

[3(2*E*), 4*S*]-3-[3-(*N*-(2-*t*-butyloxycarbonyl)-3-indolyl-1-oxopropenyl]-4-phenyl-2-oxazolidinone (14)

An oven-dried, three-necked 500 mL round-bottomed flask set up with a thermometer adapter and thermometer, was cooled under N_2. The starting material, carboxylic acid 7 (8.70 g, 30.26 mmol) was rapidly added as a solid, then dry THF (115 mL) was added via syringe and the solution cooled to −78 °C. Freshly distilled TEA (13 mL, 93.12 mmol) was added dropwise (internal temperature −60 °C), then pivaloyl chloride (4.5 mL, 34.53 mmol), dropwise. The suspension was allowed to stir, warming slowly, for 2 h and 30 min (initial temperature −40 °C, final temperature −20 °C). Lithium chloride was added (1.48 g, 34.92 mmol), followed by (*S*)-(+)-4-phenyl-2-oxazolidinone (3.80 g, 23.28 mmol). The reaction mixture was allowed to warm to room temperature, overnight, under N_2. The reaction was quenched by addition of 50 mL 0.2 M HCl. The solvent was removed under reduced pressure until only the aqueous layer remained, followed by addition of EtOAc (50 mL). The aqueous layer was extracted with EtOAc (3 × 20 mL), and the combined organic layer re-extracted with 0.2 M HCl (5 × 15 mL), $NaHCO_3$ (3 × 20 mL) and sat. NaCl (2 × 20 mL). After drying over Na_2SO_4, the solvent was removed under reduced pressure and the residue dried on a vacuum manifold overnight to yield 11.8 g crude product. The material was purified with 15% EtOAc/hexanes to yield 7.50 g (75%).

^{1}H-NMR ($CDCl_3$) δ (p.p.m.) 8.10–7.24 (arom, 10H and 2H, olefinic), 5.45 (dd, J_1 = 8 Hz, J_2 = 4 Hz, 1H), 4.61 (t, J = 8 Hz, 1H), 4.19 (dd, J_1 = 8 Hz, J_2 = 4 Hz, 1H), 1.54 (s, 9H); ESI (m/z): calcd for $C_{25}H_{24}N_2O_5$, $[M + H]^+$ expected 433, found 433, $[M + Na]^+$ expected 455, found 455, $[M - H]^-$ expected 431, found 431, $[M + Cl]^-$ expected 467, found 467; $[\alpha]_D^{25}$: −2.94° (c = 1, $CHCl_3$) TLC (EtOAc : hexanes 1 : 1, vanillin), R_f = 0.66.

[3(2*S*,3*R*), 4*S*]-3-[2-bromo-3-(*N*-(2-*t*-butyloxycarbonyl)-3-indolyl)-1-oxobutyl]-1-oxobutyl]-4-phenyl-2-oxazolidinone (15)

A solution of CuBr–Me_2S (5.35 g, 26.01 mmol) in Me_2S (26 mL) and THF (100 mL) at 0 °C was treated with CH_3-MgBr (10.4 mL, 31.21 mmol), dropwise, until the mixture turned a constant green color. The stirring was continued at 0 °C for 30 min, then the *N*-acyloxazolidinone **14** (7.50 g, 17.34 mmol, in 50 mL THF at 0 °C) was cannulated into the green suspension slowly, to result in a brown slurry. The slurry was allowed to react at 0 °C for 2 h and at room temperature for 30 min. Meanwhile, a solution of NBS (6.17 g, 34.68 mmol) was prepared and cooled to −78 °C. The starting material mixture was cooled to −78 °C and the NBS solution was cannulated into it. The slurry was stirred at −78 °C for 2 h and at 0 °C for 30 min. Solutions of 100 mL 0.5 M $NaHSO_4$ and 100 mL sat. NaCl were added, the layers were separated (organic layer-dark brown, aqueous layer-reddish brown), and the aqueous layer re-extracted with EtOAc (3 × 50 mL). The combined organic layers were

washed with 0.5 M $NaHSO_4$ (3 × 50 mL). The organic layer was further extracted with sat. NH_4Cl (4 × 50 mL), followed by sat. NaCl (3 × 50 mL), dried over Na_2SO_4, filtered, concentrated and dried overnight to provide 12.3 g crude yellow oil. The crude product contained starting material, methylated-only product and desired α-bromo-β-methylated product. Purification was effected by column chromatography with 15–20% EtOAc/hexanes, and 3.69 g (40%) of desired product was obtained, as well as 1.40 g methylated-only product.

^{1}H-NMR ($CDCl_3$) δ (p.p.m.) 8.12–7.23 (m, arom, 10H), 6.13 (d, J = 12 Hz, 1H), 5.11 (dd, J_1 = 8 Hz, J_2 = 4 Hz, 1H), 4.41 (t, J = 8 Hz, 1H), 4.12 (dd, J_1 = 8 Hz, J_2 = 4 Hz, 1H), 3.71 (m, 1H), 1.65 (s, 9H), 1.55 (d, J = 8 Hz, 3H); $[\alpha]_D^{25}$: +69° (c = 1, $CHCl_3$); IR (film, NaCl plate) 2977, 1780, 1731, 1450, 1367, 1252, 1161, 1070, 749. TLC (EtOAc : hexanes 3 : 7, vanillin), R_f = 0.66.

[3(*2R,3R*), 4*S*]-3-[2-azido-3-(*N*-(2-*t*-butyloxycarbonyl)-3-indolyl)-1-oxobutyl]-1-oxobutyl]-4-phenyl-2-oxazolidinone (16)

The α-bromo-β-methyl-*N*-acyloxazolidinone **15** (1.59 g, 3.02 mmol) was dissolved in DMSO (25 mL) and NaN_3 was added (0.79 g, 12.09 mmol). The flask was evacuated and filled with N_2 and the reaction was allowed to stir at room temperature for 7 h. Water (50 mL) was added to the mixture and a precipitate formed. The precipitate was extracted with EtOAc (5 × 20 mL). The combined organic layer was washed with sat. NaCl (2 × 20 mL), dried over Na_2SO_4, filtered, concentrated, and dried overnight to give 1.47 g slightly brown oil. The crude product was purified through a short silica gel column using 15% EtOAc/hexanes, to remove the brown impurity, and 1.03 g (70%) product was obtained.

^{1}H-NMR ($CDCl_3$) 8.20–7.22 (m, arom, 10H), 5.59 (d, J = 8 Hz, 1H), 5.50 (dd, J_1 = 8 Hz, J_2 = 4 Hz, 1H), 4.74 (t, J = 8 Hz, 1H), 4.32 (dd, J_1 = 8 Hz, J_2 = 4 Hz, 1H), 3.67 (m, 1H), 1.70 (s, 9H), 1.32 (d, J = 8 Hz, 3H); $[\alpha]_D^{25}$: +88° (c = 1, $CHCl_3$); IR (film, NaCl plate) 3439, 2977, 2110, 1780, 1731, 1450, 1367, 1260, 1153, 749. TLC (EtOAc : hexanes 3 : 7, vanillin), R_f = 0.42.

(*2R,3R*)-2-azido-3-[*N*-(2-*t*-butyloxycarbonyl))-3-indolyl]butanoic acid (17)

The α-azido-β-methyl-*N*-acyloxazolidinone **16** (1.87 g, 3.82 mmol) was dissolved in THF : H_2O (60 : 20 mL) and the yellow solution cooled to 0 °C. A solution of $LiOH{\cdot}H_2O$ (0.16 g, 15.28 mmol) in 1 mL H_2O and 30% H_2O_2 (3.5 mL, 30.56 mmol) was premixed and stirred at 0 °C for 30 min, then added dropwise to the starting material. Stirring was continued at 0 °C for 4 h. Solid Na_2SO_3 was added and the suspension was stirred for 30 min to quench the peroxide completely. The THF was removed under reduced pressure. More H_2O was added and the mixture was acidified in an ice bath with 6 N HCl. The product was extracted with EtOAc (10 × 10 mL). The organic layer was washed with sat. NaCl, dried over Na_2SO_4, filtered, concentrated, and dried overnight, resulting in 1.60 g crude oil. The crude oil was purified by column chromatography with 50% EtOAc/hexanes, followed by EtOAc and 0.2% AcOH/EtOAc, to yield 0.88 g (67%) product.

^{1}H-NMR ($CDCl_3$) δ (p.p.m.) 8.04–7.12 (m, arom, 6H), 4.13 (d, J = 8 Hz, 1H), 3.55 (m, 1H), 1.58 (s, 9H), 1.37 (d, J = 8 Hz, 3H); ESI (m/z) calcd for $C_{17}H_{20}N_4O_4$ $[M + Na]^+$ expected 367, found 367, $[M - H]^-$ expected 343, found 343; $[\alpha]_D^{25}$: +24.6° (c = 1, $CHCl_3$); IR (film on NaCl plate) 2986, 2117, 1732, 1454, 1366, 1258, 1157, 753. TLC (EtOAc : hexanes 1 : 1 vanillin), R_f = 0.14.

(*2R, 3R*)-2-amino-3-[*N*-(2-*t*-butyloxycarbonyl)-3-indolyl]butanoic acid (18)

The α-azido carboxylic acid **17** (0.71 g, 2.07 mmol) was dissolved in 10 mL MeOH, and 5% Pd/C (0.04 g) was added. The flask was evacuated and filled with H_2 and stirring at room temperature was allowed for 13 h. The mixture was filtered through Celite, which was washed extensively with MeOH (10 × 5 mL). After removal of the solvent, 0.53 g (81%) product was obtained. A sample was purified using $CHCl_3$: MeOH : AcOH 7 : 1 : 0.1 for analytical purposes.

^{1}H-NMR (CD_3OD) δ (p.p.m.) 8.16–7.24 (m, arom, 5H), 3.76–3.51 (unresolved broad multiplet, 1H), 1.69 (s, 9H), 1.53 (d, 3H, poorly resolved); the C^β-proton is possibly buried underneath the solvent peak at 3.31 p.p.m.; ^{1}H-NMR (DMSO) δ (p.p.m.) 8.0 (d, J = 8 Hz, 1H), 7.75 (m, 1H), 7.61 (m, 1H), 7.31–7.24 (m, 2H), 3.67 (broad, 2H), 1.60 (s, 9H), 1.28 (d, 3H, poorly resolved); ESI (m/z) calcd for $C_{17}H_{22}N_2O_4$ $[M + H]^+$ expected 319, found 319, $[M + Na]^+$ expected 341, found 341, $[M - H]^-$ expected 317, found 317; TLC ($CHCl_3$: MeOH : AcOH 7 : 1 : 0.1, ninhydrin), R_f = 0.19.

(*2R,3R*)-2-(9*H*-fluoren-9-yl-methoxycarbonylamino)-3-[*N*-(2-*t*-butyloxycarbonyl)-3-indolyl]butanoic acid, i.e. N^α (Fmoc)-(*2R,3R*)-β-methyl-(N^{in}-Boc)-tryptophan (19)

The free amino acid **18** (crude product from two hydrogenation reactions; (1.03 g, approximately 3.24 mmol) in AcCN (100 mL) and DMSO (10 mL) was cooled to 0 °C. A solution of 10% $NaHCO_3$ (8.2 mL, 9.72 mmol) was added dropwise, followed by solid FmocOSu (1.97 g, 5.83 mmol).

The flask was evacuated and filled with N_2 and the reaction carried out for 7 h, slowly equilibrating to room temperature. The solvent was removed under reduced pressure until only DMSO remained. The residue was diluted with H_2O (20 mL). After cooling in an ice bath, it was acidified with 0.2 M HCl, when a white precipitate formed. The precipitate was extracted with EtOAc (10 × 10 mL). The organic layer was washed with sat. NaCl (3 × 20 mL), dried over Na_2SO_4 and overnight on the vacuum manifold to result in 1.81 g crude oil. This material was purified by column chromatography with 1 : 1 EtOAc : hexanes, then 1% AcOH/EtOAc, to provide 0.77 g clear oil (approximately 36% over two steps).

^{1}H-NMR (DMSO) δ (p.p.m.) 8.02 (d, J = 7.6 Hz, 1H), 7.85 (d, J = 6.8 Hz, 2H), 7.70 (m, 2H), 7.60 (d, J = 7.6 Hz, 1H), 7.54 (d, J = 7.2 Hz), 7.51 (s, together with the previous doublet, 2H), 7.36 (m, 2H), 7.31 (t, 1H), 7.24 (m, 3H), 4.43 (m, 1H), 4.25 (m, 1H), 4.17 (m, 2.5H, contains a small impurity), 3.46 (m, 1H), 1.55 (s, 9H), 1.32 (d, J = 8 Hz, 3H); ^{13}C-NMR (DMSO) δ (p.p.m.) 172.2, 161.9 (imp.), 155.7, 148.7, 143.3, 140.3, 134.5, 129.2, 127.4, 126.7, 125.1, 124.9, 123.9, 122.6, 122.2, 121.6, 119.9, 119.8 (imp.), 119.4, 114.6, 83.4, 65.8, 57.9, 54.8 (imp.), 46.5, 35.8 (imp.), 32.5, 27.6, 17.6; MALDI-FTMS (m/z) calcd for $C_{32}H_{32}N_2O_6$, $[M + Na]^+$ expected 563.2152, found 563.2145, exact mass error 0.7 mμ, 1.2 p.p.m.; $[\alpha]_D^{25}$: +1.7° (c = 0.3, MeOH); TLC (EtOAc : hexanes 7 : 3, bromocresol green), R_f = 0.58; ($CHCl_3$: MeOH : AcOH 7 : 1 : 0.1, bromocresol green), R_f = 0.75.

Peptide synthesis

A Rink acid resin was used. The first amino acid was attached to the resin via an ester bond (51). Coupling of the first amino acid was carried out as described below. The peptide synthesis is illustrated in Fig. 3.

To a solution of resin (loading level 0.52 mmol/g, 4.9 g, 2.6 mmol theoretical loading) in 50 mL DMF were added pyridine (1.5 mL, 18.2 mmol, 7 eq), Fmoc-Phe-OH (3.0 g, 7.8 mmol, 3 eq) in DMF (25 mL), and 2,6-dichlorobenzoyl chloride (1.1 mL, 7.8 mmol, 3 eq). The resin was shaken for 20 h, and successively washed with DMF, MeOH, and DCM. This wash sequence was repeated three times. The resin was dried in a dessicator, under high vacuum, overnight. The loading level was estimated following a procedure described in the Novabiochem catalog (2000). Three resin samples of around 2.3 mg each were placed in test tubes, and 2 mL of freshly prepared 20% piperidine/DMF were added to each. The resin was agitated using a Pasteur pipette for about 2 min. The supernatant was carefully pipetted out and placed in identical UV cells. The UV absorbance of these solutions at 290 nm was measured (Abs_{sample}). A solution of 20% piperidine/DMF was used as a blank (Abs_{ref}). The substitution level was calculated according to the formula: Fmoc loading (mmol/g) = $(Abs_{sample} - Abs_{ref})/(1.65 \times mg$ resin) and found to be 0.45 mmol/g (87%). The unreacted hydroxyl groups on the resin were acylated with benzoic anhydride (2.7 g, 13 mmol, 5 eq) in pyridine/DMA 1/4 (75 mL) for 2 h.

Deprotection of Fmoc was carried out with 20% piperidine/DMF for 30 min. The peptide elongation process was continued by coupling of Fmoc-Pro-OH, Fmoc-Phe-OH, Fmoc-Thr(*t*-Bu)-OH using 2 eq amino acid, 2 eq PyBOP, 0.75 eq HOBt, 4 eq DIEA. The Kaiser test was used to assess the completion of deprotections/couplings, except in the case of Pro. The substitution level was tested again after coupling all four amino acids and was found to be 0.32 mmol/g.

An example of the chain elongation procedure is illustrated for Fmoc-Lys(Boc)-OH, which was coupled to the tetrapeptide. A portion of dry peptide-resin Fmoc-Thr(*t*-Bu)-Phe-Pro-Phe-resin (1.35 g, 0.43 mmol peptide) was swelled in DCM for 1 h and washed with DMF twice. The Kaiser test was negative. Deprotection of Fmoc was carried out with 20% piperidine/DMF for 1 h. The resin was washed 3 × DCM, 3 × DMF, 3 × DCM. The Kaiser test was positive for free amine. The amino acid Fmoc-Lys(Boc)-OH (0.81 g, 1.72 mmol, 4 eq) was dissolved in 20 mL DMF. To this solution were added PyBOP (0.89 g, 1.72 mmol, 4 eq), HOBt (0.12 g, 0.86 mmol, 2 eq), and DIEA (0.6 mL, 3.45 mmol, 8 eq) and the mixture left standing for 2 min. The solution was added to the resin and coupling was allowed to proceed overnight. The peptide-resin was washed 2 × DMF, 2× DCM, 2 × DMF, 2 × DCM and the Kaiser test was negative. The resin was dried in a dessicator under high vaccum overnight, then stored at 4 °C.

The peptide Fmoc-Lys(Boc)-Thr(*t*-Bu)-Phe-Pro-Phe-resin was thus obtained. A sample of 0.012 g peptide-resin ($3.9-5 \times 10^{-3}$ mmol peptide) was used to test if the mass of the peptide was correct. The sample was swollen in DCM for 20 min. The Kaiser test was negative. The resin sample was shaken with 20% piperidine/DMF for 30 min, then washed successively with DMF and DCM (2 × 2). The Kaiser test was positive. The peptide-resin was dried under high vacuum overnight. A solution of 10% AcOH/DCM was added and the resin shaken for 2 h. The filtrate was collected and the resin washed three times with 10% AcOH/

DCM. After removal of the solvent, H_2O was added and the residue lyophilized overnight. A white powder was obtained. MS: ESI for $C_{42}H_{62}N_6O_9$ $[M + H]^+$ calcd 794.4, found 795.4, $[M + Na]^+$ 817.5, $[M - H]^-$ 793.4.

This peptide **21** was used as a precursor for coupling the β-methyltryptophan building blocks and the procedures are illustrated in Fig. 3 for the (2R,3S) analog. Similar procedures were followed for the (2R,3R) analog.

Synthesis of c[Pro-Phe-(*2R,3S*)-β-Me-Trp-Lys-Thr-Phe] (2)

Coupling of building block Fmoc-(*2R,3S*)-β-Me-Trp(Boc)-OH (13)

A sample of Fmoc-Lys(Boc)-Thr(*t*-Bu)-Phe-Pro-Phe-resin (0.29 g, 0.093 mmol peptide) was swollen in DMF for 15 min. The Kaiser test was negative. The resin was washed with DMF once, then shaken for 30 min with 20% piperidine in DMF, washed 2 × DMF, 2 × DCM and 2 × DMF. The Kaiser test was positive. The building block **13** was coupled to the resin as follows: Fmoc-(2R,3S)-β-Me-Trp(Boc)-OH (**13**) (0.10 g, 0.18 mmol, 2 eq) was first dissolved in DMF. Coupling agents PyBOP (0.096 g, 0.18 mmol, 2 eq) and HOBt (0.014 g, 0.093 mmol, 1 eq) were added, followed by DIEA (66 μL, 0.37 mmol, 4 eq). The activated amino acid mixture was added over the peptide-resin and the vessel shaken overnight at room temperature (15 h). The resin was washed extensively (4 × DMF, 2 × DCM, three times) and the Kaiser test indicated the coupling was complete. The resin was washed with DCM and dried under high vacuum overnight.

A sample was analyzed to confirm the coupling of the building block. A portion of 0.010 g resin was cleaved with 10% AcOH/DCM for 4 h as above. After lyophilization, 0.0055 g peptide were obtained and analyzed by MS (ESI) and HPLC (PDA). For this Fmoc-protected fragment, the MS gave the following results: ESI calcd for $[M + H]^+$ 1318, $[M + Na]^+$ 1340, $[M - H]^-$ 1316; MALDI-TOF $[M + Na]^+$ 1340. RP-HPLC (PDA): 40–90% B, 40 min, $\lambda = 220$ nm, $R_t = 37.46$ min.

The entire peptide-resin was then subjected to Fmoc deprotection conditions. The resin was washed with DCM and dried in a dessicator under high vacuum overnight. The side chain-protected linear peptide **24** was cleaved from the resin with 10% AcOH/DCM for 4 h. The filtrate was collected and the solvent removed under reduced pressure. Water was added and the solution lyophilized overnight to yield a white film (0.064 g). The peptide was solubilized in 6 mL EtOAc and washed three times with 0.1 N HCl to convert the acetate salt into chloride salt. The organic layer was washed with sat. NaCl and dried over Na_2SO_4 and dried under high vacuum overnight. The yield was 0.055 g (56% relative to theoretical loading of the resin). MS: $C_{59}H_{82}N_8O_{12}$, 1094.6057, $[M + H]^+$ expected 1096, found 1096, $[M + Na]^+$ expected 1118, found 1118, $[M - H]^-$ expected 1094, found 1094; analytical HPLC (PDA) 10–90% B, 40 min, $R_t = 31$ min, one major peak.

Cyclization

The linear, side chain-protected peptide (HCl salt) **24**, NH_2-(2R,3S)-β-Me-Trp(Boc)-Lys(Boc)-Thr(*t*-Bu)-Phe-Pro-Phe-OH (0.055 g, 0.05 mmol) was dissolved in 50 mL DMF (1 mM) and the solution cooled to −20 °C in an isopropyl alcohol-dry ice bath. Solid $NaHCO_3$ was added (0.042 g, 0.50 mmol, 10 eq), followed by dropwise addition of DPPA (43 μL, 0.20 mmol, 4 eq). The mixture was stirred 4 days in the cold room at 4 °C, under N_2. The DMF was removed under reduced pressure and the residue taken up in EtOAc (20 mL) and washed with H_2O. The organic layer was washed with 0.2 M HCl (3 × 5 mL), sat. $NaHCO_3$ (3 × 5 mL) and sat. NaCl (2 × 5 mL) and dried over Na_2SO_4. The solvent was removed under reduced pressure and the residue dried on a vacuum manifold overnight to yield an oil (0.071 g).

Analytical HPLC was used to assess the completion of the reaction. The HPLC trace of the crude material (10–90% B over 40 min, $\lambda = 220$ nm) showed a major peak at $R_t = 38.61$ min (79.7%) and a minor peak $R_t = 23.29$ min (20.3%). The chromatogram was compared with a chromatogram of the linear, protected peptide in the same conditions, $R_t = 31$ min. The comparison showed that the minor peak was not linear peptide but an impurity, which was to be removed at the end of the synthesis by HPLC purification.

Final deprotection of the side chains was carried out without further purification of the cyclic-protected intermediate.

Final deprotection

The protected cyclic peptide **25** was cooled in an ice bath. The 'cleavage cocktail' was prepared as follows: 10 mL TFA were mixed with 0.25 mL H_2O and 0.1 mL anisole and the solution was chilled to 0 °C. This solution was added to the peptide and the mixture stirred at 0 °C for 30 min and room temperature for 30 min. The TFA was removed under reduced pressure. Water was added and the mixture was

lyophilized overnight to afford the product 2 (0.054 g, 98%). The product was purified by RP-HPLC using 45% B, λ = 280 nm, R_t = 9.10 min. The final yield was 0.010 g (13% based on theoretical loading of the resin).

Analytical HPLC conditions: 10–90% B, 40 min, λ = 220 nm, R_t = 21.9 min and isocratic 30% B, R_t = 11.53 min.

MS: MALDI-FTMS: $[M + H]^+$ calcd for $C_{45}H_{56}N_8O_7$ expected 821.4345, found 821.4316, $[M + Na]^+$ expected 843.4164, found 843.4146, exact mass error 1.8 mμ, 2.1 p.p.m. NMR (DMSO, 500 MHz; Table 2).

Synthesis of c[Pro-Phe-(2R,3R)-β-Me-Trp-Lys-Thr-Phe] (3)

Coupling of building block Fmoc-(2R,3R)-β-Me-Trp(Boc)-OH (19)

The building block Fmoc-(2R,3R)-β-Me-Trp(Boc)-OH **19** (0.10 g, 0.18 mmol) was used. The procedure was similar to that shown for the isomer (2R,3S) detailed above. A portion of 0.29 g peptide-resin (0.093 mmol peptide) was employed for the synthesis. The building block was coupled to the peptide for 8 h. The peptide was Fmoc-deprotected as usual and dried in the dessicator overnight. The protected linear peptide was cleaved from the resin with 10% AcOH/DCM for 4 h, and the linear, side chain-protected peptide **24A** (0.057 g, 58% relative to theoretical loading of the resin) was obtained. An analytical PDA chromatogram with 10–90% B over 40 min indicated a major product at R_t = 33.39 min (89%), and MS confirmed the presence of the correct peptide: ESI calcd for $C_{59}H_{82}N_8O_{12}$ $[M + H]^+$ expected 1096, found 1096, $[M + Na]^+$ expected 1118, found 1118, $[M - H]^-$ expected 1094, found 1094. The peptide was dissolved in EtOAc and washed three times with 0.1 N HCl to convert it to HCl salt.

Cyclization

The side chain-protected linear peptide **24A** (0.054 g) was allowed to cyclize for 3 days, using a procedure similar to the one described above. The crude product was purified by column chromatography using 7 : 3 EtOAc : hexanes, and a white oil (0.039 g, 74%) was obtained.

MS: ESI calcd for $C_{59}H_{80}N_8O_{11}$ $[M + H]^+$ expected 1077.6, found 1077.6, $[M + Na]^+$ 1099.5, found 1099.6, $[M - H]^-$ 1075.6, found 1075.6; PDA 10–90% B, 40 min, λ = 220 nm, R_t = 39.67 min.

The cyclic, protected peptide **25a** was treated with TFA at 0 °C for 30 min, under N_2, and lyophilization afforded crude product 3 (0.022 g). This was purified in isocratic conditions with 43% B at λ = 280 nm, R_t = 10.57 min, and 0.006 g pure material (8% based on theoretical resin loading) resulted.

Analytical conditions: PDA, gradient 10–90% B over 40 min, λ = 220 min, R_t = 23.51 min, and isocratic, 32% B, R_t = 20.00 min; MS: MALDI-FTMS calcd for $C_{45}H_{56}N_8O_7$ $[M + H]^+$ expected 821.4345, found 821.4312, exact mass error 3.3 mμ, 4.0 p.p.m. NMR (DMSO, 500 MHz; Table 3).

Computer simulations

Computer simulations of the two peptide diastereomers containing (2R,3S)- and (2R,3R)-β-Me-Trp were carried out to determine differences in overall conformation and energy to explain their different binding profiles. The simulations were carried out on an SGI IRIX 6.5 workstation. The INSIGHT II and DISCOVER programs were used for the molecular mechanics (energy minimization), the dynamics calculations and visualization.

The initial structures of the two isomers were generated using the Biopolymer module of INSIGHT II introducing a βII′ turn in the backbone torsional angles from the Phe^7 to the Thr^{10} residues and a βVI turn from the Phe^{11} to the Pro^6 residue, in accordance with the experimental data available from the literature (17).

The molecular dynamics calculations were carried out in vacuo with the force field CVFF91. A distance-dependent dielectric constant ($1 \times r$) was used to take into account the solvent effects. Bonds between atoms were kept fixed by the SHAKE procedure with a relative tolerance of 10^{-3}. Nonbonded interactions were treated using the double cut-off method with two radii of 0.8 and 1.4 Å. During the simulations, the peptide bonds were maintained in the *trans*-conformation. Prior to every molecular dynamics simulation, the system was equilibrated with 3 ps initialization dynamics followed by a step size of 1 fs for a 10 ns simulation, and structures were collected every 1 ps. An archive of structures was then created by sampling every 10 ps and minimizing the sampled structure to convergence (CVFF91 force field and conjugate gradients algorithm with convergence criterion of 0.001 kcal/mol).

Biologic tests

The cDNA for human somatostatin receptors (hSSTR) 1 through 4 were subcloned into the pcDNA3.1/Neo expres-

sion vector. cDNA for hSSTR5 was created as a cassette construct in pTEJ8 (52). Stable transfections of CHO-K1 cells expressing all five hSSTRs, were prepared using Superfect transfection reagent (Qiagen, Hilden, Germany) following the manufacturer's guidelines. Clones were selected and maintained in CHO-K1 medium containing Hams F12 with 10% fetal bovine serum and 700 μg/mL neomycin. Cells were harvested, homogenized using a glass homogenizer and membranes were prepared by centrifugation as previously described (52,53). Binding studies were performed with 30–40 μg of membrane protein collected from CHO-K1 cells stably expressing the receptor constructs, and ^{125}I-labeled LTT-SST28 radioligand (approximately 60 pM) in 50 mM HEPES, pH 7.5, 2 mM $CaCl_2$, 5 mM $MgCl_2$, 0.5% bovine serum albumin, 0.02% phenylmethylsulfonyl fluoride, and 0.02% bacitracin (binding buffer) for 30 min at 37 °C. Incubations were terminated by the addition of ice-cold binding buffer. Membrane pellets were quantified for radioactivity using a LKB-γ counter (LKB-Wallach, Turku, Finland). Binding data were analyzed with PRISM 3.0 (Graph Pad Software, San Diego, CA, USA) by nonlinear regression analysis. Data are presented as mean ± SEM and represent three independent experiments performed in duplicate.

Acknowledgements: Authors wish to acknowledge the NIH-DK-15410 grant to MG for financial support. We are grateful to Joseph Taulane for helpful discussions while editing and revising the manuscript, and to Robyn Swanland and Joseph for help submitting this manuscript. Authors thank Dr Lotte Hansen for her IT expertise in preparing the Supplementary material for publication.

References

1. Brazeau, P., Vale, W., Burgus, R., Ling, N., Butcher, M., Rivier, J. & Guillemin, R. (1973) Hypothalamic peptide that inhibits the secretion of immunoreactive pituitary growth hormone. *Science* **179**, 77–79.
2. Pradayrol, L., Joernvall, H., Mutt, V. & Ribert, A. (1980) N-terminally extended somatostatin. The primary structure of somatostatin-28. *FEBS Lett.* **109**, 55–58.
3. Patel, Y.C. (1999) Somatostatin and its receptor family. *Front. Neuroendocrinol.* **20**, 157–198.
4. Rohrer, S.P., Birzin, E.T., Mosley, R.T., Berk, S.C., Hutchins, S.M., Shen, D.-M., Xiong, Y., Hayes, E.C., Parmar, R.M., Foor, F., Mitra, S.W., Degrado, S.J., Shu, M., Klopp, J.M., Cai, S.-J., Blake, A., Chan, W.W.S., Pasternak, A., Yang, L., Patchett, A.A., Smith, R.G., Chapman, K.T. & Schaeffer, J.M. (1998) Rapid identification of subtype-selective agonists of the somatostatine receptors through combinatorial chemistry. *Science* **282**, 737–740.
5. Lamberts, S.W.J., Krenning, E.P. & Reubi, J.-C. (1991) The role of somatostatin and its analogs in the diagnosis and treatment of tumors. *Endocr. Rev.* **12**, 450–480.
6. Yamada, Y., Post, S.R., Wang, K., Tager, H.S., Bell, G.I. & Seino, S. (1992) Cloning and functional characterization of a family of human and mouse somatostatin receptors expressed in brain, gastrointestinal tract, and kidney. *Proc. Natl Acad. Sci. USA* **89**, 251–255.
7. Yasuda, K., Rens-Domiano, S., Breder, C.D., Law, S.F., Saper, C.B., Reisine, T. & Bell, G.I. (1992) Cloning of a novel somatostatin receptor, $SSTR_3$, that is coupled to adenylyl cyclase. *J. Biol. Chem.* **267**, 20422–20428.
8. Yamada, Y., Reisine, T. & Law, S.F. (1992) Somatostatin receptors, an expanding gene family: cloning and functional characterization of human $SSTR_3$, a protein coupled to adenylyl cyclase. *Mol. Endocrinol.* **6**, 2136–2142.
9. Bruno, J.F., Xu, J., Song, J. & Berelowitz, M. (1992) Molecular cloning and functional expression of a brain-specific somatostatin receptor. *Proc. Natl Acad. Sci. USA* **89**, 11151–11155.
10. O'Caroll, A.M., Lolait, S.J., Konig, M. & Mahon, L.C. (1992) Molecular cloning and expression of a pituitary somatostatin receptor with preferential affinity for somatostatin-28. *Mol. Pharmacol.* **42**, 939–946.
11. O'Caroll, A.M., Raynor, K., Lolait, S.J. & Reisine, T. (1994) Characterization of cloned human somatostatin receptor $SSTR_5$. *Mol. Pharmacol.* **46**, 291–298.
12. Hoyer, D., Bell, G.I., Berelowitz, M., Epelbaum, J., Feniuk, W., Humphrey, P.P.A., O'Caroll, A.M., Patel, Y.C., Schonnbrun, A., Taylor, J.E. & Reisine, T. (1995) Classification and nomenclature of somatostatin receptors. *TiPS* **16**, 86–88.
13. Hannon, J.P., Nunn, C., Stolz, B., Bruns, C., Weckbecker, G., Lewis, I., Troxler, T., Hurth, K. & Hoyer, D. (2002) Drug design at peptide receptors. *J. Mol. Neurosci.* **18**, 15–27.
14. Janecka, A., Zubrzycka, M. & Janecki, T. (2001) Somatostatin analogs. *J. Pept. Res.* **58**, 91–107.
15. Veber, D.F. (1992) Design and discovery in the development of peptide analogues. In: *Peptides, Chemistry and Biology: Proceedings of the* 12th American Peptide Symposium (Smith, J.A. & Rivier, J.E., eds), pp. 3–14. ESCOM, Leiden, the Netherlands.
16. Mierke, D.F., Pattaroni, C., Delaet, N., Toy, A., Goodman, M., Tancredi, T., Motta, A., Temussi, P.A., Moroder, L., Bovermann, G. & Wunsch, E. (1990) Cyclic hexapeptides related to somatostatin. *Int. J. Pept. Protein Res.* **36**, 418–432.
17. Huang, Z., He, Y.-B., Raynor, K., Tallent, M., Reisine, T. & Goodman, M. (1992) Main chain and side chain methylated somatostatin analogs: syntheses and conformational analyses. *J. Am. Chem. Soc.* **114**, 9390–9401.
18. Hirschmann, R., Nicolaou, K.C., Pietranico, S., Salvino, J., Leahy, E.M., Sprengeler, P.A., Furst, G., Smith, A.B., Strader, C.D., Cascieri, M.A., Candelore, M.R., Donaldson, C., Vale, W. & Maechler, L. (1992) Nonpeptidal peptidomimetics with a β-D-glucose scaffolding. A partial somatostatin agonist bearing a close structural relationship to a potent, selective substance P antagonist. *J. Am. Chem. Soc.* **114**, 9217–9218.

19. Hirschmann, R., Nicolaou, K.C., Pietranico, S., Leahy, E.M., Salvino, J., Arison, B., Cichy, M.A., Spoors, P.G., Shakespeare, W.C., Sprengeler, P.A., Hamley, P., Smith, A.B. III, Reisine, T., Raynor, K., Maechler, L., Donaldson, C., Vale, W., Freidinger, R.M., Cascieri, M.R. & Strader, C.D. (1993) De novo design and synthesis of somatostatin non-peptide peptidomimetics utilizing b-D-glucose as a novel scaffolding. *J. Am. Chem. Soc.* **115**, 12550–12568.
20. Bonner, G.G., Davis, P., Stropova, D., Edsall, S., Yamamura, H.I., Porecca, F. & Hruby, V.J. (2000) Opiate aromatic pharmacophore structure-activity relationships in CTAP analogues determined by topographical bias, two-dimensional NMR, and biological activity assays. *J. Med. Chem.* **43**, 569–580.
21. Haskell-Luevano, C., Boteju, L.W., Miwa, H., Dickinson, C., Gantz, I., Yamada, T., Hadley, M.E. & Hruby, V.J. (1995) Topographical modification of melanotropin peptide analogues with β-methyltryptophan isomers at position 9 lead to differential potencies and prolonged biological activities. *J. Med. Chem.* **38**, 4720–4729.
22. Hruby, V.J., Toth, G., Gehrig, C.A., Kao, L.-F., Knapp, R., Lui, G.K., Yamamura, H.I., Kramer, T.H., Davis, P. & Burks, T.F. (1991) Topographically designed analogues of [D-Pen2,D-Pen5]-enkephalin. *J. Med. Chem.* **34**, 1823–1830.
23. Hruby, V.J. & Agnes, R.S. (1999) Conformation-activity relationships of opioid peptides with selective activities at opioid receptors. *Biopolymers* **51**, 391–410.
24. Berk, S.C., Rohrer, S.P., Degrado, S.J., Birzin, E.T., Mosley, R.T., Hutchins, S.M., Pasternak, A., Schaeffer, J., Underwood, D.J. & Chapman, K.T. (1999) A combinatorial approach towards the discovery of non-peptide, subtype-selective somatostatin receptor ligands. *J. Comb. Chem.* **1**, 388–396.
25. Yang, L., Berk, S.C., Rohrer, S.P., Mosley, R.T., Guo, L., Underwood, D.J., Arison, B.H., Birzin, E.T., Hayes, E.C., Mitra, S.W., Parmar, R.M., Cheng, K., Wu, T.-J., Butler, B.S., Foor, F., Pasternak, A., Pan, Y., Silva, M., Freidinger, R.M., Smith, R.G., Chapman, K.T., Schaeffer, J.M. & Patchett, A.A. (1998) Synthesis and biological activities of potent peptidomimetics selective for somatostatin receptor subtype 2. *Proc. Natl Acad. Sci. USA* **95**, 10836–10841.
26. Yang, L., Guo, L., Pasternak, A., Mosley, R.T., Rohrer, S.P., Birzin, E.T., Foor, F., Cheng, K., Schaeffer, J.M. & Patchett, A.A. (1998) Spiro[1H-indene-1,4′-piperidine] derivatives as potent and selective non-peptide human somatostatine receptor subtype 2 (sst_2) agonists. *J. Med. Chem.* **41**, 2175–2179.
27. Souers, A.J., Virgilio, A.A., Rosenquist, A., Fenuik, W. & Ellman, J.A. (1999) Identification of a potent heterocyclic ligand to somatostatin receptor subtype 5 by the synthesis and screening of beta-turn mimetic libraries. *J. Am. Chem. Soc.* **121**, 1817–1825.
28. Souers, A.J., Rosenquist, A., Jarvie, E.M., Ladlow, M., Feniuk, W. & Ellman, J.A. (2000) Optimization of a somatostatin mimetic via constrained amino acid and backbone incorporation. *Bioorg. Med. Chem. Lett.* **10**, 2731–2733.
29. Reubi, J.C., Schaer, J.C., Waser, B., Hoeger, C. & Rivier, J. (1998) A selective analog for the somatostatin sst_1-receptor subtype expressed by human tumors. *Eur. J. Pharmacol.* **345**, 103–110.
30. Rivier, J., Hoeger, C., Erchegyi, J., Gulyas, J., DeBoard, R., Craig, A.G., Koerber, S.C., Wenger, S., Waser, B., Schaer, J.C. & Reubi, J.-C. (2001) Potent somatostatin undecapeptide agonists selective for somatostatin receptor 1 (sst_1). *J. Med. Chem.* **44**, 2238–2246.
31. Erchegyi, J., Hoeger, C., Low, W., Hoyer, D., Waser, B., Eltschinger, V., Schaer, J.C., Cescato, R., Reubi, J.-C. & Rivier, J. (2005) Somatostatin receptor 1 selective analogues: 2. N^{α}-methylated scan. *J. Med. Chem.* **48**, 507–514.
32. Grace, C.R.R., Durrer, L., Koerber, S.C., Erchegyi, J., Reubi, J.-C., Rivier, J. & Riek, R. (2005) Somatostatin receptor 1 selective analogues: 4. Three-dimensional consensus structure by NMR. *J. Med. Chem.* **48**, 523–533.
33. Reubi, J.-C., Schaer, J.C., Wenger, S., Hoeger, C., Erchegyi, J., Wasser, B., Rivier, J. (2000) SST_3-selective potent peptide somatostatin antagonists. *Proc. Natl Acad. Sci. USA* **97**, 13973–13978.
34. Erchegyi, J., Penke, B., Simon, L., Michaelson, S., Wenger, S., Waser, B., Cescato, R., Schaer, J.C., Reubi, J.-C. & Rivier, J. (2003) Novel sst_4-selective somatostatin (SRIF) agonists: 2. Analogues with β-methyl-3-(2-naphthyl)-alanine substitutions at position 8. *J. Med. Chem.* **46**, 5587–5596.
35. Erchegyi, J., Waser, B., Schaer, J.C., Cescato, R., Brazeau, J.F., Rivier, J. & Reubi, J.-C. (2003) Novel sst_4-selective somatostatin (SRIF) agonists: 3. Analogues amenable to radiolabeling. *J. Med. Chem.* **46**, 5597–5605.
36. Grace, C.R.R., Koerber, S.C., Erchegyi, J., Reubi, J.-C., Rivier, J. & Riek, R. (2003) Novel sst_4-selective somatostatin (SRIF) agonists: 4. Three dimensional consensus structure by NMR. *J. Med. Chem.* **46**, 5606–5618.
37. Bruns, C., Lewis, I., Briner, U., Meno-Tetang, G. & Weckbecker, G. (2002) SOM230: a novel somatostatin peptidomimetic with broad somatotropin release inhibiting factor (SRIF) receptor binding and a unique antisecretory profile. *Eur. J. Endocrinol.* **146**, 707–716.
38. Lewis, I., Bauer, W., Albert, R., Chandramouli, N., Pless, J., Weckbecker, G. & Bruns, C. (2003) A novel somatostatin mimic with broad somatotropin release inhibitory factor receptor binding and superior therapeutic potential. *J. Med. Chem.* **46**, 2334–2339.
39. Sarret, P., Nouel, D., Dal Farra, C., Vincent, J.-P., Beaudet, A. & Mazella, J. (1999) Receptor-mediated internalization is critical for the inhibition of the expression of growth hormone by somatostatin in the pituitary cell line AtT-20. *J. Biol. Chem.* **274**, 19294–19300.
40. Boteju, L.W., Wegner, K., Qian, X. & Hruby, V.J. (1994) Asymmetric synthesis of unusual amino acids: synthesis of optically pure isomers of *N*-indole-(2-mesitylenesulfonyl)-β-methyltryptophan. *Tetrahedron* **50**, 2391–2404.
41. Han, G., Lewis, A. & Hruby, V.J. (2001) Synthesis of (2S, 3S)-β-methyltryptophan. *Tetrahedron Lett.* **42**, 4601–4603.
42. Snyder, H.R. & Matteson, D.S. (1957) The synthesis of the 2-amino-3-(3-indolyl)-butyric acids (β-methyltryptophans). *J. Am. Chem. Soc.* **79**, 2217–2221.
43. Brady, S.F., Varga, S.L., Freidinger, R.M., Schwenk, D.A., Mendlowski, M., Holly, F.W. & Veber, D.F. (1979) Practical synthesis of cyclic peptides, with an example of dependence of cyclization upon linear sequence. *J. Org. Chem.* **44**, 3101–3105.
44. Evans, D.A., Britton, T.C., Ellman, J.A. & Dorow, R.L. (1990) The asymmetric synthesis of α-amino acids. Electrophilic Azidation of chiral imide enolates, a practical approach to the synthesis of (*R*)- and (*S*)-α-azido carboxylic acids. *J. Am. Chem. Soc.* **112**, 4011–4030.

45. Melacini, G., Zhu, Q., Osapay, G. & Goodman, M. (1997) A refined model for the somatostatin pharmacophore: conformational analysis of lanthionine-sandostatin analogs. *J. Med. Chem.* **40**, 2252–2258.
46. Tran, T.-A., Mattern, R.-H., Morgan, B.A., Taylor, J.E. & Goodman, M. (1999) Synthesis and binding potencies of cyclo-hexapeptide somatostatin analogs containing naphthylalanine and arylalkyl peptoid residues. *J. Pept. Sci.* **5**, 113–130.
47. Veber, D.F. (1981) *Peptides, Synthesis, Structure and Function, Proceedings of the Seventh American Peptide Symposium* (Rich, D.H. & Gross, V.J., eds), pp. 685–694. Pierce Chemical Co., Rockford, IL, USA.
48. Kaiser, E., Colescott, R.L., Bossinger, C.D. & Cook, P.I. (1970) Color test for the detection of free terminal amino groups in the solid phase synthesis of peptides. *Anal. Biochem.* **34**, 595–598.
49. Leffler, J.E. & Tsuno, Y. (1963) Some decomposition reactions of acid azides. *J. Org. Chem.* **28**, 902–906.
50. Harmon, R.E., Wellman, G. & Gupta, S.K. (1973) The reaction of arylsulfonyl azides with *N*-methylindole. *J. Org. Chem.* **38**, 11–16.
51. Sieber, P. (1987) An improved method for anchoring of 9-fluorenylmethoxycarbonyl-amino acids to 4-alkoxybenzyl alcohol resins. *Tetrahedron Lett.* **28**, 6147–6150.
52. Hukovic, N., Rocheville, M., Kumar, U., Sasi, R., Khare, S. & Patel, Y.C. (1999) Agonist-dependent up-regulation of human somatostatin receptor type 1 requires molecular signals in the cytoplasmic C-tail. *J. Biol. Chem.* **274**, 24550–24558.
53. Grant, M., Patel, R.C. & Kumar, U. (2004) The role of subtype-specific ligand binding and the C-tail domain in dimer formation of human somatostatin receptors. *J. Biol. Chem.* **279**, 38636–38643.

Supplementary material

The following supplementary material is available online for this article from http://www.Blackwell-Synergy.com

Figure S1 Starting position of the (2R,3S) peptide 2 for the 10 ns simulation

Figure S2 Starting position of the (2R,3R) peptide 3 for the 10 ns simulation.

Figure S3 Significant NOEs for the (2R,3S) peptide, c[Pro^6-Phe^7-(2R,3S)-β-MeTrp^8-Lys^9-Thr^{10}-Phe^{11}].

Figure S4 Significant NOEs for the (2R,3R) peptide, c[Pro^6-Phe^7-(2R,3R)-β-MeTrp^8-Lys^9-Thr^{10}-Phe^{11}].

Figure S5 Significant NOEs for the (2R,3R) peptide, c[Pro^6-Phe^7-(2R,3R)-β-MeTrp^8-Lys^9-Thr^{10}-Phe^{11}].

THE JOURNAL OF BIOLOGICAL CHEMISTRY
Vol. 279, No. 35, Issue of August 27, pp. 36179–36183, 2004
Printed in U.S.A.

Agonist-dependent Dissociation of Human Somatostatin Receptor 2 Dimers

A ROLE IN RECEPTOR TRAFFICKING*

Received for publication, June 30, 2004
Published, JBC Papers in Press, July 1, 2004, DOI 10.1074/jbc.M407310200

Michael Grant‡§, Brian Collier§, and Ujendra Kumar‡¶

From the ‡Fraser Laboratories for Diabetes Research, Department of Medicine, Royal Victoria Hospital, Montreal, Quebec H3A 1A1, Canada and §Department of Pharmacology & Therapeutics, McGill University, Montreal, Quebec H3G 1Y6, Canada

G-protein-coupled receptors (GPCRs) represent the largest and most diverse family of cell surface receptors. Several GPCRs have been documented to dimerize with resulting changes in pharmacology and signaling. We have previously reported, by means of photobleaching fluorescence resonance energy transfer (pbFRET) microscopy and fluorescence correlation spectroscopic analysis in live cells, that human somatostatin receptor (hSSTR) 5 could both homodimerize and heterodimerize with hSSTR1 in the presence of the agonist SST-14. By contrast, hSSTR1 remained monomeric when expressed alone regardless of agonist exposure in live cells. However, the effect of the agonist on other hSSTR members remains unknown. Using pbFRET microscopy and Western blot, we provide evidence for agonist-dependent dissociation of self-associated hSSTR2 stably expressed in CHO-K1 and HEK-293 cells. Furthermore, the dissociation of the hSSTR2 dimer occurred in a concentration-dependent manner. Moreover, blocking receptor dissociation using a cross-linker agent perturbed receptor trafficking. Taking these data together, we suggest that the process of GPCR dimerization may operate differently, even among members of the same family, and that receptor dissociation as well as dimerization may be important steps for receptor dynamics.

G-protein-coupled receptors (GPCRs)[1] represent ~1% of the human genome, an estimate exceeding 800 genes (1). The initial notion that GPCRs are present on the membrane as monomeric entities in a 1:1 stoichiometric ratio with their G-protein has since been reinterpreted. Several studies have shown by using a combination of techniques such as co-immunoprecipitation, bioluminescence resonance energy transfer, and fluorescence resonance energy transfer (FRET) that at least some GPCRs assemble on the membrane as functional homo- and heterodimers (2–4). Dimerization of GPCRs has been shown to affect a multitude of receptor functions, including ligand binding, signaling, receptor desensitization, and receptor trafficking (2–5).

The mechanism by which GPCR dimerization occurs remains obscure and controversial. One model suggests that ligand binding induces a conformational change in the receptor that favors dimer formation. In contrast to this model, the presence of GPCRs, which may be assembled as preformed dimers, has been shown for members of the class C subfamily, which includes GABAergic receptors (6–8), calcium-sensing receptor (9, 10), the metabotropic glutamate receptor (11), and the sweet taste receptors (12–14). This paradigm of GPCR assembly, however, is not consistent among the other families of GPCRs (2). Several reports have shown that agonist plays an active role in GPCR dimerization at the plasma membrane, suggesting an equilibrium between GPCR dimers or monomers that can be regulated by ligand occupancy. These receptors include the human somatostatin receptors (hSSTRs) (15, 16), the dopamine D2 receptor (17), the gonadotropin-releasing hormone receptor (18, 19), the luteinizing hormone/chorionic gonadotropin hormone receptor (20), the bradykinin B_2 receptor (21), the thyrotropin-releasing hormone receptor (22), the human cholecystokinin receptor (23), the human thyrotropin receptor (24), the chemokine receptors (25–28), the mouse δ-opioid receptor (δ-OR) (29), and the rhesus neuropeptide Y4 receptor (30).

We have previously reported that hSSTRs are capable of undergoing both homo- and heterodimerization at the cell membrane (15, 31). Recently, we have demonstrated agonist-dependent homo- and heterodimers on the plasma membrane in live cells using fluorescence correlation spectroscopy (16). One of the receptor subtypes, hSSTR1, did not form homodimers in either the absence or presence of agonist, in contrast to hSSTR5, which showed robust dimerization on agonist exposure. When both receptors were co-expressed in the same cell, two populations of dimers were observed, hSSTR5 homodimers and hSSTR1/hSSTR5 heterodimers (16). The effect of agonist on other members of the hSSTR family is currently unknown.

In the present study using both Western blot and pbFRET analysis, we determined the effect of agonist on hSSTR2 dimerization. We show that agonist induced a dissociation of preassembled hSSTR2 dimers in a concentration-dependent manner. This effect was inhibited when cell membranes were pretreated with a cross-linking agent. hSSTR2 undergoes internalization on exposure to agonist, however, inhibition of dimer dissociation resulted in impaired receptor internalization. Finally, our data provide evidence suggesting that agonist-

* This work was supported by Canadian Institute of Health Research Grants MT-10411 and MT-6911. The costs of publication of this article were defrayed in part by the payment of page charges. This article must therefore be hereby marked "*advertisement*" in accordance with 18 U.S.C. Section 1734 solely to indicate this fact.

¶ To whom correspondence should be addressed: Rm. M3.15, Royal Victoria Hospital, 687 Pine Ave. West, Montreal, Quebec H3A 1A1, Canada. Tel.: 514-842-1231 (ext. 35042); Fax: 514-843-2819; E-mail: ujendra.kumar@muhc.mcgill.ca.

[1] The abbreviations used are: GPCR, G-protein-coupled receptor; pbFRET, photobleaching fluorescence resonance energy transfer; GABA, γ-aminobutyric acid; hSSTR, human somatostatin receptor; δ-OR, mouse δ-opioid receptor; HA, hemagglutinin; FITC, fluorescein isothiocyanate; BS^3, bis(sulfosuccinimidyl) suberate; HA-hSSTR, HA-tagged hSSTR; D-PBS, Dulbecco's phosphate-buffered saline; LTT-SST-28, [Leu^8-D-Trp^{22},Tyr^{25}]SST-28.

dependent dissociation of self-associated dimers may be a requirement for proper receptor trafficking.

EXPERIMENTAL PROCEDURES

Materials—The peptides SST-14 and [Leu^8-D-Trp^{22},Tyr^{25}]SST-28 (LTT-SST-28) were purchased from Bachem, Torrance, CA. Fluorescein- and rhodamine-conjugated and non-conjugated mouse monoclonal antibodies against hemagglutinin (HA) (12CA5) were purchased from Roche Applied Science. FITC-conjugated goat anti-mouse affinity-purified secondary antibody was purchased from Jackson ImmunoResearch Laboratories, West Grove, PA. The cross-linking agent bis(sulfosuccinimidyl) suberate (BS^3) was purchased from Sigma.

SSTR Constructs and Expressing Cell Lines—Stable CHO-K1 and HEK-293 cells expressing HA-tagged hSSTR2 were prepared by LipofectAMINE transfection reagent as described previously (15). Stable transfections were made using the vectors pCDNA3.1/Neo (neomycin resistance) from Invitrogen. Clones from CHO-K1 cells were selected and maintained in medium containing Ham's F-12 with 10% fetal bovine serum and 700 μg/ml neomycin. Clones from HEK-293 cells were selected in Dulbecco's modified Eagle's medium containing 10% fetal bovine serum and 700 μg/ml neomycin.

pbFRET Microscopy—pbFRET experiments were performed at the plasma membrane of CHO-K1 cells as described previously (15, 16, 31). In brief, CHO-K1 cells expressing HA-hSSTR2 were treated with different concentrations (0, 10^{-10}, 5×10^{-9}, 10^{-7}, and 10^{-6} M) of agonist for 10 min at 37 °C, fixed with 4% paraformaldehyde in PBS for 20 min on ice, and processed for immunocytochemistry. Immunocytochemistry was performed using monoclonal anti-HA antibodies conjugated to FITC and rhodamine for the donor and acceptor, respectively, before being subjected to pbFRET analysis. The effective FRET efficiency (E) was calculated from the average photobleaching time constant of the donor obtained in the absence ($\tau_{avg\ D-A}$) and presence ($\tau_{avg\ D\ A}$) of the acceptor, according to the equation $E = 1 - (\tau_{D-A}/\tau_{D+A}) \times 100$.

Western Blot Analysis—Membranes from HA-hSSTR2 stably transfected in HEK-293 cells were prepared using a glass homogenizer in 20 mM Tris-HCl, 2.5 mM dithiothreitol, pH 7.5, as described previously (15). The membrane pellet was washed and resuspended in 20 mM Tris-HCl, pH 7.5, in the absence of dithiothreitol. Membrane protein (50 μg) was treated with SST-14 (0, 10^{-10}, 10^{-8}, and 10^{-6} M) in binding buffer (50 mM Hepes, 2 mM $CaCl_2$, 5 mM $MgCl_2$, pH 7.5) for 30 min at 37 °C. When the cross-linking agent BS^3 was used, membranes were pretreated with 5 mM BS^3 for 1 h at 4 °C, and this reaction was terminated by the addition of 50 mM Tris-HCl, pH 7.5, for 15 min at 4 °C. After treatment with SST-14, membrane protein was solubilized in Laemmli sample buffer containing 62.5 mM Tris-HCl, pH 6.8, 25% glycerol, 2% SDS, 0.01% bromphenol blue, and 710 mM 2-mercaptoethanol (Bio-Rad). The sample was heated at 85 °C for 5 min before being fractionated by electrophoresis on a SDS-7% polyacrylamide gel. The fractionated proteins were transferred by electrophoresis to a 0.2-μm nitrocellulose membrane (Trans-Blot transfer medium, Bio-Rad) in transfer buffer consisting of 25 mM Tris, 192 mM glycine, and 20% methanol. The membrane was blotted with anti-HA mouse monoclonal antibody (dilution, 1:5000). Blocking of membrane, incubation of primary antibodies, incubation of secondary antibodies, and detection by chemiluminescence were performed following WesternBreeze® (Invitrogen) according to the manufacturer's instructions. Images were captured using an Alpha Innotech FluorChem 8800 (Alpha Innotech Co., San Leandro, CA) gel box imager, and densitometry was carried out using FluorChem software (Alpha Innotech Co.).

Internalization by Radioligand and Immunocytochemistry—Receptor internalization was assessed as described previously (32). CHO-K1 cells stably expressing HA-hSSTR2 were cultured in 6-well plates to ~90% confluency (~1.5×10^6 cells/well). On the day of the experiment, medium was removed, and the cells were washed twice with Dulbecco's PBS (D-PBS) solution and incubated overnight at 4 °C in binding buffer (50 mM Hepes, pH 7.5, 2 mM $CaCl_2$, 5 mM $MgCl_2$, 0.5% bovine serum albumin, 0.02% phenylmethylsulfonyl fluoride, and 0.02% bacitracin) with ^{125}I-LTT-SST-28 (200,000 cpm) with or without 1 μM SST-14 to account for nonspecific binding. Cells were washed two times in D-PBS and warmed to 37 °C for various times (0, 15, 30, 60 min) to initiate internalization. For cross-linking experiments, cells were pretreated with 1 mM BS^3 in D-PBS for 1 h at 4 °C, and this reaction was terminated by washing the cells first with D-PBS followed by the addition of 50 mM Tris-HCl, pH 7.5, for 15 min at 4 °C. Surface-bound radioligand was removed with 1 ml of acid wash buffer (20 mM NaOAc in 1× Hanks' solution, pH 5.0) for 10 min. Internalized radioligand was measured as acid-resistant counts taken after removing cells with 1 ml of 1 N NaOH. Radioactive fractions were quantified for radioactivity using an LKB gamma counter (LKB-Wallach, Turku, Finland). Each experiment was performed three times in triplicate.

For *internalization by immunocytochemistry*, CHO-K1 cells stably expressing HA-hSSTR2 were grown on coverslips and treated with SST-14 (1 μM) for 30 min at 37 °C. When the cross-linker agent was indicated, cells were treated with 1 mM BS^3 for 1 h at 4 °C prior to the addition of SST-14. Reaction was terminated with 50 mM Tris-HCl, pH 7.5, for 15 min at 4 °C. Cells were washed two times in D-PBS and fixed for 20 min at 4 °C with 4% paraformaldehyde. After three subsequent washes in D-PBS, cells were incubated in 5% normal goat serum in D-PBS for 1 h followed by incubation with anti-HA monoclonal antibody (1:1000) in 1% normal goat serum overnight at 4 °C. Unless indicated, permeabilization of cells was performed using 0.2% Triton X-100 in D-PBS for 10 min followed by three washes in D-PBS prior to incubation with antibody. Cells were then washed three times in D-PBS followed by incubation with FITC-conjugated goat anti-mouse secondary antibody (1:800) for 1 h. After two washes in D-PBS, cells were mounted and viewed under a Leica DML microscope attached to a Cool Snap CCD camera.

RESULTS

Ligand-dependent Dissociation of hSSTR2 Homodimers by pbFRET and Western Blot—CHO-K1 cells were stably expressed with an N-terminal HA-tagged hSSTR2 (B_{max} = 435 ± 33 fmol/mg of protein, K_D = 0.3 ± 0.1 nM). Cells were treated with different concentrations of SST-14 and processed for hSSTR2 localization to study by pbFRET microscopy. pbFRET microscopy was determined by the photobleaching decay of donor on the cell surface by using monoclonal anti-HA antibodies conjugated with either fluorescein (donor) or rhodamine (acceptor). As shown in Fig. 1*A*, in the basal state, the cell surface presented with a high relative FRET efficiency, suggesting the presence of homodimers, compared with SST-14-treated cells. Treatment with SST-14 induced a concentration-dependent decrease in FRET efficiency from a maximum of 11.7 ± 1.1% under basal conditions to 2.1 ± 0.9% with 1 μM SST-14 (Table I and Fig. 1*A*). Our data indicate that unlike hSSTR1 and hSSTR5, hSSTR2 is self-associated and dissociates on agonist activation. Because FRET is sensitive to distance, changes in FRET efficiency can be perceived as either dissociation of dimers or changes in receptor conformation. To confirm whether ligand-activated hSSTR2 is associated with changes in dimer to monomer formation, we performed Western blot.

Membranes from HEK-293 cells stably expressing HA-hSSTR2 (B_{max} = 2608 ± 206 fmol/mg of protein, K_D = 0.4 ± 0.1 nM), which were chosen for their higher expression levels, were treated with various concentrations of SST-14 before being processed for Western blot. In the absence of agonist, hSSTR2 was present in both dimeric (120 kDa) and monomeric (60 kDa) forms (Fig. 1*B*). Treatment of hSSTR2 membrane with SST-14 induced a concentration-dependent decrease in dimer formation (Fig. 1*B*). Increasing concentrations of SST-14 gradually decreased the ratio of hSSTR2 dimers to monomers (Fig. 1*C*). Dissociation of the dimeric complex could be prevented when membranes were pretreated with the cross-linking agent BS^3 (Fig. 1*D*). Western blot in combination with pbFRET analysis supports the notion that hSSTR2 is a self-associated dimer under basal conditions, but on ligand activation, it preferentially dissociates into monomers. It is unclear why there was an appreciable amount of monomeric receptor found by Western blot. One reason could be the result of a solubilization artifact, because receptor dimers can be affected by the concentration of detergent used. Another reason could be the higher expression levels achieved in HEK-293 cells compared with those in CHO-K1 cells used to perform Western blot. Perhaps the monomeric receptors represent an immature intracellular pool that is only functional when the receptors are in dimeric form and are present at the cell surface. With the exception of the

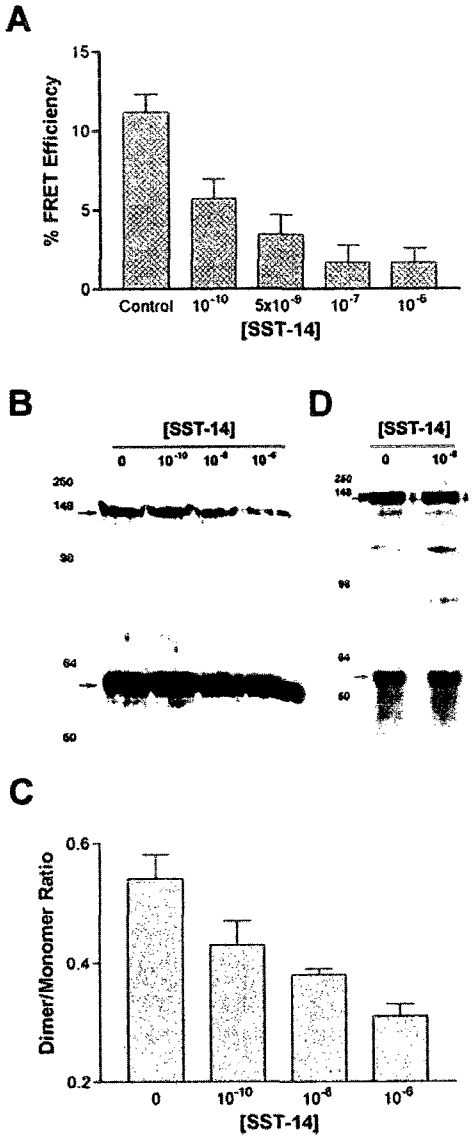

FIG. 1. **Agonist-dependent dissociation of the hSSTR2 dimer.** *A*, CHO-K1 cells stably expressing HA epitope-tagged hSSTR2 were subjected to pbFRET analysis using anti-HA monoclonal antibodies conjugated with either FITC (donor) or rhodamine (acceptor) as described under "Experimental Procedures." Control represents the FRET efficiency of cells that have not been treated with SST-14. Cells were treated with SST-14 for 10 min before being processed for pbFRET microscopy. Means ± S.E. represent three independent experiments, each taken from ~40–50 cells. *B*, HEK-293 cells stably expressing HA epitope-tagged hSSTR2 were treated with the indicated concentrations of SST-14 for 30 min before being processed and separated on a SDS-7% polyacrylamide gel. The represented blot is taken from three independent runs. *C*, immunoblots from *B* were quantified for changes in the dimeric:monomeric ratio after SST-14 treatment by densitometry using FluorChem software. *D*, immunoblot from membranes of HEK-293 cells stably expressing HA-hSSTR2 incubated with 5 mM BS^3 prior to treatment with or without 1 μM SST-14. Membranes were separated on a SDS-7% polyacrylamide gel. The immunoblot is a representation of three independent runs.

TABLE I
Concentration-dependent decrease in FRET efficiencies

CHO-K1 cells expressing HA-hSSTR2 were treated with the indicated concentrations of SST-14 and subjected to pbFRET analysis as described under "Materials and Methods." D − A and D + A, correspond to donor in the absence and presence of acceptor, respectively; τ_{avg}, mean of n photobleaching time constants; n, number of cells analyzed; E, average effective FRET efficiency. Means ± S.E. represent three independent experiments.

SST-14 concentration		τ_{avg}	n	E
Control	D − A	13.6 ± 0.3	48	
	D + A	15.4 ± 0.3	48	11.7 ± 1.1
10^{-10}	D − A	13.2 ± 0.3	48	
	D + A	14.0 ± 0.4	48	5.7 ± 1.3
5×10^{-9}	D − A	13.4 ± 0.4	48	
	D + A	13.8 ± 0.2	48	2.9 ± 1.2
10^{-7}	D − A	14.1 ± 0.3	48	
	D + A	14.3 ± 0.3	48	1.4 ± 1.1
10^{-6}	D − A	14.2 ± 0.4	48	
	D + A	14.5 ± 0.2	48	2.1 ± 0.9

δ-OR (29), little has been shown to support the functional significance for the dissociation of GPCR dimers. To determine whether dissociation of the dimeric complex is associated with changes in receptor properties, we proceeded to investigate receptor internalization.

Internalization of hSSTR2—CHO-K1 cells stably expressing HA-hSSTR2 were grown on coverslips and treated with 1 μM SST-14 for 30 min with or without prior treatment of BS^3. Because BS^3 is a hydrophilic lipid impermeable cross-linking agent and was shown to inhibit agonist-induced hSSTR2 dissociation (Fig. 1*D*), only dimeric receptors at the cell surface would be affected on treatment. Under basal conditions, hSSTR2 was mainly localized at the cell surface with little or no cytoplasmic localization of receptor in permeabilized cells (Fig. 2*A*, *left panels*). Treatment with SST-14 (1 μM) resulted in the internalization of hSSTR2 with decreases in cell surface expression (Fig. 2*A*, *middle panels*). Internalization of receptor was appreciably inhibited when cells were treated with the cross-linker prior to the exposure of SST-14 (Fig. 2*A*, *right panels*). Thus, we demonstrate that internalization of hSSTR2 can be inhibited when receptor dissociation is blocked. To determine whether receptor internalization was either completely blocked or delayed, we measured internalization kinetics.

Cells expressing hSSTR2 were treated with or without 1 mM cross-linker BS^3 to determine the effect of inhibiting receptor dissociation on the kinetics of internalization. We used the radioligand ^{125}I-LTT-SST-28, an agonist to hSSTR2, to measure internalization kinetics. Receptor binding was not inhibited on treatment with BS^3. A maximum internalization was achieved at ~30 min, when measured up to 1 h. This internalization rate was significantly altered when cells were pretreated with BS^3, consistent with the immunocytochemistry results that inhibition of dimer dissociation impairs receptor trafficking (Fig. 2*B*).

DISCUSSION

The mechanisms underlying dimerization have become paramount in the elucidation of GPCR function. There are two general models that have been proposed for the dimerization of GPCRs that have resulted in contentious debate (for reviews see Refs. 2–4). One model states that GPCRs are preassembled dimeric complexes occurring early following their synthesis in the endoplasmic reticulum, without any ensuing effect on ligand treatment in altering the dimeric state of the receptor. An example that has been well documented in this regard is the $GABA_B$ receptor, a relative of the class C subfamily of GPCRs

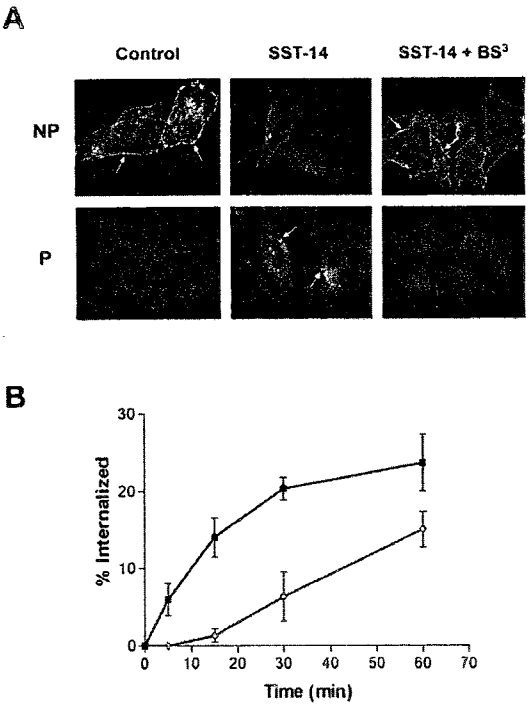

FIG. 2. **Internalization of hSSTR2.** *A*, immunocytochemistry of CHO-K1 cells stably expressing HA-hSSTR2 in the absence (*Control*) or presence of 1 μM SST-14 with or without pretreatment of 1 mM BS^3. Non-permeabilized (*NP*) cells represent cell surface distribution of receptor, and permeabilized (*P*) cells represent internalized receptor. *Arrows* indicate both surface and internalized receptors. Magnification ×630. *B*, internalization kinetics of HA-hSSTR2 stably expressed in CHO-K1 cells using the radioligand ^{125}I-LTT-SST-28 as described under "Experimental Procedures." Internalization rate of hSSTR2 without (■) or with (◇) pretreatment of 1 mM BS^3.

(6–8). In this example, the heterodimerization between the $GABA_BR1$ and $GABA_BR2$ receptor subtypes was shown to be a prerequisite for the proper trafficking and functioning at the cell surface (6–8). The other model states a ligand dependence for GPCR dimerization and has been documented for several GPCRs; therefore, a ligand-independent constitutive receptor dimerization paradigm cannot be universally accepted for all receptors (2, 3). In fact, there have been conflicting reports on the same receptor subtype, concerning its dimerization properties, as to whether or not ligand has a direct effect. Cvejic and Devi (29) have reported that ligand-activated mouse δ-OR causes dissociation of receptor dimers to monomers in stably transfected cells using co-immunoprecipitation. On the contrary, Milligan and co-workers (33) found that the human δ-OR displayed constitutive dimerization irrespective of ligand occupancy, using both bioluminescence resonance energy transfer and FRET techniques in transiently transfected cells. Whether these discrepancies are caused by the types of techniques used, transfections, or the species of receptor used is uncertain. In a recent report, transiently transfected cells resulted in the formation of mostly dimeric immature intracellular human lutropin receptors that exhibited no effect on ligand treatment (34). When stably transfected, however, mature cell surface monomeric receptors were mainly present and displayed ligand-induced increases in dimer formation. Therefore, it was suggested that these promiscuous interactions were occurring at the level of the endoplasmic reticulum in transiently transfected cells because of the accumulation of immature receptors (34).

We have previously reported that hSSTR5 can both homo- and heterodimerize with hSSTR1 and dopamine 2 receptor in a ligand-dependent manner in stably transfected cells (15, 16, 31), but the functional significance of these observations remains unclear. Dimerization of the β_2-adrenergic receptor was suggested to be a requirement for receptor activation (35). Furthermore, using a coumermycin-gyrase B-induced dimerization system on the platelet-activating factor receptor, coumermycin-induced dimerization was sufficient to cause the desensitization and internalization of platelet-activating factor receptor in an agonist-independent fashion (36). Taken together this would suggest that dimerization plays a key role in receptor activation and internalization, although this has not been exemplified for all GPCRs.

In the present study, hSSTR2 was found to be a self-associated dimer at the cell surface in stably transfected cells as observed with pbFRET microscopy. This technique was advantageous for probing receptors present only at the cell surface. Furthermore, these observations were also confirmed using Western blot analysis. Ligand activation of hSSTR2 resulted in the dissociation of receptor dimers to monomers as shown using both techniques. Other GPCRs have also been reported to undergo ligand-induced dissociation, including the δ-OR (29), the human cholecystokinin receptor (23), the human thyrotropin receptor (24), and the rhesus neuropeptide Y4 receptor (30). With the exception of the δ-OR, little has been shown to address the functional significance for the dissociation of receptor dimers. To address this issue for hSSTR2, we monitored the effect of blocking receptor dissociation on internalization kinetics. Using a cell-impermeable cross-linking agent to prevent receptor dissociation, we found that, in the presence of agonist, receptor internalization was impaired. Similarly, Cvejic and Devi (29) have also shown impaired receptor trafficking when δ-OR dissociation was not implicated.

Whether ligand-dependent receptor dissociation is involved in all SSTR2 species remains obscure. In a report on rat SSTR2 (37), self-associated receptors were shown by using Western blot, but agonist treatment did not have a considerable effect on receptor dimers. Interestingly, the same group also reported a SSTR2/SSTR3 heterodimer that, when treated with either a selective agonist for SSTR2 or SST-14 (agonist to both receptors), resulted in the dissociation of the heterodimeric complex and selective internalization of SSTR2 (37). A similar phenomenon was shown for the dopamine D1 and adenosine A1 receptor heterodimer, in which treatment with a D1 receptor agonist caused dissociation of the heterodimeric complex (38).

In conclusion, we show that hSSTR2 preferentially exists as a dimer at the basal state but on stimulation with agonist dissociates into monomeric receptors. Moreover, dissociation of receptor dimers is important for efficient receptor trafficking because inhibiting dimer dissociation alters internalization kinetics. These data provide a new level of understanding in the functioning of hSSTRs and may help elucidate the functional properties of other GPCRs.

Acknowledgments—We thank M. Correia for secretarial help and H. Alturaihi for technical assistance. This article has been dedicated to Dr. Yogesh C. Patel.

REFERENCES

1. Pierce, K. L., Premont, R. T., and Lefkowitz, R. J. (2002) *Nat. Rev. Mol. Cell. Biol.* **3**, 639–650
2. Agnati, L. F., Ferré, S., Lluis, C., Franco, R., and Fuxe, K. (2003) *Pharmacol. Rev.* **55**, 509–550
3. Angers, S., Salahpour, A., and Bouvier, M. (2002) *Annu. Rev. Pharmacol.*

Toxicol. **42,** 409–435
4. Bai, M. (2004) *Cell. Signal.* **16,** 175–186
5. Mellado, M., Rodríguez-Frade, J. M., Mañes, S., and Martínez-A, C. (2001) *Annu. Rev. Immunol.* **19,** 397–421
6. White, J. H., Wise, A., Main, M. J., Green, A., Fraser, N. J., Disney, G. H., Barnes, A. A., Emson, P., Foord, S. M., and Marshall, F. H. (1998) *Nature* **396,** 679–682
7. Jones, K. A, Borowsky, B., Tamm, J. A., Craig, D. A., Durkin, M. M., Dai, M., Yao, W. J., Johnson, M., Gunwaldson, C., Huang, L. Y., Tang, C., Shen, Q., Salon, J. A., Morse, K., Laz, T., Smith, K. E., Nagarathnam, D., Noble, S. A., Branchek, T. A., and Gerald, C. (1998) *Nature* **396,** 674–679
8. Kaupmann, K., Malitschek, B., Schuler, V., Heid, J., Froestl, W., Beck, P., Mosbacher, J., Bischoff, S., Kulik, A., Shigemoto, R., Karschin, A., and Bettler, B. (1998) *Nature* **396,** 683–687
9. Bai, M., Trivedi, S., Brown, E. M. (1998) *J. Biol. Chem.* **273,** 23605–23610
10. Jensen, A. A., Hansen, J. L., Sheikh, S. P., and Bräuner-Osborne, H. (2002) *Eur. J. Biochem.* **269,** 5076–5087
11. Romano, C., Yang, W. L., and O'Malley, K. L. (1996) *J. Biol. Chem.* **271,** 28612–28616
12. Nelson, G., Hoon, M. A., Chandrashekar, J., Zhang, Y., Ryba, N. J. P., and Zuker, C. S. (2001) *Cell* **106,** 381–390
13. Nelson, G., Chandrashekar, J., Hoon, M. A., Feng, L., Zhao, G., Ryba, N. J. P., and Zuker, C. S. (2002) *Nature* **416,** 199–202
14. Li, X., Staszewski, L., Xu, H., Durick, K., Zoller, M., and Adler, E. (2002) *Proc. Natl. Acad. Sci. U. S. A.* **99,** 4692–4696
15. Rocheville, M., Lange, D. C., Kumar, U., Sasi, R., Patel, R. C., and Patel, Y. C. (2000) *J. Biol. Chem.* **275,** 7862–7869
16. Patel, R. C., Kumar, U., Lamb, D. C., Eid, J. S., Rocheville, M., Grant, M., Rani, A., Hazlett, T., Patel, S. C., Gratton, E., and Patel, Y.C. (2002) *Proc. Natl. Acad. Sci. U. S. A.* **99,** 3294–3299
17. Wurch, T., Matsumoto, A., and Pauwels, P. J. (2001) *FEBS Lett.* **507,** 109–113
18. Cornea, A., Janovick, J. A., Maya-Nunez, G., and Conn, P. M. (2000) *J. Biol. Chem.* **276,** 2153–2158
19. Horvat, R. D., Roess, D. A., Nelson, S. E., Barisas, B. G., and Clay, C. M. (2001) *Mol. Endocrinol.* **15,** 695–703
20. Roess, D. A., Horvat, R. D., Munnelly, H., and Barisas, B. G. (2000) *Endocrinology* **141,** 4518–4523
21. Abdalla, S., Zaki, E., Lother, H., and Quitterer, U. (1999) *J. Biol. Chem.* **274,** 26079–26084
22. Kroeger, K. M., Hanyaloglu, A. C., Seeber, R. M., Miles, L. E. C., and Eidne, K. A. (2001) *J. Biol. Chem.* **276,** 12736–12743
23. Cheng, Z.-J., and Miller, L. J. (2001) *J. Biol. Chem.* **276,** 48040–48047
24. Latif, R., Graves, P., and Davies, T. F. (2002) *J. Biol. Chem.* **277,** 45059–45067
25. Rodriguez-Frade, J. M., Vila-Coro, A. J., de Ana, A. M., Albar, J. P., Martinez-A, C., and Mellado, M. (1999) *Proc. Natl. Acad. Sci. U. S. A.* **96,** 3628–3633
26. Vila-Coro, A. J., Mellado, M., de Ana, A. M., Lucas, P., del Real, G., Martinez-A, C., and Rodriguez-Frade, J. M. (2000) *Proc. Natl. Acad. Sci. U. S. A.* **97,** 3388–3393
27. Vila-Coro, A. J., Rodriguez-Frade, J. M., de Ana, A. M., Moreno-Ortiz, M. C., Martinez-A, C., and Mellado, M. (1999) *FASEB J.* **13,** 1699–1710
28. Mellado, M., Rodriguez-Frade, J. M., Vila-Coro, A. J., Fernandez, S., Martin de Ana, A., Jones, D. R., Toran, J. L., and Martinez-A, C. (2001) *EMBO J.* **20,** 2497–2507
29. Cvejic, S., and Devi, L. A. (1997) *J. Biol. Chem.* **272,** 26959–26964
30. Berglund, M. M., Schober, D. A., Esterman, M. A., and Gehlert, D. R. (2003) *J. Pharmacol. Exp. Ther.* **307,** 1120–1126
31. Rocheville, M., Lange, D. C., Kumar, U., Patel, S. C., Patel, R. C., and Patel, Y. C. (2000) *Science* **288,** 154–157
32. Hukovic, N., Panetta, R., Kumar, U., and Patel, Y. C. (1996) *Endocrinology* **137,** 4046–4049
33. McVey, M., Ramsay, D., Kellett, E., Rees, S., Wilson, S., Pope, A. J., and Milligan, G. (2001) *J. Biol. Chem.* **276,** 14092–14099
34. Tao, Y. X., Johnson, N. B., and Segaloff, D. L. (2004) *J. Biol. Chem.* **279,** 5904–5914
35. Hebert, T. E., Moffett, S., Morello, J. P., Loisel, T. P., Bichet, D. G., Barret, C., and Bouvier, M. (1996) *J. Biol. Chem.* **271,** 16384–16392
36. Perron, A., Chen, Z. G., Gingras, D., Dupré, D. J., Stanková, J., and Rola-Pleszczynski, M. (2003) *J. Biol. Chem.* **278,** 27956–27965
37. Pfeiffer, M., Koch, T., Schröder, H., Klutzny, M., Kirscht, S., Kreienkamp, H. J., Höllt, V., and Schulz, S. (2001) *J. Biol. Chem.* **276,** 14027–14036
38. Ginés, S., Hillion, J., Torvinen, M., Le Crom, S., Casadó, V., Canela, E. I., Rondin, S., Lew, J. Y., Watson, S., Zoli, M., Agnati, L. F., Vernier, P., Lluis, C., Ferré, S., Fuxe, K., and Franco, R. (2000) *Proc. Natl. Acad. Sci. U. S. A.* **97,** 8606–8611

THE JOURNAL OF BIOLOGICAL CHEMISTRY
Vol. 279, No. 37, Issue of September 10, pp. 38636–38643, 2004
Printed in U.S.A.

The Role of Subtype-specific Ligand Binding and the C-tail Domain in Dimer Formation of Human Somatostatin Receptors*

Received for publication, June 4, 2004, and in revised form, July 7, 2004
Published, JBC Papers in Press, July 9, 2004, DOI 10.1074/jbc.M406276200

Michael Grant‡, Ramesh C. Patel§, and Ujendra Kumar‡¶

From the ‡Fraser Laboratories For Diabetes Research, Royal Victoria Hospital, Department of Medicine, McGill University, Montreal, Quebec H3A 1A1, Canada and the §Department of Chemistry and Physics, Clarkson University, Potsdam, New York 13699-5810

G-protein-coupled receptors (GPCRs) represent the largest and most diverse family of cell surface receptors. Several GPCRs have been documented to dimerize with resulting changes in pharmacology. We have previously reported by means of photobleaching fluorescence resonance energy transfer (pbFRET) microscopy and fluorescence correlation spectroscopic (FCS) analysis in live cells, that human somatostatin receptor (hSSTR) 5 could both homodimerize and heterodimerize with hSSTR1 in the presence of the agonist SST-14. In contrast, hSSTR1 remained monomeric when expressed alone regardless of agonist exposure in live cells. In an effort to elucidate the role of ligand and receptor subtypes in heterodimerization, we have employed both pbFRET microscopy and Western blot on cells stably co-expressing hSSTR1 and hSSTR5 treated with subtype-specific agonists. Here we provide evidence that activation of hSSTR5 but not hSSTR1 is necessary for heterodimeric assembly. This property was also reflected in signaling as shown by increases in adenylyl cyclase coupling efficiencies. Furthermore, receptor C-tail chimeras allowed for the identification of the C-tail as a determinant for dimerization. Finally, we demonstrate that heterodimerization is subtype-selective involving ligand-induced conformational changes in hSSTR5 but not hSSTR1 and could be attributed to molecular events occurring at the C-tail. Understanding the mechanisms by which GPCRs dimerize holds promise for improvements in drug design and efficacy.

In recent years, G-protein-coupled receptors (GPCRs),[1] once believed to exist at the plasma membrane as monomers, have been shown to assemble on the membrane as functional homo- and heterodimers (1, 2). Dimerization[2] of GPCRs has been shown to affect a multitude of receptor functions including ligand binding, signaling, receptor desensitization, and receptor trafficking (1, 2). The influence of GPCR dimerization was shown to include cellular immunity, neurotransmission (1), taste (3–5), and disease (6). Although the mechanism by which GPCR dimerization occurs remains obscure, one model suggests that ligand binding of cell surface receptors induces a conformational change that favors dimer formation; while the other suggests that dimerization is an exclusive event occurring early on during receptor biogenesis most probably in the ER and is a necessary event for proper receptor trafficking and function.

This latter model has been suggested for members of the class C subfamily of GPCRs, which include the GABAergic receptors (7–9), calcium-sensing receptor (10, 11), the metabotropic glutamate receptor (12), and the sweet taste receptors (3–5). However, this paradigm of GPCR assembly is not consistent among the class A/rhodopsin-like family of GPCRs. Several reports have shown that agonist plays an active role in GPCR dimerization at the plasma membrane, suggesting an equilibrium between GPCR dimers/monomers that can be regulated by ligand occupancy. These receptors include the human somatostatin receptors (hSSTRs) (13, 14), dopamine D2 receptor (15), gonadotrophin-releasing hormone receptor (16, 17), luteinizing hormone/chorionic gonadotrophin hormone receptor (18), bradykinin B_2 receptor (19), thyrotropin-releasing hormone receptor (20), cholecystokinin receptor (21), thyrotropin receptor (22), and the chemokine receptors (23–26).

We have previously reported that hSSTRs, known to modulate neurotransmission, cell secretion, and cell proliferation (27, 28) are capable of undergoing both homo- and heterodimerization at the cell membrane (13, 14, 29). Recently, we have demonstrated ligand-dependent homo- and heterodimers on the plasma membrane in live cells in both a homogeneous and heterogeneous receptor expressing cell line, using both single and two photon dual color fluorescence correlation spectroscopy (FCS) with cross-correlation analysis (a method that discriminates based upon molecular size, number density, and average brightness/particle in femtoliter confocal volumes) (14). One of the receptor subtypes, hSSTR1, did not form homodimers in either the absence or presence of ligand. In contrast, hSSTR5 showed robust dimerization upon agonist exposure. When both receptors were co-expressed in the same cell, we were able to observe two populations of dimers, hSSTR5 homodimers and hSSTR1/hSSTR5 heterodimers (14). However, it remains unclear as to whether one or both receptor subtypes are capable of promoting heterodimerization, and which receptor motifs may be attributed to this behavior.

In the present study, using subtype-specific agonists and both photobleaching fluorescence resonance energy transfer (pbFRET) and Western blot analysis, we demonstrate that ligand-bound hSSTR5 but not hSSTR1 can promote the het-

* This work was supported by Canadian Institute of Health Research (CIHR) Grants MT-10411 and MT-6911. The costs of publication of this article were defrayed in part by the payment of page charges. This article must therefore be hereby marked "*advertisement*" in accordance with 18 U.S.C. Section 1734 solely to indicate this fact.

This article is dedicated to Dr. Yogesh C. Patel.

¶ To whom correspondence should be addressed: Room M3.15, Royal Victoria Hospital, 687 Pine Ave. West, Montreal, Quebec H3A 1A1, Canada. Tel.: 514-842-1231 (ext. 35042); Fax: 514-843-2819; E-mail: ujendra.kumar@muhc.mcgill.ca.

[1] The abbreviations used are: GPCR(s), G-protein-coupled receptor(s); hSSTR, human somatostatin receptor; SST, somatostatin; HA, hemagglutinin; CHO, Chinese hamster ovary; pbFRET, photobleaching fluorescence resonance energy transfer; FITC, fluorescein isothiocyanate; TR, Texas red; FCS, fluorescence correlation spectroscopy; TM, transmembrane domain; GABA, γ-aminobutyric acid.

[2] The terms dimerization and oligomerization are used interchangeably.

erodimerization of hSSTR1/hSSTR5. Moreover, using receptor C-tail chimeras, we were able to abrogate the homodimerization of hSSTR5 and induce the formation of hSSTR1 homodimers. The hSSTR5 subtype-specific analog of somatostatin, SMS 201-995, displayed a relatively poor signaling profile for hSSTR5 expressed alone despite having nanomolar binding affinity. Accordingly, co-expression with hSSTR1 resulted in a robust signaling efficiency by SMS 201-995 that correlated in part with its ability to induce heterodimerization. Finally, we demonstrate that not all agonists can induce heterodimerization, which was dependent upon ligand occupancy of a specific receptor subtype that can lead to alterations in pharmacology.

EXPERIMENTAL PROCEDURES

Materials and Antisera—The peptides SST-14, D-Trp-SST-14, SST-28, and [Leu (8)-D-Trp-22, Tyr-25]-SST-28 (LTT-SST-28) were purchased from Bachem, Torrance, CA; Octreotide [SMS (201-995)] was given by Sandoz, Basel, Switzerland and des-AA^{1,2,5}-[D-Trp^{8}IAmp^{9}]SS (SCH-275) was a gift from Dr. J. Rivier, Salk Institute. Fluorescein- and rhodamine-conjugated and unconjugated mouse monoclonal antibodies against hemagglutinin (HA) (12CA5) were purchased from Roche Applied Science. Anti-c-Myc monoclonal antibody was purchased from Sigma-Aldrich, Inc. Rabbit polyclonal antibodies directed against the N-terminal segment of hSSTR1 was generated and characterized as described (30). Protein A/G-agarose beads were purchased from Oncogene Research Products, La Jolla, CA.

SSTR Constructs and Expressing Cell Lines—Stable transfections of CHO-K1 cells expressing hSSTR5, hSSTR1, and both HA-tagged hSSTR5 and hSSTR1 and c-Myc-tagged hSSTR5 were prepared by LipofectAMINE transfection reagent as previously described (13). Chimeric receptors R1CR5 and R5CR1 were constructed by interchanging the C-tail of each receptor with one another. R1CR5 was created by adding the C-tail of hSSTR5, the last 46 residues, to hSSTR1 after residue 331. Similarly, R5CR1 includes the remaining 60 residues of hSSTR1 joined to hSSTR5 following residue 318 (31). Clones were selected and maintained in CHO-K1 medium containing Hams F12 with 10% fetal bovine serum and 700 μg/ml neomycin. Stable transfections of CHO-K1 and HEK-293 cells co-expressing hSSTR5 and hSSTR1 were made using the vectors pCDNA3.1/Neo (neomycin resistance) and pCDNA3.1/Hygro (hygromycin resistance) such that hSSTR5 was cloned into pCDNA3.1/Hygro and hSSTR1 was cloned into pCDNA3.1/Neo. Stable transfections were selected in CHO-K1 medium containing 700 μg/ml of neomycin with 500 μg/ml of hygromycin or, HEK-293 medium containing 700 μg/ml of neomycin and 400 μg/ml of hygromycin.

Fluorescent SST Ligands—Fluorescent-labeled SST ligands were prepared by N-terminal conjugation of D-Trp-SST-14 to fluorescein by the use of fluorescein isothiocyanate (SST-FITC) and SST-14 to Texas Red by use of Texas Red succinimidyl ester (SST-TR). The reaction of the dye with the ligand was performed in 0.2 M sodium bicarbonate, pH 7.5 for 4 h at 4 °C in the absence of light. The reaction was stopped with 1.5 M hydroxylamine followed by HPLC separation as previously described (32).

Binding Assays—Cells were harvested, homogenized using a glass homogenizer, and membranes were prepared by centrifugation as previously described (13, 31). Binding studies were performed with 20–40 μg of membrane protein collected from CHO-K1 cells stably expressing the receptor constructs, and ^{125}I-labeled LTT-SST-28 radioligand (~60 pM) in 50 mM HEPES, pH 7.5, 2 mM $CaCl_2$, 5 mM $MgCl_2$, 0.5% bovine serum albumin, 0.02% phenylmethylsulfonyl fluoride, and 0.02% bacitracin (binding buffer) for 30 min at 37 °C. Incubations were terminated by the addition of ice-cold binding buffer. Membrane pellets were quantified for radioactivity using a LKB gamma counter (LKB-Wallach, Turku, Finland). Binding data were analyzed with Prism 3.0 (Graph Pad Software, San Diego, CA) by non-linear regression analysis.

Coupling to Adenylyl Cyclase—Cells were grown in 6-multiwell plates and tested for receptor coupling to adenylyl cyclase by incubation for 30 min with 20 μM forskolin and 0.5 mM 3-isobutyl-1-methylxanthine with or without agonists (10^{-11}–10^{-6} M) at 37 °C as previously described (31). Cells were then scraped in 0.1 N HCl and quantified for cAMP by radioimmunoassay using a cAMP Kit (Inter Medico, Markham, ON) following the manufacturer's guidelines. Data were analyzed by non-linear regression analysis using Prism 3.0 (Graph Pad Software). S.E. are representative of at least three independent experiments.

PbFRET Microscopy and Immunocytochemistry—PbFRET experiments were performed on CHO-K1 cells as previously described (13, 14, 29, 33) stably co-expressing HA-hSSTR5 and hSSTR1, and mono-expressing hSSTR5, hSSTR1, and the receptor chimeras. The effective FRET efficiency (E) was calculated in terms of a percent based upon the photobleaching (pb) time constants of the donor taken in the absence (D − A) and presence (D + A) of acceptor according to $E = 1 - (\tau_D - A/\tau_{D,A}) \times 100$. CHO-K1 cells expressing HA-hSSTR5 and hSSTR1 were grown on glass coverslips for 24 h, treated with different concentrations of agonist for 15 min at 37 °C and fixed with 4% paraformaldehyde for 20 min on ice and processed for immunocytochemistry. Antibodies used were mouse monoclonal anti-HA antibody conjugated to Rhodamine directed to HA-hSSTR5 and rabbit primary antibody followed by secondary anti-rabbit IgG antibody conjugated to fluorescein-directed to hSSTR1. pbFRET in CHO-K1 cells expressing hSSTR1, hSSTR5 and the chimera receptors was performed using fluorescently labeled SST ligands. Cells were grown on coverslips as mentioned above, treated with either 20 nM SST-FITC or 20 nM SST-FITC and 20 nM SST-TR. Both reactions, either antibody or ligand resulted in specific staining at the plasma membrane. The plasma membrane region was used to analyze the photobleaching decay on a pixel-by-pixel basis as described earlier (13, 33).

Co-immunoprecipitation and Western Blot—Membranes from HA-hSSTR1, HA-SSTR5, and HA-hSSTR1/c-Myc-hSSTR5 stably transfected in HEK-293 cells were prepared using a glass homogenizer in 20 mM Tris-HCl, 2.5 mM dithiothreitol, pH 7.5 as previously described (13). The membrane pellet was washed and resuspended in 20 mM Tris-HCl, pH 7.5 in the absence of dithiothreitol. Membrane protein (300 μg) was treated with SST-14 (0 and 10^{-6} M) in binding buffer (50 mM Hepes, 2 mM $CaCl_2$, 5 mM $MgCl_2$, pH 7.5) for 30 min at 37 °C. Following treatment membrane protein was solubilized in 1 ml of radioimmune precipitation assay buffer (150 mM NaCl, 50 mM Tris-HCL, 1% Nonidet P-40, 0.1% SDS, 0.5% sodium deoxycholate, pH 8.0) for 1 h at 4 °C. Samples were centrifuged, and lysate was collected and incubated with 1 μg of anti-HA antibody overnight at 4 °C. Antibody was immunoprecipitated with 20 μl of protein A/G-agarose beads for 2 h at 4 °C. Beads were then washed three times in radioimmune precipitation assay buffer before being solubilized in Laemmli sample buffer containing 62.5 mM Tris-HCl (pH 6.8), 25% glycerol, 2% SDS, 0.01% bromphenol blue, and 710 mM 2-mercaptoethanol (Bio-Rad). The sample was heated at 85 °C for 5 min before being fractionated by electrophoresis on a 7% SDS-polyacrylamide gel. The fractionated proteins were transferred by electrophoresis to a 0.2 μm nitrocellulose membrane (Trans-Blot Transfer Medium, Bio-Rad) in transfer buffer consisting of 25 mM Tris, 192 mM glycine, and 20% methanol. Membrane was blotted with anti-HA antibody (dilution 1:5000) for detection of HA-hSSTR1 and HA-hSSTR5 from single expressions, and anti-c-Myc antibody (1:5000) for detection of c-Myc-hSSTR5 from co-expressions. Blocking of membrane, incubation of primary antibodies, incubation of secondary antibodies, and detection by chemiluminescence were performed following WesternBreeze® (Invitrogen Life Technologies) according to manufacturer's instructions. Images were captured using an Alpha Innotech FluorChem 8800 (Alpha Innotech Co., San Leandro, CA) gel box imager and densitometry was carried out using FluorChem software (Alpha Innotech Co.).

RESULTS

Ligand-dependent Heterodimerization of hSSTR1 and hSSTR5 by pbFRET—To study the heterodimerization of hSSTRs, we stably expressed hSSTR5 with an N-terminal HA tag and wild-type hSSTR1 in CHO-K1 cells (B_{max} 395 ± 12 fmol/mg of protein; K_D, 2.3 ± 0.1 nM). Cells were treated with various concentrations of the agonists: SST-14, SST-28, endogenous agonists for both the receptors, SCH-275 (subtype-agonist for hSSTR1) and SMS 201-995 (subtype-agonist for hSSTR5) for 15 min. Treatment was terminated by putting the cells on ice, washing once with phosphate-buffered saline followed by fixing in 4% paraformaldehyde for 20 min. To determine the physical association between the two receptors, we performed pbFRET microscopy on the cells by using a primary antibody followed by a secondary antibody conjugated with fluorescein (donor) to hSSTR1 and an anti-HA monoclonal antibody conjugated with rhodamine (acceptor) to hSSTR5. A panel of images depicting the co-expression of both receptor subtypes within the same cell is shown in Fig. 1. The decrease in donor fluorescence intensity due to photobleaching during prolonged exposure to excitation light was monitored in the

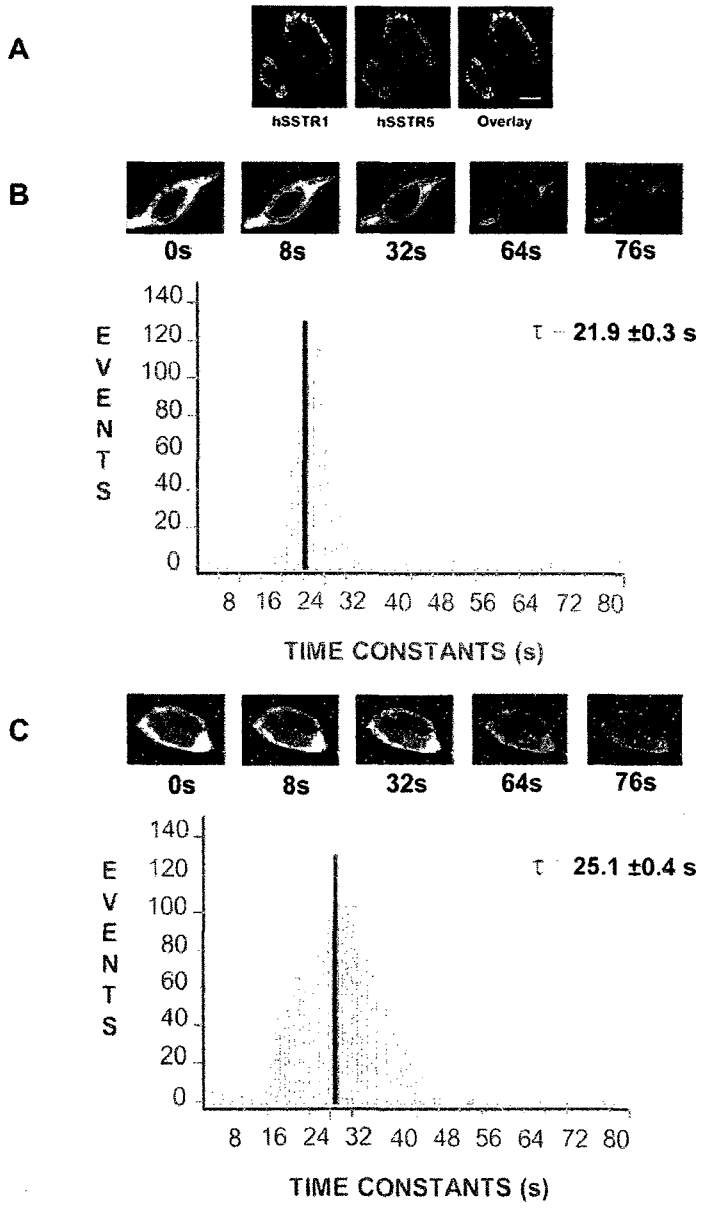

FIG. 1. **Confocal microscope images and a representative histogram time constant plot from pbFRET microscopy from CHO-K1 cells stably expressing HA-hSSTR5 and hSSTR1.** *A*, confocal photomicrographs illustrating the colocalization of hSSTR1 and HA-SSTR5 in CHO-K1 cells. Cells were incubated with primary rabbit polyclonal anti-hSSTR1 followed by secondary anti-rabbit fluorescein-conjugated antibody shown in *green*, anti-HA rhodamine-conjugated monoclonal antibody to HA-hSSTR5 shown in *red*, and colocalization of the two images shown in *yellow* (*scale bar* 25 μm). *B*, photobleaching of fluorescein (donor) in the absence of rhodamine (acceptor), *top panel*. In this representation, cells were treated with 1 μM SST14, fixed and followed by donor photobleaching with 488 nm light. A sequence of 20 images was captured, of which only a selected few are shown here. A histogram time constant plot was calculated based on a pixel-by-pixel basis of a selected area on the cell surface. The mean time constant of 21.9 ± 0.3 s is shown as a *black bar* taken by averaging the time constants from a Gaussian distribution. *C*, in this representation, cells treated with 1 μM SST14 were photobleached in the presence of the acceptor molecule. The *top panel* shows the visual delay in photobleaching of the donor and below is the histogram time constant bar plot displaying an increase in the mean time constant (25.1 ± 0.4 s).

absence and presence of acceptor fluorophore. Delays in the photobleaching decay of the donor in the presence of the acceptor related to an increase in FRET efficiency. Because FRET occurs at distances between 10–100 Å, it is a direct measure of protein-protein interaction. By taking a series of digital photographs, we analyzed the photobleaching decay of the donor on the surface of cell membranes on a pixel-by-pixel basis (Fig. 1, *B* and *C*). Cells were treated with different concentrations of four agonists, which displayed differences in their ability to induce heterodimerization. As shown in Fig. 2, in absence of agonist, a low relative FRET efficiency (<3%) was present in each condition. Treatment of SST-14 resulted in a concentration-dependent increase in heterodimer formation as indicated by increases in FRET efficiency. A maximum of 13.0 ± 1.1% at 10^{-6} M was achieved possibly suggesting a saturation in the response (EC_{50} of 3.4 ± 2.1 nM) (Fig. 2*A*). A similar phenomenon was observed for SST-28, which also induced a concentration-dependent increase in FRET efficiency however with greater efficacy (EC_{50} 0.14 ± 0.04 nM) (Fig. 2*B*). This may indicate that SST-28 is a more potent agonist at inducing heterodimerization than is SST-14. The hSSTR5 subtype agonist SMS 201-995, although capable of promoting heterodimerization, did so at

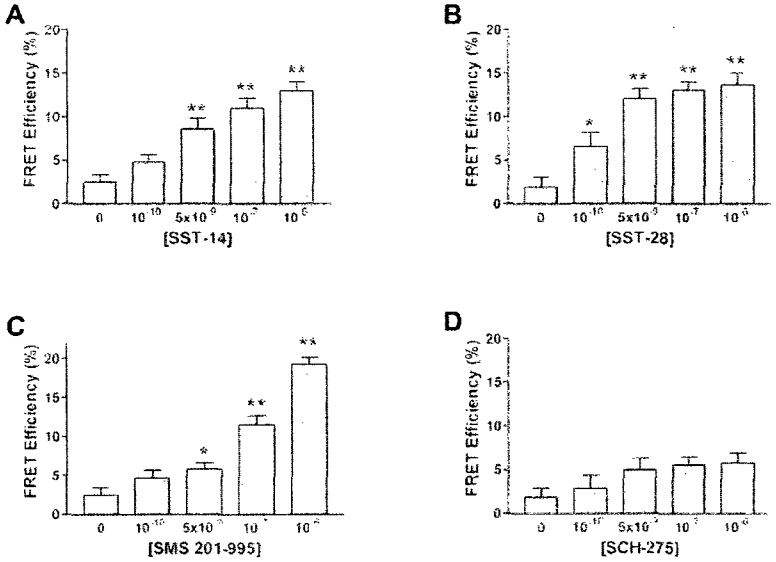

FIG. 2. **Concentration-dependent increase in effective FRET efficiencies from CHO-K1 cells stably expressing HA-hSSTR5 and hSSTR1 by different agonists.** Cells were treated with the indicated concentrations of each agonist and analyzed by pbFRET microscopy. The calculated FRET efficiencies (%) and EC_{50} values for each agonist (*A*) SST-14 (3.4 ± 2.1 nM), (*B*) SST-28 (0.14 ± 0.04 nM), (*C*) SMS 201-995 (119 ± 16 nM) were plotted and analyzed by a sigmoidal dose-response equation using Graph Pad Prism 3.0. *D*, treatment with SCH-275 did not result in a significant increase in FRET efficiency. Data were analyzed by ANOVA, posthoc Dunnett's and compared with basal conditions without treatment. Means ± S.E. are representative of three independent experiments performed in triplicate; *, $p < 0.05$; **, $p < 0.01$.

much higher concentrations as determined by its EC_{50} value (EC_{50} 119 ± 16 nM) (Fig. 2*C*). One possible explanation for this event could be that SMS 201-995 favors the formation of hSSTR5 homodimers than heterodimers; however, further studies are required. In contrast, treatment with the hSSTR1 subtype agonist SCH-275, did not result in significant increases in FRET efficiency (Fig. 2*D*). These results demonstrate that hSSTR1 is unable to promote heterodimerization. To further illustrate the active contribution of hSSTR5 in heterodimerization, we performed Western blot and co-immunoprecipitation on membranes prepared from cells either individually or co-expressing the two receptors.

Western Blot on Ligand-activated hSSTRs—To verify the receptor subtype actively involved in the heteromeric assembly of hSSTR1 and hSSTR5, we performed co-immunoprecipitation and Western blot on membranes from HEK-293 cells mono- and co-expressing the two receptors. In the absence of SST-14, hSSTR5 was found mainly as a monomer (~55 kDa) (Fig. 3). Treatment with SST-14 resulted in the formation of dimers (~110 kDa) including higher order oligomers (Fig. 3). A similar phenomenon was reported for hSSTR5 transfected in CHO-K1 cells, whereby agonist induced the dimerization of the receptor (13). Unlike hSSTR5, hSSTR1 did not form dimers in response to agonist nor was it self-associated under basal conditions (Fig. 3). This is in agreement with a previous report on hSSTR1 showing that it remained monomeric even in the presence of agonist in live cells using FCS (14). Co-immunoprecipitation of membranes expressing both receptor subtypes resulted in the detection of a weak band in the absence of agonist, however, upon agonist stimulation a strong signal was detected (~115 kDa) indicating heterodimeric interaction (Fig. 3). Taken together these results and those obtained by pbFRET (Fig. 2), suggest that hSSTR1 is not actively involved in heterodimeric assembly.

Membrane Binding Analysis of the hSSTR1 and hSSTR5 Heterodimer—To determine whether heterodimerization altered the binding properties of the receptors, we compared the binding constants for each agonist. Membranes were collected from CHO-K1 cells stably expressing hSSTR1, hSSTR5, and

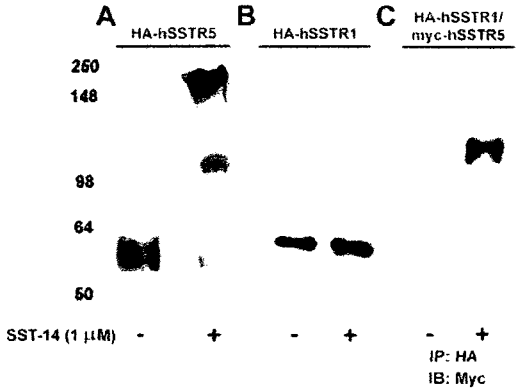

FIG. 3. **Western blot and co-immunoprecipitation of HEK-293 cells stably expressing HA-hSSTR1, HA-hSSTR5, and co-expressing HA-hSSTR1 and c-Myc-hSSTR5.** *A*, membranes from HEK-293 cells stably expressing HA epitope-tagged hSSTR5 were treated with or without 1 μM SST-14 for 30 min before being separated on a SDS-polyacrylamide gel. HSSTR5 can be seen mainly as a monomer (~55 kDa) but upon treatment with agonist self-associates into dimers (~110 kDa) and higher order oligomers. *B*, immunoblot of membranes expressing HA epitope-tagged hSSTR1 in the absence or presence of 1 μM SST-14 appearing at ~58 kDa. *C*, membranes co-expressing HA-hSSTR1 and c-Myc-hSSTR5 were incubated with or without SST-14 (1 μM) for 30 min, solubilized, and immunoprecipitated with anti-HA antibody against hSSTR1. Immunoblotting was performed with anti-c-Myc antibody for detection of hSSTR5. Note the formation of heterodimers upon agonist treatment. Immunoblots are representations of three independent experiments.

TABLE I

Comparison of the potencies of SST agonists for binding to membranes expressing hSSTR1, hSSTR5, and hSSTR1/hSSTR5

Competition analysis on membrane preparations from CHO-K1 cells stably expressing hSSTR1, hSSTR5, and coexpressing the two receptors (hSSTR5/R1). K_i values expressed in nM are the inhibitory concentration required for half-maximal inhibition of ^{125}I-LTT-SST-28 binding. Means ± S.E. represent three independent experiments performed in triplicate.

Receptors	Agonists			
	SST-14	SST-28	SMS 201-995	SCH-275
hSSTR1	0.20 ± 0.01	2.14 ± 0.40	≥1000	4.10 ± 0.56
hSSTR5/R1	0.49 ± 0.09	0.50 ± 0.04	45.1 ± 7.4	11.4 ± 0.39
hSSTR5	1.25 ± 0.22	0.95 ± 0.11	8.23 ± 0.84	≥1000

from cells co-expressing the two receptors. Saturation analysis with the radioligand ^{125}I-LTT-SST-28 gave a B_{max} of 415 ± 14 fmol/mg of protein and a K_D of 0.49 ± 0.08 nM from membranes of the co-transfectants and B_{max} and K_D values of 284 ± 5 fmol/mg, 1.4 ± 0.05 nM and 231 ± 25 fmol/mg, 1.1 ± 0.15 nM for membranes transfected with hSSTR5 and hSSTR1 respectively. Binding constants represented as K_i values for each of the four agonists from each receptor species are shown in Table I. Heteromeric assembly of hSSTR1/hSSTR5 did not result in changes in the K_i values for SST-14 as determined by the lack of statistical significance when compared with the individual receptors. Although the K_i value for SST-28 was lower for the heterodimer than for the individual receptors, indicating a higher affinity, the difference was ~2-fold in comparison to hSSTR5 and 4-fold to hSSTR1. For the subtype-specific agonists SMS 201-995 and SCH-275, K_i values were slightly higher for the heterodimer than for the individual hSSTRs. Based on our results heterodimerization did not markedly alter the binding properties of the receptors.

Signaling of the Heterodimer—To determine the signaling properties of the heterodimer we measured cAMP accumulation. HSSTRs are well known to inhibit cAMP production through $G\alpha_{i/o}$ coupling (28), we monitored the dose-dependent effect of all four agonists on the inhibition of forskolin-stimulated cAMP production in CHO-K1 cells mono or co-expressing hSSTR1 and hSSTR5. Cells were treated with each of the four agonists with the indicated concentrations in the presence of forskolin (20 μM) and measured for cAMP. Treatment of cells with SST-14 or SST-28 co-expressing hSSTR1/hSSTR5 resulted in greater signaling efficiencies when compared with treatment of cells expressing either receptor separately (Fig. 4, *A* and *B*; Table II). The signaling efficiency of SMS 201-995 in cells expressing hSSTR5 was greatly enhanced upon hSSTR1 co-expression (Fig. 4*C*). It has been previously reported that SMS 201-995 poorly stimulates hSSTR5 when expressed in CHO-K1 cells contrary to its relatively high binding affinity to the receptor (34). To verify that our results were not dependent on the cell type, we stably expressed hSSTR5 in HEK-293 cells and performed the same signaling experiments using SMS 201-995. The results were similar to those obtained in CHO-K1 cells therefore indicating that this property was independent of cell type (data not shown). Treatment with the subtype-specific agonist SCH-275 did not demonstrate changes in signaling efficiency for hSSTR1 expressed alone or when co-expressed with hSSTR5 (Fig. 4*D*).

To determine if heterodimerization resulted in a synergistic effect on adenylyl cyclase coupling efficacy, we compared the total inhibition of forskolin-stimulated cAMP production achieved by saturating concentrations of ligand from both the mono- and co-expressing cell lines. The maximum inhibition achieved in cells expressing hSSTR5 was ~85% as determined by treatment with SST-14 and SST-28 (endogenous ligands) using 1 μM concentrations (Fig. 5, *A* and *B*). The subtype agonist SMS 201-995 did not reach this receptor maximum at 1 μM concentrations (Fig. 5*C*) despite receptor saturation. The total inhibition reached by cells expressing hSSTR1 was ~25%, in agreement with what has been previously reported (Fig. 5*D*) (31). When both receptors were co-expressed the total inhibition achieved was ~50% for the agonists SST-14, SST-28, and SMS 201-995 but was unchanged upon treatment with SCH-275 (~25%). These results correlate with our pbFRET and Western blot data indicating that stimulation of hSSTR1 specifically was not sufficient to promote heterodimerization and therefore did not result in changes in signaling. Although the maximum inhibition achievable was lower for the heterodimer, the efficiency for inducing maximum stimulation was higher for agonists capable of inducing heterodimerization (Fig. 4). This indicates that heterodimerization may not always result in a synergistic effect on coupling efficiency contrary to what we have previously reported for the dopamine receptor 2 and hSSTR5 heterodimer (29). This does not rule out other possible efficacies that may be altered such as MAP kinase activation.

Homodimerization of hSSTR1, hSSTR5, hSSTR5-C-tail-R1, and hSSTR1-C-tail-R5 Using Labeled Ligands—To determine the possible molecular determinants involved in the heterodimerization of hSSTR1 and hSSTR5, we compared the pbFRET results using labeled ligands in CHO-K1 cells individually expressing hSSTR1, hSSTR5, and two chimeric receptors: hSSTR5 possessing the C-tail of hSSTR1 (R5CR1) and hSSTR1 possessing the C-tail of hSSTR5 (R1CR5). The R5CR1 chimera was created by replacing C-tail residues 319–363 and swapping them with residues 332–391 of the hSSTR1 C-tail. Similarly, R1CR5 was created by exchanging the same residues. The chimeric receptors were correctly targeted to the plasma membrane as determined by saturation binding analysis and forskolin-stimulated cAMP inhibition analysis (31). As previously reported, replacement of the hSSTR5 C-tail with the C-tail of hSSTR1 completely abolishes agonist-mediated internalization (31). The R5CR1 chimera mimicked the properties of hSSTR1, suggesting the presence of negative internalization signals in the C-tail of hSSTR1 sufficient to block the internalization of hSSTR5. Similarly, replacement of the hSSTR1 C-tail with that of hSSTR5 not only mimicked the signaling properties of hSSTR5 but also its internalization characteristics (31). We have previously reported that hSSTR1 does not undergo homodimerization contrary to hSSTR5, which is fully capable of dimerizing (13, 14). Therefore, using the chimeric receptors, R5CR1 and R1CR5, we proceeded to determine whether these receptors reflected their wild-type counterparts in undergoing homodimerization. Labeled ligands were generated by conjugation of fluorescein isothiocyanate to SST-14-D-Trp8 as the donor and Texas Red-succinamidyl ester to SST-14 as the acceptor. In this fashion, the labeled conjugates gave comparable binding affinities, similar to unconjugated SST-14, to be used together in our pbFRET studies (data not shown). CHO-K1 cells stably expressing any of the four receptors were grown on coverslips and then incubated with either the donor ligand alone or the donor ligand with the acceptor ligand, each at a concentration of 20 nM. As shown in Fig. 6, the FRET efficiencies of hSSTR1 and R5CR1 were comparable suggesting the absence of homodimerization, contrary to the FRET efficiencies obtained for hSSTR5 and R1CR5 (21.5 ± 1.7% and 14.9 ± 2.8%)

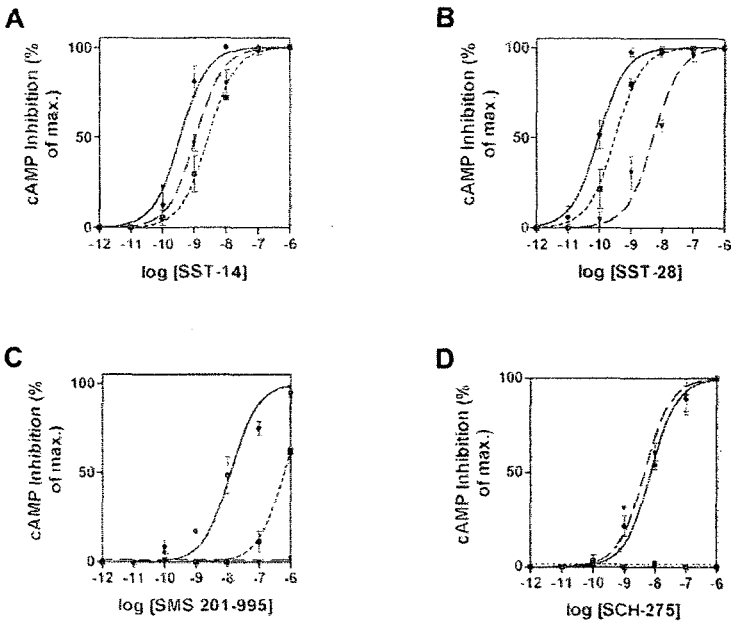

FIG. 4. **Adenylyl cyclase coupling efficiency of the hSSTR1/hSSTR5 heterodimer.** CHO-K1 cells monotransfected with hSSTR1 (▲) and hSSTR5 (■) or cotransfected with both receptors (●) were treated with forskolin (20 μM) alone or in combination with the indicated concentrations of the agonists (*A*) SST-14, (*B*) SST-28, (*C*) SMS 201-995, and (*D*) SCH-275 for 30 min. Treatment of cells with forskolin alone was taken as 0% inhibition and treatment of forskolin with 1 μM concentrations of agonist was taken as 100% inhibition. The data represent means ± S.E. from three independent experiments performed in triplicate.

TABLE II

Comparison of adenylyl cyclase coupling efficiencies by SST agonists

CHO-K1 cells stably expressing hSSTR1 and hSSTR5 or coexpressing both receptors (hSSTR5/R1) were treated with given concentrations of each agonist in the presence of forskolin and measured for cAMP accumulation. EC_{50} values represented in nM are the half-maximal inhibition of forskolin-induced cAMP production. Means ± S.E. represent three independent experiments performed in triplicate.

Receptors	Agonists			
	SST-14	SST-28	SMS 201-995	SCH-275
hSSTR1	1.21 ± 0.38	5.19 ± 0.23	≥1000	4.93 ± 1.12
hSSTR5/R1	0.37 ± 0.05	0.10 ± 0.03	12.8 ± 4.3	7.56 ± 1.50
hSSTR5	2.85 ± 1.31	0.32 ± 0.11	643 ± 99	≥1000

indicating homodimer formation. Taken together, these results suggest that the C-tail of hSSTR1 responsible for the inhibition of internalization and up-regulation may also be responsible for its inability to homodimerize.

DISCUSSION

There have been several reports documenting GPCR heterodimerization but the mechanism underlying such an event remains largely unknown (1, 2). To our knowledge this is the first time that heterodimerization has been shown to be modulated by subtype-specific agonists and more specifically through the occupancy of one receptor subtype over another. Using pbFRET microscopy, we were able to demonstrate that both the agonists, SST-14 and SST-28, endogenous ligands for both receptor subtypes, induced a dose-dependent increase in FRET efficiency. These agonists were able to efficiently induce heterodimerization at values corresponding to their binding constants. Co-immunoprecipitation and Western blot also demonstrated increases in heterodimeric interaction when agonist was present. However, this was not the case when specific activation of the individual receptor subtypes was involved. Selective activation of hSSTR1 by SCH-275 did not result in changes in FRET efficiency nor did it present as a dimer or higher order oligomer on immunoblots, an indication that by itself is monomeric and unable to induce heterodimerizaton. In contrast, selective activation of hSSTR5 resulted in increases in FRET efficiency and therefore could be the active subtype involved in this heterodimeric assembly. Immunoblots of hSSTR5 demonstrated it as being monomeric in basal conditions but displayed profound changes in receptor stoichiometry ranging from receptor dimers to higher order oligomers upon agonist activation. However, for both SST-14 and SST-28, the ligand-induced FRET based efficiency was severalfold higher (3.4 ± 2.1 nM and 0.14 ± 0.04 nM, respectively) when compared with SMS 201-995 (119 ± 16 nM). This difference could be the result of activation of both receptor subtypes simultaneously that allow for conformational changes to better stabilize the heterodimer. Another possibility could be that stimulation of hSSTR5 alone could preferentially form homodimers at lower concentrations of agonist followed by heterodimer formation at higher concentrations. In our previous study using live cells expressing hSSTR1 and hSSTR5 at least three populations of receptors may exist upon stimulation with SST-14; hSSTR1 monomers, hSSTR5 homodimers and hSSTR1/hSSTR5 heterodimers (14). It would be interesting if indeed stimulation of hSSTR5 alone preferentially stabilizes homodimers, then one could develop ways of tailoring such processes. A similar scenario has been described for the chemokine receptors CCR2 and CCR5 (26). In cells co-expressing the two receptors, selective activation of either receptor alone resulted in homodimerization whereas co-administration of agonist for both receptors induced heterodimerization.

Binding constants for all four agonists for the heterodimer in

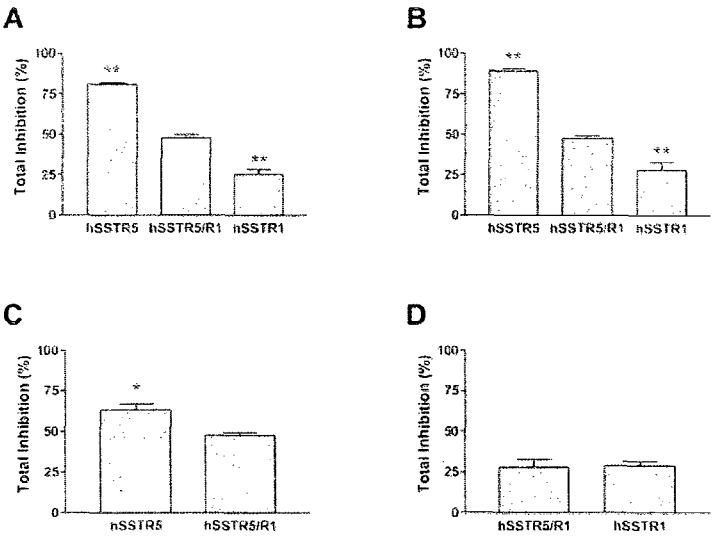

FIG. 5. **Total inhibition of forskolin-stimulated cAMP production.** Maximum coupling efficacy was calculated by treating cells with 1 μM concentrations of each agonist, SST-14 (*A*), SST-28 (*B*), SMS 201-995 (*C*), and SCH-275 (*D*), in the presence of forskolin for 30 min and comparing them with cells stimulated with forskolin alone. Treatment of cells monotransfected with hSSTR1 and hSSTR5 were compared statistically to cotransfectants. Statistical significance was determined by analysis of variance, posthoc Dunnetts, whereby control was taken as forskolin stimulation alone. There were no statistical differences resulting from treatment with SCH275. Means ± S.E. represent three independent experiments. *, $p < 0.05$; **, $p < 0.01$, compared with cotransfectants.

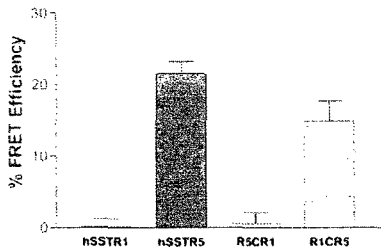

FIG. 6. **The characterization of the functional importance of the C-tail in the homodimerization of hSSTR1 and hSSTR5 by pbFRET microscopy.** CHO-K1 cells stably expressing either hSSTR1, hSSTR5, R1CR5, or R5CR1 were treated with 20 nM SST-FITC (donor) or with 20 nM SST-FITC and SST-TR (donor − acceptor) and processed for pbFRET microscopy (see text for "Experimental Procedures"). Note the significant changes in FRET efficiencies upon C-tail transposition. Homodimerization of hSSTR1 is promoted through C-tail replacement with hSSTR5.

comparison to the individual receptors did not reveal any marked differences. There was however a small but significant rightward shift in the binding curve for SMS 201-995 toward the heterodimer, indicating a decrease in binding affinity but was less apparent for SCH-275. Finally, the endogenous ligands SST-14 and SST-28 bound to all three receptor combinations (hSSTR1, hSSTR5, and hSSTR1/hSSTR5) with similar affinities. These results indicate that interacting receptor pairs may not always have a profound effect on ligand binding sites.

Heterodimerization was however reflected by changes in receptor signaling (Figs. 4 and 5). The maximum coupling efficacy determined by inhibition of forskolin-stimulated cAMP production was ~50% for the heterodimer as determined by the agonists SST-14 and SST-28. These results cannot be accounted for by the additive stimulation of both receptor subtypes separately because the maximum stimulation of hSSTR5 and hSSTR1 alone was ~80 and 25% respectively. In this context, only SMS 201-995 but not SCH-275 was able to attain this maximum inhibition in cotransfected cells, possibly indicating that SCH-275 was unable to induce heterodimerization. To further characterize these changes in signaling, we monitored coupling efficiency by comparing EC_{50} values. Using the subtype-specific agonist for hSSTR1, we were unable to observe alterations in the signaling profiles for hSSTR1 expressed alone or when co-expressed with hSSTR5. In contrast, activation of hSSTR5 by SMS 201-995 resulted in a robust increase in coupling efficiency when both hSSTR5 and hSSTR1 were co-expressed. This property correlated in part with the ability of SMS 201-995 to induce heterodimerization. The alteration in maximum coupling efficacy associated with heterodimerization may have functional implications. One possible consequence may be associated with the poor response of human prolactinomas to SMS 201-995 treatment. Human prolactinomas are pituitary adenomas that hypersecrete prolactin and predominantly express hSSTR1 and hSSTR5 (35, 36). In cultured studies of human excised prolactinomas, tumors that displayed increased expression of hSSTR1 fared poorly to treatment with SMS 201-995 in controlling prolactin release compared with those expressing lower levels of hSSTR1 regardless of hSSTR5 expression (36). However, a direct association between heterodimerization and treatment outcome in prolactinomas would be necessary to validate such claims.

HSSTR1 is the only member of the human SSTR family that does not internalize but up-regulates at the cell surface in response to prolonged agonist exposure (31). Knowing that the C-tail of hSSTR1 is responsible for its ability to up-regulate at the cell surface, we proceeded to determine whether it also mediates its monomeric state. Using receptor C-tail chimeras, whereby the C-tails of both receptors were interchanged, we attempted to characterize a putative interface involved in somatostatin receptor dimerization. Replacement of the C-tail for hSSTR5 with that of hSSTR1 was enough to antagonize homodimerization of hSSTR5. Moreover, when the C-tail of hSSTR5 was in place of the C-tail for hSSTR1, hSSTR1 was capable of forming homodimers. Surprisingly, the molecular determinant responsible for the up-regulation of hSSTR1 was also responsible for preventing its homodimerization. Unlike hSSTR1, hSSTR5 does internalize and homodimerize when in the presence of agonist, yet these properties were both inhibited when the C-tail of hSSTR1 was added. It is not the first time that the C-tail has been suggested to be implicated in the heterodimerization of GPCRs. The $GABA_B$ receptor is a het-

erodimer composed of the subtypes $GABA_BR1$ and $GABA_BR2$ (7–9). Initial attempts in its cloning have shown that heterologous expression of the individual receptor subtypes were either found essentially retained in the ER ($GABA_BR1$) or expressed at the cell surface but functionally inactive ($GABA_BR2$). When both receptors were co-expressed a retention sequence found in the C-tail of $GABA_BR1$ was masked through C-tail interaction with $GABA_BR2$. This allowed for proper trafficking and functioning of the $GABA_B$ receptor. Similarly, the C-tail of the δ-opioid receptor was found necessary for dimerization and when perturbed through C-tail deletion internalization was impaired (37). However, this does not rule out other possible domains that may also be contributing to dimerization such as the transmembrane region (38–40).

Although a general mechanism such as preformed or ligand induced dimer formation does not seem to be exclusively valid, our study highlights the importance of ligands, especially receptor specific ligands, in dimer formation. It is noteworthy that hSSTR1 homodimers cannot be formed, yet ligand bound hSSTR5 forms heterodimers with hSSTR1. Indeed, the ligand bound hSSTR1/hSSTR5 heterodimer is more stable as demonstrated by pbFRET and signaling efficiencies of SST-14 and SST-28 suggesting a preferred conformational state resulting from ligand binding. These findings are consistent with earlier results with dopamine 2/hSSTR5 (29) and hSSTR1/hSSTR5 (14) heterodimers in which a dimer containing one or two ligands could be established.

In conclusion, we have demonstrated that activation of hSSTR5 but not hSSTR1 was capable of promoting hSSTR1/hSSTR5 heterodimerization. These results also demonstrate that agonist-mediated heterodimerization may occur through ligand occupancy of only one receptor subtype. Furthermore, this process resulted in changes in maximum coupling efficacy and coupling efficiency with little changes in ligand binding. We have also demonstrated that the C-tail of hSSTR1 was responsible for preventing dimerization. However, further studies are required to define any specific residues or motifs that may account for this inhibition of interaction. Our data provide direct biophysical and functional evidence that heterodimerization is a receptor and ligand specific process. We recognize the importance of the C-tail in receptor internalization, G-protein coupling, and dimer formation. A detailed understanding of the significance on the interrelationship(s) among these events are lacking and need to be elucidated.

Acknowledgments—We thank M. Correia for secretarial help and H. Alturaihi and A. Abdallah for technical assistance.

REFERENCES

1. Agnati, L. F., Ferré, S., LLuis, C., Franco, R., and Fuxe, K. (2003) *Pharm. Rev.* **55,** 509–550
2. Angers, S., Salahpour, A., and Bouvier, M. (2002) *Annu. Rev. Pharmacol. Toxicol.* **42,** 409–435
3. Nelson, G., Hoon, M. A., Chandrashekar, J., Zhang, Y., Ryba, N. J. P., and Zuker, C. S. (2001) *Cell* **106,** 381–390
4. Nelson, G., Chandrashekar, J., Hoon, M. A., Feng, L., Zhao, G., Ryba, N. J. P., and Zuker, C. S. (2002) *Nature* **416,** 199–202
5. Li, X., Staszewski, L., Xu, H., Durick, K., Zoller, M., and Adler, E. (2002) *Proc. Natl. Acad. Sci. U. S. A.* **99,** 4692–4696
6. Abdalla, S., Lother, H., Massiery, A. E., and Quitterer, U. (2001) *Nat. Med.* **7,** 1003–1009
7. White, J. H., Wise, A., Main, M. J., Green, A., Fraser, N. J., Disney, G. H., Barnes, A. A., Emson, P., Foord, S. M., and Marshall, F. M. (1998) *Nature* **396,** 679–682
8. Jones, K. A., Borowsky, B., Tamm, J. A., Craig, D. A., Durkin, M. M., Dai, M., Yao, W. J., Johnson, M., Gunwaldsen, C., Huang, L. Y., Tang, C., Shen, Q., Salon, J. A., Morse, K., Laz, T., Smith, K. E., Nagarathnam, D., Noble, S. A., Branchek, T. A., and Gerald, C. (1998) *Nature* **396,** 674–679
9. Kaupmann, K., Malitschek, B., Schuler, V., Heid, J., Froestl, W., Beck, P., Mosbacher, J., Bischoff, S., Kulik, A., Shigemoto, R., Karschin, A., and Bettler, B. (1998) *Nature* **396,** 683–687
10. Bai, M., Trivedi, S., and Brown, E. M. (1998) *J. Biol. Chem.* **273,** 23605–23610
11. Jensen, A. A., Hansen, J. L., Sheikh, S. P., and Bräuner-Osborne, H. (2002) *Eur. J. Biochem.* **269,** 5076–5087
12. Romano, C., Yang, W. L., and O'Malley, K. L. (1996) *J. Biol. Chem.* **271,** 28612–28616
13. Rocheville, M., Lange, D. C., Kumar, U., Sasi, R., Patel, R. C., and Patel, Y. C. (2000) *J. Biol. Chem.* **275,** 7862–7869
14. Patel, R. C., Kumar, U., Lamb, D. C., Eid, J. S., Rocheville, M., Grant, M., Rani, A., Hazlett, T., Patel, S. C., Gratton, E., and Patel, Y. C. (2002) *Proc. Natl. Acad. Sci. U. S. A.* **99,** 3294–3299
15. Wurch, T., Matsumoto, A., and Pauwels, P. J. (2001) *FEBS Lett.* **507,** 109–113
16. Cornea, A., Janovick, J. A., Maya-Nunez, G., and Conn, P. M. (2000) *J. Biol. Chem.* **276,** 2153–2158
17. Horvat, R. D., Roess, D. A., Nelson, S. E., Barisas, B. G., and Clay, C. M. (2001) *Mol. Endocrinol.* **15,** 695–703
18. Roess, D. A., Horvat, R. D., Munnelly, H., and Barisas, B. G. (2000) *Endocrinology* **141,** 4518–4523
19. Abdalla, S., Zaki, E., Lother, H., and Quitterer, U. (1999) *J. Biol. Chem.* **274,** 26079–26084
20. Kroeger, K. M., Hanyaloglu, A. C., Seeber, R. M., Miles, L. E. C., and Eidne, K. A. (2001) *J. Biol. Chem.* **276,** 12736–12743
21. Cheng, Z-J., and Miller, L. J. (2001) *J. Biol. Chem.* **276,** 48040–48047
22. Latif, R., Graves, P., and Davies, T. F. (2002) *J. Biol. Chem.* **277,** 45059–45067
23. Rodriguez-Frade, J. M., Vila-Coro, A. J., de Ana, A. M., Albar, J. P., Martinez-A, C., and Mellado, M. (1999) *Proc. Natl. Acad. Sci. U. S. A.* **96,** 3628–3633
24. Vila-Coro, A. J., Mellado, M., de Ana, A. M., Lucas, P., del Real, G., Martinez-A., C., and Rodriguez-Frade, J. M. (2000) *Proc. Natl. Acad. Sci. U. S. A.* **97,** 3388–3393
25. Vila-Coro, A. J., Rodriguez-Frade, J. M., de Ana, A. M., Moreno-Ortiz, M. C., Martinez-A, C., and Mellado, M. (1999) *FASEB J.* **13,** 1699–1710
26. Mellado, M., Rodriguez-Frade, J. M., Vila-Coro, A. J., Fernandez, S., Martin de Ana, A., Jones, D. R., Toran, J. L., and Martinez-A, C. (2001) *EMBO J.* **20,** 2497–2507
27. Moller, L. S., Stidsen, C. E., Hartmann, B., and Holst, J. J. (2003) *Biochim. Biophys. Acta* **1616,** 1–84
28. Patel, Y. C. (1999) *Front. Neuroendocrinol.* **20,** 157–198
29. Rocheville, M., Lange, D. C., Kumar, U., Patel, S. C., Patel, R. C., and Patel, Y. C. (2000) *Science* **288,** 154–157
30. Kumar, U., Sasi, R., Suresh, S., Patel, A., Thangaraju, M., Metrakos, P., Patel, S. C., and Patel, Y. C. (1999) *Diabetes* **48,** 77–85
31. Hukovic, N., Rocheville, M., Kumar, U., Sasi, R., Khare, S., and Patel, Y. C. (1999) *J. Biol. Chem.* **274,** 24550–24558
32. Nouel, D., Gaudriault, G., Houle, M., Reisine, T., Vincent, J. P., Mazella, J., and Beaudet, A. (1997) *Endocrinology* **138,** 296–306
33. Patel, R. C., Lange, D. C., and Patel, Y. C. (2002) *Methods* **27,** 240–248
34. O'Carroll, A-M., Raynor, K., Lolait, S. J., and Reisine, T. (1994) *Mol. Pharmacol.* **46,** 291–298
35. Shimon, I., Yan, X., Taylor, J. E., Weiss, M. H., Culler, M. D., and Melmed, S. (1997) *J. Clin. Investig.* **100,** 2386–2392
36. Jaquet, P., Ouafik, L., Saveanu, A., Gunz, G., Fina, F., Dufour, H., Culler, M. D., Moreau, J. P., and Enjalbert, A. (1999) *J. Clin. Endocrinol. Metab.* **84,** 3268–3276
37. Cvejic, S. and Devi, L. A. (1997) *J. Biol. Chem.* **272,** 26959–26964
38. Hebert, T. E., Moffett, S., Morello, J. P., Loisel, T. P., Bichet, D. G., Barret, C., and Bouvier, M. (1996) *J. Biol. Chem.* **271,** 16384–16392
39. Overton, M. C., Chinault, S. L., and Blumer, K. J. (2003) *J. Biol. Chem.* **278,** 49369–49377
40. Pagano, A., Rovelli, G., Mosbacher, J., Lohmann, T., Duthey, B., Stauffer, D., Ristig, D., Schuler, V., Meigel, I., Lampert, C., Stein, T., Prézeau, L., Blahos, J., Pin, J. P., Froestl, W., Kuhn, R., Heid, J., Kaupmann, K., and Bettler, B. (2001) *J. Neurosci.* **21,** 1189–1202

ELSEVIER

Molecular and Cellular Endocrinology 221 (2004) 105–119

MCE
Molecular and Cellular Endocrinology

www.elsevier.com/locate/mce

Deficiency of somatostatin (SST) receptor type 5 (SSTR5) is associated with sexually dimorphic changes in the expression of SST and SST receptors in brain and pancreas

José L. Ramírez[a,1], M. Grant[a,1], M. Norman[b], X.P. Wang[b], S. Moldovan[b], F.J. de Mayo[b], C. Brunicardi[b], U. Kumar[a,*]

[a] *Fraser Laboratories, Departments of Medicine, Royal Victoria Hospital, McGill University, Montreal, Que., Canada H3A 1A1*
[b] *Department of Surgery, Baylor College of Medicine, Houston, TX 77030, USA*

Received 8 December 2003; received in revised form 30 January 2004; accepted 3 February 2004

Abstract

The actions of somatostatin (SST) are mediated through five somatostatin receptor subtypes, termed SSTR1–5. Although SSTRs commonly display an overlapping pattern of tissue distribution, subtype-selective responses have been shown to occur in the same tissue. In the present study, we have investigated the changes in SSTR subtypes at the cellular and molecular level in both the brain and the pancreatic islets of mice deficient in SSTR5 (SSTR5KO). Expression levels of insulin and glucagon were also determined in the pancreas of these mice. Semi-quantitative RT-PCR and Western blot analysis showed significant increases in the expression of SSTR2 and 3 with a corresponding reduction in SSTR4 in the brains of female SSTR5KOs, while no changes were observed in male KOs. Strikingly, SST mRNA and SST-like immunoreactivity (SST-LI) were reduced in the brain of male KO animals but not in their female counterparts. In male SSTR5KO islets, there was an increase in the number of cells immunoreactive for SSTR1–3, whereas in female islets only SSTR3 expression was increased. Pancreatic SST-LI and SST mRNA, as well as immunoreactivity for insulin were reduced in male but not in female KO mice. These data indicate that deficiency of SSTR5 leads to subtype-selective sexually dimorphic changes in the expression of both brain and pancreatic SSTRs.

Keywords: Somatostatin; Somatostatin receptor; Sexual dimorphism; Brain; Pancreas

1. Introduction

Somatostatin (SST) is a multifunctional peptide with two biologically active forms, SST-14 and SST-28, which are synthesized in neurons throughout the brain as well as in peripheral tissues such as the pancreas and the gut (Patel, 1992, 1999; Epelbaum et al., 1994). Acting via a family of five G-protein coupled receptors (GPCRs) termed SSTR1–5, SST exerts a diverse array of effects that include inhibition of endocrine secretion, modulation of neurotransmission, and regulation of cell proliferation. SSTRs are typically expressed in target tissues such as the brain, pituitary, pancreas, gut, aorta, and immune cells with overlapping patterns of expression with differences according to sex and species (Patel, 1997, 1999; Bruno et al., 1993; Feuerbach et al., 2000; Fehlmann et al., 2000). In the rat, mRNA for all of the SSTR subtypes have been localized in the brain showing patterns of regional subtype-selectivity (Bruno et al., 1993; Breder et al., 1992). SSTR1 is most abundantly expressed in rat brain, followed by SSTR2, 5, 3, and 4 (Bruno et al., 1993; Fehlmann et al., 2000; Breder et al., 1992; Kong et al., 1994; Meyerhof et al., 1992). In contrast, SSTR5 mRNA is poorly expressed in human brain. All five SSTRs are also expressed in the pituitary, pancreas, gut, and aorta of both rodent and human species (Patel, 1999; Thoss et al., 1996; Kumar et al., 1997, 1999; Khare et al., 1999; Patel et al., 1995). It has been proposed that SSTR2 mediates the effects of SST on pancreatic glucagon whilst SSTR5 plays an important role in regulating

* Corresponding author. Present address: Royal Victoria Hospital, Room M3.15, 687 Pine Avenue West, Montreal, Que., Canada H3A 1A1. Tel.: +1-514-842-1231x35042x36495; fax: +1-514-843-2819.
E-mail address: ujendra.kumar@muhc.mcgill.ca (U. Kumar).
[1] Authors equally contributed to this study.

0303-7207/$ – see front matter
doi:10.1016/j.mce.2004.02.001

insulin secretion (Rossowski and Coy, 1994; Strowski et al., 2000, 2003; Tirone et al., 2003). However, the finding that cells often express multiple SSTR subtypes and the recent demonstration that several of the SSTR subtypes associate as functional homo- and heterodimers, suggest that members of this family may be able to operate in concert (Rocheville et al., 2000; Patel et al., 2002). Concerning gender-related differences in the expression of SSTRs, it has been reported that females from both rat (Kimura et al., 1998) and mouse (Low et al., 2001) species display lower levels of mRNA for SSTR5 in the pituitary than their male counterparts. Likewise, sexual dimorphism has been reported for the expression of SSTR1–3 in the rat anterior pituitary (Senaris et al., 1996; Zhang et al., 1999) as well as for SSTR1 expression in the arcuate nucleus of adult rats (Zhang et al., 1999).

A common property of most GPCRs is their ability to be regulated by agonist occupancy (Patel, 1999; Dohlman et al., 1991). Such agonist-specific regulation involves receptor desensitization, uncoupling from G-proteins, receptor internalization, degradation and receptor recycling (Patel, 1999; Patel, 1997; Dohlman et al., 1991). Numerous studies of SSTR regulation have shown that agonist-dependent internalization and desensitization are subtype-specific (Patel, 1999; Hukovic et al., 1996). We have recently demonstrated that mice deficient in SST induced increases in mRNA for SSTR1, 2, and 5 in the brain, whereas SSTR3–5 were downregulated in the pancreas (Ramirez et al., 2002). However, little is known about whether the expression of a given member of a GPCR subfamily influences the pattern of expression of other receptors within the same family. The lack of SSTR2 in rat adrenal gland and pituitary (Hofland et al., 2000) and the lack of SSTR1 (Kreienkamp et al., 1999) in mouse brain however did not alter the expression of the other SSTRs. Recently, two SSTR5 knock out models have been described (Strowski et al., 2003; Tirone et al., 2003). The major inhibitory effect of pancreatic somatostatin on insulin secretion was found to occur via SSTR5 in an isolated perfused mouse pancreatic model. However, SSTR5KO displayed decreases in circulating basal levels of insulin and blood glucose, indicating other possible roles for SSTR5 in glucose homeostasis besides its regulation in insulin secretion (Strowski et al., 2003). In neither study were female KO mice fully examined leaving an open question as to whether or not both sexes are equally affected upon SSTR5 deficiency.

In the present study, we determined the effect of SSTR5 deficiency on the expression of other receptor subtypes. Although SSTR5KO mice were physically indistinguishable from wild-type, its deficiency played a significant role on the expression of SSTRs, SST, insulin and glucagon in both male and female mice. Unlike the knockout models for SSTR1 and 2, the deficiency of SSTR5 induces subtype-selective sexually dimorphic changes in the expression levels of SSTRs and SST in both brain and pancreas, including changes in the expression of islet hormones.

2. Materials and methods

2.1. Generation of SSTR5 deficient mice and tissue analysis

The SSTR5 gene was cloned from a M129VJ mouse genomic library constructed in pBluescript SK II (±) phagemid (Tirone et al., 2003; Moldovan et al., 1998). A targeting vector was constructed that contained a 7 kb homologue of mSSTR5 DNA flanking both sides of the neomycin gene, the positive selection marker. The DNA construct was used for electroporation in 129SV ES cells (Baylor College of Medicine, Tissue Culture Core). Positive ES cells were then microinjected into C57/B1/6J blastocysts to generate chimeric mice. Chimeric males were then selected and crossed with wild-type C57/Bl/6J females to assess for germ line transmission. Heterozygous mice were cross-bred to generate $SSTR5^{++}$, $SSTR5^{+/-}$, $SSTR5^{-/-}$ animals. Homozygous male and female $SSTR5^{-/-}$ mice were selected for the study. Animals were maintained on a 12 h light/dark cycle and fed standard chow.

SSTR5KO mice were initially screened by Southern blot analysis to identify chimeras and subsequent generations of homozygous mice were then screened by PCR assays. PCR primers for the wt were #1 ACA CCT AGC TGG AAT GCC TCA corresponding to bp 265-85 in mSSTR5 and #2 CAG TAG GAG ACA GCA TTC corresponding to bp 546-28 (GI no. 2209142). PCR primers for the KO screen consisted of #1 AAG GCA GTC TGG AGC AT corresponding to bp 2281-2297 in the PKG-Neo cassette and #2 AAC CTG CGT GCA ATC CAT CTT corresponding to bp 2806-2786. PCR amplification was carried out with *Taq* polymerase, dNTPs and $MgCl_2$ for 5 min at 94 °C then 30 cycles of 94 °C—1 min, 60 °C—1 min, 72 °C—1 min, and a final 6 min at 72 °C. Viable F2 homozygous offspring were produced in the normal Mendelian ratios. SSTR5 deficient mice presented a gross phenotype similar to that of wt animals. They had normal gestation, were born normally, grew to adulthood and reproduced with no obvious physiological abnormalities. SSTR5KO mice and matching wt adults (3–6 months old) of both sexes were sacrificed by decapitation. Whole brain and pancreas were removed and frozen immediately in liquid nitrogen for total mRNA extraction, or placed in 4% paraformaldehyde solution for immunohistological analysis.

2.2. Reverse transcriptase polymerase chain reaction (RT-PCR) of mRNA for SSTR1–5 and SST

mRNA for SSTR1–5 and SST was analyzed by semi-quantitative RT-PCR as previously described (Khare et al., 1999; Low et al., 2001; Ramirez et al., 2002). Briefly, samples of brain and pancreas were homogenized in Trizol reagent (Life Technologies Inc., Gaithersburg, MD) for total RNA isolation by use of the guanidinium

isothiocyanate phenolchloroform extraction method. For reverse transcription, 10 μg total DNA-free RNA was incubated with 400 units Moloney murine leukemia virus reverse transcriptase (Gibco-BRL, Paisley, UK) at 42 °C for 30 min in the proper buffer solution. Four microliters of resulting cDNA samples were denatured at 94 °C before initiation of PCR reaction. Primers used for mouse SSTR1–5 and SST were followed as previously described (Low et al., 2001; Ramirez et al., 2002). SSTR1–5 and SST were co-amplified with α-actin as an internal control.

2.3. Southern transfer and hybridization

PCR products (30 μl) were separated by electrophoresis on 1.5% agarose gels, transferred to gene screen plus hybridization membranes (Bristol-Myers Squibb, Billerica, MA), and hybridized with ^{32}P-labeled SSTR1–5, SST and α-actin specific cDNA probes (Ramirez et al., 2002). Autoradiograms were scanned and the hybridization signals were quantified using the Igor Pro 3.13 Analysis Software Package (Wave Metrics Inc., Lake Oswego, OR). Total intensity of the blots (average optical density × area in pixels) were corrected for background and used as an index for SSTRs and actin mRNAs. Only bands that did not reach saturation density upon X-ray film exposure were subjected to quantitative analysis. Values of SSTR1–5 and SST mRNA expression were normalized to those of actin mRNA from the same samples. All experiments were repeated four times and each mRNA quantification represented an average of at least three measurements.

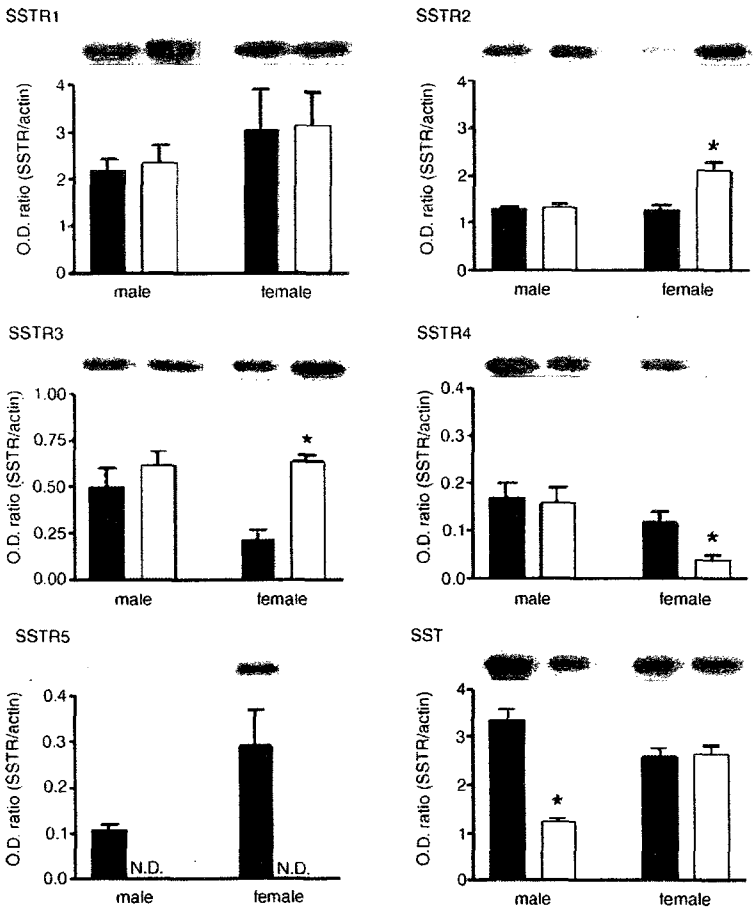

Fig. 1. mRNA expression of SSTRs and SST in whole brain. The mRNA expression levels for the SSTRs and SST taken from whole brain extract were quantified from a Southern blot hybridization signal produced by an RT-PCR product of either wild-type animals (filled columns) or SSTR5KO animals (*open columns*). The arbitrary units were normalized for background signals and expressed as a ratio of product/β-actin mRNA. The data are represented of four separate experiments and each experiment was analyzed in triplicate. * $P < 0.05$; N.D., not detectable.

2.4. Binding analysis

Brain membranes were prepared as previously described (Ramirez et al., 2002). Briefly, whole brains were homogenized in 0.32 M sucrose, 20 mM Tris–HCl, 2.5 mM DTT, pH 7.5 with a glass homogenizer. After several centrifugation steps, the final pellet was resuspended in 20 mM Tris–HCl buffer, an aliquot removed for determination of protein content by the Bradford Method, and the remaining sample was kept for saturation analysis of membrane SSTRs. Saturation analysis was carried out in culture tubes using 40 μg of membrane and [^{125}I]-LTT-SST-28 radioligand at 37 °C for 30 min in the appropriate buffer as previously described (Ramirez et al., 2002). Specific binding was defined as the difference between the amounts of radioligand bound in the absence and presence of 100 nM SST-14 (Bachem, Torrance, CA). Radioactivity associated with membrane pellets was quantified using a LKB gamma counter (LKB-Wallach, Turku, Finland). Kinetic constants were calculated by non-linear regression analysis using Graph Pad Prism 3.0 (Graph Pad Software, San Diego, CA). Saturation analysis on both *wt* and SSTR5KO membranes were repeated at least four times.

2.5. Western blot analysis

Brain membranes were prepared from cerebrocortical tissue of both *wt* and SSTR5KO using a glass homogenizer in 0.32 M sucrose, 20 mM Tris–HCl, 2.5 mM DTT, pH 7.5 as previously described (Ramirez et al., 2002). The membrane pellet was washed and resuspended in 20 mM Tris–HCl, 2.5 mM DTT, pH 7.5 in the absence of sucrose. Membrane protein (50 μg) was solubilized in Laemmli sample buffer containing 62.5 mM Tris–HCl (pH 6.8), 25% glycerol, 2% SDS, 0.01% Bromophenol Blue and 710 mM 2-mercaptoethanol (Bio-Rad, Hercules, CA). The sample was heated at 99 °C for 5 min before being fractionated by electrophoresis on a 7.5% SDS polyacrylamide gel. The fractionated proteins were transferred by electrophoresis to a 0.2 μm nitrocellulose membrane (Trans-Blot Transfer Medium, Bio-Rad) in transfer buffer consisting of 0.025 mol/l Tris, 0.192 mol/l glycine and 20% methanol. Membrane was blotted with SSTR affinity-purified primary antibodies (dilution 1:400) as previously described (Kumar et al., 1999). Blocking of membrane, incubation of primary SSTR antibodies, incubation of secondary antibodie and detection by chemiluminescence were performed following WesternBreeze® (Invitrogen Life Technologies) manufacturer instructions. Images were captured using an Alpha Innotech FluorChem 8800 (Alpha Innotech Co., San Leandro, CA) gel box imager and densitometry was carried out using FluorChem software (Alpha Innotech Co.); α-tubulin was used as an internal control.

Table 1
Binding analysis of SSTRs in whole brain membranes from SSTR5$^{+/+}$ and SSTR5$^{-/-}$ male and female mice

	Kd (nM)	B_{max} (fmol/mg protein)
Male +/+	1.43 ± 0.49	219 ± 25
Male −/−	1.65 ± 0.43	172 ± 12
Female +/+	0.70 ± 0.45	86 ± 5.8
Female −/−	1.35 ± 0.38	224 ± 20[a]

Quantification of total SST binding sites in membrane extracted from whole mouse brain was carried out by saturation binding using the radioligand [^{125}I]-LTT-SST-28. Data are expressed as mean ± S.E.M. of three independent experiments.

[a] $P < 0.05$ vs. other genotype in the same sex.

2.6. Radioimmunoassay of SST

Immunoreactive SST (SST-LI) was measured using a SST radioimmunoassay (RIA) as described earlier (Patel and Reichlin, 1978). Brain and pancreas samples were homogenized in 1 M acetic acid by sonication, boiled for 5 min, sampled for protein quantification using the Bradford Assay. The remaining extract was centrifuged at 8000 × *g* for 30 min, the supernatant neutralized and sampled using RIA. RIA was performed using the rabbit anti-SST antibody (R149) directed against the central segment of SST-14. Synthetic SST-14 standards and a bovine serum albumin-coated charcoal separation method were used. Antibody R149 recognizes both SST-14 and SST-28 with equal affinity (Patel and Reichlin, 1978).

2.7. Immunohistochemistry

Sections of brain and pancreas from wild-type and SSTR5KO mice were analyzed for the expression of SSTR1–5 by peroxidase immunohistochemistry. Pancreatic samples were further characterized for islet expression of insulin, glucagon and SST by indirect immunofluorescence method. Anti-peptide rabbit polyclonal antibodies specific to SSTR1–5, SST, insulin and glucagon were produced and

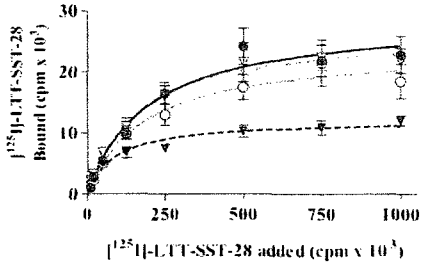

Fig. 2. Saturation isotherms of [^{125}I]-LTT-SST-28 binding to membranes prepared from whole brain. Membranes were incubated with increasing concentrations of radioligand and assayed for binding using 100 nM SST-14 as the cold peptide to quantify total SSTR population. Male wild-type, solid black line, filled circles; male KO, gray solid line, open circles; female wild-type, dotted black line, filled triangles; female KO, gray dotted line, open triangles. Data represent the mean ± S.E.M. of three independent experiments.

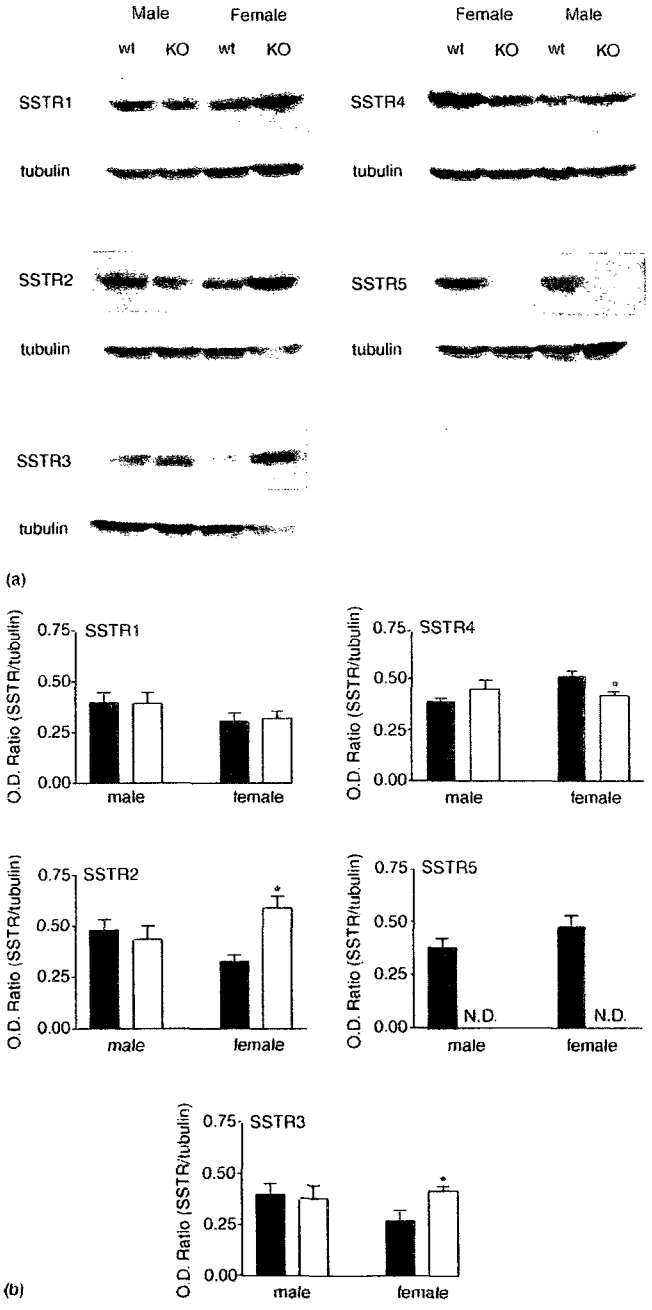

Fig. 3. Western blot analysis of all five SSTRs taken from whole brain. Western blot analysis on all five SSTRs were preformed on both wild-type and knockout mice from both sexes, male and female, using polyclonal SSTR subtype-specific antibodies. (a) Representative blots from one of three experiments (upper panels), α-tubulin was assayed for protein loading (lower panels). (b) Bar plots taken by densitometry analysis from SSTR immunoblots were normalized for protein loading using α-tubulin. Means ± S.E.M. were taken from three independent experiments; $^{*}P < 0.05$; N.D., not detectable.

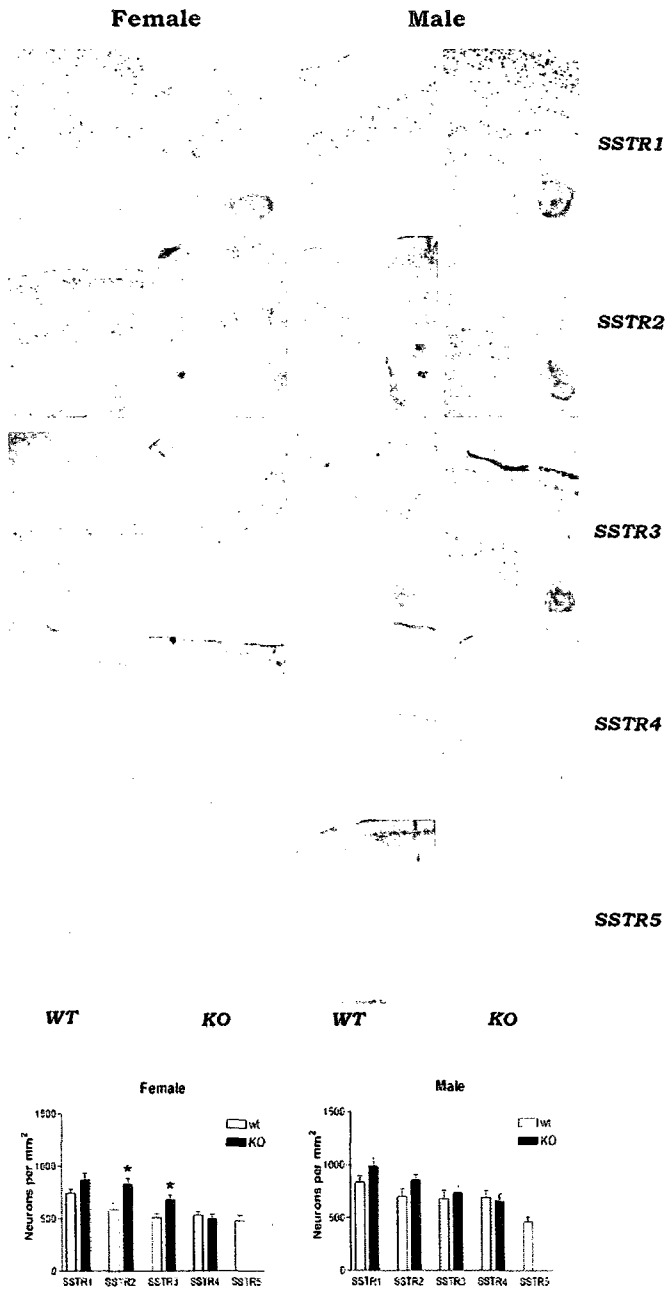

Fig. 4. Photomicrographs illustrating immunohistochemical expression of SSTR1–5 in brain cortex. SSTRs were visualized in the coronal sections of cortex from both wild-type ($SSTR5^{+/+}$) and SSTR5KO ($SSTR5^{-/-}$) male and female mice. SSTRs were visualized as a brown reaction product by peroxidase immunohistochemistry using SSTR1–5 subtype-specific rabbit antibodies and secondary anti-IgG rabbit biotinylated antibody followed by exposure to avidin–biotinylated–peroxidase complex. Note the significant changes in subcellular expression in cortical layer. Bottom panel depicts the number of immunopositive neurons per mm^2 for each SSTR subtype in male and female mice. Magnification 100× and inset 400×; $^*P < 0.05$.

characterized as previously described (Kumar et al., 1997, 1999; Khare et al., 1999; Ramirez et al., 2002; Patel and Reichlin, 1978). Mouse brain and pancreatic tissue samples were fixed in 4% paraformaldehyde overnight. Thick brain sections (30–40 μm) from each animal were cut on a vibratome and collected in Tris buffered saline (TBS), containing 50 mM Tris–HCl and 0.9% NaCl, pH7.5. Sections were then treated with 1.5% H_2O_2 and 10% methanol for 10 min to block endogenous peroxidase. Sections were washed in TBS and incubated with 5% normal goat serum followed by incubation with primary antibodies to SSTR1–5 (diluted 1:400) at 4 °C for 24 h. After washing with Tris buffered saline (TBS), sections were incubated with biotinylated goat anti-rabbit secondary antibody (diluted 1:200) at room temperature for 1.0 h, followed by exposure to avidin–biotinylated–peroxidase complex (Vector Laboratories, Burlingamine, CA, USA) in TBS for 1 h at room temperature. The final product was revealed by chromogen 3.3′-diaminobenzidine (DAB) 0.5 mg/ml (Sigma) containing 0.01% hydrogen peroxide yielding a brown-black reaction product. After three subsequent washes, sections were mounted and viewed under a Leica DML microscope attached to a Cool Snap CCD camera. Neurons showing SSTRs like immunoreactivity were counted from 10 to 12 randomly selected areas from the cortical region.

For immunostaining of insulin, glucagon, and SST in pancreatic tissue, samples were deparaffinized and incubated in 5% normal goat serum for 1 h at room temperature. Sections were then incubated overnight in the presence of insulin anti-guinea pig (1:800), glucagon anti-sheep (1:1000) and SST anti-mouse monoclonal (1:100) antibodies, as previously described (Kumar et al., 1999). After three washes in buffer, sections were incubated with FITC-conjugated goat anti-guinea pig, FITC-conjugated goat anti-sheep or rhodamine-conjugated goat anti-mouse secondary antibodies to visualize insulin, glucagon and SST, respectively. Section were mounted on Immunofluor and visualized using a Zeiss LSM 410 inverted confocal microscope (Carl Zeiss, Inc., Thornwood, NY) (Kumar et al., 1999).

Controls used to validate the specificity of the immunoreactivity included pre-immune serum in place of primary antibody and primary antibody adsorbed with excess antigen. For quantitative analysis in pancreas, 8–10 islets were selected per slide from which immunopositive cells were counted from randomly selected regions. The results are presented as percentage of total islet cells; mean ± S.E.M. were taken from three independent experiments. A mean of 2044 ± 52 β-cells, 584 ± 29 α-cells, and 198 ± 36 δ-cells were analyzed per experiment.

2.8. Statistical analysis

Results are presented as mean ± S.E.M. Statistical comparisons between genotypes were made by Student's unpaired *t*-test. SSTR5KO samples were compared with their counter part wt values as paired data groups within the same experimental procedure. P values <0.05 were considered statistically significant. All tests were performed using Graph Pad Prism 3.0, San Diego, CA.

3. Results

3.1. Expression of SST and SSTR1–5 in Brain

SST mRNA was readily detected in brain of all mice analyzed in this study. All five SSTR mRNA were detected in whole brain extracts from animals of both sexes, with the exception of mRNA for SSTR5 in KO animals (Fig. 1). The relative abundance of mRNA for the different subtypes were as follows: SST > SSTR1 > SSTR2 > SSTR3 > SSTR4 > SSTR5, for wt male animals, and SST ≈ SSTR1 > SSTR2 > SSTR3 ≈ SSTR5 > SSTR4 for wt females.

There were no differences in the levels of expression for SSTR1 mRNA between wt and KO animals for both sexes. In contrast, SSTR2 and SSTR3 mRNA expression was increased in the brain of SSTR5KO female mice, while mRNA levels for SSTR4 were reduced. There were no significant differences in the expression levels of SSTRs between the brains of both male *wt* and KO animals. As expected, expression of SSTR5 was undetectable in the brain of KO animals. Control female mice displayed lower expression levels for SST than males. Surprisingly, there was a dramatic reduction in SST mRNA of male KO mice, with no significant changes with that in females (Fig. 1). These data indicate that the SSTR5 deficiency induces an upregulation of SSTR2 and 3 mRNA, with a downregulation of SSTR4 in female SSTR5KO mice brain only. Furthermore, SST mRNA was only found to be down regulated in male KO brain.

We further extended our study and analyzed the expression levels of SSTRs by other approaches. First, we estimated the total binding population of SSTRs in brain by saturation binding analysis using the radioligand

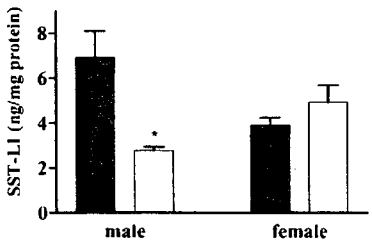

Fig. 5. Somatostatin-like immunoreactivity (SST-LI) in whole brain from wild-type and SSTR5KO mice. RIA was used to quantify SST from homogenate of whole brains from wild-type (filled columns) and SSTR5KO mice (open columns). Results are expressed in nanograms (ng) of immunoreactive protein per milligram (mg) of total protein. Data are expressed as mean ± S.E.M. of nine animals, quantified in three separate experiments; $^*P < 0.05$.

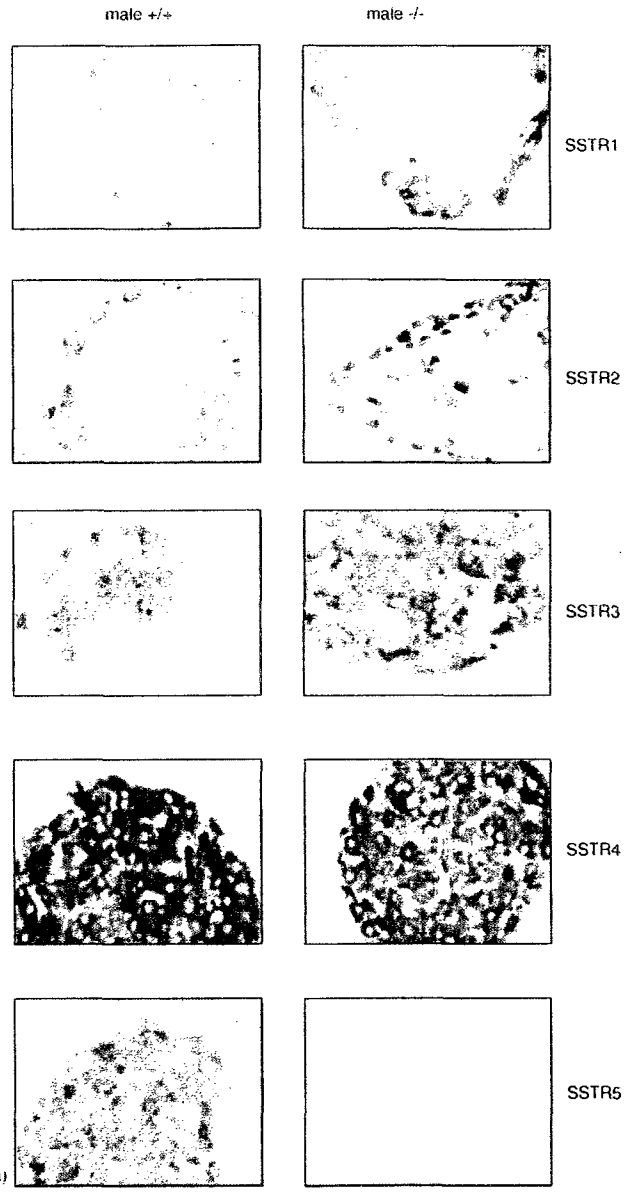

Fig. 6. Immunoperoxidase photomicrographs illustrating the distribution of SSTR immunoreactivity in male and female pancreas. Photographs were captured by light microscopy using a Leica DML microscope attached to a Cool Snap CCD camera using a Leica DmLB microscope. (a) Photomicrographs show details of immunostaining for SSTRs in selected pancreatic islets of wild-type ($SSTR5^{+/+}$, left-hand panels) and SSTR5KO ($SSTR5^{-/-}$, right-hand panels) male mice. (b) Similarily, photomicrographs taken from female mice show details of immunostaining for SSTRs in pancreatic islets of wild-type ($SSTR5^{+/+}$, left-hand panels) and SSTR5KOs ($SSTR5^{-/-}$, right-hand panels). All five receptor subtypes displayed specific and selective distribution in islets. Magnification 400×.

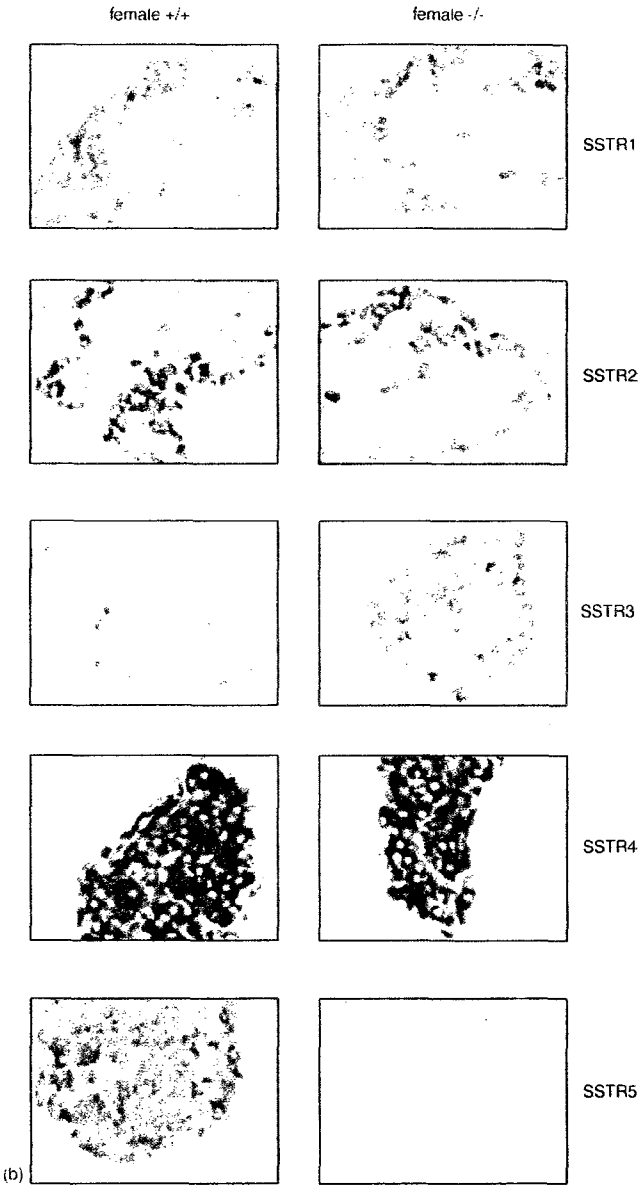

Fig. 6. (*Continued*).

[^{125}I]-LTT-SST-28. Secondly, Western Blot analysis was used to quantify the individual expressions of each subtype in the brains of both *wt* and KOs from both sexes. Thirdly, we determined SSTR protein expression by immunohistochemistry in brain sections using specific antibodies to SSTR1–5. Control male mice displayed a 2.5-fold higher level of SST binding sites in brain compared to females (B_{max} 219 ± 25 versus 86 ± 5.8, Table 1). Interestingly, deletion of the SSTR5 gene resulted in a 160% net increase in the level of expression of SST binding sites in female SST5KO mice reaching values similar to those found in both male genotypes (Fig. 2, Table 1). In contrast to the changes in B_{max}, the ligand binding affinity (Kd) for the SST binding sites was unaffected by SSTR5 deficiency (Table 1).

In order to quantify the changes in the pattern of expression of individual SSTRs in the brains of both *wt* and SSTR5KO male and female mice, Western Blot analysis was performed. As shown in Fig. 3a and b, Western Blot displayed changes in the pattern of expression of SSTRs in female SSTR5KO animals were comparable as demonstrated by Southern blot analysis. More specifically, changes were observed for SSTR2–4 in female KOs compared to their *wt* counterparts with no changes in SSTR1. Taken together, these results demonstrate that SSTR5 deficiency causes a change in the pattern of expression of SSTRs at both the mRNA and protein levels in a sexually deterministic manner.

Peroxidase immunohistochemistry for SSTR1–5 on coronal sections of cortex from *wt* and KO male and female mice are illustrated in Fig. 4. Consistent with the results obtained by mRNA, binding and Western Blot analysis, there were no discernable changes in the intensity or number of immunopositive neurons between male wt and SSTR5KO mice. There were no apparent differences in immunoreactivity for SSTR1 between female *wt* and KO brain sections. In females, however, there was an apparent increase in the intensity of immunostaining for SSTR2 and 3 and a slight reduction in the staining for SSTR4. Changes in the subcellular distribution of SSTRs mainly occurred in upper as well as in deeper cortical layers (Fig. 4). As expected, SSTR5 immunoreactivity was undetectable in the brain of KO animals. No immunoreactivity was seen in the presence of primary antibody adsorbed with excess antigen, pre-immune serum in place of primary antibodies or by the omission of primary antibodies (data not shown). Quantitative analysis of SSTR immunoreactive neurons is shown in Fig. 4 (bottom panel).

Changes in the level of expression of brain SST was also analyzed using RIA (Fig. 5). In male animals, deletion of the SSTR5 gene resulted in a 60% decrease of total SST-like immunoreactivity (SST-LI). There were no significant changes in brain SST-LI between female *wt* and KO mice. However, female *wt* mice generally displayed lower levels of brain SST-LI than male animals as was also demonstrated by Southern Blot analysis (Fig. 1).

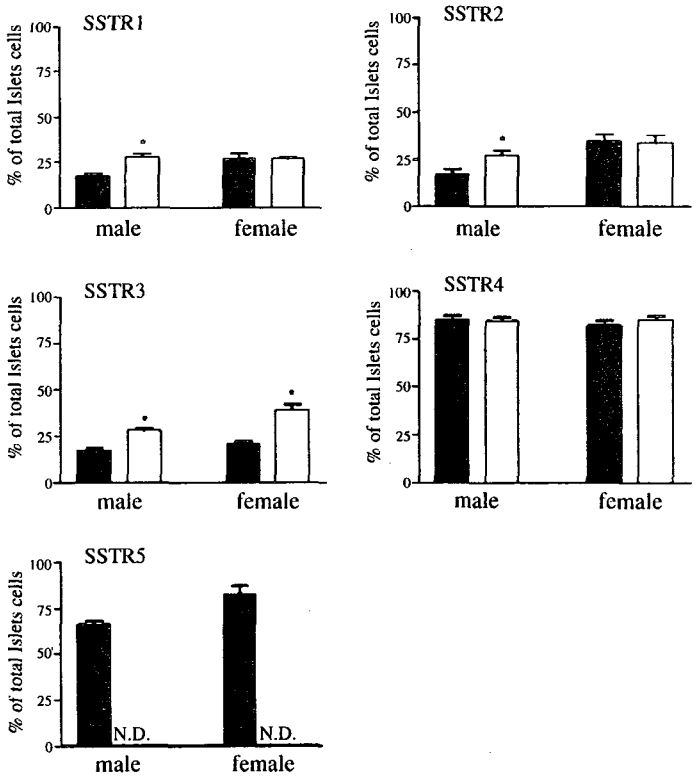

Fig. 7. Quantitative analysis on the expression of SSTR1–5 in pancreatic islet cells. Bars represent the mean ± S.E.M. in percent of cells positive for a given SSTR subtype in respect to total number of islet cells. A total of 8–10 islets were counted per slide in three independent experiments performed in triplicate. $^{*}P < 0.05$; N.D., not detectable.

3.2. Pancreatic expression of SSTR1–5 insulin, glucagon and SST

SSTR expression in pancreas of both *wt* and SSTR5KO mice was illustrated by use of peroxidase immunohistochemistry (Fig. 6a and b). Islets of both sexes displayed SSTR1 and 2 immunoreactivity concentrated mainly in the periphery and to a small extent in some cells scattered within the islet. Females of both genotypes exhibited higher levels of immunostaining for both of these two receptor subtypes than their male counterparts. SSTR3–5 displayed localizations throughout the islets of male mice, with similar patterns of distribution for females save for SSTR3, which was localized mainly in the periphery. Surprisingly, SSTR4 displayed intense staining in the majority of islet cells of both sexes that differed according to human islets (13). An increase in the number of SSTR1 and 2 positive cells was shown in islets of male KO mice however; in female KOs no changes were apparent. The number of SSTR3 positive cells was increased in both sexes of the KO mice, however there were no significant changes in the number of positive cells for SSTR4 (Fig. 7).

Pancreatic SST was analyzed for mRNA expression and SST-LI in whole pancreatic extracts. Islets were additionally analyzed for the expression of insulin, glucagon and SST by semi-quantitative assessment by the identification of fluorescently labeled cells, and quantitatively by morphometry on the positive islet cell types expressed as a percent of the total islet cell population. Both SST mRNA levels (Fig. 8A) as well as SST-LI (Fig. 8B) were selectively reduced in male pancreas from SSTR5KO animals whilst levels in females remained unchanged. Wild-type females showed lower levels of both SST mRNA and SST-LI in comparison to their male counterparts. Immunohistochemical analysis of islet cells revealed a significant decrease in the intensity of insulin and SST immunostaining in male KO mice with only moderate reductions in SST immunostaining in females (Fig. 9). No significant changes were observed in glucagon staining for either sex. Quantitative analysis of the total number of immunopositive cells showed that β-cells represented ~80% of total islet cells whereas α-cells and δ-cells, accounted for ~18% and 8%, respectively (Fig. 10). Lack of the SSTR5 subtype induced a significant decrease in the number of SST positive (Fig. 10A) and insulin positive (Fig. 10B) cells in male islets. The levels of glucagon from both sexes remained the same (Fig. 10C).

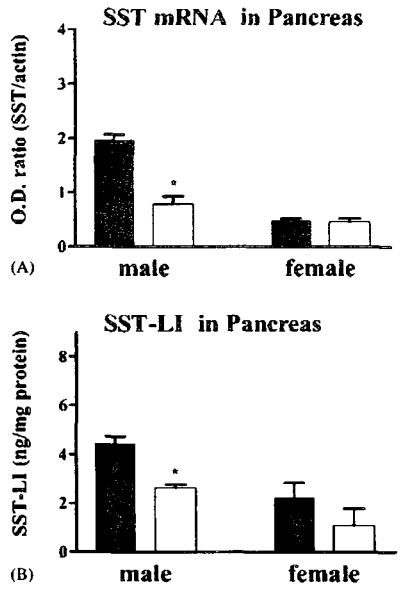

Fig. 8. SST mRNA expression and SST-like immunoreactivity (SST-LI) in pancreas of wild-type (filled columns) and SSTR5KO (open columns) mice. SST mRNA expression was analyzed by semi-quantitative RT-PCR from the pancreas of both sexes and genotypes (A). SST peptide from pancreas homogenate was quantified by RIA as described in the material and methods (B). Mean ± S.E.M. of four independent experiments; $^{*}P < 0.05$.

4. Discussion

Since the initial cloning and pharmacological characterization of SSTR subtypes, there has been some speculation about the physiological significance of the individual receptors in vivo due to their overlapping expression patterns and signaling characteristics. Mice lacking either SSTR1 (Kreienkamp et al., 1999) or SSTR2 (Strowski et al., 2000) have been generated with no aberrant changes in gross morphology. Upon close examination, SSTR1 was shown to be involved in basal growth hormone release while SSTR2 demonstrated to be a critical regulator of glucagon secretion and recently, SSTR5 has been shown to regulate insulin secretion and glucose homeostasis (Strowski et al., 2003; Tirone et al., 2003). However, there is a paucity of literature regarding the sexual dimorphism in the expression patterns of SSTRs and hormones by loss of one of either factor. We have recently shown that somatostatin knock-out (SST-KO) mice exhibited sexual differences in the mRNA expression for SSTR1, 2, and 5 in the pituitary and the hypothalamus (Low et al., 2001). Other hormones such as estrogen have been shown to effect the expression of SSTR2 and 5 in the pituitaries of rats such that SSTR5 is down regulated and SSTR2 is up-regulated (Kimura et al., 1998). Finally, SSTR1 mRNA levels have been shown to up-regulate in the presence of testosterone in male rat pituitaries (Senaris et al., 1996). In the present study, we have demonstrated a sexual dimorphism in the expression patterns of SSTRs and SST in the brains and in the pancreas of both *wt* and SSTR5 deficient mice. Total SST binding sites in the brains of *wt* animals were higher in male compared to female mice. SSTR5 deficiency resulted in an increase in the total SST binding sites in the brains of female KO mice to those comparable to *wt*

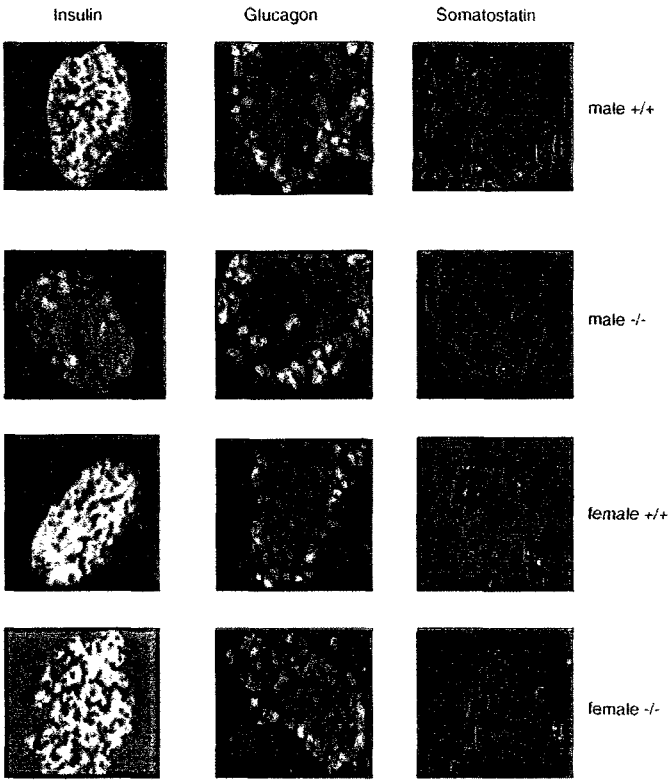

Fig. 9. Immunofluorescent photomicrographs of pancreatic islet cells showing the expression of insulin, glucagon and somatostatin. Insulin and glucagon positive cells were identified by green immunofluorescence (left-hand panels for insulin, middle panels for glucagon) and SST immunoreactivity was localized with red fluorescence (right-hand panels) in both sexes from *wt* and SSTR5KO mice. Magnification 400×.

males, whereas there were no discernable changes amongst male KO mice and their wild-type counterparts. Receptor analysis using RT-PCR, Western blot and immunocytochemistry, have shown that the increase in SST binding sites in the brains of female KO mice was due to an up-regulation of both SSTR2 and 3 despite a down-regulation in SSTR4.

Total SST mRNA and SST-like immunoreactivity by both RT-PCR and RIA analysis, respectively, were lower in the brains of female compared to male *wt* animals. These results are consistent with previous studies of both the rat hypothalamus (Argente et al., 1991; Chowen-Breed et al., 1989) and the hypothalamus and pituitary of mice (Low et al., 2001). Furthermore, SST deficiency resulted in a feminization of hepatic gene expression in male mice due to identical profiles in GH-regulated hepatic mRNAs as seen in females. SST was required for masculinization of the ultradian GH rhythm by suppression of interpulsatory GH levels (Low et al., 2001) consistent with the notion that SST expression is higher in male rather than female mice. Lack of SSTR5 did not result in significant changes in the expression levels of SST in female however; SST was significantly reduced in male KOs. On the other hand, we have previously shown that male SST-KO mice exhibited an up-regulation of SSTR5 in several brain regions (Ramirez et al., 2002) including the pituitary (Low et al., 2001). There may be an underlying relationship between the expression patterns of SST and SSTR5 in the brains of male mice that is absent in females.

In addition to its implication in physiological and pathological processes in the central nervous system, SST is also an important factor in the regulation of pancreatic hormone secretion (Patel, 1999; Reichlin, 1983; Patel et al., 2001). In our study, mouse islets from both sexes expressed all five somatostatin receptor subtypes, in accordance with previously reported studies in the rat and human pancreas (Fehlmann et al., 2000; Kumar et al., 1999; Patel et al., 1995). Although there is no absolute specificity of any SSTR for a given islet cell type (Kumar et al., 1999), it has been proposed that somatostatin inhibition of insulin release is mainly mediated via SSTR5 in rat (Rossowski and Coy, 1994) and mouse (Strowski et al., 2000) and via SSTR1 and 5 in human islets (Kumar et al., 1999), whereas glucagon secretion is primarily regulated via SSTR2 in all the species (Kumar et al.,

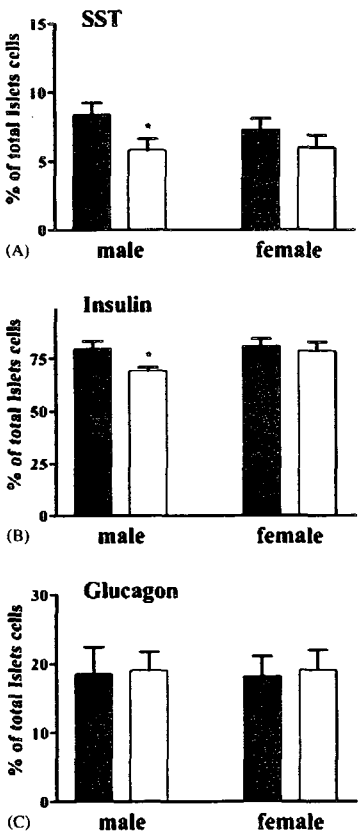

Fig. 10. Immunoquantitative analysis of the expression of SST (A), insulin (B) and glucagon (C) in pancreatic islet cells. Bars represent the mean ± S.E.M. in percent of cells positive for a given pancreatic hormone in respect to the total number of islet cells. A total of 8–10 islets were counted per slide in three independent experiments performed in triplicate. * $P < 0.05$.

1999; Rossowski and Coy, 1994; Strowski et al., 2000). Our immunocytochemical studies demonstrated that SSTR4 is the most abundant SSTR subtype in mouse pancreas, which differs from that previously found in rat and human (Patel, 1999; Kumar et al., 1999; Patel et al., 1995). These data suggest a more important role for SSTR4 in the control of mouse pancreatic functions than previously thought. Furthermore, deficiency in SSTR5 resulted in an up-regulation of immunopositive cells for SSTR1–3 in islets of male mice, whereas in female mice only SSTR3 was up-regulated. In addition, wild-type females presented a higher number of immunostained cells for SSTR1–3 and 5 compared to that of males. As demonstrated by the expression patterns of SSTRs in the brain, the regulation of the somatostatinergic system in the pancreas is also found to be sexually dimorphic.

The SSTR5 deficient condition resulted in a significant reduction in the basal levels of immunodetectable insulin in the pancreas of male mice with a decreased expression of SST. A similar occurrence has also been reported recently by Strowski et al. (2003) upon examination of circulating insulin levels in their SSTR5KO model. On the other hand, cultured islets from SSTR5KO displayed a higher content of insulin when compared to islets from *wt* animals (Strowski et al., 2003). One reason for this discrepancy can be due to the culturing conditions themselves, which introduce a higher than physiologically relevant glucose concentration during incubation, and may possibly mimic a hyperglycemic state as previously mentioned (Zhou et al., 2003). In a report by Tirone et al. (2003) using an isolated perfused pancreas from SSTR5KO mouse, insulin secretion was dysregulated upon glucose stimulation and not in a fasted state. Aside from its role on insulin secretion, other factors may be regulated by SSTR5 including insulin sensitivity and glucose homeostasis as mentioned by Strowski et al. However, what has been reported in male mice may not adequately be reflected in female mice as suggested by our results. This is based on the lack of differences observed in the expression patterns of SST and insulin in the islets of both female *wt* and KO mice. The expression levels for glucagon however, remained the same for both sexes between the two conditions *wt* and SSTR5KO. Further studies are required in order to elucidate the functional role of SSTR5 in pancreas. An example of sexually based differences has been shown for the free fatty acid-induced insulin resistance model in rats (Hevener et al., 2002). In this study, sexual determinants were found between male and female rats that were responsible for female tolerance towards insulin resistance from elevated free fatty acids. We have also reported gender-related differences in the expression of SSTRs in a SST deficient mouse model with changes in growth and stress axes (Low et al., 2001; Ramirez et al., 2002). Therefore, it would be interesting to determine whether our observations in female KO mice correspondingly relate to differences in insulin sensitivity and glucose homeostasis when compared to the male SSTR5KO model described by Strowski et al.

In conclusion, we have demonstrated that SSTR5 deficiency lead to a subtype-selective sexually dimorphic change in the expression patterns of SSTRs in the brain and pancreas of mice. SSTR5 may be important in the regulation of brain and pancreatic SST as well as in the regulation of insulin in male mice. Despite the obvious overlap in the function of SSTRs, this study sheds light on a possible intricate balance between the regulation of somatostatin and its receptors in a subtype-, tissue-, species-, and gender-specific manner that should not be overlooked. Due to the overlapping expressing patterns and compensatory roles amongst SSTRs, double knockouts may be necessary to delineate the subtype-selective and tissue-specific roles for these receptors. However, further studies are required to define the molecular mechanism and physiological consequences of these observations.

Acknowledgements

This work was supported by grants from Canadian Institutes of Health Research (#MT-10411 and #MT-6196). J.L.R. is a Fellow of the Fonds de la Recherche en Sante du Quebec (FRSQ) and Ministerio de Educacion y Cultura (MEC, Spain). We thank M. Correia for secretarial help. This article is dedicated to the memory of Dr. Yogesh C. Patel.

References

Argente, J., Chowen, J.A., Zeitler, P., Clifton, D.K., Steiner, R.A., 1991. Sexual dimorphism of growth hormone-releasing hormone and somatostatin gene expression in the hypothalamus of the rat during development. Endocrinology 128, 2369–2375.

Breder, C.D., Yamada, Y., Yasuda, K., Seino, S., Saper, C.B., Bell, G.I., 1992. Differential expression of somatostatin receptor subtypes in brain. J. Neurosci. 12, 3920–3934.

Bruno, J.F., Xu, Y., Song, J., Berelowitz, M., 1993. Tissue distribution of somatostatin receptor subtype messenger ribonucleic acid in the rat. Endocrinology 133, 2561–2567.

Chowen-Breed, J.A., Steiner, R.A., Clifton, D.K., 1989. Sexual dimorphism and testosterone-dependent regulation of somatostatin gene expression in the periventricular nucleus of the rat brain. Endocrinology 125, 357–362.

Dohlman, H.G., Thorner, J., Caron, M.G., Lefkowitz, R.J., 1991. Model systems for the study of seven transmembrane segment receptors. J. Biol. Chem. 268, 337–341.

Epelbaum, J., Dournaud, P., Fodor, M., Viollet, C., 1994. The neurobiology of somatostatin. Crit. Rev. Neurobiol. 8, 25–44.

Fehlmann, D., Langenegger, D., Schuepbach, E., Siehler, S., Feuerbach, D., Hoyer, D., 2000. Distribution and localization of somatostatin receptor mRNA and binding sites in the brain and periphery. J. Physiol. Paris 94, 265–281.

Feuerbach, D., Fehlmann, D., Nunn, C., Siehler, S., Langenegger, D., Bouhelal, R., Seuwen, K., Hoyer, D., 2000. Cloning, expression and pharmacological localization of the mouse somatostatin SST(5) receptor. Neuropharmacology 39, 1451–1462.

Hevener, A., Reichart, D., Janez, A., Olefsky, J., 2002. Female rats do not exhibit free fatty acid-induced insulin resistance. Diabetes 51, 1907–1912.

Hofland, L.J., Lamberts, S.W.J., Lichtenauer-Kaligis, E.G.R., Waaijers, M., van Koetsveld, P.M., van Hagen, M., Schaeffer, J.M., Krenning, E.P., Breeman, W.A.P., 2000. Somatostatin receptor subtype 2-dependent uptake of [^{111}In-DTPA^{0}] octreotide: studies in SST2 knock out mice. In: Program 82nd Annual Meeting US Endocrine Society. Toronto, p. 188 (Abstract).

Hukovic, N., Panetta, R., Kumar, U., Patel, Y.C., 1996. Agonist-dependent regulation of cloned human somatostatin receptor types 1–5 (hSSTR1–5): subtype selective internalization or upregulation. Endocrinology 137, 4046–4049.

Khare, S., Kumar, U., Sasi, R., Puebla, L., Calderon, L., Lemstrom, K., Hayry, P., Patel, Y.C., 1999. Differential regulation of somatostatin receptor type 1–5 in rat aorta after angioplasty. FASEB J. 13, 387–391.

Kimura, N., Tomizawa, S., Arai, K.N., Kimura, N., 1998. Chronic treatment with estrogen up-regulated expression of SST2 messenger ribonucleic acid (mRNA) but down-regulates expression of SST5 mRNA in rat pituitaries. Endocrinology 139, 1573–1580.

Kong, H., De Paoli, A.M., Breder, C.D., Yasuda, K., Bell, G.I., Reisine, T., 1994. Differential expression of messenger RNAs for somatostatin receptor subtypes SSTR1, SSTR2, and SSTR3 in adult rat brain: analysis by RNA blotting and in situ hybridization histochemistry. Neuroscience 59, 175–184.

Kreienkamp, H.-J., Akgun, E., Baumeister, H., Meyerhof, W., Richter, D., 1999. Somatostatin receptor subtype 1 modulates basal inhibition of growth hormone release in somatotrophs. FEBS Lett. 462, 464–466.

Kumar, U., Laird, D., Srikant, C.B., Escher, E., Patel, Y.C., 1997. Expression of the five somatostatin receptor (SSTR1–5) subtypes in rat pituitary somatotrophes: quantitative analysis by double-immunofluorescence confocal microscopy. Endocrinology 138, 4473–4476.

Kumar, U., Sasi, R., Suresh, S., Patel, A., Thangaraju, M., Metrakos, Patel, S.C., Patel, Y.C., 1999. Subtype-selective expression of the five somatostatin receptors (hSSTR1–5) in human pancreatic islet cells. A quantitative double-label immunohistochemical analysis. Diabetes 48,77–85.

Low, M.J., Otero Corchon, V., Ramirez, J.L., Kumar, U., Patel, Y.C., Rubinstein, M., 2001. Somatostatin is essential for sexual dimorphism of growth and stress axes. J. Clin. Invest. 107, 1571–1580.

Meyerhof, W., Wulfsen, I., Schonrock, C., Fehr, S., Richter, D., 1992. Molecular cloning of a somatostatin-28 receptor and comparison of its expression pattern with that of somatostatin-14 receptor in rat brain. Proc. Natl. Acad. Sci. U.S.A 89, 10267–10271.

Moldovan, S., DeMayo, F., Brunicardi, F.C., 1998. Cloning of the mouse *SSTR5* gene. J. Surg. Res. 76, 57–60.

Patel, Y.C., Reichlin, S., 1978. Somatostatin in hypothalamus, extrahypothalamic brain and peripheral tissues of the rat. Endocrinology 102, 523–530.

Patel, Y.C., Greenwood, M.T., Panetta, R., Demchyshyn, L., Niznik, H., Srikant, C.B., 1995. The somatostatin receptor family: a mini review. Life Sci. 57, 124–1265.

Patel, Y.C., Liu, J.L., Galanopoulou, A., Papachristou, D.N., 2001. Production, action, and degradation of somatostatin. In: Jefferson, L.S., Cherrington, A.D. (Eds.) The Handbook of Physiology, The Endocrine Pancreas and Regulation of Metabolism. Oxford University Press, NY, pp. 267–302.

Patel, R.C., Kumar, U., Lamb, D.C., Eid, J.S., Rocheville, M., Grant, M., Rani, A., Hazlett, T., Patel, S.C., Gratton, E., Patel, Y.C., 2002. Ligand binding to somatostatin receptors induces receptor-specific oligomer formation in live cells. Proc. Natl. Acad. Sci. U.S.A 99, 3294–3299.

Patel, Y.C., 1992. General aspect of the biology and function of somatostatin. In: Weil, C., Muller, E.E., Thorner, M.O. (Eds.), Basic and Clinical Aspects of Neuroscience. Springer-Verlag, Berlin, vol. 4, pp. 1–16.

Patel, Y.C., 1997. Molecular pharmacology of somatostatin receptor subtypes. J. Endocrinol. Invest. 20, 348–367.

Patel, Y.C., 1999. Somatostatin and its receptor family. Frontiers Neuroendocrinol. 20, 157–198.

Ramirez, J.L., Mouchantaf, R., Kumar, U., Otero Corchon, V., Rubinstein, M., Low, M.J., Patel, Y.C., 2002. Brain somatostatin receptors are upregulated in somatostatin deficient mice. Mol. Endocrinol. 16 (8), 1951–1963.

Reichlin, S., 1983. Somatostatin. N. Engl. J. Med. 309, 1495–1501.

Rocheville, M., Lange, D.C., Kumar, U., Sasi, R., Patel, R.C., Patel, Y.C., 2000. Subtypes of the somatostatin receptor assemble as functional homo- and heterodimers. J. Biol. Chem. 275, 7862–7869.

Rossowski, W.J., Coy, D.H., 1994. Specific inhibition of rat pancreatic insulin or glucagon release by receptor-selective somatostatin analogs. Biochem. Biophys. Res. Commun. 250, 341–346.

Senaris, R.M., Lago, F., Dieguez, C., 1996. Gonadal regulation of somatostatin receptor 1, 2 and 3 mRNA in the rat anterior pituitary. Brain Res. Mol. Brain Res. 38 (1), 171–175.

Strowski, M.Z., Parmar, R.M., Blake, A.D., Schaeffer, J.M., 2000. Somatostatin inhibits insulin and glucagon secretion via two receptor subtypes: an in vitro study of pancreatic islet from somatostatin receptor 2 knock-out mice. Endocrinology 141, 111–117.

Strowski, M.Z., Kohler, M., Chen, H.Y., Trumbauer, M.E., Li, Z., Szalkowski, D., Gopal-Truter, S., Fisher, J.K., Schaeffer, J.M., Blake, A.D., Zhang, B.B., Wilkinson, H.A., 2003. Somatostatin receptor sub-

type 5 regulates insulin secretion and glucose homeostasis. Mol. Endocrinol. 17, 93–106.

Thoss, V.S., Perez, J., Probst, A., Hoyer, D., 1996. Expression of five somatostatin receptor mRNAs in the human brain and pituitary. Arch. Pharmacol. 354, 411–419.

Tirone, T.A., Norman, M.A., Moldovan, S., Demayo, F.J., Wang, X.P., Brunicardi, F.C., 2003. Pancreatic somatostatin inhibits insulin secretion via SSTR-5 in the isolated perfused mouse pancreas model. Pancreas 26, e67–e73.

Zhang, W.-H., Beaudet, A., Tannenbaum, G.S., 1999. Sexually dimorphic expression of SST1 and SST2 somatostatin receptor subtypes in the arcuate nucleus and anterior pituitary of adults rats. J. Neuroendocrinol. 11, 129–136.

Zhou, Y.-P., Marlen, K., Palma, J.F., Schweitzer, A., Reilly, L., Gregoire, F.M., Xu, G.G., Blume, J.E., Johnson, J.D., 2003. Overexpression of repressive cAMP response element modulators in high glucose and fatty acid-treated rat islets. J. Biol. Chem. 278, 51316–51323.

Ligand binding to somatostatin receptors induces receptor-specific oligomer formation in live cells

Ramesh C. Patel*†‡, Ujendra Kumar*‡, Don C. Lamb§, John S. Eid§, Magalie Rocheville*, Michael Grant*, Aruna Rani*, Theodore Hazlett§, Shutish C. Patel¶, Enrico Gratton§, and Yogesh C. Patel*‖

*Fraser Laboratories, Departments of Medicine, Pharmacology, and Therapeutics and Neurology and Neurosurgery, McGill University, and Royal Victoria Hospital, Montreal, QC, Canada H3A 1A1; †Department of Chemistry and Physics, Clarkson University, Potsdam, NY 13699, and Neural Connections, Potsdam, NY 13676; §Fluorescence Dynamics Laboratory, University of Illinois, Champaign-Urbana, IL 61801-3080; and ¶New England Biomedical Research Center, Newington, CT 06111

Communicated by Susan E. Leeman, Boston University School of Medicine, Boston, MA, December 27, 2001 (received for review October 2, 2001)

Heptahelical receptors (HHRs) are generally thought to function as monomeric entities. Several HHRs such as somatostatin receptors (SSTRs), however, form homo- and heterooligomers when activated by ligand binding. By using dual fluorescent ligands simultaneously applied to live cells monotransfected with SSTR5 (R5) or SSTR1 (R1), or cotransfected with R5 and R1, we have analyzed the ligand receptor stoichiometry and aggregation states for the three receptor systems by fluorescence resonance energy transfer and fluorescence correlation spectroscopy. Both homo- and heterooligomeric receptors are occupied by two ligand molecules. We find that monomeric, homooligomeric, and heterooligomeric receptor species occur in the same cell cotransfected with two SSTRs, and that oligomerization of SSTRs is regulated by ligand binding by a selective process that is restricted to some (R5) but not other (R1) SSTR subtypes. We propose that induction by ligand of different oligomeric states of SSTRs represents a unique mechanism for generating signaling specificity not only within the SSTR family but more generally in the HHR family.

Heptahelical receptors (HHRs) constitute the largest single family of transmembrane signaling molecules that respond to diverse external stimuli such as hormones, neurotransmitters, chemoattractants, odorants, and photons. Although these receptors have been generally thought to function as monomeric entities, there is growing evidence that a number of HHRs assemble as functional homo- and heterooligomers (1, 2). Dimerization seems to be necessary for function of the class C subfamily of HHRs comprising the metabotropic glutamate, calcium sensing, the GABAB, and pheromone receptors that are targeted to the plasma membrane as preformed dimers which are stabilized by ligand binding (3–7). Several HHRs such as somatostatin receptors (SSTRs), dopamine receptors, gonadotrophin-releasing hormone receptor (GnRHR), luteinizing hormone/chorionic gonadotrophin hormone receptor, and chemokine receptors, however, which belong to the rhodopsin-like class A subfamily of HHRs, assemble on the membrane as homo- and heterooligomeric species in response to agonist activation (8–15).

In the case of SSTRs, we have shown by photobleaching fluorescence resonance energy transfer (pbFRET) that the human (h) type 5 receptor (hSSTR5 or R5) exists in the basal state as a monomer, and that activation by ligand induces dose-dependent oligomerization (8). When coexpressed with another SSTR (hSSTR1 or R1) or an unrelated HHR such as the dopamine 2 receptor (D_2R), R5 also forms a heterooligomer that displays pharmacological properties distinct from those of either of the separate receptors (9). Little is known about the stoichiometry of ligand-receptor reactions or the specificity for homo- and heterooligomeric interactions between two receptors that are coexpressed in the same cell. By using dual fluorescent ligands simultaneously applied to live cells monotransfected with R5 or R1, or cotransfected with R5 and R1, we have analyzed the ligand-receptor stoichiometry and aggregation states for the three receptor systems by FRET and fluorescence correlation spectroscopy (FCS). We demonstrate the presence of monomeric, homooligomeric, and heterooligomeric receptor species in the same cell cotransfected with two SSTRs. We show that both homo- and heterooligomeric receptors are occupied by two ligand molecules, and that oligomerization of SSTRs is regulated by ligand binding by a selective process that is restricted to some (R5) but not other (R1) SSTR subtypes.

Methods

Peptides and Antisera. SST-14, SST-28, and [Leu (8)-D-Trp-22, Tyr-25] SST-28 (LTT-SST-28) were obtained from Peninsula Laboratories. Anti-hemagglutinin (HA) mouse mAb (12CA5) and fluorescein- and rhodamine-conjugated mAbs against HA were from Roche Molecular Biochemicals. Rabbit polyclonal Ab directed against the NH_2-terminal segment of hR1 was produced and characterized as described (16).

SSTR-Expressing Cells. Stable Chinese hamster ovary (CHO)-K1 cells expressing HA-R5, wild-type (wt) R1, or coexpressing HA-R5/wt R1 were prepared by lipofectin transfection as described (8).

Fluorescent SST Ligands and Binding Studies. Fluorescent SST ligands were prepared by N-terminal conjugation of SST-14 to FITC and Texas red (TR) followed by HPLC separation (17, 18). Radioligand binding studies were carried out by reacting [^{125}I-LTT] SST-28 for 30 min at 37°C with cell membrane protein as reported (8, 9).

pbFRET. pbFRET analysis was performed as described (8, 9, 19). The effective FRET efficiency E was calculated from the pb time constants of the donor obtained in the absence (D − A) and presence (D + A) of acceptor according to $E = 1 - (\tau_{D\text{-}A}/\tau_{D+A})$. CHO-K1 cells stably cotransfected with HA-R5 or R1 were grown on glass coverslips for 24 h, treated with SST-14 for 30 min at 37°C, and fixed and processed for immunocytochemistry. HA-R5 and R1 were specifically labeled with FITC and rhodamine, respectively, by using mouse monoclonal HA Abs and rabbit polyclonal R1 Ab followed by reaction with conjugated secondary Abs. Both reactions resulted in specific plasma membrane staining. The pb decay was analyzed for the plasma membrane region on a pixel by pixel basis as well as averaged over the entire image. Image analysis procedures and instrumental setup are described in ref. 8.

Abbreviations: HHR, heptahelical receptor; SSTR, somatostatin receptor; pbFRET; photobleaching fluorescence resonance energy transfer; FCS, fluorescence correlation spectroscopy; HA, hemagglutinin; CHO, Chinese hamster ovary; TR, Texas red; GP, generalized polarization.

‡R.C.P. and U.K. contributed equally to this work.

‖To whom reprint requests should be addressed. E-mail: yogesh.patel@mcgill.ca.

The publication costs of this article were defrayed in part by page charge payment. This article must therefore be hereby marked "*advertisement*" in accordance with 18 U.S.C. §1734 solely to indicate this fact.

www.pnas.org/cgi/doi/10.1073/pnas.042705099

FRET Analysis by Single-Photon Excitation. CHO-K1 cells expressing SSTRs were cultured in chamber slides, treated with fluorescent SST ligands, and examined directly. One-photon experiments were performed by using the 488-nm output of an argon-ion laser coupled to an Olympus (New Hyde Park, NY) 1× 70 epifluorescence microscope with confocal optics. The resulting emission was separated spectrally and detected on two avalanche photodiodes. The sample was scanned through the excitation volume by using a Piezo scanner (Physik Instrumente, Karlsruhe/Palmbach, Germany), and an image was recorded. The resolution of the system is determined by the width of the point-spread function of the laser (~500 nm for the measurements presented here). Each pixel represents a movement of the sample of ~200 nm. Variations in the relative intensity of TR and FITC fluorescence were observed by plotting a generalized polarization (GP) image (20). GP is determined as $GP = (I_1 - I_2)/(I_1 + I_2)$, where I_1 and I_2 are the intensities of channel 1 (TR) and 2 (FITC), respectively. The GP image was obtained by performing this operation on each pixel of the two-channel image. The GP value ranges from −1 to +1, reflecting the relative intensity of each channel (−1 and +1 correspond to signal from only the FITC and TR channels, respectively, and being a ratio is independent of intensity). Changes in GP can arise from (*i*) changes in the ratio of the labeled ligands, (*ii*) changes in the molecular brightness of either fluorophore, or (*iii*) changes in the FRET efficiency between the fluorescent labels. Different information can be obtained from the GP image depending on which process is dominant. A change in ligand concentration cannot lead to a change in GP because the GP function is defined to be intensity independent; a change in the ratio of labeled ligands can (but does not necessarily have to) lead to a change in GP. Because direct excitation of the acceptor is negligible, changes in the ratio of donor- and acceptor-labeled ligands cannot cause changes in GP. Furthermore, we have no evidence for changes in the molecular brightness of the fluorophores and thus attribute changes in the GP to variations in the FRET efficiency of the labeled ligands. To correctly determine the FRET efficiency in the presence of direct TR excitation, the relative intensity of the two channels in the absence of FRET was taken to be the GP value measured in buffer where the ligands do not dimerize.

Fluorescence Correlation Spectroscopy. CHO-K1 cells expressing SSTRs were cultured in chamber slides, treated with dual fluorescent SST ligands, and analyzed directly for FCS (21, 22). A mode-locked Ti-Sapphire laser, which generated ~100 fsec-wide pulses at an 80-MHz frequency, was used as an efficient two-photon excitation light source directed by means of a Zeiss microscope to a confocal sample volume. The resulting fluorescence was spectrally separated by two avalanche photodiodes. The general equation for the normalized correlation function expressing the level of correlation between two photons separated by a time τ is given by

$$G_{ij}(\tau) = \frac{\delta F_i(t)\,\delta F_j(t+\tau)}{\langle F_i(t)\rangle\,\langle F_j(t)\rangle}, \qquad [1]$$

with $i = j$ for autocorrelation and $i \neq j$ for cross correlation. $F(t)$ is the fluorescence intensity at time t, and the $\langle\ \rangle$ indicate time averaging (23). At $\tau = 0$ [i.e., G (0), the y intercept of an FCS curve], the autocorrelation is inversely proportional to the average number of fluorescent particles. For τ approaching infinity, the above equation should vanish because the temporal separation of the two photons is large enough that there is no longer any correlation between them. Because the excitation volume is known, the correlation resulting from the time it takes for a dye to cross this volume intrinsically yields a diffusion coefficient. In addition, any property that causes fluctuations in the fluorescence intensity of the dye at a rate fast enough to occur during the fraction of time when the dye is in the excitation volume should be observable in the autocorrelation function.

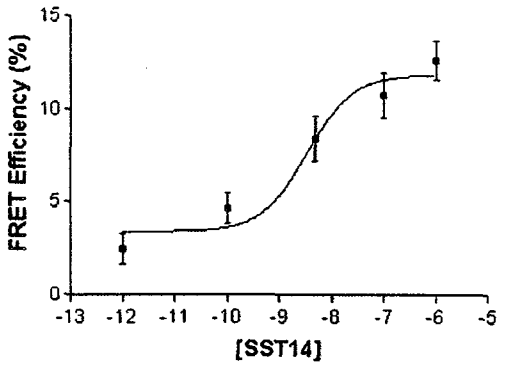

Fig. 1. pbFRET analysis of R5/R1 receptors. Dose-dependent increase in effective FRET efficiency induced by treatment with SST-14 of CHO-K1 cells coexpressing HA-R5 and wild-type R1. CHO-K1 cells were treated with increasing concentrations of SST-14 for 30 min at 37°C and analyzed for pbFRET by using FITC-labeled mouse monoclonal anti-HA Abs and rabbit polyclonal R1 Ab directed against the receptor N-terminal segment followed by reaction with rhodamine-conjugated secondary Ab. Thirty to forty cells were analyzed for each experimental condition.

Results

Ligand-Dependent Oligomerization of SSTRs: Analysis by pbFRET. To study SSTR homooligomers, we expressed R5 at low levels in CHO-K1 cells (B_{max} 160 ± 30 fmol/mg of protein; K_d 1.1 ± 0.2 nM for SST-14 binding) by stable transfection of R5 tagged at the NH_2 terminus with the nonapeptide of HA (8). By pbFRET, using fluorescein (donor)- and rhodamine (acceptor)-labeled monoclonal anti-HA Abs, we have shown that in the absence of ligand, the receptor expressed in these cells displays low effective FRET efficiency consistent with a monomeric state (8). Addition of SST-14 induces a dose-dependent increase in FRET (EC_{50} 3.9 ± 2.8 nM) (8). Treatment of live R5 cells with the dual fluorescent anti-HA Abs for 4 h did not result in any observable FRET, indicating that NH_2-terminal Ab binding to the receptor does not induce aggregation in the absence of SST ligand. To characterize SSTR heterooligomers, we stably coexpressed HA-R5 with wild-type R1 in CHO-K1 cells. Membrane-binding analysis with the common radioligand [^{125}I-LTT] SST-28 gave a B_{max} of 250 ± 19 fmol/mg of protein and a K_d of 0.65 ± 0.12 nM for SST-14 binding. Physical association of the two receptors to form heterooligomers was demonstrated by pbFRET microscopy (8, 9). As in the case of R5 homooligomers, we found a low relative FRET efficiency in the basal state reflecting a low level of preformed heterooligomers (Fig. 1). Treatment with SST-14 induced dose-dependent increase in FRET efficiency with a maximum of 12.6 ± 1.0% at 10^{-6} M (EC_{50} 3.4 ± 2.1 nM), indicating agonist-induced microaggregation (physical association within 100–120 Å) of the two receptors to form a heterooligomer.

FRET Analysis of Interaction of SSTR Oligomers with Dual Fluorescent Ligands. To determine whether SSTR oligomers interact with two ligand molecules, we used a single-photon confocal system with two-channel detection (channel 1 for TR and channel 2 for FITC) for direct FRET analysis by using two fluorescent ligands, SST-FITC and SST-TR. The two ligands were simultaneously

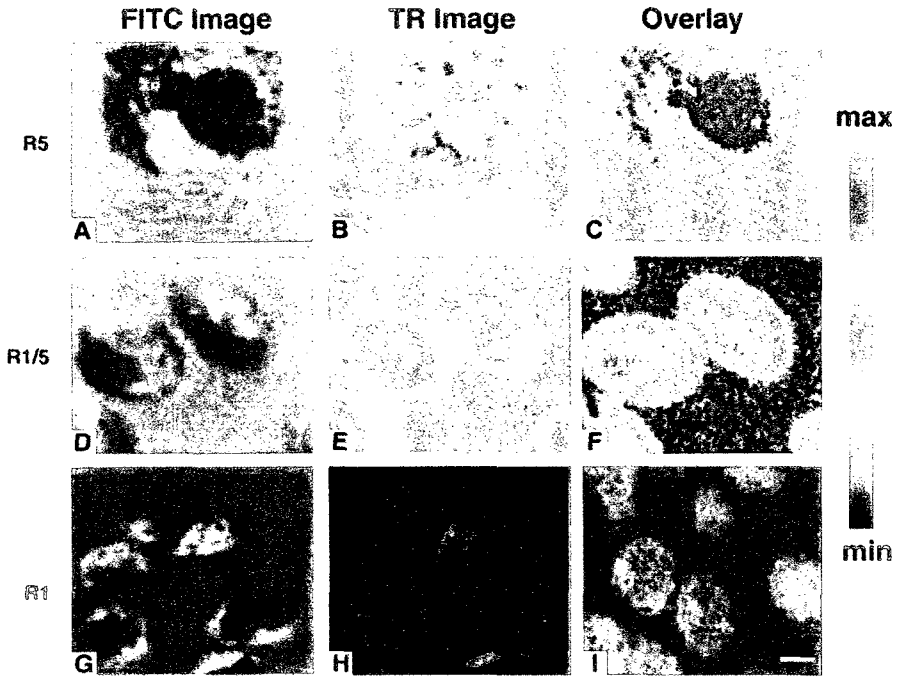

Fig. 2. FRET analysis of dual-fluorescent SST ligands interacting with R5, R5/R1, and R1 in live cells. The FITC fluorescence emission (*Left*), TR fluorescence emission (*Center*), and GP image (*Right*) are shown for CHO-K1 cells individually transfected with R5 (*Top*), coexpressing R5/R1 (*Middle*), or R1 (*Bottom*). The GP image was calculated on a pixel by pixel basis from the FITC and TR images as described (18). The R5 and R5/R1 cells were measured by using single-photon excitation, and the R1 cells were measured with two-photon excitation. [Bar = 10 μm (*A–C*) and 25 μm (*D–I*).]

applied at low concentrations (SST-FITC ~ 12–15 nM, SST-TR ~ 5 nM) to cultured CHO-K1 cells stably expressing HA-R5, and signals from both channels were recorded 1–2 min later. The relative intensities of the two fluorescent labels were calculated for individual pixels in given areas of the cell membrane and expressed quantitatively as GP. Confocal images of R5/CHO-K1 cells treated with SST-FITC and SST-TR revealed specific labeling and colabeling of plasma membrane receptors by the two ligands (data not shown). Selective FITC excitation at 488 nm resulted in energy transfer from FITC to TR, and hence, a quenching of the FITC signal and associated increase in the TR emission (Fig. 2*A* and *B*). The GP images obtained (Fig. 2*C*) reveal a highly structured but uneven pattern over the cell surface with the red areas corresponding to regions of high FRET efficiency.

The results of single-photon experiments with the dual fluorescent SST-FITC and SST-TR ligands applied to HA-R5/R1 cell cotransfectants are depicted in Fig. 2 *D–F*. Confocal images showed specific labeling of plasma membrane receptors by both ligands (data not shown). As in the case of HA-R5, GP analysis of R5/R1 cell cotransfectants after simultaneous application of the two fluorescent ligands showed strong TR emission from channel 1 after FITC excitation (Fig. 2 *D* and *E*). The GP image (shown in red) over the cell surface for the R5/R1 heterooligomer is uneven comparable to that of the R5/R5 homooligomer, but with noticeably reduced GP values (Fig. 2*F*).

The histogram of GP values for Fig. 2 *C* and *F* masked via intensity to include only the membrane region of the cell are shown in Fig. 3*A*. Analysis of the membrane region revealed a broad monophasic curve for the R5 homooligomer with a relatively high mean GP value of 0.75. The GP distribution for the R5/R1 heterooligomer showed a bimodal curve comprising a major peak, with a mean GP value of 0.45, and a smaller peak with a mean GP value of 0.75, overlapping the single peak obtained with the R5 homooligomer. A distribution of GP values in the histogram arises from variations in the number of monomeric, homooligomeric, and (when relevant) heterooligomeric receptors within each pixel. Although the absolute GP value can be affected by direct excitation of the acceptor, crosstalk of the donor in the acceptor channel, and fluorescent background, it should be stressed that these results depend on the shape of the GP distribution function and the relative GP values of the two measurements. Provided the amount of direct excitation, background, and crosstalk are known, FRET efficiency can still be calculated. That FRET is observed between the two ligands implies they are in close proximity to each other (24, 25). The Förster distance for the FITC/TR donor-acceptor pair is Ro ≅ 50 Å with an uncertainty of about 5%. Hence, the homo- and the heterooligomer must be occupied by the two fluorescent ligand molecules, and the ligands must reside within 100 Å of each other. In view of the limitations and uncertainties in determination of the donor-acceptor separation, we roughly estimate the distance between the two fluorophores in the R5 homooligomer to be ~50 Å, and approximately 60 Å in the case of the R5/R1 heterooligomer (24, 25). Furthermore, the biphasic distribution plot obtained for the R5/R1 cotransfectants suggests a mixed

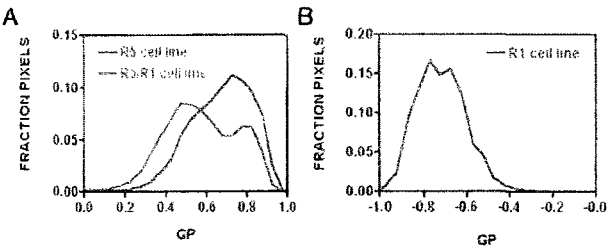

Fig. 3. Calculated FRET efficiencies for R5, R5/R1, and R1 cell lines. Normalized histograms of GP values occurring in the cell portion of the GP images in Fig. 2 *C*, *F*, and *I* are plotted. The cellular portion of the image was determined by visual assessment. The GP value is a measure of fractional intensity. A GP value of −1, 0, and 1 corresponds to signal entirely in the FITC channel, equally split between the two channels, or entirely in the TR channel, respectively. (*A*) Histogram of the R5 (red line)- and R5/R1 (green line)-transfected cell lines. Only pixels above a certain threshold intensity in the TR channel were included in the histogram to investigate the cell portion of the GP images. (*B*) Histogram of GP values for R1-transfected cell lines.

population of both R5/R1 heterooligomers and R5/R5 homooligomers in the same cells.

Although these results confirm the theoretical prediction that cotransfection of R5 with another SSTR subtype to produce a heterooligomer should also result in a population of R5 homooligomers, we were surprised not to see a third peak in the GP distribution plot of the R5/R1 cotransfectants corresponding to R1 homooligomers. This finding could be the result of an absence of R1 homooligomers or an R1 homooligomer peak that overlaps the R5/R5 or R5/R1 peaks detected. To distinguish between these two possibilities, direct studies were carried out in CHO-K1 cells monotransfected with R1 (B_{max} 229 ± 10 fmol/mg of protein; K_d 0.62 ± 0.13 nM for SST-14). We first conducted pbFRET analysis of HA-R1 stably expressed in CHO-K1 cells with fluorescein- and rhodamine-conjugated monoclonal HA Abs. We obtained effectively no energy transfer both in the absence (1.1 ± 1.1%) and presence (1.0 ± 0.7%) of SST-14 (10^{-6} M), indicating that unlike R5, R1 exists only as a monomer in these cells. This result was confirmed by two-photon experiments with the dual fluorescent SST ligands, which showed that although both ligands were specifically colocalized on the plasma membrane (data not shown), there was no TR emission after FITC excitation (Fig. 2 *G* and *H*). GP analysis revealed a monophasic curve with a negative GP value consistent with the absence of FRET between the two ligands (Figs. 2*I* and 3*B*).

FCS Analysis of SSTR Oligomers. Although FRET represents a powerful tool for probing dimer formation, it is less effective for analyzing monomeric species and for ligand-induced aggregation that extends beyond dimerization to oligomer formation. To address these issues, we applied two-photon dual color FCS with auto- and crosscorrelation analysis as described (21). With this method, a discrimination based on molecular size, number density, and average brightness/particle can be analyzed from experimental parameters totally independent of FRET. By using this technique, a sharply focused laser beam illuminates a femtoliter confocal volume in live cells, and emitted light quanta from single molecules are detected over time via a scanning dual channel two-photon system (21–23). Fluctuations in fluorescence intensity caused by translational and rotational diffusion, chemical reactions, and conformational changes of the molecules are revealed by autocorrelation analysis. In addition, fluorescence crosscorrelation analysis can be used to detect only those molecules that carry two different fluorophores so as to monitor oligomerization and aggregation. The maximum amplitude of the crosscorrelation function $G_{1\,2}$ (0) is directly proportional to the concentration of double-labeled molecules (23). Independent diffusion of two unattached different color-labeled ligands into the open two-photon volume will not contribute to the crosscorrelation, because these events are random and vanish when averaged.

Fig. 4*A* depicts a computer-simulated theoretical crosscorrelation analysis that would result from a purely monomeric sample. The simulations were performed by using the "Monte Carlo in a Grid" algorithm (26). The parameters selected were closely matched to those analyzed experimentally except for the number of particles, which was chosen to be much smaller than the experimental value to speed up the simulation time. The sole effect of this discrepancy is that the overall magnitude of the autocorrelation and crosscorrelation curves is larger in the simulation compared with the experiment. Therefore, to compare the results of the simulation to the experiment, the ratio of the crosscorrelation amplitude to that of the autocorrelation was used. The simulated minimum $G_{1\,2}$ (0)/G_1 (0) value obtained (0.22) is greater than 0 only because unavoidable color leakage creates a background level of crosstalk between the two channels (Fig. 4*A*). Simulated crosscorrelation analysis for a purely dimeric sample yields a maximum $G_{1\,2}$ (0)/G_1 (0) ratio of 0.71 (Fig. 4*B*). These values match very well with theoretical expectation. The experimental values should lie somewhere between these two extremes, because both monomeric and dimeric species are expected to be present. Consequently, for any given pair of experimental autocorrelation curves a maximum and minimum crosscorrelation value can be calculated by using simulation.

To determine the oligomerization status of R1, R5, and R5/R1 receptors, SST-FITC and SST-TR (5–15 nM) were applied to live CHO-K1 cells expressing R1 or R5, or coexpressing R5/R1 and FCS autocorrelation curves derived from selected cell regions (Fig. 5). Unlike the well defined curves obtained for the fluorescent ligands in solution (data not shown), sampling of different membrane regions from all three cell lines revealed a variation in FCS autocorrelation curves (shown in green and red) corresponding to a heterogeneous distribution of diffusion constants (Fig. 5 *B* and *D*). Crosscorrelation analysis (black curves) gave $G_{1\,2}$ (0) values of 0.02 for the R1 and 0.07 for the R5/R1-expressing cells. More importantly, the R5/R1-expressing cells displayed a greater crosscorrelation relative to the simulated boundaries (represented by the horizontal blue lines in Fig. 5 *B* and *D*) than the R1-expressing cells, suggesting a higher level of dimerization/oligomerization for R5/R1 compared to R1 (Fig. 5 *B* and *D*). In the case of R5, we were unable to obtain sufficiently noise-free curves to enable a crosscorrelation calculation, possibly because of the presence of a heterogeneous and highly aggregated system. Overall, these results are in agreement with our FRET data showing progressively increasing oligomer formation from R1 to R5/R1 and (probably) R5.

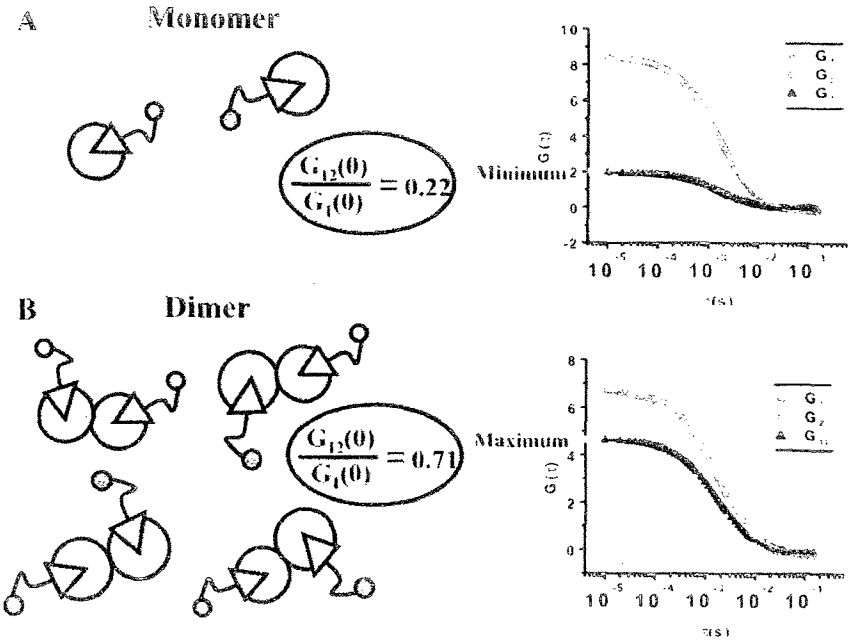

Fig. 4. Theoretical auto- and crosscorrelation FCS curves for monomeric and dimeric receptor species derived by using a Monte Carlo in a Grid simulation adapted to FCS measurements (using the SIMFCS program written by E.G.). The two-channel autocorrelation curves shown in green and red are coincident because the number of particles simulated was equally divided between the two species. (*A*) For the monomer case, the ratio of $G_{12}(0)$ (crosscorrelation curve shown in black) to $G_1(0)$ should theoretically be zero but shows a finite minimum value because of the crosstalk between the two channels. (*B*) The curves for the dimeric case reveal the maximum possible ratio of $G_{12}(0)$ to $G_1(0)$. These two scenarios set the minimum and maximum ratios for the set of experimental conditions simulated.

Discussion

By using three independent techniques, we present conclusive evidence that membrane SSTRs exist in the basal state as a monomeric species, and that activation by ligand induces both homo- and heterooligomerization. In the case of R5, our FRET and FCS results suggest that ligand binding triggers a receptor-clustering process in the cell membrane that extends beyond dimers to higher order oligomers. A similar model of ligand-induced microaggregation has been proposed for the gonadotropin-releasing hormone receptor based on Ab crosslinking and pb recovery experiments (10, 27). It is possible that ligand-bound R5 clusters aggregate in membrane rafts similar to the reported association of receptors for IgA, epidermal growth factor, and tissue factor, which have been shown to selectively associate with such membrane microdomains (28).

In contrast to R5, R1 did not form a homooligomer. Because this receptor binds and signals effectively when expressed as a monotransfectant, this means that a monomeric SSTR can be active and that homooligomerization is not an obligatory requirement for activation of all SSTRs (29). Interestingly, unlike other SSTRs, R1 is resistant to agonist-induced endocytosis but is instead up-regulated at the membrane in response to continued agonist exposure (29). Whether this or another property is linked to the inability of R1 to form homooligomers remains to be determined. We speculate that ligand-induced conformational change does not expose a hydrophobic interface, which can facilitate dimer formation in the case of R1. The observation that this receptor remains monomeric provides an important reference point against which precise molecular parameters such

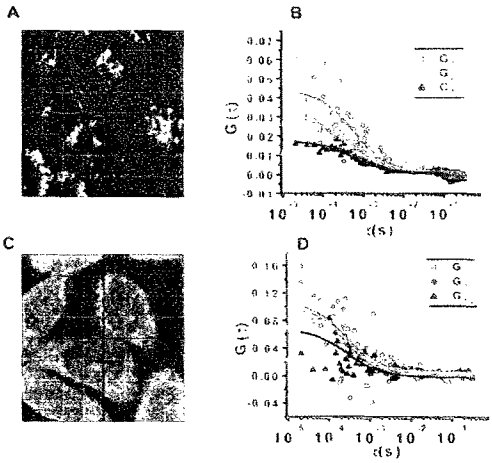

Fig. 5. Experimentally derived auto- and crosscorrelation curves from live R1- and R5/R1-expressing CHO-K1 cells using dual-color two-photon FCS. (*A* and *C*) The spots sampled are marked by a pink cross. (*B* and *D*) Autocorrelation curves are shown in red and green, and crosscorrelation is shown in black. The R5/R1-expressing cells have a greater crosscorrelation relative to the simulated boundaries (represented by the horizontal blue lines on the *y* axis) than the R1-expressing cells, indicating a higher level of dimer/oligomer formation.

as aggregation kinetics, conformational states, and translational/rotational diffusion can be evaluated and compared with an oligomeric receptor such as R5 in live cells. Interestingly, although R1 did not form a homooligomer when expressed alone, it did associate with R5 as a heterooligomer when coexpressed with this receptor. Although the precise receptor domains that dictate such specificity for oligomerization remain to be elucidated, our distance estimates showing that the relative distance between the two ligand molecules in the ligand-bound form of the R5/R1 heterooligomer is greater than the distance between the same two ligand molecules in the R5 homooligomer suggests that the R5 homooligomer is a more compact structure than the R5/R1 heterooligomer, assuming that clusters with the same stoichiometry are compared. In this particular system, the GP data suggest a relationship between the proximity of binding sites and ease of dimer formation. The use of fluorescent ligands to probe distance relationships at the nanometer level provides a powerful approach that could be extended to other HHR oligomeric combinations to test the general validity of this observation.

Concerning ligand-receptor stoichiometry, we have described pharmacological evidence for the interaction of one ligand per receptor oligomer based on functional complementation of two partially active R5 mutants where only one of the mutants is binding competent, by functional complementation of a signaling-deficient R5 mutant with R1 by using a selective agonist that binds to only one of the two receptors, and by demonstrating that either SST or dopamine induces heterodimerization of R5 with the D2 receptor (8, 9). On the other hand, the finding that the R5/D2R heterooligomer displays enhanced signaling when simultaneously activated by both SST and dopamine ligands provides pharmacological evidence for the occupancy of the heterooligomer by two ligand molecules (9). Here we provide direct evidence with FRET that activated R5 homooligomers and R5/R1 heterooligomers interact with two ligand molecules. The association of SSTR homo- and heterooligomers with two ligand molecules is comparable to the model revealed by the crystal structure of the extracellular domain of the metabotropic glutamate receptor whose active form has binding sites for two glutamate molecules (6). Overall, our model suggests that a single ligand molecule is sufficient to trigger oligomerization but that a second physical state exists in which the oligomer is occupied by two ligand molecules. Functionally, the induction by ligand binding of different oligomeric states of SSTRs with different rates of lateral diffusion in the plasma membrane may be a mechanism for generating signaling specificity not only within the SSTR family but more generally in the HHR family.

We thank M. Correia for secretarial help. This study was supported by National Institutes of Health Grants NS32160 and NS34339 and by Canadian Institutes of Health Research Grant MOP-10411. Y.C.P. is a Distinguished Scientist of the Canadian Institutes of Health. M.R. is supported by a studentship from the Fonds de la Recherche en Sante du Quebec (FRSQ).

1. Milligan, G. (2001) *J. Cell Sci.* **114,** 1265–1271.
2. Salahpour, A., Angers, S. & Bouvier, M. (2000) *Trends Endocrinol. Metab.* **11,** 163–168.
3. Marshall, F. H., Jones, K. A., Kaupmann, K. & Bettler, B. (1999) *Trends Pharmacol. Sci.* **20,** 396–399.
4. Herrada, G. & Dulac, C. (1997) *Cell* **90,** 763–773.
5. Matsunami, H. & Buck, L. B. (1997) *Cell* **90,** 775–784.
6. Kunishima, N., Shimada, Y., Tsuji, Y., Sato, T., Yamamoto, M., Kumasaka, T., Nakanishi, S., Jingami, H. & Morikawa, K. (2000) *Nature (London)* **407,** 971–977.
7. Bai, M., Trivedi, S. & Brown, E. M. (1998) *J. Biol. Chem.* **273,** 23605–23610.
8. Rocheville, M., Lange, D., Kumar, U., Sasi, R., Patel, R. C. & Patel, Y. C. (2000) *J. Biol. Chem.* **275,** 7862–7869.
9. Rocheville, M., Lange, D., Kumar, U., Patel, S. C., Patel, R. C. & Patel, Y. C. (2000) *Science* **288,** 154–157.
10. Horvat, R. D., Roess, D. A., Nelson, S. E., Barisas, B. G. & Clay, C. M. (2001) *Mol. Endocrinol.* **15,** 695–703.
11. Cornea, A., Janovick, J. A., Maya-Nunez, G. & Conn, P. M. (2001) *J. Biol. Chem.* **276,** 2153–2158.
12. Roess, D. A., Horvat, R. D., Munnelly, H. & Barisas, B. G. (2000) *Endocrinology* **141,** 4518–4523.
13. Rodriguez-Frade, J. M., Vila-Coro, A. J., Martin de Ana, A., Albar, J. P., Martinez-A C. & Mellado, M. (1999) *Proc. Natl. Acad. Sci. USA* **96,** 3628–3633.
14. Vila-Coro, A. J., Rodriguez-Frade, J. M., Martin De Ana, A., Moreno-Ortiz, M. C., Martinez-A, C. & Mellado, M. (1999) *FASEB J.* **13,** 1699–1710.
15. Vila-Coro, A. J., Mellado, M., Martin de Ana, A., Lucas, P., del Real, G., Martinez-A, C. & Rodriguez-Frade, J. M. (2000) *Proc. Natl. Acad. Sci. USA* **97,** 3388–3393.
16. Kumar, U., Sasi, R., Suresh, S., Patel, A., Thangaraju, M., Metrakos, P., Patel, S. C. & Patel, Y. C. (1999) *Diabetes* **48,** 77–85.
17. Nouel, D., Gaudriault, G., Houle, M., Reisine, T., Vincent, J. P., Mazella, J. & Beaudet, A. (1997) *Endocrinology* **138,** 296–306.
18. Cornea, A., Janovick, J. A., Lin, X. & Conn, P. M. (1999) *Endocrinology* **140,** 4272–4280.
19. Jovin, T. M. & Arndt-Jovin, D. (1989) in *FRET Microscopy: Digital Imaging of Fluorescence Resonance Energy Transfer. Application in Cell Biology in Cell Structure and Function by Microspectro-Fluometry*, Kohen, E., Ploem, J. S. & Hirschberg, J. G., eds. (Academic, Orlando, FL), p. 99.
20. Bagatolli, L. A. & Gratton, E. (2000) *Biophys. J.* **79,** 434–447.
21. Berland, K. M., So, P. T. C. & Gratton, E. (1995) *Biophys. J.* **68,** 694–701.
22. Magde, D., Elson, E. & Webb, W. W. (1972) *Phys. Rev. Lett.* **29,** 705–708.
23. Kettling, U., Koltermann, A., Schwille, P. & Eigen, M. (1998) *Proc. Natl. Acad. Sci. USA* **95,** 1416–1420.
24. Forster, T. (1948) *Ann. Phys.* **2,** 55–75.
25. Wu, P. & Brand, L. (1994) *Anal. Biochem* **218,** 1–13.
26. Fishkin, J. B. & Gratton, E. (1993) *J. Opt. Soc. Am. A.* **10,** 127–140.
27. Conn, P. M., Rogers, D. C., Stewart, J. M., Neidel, J. & Sheffield, T. (1982) *Nature (London)* **296,** 653–655.
28. Simons, K. & Toomre, D. (2000) *Nat. Rev. Mol. Cell. Biol.* **1,** 31–39.
29. Hukovic, N., Rocheville, M., Kumar, U., Sasi, R., Khare, S. & Patel, Y. C. (1999) *J. Biol. Chem.* **274,** 24550–24558.